Terms and Conditions of Use of Digitised Theses from Trinity College Library Dublin

Copyright statement

All material supplied by Trinity College Library is protected by copyright (under the Copyright and Related Rights Act, 2000 as amended) and other relevant Intellectual Property Rights. By accessing and using a Digitised Thesis from Trinity College Library you acknowledge that all Intellectual Property Rights in any Works supplied are the sole and exclusive property of the copyright and/or other IPR holder. Specific copyright holders may not be explicitly identified. Use of materials from other sources within a thesis should not be construed as a claim over them.

A non-exclusive, non-transferable licence is hereby granted to those using or reproducing, in whole or in part, the material for valid purposes, providing the copyright owners are acknowledged using the normal conventions. Where specific permission to use material is required, this is identified and such permission must be sought from the copyright holder or agency cited.

Liability statement

By using a Digitised Thesis, I accept that Trinity College Dublin bears no legal responsibility for the accuracy, legality or comprehensiveness of materials contained within the thesis, and that Trinity College Dublin accepts no liability for indirect, consequential, or incidental, damages or losses arising from use of the thesis for whatever reason. Information located in a thesis may be subject to specific use constraints, details of which may not be explicitly described. It is the responsibility of potential and actual users to be aware of such constraints and to abide by them. By making use of material from a digitised thesis, you accept these copyright and disclaimer provisions. Where it is brought to the attention of Trinity College Library that there may be a breach of copyright or other restraint, it is the policy to withdraw or take down access to a thesis while the issue is being resolved.

Access Agreement

By using a Digitised Thesis from Trinity College Library you are bound by the following Terms & Conditions. Please read them carefully.

I have read and I understand the following statement: All material supplied via a Digitised Thesis from Trinity College Library is protected by copyright and other intellectual property rights, and duplication or sale of all or part of any of a thesis is not permitted, except that material may be duplicated by you for your research use or for educational purposes in electronic or print form providing the copyright owners are acknowledged using the normal conventions. You must obtain permission for any other use. Electronic or print copies may not be offered, whether for sale or otherwise to anyone. This copy has been supplied on the understanding that it is copyright material and that no quotation from the thesis may be published without proper acknowledgement.

INVESTIGATIONS INTO BILE ACID EFFECTS ON THE GOLGI APPARATUS, CELL VIABILITY AND GLUCOCORTICOID RECEPTOR DISTRIBUTION IN ESOPHAGEAL CELLS

A thesis submitted for the degree of Doctor of Philosophy (PhD)

by

Ruchika Sharma

B. Sc (Pharm), MPSI

at

University of Dublin, Trinity College

2010

Supervisors:

Dr. John Gilmer, PhD

Lecturer,

School of Pharmacy and Pharmaceutical Sciences,

Trinity College Dublin,

Ireland.

Dr. Aideen Long, PhD

Senior Lecturer,

Department of Clinical Medicine,

Trinity College Dublin,

Ireland.

Declaration

I hereby declare that this thesis has not been previously submitted for a degree at this or any other university and that the work described in this thesis is entirely my own work. I hereby give my permission to the library of Trinity College Dublin to lend or copy this thesis upon request for the purpose of study.

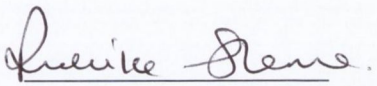

Ruchika Sharma

For my parents

Summary

Bile acids are a family of steroidal molecules derived from cholesterol and biosynthesised in the pericentral hepatocytes in the liver. In recent years there has been a renaissance in bile acid based research as it has emerged that bile acids have a wide range of biological effects, which extend beyond their traditional role as solubilising agents in the gut.

Bile acids have been shown to activate apoptotic, carcinogenic, inflammatory and anti-inflammatory signalling pathways. Using a chemical biology approach this thesis sought to investigate some of the biological effects of bile acids in an esophageal cancer model.

Previous studies have demonstrated the cytotoxicity of bile acids in hepatic, colonic and esophageal cell lines. Bile acid hydrophobicity is believed to be an important cytotoxicity determinant but this relationship is not well characterised. Chapter three of this thesis describes an investigation into the relationship between bile acid hydrophobicity and effects on cell viability.

In this study we synthesised new azido and other hydrophobic bile acid derivatives. We assembled a panel of 37 bile acids with a good range of hydrophobicities as determined by reverse phase thin layer chromatography. R_{Mw} which is extrapolated retention in 100% aqueous phase was used as a measure of hydrophobicity. The MTT cell viability assay was used to assess cytotoxicity over 24 h in the HET-1A cell line, a normal esophageal cell line.

R_{Mw} values inversely correlated with cell viability for the entire panel of compounds (r^2=0.6) but this became more significant when non-acid compounds were excluded (r^2=0.82, n= 29). The association in more homologous subgroups was stronger still (r^2>0.96). None of the polar compounds were cytotoxic at 500 μM, however, not all lipophilic bile acids were cytotoxic. Finally, chenodeoxycholic acid, deoxycholic acid and lagodeoxycholic acid were prominent outliers being more toxic than predicted by R_{Mw}. The study showed that there is an inverse correlation between R_{Mw} and toxicity that has good predictive value in homologous sets and that hydrophobicity is a necessary but not sufficient characteristic for bile acid cytocidal activity.

In Chapter four we investigated the potential of ursodeoxycholic acid derivatives as modulators of the glucocorticoid receptor. Ursodeoxycholic acid, a tertiary bile acid, is clinically used for the treatment of hepatic inflammatory diseases and recent studies have shown that its biological effects are mediated via the glucocorticoid receptor.

A series of UDCA derivatives were synthesised and screened for ability to induce translocation of the glucocorticoid receptor from the cytoplasm to the nucleus, in a high content screening assay using the SKGT-4 cell line, an esophageal cancer cell

line. The most potent derivative was tested for transactivation and transrepression potential using reporter based assays. Coactivator recruitment ability was assessed using a time-resolved fluorescence energy transfer assay.

UDCA derivatives induced glucocorticoid receptor translocation in a time dependent manner with equal efficacy to that of dexamethasone 100 nM. Several of the derivatives had low micro molar potency for translocation. The most potent derivative could suppress TNF-α induced NF-κB transcriptional activity and also induced glucocorticoid response element transactivation. Interestingly the derivative was unable to displace dexamethasone from the glucocorticoid receptor ligand binding domain in a competition binding experiment but was capable of co-activator recruitment. Using ursodeoxycholic acid as a lead we produced a series of derivatives which demonstrate a novel mechanism for glucocorticoid receptor activation. These derivatives could result in a new class of anti-inflammatory compounds.

Certain bile acids are also regarded as causative agents in the pathogenesis of colon and esophageal cancer. In Chapter five of this work we investigated if bile acid induced carcinogenesis in the colon and esophagus could be mediated via the secretory pathway. Using the HCT116, colon cancer cell line, we found that the bile acid, deoxycholic acid could induce fragmentation of the Golgi apparatus and that this resulted in a decrease in the secretory capacity of the cell line. We also found that deoxycholic acid induced Golgi fragmentation was inhibited by ursodeoxycholic acid via a glucocorticoid receptor pathway.

The Golgi assay was then adapted to an esophageal model using the HET-1A cell line. A panel of thirteen physiological bile acids were screened for effects on the Golgi apparatus. These bile acids were also screened for effects on markers of the ER stress response using real-time PCR.

We found that only the toxic bile acids deoxycholic acid, lithocholic acid and chenodeoxycholic acid induced ER stress response proteins and Golgi fragmentation, at sublethal concentrations. Furthermore we found that inhibition of ER stress with the inhibitor salubrinal decreased bile acid induced Golgi fragmentation.

This work indicates that bile acids effect the secretory pathway of the HET-1A cell line which manifests as an ER stress response and Golgi fragmentation. We propose that these changes could contribute to bile acid induced carcinogenesis in the esophagus.

Acknowledgements

I would firstly like to extend my gratitude to my supervisors, Dr. John Gilmer and Dr. Aideen Long for giving me the opportunity to work on this project. During these three years I have learned an incredible amount from them and their constant support and encouragement has guided me through this work.

I would also like to thank Prof. Dermot Kelleher for the opportunity to work in the IMM and for his many useful suggestions and insights.

A special thanks to Dr. Annemarie (Golgi) Byrne for her enthusiasm, help and advice over the past three years.

Thanks to the rest of the "Bile acid group", Shane, Fiona and Dave for all their advice, useful suggestions and for being a source of cells when needed. Thanks to Dave especially for help with the GR assay. A special thanks to Feri, for being my fellow bile acid chemist and for synthesis of compounds which have helped complete this work.

Thanks to Jun for assistance with modelling work. Thank you to Dr. John O' Brien and Dr. Manuel Ruether for NMRs, Dr. Martin Feeney and Dilip Rai for mass specs and Ray Keaveney for HPLC work.

Thank you to all the post docs in the IMM and Trinity for their constant help, advice and wise words of encouragement-Mike F (thanks for counting all those Golgi), Eugene, Dara, Steve, Antje, Emily, Martina, Jen, Seonadh, Lara, Mike J, Juan, Shona, Miriam and Niall. Thanks especially to Seow Theng and Sinead for helping me with transfections and plasmid preps. Thanks to Tony and Connla for assistance with the InCell.

To all the reading room gang Ruth, Kunal, Ramon, Christine (Chrissie Lynn), Cormac, Gosia and Sarah, thank you for being such great company in the basement and for providing welcome distraction. Thank you to Danijela for her good humour and Navin especially for advice on Photoshop. Special thanks to Stephanie for her friendship and for her crazy dancing! Thanks to Paul, Billy, Pat, Wei, Jun, Shu, Ciaran, Kinga, Orla, Deirdre, Jenny, Tom and all the other postgrads past and present in the pharm chem and pharmacognosy labs for their support and friendship. Thanks to Yvonne, Mike J and Eugene in particular for being my tequila buddies. Thanks to Fiona for teaching me about rugby, despite my lack of enthusiasm. Thanks to Sheila and Anthony for reminding me of life outside the lab.

Finally a special thanks to John for his patience and for learning to cope so well with my "rants". Thanks to Niamh for her friendship and for sticking with me through two degrees, seven apartments and sixteen balls! A big thank you to Brian for his support and for readily accepting his second place to bile acids! Thanks to Manuj for his constant support and advice, especially through all the hard times.

Thank you to Mum and Dad for teaching me the importance of hard work and learning, for your continuous love and kindness and for supporting me through everything I do.

Associated Publications

Publications

Byrne A.M, Foran E., **Sharma R.**, Davies A., Mahon C., O'Sullivan J., O'Donoghue D., Kelleher D., Long A. Bile acids modulate the Golgi membrane fission process via a protein kinase Cη and protein kinase D-dependent pathway in colonic epithelial cells *Carcinogenesis* 2010 Apr;31(4):737-44

Sharma R., Majer F., Peta V., Wang J., Keaveney R., Kelleher D., Long A., Gilmer J.F. Bile acid toxicity SAR: Correlations between cell viability and chromatographic lipophilicity in a panel of new and known bile acids. *Bioorg Med Chem* 18, 6886-95 (2010).

Sharma R., Majer F., Prichard D., Kelleher D., Long A., Gilmer J.F. Simple analogs of ursodeoxycholic acid cause translocation of the glucocorticoid receptor. *J Med Chem* Publication Date (Web) Dec 15, 2010.

Sharma R., Byrne A.M, Gilmer J.F., Long A. Bile acid induced Golgi fragmentation is mediated via an ER stress pathway. *Manuscript in preparation.*

Byrne A.M, **Sharma R.**, Kelleher D., Long A. Bile acid induced Golgi fragmentation results in aberrant secretion and glycosylation patterns in an esophageal cell line model. *Manuscript in preparation.*

Sharma R., Long A., Gilmer J.F. Trends in Bile Acid Medicinal Chemistry. Review in preparation. *Manuscript in preparation.*

Oral Presentations

Sharma, R. An Investigation in to the effect of Ursodeoxycholic acid and derivatives on the Golgi apparatus. *School of Medicine Clinical Research Day*, November 2008, Adelaide and Meath Hospital Incorporating the National Children's Hospital, Dublin, Ireland.

Sharma, R. An Investigation into the effect of Ursodeoxycholic acid and derivatives on the Golgi apparatus. *All Ireland Schools of Pharmacy Research Symposium*, April 2008, University College Cork, Cork, Ireland.

Sharma, R. An Investigation into the effect of bile acids on Golgi morphology in a model of esophageal cancer. *Royal Academy of Medicine in Ireland, Summer Meeting*, June 2007, University College Cork, Cork, Ireland.

Poster Presentations

Sharma R., Majer F., Peta V., Wang J., Keaveney R., Kelleher D., Long A., Gilmer J.F. Quantification of bile acid toxicity in an esophageal cell line: is there a relationship between hydrophobicity and biological effect? *12th Annual Meeting of IMM.* Nov 2009. Institute of Molecular Medicine, Trinity Centre for Health Sciences, Dublin, Ireland.

Sharma R., Byrne A.M., Kelleher D., Long A, Gilmer J.F. An Investigation into the effect of Ursodeoxycholic acid and derivatives on the Golgi apparatus. *American Chemical Society National Meeting*, August 2009, Washington DC, USA.

Sharma R., Byrne A.M., Kelleher D., Long A, Gilmer J.F. Effects of Ursodeoxycholic acid and derivatives on the Golgi apparatus. *10th Tetrahedron Symposium*, June 2009, Paris, France.

Sharma R., Byrne A.M., Kelleher D., Long A, Gilmer J.F. An Investigation into the effect of Ursodeoxycholic acid and derivatives on the Golgi apparatus. *Drug Discovery and Therapeutics Conference*, August 2008 Boston, Massachusetts, USA.

Sharma R., Byrne A.M., Kelleher D., Long A, Gilmer J.F. An Investigation into the effect of Ursodeoxycholic acid and derivatives on the Golgi apparatus. *European Federation of Medicinal Chemistry Symposium*, September 2008, Vienna, Austria.

Sharma R., Byrne A.M., Kelleher D., Long A, Gilmer J.F. An Investigation into the effect of Ursodeoxycholic acid and derivatives on the Golgi apparatus. *20th International Bile Acid Meeting*, June 2008, Amsterdam, Netherlands.

Sharma R., Byrne A.M., Kelleher D., Long A, Gilmer J.F. An Investigation into the effect of Ursodeoxycholic acid and derivatives on the Golgi apparatus. *Irish Society of Gastroenterology, Winter Meeting*, November 2007, Dublin, Ireland.

Abbreviations

11βHSD	11 β hydroxysteroid dehydrogenase
AATF	Apoptosis antagonizing transcription factor
AF1	Activation function1
AP-1	Activator protein-1
AR	Androgen receptor
ASBT	Apical sodium dependent bile acid transporter
ATCC	American Type Culture Collection
BA	Bile acid
BEBM	Bronchial epithelial cell basal medium
BSEP	Bile salt export pump
CA	Cholic acid
CAT	Chloramphenicol acetyltransferase
CCK	Cholecystikinin
CDCA	Chenodeoxycholic acid
CGN	cis-Golgi network
CMC	Critical micelle concentration
COX	Cyclooxygenase
CPA	Cyclopropylamide, compound **77**
CREB	cAMP response element binding protein
DBD	DNA binding domain
DCA	Deoxycholic acid
DMEM	Dulbecco's Modified Eagle Medium
DMSO	Dimethylsulfoxide
EC50	half maximal effective concentration
EcR	Ecdysteroid nuclear receptor
EGFP	Enhanced green fluorescent protein
EGFR	Epidermal growth factor receptor
EIF2α	Eukaryotic translation initiation factor 2
ER	Estrogen receptor

ER	Endoplasmic reticulum
ERK	Extracellular signal regulated kinases
F.luc	Firefly luciferase
FXR	Farnesoid X Receptor
GA	Golgi apparatus
GAPDH	Glyceraldehyde-3-phosphate dehydrogenase
GCA	Glycocholic acid
GCs	Glucocorticoids
GERD	Gastro-esophageal reflux disease
GIT	Gastrointestinal tract
GFP	Green fluorescent protein
GPCR	G-protein coupled receptor
GR	Glucocorticoid receptor
GRE	Glucocorticoid response element
GST	Glutathione S Transferase
GTM	General Transcription Machinery
HBSS	Hank's Balanced Salt Solution
HCA	High content analysis
HCA	Hyocholic acid
HCS	High content screening
HDACs	Histone deacetylases
HPLC	High performance liquid chromatography
HRMS	High resolution mass spectrometry
HSA	Hydrophobic surface area
Hsp	Heat shock protein
IBABP	Intestinal Bile acid binding protein
IUPAC	International Union of Pure and Applied Chemistry
JNK	c-Jun N-terminal kinases
LB	Luria Bertani
LBD	Ligand binding domain
LCA	Lithocholic Acid

LD_{50}	Half Maximal Lethal Dose
LXR	Liver X Receptor
MAPK	Mitogen activated protein kinase
MHC	Myosin Heavy Chain
MLC	Myosin Light Chain
MOE	Molecular operating environment
MMPT	Mitochondrial membrane permeability transistion
MR	Mineralocorticoid receptor
MRP	Multidrug resistance associated protein
MSK1	Mitogen and stress activated protein kinase 1
NCA	Nutriacholic acid
NCoR	Nuclear receptor co-repressor
NF-κB	Nuclear factor kappa light chain enhancer of activated B cells
NLS	Nuclear localisation signal
NRs	Nuclear receptors
NTCP	Sodium-taurocholate cotransporting polypeptide
OATP	Organic anion transporter
ODS	Octadecyl silanized
OST	Organic Solute Transporter
PBC	Primary biliary cirrhosis
PC	Phosphatidylcholine
PCC	Pyridinium chlorochromate
PCR	Polymerase chain reaction
PGs	Prostaglandins
PI	Propidium iodide
PI3K	Phosphatidylinositol 3-kinase
pK_a	-log acid dissociation constant
PKC	Protein Kinase C
PPAR	Peroxisome proliferator activated receptor
PMA	Phorbol Myristate Acetate
PR	Progesterone receptor

PSA	Polar surface area
PSC	Primary sclerosing cholangitis
RacK	Rac Kinase
RhoK	Rho Kinase
R.luc	Renilla luciferase
ROS	Reactive oxygen species
RPHPLC	Reverse phase high performance liquid chromatography
RP-TLC	Reverse phase thin layer chromatography
RT-PCR	Reverse transcriptase polymerase chain reaction
RXR	Retinoid X receptor
SAR	Structure activity relationship
SLCA	Sulfo-lithocholic acid
SMRT	Silencing mediator of retinoid and thyroid receptors
SRC	Steroid receptor co-activator
TBP	Tata box binding protein
TCA	Taurocholic acid
TIF-2	Transcription intermediary factor 2
TLCA	Taurolithocholic acid
TNF	Tumour necrosis factor
TPR	Tetratricopeptide repeat protein
TR	Thyroid hormone receptor
TRAIL-R1	TNF-related apoptosis-inducing ligand receptor 1
TR-FRET	Time resolved fluorescence resonance energy transfer
UCA	Ursocholic acid
UDCA	Ursodeoxycholic acid
UPR	Unfolded protein response
VDR	Vitamin D receptor

Table of Contents

List of Figures

List of Tables

1 CHAPTER ONE

GENERAL INTRODUCTION

Chapter I

1.1 Bile acids

Bile acids (BAs) are steroidal chemicals derived from cholesterol, biosynthesised by the pericentral hepatocytes in the liver (Hofmann, 1999). They are amphiphilic molecules which allows them to carry out vital physiological functions, including absorption of dietary lipids from the gut through the formation of mixed micelles (Roda, Hofmann & Mysels, 1983). It is only recently that BAs have been identified as ligands for the farnesoid X receptor (FXR) (Makishima *et al.*, 1999; Parks *et al.*, 1999), a nuclear receptor involved in various aspects of liver and glucose metabolism (Claudel, Staels & Kuipers, 2005). Furthermore a number of studies have shown that BAs are involved in a variety of disease processes including cholestatic diseases (Hofmann, 2002). They are also regarded as causative agents in the progression of colon and liver cancer and more recently in esophageal cancer (Bernstein *et al.*, 2005; Jenkins *et al.*, 2004). On the other hand, certain BAs are used therapeutically for gallstone dissolution (Tint *et al.*, 1982) and treatment of primary biliary cirrhosis (PBC) (Poupon, Poupon & Balkau, 1994). Hence BAs can be regarded as regulators of diverse cellular functions (Scotti *et al.*, 2007). Much research by scientists from wide ranging disciplines has been done to help understand the multiple cellular processes regulated by BAs and the mechanisms and consequences of these processes.

1.2 Structure of BAs

Studies on compounds present in bile began in the early nineteenth century but it was only Bernal's elucidation of the cyclopentanoperhydrophenanthrene structure of cholesterol in 1932 that allowed Rosenheim and King to propose the correct structure of BAs (Hofmann, 1985; Maitra & Mukhopadhyay, 2004). All BAs consist of two connecting units, a rigid steroid nucleus and a short aliphatic side chain, Figure 1.1. The BA nucleus has the tetracyclic cyclopentanoperhydrophenanthrene ring common to all steroids containing the six-membered A, B and C rings and a five-membered D ring. Numbering begins in ring A at C1 and proceeds around A and B to C10, then into ring C beginning with C11 and around C and D to C17. The angular methyl groups attached to C13 and C10 are numbered 18 and 19 respectively. The 17 side chain begins with C20 and finishes in sequential order (Williams & Lemke, 2002).

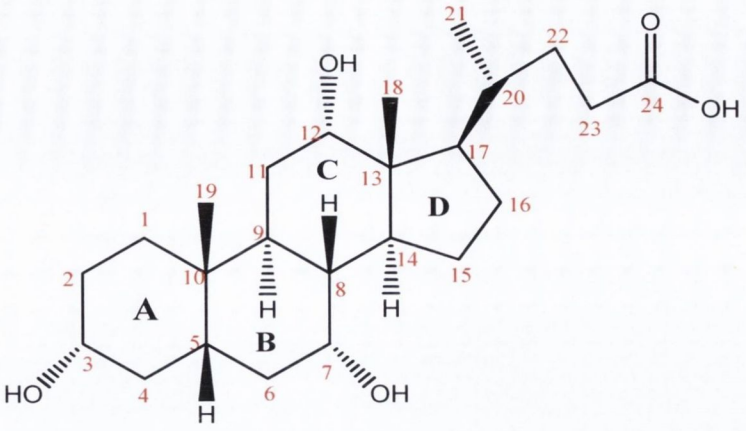

Figure 1.1 Chemical structure and numbering of cholic acid. *Bile acid numbering begins at C1 in ring A and proceeds around A and B into C and D, finishing in the side chain.*

Using a planar representation for drawing, the steroid nucleus forms a flat plane with two surfaces. Groups pointing below this steroidal plane are referred to as α-substituents and those above the plane are β substituents.
The 5α notation is used to denote the configuration of the hydrogen atom at C5, opposite to the C19 β-angular methyl group, making the A/B ring junction trans fused. Steroid families having a 5α-configuration include the 5α-pregnanes (adrenocorticoids), 5α-estranes and 5α-androstanes, Figure 1.2.

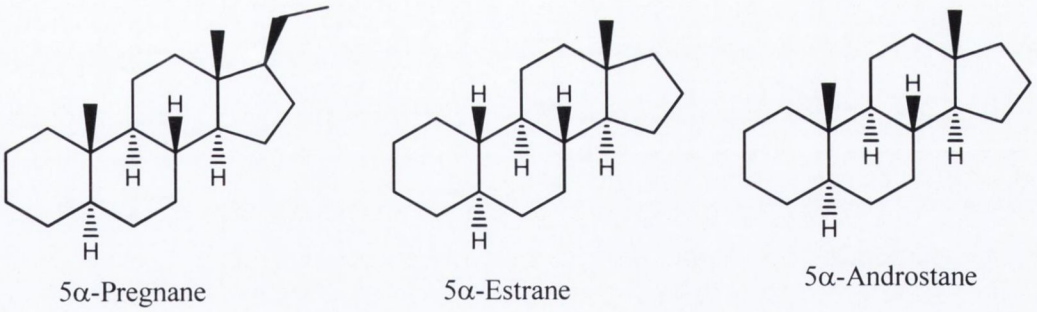

Figure 1.2 Steroid families with a 5α-configuration. *These include the 5α-pregnanes exemplified by the adrenocorticoids, the 5α-estrane family and the 5α-androstanes.*

The A/B ring junction in BAs of higher vertebrates is in the cis-configuration with a 5-β H and 19-β methyl group. This configuration gives the molecules a curved or beaked shape (Maitra & Mukhopadhyay, 2004). However in some reptiles and mammals the

A/B configuration is trans, denoted by a 5-α H. Such BAs are relatively flat and are described as allo-BAs in trivial nomenclature (Hofmann & Hagey, 2008).

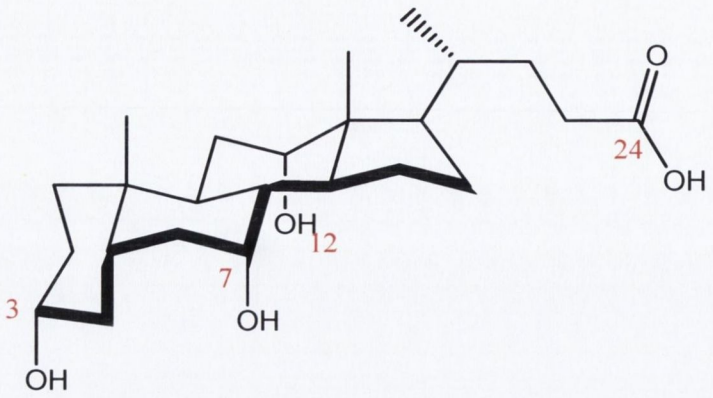

Figure 1.3 Curved structure of BAs. *BAs have a curved beaked structure due to the cis-fusion at the A/B ring junction.*

The side chain structure determines whether the compound is a BA or a bile alcohol. There are four different types of bile alcohol (C_{27}, C_{26}, C_{25} and C_{24}) and two major classes of BAs determined by the length of the side chain, the C_{27} and C_{24} BAs. The term "cholestanoid" is used to refer to all C_{27} containing bile alcohols and BAs as these contain the C_8 side chain of cholesterol whereas the term "cholanoid" is used for C_{24} compounds which only have a C_5 side chain. These two groups constitute the end products of cholesterol biosynthesis in the majority of vertebrates although certain species of frogs have BAs and bile alcohols containing C_7 and C_9 (Hofmann & Hagey, 2008) side chains. In the 1960's Haslewood conducted a series of comparative studies on BAs and bile alcohols from different species (Anderson & Haslewood, 1964; Haslewood, 1964a; Haslewood, 1964b). He proposed that the BA structure could be used as an aid to understanding the evolutionary process, noting the changing patterns in BA structure along the line of vertebrate evolution (Maitra & Mukhopadhyay, 2004). There is clear evidence of evolution of BAs through the stages: C_{27} alcohols $\rightarrow C_{27}$ acids $\rightarrow C_{24}$ acids. Bile alcohols therefore are only a major component of the bile pool in lower vertebrates. Allo-BAs are more common in lower species as well whereas the more evolved mammals have BAs with a 5β configuration. Hence, the bile composition of humans largely consists of C_{24} BAs with a 5β configuration, although recent studies have identified C_{27} BAs in human blood and cerebrospinal fluid (Ogundare *et al.*, 2010).

1.3 BA Biosynthesis in humans

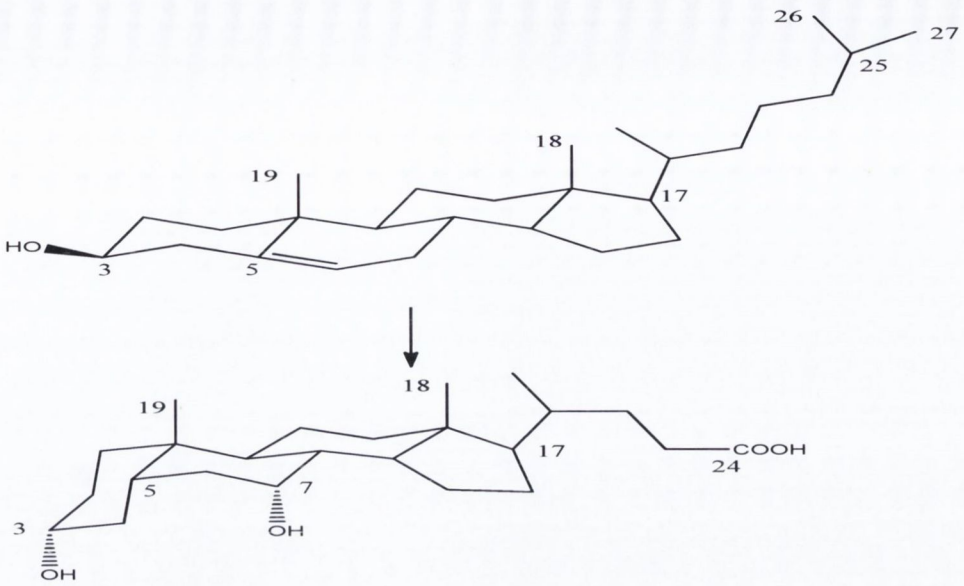

***Figure 1.4 Conversion of cholesterol to chenodeoxycholic acid (CDCA)**. CDCA biosynthesis from cholesterol involves multiple enzymatic steps which results in a change from a sp2 hybridised system to 5β configuration.*

BAs directly synthesised from cholesterol in the hepatocyte are referred to as *primary BAs.* Cholesterol is a C_{27} sterol with a double bond at C_5 and has an isooctane side chain, Figure 1.4. There is a complex series of hydroxylation, epimerisation and reduction steps required on both the nucleus and side chain to convert the flat sterol to the curved root BA, CDCA. The first step, believed to be the rate limiting step, is the oxidation of cholesterol to 7α-hydroxycholesterol catalysed by the enzyme 7α-hydryoxylase (CYP7a1) (step i, Figure 1.5). 7α-Hydroxycholesterol is then converted to cholest-7α-hydroxy-Δ^4-3-one through isomerase and reductase enzymes (step ii). This oxo derivative is a key intermediate as it is the branching point for the biosynthesis of the primary BAs CDCA and Cholic acid (CA). For the synthesis of CA, hydroxylation now occurs at C_{12} forming the backbone of the BA (step iii). The enzyme involved is sterol-12α-hydroxylase (CYP8b1). The remaining steps are the same for the synthesis of CDCA and CA. The activity of the enzyme, CYP8b1 determines the ratio of CDCA to CA (Vlahcevic *et al.*, 2000). Stereoselective reduction of the double bond forms the 5-β BA skeleton. Hydroxylation at C_{27}, followed by oxidation, affords the C_{27} carboxylic acid. This step is thought to occur in the mitochondrion and is mediated by a P-450 hydroxylase. Oxidative cleavage of the side chain from C_{27} to C_{24} by peroxisomal enzymes produces CDCA and CA. Seventeen enzymes are involved in the synthesis of the full complement of BAs (Maitra & Mukhopadhyay, 2004). Mutations in these enzymes are thought to be responsible for a number of liver disorders (Russell, 2003).

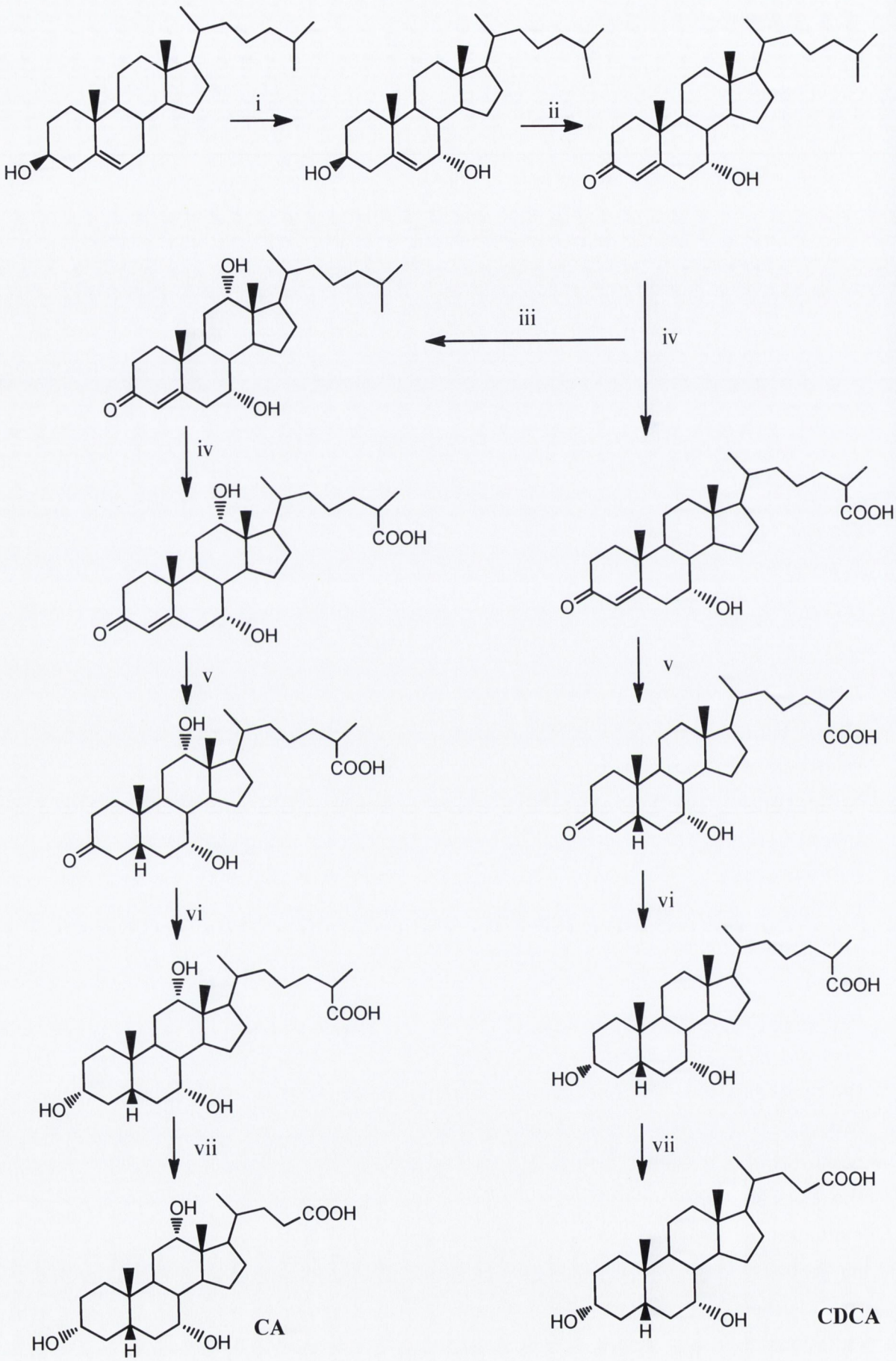
i
ii
iii
iv
v
vi
vii
HO
OH
O
COOH
H
CA
CDCA

Figure 1.5 Biosynthesis of BAs from cholesterol. *The primary BAs CDCA and CA are synthesised from cholesterol in a complex series of enzyme catalysed reactions, (i) 7-hydroxylation (CYP7A1), (ii) oxidation/isomerisation to 3-oxo, (iii) 12-hydroxylation (CYP8B1), (iv) side chain oxidation to C_{27} acid, (v) saturation to form A/B cis-fused ring, (vi) reduction of 3-oxo to 3-OH, (vii) oxidative cleavage of side chain to C_{24} acid.*

BA biosynthesis is regulated at multiple levels. Cholesterol controls its own conversion to BAs at the transcriptional level through activation of the nuclear, Liver X receptor (LXR). LXR in turn increases the expression of the enzyme CYP7A1. BAs themselves exert a negative feedback regulation of their own synthesis. The FXR has been shown to mediate this negative feedback effect again through downstream inhibition of biosynthetic enzymes. Hormones such as insulin may also affect BA synthesis. Insulin is known to down-regulate CYP7A1, for example (Roda *et al.*, 1994). Average bile acid synthesis is 0.3 g/day (Hofmann, 1999).

1.4 Classification of BAs

BAs can be classified into primary, secondary and tertiary BAs. As already mentioned, BAs that are synthesised from cholesterol in the hepatocyte are referred to as primary BAs. In humans these are CDCA and CA although traces of the 7-β epimer of CA, ursocholic acid can also be present in some individuals (Hofmann & Hagey, 2008). The primary BAs can then be modified by enzymes of anaerobic bacteria in the caecum. These modifications include removal, oxidation or epimerisation of the nuclear hydroxyl groups. BAs resulting from such modifications are referred to as secondary BAs (Hofmann & Hagey, 2008). In humans the secondary BAs lithocholic acid (LCA) and deoxycholic acid (DCA) are formed by bacterial 7-dehydroxylation of CDCA and CA respectively. LCA can then be transformed to the tertiary BAs sulfo-lithocholic acid (SLCA) by sulfation at the 3-OH. LCA is also converted to ursodeoxycholic acid (UDCA), although a certain amount of UDCA is also formed by 7-epimerisation of CDCA, Figure 1.6. These are the predominant BAs in humans but others have been found in trace amounts and there are a number of other BAs common in other mammals as shown in Table 1.1.

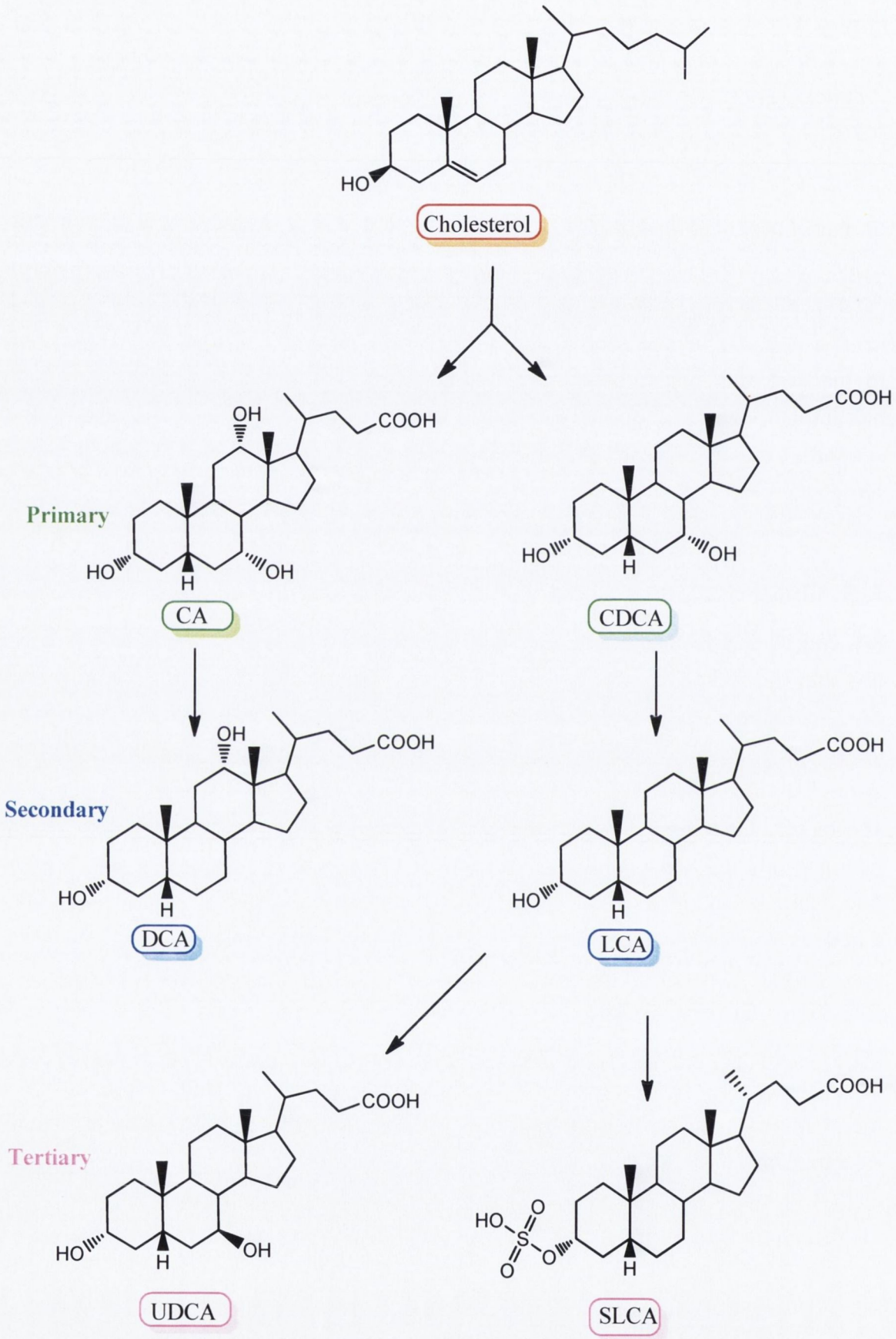

Figure 1.6 Classification of BAs. *Bile acids are classified into primary (CDCA and CA), secondary (DCA and LCA) and tertiary BAs (UDCA and SLCA).*

Table 1.1 C_{24} BAs of mammals. *There are a number of different BAs found in mammals. The A/B ring configuration, substituents on the steroid ring and side chain along with the species in which they occur are detailed for the listed BAs. Adapted from (Hofmann & Hagey, 2008).*

Trivial Name	A/B Configuration	A ring	B ring	C &D ring	C_5 side chain	Species
AlloCA	Trans (5α)	3αOH	7αOH	12αOH	None	Minor BA in newborn rabbit
Ursocholic	Cis (5β)	3αOH	7βOH	12αOH	None	Trace BA in man
LagoDCA	Cis (5β)	3αOH		12βOH	None	Trace BA in rabbit
α-Muricholic	Cis (5β)	3αOH	6βOH 7αOH		None	Rodents (minor BA)
Hyocholic	Cis (5β)	3αOH	6αOH 7αOH		None	Pigs
Phocecholic	Cis (5β)	3αOH	7αOH		23-(R)-OH	Minor BA in sea mammals
IsoLCA	Cis (5β)	3βOH				Major fecal BA in man
IsoDCA	Cis (5β)	3βOH		12αOH		Major fecal BA in man
IsoCDCA	Cis (5β)	3βOH	7αOH			Major fecal BA in man
IsoUDCA	Cis (5β)	3βOH	7βOH			Major fecal BA in man
IsoDCA	Cis (5β)	3βOH	7αOH	12αOH		Major fecal BA in man

1.5 BA conjugation

Free BAs only account for 2% of bile. They are present in the enterohepatic circulation but are precipitated at low pH. The reason for this is their acidity. pK_a is the negative logarithm of the acid dissociation constant, K_a. Therefore the pK_a is a measure of the equilibrium between the ionised and unionised acid. The pK_a of most free natural BAs is 5.1 as determined by Roda *et al* (Roda & Fini, 1984). When the pH reaches the pK_a of an acid, the molecule is 50% ionised. At pHs below this value the species will

predominantly exist as the unionised form resulting in precipitation due to poor solubility.

The majority of the BA pool consists of conjugated BAs. Five types of conjugation of C_{24} BAs are currently known. The first is N-acyl amidation with the amino acids glycine or taurine at the acid side chain, Figure 1.7.

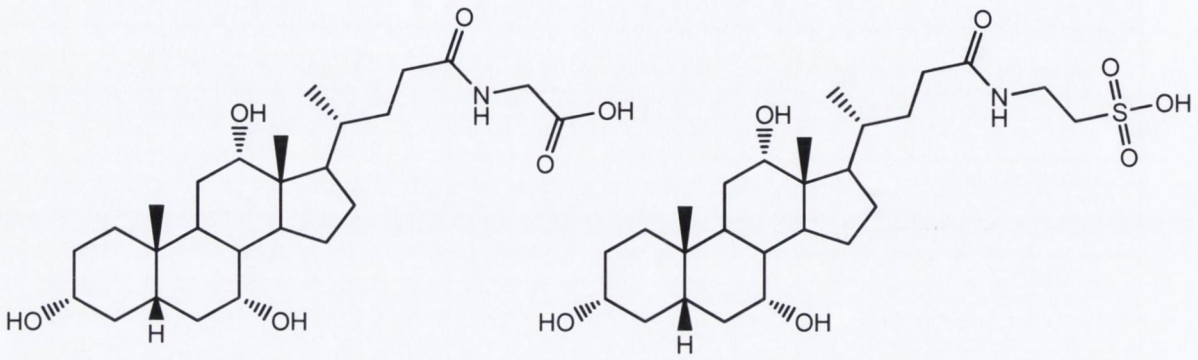

***Figure 1.7 Structure of glycocholic acid (GCA) and taurocholic acid (TCA)**. N-acyl amidation to the amino acids glycine and taurine is the most common type of BA conjugation.*

Conjugation to taurine decreases the pK_a of the natural BAs to below 2 (Hofmann & Mysels, 1992). This is because the sulfonic acid moiety is strongly electron withdrawing and converts weak acids to strong acids which are ionised at the intestinal pH (pH 6-7) and hence present as the negatively charged BA anion which has increased solubility. This negatively charged form of the BA is impermeable to cell membranes. The conjugated BA molecule is too large to diffuse through the paracellular junctions of the biliary tract and small intestine. This impermeability to cell membranes and paracellular junctions is a key factor in promoting the high intraluminal concentration of conjugated BAs in the biliary tract and small intestine (Jenkins & Hardle, 2008). On the other hand in the acidic stomach they are soluble and unionised and hence can enter the gastric epithelium. Taurine conjugated BAs represent > 20% of bile (Jenkins & Hardle, 2008).

Glycine conjugated BAs are the most abundant conjugated BAs representing 70% of bile. Conjugation to glycine results in more soluble ionised products which again are restricted to the intestinal lumen due to low epithelial permeability. However the higher pK_a of the glycine conjugates (3.8 to 4.8) means that they can cross intestinal membranes to a certain extent when the pH approaches their pK_a (Jenkins & Hardle, 2008).

The second type of conjugation which BAs undergo is sulfation which can occur at C-3 or C-24. Other types of conjugation include ester glucuronidation at C-24 and ethereal conjugation predominantly at C-3 but also at other nuclear sites.

The fifth form of conjugation is N-acetyl conjugation at C-7 which occurs in BAs such as UDCA with a 7β hydroxyl group. BAs may undergo conjugation on both the steroid nucleus and side chain (Hofmann & Hagey, 2008). LCA for example is conjugated with glycine or taurine and may be sulfated at the C-3 position. This double conjugation promotes the excretion of LCA. The percentage composition of the BAs in human bile are shown in Table 1.2.

Table 1.2 Human BA composition. *Glycine conjugated BAs are the most predominant form of BAs found in human bile, followed by taurine conjugates. Free unconjugated BAs only form 2% of the bile.*

Class	Name	Forms of Conjugates	Percent of Total Bile
Primary	Cholic acid Chenodeoxycholic Acid	Glycine or Taurine	36- 38 % Or 32 - 34%
Secondary	Deoxycholic acid Lithocholic acid	Glycine or Taurine	26 -28% 1-2 %
Tertiary	Ursodeoxycholic acid	Glycine or Taurine	1-2 %

1.6 Enterohepatic Circulation of BAs

BAs undergo a process of enterohepatic circulation which involves secretion into the small intestine and then re-absorption from the distal intestine where they are re-absorbed via both passive and active transport mechanisms and then returned to the liver where they are secreted once more into the bile. Figure 1.8 illustrates the transport mechanisms of these BAs through the liver and intestine (Hofmann & Hagey, 2008).

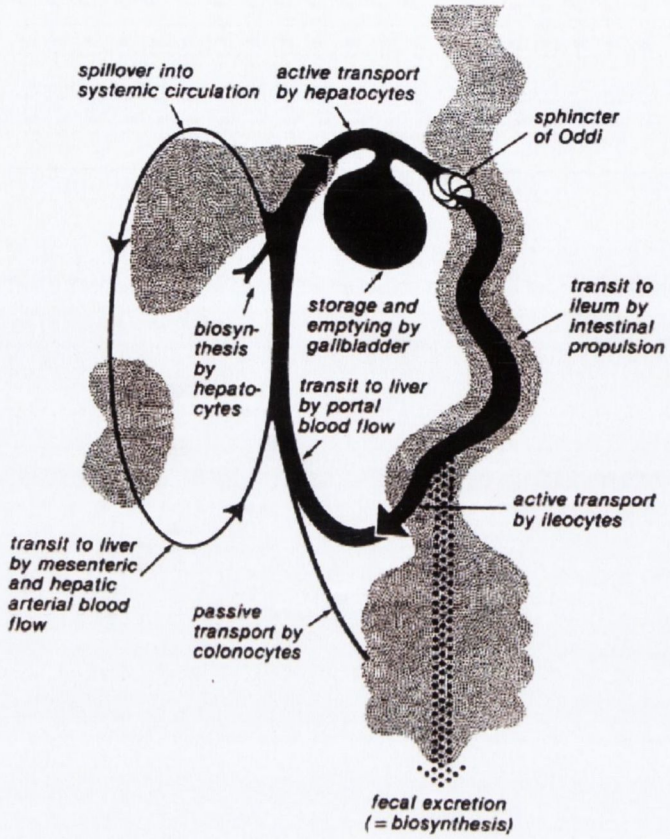

Figure 1.8 Enterohepatic circulation of BAs. *BAs undergo a process of enterohepatic circulation where they are secreted into the small intestine from the liver, then re-absorbed from the distal intestine and then returned to the liver where they can be recycled and secreted again into the bile, taken from (Hofmann & Hagey, 2008).*

The primary BAs, CDCA and CA are secreted in their conjugated form into the canalicular spaces between hepatocytes. Bile then flows distally into the bile ducts and the majority is stored in the gall bladder although some enters the intestine. On ingestion of a meal gradual gallbladder emptying occurs in response to the gastrointestinal hormone cholecystikinin resulting in BA delivery to the small intestinal lumen (Hofmann & Hagey, 2008). In man about 85% of these secreted BAs are absorbed by active and passive mechanisms and returned to the liver for re-secretion into the canaliculi (Jenkins & Hardle, 2008). Only 15% of the secreted BAs reach the distal ileum and colon. As mentioned, the secondary BAs are derived from these BAs by deconjugation followed by dehydroxylation to yield LCA, DCA and UDCA. The overall result is an increase in the hydrophobicity of the BA pool. Formation of BAs of a more hydrophobic nature ensures passive absorption of those BAs not reabsorbed in the ileum. In the normal adult only 1-3% of BAs secreted by the liver are present in the faeces (Jenkins & Hardle, 2008). The composition of the BA pool varies when

conditions of biotransformation are altered, for example by changes in transit time through the gastrointestinal tract or changes in the bacterial flora brought about by drugs and diet. For example, increased fat and reduced fibre can increase the amount of taurine conjugated BAs reaching the colon by almost tenfold resulting in much higher concentrations of the secondary BAs through dehydroxylation. DCA and LCA can accumulate in the colon as 7-dehydroxylation cannot be reversed. However double conjugation of LCA in the liver at the 3 and 24 positions produces a highly water soluble ionised derivative which cannot be reabsorbed by the colonic mucosa. Hence it is not present in very high quantities in the bile (Martinez-Augustin & Sanchez de Medina, 2008).

BA concentrations in the intestinal lumen are in the medium millimolar range. The entire mass of circulating BAs is called the BA pool and is about 2-3 g in normal size adults. As the pool cycles several times a day as described, BA secretion is 4 to 6 g per meal averaging 12 to 18 g/day (Hofmann, 1999; Hofmann & Hagey, 2008).

In plasma, BAs are found mainly bound to the plasma protein albumin, but can also bind to high density lipoprotein as determined by Kramer *et al* (Jenkins & Hardle, 2008; Kramer *et al.*, 1979). Aldini *et al* used equilibrium dialysis experiments to determine the percentage of a series of BAs bound to albumin and found that increasing hydrophobicity was associated with higher affinity binding constants (Aldini *et al.*, 1982). Binding minimises the free concentrations of BAs in plasma resulting in concentrations below 1 μM (Costarelli *et al.*, 2002; El-Mir *et al.*, 2001).

1.7 BA Transporters

In order for enterohepatic cycling of BAs to occur, the expression of BA transporters on the liver hepatocytes and ileal enterocytes is essential, as passive diffusion only accounts for a minimal amount of BA uptake. The terminal ileum has an apical bile salt transporter (ASBT) that mediates sodium dependent co-transport of BAs (Hofmann & Hagey, 2008). Different BA molecules are transported to different degrees by the ASBT as it has greater affinity for the conjugated form of BAs (Martinez-Augustin & Sanchez de Medina, 2008). Basolateral transport out of the enterocyte into portal blood for transport back to the liver is mainly mediated by a heterodimer of two proteins, organic solute transporter (OSTα/OSTβ). Efflux may also involve a truncated form of the ASBT and the multidrug resistance-associated protein 3 (MRP3) although this remains to be defined (Jenkins & Hardle, 2008). Within the enterocyte it is unlikely that BAs traverse the enterocyte as free monomers. A binding protein for BAs has been identified, called intestinal BA binding protein (IBABP) (Jenkins & Hardle, 2008). It is thought that this protein functions along with ASBT to regulate BA levels

within the enterocyte and therefore its expression is up-regulated by increased flux of BAs whereas that of ASBT is down regulated.

As described, BAs are transported to the liver in the portal vein partly bound to albumin. Conjugates of CA are 60-80% bound whereas those of CDCA are more tightly bound, >95% (Hofmann & Hagey, 2008). Uptake at the hepatocyte is mediated by the Na-taurocholate co transporting polypeptide (NTCP) which shares homology with the ASBT. The organic anion transporter family (OATP) may also be involved in the uptake process although NTCP is more efficient at transporting trihydroxy BAs (Jenkins & Hardle, 2008). Both these transporters bind not only to BAs but also to other steroids and thyroid hormone. Transport across the hepatocyte occurs in monomeric form although vesicular transport may also occur (Hofmann & Hagey, 2008). The protein involved in transport of BAs out from the hepatocyte to the canaliculus is the ATP-energised pump, called the bile-salt export pump (BSEP) (Jenkins & Hardle, 2008).

These transporters mainly transport conjugated BAs although unconjugated forms may also be transported by the NTCP and OATP (Hofmann & Hagey, 2008). Unconjugated BAs have also been shown to be substrates for a fatty acid transport protein, FATP5. This has been shown for UDCA and its conjugates (Maeda *et al.*, 2006). The high specificity of all these transporters for BAs also accounts for the low levels of BAs in peripheral blood.

1.8 BA micellisation and physicochemical properties

BAs are amphiphatic molecules possessing polar and non-polar parts which gives them the ability to aggregate in solution to form micelles. The more hydrophobic hydrocarbon surface lies on the convex β side of the steroid nucleus whereas the concave α side is less hydrophobic due to its smaller total surface area and principally due to hydroxyl groups at various positions. Furthermore, the aliphatic side chain and conjugated amide function (taurine or glycine) contains a strong ionic polar group, which also contributes a strong hydrophilic moiety to the less hydrophobic α side. Hence, BAs have two functionally different sides (Armstrong & Carey, 1982). BA aggregation in solution is largely driven by the association of the non-polar β hydrophobic faces while further aggregation can occur through the hydrogen bonding interactions of the α hydroxyls and the carboxylic acid group as shown in Figure 1.9 (Maitra & Mukhopadhyay, 2004).

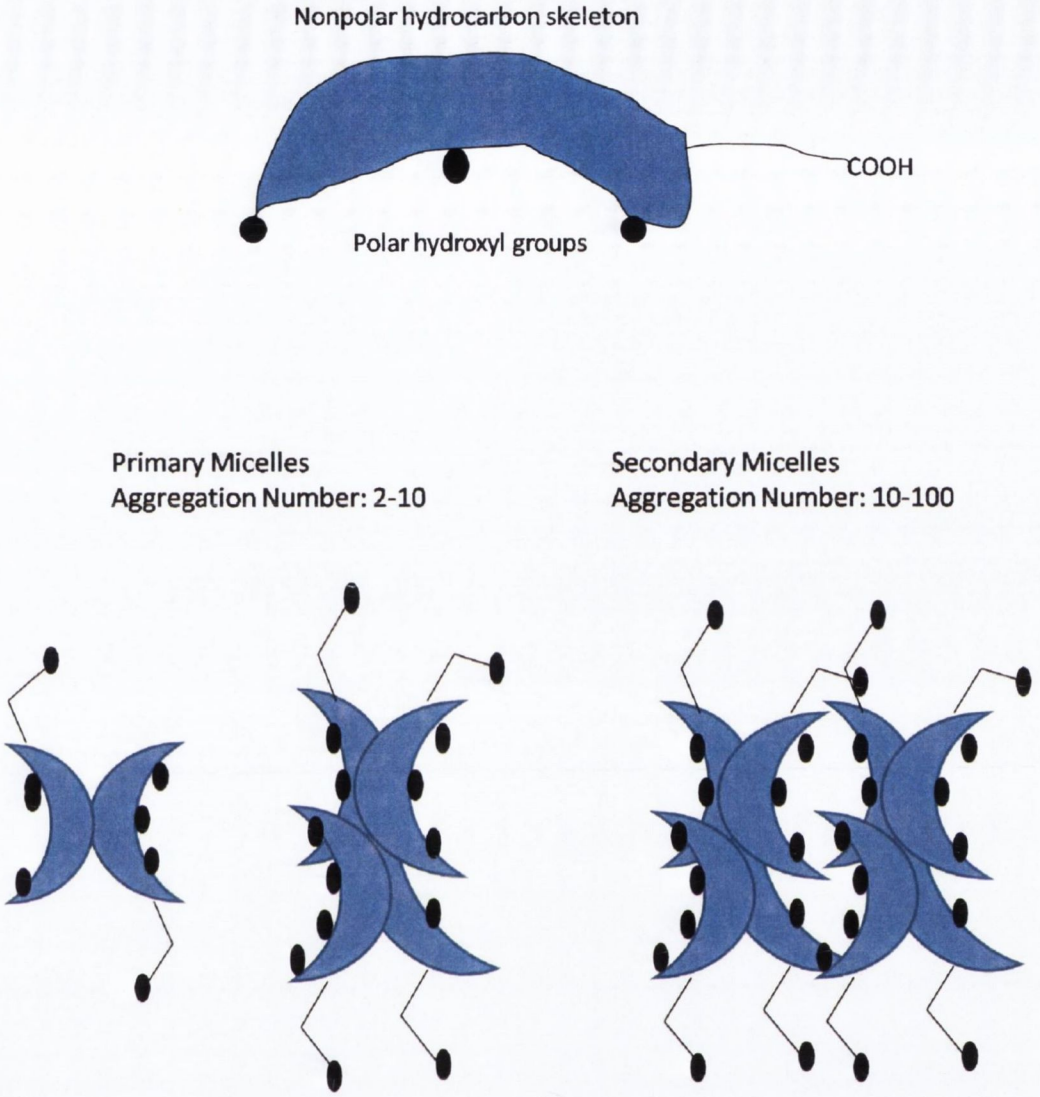

Figure 1.9 Cartoon representation of BA micellisation. *BAs are amphiphatic molecules possessing a hydrophobic convex β side and a polar concave α side. This gives them the ability to aggregate in solution to form micelles. Adapted from (Maitra & Mukhopadhyay, 2004).*

BAs self associate over a narrow concentration range to form micelles. The approximate midpoint of this concentration range is referred to as the critical micelle concentration (CMC) (Hofmann & Hagey, 2008). Below the CMC, BAs exist as monomers in the bulk solution and also at the air-water interface. The presence of the amphiphiles at the air water interface reduces surface tension, γ, at the surface layer. A point is reached at which both the air-water interface and the bulk solution become saturated with monomers. This is the CMC. After this point, increasing concentration of BA aggregate to form micelles in the bulk phase (Sinko & Singh, 2006). The

concentration of BA molecules at the surface layer remains constant in the presence of the micelles and so a plot of γ vs log concentration becomes horizontal as shown in Figure 1.10 (Florence & Attwood, 2006).

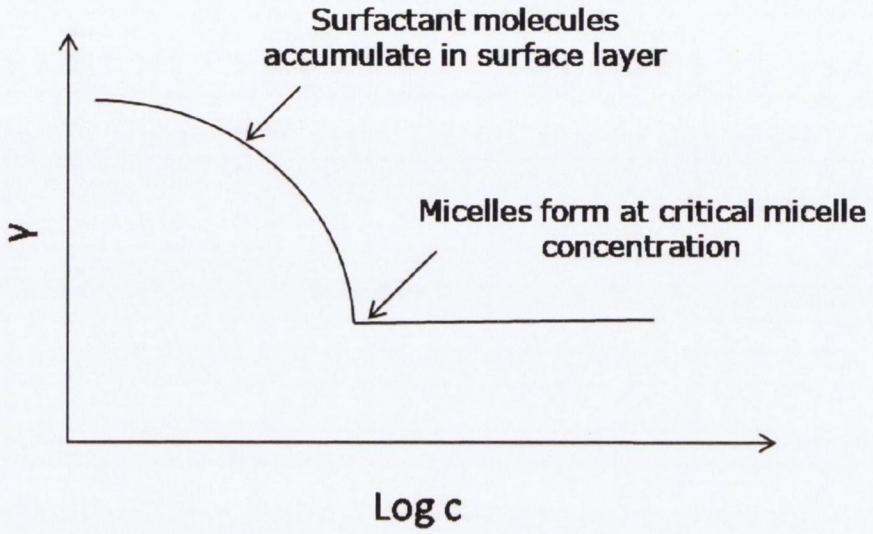

Figure 1.10 Critical Micelle Concentration. *The concentration at which micelles first form in solution is referred to as the critical micelle concentration, adapted from (Florence & Attwood, 2006).*

Multiple techniques exist for the measurement of BA CMCs. These include dye solubilisation, light scattering or changes in the fluorescence of a probe molecule. It is best measured however with the maximum bubble pressure method (Hofmann & Hagey, 2008; Roda *et al.*, 1983). Sodium ions lower the CMC and hence CMC measurements are often made at 0.15M Na^+ in order to simulate *in vivo* conditions (Roda *et al.*, 1983). Table 1.3 shows the CMC values of the common BAs in water and in 0.15M Na^+. The CMC values of the dihydroxy BAs tend to be lower than those of the trihydroxy derivatives. This is why CA has a higher CMC than DCA and CDCA. The CMC inversely correlates with the area of the hydrophobic β face of the BA molecule. The 7β-OH on UDCA interrupts the hydrophobic area of the β face and so results in a higher CMC. Therefore CMC is thought to correlate with the hydrophobic-hydrophilic balance of the BA molecule.

Table 1.3 Water Solubility and CMCs of conjugated and unconjugated BAs. *Hofmann et al determined CMC values of the sodium salts of a series of BAs in water. CMC correlates with the area of the hydrophobic face of the BA molecule, adapted from (Hofmann & Roda, 1984).*

Compound	Solubility (H_20) mM	CMC (mM) (0.15M Na)
CDCA	0.027	9 (4)
GCDCA		3(0.6)
TCDCA		1.8(0.5)
CA	0.273	13(11)
GCA		12(10)
TCA		10(6)
UDCA	0.009	19(7)
GUDCA		12(4)
TUDCA		8(2.2)
DCA	0.028	10(3)
GDCA		6(2)
TDCA		6(2.4)
LCA	0.00005	0.9 (0.5)

Like the CMC, hydrophilicity of the common free and conjugated bile salts decreases in the order UDCA > CA > CDCA > DCA > LCA, and taurine-conjugated > glycine-conjugated > free species. Natalini *et al* have correlated CMC values with hydrophobicity indices, which were determined chromatographically by extrapolating the retention factors back to a virtual pure water-containing mobile phase (Carey, 1983; Natalini *et al.*, 2007). Ultracentrifugation and quasi-elastic light scattering techniques have shown that primary BA micelles consist of 2-10 molecules which then go on and form larger secondary aggregates containing anything between 10-100 molecules. Small was the first person to propose a model for the primary and secondary aggregation of BAs (Small, 1971). Micelles consisting of only these BA anions are called simple micelles but they do not occur in this form *in vivo* as simple micelles possess the ability to solubilise lipid bilayers and form mixed micelles. The primary lipid in mixed micelles is phosphatidylcholine. The mixed micelle is thought to be spherical in shape and can have a radius in the nanometre range. The ionised head groups of the BAs repel each other making the micelle a polyanion. The mixed micelle

within the enterocyte and therefore its expression is up-regulated by increased flux of BAs whereas that of ASBT is down regulated.

As described, BAs are transported to the liver in the portal vein partly bound to albumin. Conjugates of CA are 60-80% bound whereas those of CDCA are more tightly bound, >95% (Hofmann & Hagey, 2008). Uptake at the hepatocyte is mediated by the Na-taurocholate co transporting polypeptide (NTCP) which shares homology with the ASBT. The organic anion transporter family (OATP) may also be involved in the uptake process although NTCP is more efficient at transporting trihydroxy BAs (Jenkins & Hardle, 2008). Both these transporters bind not only to BAs but also to other steroids and thyroid hormone. Transport across the hepatocyte occurs in monomeric form although vesicular transport may also occur (Hofmann & Hagey, 2008). The protein involved in transport of BAs out from the hepatocyte to the canaliculus is the ATP-energised pump, called the bile-salt export pump (BSEP) (Jenkins & Hardle, 2008).

These transporters mainly transport conjugated BAs although unconjugated forms may also be transported by the NTCP and OATP (Hofmann & Hagey, 2008). Unconjugated BAs have also been shown to be substrates for a fatty acid transport protein, FATP5. This has been shown for UDCA and its conjugates (Maeda *et al.*, 2006). The high specificity of all these transporters for BAs also accounts for the low levels of BAs in peripheral blood.

1.8 BA micellisation and physicochemical properties

BAs are amphiphatic molecules possessing polar and non-polar parts which gives them the ability to aggregate in solution to form micelles. The more hydrophobic hydrocarbon surface lies on the convex β side of the steroid nucleus whereas the concave α side is less hydrophobic due to its smaller total surface area and principally due to hydroxyl groups at various positions. Furthermore, the aliphatic side chain and conjugated amide function (taurine or glycine) contains a strong ionic polar group, which also contributes a strong hydrophilic moiety to the less hydrophobic α side. Hence, BAs have two functionally different sides (Armstrong & Carey, 1982). BA aggregation in solution is largely driven by the association of the non-polar β hydrophobic faces while further aggregation can occur through the hydrogen bonding interactions of the α hydroxyls and the carboxylic acid group as shown in Figure 1.9 (Maitra & Mukhopadhyay, 2004).

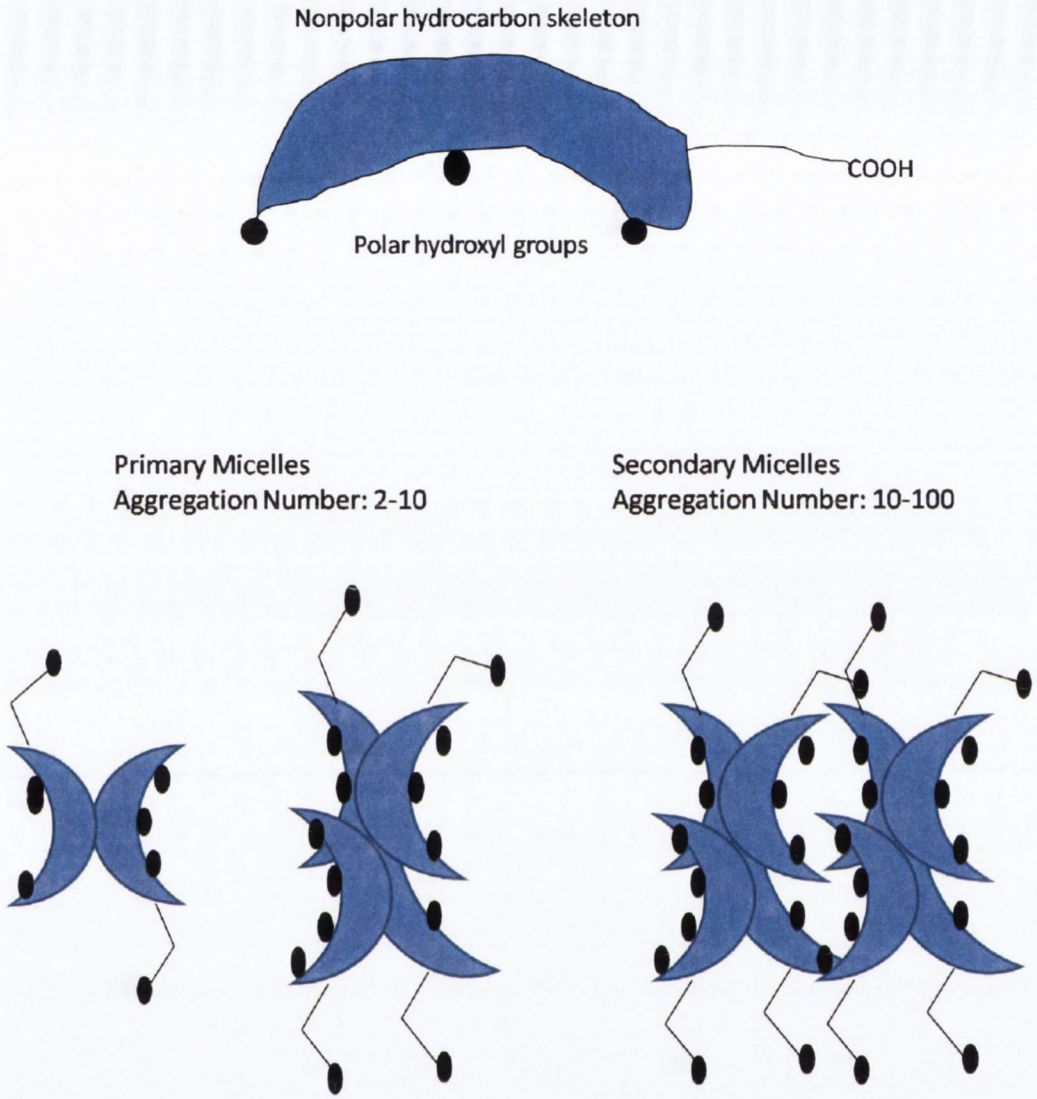

Figure 1.9 Cartoon representation of BA micellisation. *BAs are amphiphatic molecules possessing a hydrophobic convex β side and a polar concave α side. This gives them the ability to aggregate in solution to form micelles. Adapted from (Maitra & Mukhopadhyay, 2004).*

BAs self associate over a narrow concentration range to form micelles. The approximate midpoint of this concentration range is referred to as the critical micelle concentration (CMC) (Hofmann & Hagey, 2008). Below the CMC, BAs exist as monomers in the bulk solution and also at the air-water interface. The presence of the amphiphiles at the air water interface reduces surface tension, γ, at the surface layer. A point is reached at which both the air-water interface and the bulk solution become saturated with monomers. This is the CMC. After this point, increasing concentration of BA aggregate to form micelles in the bulk phase (Sinko & Singh, 2006). The

concentration of BA molecules at the surface layer remains constant in the presence of the micelles and so a plot of γ vs log concentration becomes horizontal as shown in Figure 1.10 (Florence & Attwood, 2006).

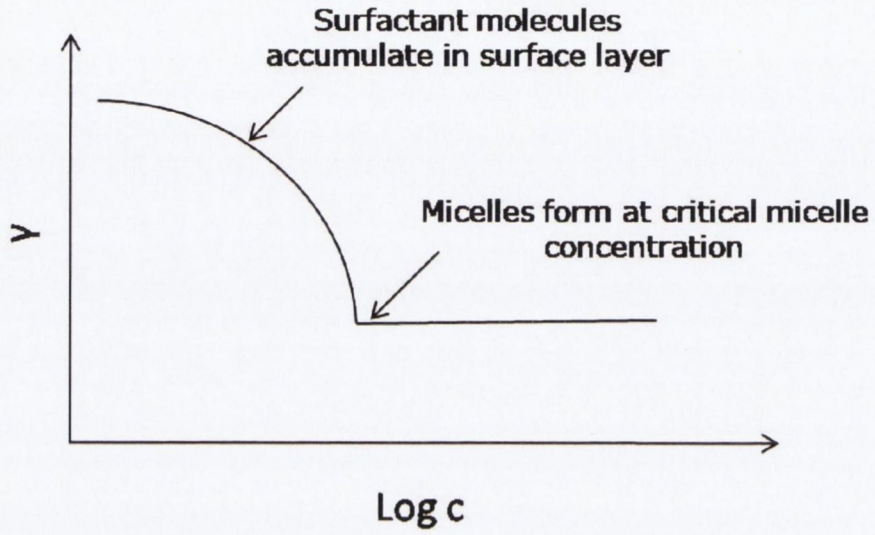

Figure 1.10 Critical Micelle Concentration. *The concentration at which micelles first form in solution is referred to as the critical micelle concentration, adapted from (Florence & Attwood, 2006).*

Multiple techniques exist for the measurement of BA CMCs. These include dye solubilisation, light scattering or changes in the fluorescence of a probe molecule. It is best measured however with the maximum bubble pressure method (Hofmann & Hagey, 2008; Roda *et al.*, 1983). Sodium ions lower the CMC and hence CMC measurements are often made at 0.15M Na^+ in order to simulate *in vivo* conditions (Roda *et al.*, 1983). Table 1.3 shows the CMC values of the common BAs in water and in 0.15M Na^+. The CMC values of the dihydroxy BAs tend to be lower than those of the trihydroxy derivatives. This is why CA has a higher CMC than DCA and CDCA. The CMC inversely correlates with the area of the hydrophobic β face of the BA molecule. The 7β-OH on UDCA interrupts the hydrophobic area of the β face and so results in a higher CMC. Therefore CMC is thought to correlate with the hydrophobic-hydrophilic balance of the BA molecule.

Table 1.3 Water Solubility and CMCs of conjugated and unconjugated BAs. *Hofmann et al determined CMC values of the sodium salts of a series of BAs in water. CMC correlates with the area of the hydrophobic face of the BA molecule, adapted from (Hofmann & Roda, 1984).*

Compound	Solubility (H_20) mM	CMC (mM) (0.15M Na)
CDCA	0.027	9 (4)
GCDCA		3(0.6)
TCDCA		1.8(0.5)
CA	0.273	13(11)
GCA		12(10)
TCA		10(6)
UDCA	0.009	19(7)
GUDCA		12(4)
TUDCA		8(2.2)
DCA	0.028	10(3)
GDCA		6(2)
TDCA		6(2.4)
LCA	0.00005	0.9 (0.5)

Like the CMC, hydrophilicity of the common free and conjugated bile salts decreases in the order UDCA > CA > CDCA > DCA > LCA, and taurine-conjugated > glycine-conjugated > free species. Natalini *et al* have correlated CMC values with hydrophobicity indices, which were determined chromatographically by extrapolating the retention factors back to a virtual pure water-containing mobile phase (Carey, 1983; Natalini *et al.*, 2007). Ultracentrifugation and quasi-elastic light scattering techniques have shown that primary BA micelles consist of 2-10 molecules which then go on and form larger secondary aggregates containing anything between 10-100 molecules. Small was the first person to propose a model for the primary and secondary aggregation of BAs (Small, 1971). Micelles consisting of only these BA anions are called simple micelles but they do not occur in this form *in vivo* as simple micelles possess the ability to solubilise lipid bilayers and form mixed micelles. The primary lipid in mixed micelles is phosphatidylcholine. The mixed micelle is thought to be spherical in shape and can have a radius in the nanometre range. The ionised head groups of the BAs repel each other making the micelle a polyanion. The mixed micelle

can then solubilise lipids, lecithin, cholesterol and fat soluble vitamins (Maitra & Mukhopadhyay, 2004; Ueno, 1997; Wiedmann & Kamel, 2002).

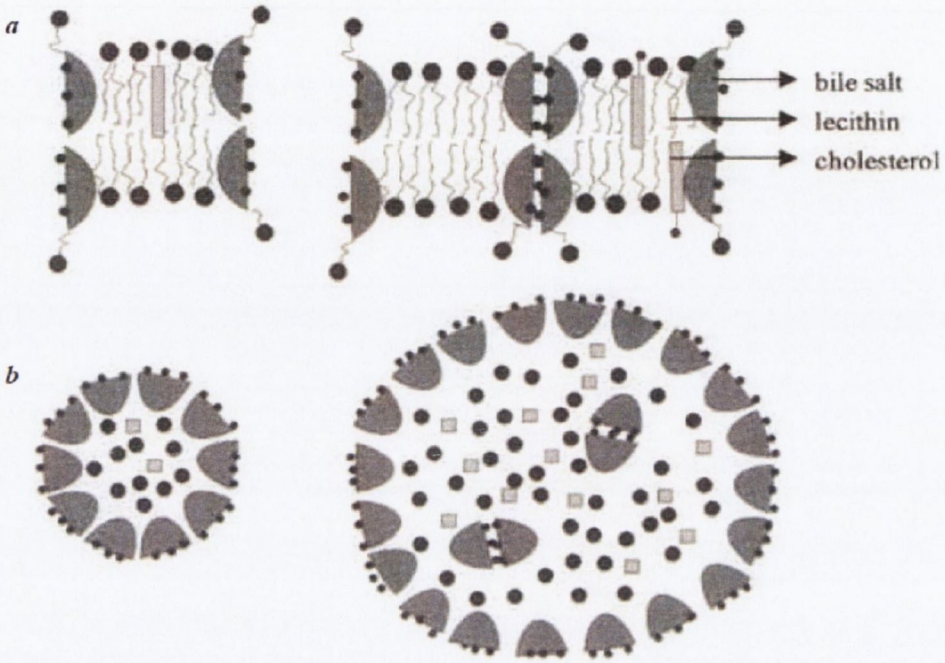

Figure 1.11 Proposed molecular arrangement of bile-salt-lecithin cholesterol mixed micelles. *a) Longitudinal view and b) Cross-sectional view of mixed micelles, taken from (Maitra & Mukhopadhyay, 2004).*

1.9 Physiological Functions of BAs

The main physiological role of BAs is in solubilisation of dietary lipids in the intestine. These digestive functions of BA are summarised in Table 1.4.

Table 1.4 The digestive functions of BAs. *Adapted from (Hofmann, 1999).*

Process	Site	Mechanism
Cholesterol elimination	Hepatocyte	Conversion to BAs Stimulation of biliary cholesterol secretion
	Biliary tract	Solubilisation of cholesterol in mixed micelles
	Intestine	Fecal excretion of cholesterol and BAs
Stimulation of bile flow	Hepatocyte	Canalicular secretion of osmotically active molecules
	Cholangiocyte	Potentiation of secretin-stimulated bicarbonate Secretion
Stimulation of PC * Secretion	Hepatocyte	Detachment of PC from canalicular membrane
	Biliary tract	Solubilisation of PC in mixed micelles
Feedback inhibition	Hepatocyte	Repression of cholesterol 7α-hydroxylase and HMG-CoA reductase
Enhancement of lipid absorption	Small intestine	Formation of mixed micelles
Cleaning of absorptive surface	Small intestine	Surface activity of BA anions
Stimulation of intestinal motility	Large intestine	Neural arc

**PC indicates phosphatidylcholine.*

In addition to the above digestive functions, recent findings have suggested the participation of BAs in many other body functions. At the intestinal level BAs are known to modulate pancreatic enzyme secretion and cholecystikinin (CCK) release (Koop *et al.*, 1996; Monte *et al.*, 2009). Interestingly they have been shown to have anti-microbial properties that prevent the over-growth of bacterial flora in the intestine (Begley, Gahan & Hill, 2005). Furthermore discovery of BAs as ligands of the FXR and the G-protein coupled receptor, TGR5 and subsequent work characterising the activity of these receptors has unearthed a number of endocrine functions of BAs. For example, BAs regulate their own synthesis through the FXR and have also been found to have roles in the control of general energy-related metabolism, and in hepatic glucose handling (Ma *et al.*, 2006; Monte *et al.*, 2009).

1.10 BAs as agonists

The mechanism of action through which the diverse range of BAs mediate their biological effects remains unknown. However, two signalling pathways are known to be directly activated by BAs. These are the TGR5 pathway and activation of the members of the nuclear hormone receptor super family, which includes the FXR.

TGR5 is a member of the rhodopsin-like superfamily of GPCRs and was identified as an LCA-activated receptor (Kawamata *et al.*, 2003). Primary and secondary BAs activate the receptor at nanomolar concentrations (Table 1). LCA and taurolithocholic acid (TLCA) activate the receptor with an EC_{50} of 600 and 300 nM, respectively, and should be considered physiological ligands for TGR5 (Kawamata *et al.*, 2003). Furthermore Pelliciari *et al* have performed comprehensive SAR studies and have identified novel synthetic TGR5 ligands. Some of these natural and synthetic TGR5 agonists are shown in Table 1.5 (Pellicciari *et al.*, 2007; Sato *et al.*, 2008).

Table 1.5 Natural and synthetic TGR5 agonists. *TGR5 is a potential therapeutic target for treatment of metabolic disorders, adapted from (Fiorucci et al., 2009).*

Natural	Synthetic
TLCA	6-ECDCA
LCA	23-(S)-methyl CA
DCA	
CA	
UDCA	
CDCA	

There is much current interest in TGR5 as a therapeutic target as TGR5 ligands decrease blood glucose levels and increase energy expenditure by promoting intracellular thyroid hormone activation in thermogenically competent tissues (Fiorucci *et al.*, 2009). Hence these BAs may be useful in treatment of metabolic disorders.

The FXR is another protein known to be activated by BAs. Indeed most BA homeostasis is thought to occur through the FXR as it is known to regulate the expression of enzymes involved in BA synthesis (Lu *et al.*, 2000) as well as expression of BA transporters such as the IBABP (Sinal *et al.*, 2000).

Table 1.6 Natural and synthetic FXR agonists. *These FXR agonist are interesting lead molecules in developing therapies for glucose and lipid metabolic disorders, adapted from (Fiorucci et al., 2009).*

Natural	Synthetic
DCA	6-ECDCA
LCA	23-(S)-methyl CA
CDCA	Fexeramine
	GW4064
	MeCA
	MeDCA
	WAY-362450

FXR is also known to alter the transcription of several genes involved in fatty acid and triglyceride synthesis and lipoprotein metabolism. Administration of FXR agonists [GW4064, 6α-ethyl-chenodeoxycholic acid (6-ECDCA) and WAY- 362450] to rats and mice reduces plasma triglyceride and cholesterol levels (Kast *et al.*, 2001; Lefebvre *et al.*, 2009) again making BAs and their derivatives interesting lead molecules in the search for treatments for lipid and glucose metabolic disorders.

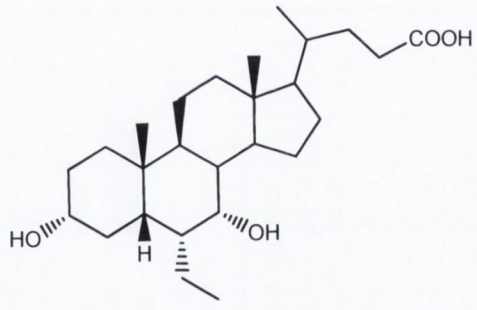

6-ECDCA

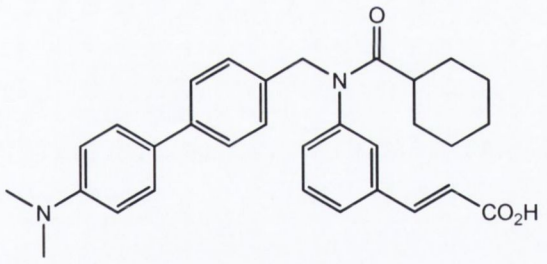

Fexeramine

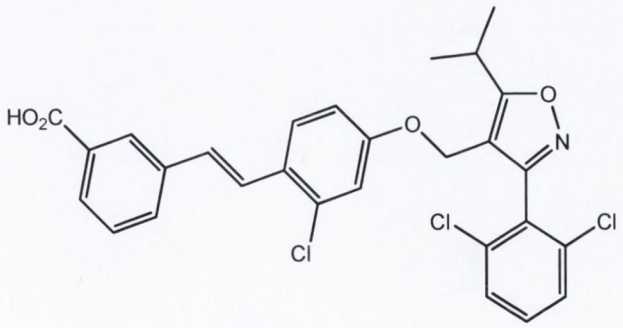

GW4064

Figure 1.12 Structures of synthetic FXR and TGR5 agonists. *6-ECDCA is a potent TGR5 and FXR agonist, Fexeramine and GW4064 are potent FXR agonists.*

UDCA does not bind to the FXR but interestingly inhibits its activation by other BAs (Makishima *et al.*, 1999). Another member of the nuclear receptor family shown to be activated by the BA UDCA is the glucocorticoid receptor (GR). Ligand dependent activation of the GR alters the transcriptional activity of several genes, which regulate vital bodily functions, including metabolism, bone turnover and homeostasis of the immune system. The mechanism of action of UDCA remains unknown although many of its effects are thought to occur via activation of the GR. The functions of the GR and its activation by UDCA will be covered in more detail in Chapter 4.

1.11 BAs and disease pathology

Despite being essential physiological regulators, it is now well recognised that BAs play a central role in the pathology of hepatic, biliary and intestinal diseases (Hofmann, 1999). *In vitro* hydrophobic bile salts have been shown to be cytotoxic against a variety of different cell types including hepatocytes (Spivey, Bronk & Gores, 1993), erythrocytes (Heuman *et al.*, 1991), mast cells (Quist *et al.*, 1991) and gastric and intestinal cells (Ota *et al.*, 1991). Leading on from this, it is now generally accepted that secondary hydrophobic BAs are cytotoxic when their concentrations increase to abnormally high levels either intracellularly or extracellularly (Hofmann, 1999). As a result they have been thought to significantly contribute to the development of a number of hepatobiliary cholestatic disorders. In cholestasis bile cannot flow from the liver to the small intestine. It may be caused by an impairment of bile secretion, an obstruction of bile flow or a combination of the two. It is a symptom of many diseases including acute hepatitis, primary biliary cirrhosis (PBC) and primary sclerosing cholangitis (PSC) (Beers, 2004). The common consequence of all forms of cholestasis is retention of BAs and other potentially toxic compounds in the hepatocytes. This can lead to high concentrations of cytotoxic BAs which can induce cellular membrane damage but also can induce apoptosis or necrosis of hepatocytes. Continuous insult eventually results in a chronic cholestatic liver disease. In certain cholestatic disorders there is also leakage of BAs into the peribiliary space causing portal inflammation and fibrosis (Hofmann, 1999; Hofmann, 2002; Paumgartner, 2006).

1.12 BAs and Cancer

In experimental and epidemiological studies BAs have been identified as causative agents in the development of colon cancer and liver cancer (Thompson, 1996). BAs were first proposed to be carcinogens in 1939 and 1940 by Cook and Kennaway

(Cook, Kennaway & Kennaway, 1940). More recent evidence supports this view. At least 15 reports, from 1980 through 2003, indicate that BAs cause DNA damage. Patients with colorectal adenomas and carcinomas exhibit high blood and fecal levels of secondary BAs (Bayerdorffer *et al.*, 1994). These cancers are associated with diets rich in fat which is a powerful stimulant of BA secretion. Thus many investigators have studied the effects of BAs, particularly secondary BAs (DCA and LCA) on intestinal epithelial cell proliferation, apoptosis and mutagenesis *in vitro*, as well as on cancer promotion *in vivo*. Reports, from 1994 through 2002, indicate that BAs, at the increased concentrations which would be found in high fatty western diets, can induce apoptosis. Those cells within the exposed population which display resistance to apoptosis may survive and selectively proliferate (Bernstein *et al.*, 2005).

A number of mechanisms have been proposed to explain the induction of carcinogenesis by BAs. DCA has been shown to activate a number of mitogenic and apoptotic signaling pathways. The cascades activated include the epidermal growth factor receptor and the Raf/Mek/Erk pathway (Bernstein et al., 2005; Im & Martinez, 2004), the activator protein -1 (AP-1) transcription factor (Hirano et al., 1996; Im & Martinez, 2004), and the protein kinase C (PKC) family (Shah *et al.*, 2005) all of which are known to be deregulated during colon tumourigenesis. Activation of the AP-1 proto-oncogene has been shown to occur by co-operate activation of PKCs and extracellular signal-regulated kinases (ERKs) in HCT-116 human colorectal cancer cells (Qiao *et al.*, 2000). The AP-1 complex activated by BAs consists of JunD, Fra-1 and c-Fos (Looby *et al.*, 2009). These transcription factors are also involved in invasion pathways (Ozanne *et al.*, 2000). An important target gene of BA signaling is the gene that encodes cyclooxygenase 2 (COX-2) (Zhang *et al.*, 1998). Treatment of rats with DCA via an intracolonic instillation procedure resulted in increased colonic accumulation of prostaglandin E and thromboxane B2. COX-2 enzyme activity is responsible for the conversion of arachidonic acid to prostaglandins (PGs) (DeRubertis, Craven & Saito, 1984).

COX-2 may contribute to carcinogenesis in several ways. COX-2 activity can lead to an inhibition of apoptosis, as indicated by the induction of resistance to butyrate-induced apoptosis in rat intestinal epithelial cells after successful transfection with COX-2 (Tsujii & DuBois, 1995). COX-2 expression can also stimulate colorectal cancer cells to secrete proangiogenic prostaglandins (PGs) (Tsujii *et al.*, 1998) and stimulates expression of MMP-2 and invasion into matrigel of Caco-2 human colorectal cancer cells (Tsujii, Kawano & DuBois, 1997). Pathways potentially involved in BA induced carcinogenesis are shown in Figure 1.13.

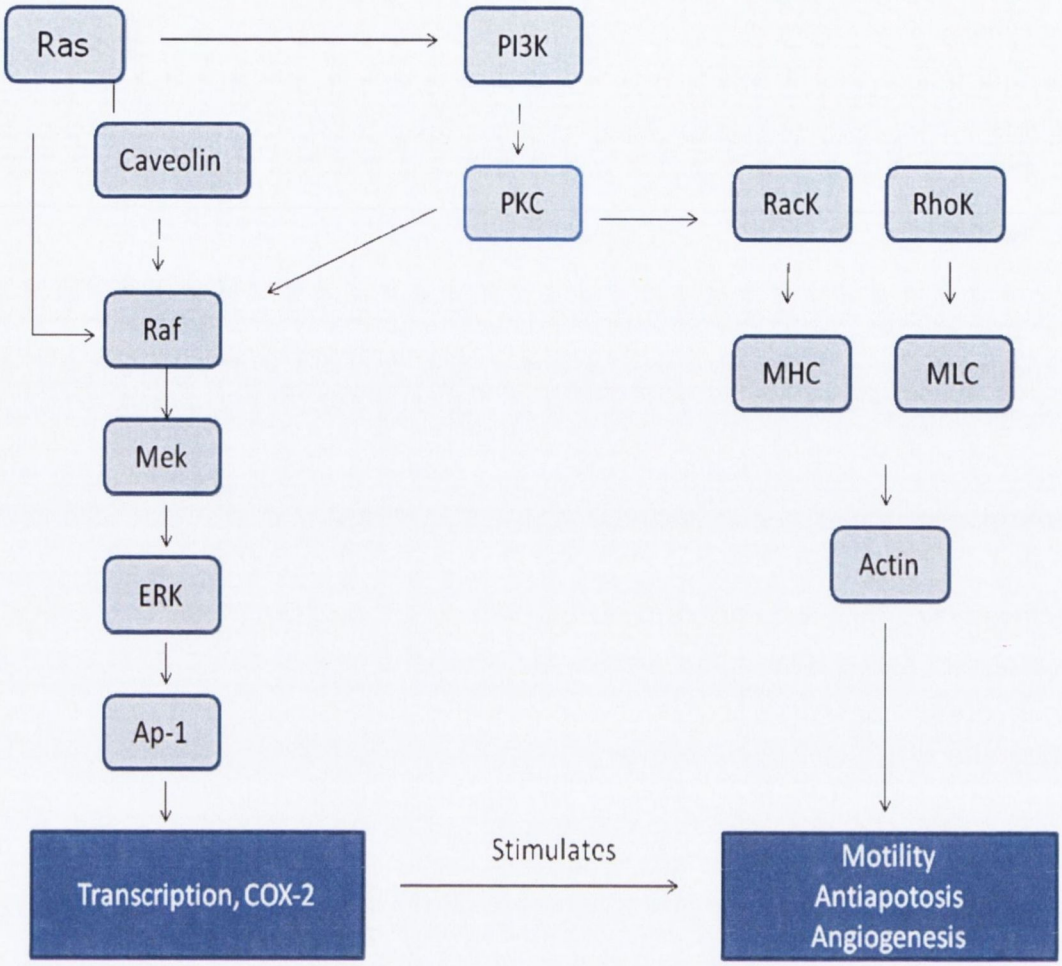

Figure 1.13 Potential signaling pathways of BAs in pre-cancerous and cancerous colonic cells. *AP1 is activated via a PKC and ERK pathway. AP-1 can then increase expression of COX-2. Activation of the phosphatidylinositol 3-kinase (PI3K) pathway can up regulate proteins such as, Rac kinase (RacK), Rho kinase (RhoK) and the myosin heavy and light chains (MHC and MLC) which are involved in motility and invasion. Ras and caveolins are upstream regulators of PI3K and the Raf/Mek/Erk pathway which regulate cell proliferation, growth and migration. Adapted from (Debruyne et al., 2001).*

1.13 BAs and Esophageal Cancer

Barrett's esophagus is a metaplastic condition in which columnar epithelium containing goblets cells, replaces the squamous epithelium normally found in the esophagus. It is a prevalent complication of chronic gastro-esophageal reflux disease (GERD) and is the single most important risk factor for the development of esophageal adenocarcinoma, increasing the risk by at least 30 fold (Fitzgerald, Lascar & Triadafilopoulos, 2001). Adenocarcinoma of the distal esophagus and gastro-esophageal junction has increased in incidence over the last several decades at a rate exceeding that of any other cancer (Cameron, 1997).

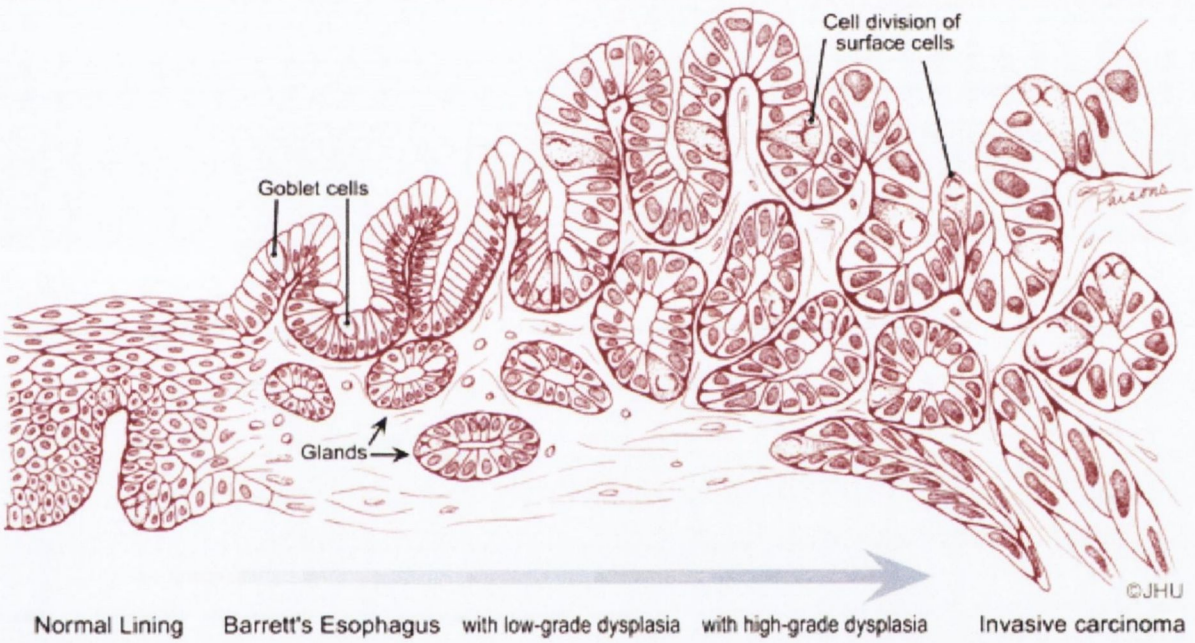

Figure 1.14 Progression of esophageal adenocarcinoma. *Chronic exposure to reflux containing bile and acid can result in Barrett's esophagus in which the squamous epithelium is replaced by a columnar epithelium. Barrett's esophagus greatly increases the risk of full blown invasive carcinoma. Taken from http://pathology2.jhu.edu/beweb/Definition.cfm.*

Currently the only strategies available to diminish adenocarcinoma rates are surveillance endoscopy, endoscopic thermal or photodynamic ablation or tissue resection. Therefore approaches are required that remove or prevent stimuli considered prime candidates in the development of esophageal adenocarcinoma (Jankowski & Anderson, 2004).

Both gastric acid and BAs have been reported as potential insults involved in the pathogenesis of Barrett's esophagus and the development of esophageal adenocarcinoma (Jankowski & Anderson, 2004). It is thought that chronic exposure to

reflux containing acid and bile salts in conditions such as GERD may be crucial in the pathogenesis of the disease (Attwood *et al.*, 1992; Gillen *et al.*, 1988). Barrett's metaplasia patients have increased bile exposure and increased proportions of secondary BAs in their refluxate (Nehra *et al.*, 1998). Furthermore, Barrett's patients with early adenocarcinoma have higher exposure to BAs than uncomplicated Barrett's patients (Stein *et al.*, 1998). Unconjugated BAs in particular have been suggested as an important factor in the progression of the neoplastic sequence in Barrett's cancers (Jankowski *et al.*, 1993). Opinions are still conflicting regarding the relative roles of BAs and stomach acid (Triadafilopoulos, 2001). However the fact that patients undergoing acid suppression therapy can progress to adenocarcinoma suggests that factors other than acid are important in Barrett's carcinogenesis. Furthermore compensatory proliferation has been postulated to occur *in vivo* as a result of BA induced apoptosis (Lapre *et al.*, 1992), which indicates that BAs may be initiators as well as promoters of cancer progression.

BAs have been found to initiate a number of cell signalling cascades in esophageal cancer cell lines in a manner analogous to colon cancer. Jenkins *et al* have shown that exposure of an esophageal cancer cell line to DCA at neutral pH activates the transcription factor nuclear factor kappa light chain enhancer of activated B cells (NF-κB), a candidate cancer promoting gene (Jenkins *et al.*, 2004). Other molecules involved include COX-2, c-myc and the mitogen-activated protein kinase (MAPK) pathway.

COX-2 upregulation has been reported in esophageal adenocarcinoma (Deasy *et al.*, 2007; Kaur *et al.*, 2000). PGs have also been found to be overexpressed in esophageal tumours as a consequence of enhanced COX-2 expression (Buttar *et al.*, 2002). Moreover, COX-2 expression levels have been found to be elevated in Barrett's esophagus (Lagorce *et al.*, 2003) and have been reported to increase with the progression from metaplasia to dysplasia to adenocarcinoma (Morris *et al.*, 2001). Following on from this a phase III trial is currently being conducted by Raj Jankowski, the Aspect Trial, which is a randomised study, looking at the effect of aspirin and esomeprazole chemoprevention in Barrett's metaplasia. Interim analysis of this trial is due in 2011 (Das, Chilton & Jankowski, 2009).

1.14 UDCA

The tertiary BA UDCA has properties distinct from those of the other BAs. While the secondary BAs are recognised as toxic and carcinogenic agents, UDCA has been shown to have numerous beneficial effects in the treatment of liver diseases in particular. The use of UDCA in the treatment of liver maladies originates in ancient Chinese folk

medicine. For centuries the Chinese used a drug called "yutan", a dried powder derived from the bile of adult bears to cure hepatobiliary disorders (Lazaridis, 2001). In 1927 Shoda was the first person to describe the chemical form of UDCA from the bile of the Chinese black bear (Shoda, 1927). He named this BA urso-deoxycholic acid because of its discovery in the bile of the bear ("ursus" meaning bear in Latin) and his belief that it was an isomer of DCA which was confirmed later by Iwasaki in 1936 (Iwasaki, 1936).

1.14.1 Clinical Usage and Efficacy of UDCA

Following oral administration UDCA absorption in the gut varies from 30-60% (Lazaridis, 2001). The degree of UDCA enrichment in bile following chronic ingestion correlates with its daily-administered dose. UDCA given at 8-10 mg/kg per day causes an expected enrichment of approximately 40% in biliary Bas (Hofmann, 1994). A UDCA dose above 10-12 mg/kg per day does not further increase its proportion in bile due to its epimerization to CDCA (Hofmann, 1994; Rubin *et al.*, 1994). In humans, the half-life of UDCA is 3.5 to 5.8 days (Ward *et al.*, 1984). UDCA is currently licensed and used for treatment of a variety of hepatic disorders.

1.14.1.1 Cholestatic Hepatic Diseases

UDCA is used for treatment of PBC and PSC which are autoimmune diseases affecting the liver and biliary ducts. A number of studies have been conducted showing the positive outcome of UDCA therapy. A multicenter controlled trial of patients with PBC by Poupon *et al* demonstrated that UDCA therapy for two years leads to reduction of clinically overt disease, improvement of liver blood tests but mean histologic score of liver biopsies in the UDCA treated group compared to placebo (Poupon *et al.*, 1991). Subsequent studies have shown that UDCA delays the progression rate of PBC resulting in a decreased need for liver transplantation (Poupon *et al.*, 1994). Lindor *et al* reported a 2.6-fold decrease in mortality or need for liver transplantation in the UDCA treatment group compared to patients receiving placebo (Lindor *et al.*, 1996). UDCA has been used in combination with either colchicine or prednisone and compared to UDCA alone. These studies did not show an additional favorable outcome compared to UDCA monotherapy (Leuschner *et al.*, 1996; Poupon *et al.*, 1996).

1.14.1.2 Gallstone dissolution

Due to its chemical and structural resemblance to CDCA, a BA studied extensively for dissolving gallstones, it was proposed that UDCA might also be suitable for this role. In a pivotal study, Makino *et al* reported gallstone dissolution with UDCA (Makino *et*

al., 1975). Since then UDCA has been used in the treatment of certain types of gallbladder stones as an alternative to cholecystectomy (Tint *et al.*, 1982). The proposed mechanism of action involves saturation of bile by UDCA leading to gallstone dissolution by solubilizing cholesterol from the stone surface (Rubin *et al.*, 1994). Given that UDCA has a much higher CMC, and is a poorer surfactant than other BAs it is remarkable that it is a better agent for dissolution.

1.14.1.3 Other Diseases

UDCA trials have been conducted showing varying degrees of success in treatment for a number of diseases. These include treatment for other forms of cholestasis such as drug induced cholestasis, total parenteral nutrition induced cholestasis, benign recurrent intrahepatic cholestasis and intrahepatic cholestasis of pregnancy (Lazaridis, 2001). Paediatric patients with conditions such as cystic fibrosis and progressive familial intrahepatic cholestasis also responded favourably to trials using UDCA treatment (Lazaridis, 2001). Following evidence that UDCA can activate the GR (Weitzel *et al.*, 2005), it has been proposed to have immunomodulatory properties and therefore UDCA was suggested in the treatment of liver allograft rejection, specifically of acute cellular rejection. This hypothesis was supported by promising data from uncontrolled studies (Lazaridis, 2001). Following this, four randomized placebo controlled trial tested UDCA as a prophylactic agent in reducing the incidence of cellular rejection following liver transplantation. In three of these studies UDCA failed to prevent rejection (Fleckenstein, Paredes & Thuluvath, 1998; Keiding *et al.*, 1997; Pageaux *et al.*, 1995).

However in one study, addition of UDCA in the immunosuppression regimen resulted in fewer episodes of acute cellular rejection, shorter hospital stay and better 90-day and 1-year survival (Barnes *et al.*, 1997). Hence the use of UDCA in acute cellular rejection remains to be established.

1.14.2 UDCA as a chemopreventative agent

UDCA has been shown to act as a chemopreventative agent. In an azoxymethane colon cancer model dietary supplementation with 0.2% UDCA inhibited CA induced tumour incidence by more than 50% (Earnest *et al.*, 1994). A similar study by Ikegami suggested that the effect may be mediated via attenuation of phospholipase A_2 (Ikegami *et al.*, 1998). UDCA treatment has been shown to decrease the risk of developing colorectal cancer in patients with PSC and ulcerative colitis (Pardi *et al.*, 2003; Tung *et al.*, 2001). In another study by Serfaty *et al* UDCA treatment did not significantly decrease prevalence of colon adenoma formation in patients with PBC but

it did significantly reduce the probability of recurrence following removal of the adenoma (Serfaty *et al.*, 2003). A phase III trial with 1285 patients produced similar findings as UDCA treatment was associated with a non-statistically significant reduction in total colorectal adenoma recurrence but with a statistically significant 39% reduction in recurrence of adenomas with high-grade dysplasia (Alberts *et al.*, 2005).

1.14.3 Mechanisms of UDCA action

Despite its extensive clinical usage, the exact mechanism of UDCA action remains elusive. It does not exhibit the properties of a modern day pharmacological agent. It does not display a typical dose response relationship and a protein target for the drug remains unknown. There are many proposed mechanisms of action by which UDCA is thought to elicit its pharmacological effects. These are outlined below:

1.14.3.1 Expansion of Hydrophilic BA Pool

The intracellular accumulation of hydrophobic BAs leads to an array of cell damaging events ranging from physical damage, increasing cell-membrane fluidity and permeability, to apoptosis and necrosis (Poupon & Poupon, 1995) . It has been proposed that one of the main therapeutic mechanisms of UDCA in cholestatic liver diseases is due to enrichment of the BA pool by UDCA leading to displacement of the endogenous hepatotoxic bile by the more hydrophilic BA. This displacement effect may occur either at the level of the ileum or at the hepatocyte membrane or within the cell in the organelles (Stiehl, Benz & Sauer, 1999). The fact that UDCA is orally administered indicates that competition occurs for absorption of endogenous BAs at the level of terminal ileum (Stiehl *et al.*, 1999). However, in the bile fistula rat model, intravenous infusion of conjugated UDCA decreased the hepatotoxicity induced by toxic BAs. It therefore seems likely that UDCA exerts its protective action at the level of the liver (Heuman, 1993; Poupon & Poupon, 1995). The importance of this `displacement' of hepatotoxic BAs as a mechanism in preventing liver damage remains unclear. Beuers *et al* showed an improvement in the liver blood tests of patients with cholestatic liver diseases following one month therapy with UDCA without a change in the pool size and serum levels of the main hydrophobic BAs (Beuers *et al.*, 1992). Similarly in another study of patients with PSC, treated with UDCA for three months, there was no change observed before and after therapy in the pool size of BAs and in the serum concentration of CDCA (Rudolph *et al.*, 1993). Taking these studies into account it seems unlikely that UDCA's effects arise solely from displacement of the hydrophobic toxic BAs.

1.14.3.2 Choleresis

UDCA is known to induce the secretion of BAs and other organic compounds in isolated hepatocytes, and in models such as the isolated perfused rat liver and bile fistula rat model (Trauner & Graziadei, 1999). A similar and comparable effect is seen with the hydrophobic BAs but UDCA lacks the toxicity of these and this makes it a useful drug in the treatment of cholestatic conditions where bile flow may be impaired. A study by Jazrawi *et al* demonstrated that in patients with PBC and PSC, UDCA therapy improved the net and absolute hepatic excretory rates and transit time of a BA analog (^{75}Se labelled homocholic acid taurine) (Jazrawi *et al.*, 1994).

In cholestatic hepatocytes, vesicular exocytosis is impaired. TUDCA induces vesicular exocytosis at the canalicular domain of hepatocytes. Exposure of isolated rat hepatocytes to TUDCA at concentration ranges of 5-50 μmol/l causes an increase of cytosolic free Ca^{2+} by mobilizing intracellular stores and increasing the influx of extracellular Ca^{2+} (Beuers, Nathanson & Boyer, 1993). There is a hypothesis that induction of the Ca^{2+}-dependent hepatocyte exocytosis is mediated by activation and translocation of PKCα from the cytosol to the plasma membrane (Beuers *et al.*, 1996). Therefore, the mechanism of TUDCA-induced choleresis and subsequent cytoprotection in cholestasis may be related to the fact that it can promote apical exocytosis and thus create an increase in canalicular transport. This improvement in canalicular transport helps restore bile flow, promoting the excretion of toxic hydrophobic bile salts from the hepatocyte. In another study it was proposed that activation of the MAPK pathway leads to the increase in canalicular transport (Schliess *et al.*, 1997). However despite these studies it is clear that UDCA bears protective effects on the liver which cannot be solely explained by choleresis or expansion of the BA pool.

1.14.3.3 Potential UDCA targets?

In addition to the aforementioned there are a number of carcinogenic signaling cascades induced by other BAs which UDCA has been shown to inhibit. In work done by Shah *et al* in HCT116 colon cancer cells, DCA has been found to stimulate translocation of PKC β1-, ε- and δ from the cell cytosol to the plasma membrane (Shah *et al.*, 2005). UDCA however was found to inhibit DCA induced translocation of all these isoenzymes (Shah *et al.*, 2005). Furthermore UDCA has been found to inhibit DCA induced activation of AP-1 and NF-κB transcription in a colon cancer cell line (Shah *et al.*, 2006b) and its taurine conjugate has been shown to reduce toxic BA induced apoptosis through modulation of AP-1 in liver cells (Pusl *et al.*, 2008). In a recent study it has been shown that dietary UDCA can block the development of tumours with activated Ras and suppress COX-2 up regulation in azoxymethane

induced tumours (Khare *et al.*, 2008). It has been proposed that a possible mechanism for induction of BA induced apoptosis is through activation of Bax and induction of the MMPT (Imberti *et al.*, 1993; Schaffner *et al.*, 1971).

In a recent study it has been shown that UDCA modulates transcriptional activity of the pro-apoptotic regulator p53, thereby preventing its ability to induce Bax expression, mitochondrial translocation, cytochrome c release, and apoptosis in primary rat hepatocytes. More importantly, UDCA inhibition of p53-induced apoptosis was associated with decreased p53 DNA binding activity. Subcellular localization of p53 was also altered by UDCA. Both events appear to be related to an increased association between p53 and its direct repressor, Mdm-2 (Amaral *et al.*, 2007).

1.14.3.4 Immune Modulation

The immunomodulatory properties of UDCA will be discussed in Chapter 4.

1.15 Thesis Aims and Objectives

Traditionally BAs have been known for their function as solubilising agents in the dissolution of dietary lipid in the gut. In recent years there has been a renewed interest in BAs due to their emergence as regulators of diverse cellular functions and particularly due to the role they play in disease aetiology and pathogenesis of gastrointestinal cancers.

The discovery of BAs as ligands for the FXR and TGR5 receptor has initiated a number of drug discovery programmes using the BA structure as a lead for treatment of metabolic and liver disorders. Our interest in BAs stemmed from the use of UDCA for the treatment of inflammatory liver disorders. The biological effects of UDCA stand in contrast to the other BAs which are regarded as cytotoxic agents. UDCA is cytoprotective and has demonstrated immunomodulatory properties. Several of these properties resemble those of glucocorticoids (GCs) and indeed UDCA has been shown to activate the GR (Weitzel *et al.*, 2005). Taking UDCAs clinical usage and long history of minimal side effects into account we hypothesised that UDCA would make an excellent lead for the development of a novel GR modulator. UDCAs mechanism of action has not been fully elucidated and we felt that UDCA derivatives might also prove useful as tools in understanding the mechanism of UDCAs effects.

We were also interested in the chemopreventative effects of UDCA in colon cancer and in the potential of translating this to esophageal cancer. We decided to investigate the effect of BAs on the secretory pathway and the potential role of this in esophageal cancer pathogenesis. The work focuses on changes in the morphology of the Golgi

apparatus and investigates the potential of UDCA and our UDCA derivatives to inhibit these effects.

The BA structure has also been used as a lead for the development of novel cytotoxic agents. These programmes take advantage of the known toxicity of the BAs, DCA, CDCA and LCA. These BAs are considered to be cytotoxic due to their relative hydrophobicity compared to the other BAs. During the course of our studies on UDCA we discovered that manipulation of the BA side chain produced hydrophobic agents which were not cytotoxic. Although there is a general consensus in the literature that BA hydrophobicity is a determinant of toxicity there are few studies which correlate these properties.

Hence the aims of this thesis were:

1) To investigate the relationship between BA hydrophobicity and cytotoxicity.

2) To synthesise a series of UDCA derivatives and investigate their ability to modulate the GR.

3) To investigate the effect of BAs on the secretory pathway and the implications of this in esophageal cancer pathogenesis.

2 CHAPTER TWO

MATERIALS AND METHODS

Chapter II

Lists of reagents and antibodies along with their sources are provided in tabular form in Appendix 1. Constituents of buffers used are also listed.

2.1 BAs

BAs or BA derivatives were synthesised according to procedures described in the Experimental section, Chapter 7. Commercial BAs were obtained from sources listed in Appendix 1. Ursocholic acid and hyocholic acid were a gift from Prof B. Natalini (University of Perugia). BAs to be tested in biological assays were maintained as 200 mM stock solutions in dimethyl sulfoxide (DMSO). The compounds were diluted to the required concentrations with medium. No change in pH was observed on addition of BAs to the medium.

2.2 High Performance Liquid Chromatography (HPLC)

HPLC of BAs was carried out on a Waters Breeze System 1525. The chromatography was conducted on a Varian pursuit C-18 reverse-phase column (150 mm x 4.6 mm; 3 µm particle size) and a Waters 2414 refractive index detector. The BAs were dissolved in methanol (1 mg/ml) and injected into the HPLC column. The injection volume was 50 µl. The eluent consisted of methanol: 15 mM ammonium acetate at pH 7.4. Chromatography was performed at three different mobile phase strengths in the range 70-80% methanol. Flow rate was maintained at 0.9 ml/min. The chromatographic index k_w was determined by linear extrapolation from: $\log k' = -S\varphi + \log k_w$.

2.3 Reverse Phase Thin Layer Chromatography (RP-TLC)

TLC was performed on precoated C18 reverse-phase high performance TLC (20x10, F254) plates (Merck, Darmstadt, Germany). Plates were developed in a closed chamber at room temperature across a development distance of 15 cm. Methanol: 15 mM ammonium acetate was used as the mobile phase adjusted to required pH with acetic acid. Chromatography was performed at four different mobile phase strengths in the range 50-80% methanol. After development, the plates were dried in air, stained with a vanillin solution and dried with a heat gun to visualize the spots.

2.4 Calculation of Physicochemical Descriptors

UDCA was extracted from the X-ray crystal structure bound to AKR1C2 (PDB entry 1IHI) and visualized in molecular operating environment (MOE 2007.09, Chemical Computing Group, Montreal, Canada). Energy minima for the other test BAs were generated from this by modification in MOE using sequential SD (100 steps) and TN (1000 steps or to an RMS gradient of <0.01 kcal/ (mol*A)) using the PM3 algorithm. Stochastic searches were performed for the conjugates using PM3 over 1000 steps. Physicochemical descriptor parameters including hydrophobic surface area (ASAH) and polar surface area (ASAP) were calculated based on the minimised steroid molecules following a stochastic conformational search procedure using the database functions of MOE.

2.5 Cell culture techniques

Five cell lines were used for the experimental work carried out in this thesis.

1. HET-1A a normal esophageal cell line.
2. SKGT-4, an esophageal adenocarcinoma cell line.
3. Qh-tert, a benign Barrett's epithelial cell line.
4. HEK-293, a human embryonic kidney cell line.
5. HCT-116, a colon cancer cell line.

2.5.1 Culture of HET-1A

HET-1A is an adherent epithelial cell line derived in 1986 from human esophageal autopsy tissue of a 25 year old man. The cell line was purchased from American Type Culture Collection (ATCC, Rockville, MD). Cells were cultured in bronchial epithelial cell basal medium (Lonza Group Ltd, Switzerland) supplemented with triiodothyronine, insulin, transferrin, retinoic acid, hydrocortisone, human recombinant epidermal growth factor, epinephrine and bovine pituitary extract. Cultures were maintained at 37 °C in a humidified atmosphere containing 5% CO_2 and routinely maintained in T-75 cm^2 cell culture flasks (Nunclon, Roskilde, Denmark) in a volume of 10 ml medium. Cells were passaged twice a week (1/3 dilution). Cells were washed with Hanks balanced salt solution (HBSS) and removed from plastic surface using trypsin (1 ml, 0.05% w/v) (Gibco, Invitrogen Ltd., Paisley, UK) to form a cell suspension. The trypsin was neutralised with soya bean trypsin inhibitor (1 ml, 0.05% w/v) (Sigma-aldrich, St. Louis, MO, USA). A cell pellet was obtained by centrifuging at 1200 rpm for 3 min. The pellet was resuspended in culture media and divided into cell culture flasks for

maintenance of cell stock or enumerated in the conventional way using a haemacytometer prior to use in an experiment.

2.5.2 Culture of SKGT-4

The SKGT4 cell line, an adherent cell line derived from a well-differentiated adenocarcinoma arising in Barrett's epithelium of the distal esophagus was generously provided by Dr. David Schrump (Bethesda, MA) (Altorki *et al.*, 1993). Cells were maintained in RPMI 1640 medium supplemented with 10% heat-inactivated fetal bovine serum (FBS) and 4 mM L-Glutamine (GIBCO, Invitrogen Ltd., Paisley, UK) at 37 °C in a humidified atmosphere containing 5% CO_2 and routinely maintained in T-75 cm^2 cell culture flasks (Nunclon, Roskilde, Denmark) in a volume of 10 ml medium. Cells were passaged three times a week (1/3 or 1/6 dilution). Cells were washed with PBS and removed from plastic surface using trypsin (2 ml, 0.05% w/v) to form a cell suspension which was diluted by adding double the volume of cell culture medium. A cell pellet was obtained by centrifuging at 1200 rpm for 3 min. The pellet was resuspended in culture media and divided into cell culture flasks for maintenance of cell stock or enumerated in the conventional way using a haemacytometer prior to use in an experiment.

2.5.3 Culture of HEK-293

HEK-293 cells, an adherent human embryonic kidney cell line, were grown in Dulbecco's Modified Eagle's medium (DMEM, GIBCO, Invitrogen Ltd., Paisley, UK), supplemented with 10% heat-inactivated FBS. Cultures were maintained at 37 °C in a humidified atmosphere containing 5% CO_2 and routinely maintained in T-75 cm^2 cell culture flasks (Nunclon, Roskilde, Denmark) in a volume of 10 ml medium. Cells were passaged three times a week (1/6 dilution). Cells were washed with PBS and removed from the plastic surface using trypsin (2 ml, 0.05% w/v) to form a cell suspension which was diluted by adding double the volume of cell culture medium. A cell pellet was obtained by centrifuging at 1200 rpm for 3 min. The pellet was resuspended in culture media and divided into cell culture flasks for maintenance of cell stock or enumerated in the conventional way using a haemacytometer prior to use in an experiment.

2.5.4 Culture of Qh-tert

The benign Barrett's epithelial cell line, Qh-tert was obtained from American Type Culture Collection (ATCC, Rockville, MD-check source). Cells were cultured in bronchial epithelial cell basal medium (BEBM) (Lonza Group Ltd, Switzerland) supplemented with triiodothyronine, insulin, transferrin, retinoic acid, hydrocortisone, human recombinant epidermal growth factor, epinephrine and bovine pituitary extract and 5% heat-inactivated FBS. Cultures were maintained at 37 °C in a humidified atmosphere containing 5% CO_2 and routinely maintained in T-75 cm^2 cell culture flasks (Nunclon, Roskilde, Denmark) in a volume of 10 ml medium. Cells were passaged three times a week (1/3 or 1/6 dilution). Cells were washed with HBSS (Sigma-Aldrich, St. Louis, MO, USA) and removed from plastic surface using trypsin (1 ml, 0.05% w/v) to form a cell suspension. The trypsin was neutralised with soya bean trypsin inhibitor (1 ml, 0.05% w/v). A cell pellet was obtained by centrifuging at 1200 rpm for 3 min. The pellet was resuspended in culture media and divided into cell culture flasks for maintenance of cell stock or enumerated in the conventional way using a haemacytometer prior to use in an experiment.

2.5.5 Cryopreservation and revival of cell lines

Freshly made medium consisting of 5% DMSO in FCS was used in all cases as cryoprotectant. Cells in a T-75 culture flask (Nunclon, Roskilde, Denmark) were removed from plastic surface using trypsin (1 ml, 0.05% w/v) and a cell pellet was obtained as described in Section 2.5.1. After removal of supernatant and resuspension of cells, ice cold cryoprotectant was slowly added to the pellet which was then transferred into sterile cryovials (Nunclon, Roskilde, Denmark) and placed in a -80°C freezer for 24 h and then transferred to the vapour phase of a liquid nitrogen tank for longer term storage.

For revival of cell lines cryovials were removed from the liquid nitrogen tank and thawed at 37 °C in a water bath. Upon thawing the cell solution was slowly added to warmed medium. The cell suspension was centrifuged at 1200 rpm for 3 min to form a pellet and remove DMSO. The cell pellet was resuspended in warm medium and transferred to a T-25 cm^2 (Nunclon, Roskilde, Denmark) flask for cell culture maintenance.

2.6 Cell viability and Apoptosis Assays

2.6.1 MTT Assay

Cell viability was measured using the 3-[4,5-dimethylthiazol-2-yl]-2,5-diphenyltetrazolium bromide (MTT) assay. Cells were plated into 96 well plates at a concentration of 8×10^4 cells/ml (in a 100 µl volume). After 24 h the cells were treated with various BAs at indicated concentrations for the appropriate time in supplement free medium. Control wells were treated with BEBM without supplements or with phorbol myristate acetate (PMA) 1 µg/ml as a positive control for cell death. Vehicle control wells were treated with DMSO 1%. After 22 h cells were incubated with 20 µL of MTT solution for a further 2 h. The medium was aspirated from the wells and DMSO (100 µL) added to each well to lyse the cells. The plates were shaken for 10 min to dissolve the formazan crystals and then read on a $VERSA_{max}$ Microplate Reader (Molecular Devices, Sunnyvale, CA, USA) at a wavelength of 570 nm. Cell survival rates were determined by calculating:

$$\frac{(T-B)}{(V-B)}$$

where T (treated) is the absorbance of BA treated cells, B (blank) is the absorbance of medium plus MTT, and V (vehicle) is the absorbance of vehicle control treated cells.

2.6.2 Caspase-Glo 3/7 Assay

The Caspase-Glo® 3/7 Assay (Promega Corporation, Madison, USA) is a luminescent assay that measures activation of caspase 3/7 during apoptosis. The assay provides a proluminescent caspase-3/7 DEVD-aminoluciferin substrate and a proprietary thermostable luciferase. Addition of Caspase-glo® 3/7 reagent results in cell lysis followed by caspase-mediated cleavage of the substrate. This liberates free aminoluciferin, which is consumed by the luciferase creating a luminescent signal which is proportional to caspase 3/7 activity. Cells were plated into 96 well plates at a concentration of 8×10^4 cells/ml (in a 100 µl volume). After 24 h cells were treated with various concentrations of BAs for the indicated time. After the appropriate time point the cells were allowed to equilibrate to room temperature. 100 µL of Caspase-glo® 3/7 reagent was added to each well and the luminescence measured using the Wallac 1420 $Victor^2$ luminometer (Perkin Elmer, Waltham, Massachusetts, USA).

2.7 High Content Screening and Analysis

High content screening (HCS), sometimes to referred to as high content analysis (HCA), is the use of automated microscopy and image analysis in drug discovery and cell biology (Zock, 2009). The method allows for rapid image acquisition and subsequent objective analysis of a variety of cellular phenotypes and morphologies. Traditionally HCS has its foundation in drug discovery where it provides novel secondary assay formats, selectivity screens, and cytotoxicity profiling using the multi-parameter and individual cell attributes of the approach (Zock, 2009). However in recent years the technique has gained widespread acceptance in other areas including cell signalling, oncology, *in vitro* toxicology and RNAi screening. Furthermore it is becoming increasingly common to replace difficult assays with HCS as it offers advantages such as increased sensitivity over existing methods, increased throughput and safety and in certain instances decreased cost (Baniecki, Wirth & Clardy, 2007).

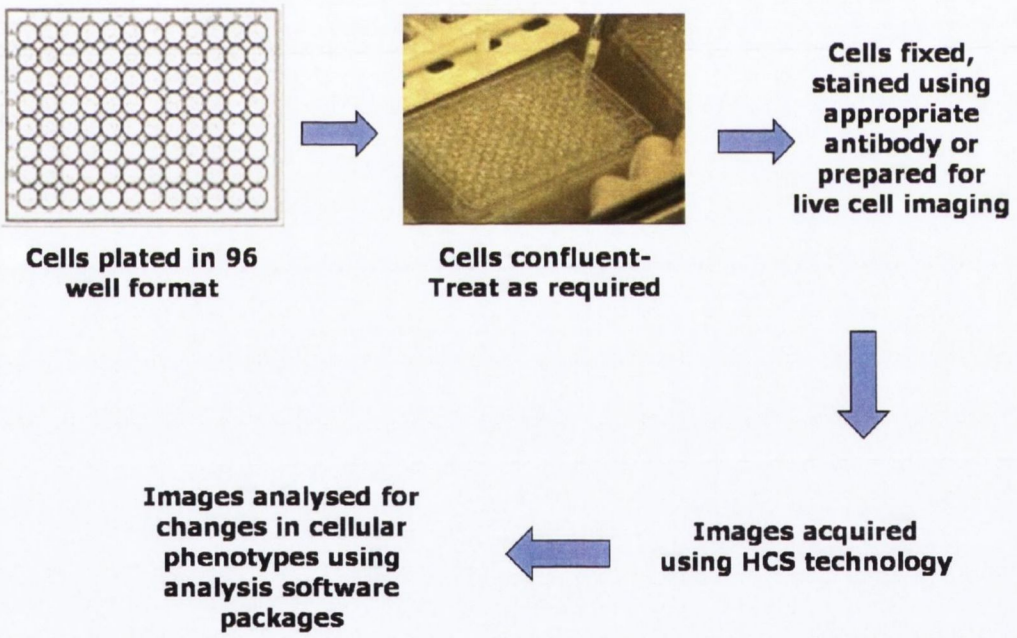

Figure 2.1 General protocol for HCS experiments. *HCS allows for rapid image acquisition and subsequent objective analysis of acquired images.*

2.7.1 In Cell Analyser

There are currently a variety of HCS instruments available on the market. These include the Cellomics Arrayscan, ImagexPress MICRO (Molecular Devices, Union City,

USA) and Scanalyzer (Scanalyzer LemnaTec, Aachen Germany). The instrument used during this thesis was the In Cell Analyser 1000.

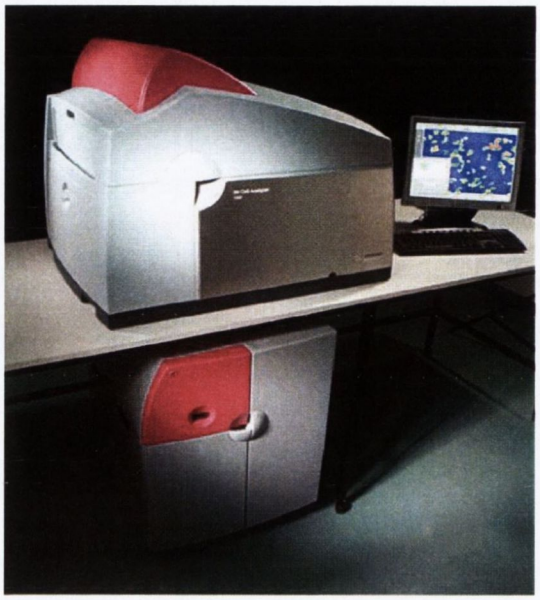

Figure 2.2 GE In cell Analyser 1000. *The GE In Cell Analyser 1000 is a high content microscope capable of rapid image acquisition in a 96 well format.*

The GE IN Cell Analyser 1000 is a microscope based screening platform capable of large scale objective analysis of fluorescently labelled cells using automated image acquisition, data management and multi-parametric analysis. The compact bench-top instrument comprises an automated Nikon™ microscope, high-resolution CCD camera, xenon lamp-based illumination, filter wheel based wavelength control, and laser based auto focus. The In Cell 1000 has been used for image acquisition in a number of experiments in this project. Analysis of acquired images was performed with the Investigator software package (GE Healthcare, Piscataway, NJ, USA) using a variety of different protocols as outlined below.

2.8 Membrane Permeability Assays

In order to determine the effect of BAs on membrane integrity a series of experiments were carried out using a combination of HCS and fluorometry based assays.

2.8.1 Propidium Iodide Staining

Het-1A cells were plated into 96 well plates at a concentration of 8×10^4 cells/ml (in 100 µl volume). After 24 h the cells were treated with Triton X-100 (0.1% v/v) and

with various concentrations of BAs as indicated for varying time points. After the appropriate time point propidium iodide (PI) (5 µg/ml) and Hoechst 33342 (5 µg/ml) were added to each well and the cells were visualized live on the GE IN Cell Analyser 1000. Six fields of view per well were acquired using a 20 × objective in duplicate wells for n=3 experiments.

2.8.1.1 Quantification of PI Uptake using High Content Analysis

PI uptake, a measure of cell permeability was determined using the Investigator software package (GE Healthcare, Piscataway, NJ, USA). The analysis was based on the intensity of PI within the nucleus. The dual object area analysis algorithm was optimised for detection of nuclei within a cell. Untreated cells with intact membranes were used as a negative control and Triton X-100 treated cells as a positive control for membrane perturbation. An intensity threshold was set to determine the percentage of cells in each well which were PI positive and had perturbed membranes.

2.8.2 Cell Tracker Staining

Cell tracker staining was also used to determine disruption of cell membrane integrity. HET-1A cells were plated into 96 well plates at a concentration of 8×10^4 cells/ml (in a 100 µl volume). After 24 h the cells were treated with 5-chloromethylfluorescein diacetate (Cell Tracker Green CMFDA, Molecular Probes, Invitrogen Life Sciences, 25 µM) for 30 min. Cell tracker reagents are chloromethyl derivatives that freely diffuse through the membranes of live cells. Once inside the cell, they react with intracellular components to produce cell impermeant dye-thioether adducts that are both fluorescent and viable for at least 24 h after loading, Figure 2.3.

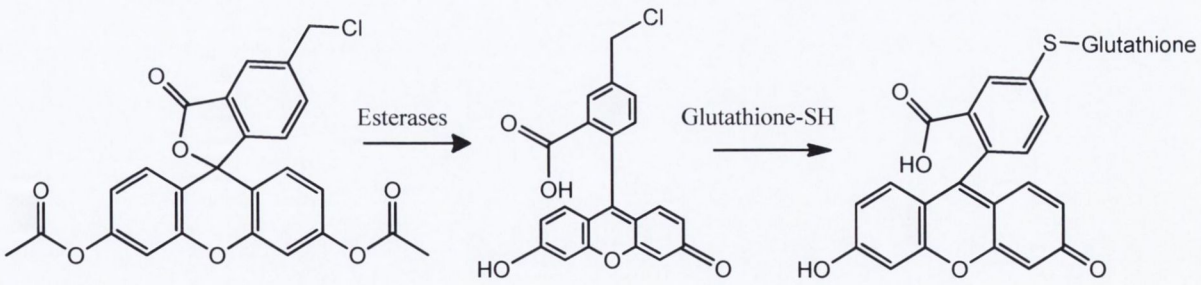

Figure 2.3 Intracellular reactions of the CellTracker Green CMFDA reagent. *Reaction with glutathione may occur prior to the hydrolysis reaction but the product is non fluorescent until the esters are cleaved.*

After washing with warmed HBSS to remove excess cell tracker these cells were then treated with Triton X-100 (0.1% v/v) and various concentrations of BAs for different time points as indicated. Hoechst 33342 (5 µg/ml) was added to the cells to visualise the nucleus. After the appropriate time point cells were imaged live on the GE IN Cell Analyser 1000. Six fields of view per well were acquired using a 20× objective in duplicate wells for n=3 experiments.

2.8.2.1 Quantification of Cell tracker Intensity using HCS

Cell Tracker intensity was measured using the Investigator software package based on the intensity of Cell Tracker within the nucleus as detected by the dual object area analysis algorithm. The dual object area analysis algorithm was optimised to detect intensity of cell tracker fluorescence within a cell using untreated cells with intact membranes as negative control and Triton X-100 treated cells as positive control for membrane perturbation and consequent cell tracker leakage. The fluorescence intensity of the BA treated cells was determined and expressed as cell intensity normalised to untreated control.

2.8.2.2 Quantification of Cell tracker Intensity in cellular supernatants

The Wallac 1420 Victor^2 fluorometer (Perkin Elmer, Waltham, Massachusetts, USA) was used to measure the fluorescence intensity in the supernatants of cell tracker treated cells after exposure to BAs at indicated concentrations and time.

2.9 GR translocation assay

SKGT-4 cells were plated into 96 well plates at a concentration of 6 × 10^4 cells/ml (in a 100 µL volume). After 48 h cells were treated with BA derivatives in supplement free medium at the required concentration for the indicated time points. Control wells were left untreated or treated with 1% DMSO as a vehicle control or dexamethasone 100 nM as positive control. After the appropriate treatment time cells were fixed with 4% paraformaldehyde/PBS (15 min) then permeabilised with 0.1% (v/v) Triton X-100/PBS (5 min) followed by blocking with 3% BSA/PBS (30 min-overnight). Cells were incubated with purified monoclonal mouse anti-glucocorticoid receptor (GR) antibody (0.5 µg/ml, 50 µl, 1 h) (BD Biosciences, San Jose, California, USA) then incubated with AlexaFluor-488-conjugated secondary antibody (80 µg/ml ,50µl, 30 min) (Invitrogen, Carlsbad, CA, USA) protected from light. Finally the nuclei were stained with Hoechst 33342 (10 µg/ml, 50 µl, 5 min) (Invitrogen, Carlsbad, CA, USA) and additionally in some experiments actin filaments were stained with 0.1 mM phalloidin-TRITC (Sigma-Aldrich, St. Louis, MO, USA) for 40 min at room temperature. Images

were acquired using the GE In Cell Analyser 1000. Four fields of view per well were acquired using a 10× objective for n=3 experiments.

2.9.1 Quantification of GR translocation using HCA

Nuclear to cytoplasmic ratio of GR distribution within the cells stained was measured using the Investigator software package (GE Healthcare, Piscataway, NJ, USA). The analysis was based on the ratio of the intensities of GR within the nucleus and cytoplasm. The multiparametric analysis algorithm was optimised to detect GR within the nucleus and the cytoplasm using vehicle only treated cells as negative control and dexamethasone treated cells as positive control. Hoechst staining enabled identification of the nucleus. The nuclear to cytoplasmic ratios were determined by calculating

(Nuclear Intensity of GR-Background Intensity)
(Cytoplasmic Intensity of GR-Background Intensity).

2.10 Golgi Assay

HET-1A cells were plated into 96 well plates at a concentration of 8×10^4 cells/ml (100 µL volume). After 48 h cells were treated with BA derivatives in supplement free medium at the required concentration for the indicated time points. In cases where cells were treated with agents prior to addition of BAs, cells were treated with the appropriate compound for 18 h prior to this. Control wells were left untreated or treated with brefeldin A (1 µg/ml) as positive control. Brefeldin A is a fungal metabolite which blocks transport of proteins from the endoplasmic reticulum to the Golgi complex and is known to induce fragmentation of the Golgi apparatus (Fujiwara *et al.*, 1988).

After the appropriate treatment time cells were fixed with 4% paraformaldehyde/PBS (15 min) then permeabilised with 0.1% Triton X-100/PBS (5 min) followed by blocking with 3% BSA/PBS (30 min-overnight). Cells were incubated with purified polyclonal rabbit anti-GM130 antibody (0.4 µg/ml, 50µl, 1 h), washed then incubated with AlexaFluor-488-conjugated secondary antibody (80 µg/ml, 50µl, 30 min) (Invitrogen, Carlsbad, CA, USA) protected from light. Anti-GM130 recognises the rat, mouse and human forms of the GM130 protein. GM130 is a peripheral cytoplasmic protein that is tightly bound to the Golgi membrane, predominantly localised to the cis-Golgi network (CGN) and is used as a CGN marker (Nakamura *et al.*, 1995).

Finally the nuclei were stained with Hoechst 33258 (10 µg/ml, 50µl, 5 min). Images were acquired using the GE In Cell Analyser 1000. Six fields of view per well were acquired using a 20 × objective for n=3 experiments.

2.10.1 Quantification of Golgi fragmentation using High Content Analysis

Golgi fragmentation was measured using the Investigator software package, (GE Healthcare, Piscataway, NJ, USA) using an algorithm specific for detection of objects within the cell called the multi-target analysis algorithm. This was optimised to detect objects (Golgi fragments) within a cell using untreated cells with intact Golgi as negative control and brefeldin A treated cells as positive control for Golgi fragmentation. A significant decrease in the mean area of the objects (Golgi fragments) relative to control was representative of Golgi fragmentation. In certain experiments the "object mean area" was used to classify cells as having intact or fragmented Golgi with an object mean area > 0.5 µm defining cells with intact Golgi and object mean area <0.5 µm defining cells with fragmented Golgi.

2.11 Reporter Gene Assays

Reporter gene assays are used to study the regulation of a gene of interest. The pattern of gene expression can be determined by replacing the coding portion of the gene of interest under study with a reporter gene. This involves cloning the regulatory elements of the gene of interest upstream of the reporter gene (Alberts *et al.*, 2008). The most commonly used reporter genes are green fluorescent protein (GFP), chloramphenicol acetyltransferase (CAT) and luciferase. The most commonly used luciferase reporter genes are firefly luciferase (F.luc) and renilla luciferase (R.luc) although gaussia luciferase (G.luc) is also increasingly being used as it has been shown to produce a greater luminescent signal than F.luc and R.luc (Badr *et al.*, 2007).

The regulatory element of the gene of interest linked to the reporter gene is introduced into the cell as a plasmid DNA construct. mRNA is transcribed from active promoters once the plasmid is in the nucleus and depends on the experimental control of the promoter, Figure 2.4. The amount of the expressed reporter gene can then be measured as a function of the reporter activity, typically in luminescence based assays. Such experiments involve co-transfection of a DNA construct producing a constitutively active protein. Measuring the activity of this protein controls for transfection efficiency and cytotoxicity.

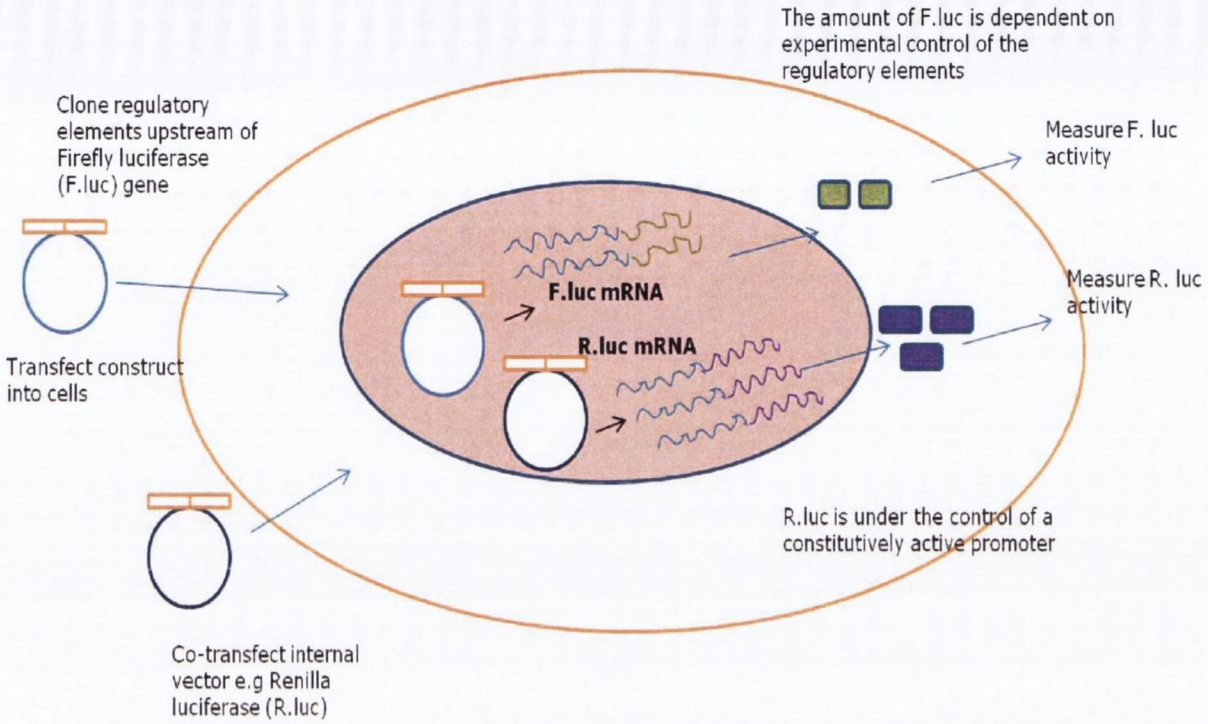

Figure 2.4 Theory of reporter gene assay. *Regulatory elements of the gene of interest are cloned upstream of a firefly luciferase (F.luc) reporter gene. Activation of the promoter results in production of F.luc mRNA which can be measured in a luminescence assay. F.luc activity is normalised to an internal vector control, such as Renilla luciferase (R.luc) which is under the control of a constitutively active promoter (Alberts et al., 2008).*

2.11.1 Preparation of reporter plasmids

A number of reporter assays were used during the course of this thesis. These include NF-κB and glucocorticoid responsive element (GRE) reporter assays.

2.11.1.1 Bacterial Transformation

The appropriate DNA construct (50 ng) (κB-CONA-Luc vector or pCMV-Gluc) was added to competent E. coli cells (40 µl) and left on ice for 30 min. The competent cells were heat shocked at 42 °C for 1 min and then returned to ice for 2 min to avoid excessive damage to the bacterial cells. Antibiotic free Luria Bertani (LB) broth (1 ml) was added to the competent cells and incubated in a shaking incubator at 37 °C for 1 h. After 1 h, 100 µl of the culture was spread onto an LB agar plate with ampicillin (60 µg/ml). The plate was incubated at 37 °C overnight to allow bacteria to grow to form single colonies.

2.11.1.2 Plasmid Amplification and Purification

A single colony was taken from a streaked selective plate and used to inoculate a starter culture of LB broth with ampicillin (5 ml). This was incubated at 37 ^{o}C for 8 h and then transferred into a conical flask with LB broth (100 ml) to be incubated overnight. The bacterial cells were harvested by centrifugation at 6000 x g for 15 min at 4 ^{o}C. The plasmid was purified using a Qiagen midi prep plasmid purification kit (Qiagen Inc., Valencia, CA, USA) using the protocols described below:

1. The bacterial pellet was lysed by dissolving in buffer P1 (4 ml) followed by buffer P2 (4 ml) after which the lysate was vigorously shaken (Appendix 1).
2. Chilled buffer P3 (4 ml) was added to the lysate and vigorously mixed. This lysate contains genomic DNA, proteins and cell debris (Appendix 1).
3. The lysate was transferred to a QIAfilter cartridge and following a 10 min incubation period was filtered through a Qiagen-tip (column) which binds to only DNA.
4. The QIAgen tip was washed multiple times with buffer QC (2 × 10 ml) followed by elution of the DNA with buffer QF (5 ml).
5. The DNA was then precipitated by addition of isopropanol (3.5 ml) to this mixture followed by centrifugation at 15000 x g for 30 min at 4 ^{o}C to form a DNA pellet.
6. The pellet was washed with 70% ethanol (2 ml) and centrifuged once more at 15,000 x g for 10 min.
7. After air-drying the pellet was resuspended in sterile water (40 µl).
8. The DNA obtained was quantified using a NanoDrop spectrophotometer (Nanodrop Technologies, Wilmington, USA).

2.12 Measurement of NF-κB activity

HEK-293 cells were transiently co-transfected with an inducible NF-κB responsive construct, which contains three kappa B elements upstream of a minimal conalbumin promoter linked to the firefly luciferase gene (Arenzana-Seisdedos *et al.*, 1993) and a constitutively expressing β-galactosidase construct (Clontech, Saint-Germain-en-Laye, France) as an internal control for transfection efficiency (ratio of 4:1). A reverse transfection procedure was carried out using lipofectamine as a transfection reagent at a ratio of 3:2 (lipofectamine:DNA). DNA and lipofectamine were diluted in OptiMem and this mixture was added to 48-well plates to give 500 ng DNA per well. HEK-293 cells at a density of 7 x 10^5 cells/ml (in a 200 µl volume) were added to this mixture.

After 24 h the cells were treated with TNF-α 10 ng/μl alone or with TNF-α 10 ng/μl and varying concentrations of the indicated compounds for 16 h.
After the appropriate time the cells were lysed with 1× Promega lysis buffer (50 μl). The lysates were then assayed for F.luc activity (Promega Corporation, Madison, USA) by addition of 100 μl F.luc substrate to 20 μl cell lysate. Luminescense was measured using Wallac 1420 Victor^2 luminometer (Perkin Elmer, Waltham, Massachusetts, USA).

2.12.1 Measurement of β-galactosidase activity

The lysates were then assayed for β-galactosidase activity using o-nitrophenyl-β-D-galactopyranoside (ONPG) as a substrate using methods described by Sambrook *et al*, "Molecular Cloning: A Laboratory Manual" (Sambrook & Russel, 2001). Briefly cell lysate (30 μl) was added to a mixture of a magnesium buffer (3 μl) and an ONPG solution in 0.1M sodium phosphate buffer (267 μl). This mixture was incubated at 37 ^{o}C until the appearance of a faint yellow colour. Sodium carbonate (500 μl, 1M) was added to this mixture to quench the reaction and the optical density of the solutions was measured at a wavelength of 420 nm in a VERSA$_{max}$ Microplate Reader (Molecular Devices, Sunnyvale, CA, USA).
F.luc values were normalised to β-galactosidase activity to control for transfection efficiency.

2.13 Measurement of GRE activity

SKGT-4 cells were transiently transfected with a mixture of an inducible GRE linked to an F.luc reporter and a constitutively expressing Renilla construct (Pcmv-R.luc) (40:1). (SABiosciences Corporation, Executive Way, Frederick, USA). A reverse transfection procedure was optimised using fugene HD as a transfection reagent at a ratio of 4:1 (fugene HD: DNA). DNA and fugene HD were diluted in OptiMem and this mixture was added to 96 well plates to give 100 ng DNA per well. SKGT-4 cells at a density of 7 x 10^4 cells/ml (in a 100 μl volume) were added to this mixture. After 24 h the cells were treated with varying concentrations of indicated compound for the indicated time.
After this time the cells were lysed using 1× Promega passive lysis buffer 50 μl (Promega Corporation, Madison, USA) and incubated at room temperature for 15 min. The lysates were then assayed for F.luc and R.luc activity (Promega Dual-Luciferase® Reporter Assay System) using a Wallac 1420 Victor^2 luminometer (Perkin Elmer, Waltham, Massachusetts, USA). This involved addition of 100 μl F.luc substrate to 20 μl of cell lysate. The luminescence was measured and then 100 μl of stop and glow®

reagent was added to quench this reaction and measure the luminescence produced from reduction of a Renilla substrate by R.luc.
F.luc values were normalised to R.luc to control for transfection efficiency.

2.14 Measurement of secretory activity using Gaussia luciferase reporter assay

The HET-1A, QHs and HCT-116 cell lines were used for this experiment. Cells were transiently transfected with a mixture of a constitutively expressing Gaussia luciferase (G.luc) construct (pCMV-Gluc) (New England Biolabs, Ipswich, MA, USA) and a constitutively expressing firefly luciferase construct (SABiosciences Corporation, Executive Way, Frederick, USA)(1:1). G.luc is processed through the secretory pathway and secreted into the cell medium. Hence effects in the secretory pathway can be measured by assaying G.luc activity in the cell supernatant. A reverse transfection procedure was optimised using fugene HD as a transfection reagent at a ratio of 4:1 (fugene HD: DNA). DNA and fugene HD were diluted in OptiMem and this mixture was added to 96-well plates to give 200 ng DNA per well. HET-1A cells or QH cells at a density of 1 x 10^5 cells/ml (100 µl) or HCT116 cells at a density of 8 × 10^4 cells/ml were added to this mixture. After 24 h the cells were treated with varying concentrations of indicated compounds for the indicated time.
After this time the supernatants were removed and the cells were lysed using passive lysis buffer 50 µl (Promega Corporation, Madison, USA) and incubated at room temperature for 15 min. The supernatants were assayed for G.luc activity using a G.luc assay kit (New England Biolabs, Ipswich, MA, USA) using the Wallac 1420 Victor^2 luminometer (Perkin Elmer, Waltham, Massachusetts, USA). This involved addition of 50 µl G.luc substrate to 20 µl of cell lysate and measurement of luminescence. The lysates were separately assayed for F.luc activity (Promega Corporation, Madison, USA) as previously described. The lysates were also assayed for protein content using a Pierce BCA protein assay kit (Pierce Biotechnology, Meridian Rd, Rockford, USA). G.luc activity was normalised to F.luc and protein content to act as internal controls.

2.14.1 BCA protein Assay

The BCA protein assay is a detergent compatible formulation based on bicinchonic acid (BCA) for the colorimetric detection of total protein. The method combines the reduction of Cu^{2+} to Cu^{1+} by protein in an alkaline medium (the biuret reaction) with the highly sensitive and selective colorimetric detection of the Cu^{1+} cation using a unique reagent containing bicinchonic acid. 50 parts of BCA reagent A were added to 1

part BCA reagent B. 200 µl of this solution was added to 10 µl of protein lysate in a 96 well plate. The solutions were incubated at 37 °C for 30 min followed by cooling to room temperature and then read in a $VERSA_{max}$ Microplate Reader (Molecular Devices, Sunnyvale, CA, USA) at 570 nm.

2.15 Ad-A-Gene GR assay

Adenoviruses are a family of DNA viruses that are used as a vehicle for the delivery of genes into cultured cells. They are an alternative to the use of lipid based transfections. We used a replication defective recombinant adenoviral preparation containing a GR gene encoding a protein fused to an enhanced green fluorescent protein (EGFP) (GE Healthcare, Piscataway, NJ, USA). The SKGT-4 cells were cultured, harvested and re-seeded in 96-well plates at a density 1×10^5 cells/ml (in a 100 µl volume) in RPMI medium containing 10% fetal bovine serum and the GR vector at a multiplicity of infection of 50 (ratio of infectious agent to cell number). These cells were left for 48 h and then treated with dexamethasone (50 nM) or UDCA (300 µM) for 2 h. The cells were then fixed in formaldehyde 2% for 10 min. Cells were stained with Hoechst solution for 5 min to visualise the nuclei and then screened and analysed using the GE In Cell Analyser following protocols described in section 2.9.1.

2.16 Radioligand Binding Assay

This assay was carried out by MDS pharma in order to determine if UDCA and derivatives could bind to the GC binding site. Human HeLa S3 cells enriched with glucocorticoid receptors are used in HEPES/RPMI-1640 buffer pH 7.2. Cells (3×10^6) are incubated with 3 nM [^{3}H]Dexamethasone for 120 min at 25 °C. Non-specific binding is estimated in the presence of 10 µM dexamethasone. Cells are filtered and washed, the filters are then counted to determine [^{3}H]Dexamethasone specifically bound. UDCA derivatives were screened at 10 µM and UDCA at 10 µM and 50 µM.

2.17 Time-resolved Fluorescence Resonance Energy Transfer Assay (TR-FRET)

TR-FRET was used in order to determine if UDCA and its derivatives were able to induce a conformational change in the GR-ligand binding domain resulting in recruitment of co-activators. TR-FRET is based on the principle that when a suitable pair of fluorophores is brought within close proximity of one another, excitation of the first fluorophore can result in energy transfer to the second fluorophore which can be

detected by an increase in the fluorescence emission of the acceptor molecule and decrease in the fluorescence emission of the donor molecule. We used a Lanthascreen™ TR-FRET Glucocorticoid Receptor (GR) Co-activator Assay kit (Invitrogen, Carlsbad, CA, USA) which provides a GR-ligand binding domain tagged with a glutathione-S-transferase (GST), a terbium-labelled anti-GST antibody (Tb-anti-GST Ab) and a fluorescein labelled steroid co-activator-1-4 peptide (Fl-SRC-1-4). Binding of agonist to the nuclear receptor causes a conformational change in the LBD of the GR which results in recruitment of the co-activator peptide. When the terbium label on the anti-GST antibody is excited at 340 nm, energy is transferred to the fluorescein label on the co-activator peptide. This energy transfer is detected by an increase in the fluorescence emission of the acceptor molecule (fluorescein, 520 nm) and a decrease in the emission of the donor molecule (terbium, 495 nm).

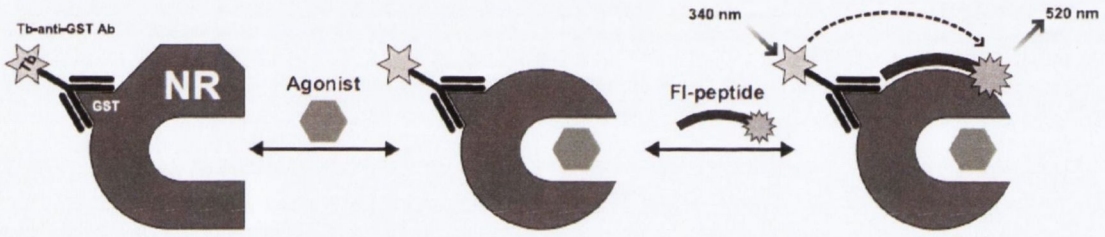

Figure 2.5 Principle of the GR co-activator peptide recruitment assay. *Interaction of agonist with the nuclear receptor induced a conformational change in the GR-LBD resulting in co-activator recruitment. Excitation of the terbium label on the anti-GST antibody transfers energy to the fluorescein label on the co-activator peptide and detected as emission at 520 nm.*

The GR-LBD was added to the indicated concentration of test compound, for example UDCA or 1% DMSO as a negative control in TR-FRET coregulator buffer (proprietary formulation) in a 384-well black assay plates (Thermofisher Scientific, Waltham, USA) followed by addition of a mixture of the fluorescein labelled co-activator peptide and the terbium labelled anti-GST antibody. The plates were incubated at room temperature for 3 h and then measured for TR-FRET activity using the LanthaScreen™ ^{optic} filter module on the BMG pherastar (BMG Labtech GmBH, Offenburg, Germany). The TR-FRET ratio was calculated by dividing the emission signal at 520 nm by the emission signal at 495 nm.

Component	Volume per well	Final Concentration
Test compound 2x	10 µl	1×
4 nM GR-LBD	5 µl	1 nM
1.2 µM Fl-SRC-1	5 µl	300 nM
Tb-anti-GST Ab	5 µl	5 nM

2.18 Quantitative Real-time polymerase chain reaction (PCR)

Real-time PCR quantifies gene expression by measuring mRNA levels in cells. The method involves extraction of mRNA from cells and purification and enzymatic degradation of DNA. Reverse transcription converts mRNA to cDNA. A series of heating and cooling cycles allows for the amplification of that DNA strand by polymerase chain reaction (Alberts *et al.*, 2008).

2.18.1 RNA Extraction and Reverse Transcription

For these experiments HET-1A cells were seeded at 2 × 10^5 cells/T-25 cm^2 flask. 48 h after cells were treated with BAs as indicated. Total cellular RNA was isolated using a Nucleospin® RNA II Kit (Macherey-Nagel GmBH & Co. KG, Düren, Germany) according to the manufacturer's instructions. Briefly,

1. Cells were lysed by addition of RA 1 buffer (350 µl) and β-mercaptoethanol (3.5 µl).
2. The lysate was applied to the Nucleospin® Filter unit and centrifuged for 1 min at 11,000 x g.
3. The filter unit was discarded and ethanol 70 % (350 µl) was added to the lysate.
4. The lysate was loaded onto a Nucleospin® RNA II column and centrifuged at 11,000×g for 30 s.
5. Membrane desalting buffer (350 µl) was added to the membrane and the column spun once more at 11,000×g for 1 min.
6. DNase reaction mixture (95 µl) was added to the column and the column incubated at room temperature for 15 min.
7. The column was washed with Buffer RA2 (200 µl, centrifuge 11,000×g for 30 s) and buffer RA3 (600 µl, centrifuge 11,000×g for 30 s). The eluent was discarded in both cases.
8. Finally RNase-free water (40 µl) was added to the column and the column was centrifuged at 11,000×g for 1 min to elute highly pure RNA. This RNA solution

was reapplied to the column and centrifuged once more to ensure maximum yield of RNA.

9. RNA was quantified using a NanoDrop Spectrophotometer (NanoDrop Technologies).

2.19 Reverse transcription of RNA to cDNA

Total RNA was transcribed to cDNA by following the first step of the Verso™ SYBR® Green 2-step quantitative real time-PCR Rox kit (Thermofisher Scientific, Waltham, USA). RNA (500 ng) was added to PCR grade water to form a total volume of 11 µl. The RNA was incubated at 70 °C for 5 min to remove secondary structure and then immediately placed on ice for 2 min. After this the following components were added to the reaction mixture shown below to give a final volume of 20 µl.

Component	**Volume per well**
RNA 500 ng	Variable (depends on sample conc.)
cDNA synthesis buffer	4 µl
dNTP mix (nucleotides)	2 µl
Random hexamers	1 µl
Reverse transcriptase	
E8nhancer (to eliminate DNA)	1 µl
Verso Enzyme Mix (Reverse transcriptase)	1 µl
PCR grade Water	Variable
Total Volume	20 µl

The following cycling programme was used:

cDNA synthesis	42 °C	1 h
Inactivation	95 °C	2 min

These cDNA samples could now be stored at -20 °C or be used in PCR reactions.

2.20 Quantitative real time PCR

Quantitative real time PCR was performed to quantify the expression of mRNA for XBP-1, Bip, CHOP and ATF3 (Primers for all the genes are listed in the appendix). The PCR reactions were prepared in 384 well clear reaction plates (Applied Biosystems, Foster City, CA). The PCR reaction was carried out using the Taqman Master Mix kit

(Applied Biosystems, Foster City, CA) and a mix of primers and fluorescently labelled Taqman MGB probes for the target gene and the housekeeping gene glyceraldehyde-3-phosphate dehydrogenase (GAPDH) which was used as endogenous control. cDNA (4.5 µl) was added to the 384-well plate followed by the addition of the RT-PCR mix (0.5 µl primer and 5 µl of Taqman Master mix). The reaction was performed in an ABI Prism 7900HT real time thermocycler (Applied Biosystems, Foster City, CA) using the following cycling program:

First step	50 °C	3 min
Second step	95 °C	10 min
Third step	95 °C	15 sec
Fourth step	60 °C	1 min

Step 3 and 4 were repeated for 40 cycles. Fold inductions were calculated using the comparative C_T method of Livak *et al* (Livak & Schmittgen, 2001) as described in the ABI Prism manual using GAPDH as the internal control.

2.21 EC_{50} curves

EC_{50} values were estimated from concentration-effect curves generated using non-linear regression models in GraphPad Prism 5 (La Jolla, CA, USA).

2.22 Statistical analysis

Statistical comparison between groups was carried out using one sample t-tests or one way ANOVA with Dunnett's or Tukey post-hoc correction to examine differences between groups. In all cases data are graphically represented as the mean ± standard error of the mean (SEM). All data were analysed using GraphPad Prism 5 (La Jolla, CA, USA).

3 CHAPTER THREE

RESULTS

Bile acid toxicity SAR: Correlations between cell viability and chromatographic lipophilicity in a panel of new and known bile acids

Chapter III

3.1 Introduction

BAs are known to regulate multiple cellular functions but perhaps the area of BA biology which has attracted most attention by investigators is their effects on cell viability and cytotoxicity. Central to the development of cholestatic liver disease and intestinal carcinogenesis is the peculiar effect BAs have on cell proliferation, both negative and positive. Retention of high concentrations of cytotoxic BAs in the liver is known to induce apoptosis or necrosis in hepatocytes eventually leading to cholestatic liver disease. Similarly the tumour promoting properties of BAs are thought to arise due to their ability to disturb the fine balance between cell proliferation, differentiation and apoptosis (Milovic *et al.*, 2002). Continual exposure of cells to cytotoxic BAs is eventually thought to lead to a resistance to apoptosis (Yui, Kanamoto & Saeki, 2009) allowing for selective growth of apoptosis resistant cell populations. Furthermore in recent years the cytotoxicity of BAs has inspired many medicinal chemistry programmes focussed on harnessing this property pharmacologically to design selective cytocidal agents (Choi *et al.*, 2001; Choi *et al.*, 2003; El Kihel *et al.*, 2008; Kim *et al.*, 2006; Liu *et al.*, 2008). For example the following LCA and CDCA piperazinylcarboxamides illustrated below (**1,2**) were shown to have low micro molar LD_{50} values in multiple myeloma and colon cancer cell lines (El Kihel *et al.*, 2008) (**1**, LD_{50}= 8.5 μM).

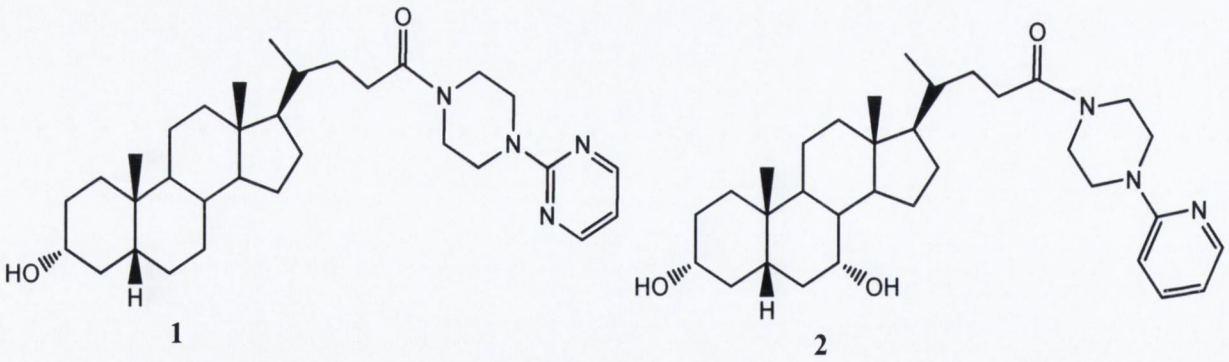

Figure 3.1. Structures of BA amides. *LCA (**1**) and CDCA (**2**) piperazinylcarboxamides, synthesised by (El Kihel et al., 2008).*

Hence an understanding of the mechanisms of BA induced cytotoxicity and the structural basis for such effects is important in elucidating the basis for BA induced carcinogenesis and for the rational design of compounds to counteract it.

3.1.1 BA induced apoptosis-Intrinsic and Extrinsic pathway

Apoptosis or programmed cell death is defined as an active physiologic process of cellular self-destruction, with specific morphologic and biochemical changes in the nucleus and cytoplasm (Steller, 1995). Apoptosis, in contrast to cellular necrosis, is a controlled form of cell death that allows for maintenance of cellular ATP content. Apoptosis involves activation of caspase enzymes, a family of cysteine proteases that act as common death effector molecules in various forms of cell death (Fulda & Debatin, 2006).

Much of the work investigating BA induced apoptosis has been conducted in hepatocytes (Benz *et al.*, 2000; Iizaka *et al.*, 2007; Oglodek *et al.*, 2009; Perez & Briz, 2009; Sola *et al.*, 2006; Tsuchiya *et al.*, 2006) although intensive investigation has also been done in colonic (Powell *et al.*, 2001; Qiao *et al.*, 2002; Qiao, Stratagouleas & Martinez, 2001a) and esophageal cell lines (Jenkins *et al.*, 2007; Kaur *et al.*, 2000; Zhang *et al.*, 2005). These studies identify a number of pathways and molecules as mediators of BA induced apoptosis.

Apoptosis signalling pathways can be initiated through two principal pathways. These are referred to as the extrinsic and intrinsic pathway of apoptosis. In the extrinsic pathway of apoptosis stimulation of death receptors results in receptor aggregation and recruitment of the initiator caspase 8 which can initiate apoptosis by direct cleavage and activation of downstream effector caspases (Fulda & Debatin, 2006; Harmand *et al.*, 2005), Figure 3.2. The death receptors are members of the tumor necrosis factor (TNF) receptor gene superfamily that consists of more than 20 proteins. The best characterised death receptors include CD95 (APO-1/Fas), TNF receptor 1 (TNFR1) and TNF-related apoptosis-inducing ligand receptor 1 (TRAIL-R1) and TRAIL-R2 (Fulda & Debatin, 2006).

The intrinsic pathway or mitochondrial pathway of apoptosis is initiated by stress signals that converge on the mitochondria leading to mitochondrial membrane permeabilisation (MMP) and release of apoptogenic proteins resulting in disruption of the mitochondrial membrane potential. This disruption culminates in activation of caspases and cell death (Amaral *et al.*, 2009c; Fulda & Debatin, 2006).

Both the extrinsic and intrinsic pathway of apoptosis have been shown to be activated by BAs, Figure 3.2 (Perez & Briz, 2009).

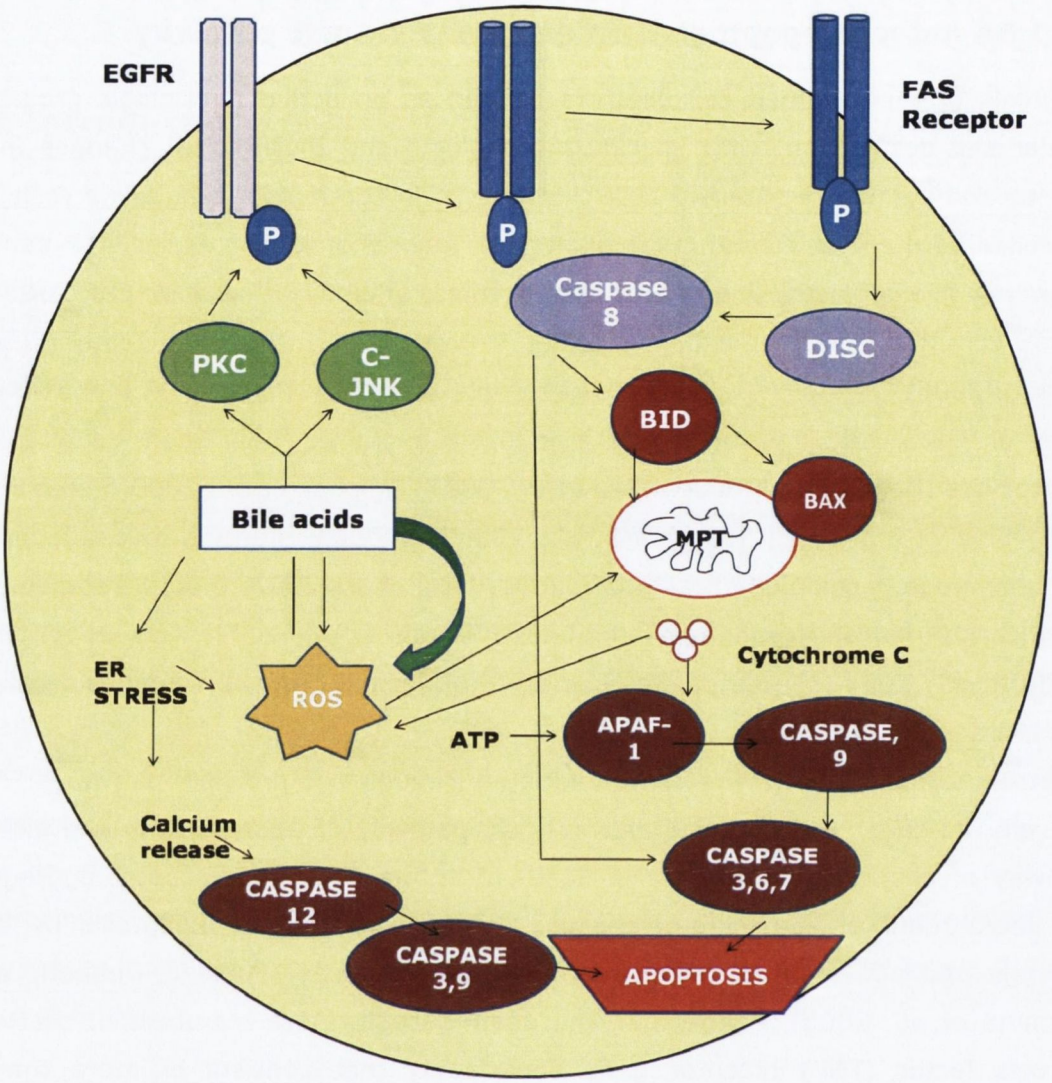

Figure 3.2. BAs induce apoptosis through the intrinsic and extrinsic pathway. *The extrinsic pathway involves activation of the CD95 death receptor and the intrinsic pathway involves induction of intracellular stresses principally arising in the mitochondria. BAs can also increase production of reactive oxygen species (ROS) and induce apoptosis through ER stress. These pathways are explained in section 3.1.1, image adapted from (Fulda & Debatin, 2006; Perez & Briz, 2009).*

3.1.1.1 Intrinsic pathway of apoptosis

Most cell death in vertebrates proceeds via the intrinsic or mitochondrial pathway of apoptosis. This pathway is ligand independent but is induced by intracellular stresses principally arising in the mitochondria (Harmand *et al.*, 2005) and resulting in MMP. MMP can occur as a result of the opening of the mitochondrial permeability transition (MPT) pore or through the formation of specific channels in the outer mitochondrial

membrane. This is promoted by the pro-apoptotic members of the Bcl-2 family of proteins (Amaral *et al.*, 2009c).

The Bcl-2 family of proteins consists of both pro- and anti-apoptotic proteins. In normal conditions the anti-apoptotic proteins, including Bcl-2 and Bcl-xL, are localised in the outer mitochondrial membrane whereas the pro-apoptotic members are in the cytosol (Amaral *et al.*, 2009c). Pro-apoptotic members include Bid and Bax. Induction of apoptosis results in a conformational change in the pro-apoptotic proteins leading to their oligomerisation and translocation to the mitochondrial membrane where they can induce formation of specific pores in the outer membrane (Kroemer, Galluzzi & Brenner, 2007).

Pore formation in the mitochondria allows for the release of cytochrome c. Cytochrome c is normally found in the inner mitochondria where it functions as an electron shuttle in the respiratory chain (Kroemer *et al.*, 2007). Once released into the cytosol, it oligomerises with apoptosis protease activating factor 1 (APAF-1). This complex leads to cleavage and activation of caspase 9 which can then cleave the downstream effector caspases 3, 6 and 7 (Fulda & Debatin, 2006).

3.1.1.2 Extrinsic pathway of apoptosis

BA associated hepatocyte and colonic apoptosis has also been shown to occur through ligand-independent phosphorylation of the death receptors including Fas and TRAIL-R2 (Faubion *et al.*, 1999; Higuchi & Gores, 2003; Katona *et al.*, 2009; Perez & Briz, 2009).

BAs are not known to be Fas agonists but they promote trafficking of the protein to the cell membrane (Higuchi & Gores, 2003; Katona *et al.*, 2009). This results in Fas oligomerisation due to increased density on the cell surface (Sodeman *et al.*, 2000) but also sensitises the cell to Fas-agonist induced cell death (Qiao *et al.*, 2001b).

A mechanism by which BAs increase Fas density on the cell surface is by sequestering the death receptor within intracellular pools, especially vesicles associated with the Golgi complex and the trans Golgi network (Bennett *et al.*, 1998; Graf *et al.*, 2002). On stimulation, these Fas-containing vesicles can be shuttled to the plasma membrane, presumably by a microtubule transport pathway, to initiate cell death signals. During BA-induced hepatocyte apoptosis, a Golgi-associated and microtubule-dependent pathway has been implicated in the trafficking of Fas to the cell surface (Sodeman *et al.*, 2000). Both PKC and JNK kinase have been implicated in this vesicle trafficking (Graf *et al.*, 2002).

BA generated reactive oxygen species (ROS) have also been implicated in Fas-translocation to the membrane (Perez & Briz, 2009). ROS is a general term used to describe radical and non-radical reactive oxygen derivatives such as superoxide and

nitric oxide. Oxidative stress occurs when the generation of ROS is excessive and the body can no longer adequately neutralise and eliminate them. ROS can activate c-Jun-N-terminal kinases (JNKs) and PKC which can then further activate the epidermal growth factor receptor (EGFR). EGFR then induces phosphorylation of Fas via JNK resulting in its translocation to the membrane (Reinehr *et al.*, 2005). The mitochondria have been proposed as the major source of oxidative stress induced by BAs (Perez & Briz, 2009; Sokol *et al.*, 2005). Hepatic mitochondria have been shown to undergo lipid peroxidation, an indicator of ROS, during cholestasis and toxicity in rats (Sokol *et al.*, 2005; Sokol, Devereaux & Khandwala, 1991). The mechanism involved includes impairment of respiration and electron transport in the mitochondria (Rolo *et al.*, 2000). Interestingly the antioxidant α-tocopherol (Vitamin E) is able to reduce both hydrophobic BA induced ROS generation and injury to hepatocytes *in vitro* (Sokol *et al.*, 1993) and *in vivo* (Sokol *et al.*, 1998). It has recently been shown that BAs may induce ROS production in esophageal cells via a TGR5 dependent pathway (Hong *et al.*, 2010).

Activation of Fas or any of the other death receptors causes the recruitment and oligomerisation of the adapter molecule FADD (Fas-associating death domain-containing protein) within the death-inducing signalling complex (DISC). DISC can then bind to and activate the initiator caspase 8 (Kroemer *et al.*, 2007).

In type 1 cells sufficient quantities of caspase 8 are activated to directly cleave and activate effector caspases (caspase 3, 6, 7). However in type 2 cells, such as hepatocytes, a mitochondrial amplification loop is required for full activation of the effector caspases (Scaffidi *et al.*, 1998). This involves cleavage of inactive Bid in the cytosol by caspase 8 and MMP resulting in apoptosis as described in Section 3.1.1.1 (Katona *et al.*, 2009; Yin & Ding, 2003).

3.1.1.3 ER stress pathway of apoptosis

BAs can also induce apoptosis via an endoplasmic reticulum (ER) stress pathway. Tsuchiya *et al* have shown that ER stress induced by the BA, GCDCA resulted in Ca^{2+} release from the ER which led to activation of caspase 12 as shown in Figure 3.2. The key protein in ER stress mediated apoptosis is CHOP. CHOP alters the balance between pro-survival and pro-apoptotic Bcl-2 family members thus promoting apoptosis through the mitochondrial pathway (Healy *et al.*, 2009; McCullough *et al.*, 2001). CHOP deficiency has been shown to attenuate cell death in hepatocytes (Tamaki *et al.*, 2008). The ER stress pathway and its activation by BAs will be discussed in detail in Chapter 5.

3.1.2 Effect of BAs on biological membranes

Despite there being substantial evidence in a variety of cell lines for BAs triggering apoptotic processes, a specific binding target responsible for BA induced cell death remains elusive. There is however evidence that BAs can induce cell death through direct damage to the cell membrane and cell organelle membranes (Perez & Briz, 2009). High concentrations of BAs result in necrosis or cell lysis through a detergency effect in which the membrane is completely ruptured (Hofmann, 1999). Even at low concentration, BAs aggregate with lipids in the outer membrane monolayer, the binding strength depending on the particular BA and lipid involved. As the concentration of BA increases, binding to the membrane continues to increase until a critical threshold concentration is reached. Following this, the BA-membrane interaction results in the formation of transient membrane holes leading to the disruption of plasma membrane integrity and subsequently cell lysis (Schubert & Schmidt, 1988). The concentration at which this occurs is related to the critical micelle concentration (CMC) of the BA (Hofmann, 1999). Hence as CDCA and DCA have a lower CMC than CA they are more cytotoxic at a given concentration (Hofmann, 1999). As BAs associate with phosphatidylcholine and other fatty acids in the intestinal lumen to form mixed micelles they do not cause damage in the biliary tract of healthy people.

However even before membrane integrity is compromised BAs have been shown to modify membrane fluidity and composition (Asamoto *et al.*, 2001; Garidel *et al.*, 2007; Vlahcevic *et al.*, 1990). For example bile salts increased membrane phospholipids and fluidity as well as increasing the expression of multidrug-resistance proteins (Mrp2, Mrp3) and the ASBT bile transporter (Asamoto *et al.*, 2001). BAs can also increase transfer of cholesterol from the membrane to high density lipoprotein vesicles (Vlahcevic *et al.*, 1990). Furthermore Akare *et al* have shown that these alterations in the lipid composition of the membrane occur without directly affecting the barrier function of the membrane (Akare & Martinez, 2005). Some of these effects resemble those observed with non-BA hydrophobic solutes such as cholesterol myristate and detergents *n*-octylglycoside and Triton-X, at sub-lytic concentrations (Strupp *et al.*, 2000). Strupp *et al* showed that these detergents can induce typical signs of apoptosis such as DNA fragmentation and cleavage of the DNA repair enzyme poly (ADP-ribose) polymerase (PARP) across human and other vertebrate cell lines in a concentration dependent manner. The apoptosis was found to be caspase dependent as treatment with peptide inhibitors blocked it. They suggest that detergents can mediate apoptosis by initiating nonspecific alterations at the cell membrane level.

3.1.3 Biological effects of BAs: hydrophilic Vs hydrophobic BAs?

Evidence from BA studies on the membrane and the lack of a receptor for BA induced apoptosis, indicate that even at sublytic concentrations BA induced apoptosis may be mediated by non-specific effects on the cell membrane.

An influential early observation about the SAR of BA toxicity was that DCA causes more membrane damage than CA and its conjugates (Vyvoda, Coleman & Holdsworth, 1977).

Numerous studies have since shown that DCA, CDCA and LCA are markedly more cytotoxic than other BAs and their own glyco and tauro-conjugates (Perez & Briz, 2009). In partitioning experiments these BAs are lipophilic relative to other less toxic physiological BAs suggesting that lipophilicity and toxicity are associated or even correlated. Hydrophobic BAs are expected to accumulate to a greater extent within the cell membrane where they can associate with the lipid bilayers and interact non-specifically with membrane components to alter their physical properties (Attili *et al.*, 1986; Billington *et al.*, 1980; Katona *et al.*, 2009). This has led to the general consensus that the physicochemical effects of BAs, principally their hydrophobicity are ultimately determinants of cytotoxicity (Akare & Martinez, 2005; Martinez *et al.*, 1998; Powell *et al.*, 2001; Yui *et al.*, 2009; Yui *et al.*, 2005).

This view has been substantiated by the fact that the relatively hydrophilic BA UDCA is used in the treatment of liver diseases and is regularly referred to as "non-toxic". Indeed unlike LCA, CDCA and DCA which are the prototypical hydrophobic toxic BAs the hydrophilic UDCA has been shown to have cytoprotective properties. In numerous studies UDCA has been shown to inhibit DCA and CDCA induced apoptosis (Amaral *et al.*, 2009c; Pusl *et al.*, 2008; Rodrigues CMP, 1998; Silva, Rodrigues & Brites, 2001; Sola *et al.*, 2004). Numerous mechanisms have been proposed for this cytoprotective effect, including, down regulation of the proteins Bax and caspase-3 (Ji *et al.*, 2009) and modulation of mitochondrial MPT (Rodrigues CMP, 1998). Other mechanisms include up regulation of basolateral export pump (Paolini *et al.*, 2002) and modulation of the EGFR/Raf-1/ERK signalling pathway (Im & Martinez, 2004). The taurine conjugate of UDCA, TUDCA inhibits apoptosis associated with ER stress by modulating intracellular calcium levels and inhibiting calpain and caspase-12 activation (Amaral *et al.*, 2009c). UDCA also interacts with nuclear steroid receptors which leads to nuclear translocation of the UDCA/NSR complex. Once in the nucleus, UDCA can modulate the E2F-1/p53/Bax pathway. Transcriptional activation of p53 induces Bax expression, mitochondrial translocation, cytochrome c release, and apoptosis in primary rat hepatocytes (Amaral *et al.*, 2009a). UDCA inhibition of p53-induced apoptosis is associated with decreased p53 DNA binding activity (Amaral *et al.*, 2007) although UDCA does not bind to the p53 DNA-binding domain (Amaral *et al.*, 2009b).

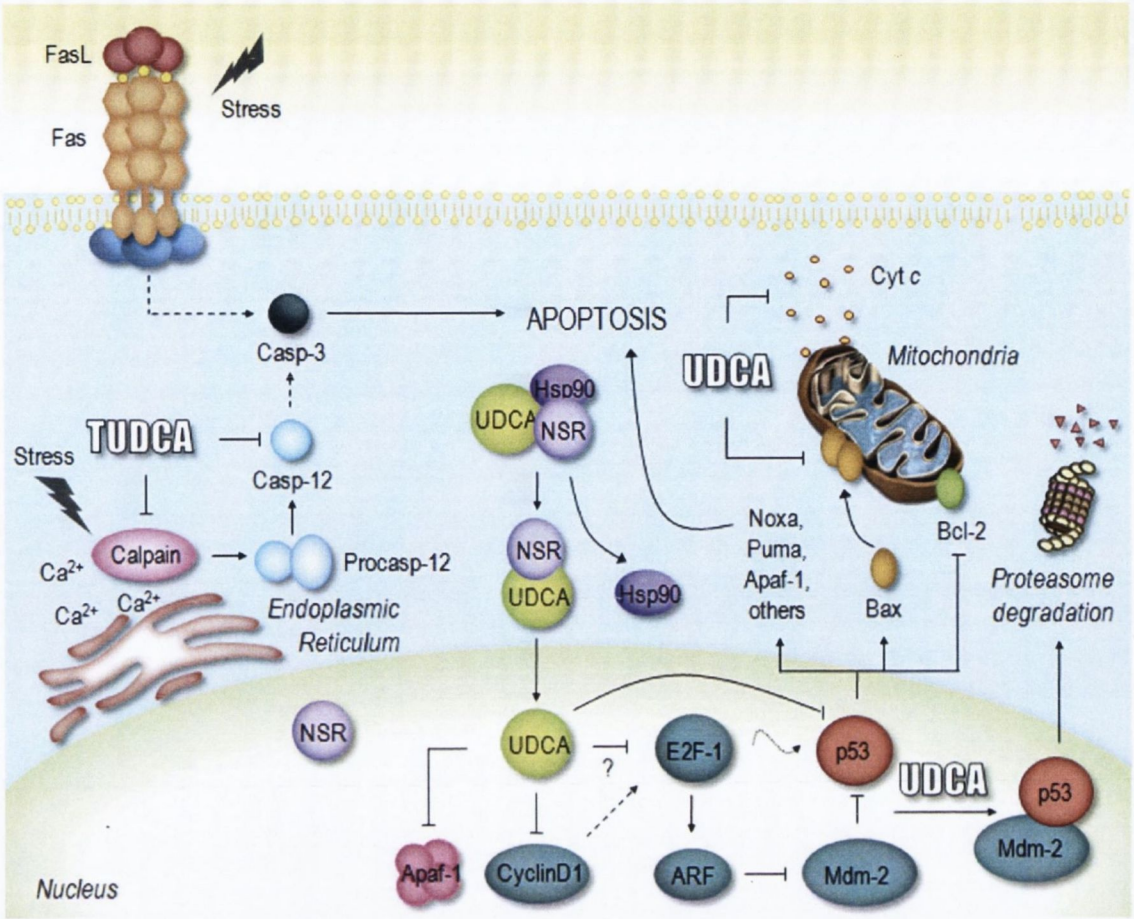

Figure 3.3 UDCA inhibits BA induced apoptosis. *Multiple mechanisms have been proposed for UDCAs inhibitory effects on apoptosis, taken from (Amaral et al., 2009c).*

It has also been proposed that the cytoprotective effects of UDCA are due to its displacement of hydrophobic toxic BAs. Indeed one of the main therapeutic mechanisms of UDCA in cholestatic liver diseases is due to enrichment of the BA pool by UDCA leading to displacement of the endogenous hepatotoxic BA (Stiehl et al., 1999).

Despite the generally held view that hydrophobicity and toxicity are correlated, few studies have been done specifically investigating the relationship between hydrophobicity and BA toxicity or other BA biological effects. Rao *et al* demonstrated that activation of PKC α and δ *in vitro* in constituted micelles correlated with chromatographic measures of hydrophobicity for DCA, UDCA, CA and CDCA and their taurine conjugates (Rao *et al.*, 1997) (r^2 of 0.6 and 0.8 for PKC α and δ respectively). More recently Martinez *et al* reported a correlation between induction of apoptosis and BA hydrophobicity in a colon cancer cell line (Powell *et al.*, 2001). In this study the researchers determined the effects of 16 BAs on the ability to induce apoptosis and

inhibit cell proliferation in the HCT116 cell line. Hydrophobicity was determined by HPLC retention time, Figure 3.4.

Bile acid	HPLC retention time (min)
DCA	31.68
CDCA	24.48
NorDCA	19.44
HomoUDCA	14.54
LagoDCA	12.88
HyoDCA	12.12
UDCA	10.52
IsoUDCA	9.7
Cholic acid	15.26
IsoCDCA	14.76
NorCDCA	14.76
Murocholic acid	8.32
β-Muricholic acid	7.65
ω-Muricholic acid	7.18
NorUDCA	6.27
Ursocholic acid	5.01

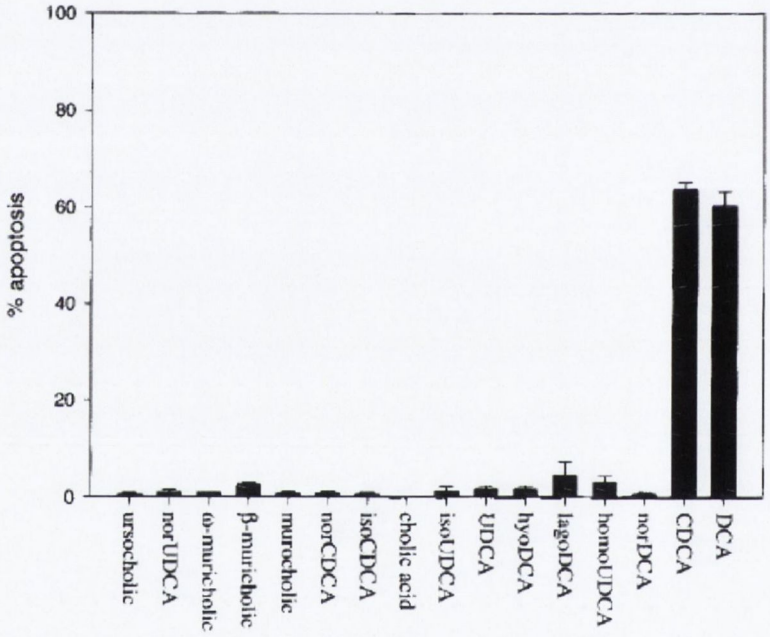

Figure 3.4 Relationship between BA hydrophobicity and toxicity. *This study by Martinez et al characterised the hydrophobicity of a panel of 16 BAs as determined by HPLC retention time and correlated this with induction of apoptosis in a HCT116 colon cancer cell line, image taken from (Powell et al., 2001).*

Although they find that the most hydrophobic BAs DCA and CDCA induce the greatest apoptosis and inhibit cell proliferation to the greatest degree as measured by thymidine uptake, these findings are not contiguous with the rest of the BA series as shown in Figure 3.4. The study did not establish a direct correlation for the relationship between toxicity and apoptosis or inhibition of proliferation and hence the observations remain qualitative.

Furthermore there is evidence that the picture is more complex than a simple direct relationship between hydrophobicity and toxicity (Araki Y, 2001; Patel T, 1994). For example, using a hepatocyte cell line, Carubi *et al* compared the toxicity of taurohyodeoxycholic acid and TDCA which have similar hydrophobicity characteristics and found varying degrees of cytotoxicity (Carubbi *et al.*, 2002). Hence although LCA, DCA and CDCA occupy both the toxic and hydrophobic end of the spectrum of common BAs, their toxicity may not be attributable to their hydrophobicity alone. Recent work by Katona *et al* has involved the synthesis and biological characterisation of enantiomeric DCA, CDCA and LCA (Katona *et al.*, 2009).

A) **B)**

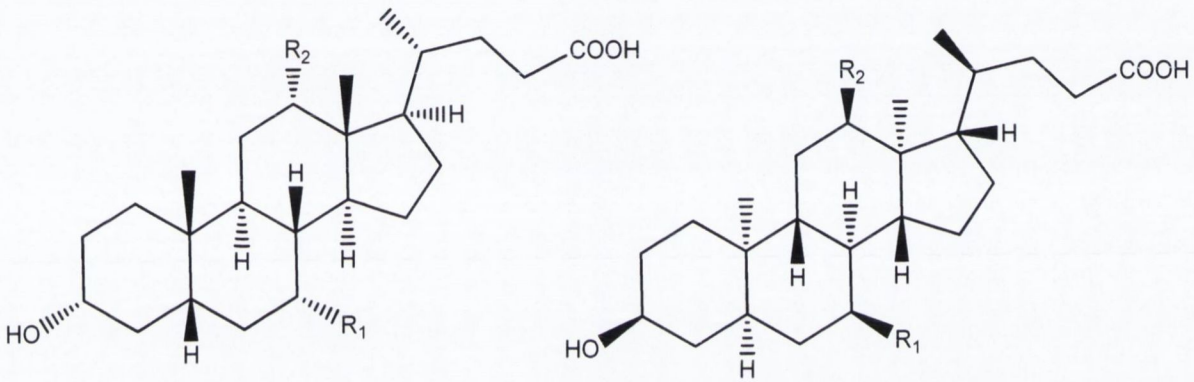

LCA R_1=H R_2=H (**3**)
DCA R_1=H R_2=OH (**4**)
CDCA R_1=OH R_2=H (**5**)

ent-LCA R_1=H R_2=H (**6**)
ent-DCA R_1=H R_2=OH (**7**)
ent-CDCA R_1=OH R_2=H (**8**)

Figure 3.5 Natural and enantiomeric BAs. *A) The natural BAs LCA (**3**), DCA (**4**) and CDCA (**5**). B) enantiomeric BAs, ent-LCA (**6**), ent-DCA (**7**) and ent-CDCA (**8**) synthesised by Katona et al (Katona et al., 2009).*

The natural BAs LCA, CDCA, and DCA were reported to initiate more apoptosis than their enantiomers ent- LCA, ent-CDCA, and ent-DCA in HT-29 and HCT-116 (Katona *et al.*, 2009). Hydrophobic interactions are identical in enantiomeric pairs unless the environment is itself chiral. Hence the enantiospecificity of apoptosis indicates that hydrophobicity alone is not the sole determinant of cell death.

3.2 Aims and Objectives

There is a dearth of quantitative information on BA toxicity in the literature to allow comparative analysis and to enable assessment of the role of BAs in the disease etiology. In particular BA structure activity relationship (SAR) studies regarding toxicity have not been studied. Furthermore having done preliminary studies investigating the effects of our synthetic BA derivatives on GR activity and Golgi morphology we realised that an increase in hydrophobic character did not always lead to increased toxicity. Hence we decided to initiate an investigation examining the effects of our panel of compounds on esophageal cell viability with a view to determining the physicochemical and structural requirements for BA toxicity in the HET-1A cell line.

The specific aims of this study were as follows:

1) To construct a panel of naturally occurring and synthetic BAs which displayed a spectrum of physicochemical characteristics.

2) To evaluate the relative polarity of these BAs using reverse-phase HPLC, revere-phase TLC and to determine physico-chemical descriptor parameters using *in silico* computational methods.

3) To evaluate the effect of this panel of BAs on the cell viability of the HET-1A, esophageal cell line. This cell line represents "normal" esophageal epithelial cells and thus is a good model to investigate how BAs may initiate intracellular signalling resulting in toxicity, which could in turn lead to activation of carcinogenic cascades.

4) To characterise the relationship between cytotoxicity and BA polarity and to investigate if BA toxicity is related to functional group type and arrangement in synthetic and natural BAs.

3.3 Results

3.3.1 BA toxicity panel

A panel of 37 BAs were studied, the structures of which are shown in Figure 3.6 below. The panel principally consisted of UDCA and DCA derivatives as these are the prototypical cytoprotective and cytotoxic BAs respectively. Twenty-five of these BAs were assembled from commercially available products and gifts donated by Prof. Natalini and Mr Ferenc Majer as outlined in Table 3.1. This was augmented with 11 compounds synthesised as outlined below. The structures of these compounds are shown in Figure 3.6. LagoDCA and 3-deoxy UDCA were particularly important compounds in the panel. LagoDCA has a 3α-OH and 12β-OH and hence has the same position of hydroxyls as DCA but was expected to have similar physicochemical behaviour to UDCA which also has one alpha and one beta hydroxyl (3α-OH and 7β-OH). On the other hand 3-deoxy UDCA is a 7β-OH BA and hence would have similar lipophilicity to the monohydroxy BA LCA (3α-OH).

Table 3.1 BAs screened in toxicity studies. *Thirty seven compounds were assembled for these studies.*

LCA (**3**)	commercial	UDCA3αN_3 (**21**)	Gift	NCA (**36**)	scheme 3.5
DCA (**4**)	commercial	UDCA3βN_3 (**22**)	Gift	NCA3-acetate (**37**)	scheme 3.5
CDCA (**5**)	commercial	3deoxyUDCA (**23**)	Gift	3,7,12-ketone (**38**)	commercial
TCDCA (**9**)	commercial	Nor UDCA (**24**)	scheme 3.7A	3,7-diketone (**39**)	scheme 3.6
GCDCA (**10**)	commercial	BisnorUDCA (**25**)	scheme 3.7B	3αOH,7βN_3 (**40**)	scheme 3.3
CA (**11**)	commercial	UDCA24CN (**26**)	scheme 3.8	UCA (**41**)	Gift
TCA (**12**)	commercial	BisnorUDCACN (**27**)	scheme 3.7B	HCA (**42**)	Gift
GCA (**13**)	commercial	UDCA-24OH (**28**)	scheme 3.4		
UDCA (**14**)	commercial	UDCA-24N_3 (**29**)	scheme 3.4		
TUDCA (**15**)	commercial	MeDCA (**30**)	Gift		
GUDCA (**16**)	commercial	DCA-24NH_2 (**31**)	Gift		
TDCA (**17**)	commercial	DCA3αN_3 (**32**)	Gift		
GDCA (**18**)	commercial	DCA3βN_3 (**33**)	Gift		
MeUDCA (**19**)	scheme 3.1	LagoDCA (**34**)	Gift		
UDCA-24NH_2 (**20**)	Gift	12KetoLCA (**35**)	Gift		

A)

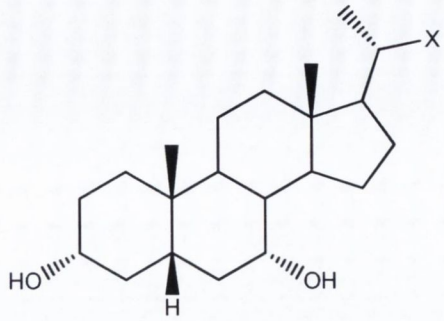

5 (CDCA) X= CH_2CH_2COOH
9 (TCDCA) X=$CH_2CH_2CONH(CH_2)_2SO_3H$
10 (GCDCA) X=$CH_2CH_2CONHCH_2COOH$

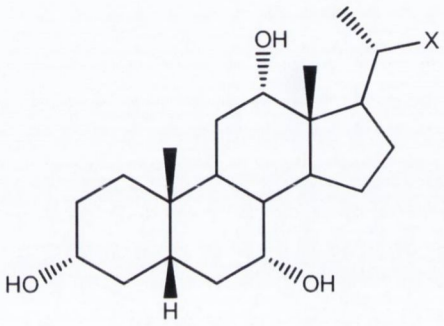

11 (CA) X= CH_2CH_2COOH
12 (TCA) X=$CH_2CH_2CONH(CH_2)_2SO_3H$
13 (GCA) X=$CH_2CH_2CONHCH_2COOH$

UDCA panel

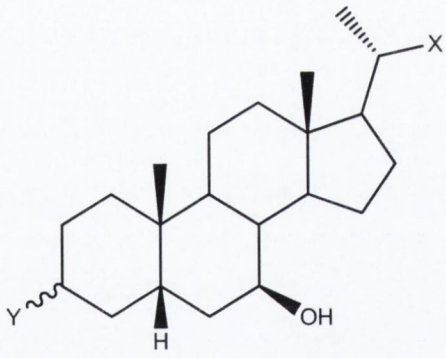

14 (UDCA) X=$(CH_2)_2COOH$, Y=αOH
15 (TUDCA) X=$(CH_2)_2CONH(CH_2)_2SO_3H$, Y=αOH
16 (GUDCA) X=$(CH_2)_2CONHCH_2COOH$, Y=αOH
19 X=$(CH_2)_2COOMe$, Y=αOH
20 X=$CH_2CH_2CONH_2$,Y=αOH
21 X=$(CH_2)_2COOH$, Y=αN_3
22 X=$(CH_2)_2COOH$, Y=βN_3
23 X=$(CH_2)_2COOH$, Y=H
24 X=CH_2COOH, Y=αOH
25 X=COOH, Y=αOH
26 X=$(CH_2)_2CN$, Y=αOH
27 X= CN, Y=αOH
28 X=$(CH_2)_3OH$, Y=αOH
29 X=$(CH_2)_3N_3$, Y=αOH

B)

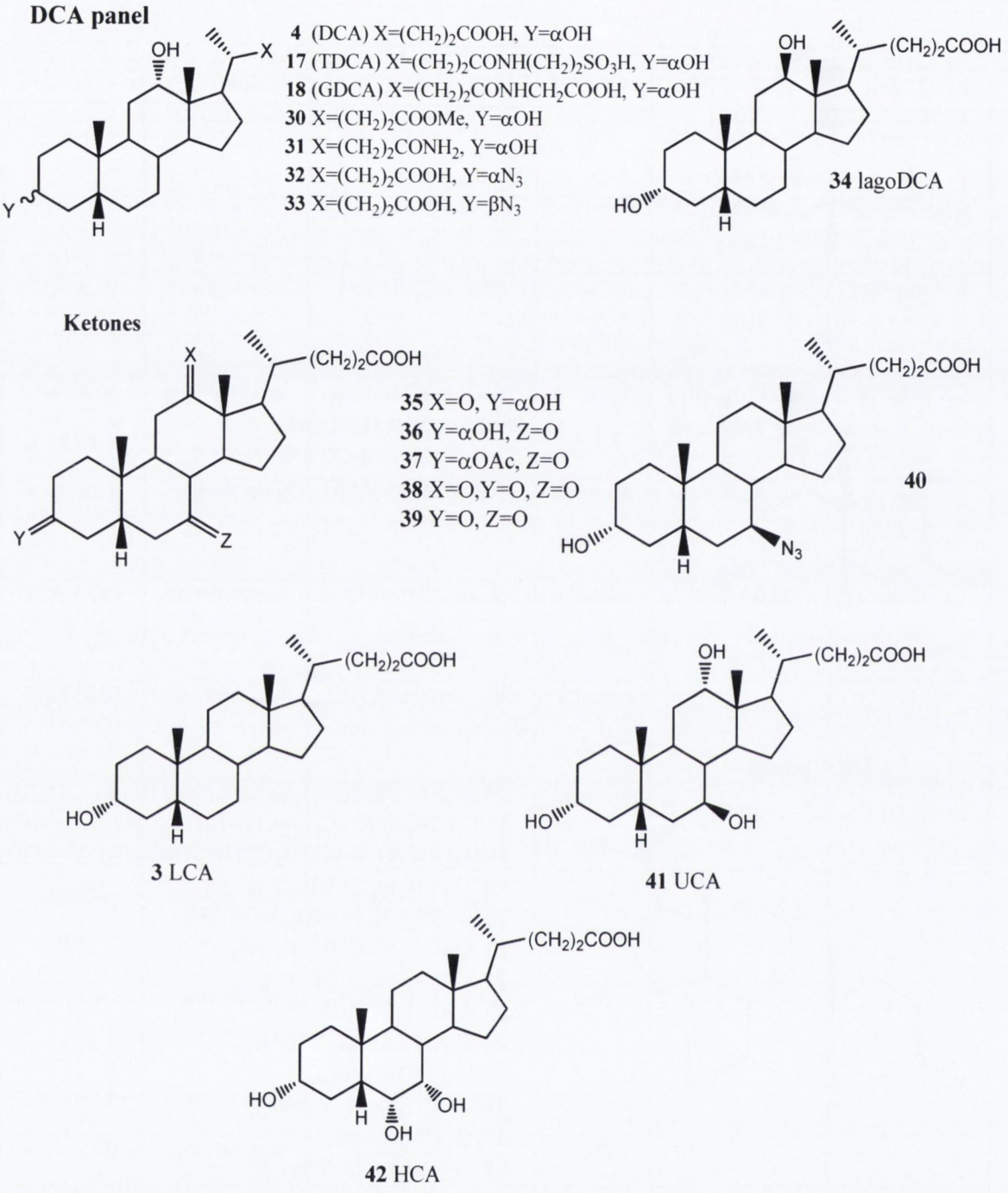

Figure 3.6 Structures of BAs studied for investigating the relationship between cytotoxicity and hydrophobicity. *A) CDCA, CA and UDCA derivatives B) DCA panel, ketones and other compounds assembled for the study.*

3.3.2 Chemical Synthesis

3.3.2.1 Preparation of BA esters

Esters of BAs were originally prepared to study the effect of esterification on the ability of BAs to induce GR translocation. This is described in Chapter 4. We decided to include the DCA and UDCA methyl esters (**19, 30**) in our panel for toxicity screening as well as they were compounds with a more hydrophobic character than the parent BAs. They were also useful compounds for protection of the carboxylic acid moiety. Dry methanol and acetyl chloride were used to generate anhydrous HCl *in situ* to generate 24-methyl UDCA (**19**), 24-methyl CDCA (**44**) and 24-methyl DCA (**30**) through acid catalysed esterification.

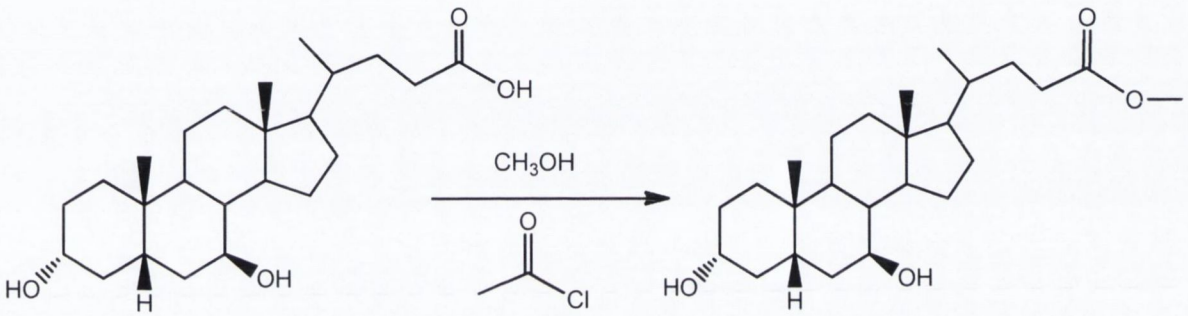

UDCA (**14**) **19**

Scheme 3.1. Synthesis of BA methyl esters showing UDCA as a representative example.

The benzyl esters of CDCA (**52**) and UDCA (**42**) were also prepared. This was achieved through base catalysed esterification using benzyl bromide and $CsCO_3$. The mechanism involves nucleophilic attack by the BA anion on benzyl bromide.

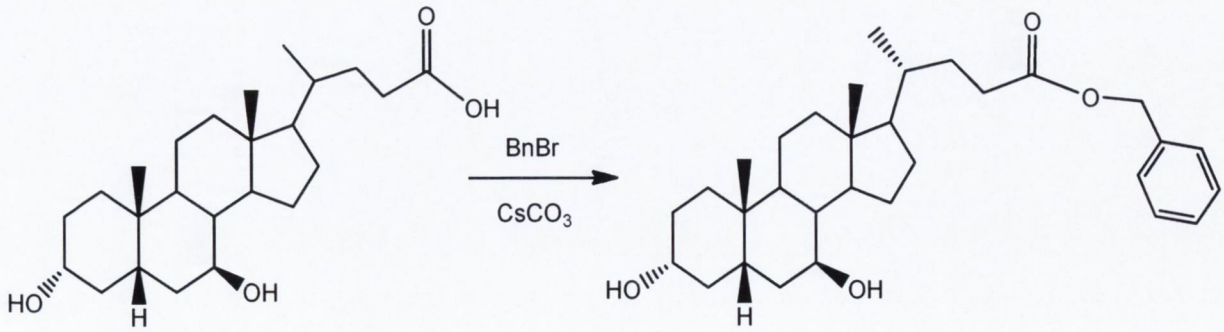

UDCA (**14**) **42**

Scheme 3.2. Synthesis of BA benzyl esters showing UDCA as a representative example.

3.3.2.2 Preparation of UDCA azides

A panel of azido BAs were included in our hydrophobicity studies due to the hydrophobic nature of the azide moiety. The 7β-azide UDCA (**40**) and 24-azido UDCA (**29**) derivatives were prepared to add to the panel of azide derivatives donated as gifts with modifications at the 3-OH position of DCA and UDCA. The 7β-azide was generated by an SN2 substitution reaction of the α-mesylate of CDCA (**46**). Carboxylic acid protection of CDCA was achieved through methyl esterification (**44**). Acetic anhydride with pyridine as an acylation catalyst was used for selective acetylation of the 3α-OH (**45**). SN2 substitution reactions can only proceed in the presence of a good leaving group. Aryl and alkyl sulfonic acids or their derivatives are commonly used for conversion of alcohols to good leaving groups through formation of sulfonates which are weak bases. Hence we used methanesulfonyl chloride to generate the 7-α mesylate (**46**). This could then be treated with NaN_3 in DMSO followed by deprotection in aqueous base to generate the 7β-azido analogue of UDCA (**40**) as shown, Scheme 3.3.

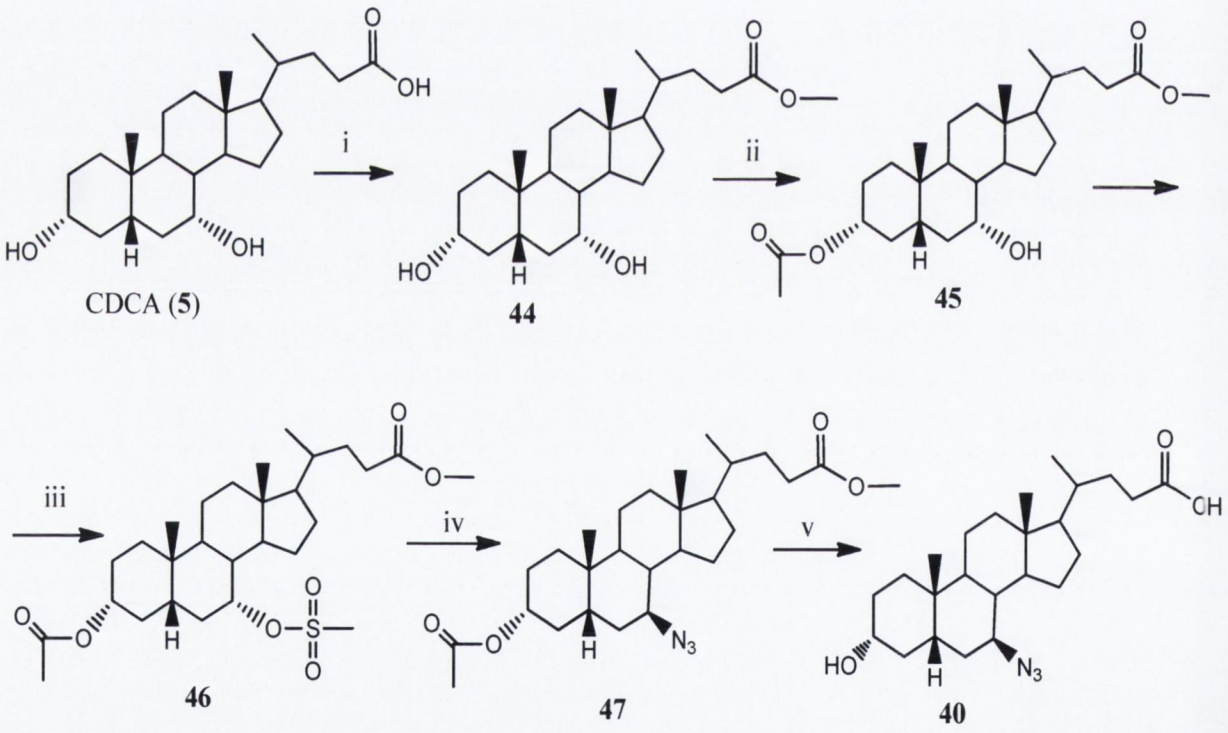

(i) Acetyl chloride, methanol, RT, 16 h; (ii) Acetic anhydride, pyridine, DCM, 0 °C-RT, 16 h; (iii) MsCl, dry pyridine, 0 °C-RT, 16 h; (iv) NaN_3, DMSO, RT, 7d (v) 2M NaOH/MeOH (pH~14), RT, 16 h.

*Scheme 3.3. Synthesis of 7β-azido UDCA (**40**)*

The 24-azido UDCA (**29**) analogue was prepared in three steps. Nucleophilic acyl substitution with $LiAlH_4$ reduced UDCA to its alcohol (**28**). Regioselective mesylation of this primary alcohol in cold solvent followed by chromatographic isolation yielded pure 24-mesylate (**48**) and 3α, 24 dimesyloxy UDCA. Finally azide substitution with NaN_3 in DMF afforded 24-azido UDCA.

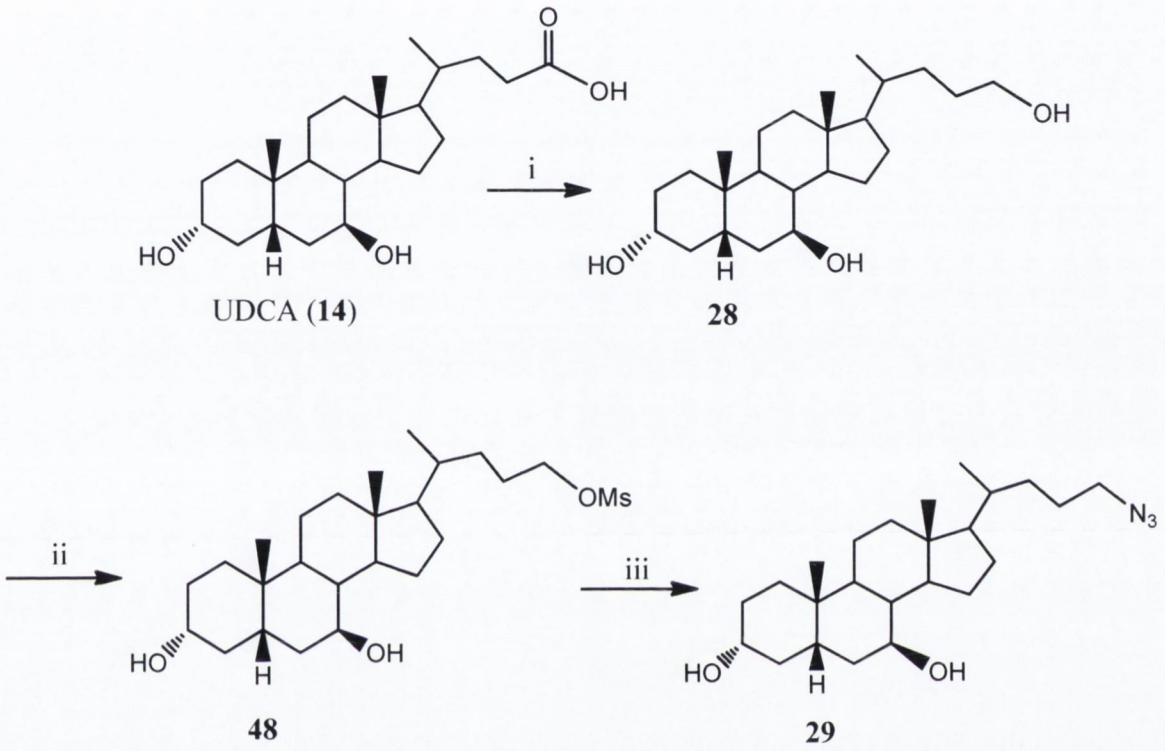

UDCA (**14**) **28**

48 **29**

(i) $LiAlH_4$, dry THF, reflux, 3 h; (ii) MsCl, NEt_3, DCM, 0 °C, 20 min; (iii) NaN_3, DMF, 60 °C, 2 d.

*Scheme 3.4. Synthesis of 24-azido UDCA (**29**).*

3.3.2.3 Synthesis of oxo-derivatives

We constructed a panel of keto derivatives for this study as introduction of keto (oxo) groups at the 3, 7 and 12 positions of BAs has the effect of depressing hydrophobicity. This is because conversion of a tetrahedral sp3 carbon to a flat sp2 carbon promotes water access to both faces of the steroid (Posa & Kuhajda, 2010). The 7-ketone (nutriacholic acid) (**36**) was obtained from benzyl CDCA monoacetate (**49**) through a pyridinium chlorochromate (PCC) oxidation reaction as shown in scheme 3.5. Hydrolysis in strong aqueous base afforded **36**. However hydrolysis, in mild basic conditions allowed for selective removal of the acetoxy group and generated **51** and similarly hydrogen reduction allowed for removal of the benzyl group only to produce 3-acetate NCA (**37**). The 3-acetate NCA was also included in our panel as it provides a highly lipophilic acid.

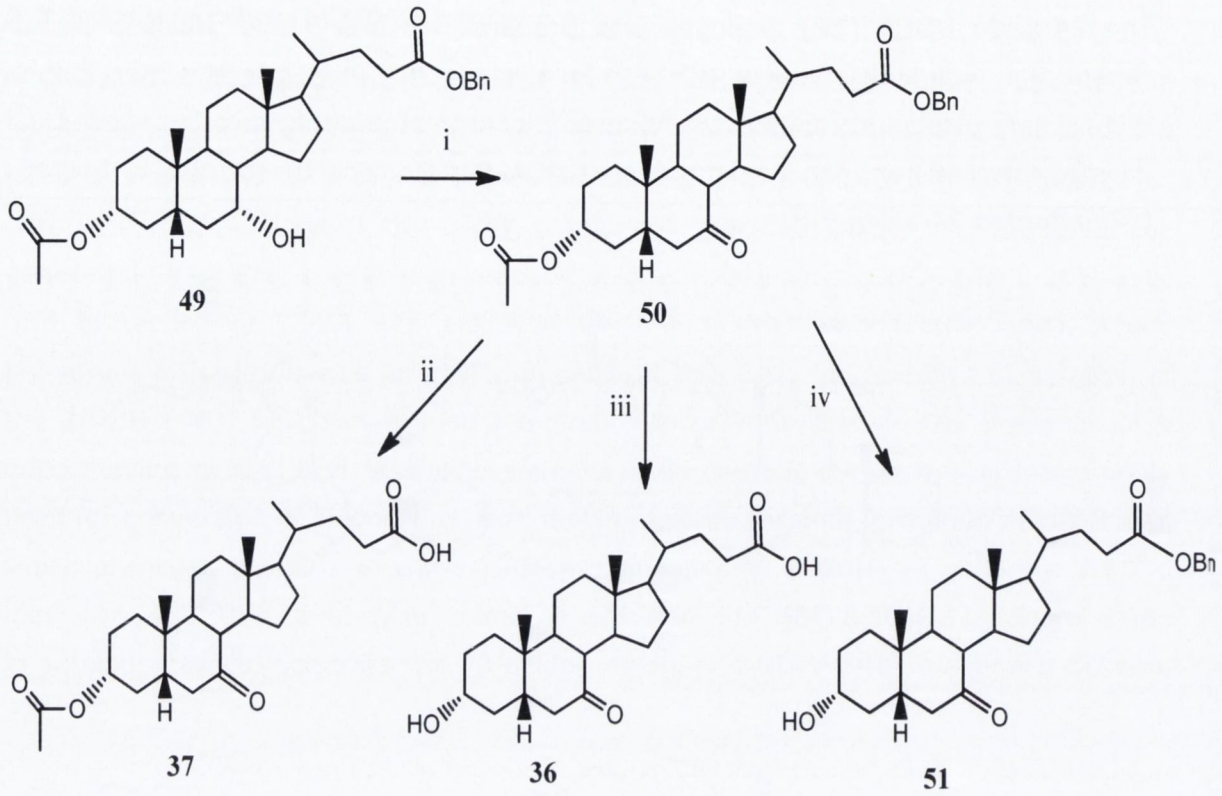

(i) PCC, DCM, RT, 16 h; (ii) 2M $NaHCO_3$/MeOH (pH~10), RT, 12 h; (iii) 2M NaOH/MeOH (pH~14), RT, 16 h; (iv) Pd/C, H_2, EtOAc, RT, 8 h.

*Scheme 3.5. Synthesis of UDCA oxo derivatives from protected CDCA (**49**).*

Oxidation of the CDCA benzyl ester (**52**) produced the 3,7-diketo acid (**39**) as shown in Scheme 3.6. The benzyl CDCA ester (**52**) was oxidised with PCC to produce the protected diketone (**53**). Hydrogen reduction removed the benzyl protection to generate the diketo acid (**39**).

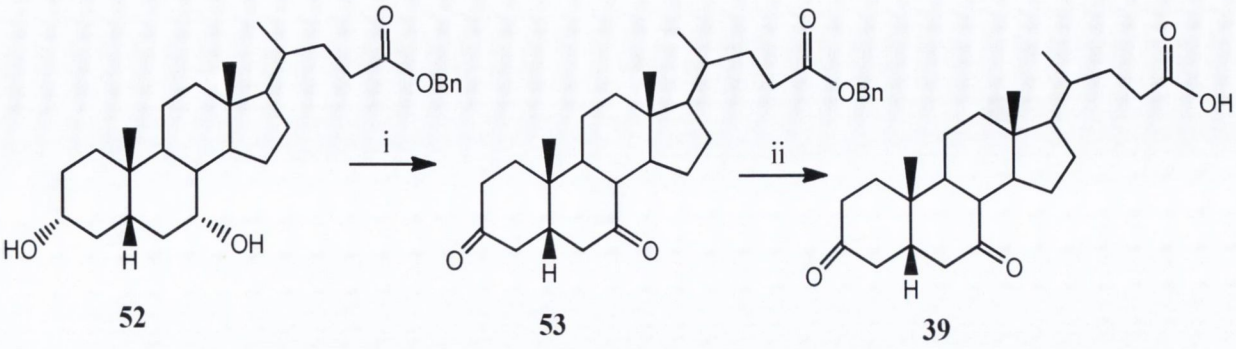

52 53 39

(i) PCC, DCM, RT, 16 h; (ii) Pd/C, H_2, EtOAc, RT, 8 h.

*Scheme 3.6. Synthesis of the 3, 7 diketone (**39**) from benzyl protected CDCA (**52**).*

3.3.2.4 Side chain degradation of UDCA

Side chain degradation of UDCA to norUDCA (**24**) and bisnorUDCA (**25**) was carried out to determine the effects of these compounds on GR translocation to the nucleus, as described in Chapter 4. These derivatives were also included in the panel of compounds to be screened for cytotoxicity. The acid derivatives were prepared via a degradation reaction involving a second order Beckmann rearrangement. This reaction also produced the nornitrile and bisnornitrile (**55**, **27**) derivatives of UDCA. We decided to include the latter along with the 24-nitrile (**26**) of UDCA, to increase the range of hydrophobicities in our panel of compounds.

The 3 and 7-OH groups of UDCA were formyl protected (**54**). **54** was then treated with trifluoroacetic acid, trifluoroacetic anhydride and sodium nitrite followed by deprotection in sodium methoxide to yield the nornitrile (**55**). Nucleophilic addition of hydroxide ion to the nornitrile was achieved through harsh aqueous base conditions involving reflux for 96 h to hydrolyse the cyano group to an acid, scheme 3.7A. These steps were then repeated on the noracid (**24**) to produce the bisnornitrile (**27**) and bisnoracid (**25**) derivatives of UDCA, scheme 3.7B.

A)

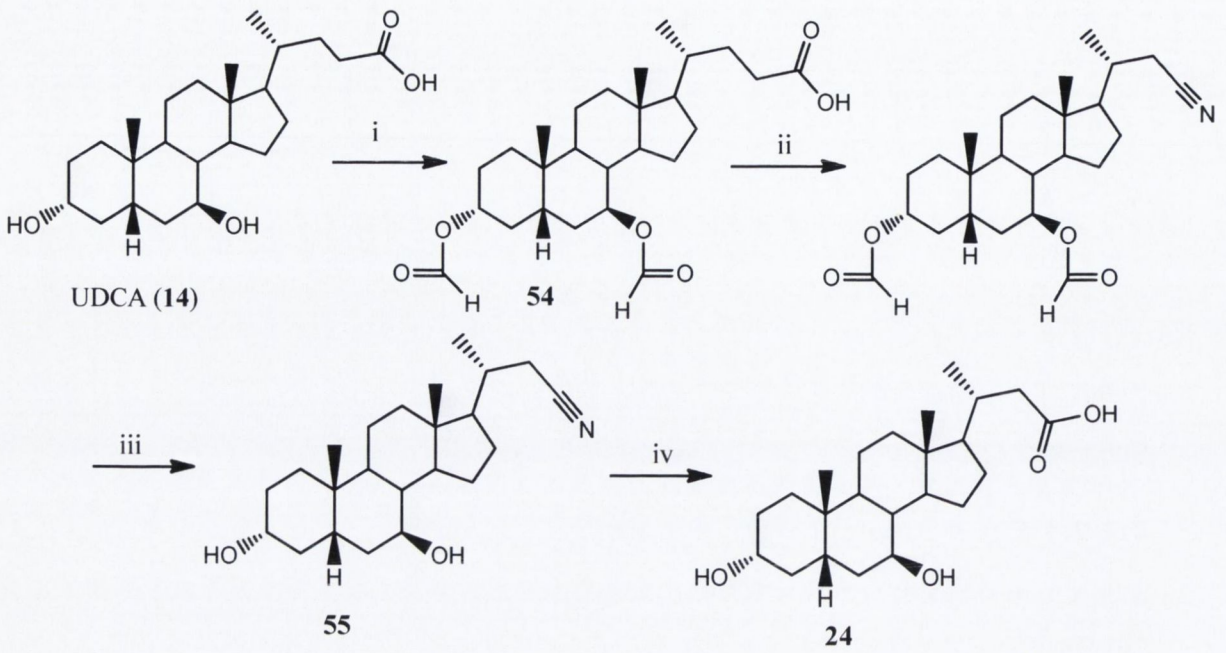

B)

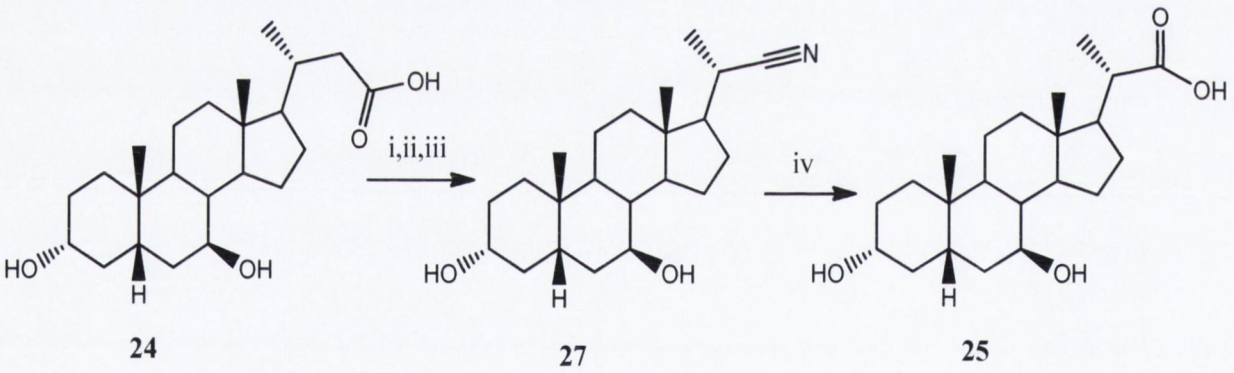

(i) Formic acid/perchloric acid, 50 ºC, 3 h; (ii) TFA, TFAA, $NaNO_2$, 0-5 ºC 1 h, 40 ºC 2 h; (iii) Na/MeOH, reflux, 2 h; (iv) 10% KOH ethanol-water 1:1, reflux, 96 h.

*Scheme 3.7 Side chain degradation of UDCA. Side chain degradation of UDCA generated A) the nornitrile (**55**) and norUDCA (**24**). B) Repeating these steps on norUDCA produced **27** and **25**.*

3.3.2.4.1 Mechanism of side chain degradation

The mechanism involved in the degradation reaction was proposed by Schteingart and Hofmann and the reaction provides a good alternative to the conventional Barbier Wieland degradation for carbon side chains. Formation of a mixed anhydride with trifluoroacetic anhydride at cold temperatures activates the α-carbon of the BA and

allows for nitrosation with trifluoroacetyl nitrite to form a nitroso anhydride. The nitrosation step is thought to only occur at moderately high temperatures which is why the temperature is increased to 40 °C. This group then tautomerises to an oxime group which can be acylated by a trifluoroacetate. This acyl intermediate now undergoes a Beckmann rearrangement in which an oxime is converted to a nitrile. Firstly the trifluoroacetate group is eliminated from the oxime, and subsequent shift of an electron pair forms the carbon-nitrogen triple bond. Carbon dioxide is liberated resulting in a decrease in chain length by one carbon. Trifluoroacetic anhydride is reformed by attack of trifluoroacetate as shown (Schteingart & Hofmann, 1988).

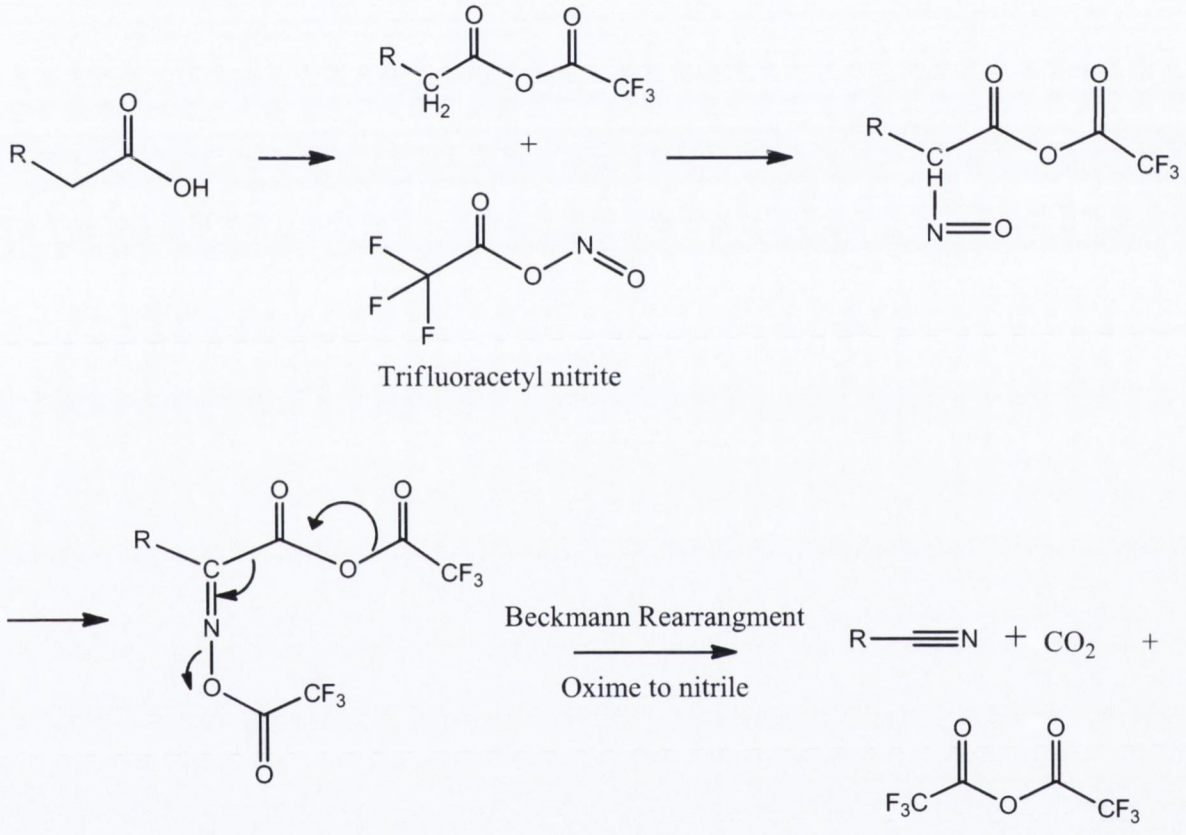

Figure 3.7 Second order Beckmann re-arrangement mechanism.

3.3.2.5 Preparation of 24-nitrile UDCA

The UDCA nitrile was prepared by formyl protection of the 3 and 7 alcohol groups with formic acid and perchloric acid (**54**). Amidation with ammonium bicarbonate produced **56** which was then dehydrated using trifluoroacetic anhydride and pyridine as a base to form the formyl nitrile. Deprotection of the formyl nitrile with sodium methoxide produced the 24-UDCA nitrile as shown in scheme 3.8.

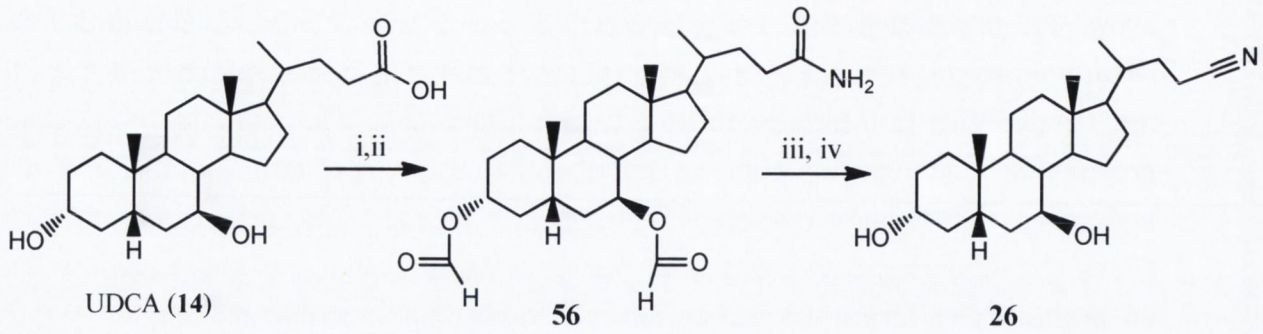

(i) Formic acid/perchloric acid, 50 °C, 3 h; (ii) NH_4CO_3, pyridine, Boc_2O, DCM, RT, 24 h; (iii) Trifluoroacetic anhydride, pyridine, dry THF, RT, 10 h; (iv) Na/MeOH, reflux, 2 h.

*Scheme 3.8. Synthesis of 24-nitrile UDCA (**26**).*

3.3.3 Determination of the relative hydrophobicity of BAs

3.3.3.1 Methods for measuring hydrophobicity

Having constructed a panel of hydrophobic and hydrophilic BA derivatives we next turned our attention to the determination of the relative polarity of these derivatives. Hydrophobicity can be defined as the association of non-polar groups or molecules in an aqueous environment which arises from the tendency of water to exclude non-polar molecules (IUPAC gold book). It is generally described by its partition coefficient (P) which refers to the distribution of compound between two immiscible phases, generally octanol and water, Equation 3.1:

$$P = \frac{[BA]_{octanol}}{[BA]_{water}} \qquad (Eq.\ 3.1)$$

However when a substance can exist in both an ionised and unionised state then the term distribution coefficient (D) is used. This is the ratio between the total concentration of both the protonated and ionised species in octanol and water phases (A. Roda, 1990).

$$D = \frac{[BA] + [A^-]_{octanol}}{[BA] + [A^-]_{water}} \qquad (Eq.\ 3.2)$$

Partition coefficients are expressed in their logarithmic form and therefore substances that display preference for the non-polar or octanol phase are considered lipophilic or hydrophobic (log $P>0$) while they are described as hydrophilic when log $P<0$.

It is generally assumed that the amount of ionised species that partitions into the octanol phase is minimal however it has been shown by Roda *et al* that a substantial amount of ionised BAs distribute into the non-polar phase (A. Roda, 1990). The BA structure accounts for this phenomenon as a strong hydrophobic steroid backbone is the principal determinant of the lipophilic character of BAs with the ionisation of the C-24 carboxy group playing a minor role (A. Roda, 1990).

The classical and most direct measurement of log P is the shake-flask experiment in which the concentration of a substance that distributes into the octanol and water phases is determined. Before the chemical substance is added to the solvent system it is necessary to equilibrate and shake the two phases together so as to achieve mutual saturation of the two phases. The quantity of substance in each phase can then be measured by a photometric method, gas chromatography or HPLC. The Nernst Partition Law applies only at constant temperature, pressure and pH for dilute solutions. It strictly applies to a pure substance dispersed between two pure solvents. If several different solutes occur in one or both phases at the same time, this may

affect the results. Hence it is essential to ensure purity of the test substance. Although the shake-flask method provides an accurate measurement of log P it is both tedious and time consuming. Pre-equilibration of phases requires at least 24 h. Incubation times of the test sample with the pre-saturated octanol and water vary but in the case of BAs up to two weeks have been used (A. Roda, 1990). Furthermore difficulties are encountered due to impurities in the test substance and the requirement of a large amount of test material.

Partition chromatographic techniques including reverse-phase HPLC (RPHPLC) and reverse-phase TLC (RPTLC) allow for rapid measurement of various indices that provide information on the lipophilic behaviour of chemicals (Cazes, 2005). Chromatographic experiments provide a lot of practical advantages over the direct determination of a physicochemical property (Natalini *et al.*, 2007). The methods are compound sparing and are less sensitive to impurities as these can be separated out during the experiments. Furthermore there is no need to determine the absolute concentration and the methods allow for automation (Natalini *et al.*, 2007).

3.3.3.2 Calculating hydrophobicity from Chromatographic Methods

In theory chromatographic methods provide similar information as traditional log P measurements (Heuman, 1989). The thermodynamic equilibrium partition coefficient K of a BA calculated from the polar mobile phase of a reversed-phase liquid chromatographic system is defined in Equation 3.3, where $[BA]_{st}$ and $[BA]_{mo}$ refer to the equilibrium concentration of BA in the stationary and mobile phases respectively (Armstrong & Carey, 1982).

$$K = \frac{[BA]_{st}}{[BA]_{mo}} \qquad \textit{(Eq. 3.3)}$$

Octadecyl-silanized (ODS) silica gel in which the silanol groups are etherified with alkyl groups containing 8 (C_8) or 18 (C_{18}) carbon atoms usually provide the non-polar stationary phase. The polar mobile phase consists of water or buffer with an organic modifier such as methanol in the case of highly retained solutes (Cazes, 2005).

The basic measure of retention in isocratic HPLC is the capacity factor, *k'*, which is defined in Equation 3.4 where t is the length of time it takes for the BA to elute and t_0 is the time required to elute a non-retained solute:

$$k' = \frac{(t_{ba}-t_0)}{t_0} \quad \text{or} \quad \log k' = \left[\log \frac{(t_{ba}-t_0)}{t_0}\right] \qquad \textit{(Eq. 3.4)}$$

The less polar a BA is the stronger its interaction with the stationary phase and hence the greater its retention time. Log *k'* values are directly related to octanol-water log P

via Colander-type equations, Equation 3.5, where the coefficients a′ and b′ are determined through regression analysis.

$\log P = a' \log k' + b'$ *(Eq. 3.5)*

However instead of isocratic capacity factors which are derived for a selected mobile phase composition, the use of a capacity factor extrapolated to pure water as mobile phase, is considered to be a more representative lipophilicity index. This is expressed as log k_w. Extrapolated capacity factors are in the same order as octanol-water log P values. Linear extrapolation gives log k_w from Equation 3.6, where φ is the fraction of organic modifier present in the mobile phase and S is the slope of the line.

$\text{Log } k' = -S'\varphi + \log k_w$ *(Eq.3.6)*

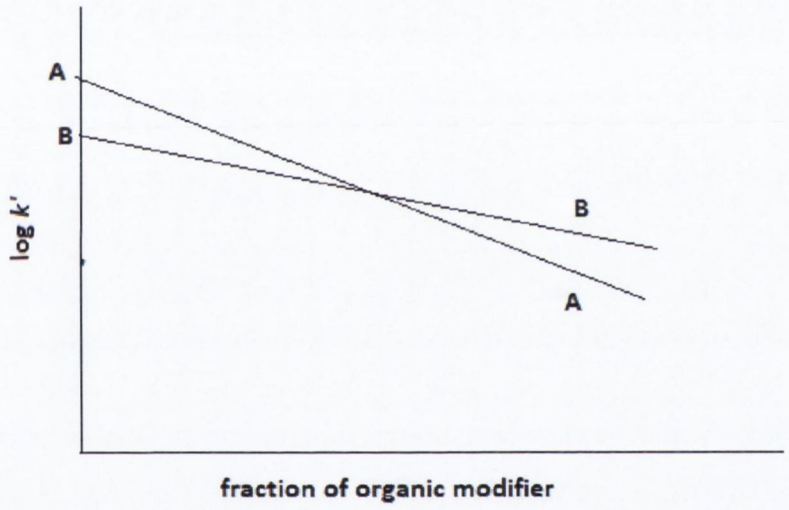

Figure 3.8 Log k′ Vs Fraction of Organic Modifier. *Inversion of lipophilicity can occur at high organic modifier concentrations.*

Figure 3.8 demonstrates that the slopes in Equation 3.6 of lines A and B may vary and so at high concentrations of organic modifier it is possible to get an inversion of lipophilicity. This is why a proper expression of lipophilicity is found only at 100% aqueous phase composition. Good correlation between chromatographic data and log P can be obtained in many cases with the coefficients, a′ and b′ being close to 1 and 0 respectively (Bechalany, 1991).

$\log P = a' \log k_w + b'$ *(Eq. 3.7)*

3.3.3.3 Results of RPHPLC

We initially decided to use RPHPLC to determine relative polarity of our panel of BAs. HPLC has widely been used for estimation of lipophilicity (Armstrong & Carey, 1982; Heuman, 1989; Roda et al., 1990) although Roda *et al* were only able to show a moderate correlation between log P and k' (r^2=0.64) (Roda et al., 1990). k_w was not assessed in this study. Good correlations between log P and k' were achieved between the highly hydrophilic or highly hydrophobic BAs such as UCA and DCA. However, they found that the correlation failed when comparing CA and UDCA and their conjugates, with the HPLC data giving longer retention times for CA, TCA and GCA despite an extra hydroxyl group. The authors suggest that the reason for this is that the partition equilibrium in HPLC is mainly driven by an apolar interaction between the β face of the BA molecule and the stationary phase. As CA has a greater amount of accessible β face than UDCA it has a longer retention time (Roda et al., 1990). More recently Natalini *et al* investigated a correlation between RPHPLC k_w values and CMC which can be considered as a measure of the hydrophobic self-aggregation of the bile salt. In this study they obtained similar r^2 values of 0.68 when correlating CMC and k_w of all BAs (Natalini *et al.*, 2007) however the correlation was found to be greater, when only the unconjugated BAs or conjugated BAs were considered, 0.94 and 0.88 respectively. We felt that the saving in experimental time and reagent justified the use of RPHPLC over shake-flask methods or similar experiment. However we encountered a series of problems during the course of our HPLC experiments. These principally arose due to the UV transparency of the majority of BAs assembled in this panel. Use of a refractive index (RI) detector solved this problem to an extent. However RI detectors are extremely sensitive to changes in ambient temperature, pressure changes and flow rate. k_w values were determined for the following 15 BAs, Table 3.2, as they provided as good range of hydrophobicity.

Table 3.2 BA k_w values obtained with RPHPLC

BA	k_w
LCA **(3)**	45.63
DCA **(4)**	21.77
CDCA **(5)**	19.09
CA **(11)**	8.55
TCDCA **(9)**	7.66
LagoDCA **(34)**	7.45
12-keto LCA **(35)**	7.12
NCA **(36)**	6.25
HCA **(42)**	6.23
UDCA **(14)**	5.30
TDCA **(17)**	4.92
3,7-diketone **(39)**	4.18
norUDCA **(24)**	2.73
GUDCA **(16)**	2.27
UCA **(41)**	2.06

The relative polarity of the BAs in this panel was in accordance with literature values. However we found very poor correlations with *in silico* descriptor parameters for hydrophobic surface area (HSA) and polar surface area (PSA) (r^2= 0.023, 0.2 and 0.43 for HSA, PSA and ratio of HSA to PSA). Although the *in silico* parameters are an expression of absolute hydrophobicity and polarity they are less sensitive to the influence of conformation on BA hydrophobicity than a chromatographic parameter. Nevertheless such a poor correlation was unexpected particularly as good correlations between log P and total HSA have been previously demonstrated (A. Roda, 1990).

3.3.3.4 Use of RPTLC for hydrophobicity determination

Taking the problems we encountered with HPLC into account we turned our attention to the use of reverse-phase TLC as an alternative to HPLC. RPTLC has been used widely for lipophilicity determination including for BAs (Posa & Kuhajda, 2010; Sarbu, Kuhajda & Kevresan, 2001; Sarbu *et al.*, 2008). It has multiple advantages including higher throughput relative to HPLC and it permits simple post-chromatographic derivitisation, which overcomes the UV transparency issue in HPLC, Figure 3.9. Furthermore it has been shown to correlate well with log P values of BAs (Sarbu *et al.*, 2001).

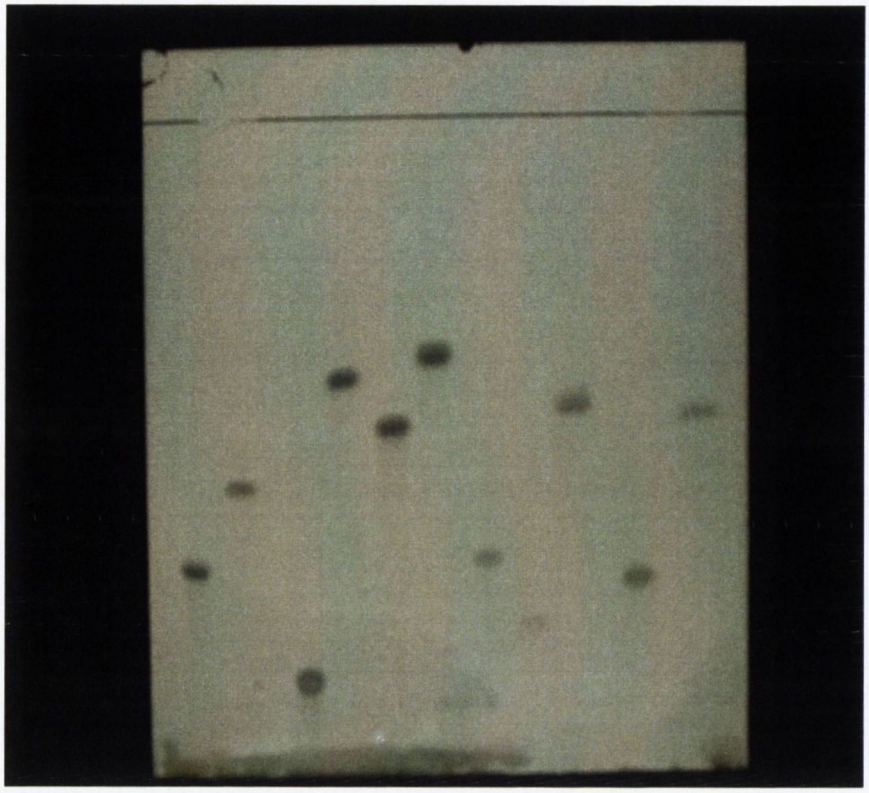

Figure 3.9 Representative example of reverse phase TLC plate of BAs. *BA test solutions were applied in DMSO. The plates were then dried at 40 °C for 1 h. Plates were developed in a closed chamber at room temperature across a development distance of 15 cm. After development, the plates were dried under ambient conditions and stained with a vanillin solution to visualize spots.*

The RPTLC approach was developed using commercially available BAs UDCA, CDCA, CA and DCA along with their glycine and taurine conjugates (**4, 5, 9-18**). The approach was optimised with respect to pH and solvent composition before application to the wider panel of compounds.

R_f is the retention factor or retardation factor. R_f is determined by dividing the distance travelled for each compound by the development distance. The less polar a solute is the stronger its interaction with the stationary phase and so the lower its R_f. R_M which is analogous to HPLC capacity factor was determined using Equation 3.8:

$$R_M = \text{Log}\ (1/R_f - 1) \qquad \textit{(Eq. 3.8)}$$

Over four concentration levels in the organic modifier concentration range (φ) 50-80% the relationship with R_M was linear for this set of 12 as shown in Figure 3.10 with r^2 >0.9 in all cases.

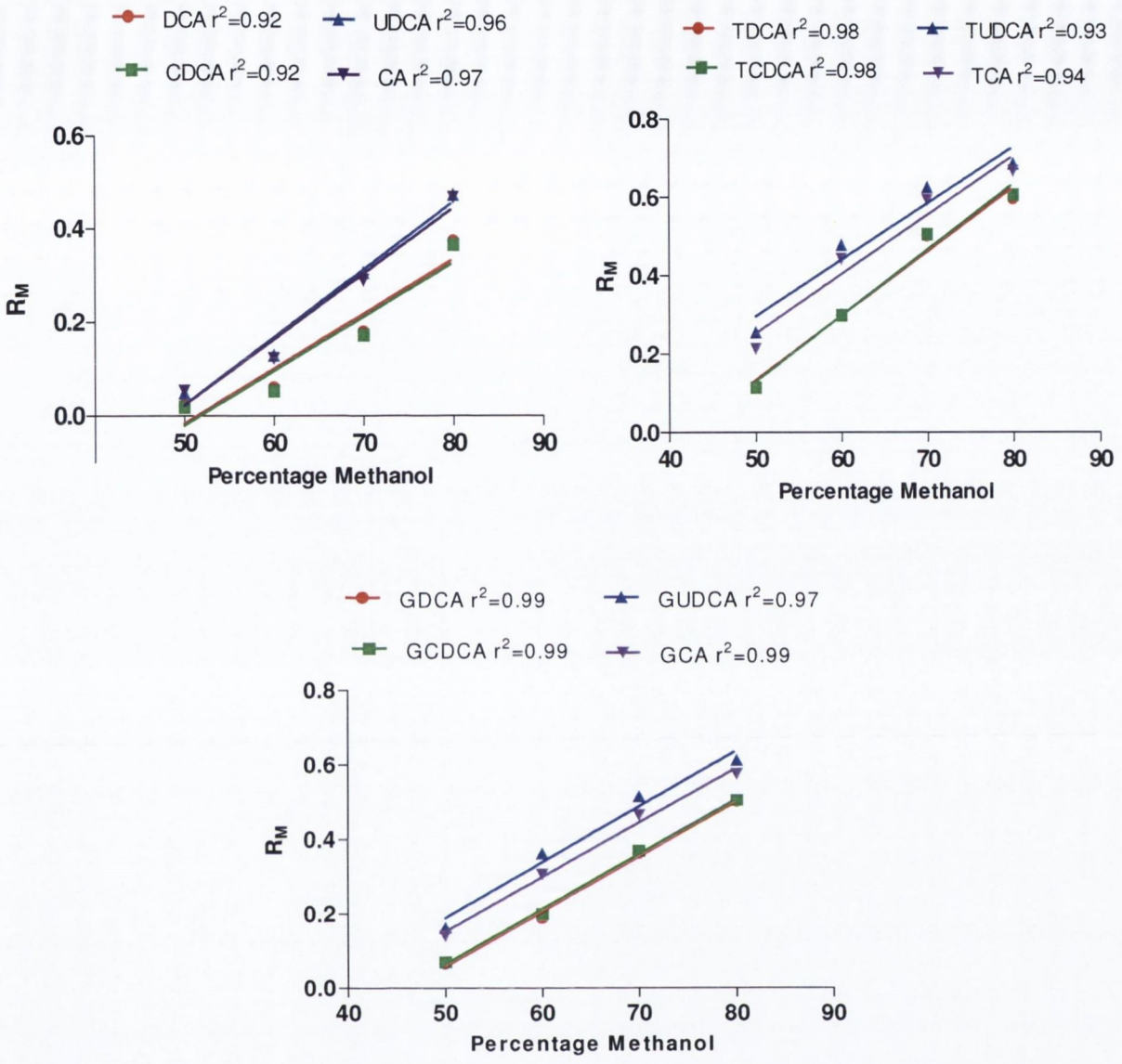

Figure 3.10 Relationship of R_M with organic modifier concentration at pH 7.4.
The relationship of R_M with percentage methanol was found to be linear at pH 7.4. Similar graphs were obtained at pH 5.4 and 8.4.

The R_{Mw}, or extrapolated retention, analogous to log k_w is the retention in 100 % aqueous phase and was estimated using Equation 3.9:

$$R_M = -S\varphi + R_{Mw} \qquad (Eq.\ 3.9)$$

Therefore the slope and intercept of the lines in Figure 3.10 was –S and R_{Mw} respectively. The slope *S* is thought to express information regarding the solute and solvent interactions. It can be thought of as a measure of the degree of responsiveness to changes in mobile phase composition. If there are no considerable differences in hydrogen-bonding capacity within a series of compounds, a good

relationship between the slope and the intercept should be found. The relationship of S with R_{Mw} was found to be linear for the development set of compounds (**4, 5, 9-18**).

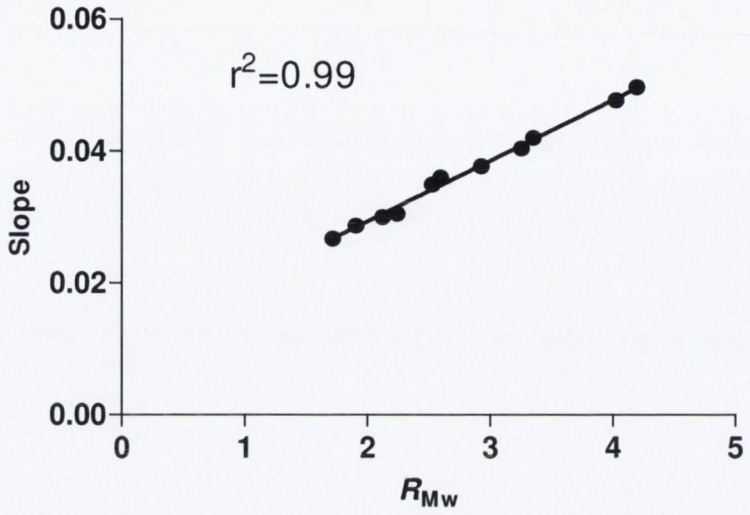

Figure 3.11 Relationship of R_{Mw} with Slope.

The relationship between retention and pH was assessed in the pH range 5.4- 8.4 for this group. For the set of 12 development compounds (**4**, **5**, **9-18**) the R_{Mw} values were estimated at pH 5.4, 7.4, 8.4, Table 3.3.

Table 3.3 R_{MW} values for the development set at pH 5.4, 7.4, 8.4.

	pH 5.4	pH 7.4	pH 8.4
DCA **(4)**	4.12	4.02	4.21
CDCA **(5)**	4.1	4.2	4.2
UDCA **(14)**	3.32	3.35	3.31
CA **(11)**	3.43	3.25	3.3
GDCA **(18)**	3.16	2.93	3.1
GCDCA **(10)**	3.08	2.93	3.1
GUDCA **(16)**	2.26	2.12	2.23
GCA **(13)**	2.4	2.24	2.43
TDCA **(17)**	2.72	2.53	2.66
TCDCA **(9)**	2.8	2.6	2.74
TUDCA **(15)**	2	1.72	1.89
TCA **(12)**	2.13	1.91	2.1

As expected in most cases the R_{Mw} values were higher at pH 5.4 than at the latter two pH values, which were similar. This is because the lower pH generates a greater percentage of unionised BA species which is relatively non-polar and has a greater interaction with the stationary phase and hence a lower R_f value. Surprisingly, we found that the R_{Mw} for the taurine conjugates also consistently followed this trend. The unconjugated BAs have a pK_a of 5.1 and the glyco conjugates have a pK_a of 4 and so the above theory applies to them. However the pK_a of the taurine conjugates is <1 and therefore this shift to lower R_f is unexpected as the BA would still be predominantly ionised.

It was decided to assess the retention for all compounds at pH 7.4 since this was the pH at which toxicity was to be determined in the cell-based assay and variations due to shifts in pK_a in methanol mixtures had been shown to be marginal. The rank order at pH 7.4 for the development set of compounds was: CDCA(**5**)~DCA(**4**)>>UDCA (**14**) >CA (**11**) >GDCA (**18**) >GCDCA (**10**) >TCDCA (**9**) >TDCA (**17**) >GCA (**13**) >GUDCA (**16**) >TCA (**12**) >TUDCA (**15**). This is roughly as expected and in accordance with numerous studies on the relative chromatographic retention of these BAs and their conjugates (A. Roda, 1990; Armstrong & Carey, 1982; Sarbu *et al.*, 2001). Retention in RP chromatographic systems is a function of the number of hydroxyl groups, their topological arrangement and extent of ionisation, bearing in mind the differences between glyco and tauro conjugates. Relative retention of the BAs is also influenced by organic modifier and stationary phase identity. The relative retention of unconjugated CA to UDCA was found to be pH dependent in our system but at pH 7.4 CA (3.25) was slightly more polar than UDCA (3.35) which accords with its greater hydrophilicity in other measures such as Log D and water solubility. On the other hand

the UDCA conjugates GUDCA (**16**) and TUDCA (**15**) were more polar than the corresponding CA conjugates as has been reported previously (A. Roda, 1990). We next investigated the relationship between R_{Mw} and *in silico* physicochemical descriptor parameters for this set. We found that there was a significant negative correlation between R_{Mw} and estimated PSA (r^2=0.82), little correlation with HSA (r^2=0.20) and a moderate positive correlation with the ratio of HSA to PSA (r^2=0.65).

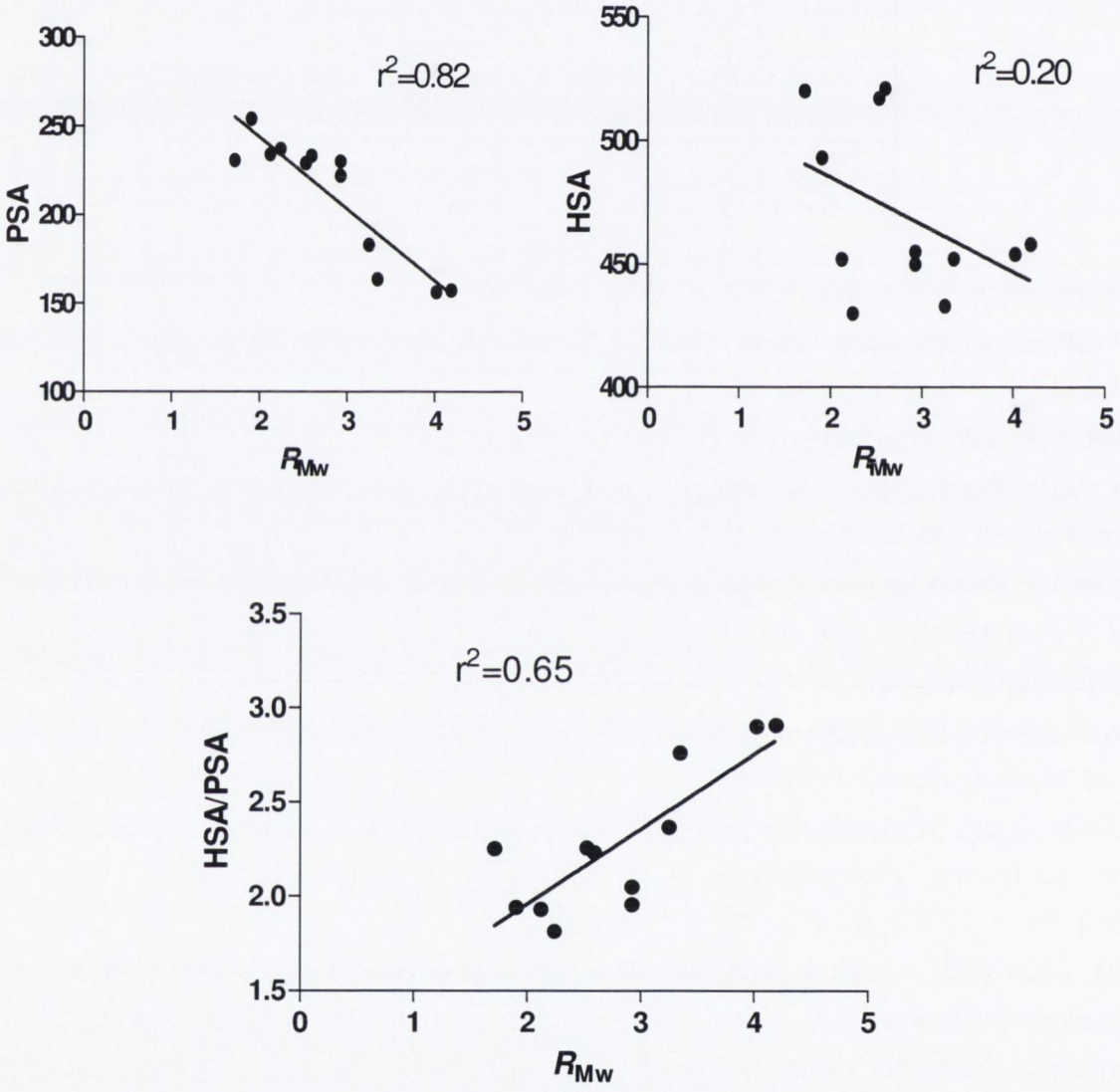

Figure 3.12 Correlation of PSA, HSA and ratio of HSA to PSA with R_{Mw}.

R_{Mw} together with HSA and PSA data for the whole set at pH 7.4 is presented in Table 3.4. It is important to bear in mind that associations with these global properties are fraught with problems of molecular size and substitution pattern. For example tauro-

and glyco-conjugates have increased HSA and PSA relative to the unconjugated compounds and hence the HSA:PSA ratio does not reflect the decreased R_{Mw}.

Linear regression of R_M Vs percentage methanol gave r^2 of >0.9 for every BA screened. The panel as a whole exhibited satisfactory dispersion and range in lipophilicity as reflected in R_{Mw} (1.717 – 5.466), Table 3.4.

Table 3.4 BA R_{Mw}, HSA, PSA and PSA/HSA, CMC arranged in order of decreasing R_{Mw}.

Compound	R_{Mw}	HSA (Å^2)	PSA (Å^2)	PSA/HSA	CMC (Roda *et al.*, 1983) (mM) (0.15 M Na^+)
37 NCA3-acetate	5.63	480	172	0.358	
40 3OH,7βN_3	5.46	440	203	0.461	
33 DCA3βN_3	5.45	452	193	0.426	
22 UDCA3βN_3	5.45	446	194	0.434	
21 UDCA3αN_3	5.41	445	205	0.460	
32 DCA3αN_3	5.40	441	196	0.444	
23 3deoxyUDCA	5.30	475	145	0.305	
29 UDCA-24N_3	5.29	476	181	0.380	2.8(0.6)
3 LCA	5.27	479	130	0.271	0.9(0.5)
28 UDCA-24OH	5.03	480	140	0.291	
26 UDCA24CN	4.93	449	162.3	0.361	
19 MeUDCA	4.77	514	146	0.284	
30 MeDCA	4.69	512	137	0.267	
20 UDCA-24NH_2	4.54	447	185	0.413	
36 NCA	4.46	452	155	0.342	25(18)
42 HCA	4.40	428	188	0.439	14(6)
5 CDCA	4.19	458	157	0.342	9(4)
4 DCA	4.02	454	156	0.343	10(3)
31 DCA-24NH_2	3.89	451	176	0.390	
34 LagoDCA	3.89	457	158	0.345	18(10)
35 12-KetoLCA	3.66	457	157	0.343	26(16)
19 BisnorUDCA	3.62	416	147	0.353	
25BisnorUDCACN	3.62	413	155	0.375	

Compound	R_{Mw}	HSA (Å^2)	PSA (Å^2)	PSA/HSA	CMC (Roda *et al.*, 1983) (mM) (0.15 M Na^+)
24 Nor UDCA	3.39	427	158	0.370	17
14 UDCA	3.35	452	164	0.362	19(7)
39 3,7-diketone	3.26	447	152	0.340	84(70)
11 CA	3.25	433	183	0.422	13(11)
41 UCA	3.01	429	186	0.433	60(39)
10 GCDCA	2.92	450	230	0.511	3(0.6)
18 GDCA	2.92	455	222	0.487	6(2)
9 TCDCA	2.59	521	233	0.447	1.8(0.5)
17 TDCA	2.52	517	229	0.442	6(2.4)
13 GCA	2.24	430	237	0.551	12(10)
16 GUDCA	2.12	452	234	0.517	12(4)
38 3,7,12-ketone	1.92	425	175	0.411	>250
12 TCA	1.90	493	254	0.515	10(6)
15 TUDCA	1.71	520	231	0.444	8(2.2)

The six azido-analogs (**21**, **22**, **29**, **31**, **32**, and **40**) were highly lipophilic as well. Indeed the azides with ionisable side chains were more highly retained than some of the non-azido neutral compounds such as the UDCA alcohol (**28**) and UDCA nitrile (**26**). 3-deoxy UDCA (**23**) showed similar retention behaviour to LCA (**3**).

On the whole the neutral compounds such as the esters and amides yielded R_{Mw} values above the median. Specifically these were the UDCA alcohol (**28**), UDCA nitrile (**26**), methyl esters (**19**, **30**) and amides (**20**, **31**) of UDCA and DCA respectively. Although the DCA amide had higher retention than the median it could not be explained why the R_{Mw} was lower than that for the UDCA neutral derivatives and even DCA (**4**) itself. Introduction of keto (oxo) groups at the 3, 7 and 12 positions has the effect of depressing hydrophobicity by promoting water access to both faces of the steroid (Posa & Kuhajda, 2010). Hence the 3, 7-diketone (**39**) was hydrophilic relative to UDCA (**14**) and particularly CDCA (**5**). In the same vein the 3,7,12 triketone (**38**) had an R_{Mw} of 1.9 compared to 3.2 for CA (**11**). 12-keto LCA (**35**) was also more hydrophilic than DCA; however there was an anomaly with NCA or 7-keto LCA (**36**) which showed a surprisingly high R_{Mw} which we could not explain. This might explain

the high hydrophobicity of 3-acetoxy NCA (**37**) (the most hydrophobic compound). This compound has a hydrophobic acetate ester and a keto group in the 7 position.

LagoDCA (**34**) showed hydrophobicity intermediate between that of UDCA (**14**) and DCA (**4**) in our system. Hence the positioning of hydroxyl groups as well as their orientation may influence the retention of a BA. Furthermore chain shortening did not have the expected effect on retention either. Reduction in the number of carbons was expected to decrease the hydrophobicity of the compounds. This is evident when comparing the bisnornitrile (**27**) and 24-nitrile (**26**) of UDCA, with the latter having higher $R_{Mw.}$ Decreasing the chain length of UDCA by one to norUDCA (**24**) did not significantly affect retention, however the bisnorUDCA (**25**) had a higher R_{Mw} to UDCA and norUDCA. In fact the retention was the same as the bisnornitrile (**27**). Interestingly this higher hydrophobicity is reflected in the ratio of HSA to PSA. This indicates that chain shortening changes the shape of the molecule such that its hydrophobic character is augmented. This is possibly because the closer proximity of the hydroxyl to the concave hydrocarbon skeleton decreases its access and interaction with the aqueous phase.

UCA (**41**), the conjugates and the triketone (**38**) were the most polar derivatives in the set.

3.3.4 BA effects on Cell Viability

3.3.4.1 Natural BAs decrease viability of HET-1A cells

Our next aim was to determine the effect of BAs on the cell viability of the normal esophageal cell line, HET-1A. As a first step, the objective was to study the effect of eight natural BAs on the viability of HET-1A cells over a 24 h period. These were UDCA (**14**), CA (**11**), DCA (**4**), CDCA (**5**), GUDCA (**16**), LCA (**3**), TDCA (**17**) and TCDCA (**9**). We decided to use a very wide concentration range (4 μM to 10 mM), which permitted a genuine comparison of BA toxicity. The MTT assay (Section 2.6.1) which is based on the activity of the mitochondrial dehydrogenase enzymes in cells was chosen for measurement of cell viability. This has been widely used for cytotoxicity studies in numerous cell lines (Ahmadian *et al.*, 2009; Fraga *et al.*, 2008; Han, Lin & Ru, 2009).

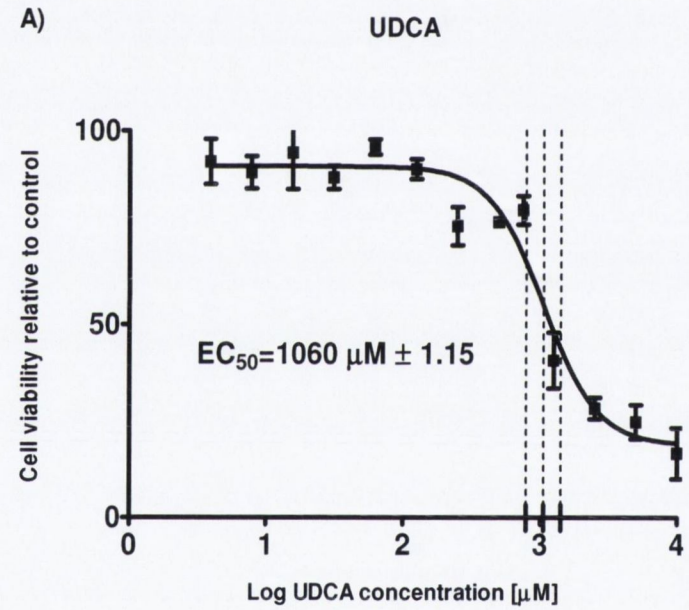

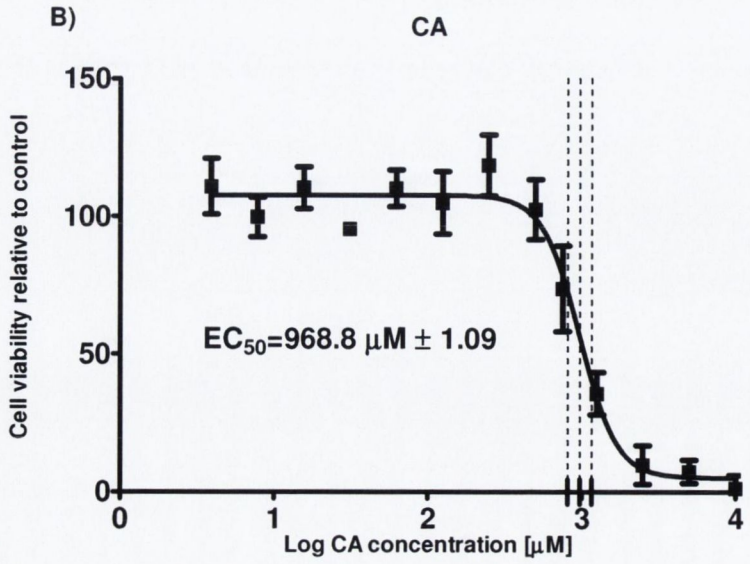

C)

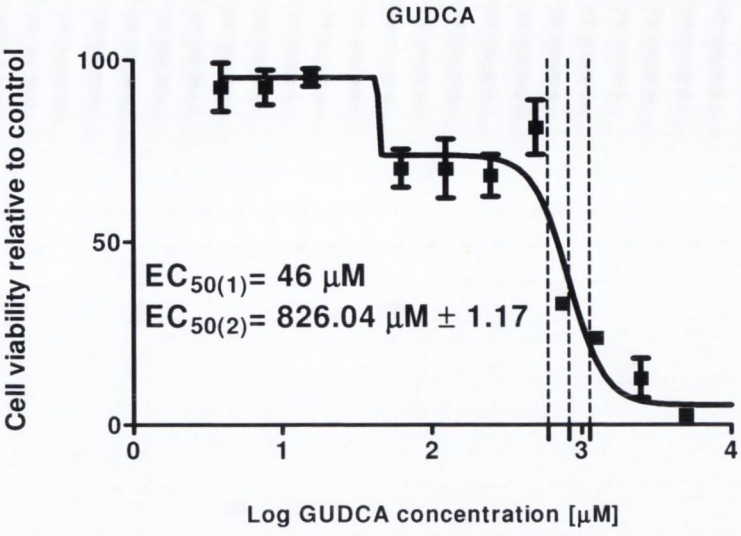
GUDCA
Cell viability relative to control
100
50
0
0
1
2
3
4
EC50(1)= 46 µM
EC50(2)= 826.04 µM ± 1.17
Log GUDCA concentration [µM]

D)

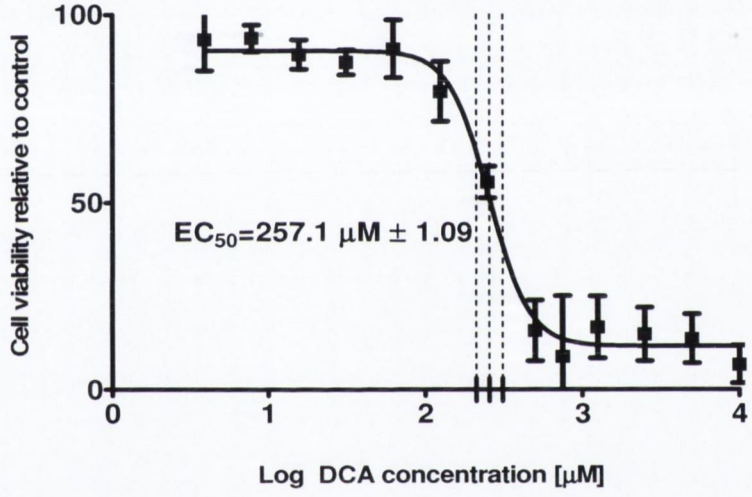
DCA
Cell viability relative to control
100
50
0
0
1
2
3
4
EC50=257.1 µM ± 1.09
Log DCA concentration [µM]

E)

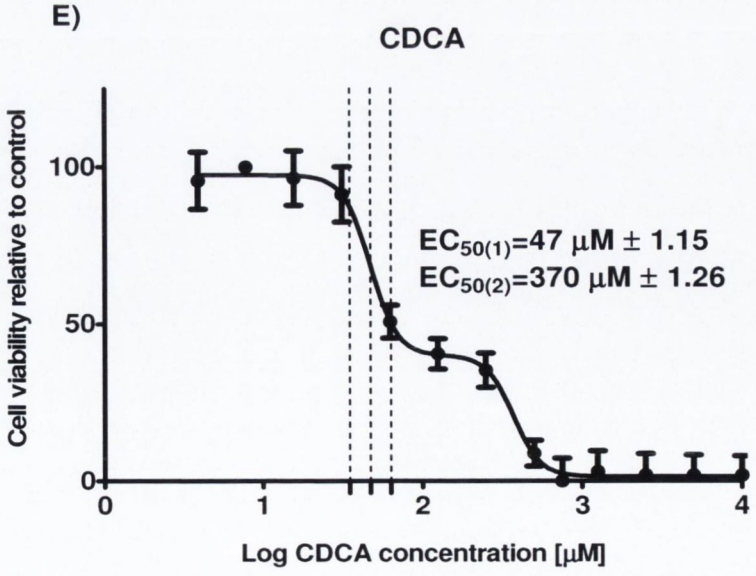
CDCA
Cell viability relative to control
100
50
0
0
1
2
3
4
EC50(1)=47 µM ± 1.15
EC50(2)=370 µM ± 1.26
Log CDCA concentration [µM]

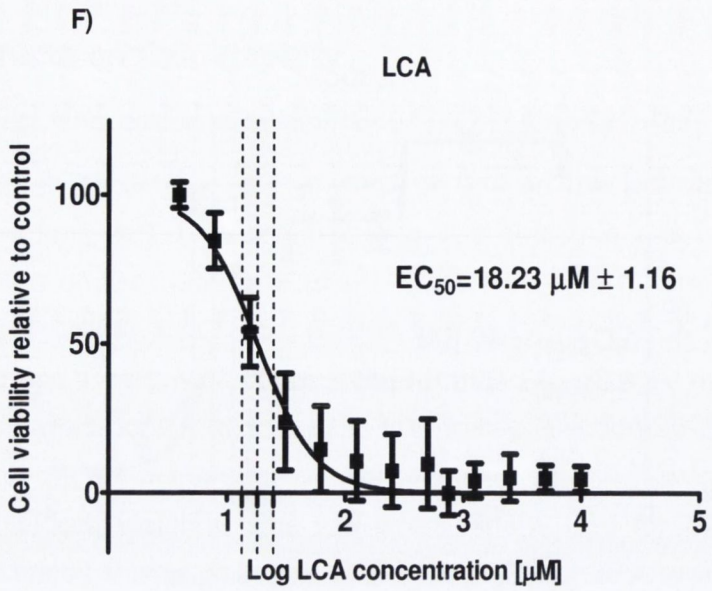

Figure 3.13 Cell viability of HET-1A cells in response to natural BAs. *HET-1A cells were treated with varying concentrations (4 µM, 8 µM, 16 µM, 32 µM, 64 µM,125 µM, 250 µM, 500 µM, 750 µM, 1.25 mM, 2.5 mM, 5 mM, 10 mM) of A) UDCA (**14**), B) CA (**11**), C) GUDCA (**16**), D) DCA (**4**), E) CDCA (**5**), or F) LCA (**3**). BAs were applied for 24 h. Cell viability was assessed in each case by the metabolism of the formazan salt, 3-(4,5 dimethylthiazol-2-yl)-2,5 diphenyltetrazolium bromide (MTT) and is expressed relative to untreated control. Values represent the mean ± SEM of three experiments performed in triplicate.*

There was a clear concentration dependent effect on cell viability for all BAs studied. The data were analysed using monophasic sigmoidal curves in the case of UDCA, CA, DCA and LCA and biphasic sigmoids for CDCA and GUDCA, Figure 3.13 A-F (r^2>0.82-0.95). EC_{50} values were determined for each of the inflection points.

In the case of LCA, DCA and CDCA there was significant decrease in viability at concentrations of 125 µM. In the other cases the onset of cell death occurred at higher concentration (>250 µM). LCA was the most potent cytotoxic BA (EC_{50} of 18.23 µM). DCA was ten fold less potent than LCA (EC_{50} of 257 µM). CDCA displayed biphasic behaviour with an initial decrease in viability to around 50% of control with an EC_{50} of 47 µM. There was a further decrease at higher concentration (370 µM) to zero viability. The curve for GUDCA showed a small sharp drop in viability at low concentration (46 µM) followed by a plateau and a later more significant decrease with an EC_{50} of 826 µM. This was preceded by an increase in viability at around 700 µM compared with control and lower concentrations. UDCA and CA were toxic at higher concentration (1060 and 968 µM respectively) with no statistically significant difference between the two BAs ($CI_{(UDCA)}$ =792-1415 µM, $CI_{(CA)}$ =807-1101 µM). CA

and GUDCA were equally toxic as there was no statistically significant difference between the EC_{50} values.

Overall in this panel, the rank order effect on cell viability was roughly as expected taking account of known tendencies towards cytotoxicity. The observed pattern however is more consistent with BA mediated alterations in cell signalling than a detergency mode, where cellular effects would be expected to follow a more abrupt course at critical concentrations. This was observed when HET-1A cells were treated with increasing concentrations of TDCA (**17**) and TCDCA (**9**).

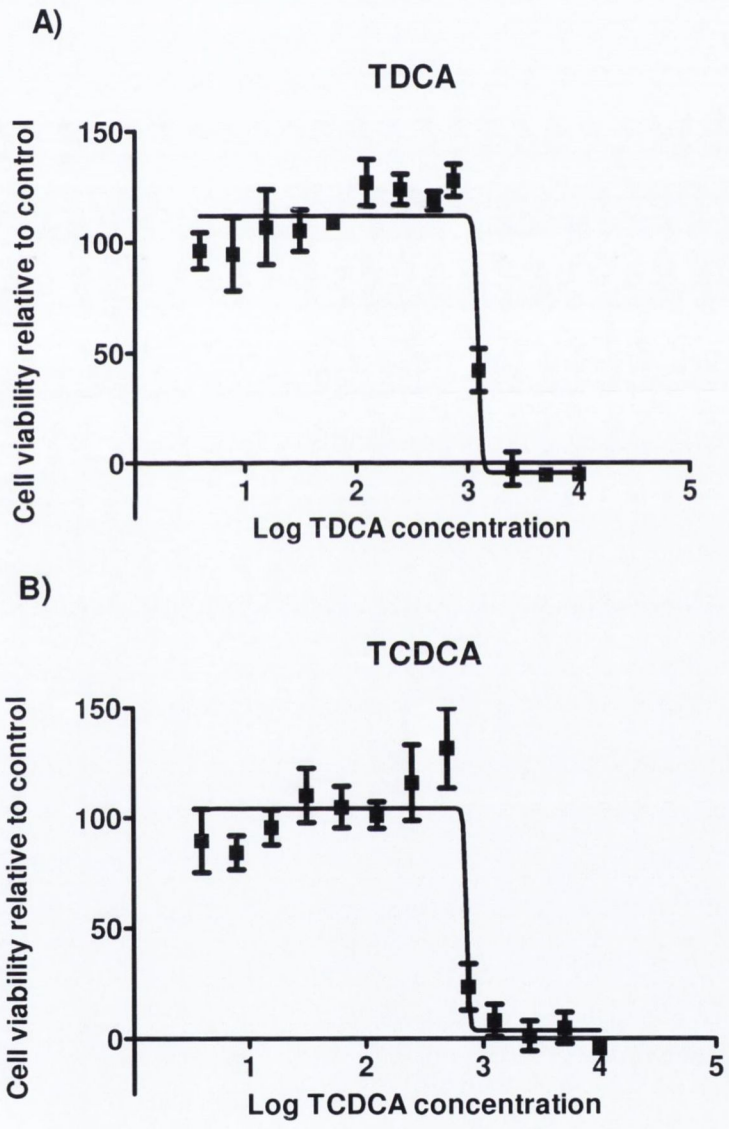

Figure 3.14 Cell viability of HET-1A cells in response to taurine conjugated BAs. *HET-1A cells were treated with varying concentrations (4 μM, 8 μM, 16 μM, 32 μM, 64 μM, 125 μM, 250 μM and 500 μM, 750 μM, 1.25 mM, 2.5 mM, 5 mM, 10 mM) of A) TCDCA and B) TDCA as described in Figure 3.13.*

There was no effect on cell proliferation at low concentrations with slight increases occurring at 125–750 μM (TDCA) and 250–500 μM (TCDCA), Figure 3.14, which is consistent with previous studies (Yamaguchi *et al.*, 2004; Zhang *et al.*, 2005). However unlike the other BAs tested which could be fitted to sigmoids, there was an all or nothing effect with a markedly sharp decline occurring in cell viability at higher concentration (~1 mM). The taurine conjugated BAs are fully ionized at pH 7.4 and are unable to cross the cell membrane in the absence of BA transporters. As there are no known transporters in the HET-1A cell line the conjugates accumulate extracellularly until a critical concentration is reached which results in cell lysis as described by Hofmann (Hofmann, 1999). In hepatocytes (Chieco *et al.*, 1997) and biliary epithelial cells (Lamireau *et al.*, 2003) which would be expected to have BA transporters the taurine conjugates have been reported to induce apoptosis. This difference in behaviour of the taurine conjugates in different cell lines is indicative that at relatively low concentrations BAs require interaction with an intracellular protein to induce cell death. The increased proliferation observed at low concentrations may be due to interaction with a cell surface receptor such as the epidermal growth factor receptor and is consistent with previous studies (Avissar NE, 2009; Raufman et al., 2008).

Another interesting observation was that the key BAs CDCA and DCA were only 3-4 fold more toxic than UDCA in this cell line, indicating that these differ more in potency than in qualitative effect. UDCA's effects could be fitted to a sigmoidal toxicity curve possibly indicative of weaker agonism of apoptotic pathways. This is consistent with studies conducted by Rolo *et al* investigating the effect of UDCA on liver mitochondria. The investigators found that at high concentrations (> 300 μM) UDCA decreased mitochondrial membrane potential and that it augmented LCA, DCA and CDCA induced MPT. This was determined by estimating mitochondrial swelling using light scattering techniques (Rolo *et al.*, 2000).

3.3.4.2 Mechanism of cell death induced by BAs: apoptosis vs. necrosis?

The concentration effect curves for the natural BAs indicated that all BAs can induce cell death but the mechanism of cell death is concentration dependent. Higher concentrations of BAs induce cell death through a detergency phenomenon which is particularly evident in the case of the taurine conjugates of DCA and CDCA where we see a sharp decrease in cell viability at ~ 1 mM. Cell death at this concentration would

be expected to depend on the individual CMC of the BAs and hence correlate with hydrophobicity (Hofmann, 1999). On the other hand cell death at lower concentrations predicted to include activation of the extrinsic and intrinsic apoptotic pathways would be expected to occur at lower concentrations. Although these effects may be mediated via the membrane they would not be expected to compromise barrier function through cell lysis. When screening our panel of 37 BAs for toxicity it was critical that we choose a concentration that induced apoptosis but did not affect membrane integrity. Akare *et al* have shown that BAs can induce PKCα activation without perturbing membrane function in experiments involving exclusion of the dye trypan blue in the HCT-116 cell line (Akare & Martinez, 2005). Hence we decided to conduct a series of similar experiments to determine a concentration at which BAs could induce apoptosis without affecting membrane integrity. In order to do this we investigated the effect of the tumour promoting BA, DCA, at low and high concentrations on HET-1A cells in assays measuring apoptosis and necrosis. Firstly we investigated the ability of DCA to induce caspase activation. We analysed activation of caspase 3/7 by DCA at 500 μM and 2 mM because DCA 2 mM induced complete cell death in the MTT assay. DCA 500 μM induced activation of caspase 3/7 in a time dependent manner, Figure 3.15, peaking at 1 h and then decreasing slightly at 6 h and 24 h. However when cells were treated with DCA 2 mM there was no evidence of caspase 3/7 activation at any of the time points indicating that at this concentration cell death is due to an immediate cell lysis and necrosis. Indeed there was decreased levels of caspase relative to control possibly because necrosis can lead to destruction of cellular enzymes (Sokol *et al*., 2005).

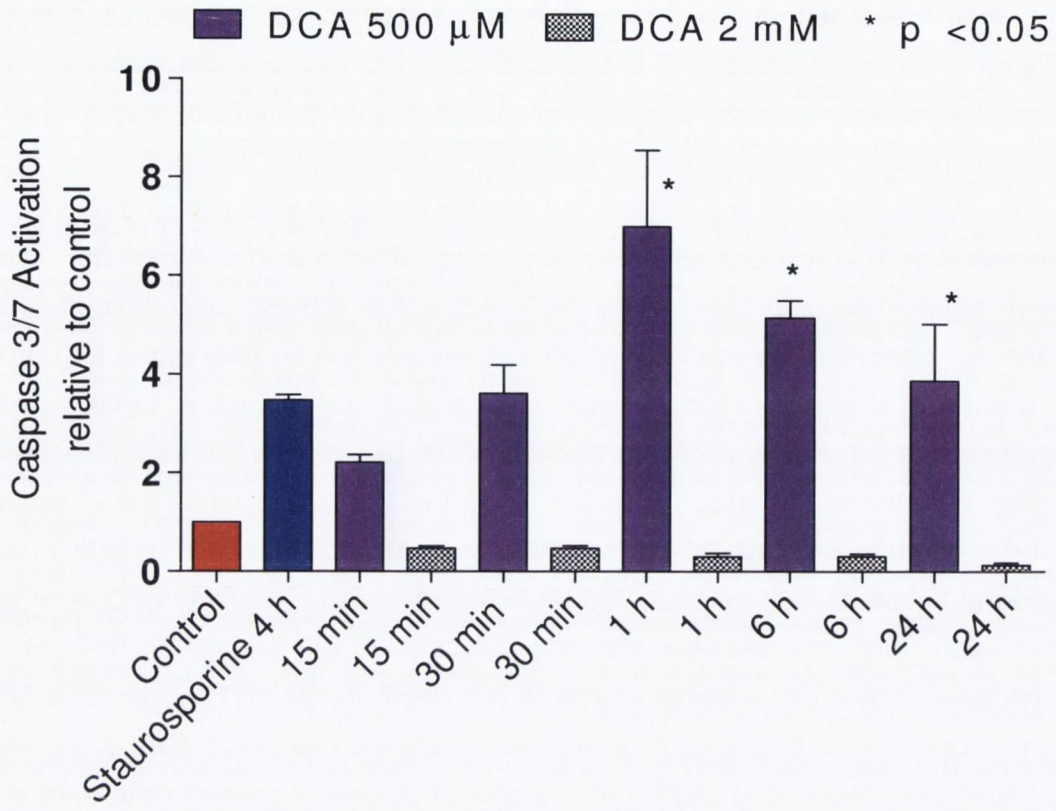

Figure 3.15 Caspase 3/7 activation by DCA in the HET-1A cell line. *HET-1A cells were treated with staurosporine or DCA 500 µM or DCA 2 mM for 15 min, 30 min, 1 h, 6 h or 24 h. After the appropriate treatment time 100 µL of caspase-Glo 3/7 reagent (Promega Corporation, Madison, USA) was added to each well and the luminescence was determined. The values are reported as fold increases over the untreated control cells. The values are reported as the mean ± SEM of three experiments performed in duplicate, * p< 0.05, as determined by a one-way ANOVA with Tukey post-hoc correction.*

Our next aim was to determine the effect of the same concentrations of DCA on the integrity of the membrane. We firstly looked at the cellular uptake of PI. PI is membrane impermeant and excluded from viable cells. PI can penetrate cells and enter the nucleus when the membrane is permeabilised. When cells were treated with the detergent Triton X-100 for 1 h extensive PI penetration was observed, Figure 3.16C, 3.16D. However when cells were treated with increasing concentrations of DCA (500 µM-1.25 mM) for 1 h there was no significant increase in the percentage of PI permeable cells relative to untreated control cells as determined by the GE Investigator software package, Figure 3.16A. Cells treated with DCA 2 mM could not be imaged at 1 h indicating complete loss of integrity. Longer exposure times to DCA 500 µM increased the percentage of PI permeable cells to a significant extent, Figure

3.16B. PI is conventionally used as a late marker of apoptosis or secondary necrosis (Rieger *et al.*, 2010; Span *et al.*, 2002). Intact membranes exclude PI, and thus live and early apoptotic cells are not stained (Vermes, Haanen & Reutelingsperger, 2000). However, when cells undergo apoptosis changes occur in the plasma and nuclear membrane secondary to activation of apoptotic cascades which results in disruption of nuclear and membrane integrity. Therefore, in late apoptotic and necrotic cells, PI can enter the cell and pass through the disrupted nuclear membrane and intercalate with DNA. Hence, the gradual increase in PI permeability at 6 h and 24 h on exposure to DCA 500 μM is also due to a loss in membrane integrity but is distinguishable from the earlier effects at 2 mM as it occurs secondary to activation of apoptotic cascades as opposed to an immediate cell lysis.

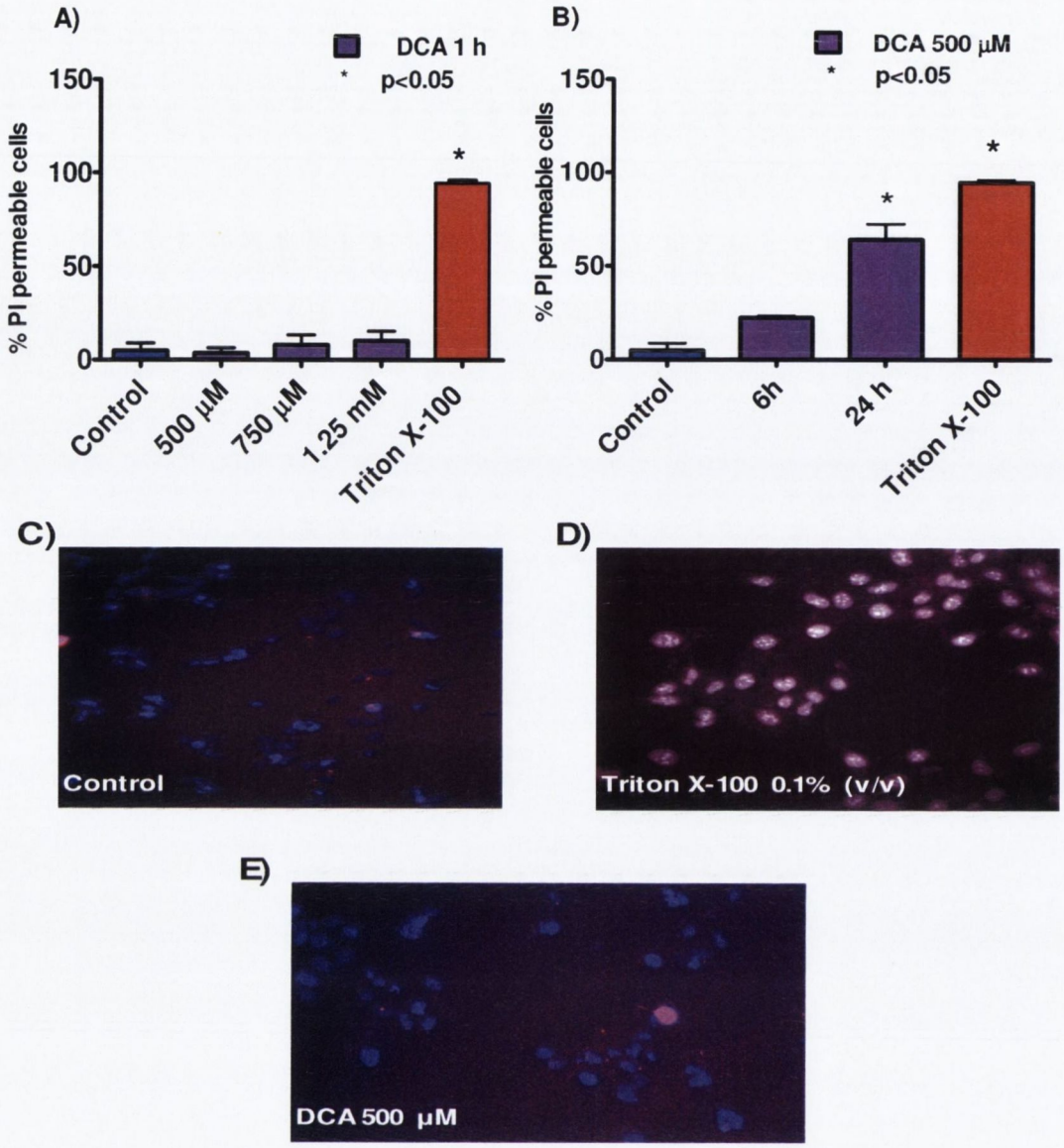

Figure 3.16 Propidium iodide staining of HET-1A cells treated with DCA. *HET-1A cells were treated with A) DCA 500 µM, 750 µM, 1.25 mM or Triton X-100 0.1%(v/v) for 1 h or B) DCA 500 µM for 6 h or 24 h. After the appropriate treatment time PI 1 µg/ml was added to each well. Live cells were visualized on the GE IN Cell Analyser 1000. PI uptake was measured using the Investigator software package (GE Healthcare, Piscataway, NJ, USA). The values are expressed as mean ± SEM of three experiments performed in duplicate, * p< 0.05 as determined by a one-way ANOVA with Tukey post-hoc correction. C) PI stained control untreated cells visualised on the IN Cell 1000. D) PI stained Triton X-100 0.1% (v/v) treated (1 h) cells visualised on the IN Cell 1000. E) PI stained DCA 500 µM (1 h) treated cells visualised on the IN Cell 1000, original magnification, x10.*

Our observations on the effect of PI on cell membrane permeability were confirmed with a similar experiment using Cell Tracker green, CMFDA. Cell Tracker reagents are chloromethyl derivatives that freely diffuse through the membranes of live cells. Once inside the cell, they react with intracellular components to produce cell impermeant dye-thioether adducts that are both fluorescent and viable for at least 24 h after loading. When cells were treated with DCA 500 μM or DCA 750 μM for 1 h there was no change in the fluorescence intensity of cell tracker within the cells, as measured using the Investigator software package, Figure 3.17A. DCA 1.25 mM however caused a significant decrease in cell intensity of cell tracker green relative to control. When fluorescence was determined in the supernatants of these cells there was no significant difference in DCA 500 μM, 750 μM and DCA 1.25 mM relative to control indicating no leakage of Cell Tracker into the medium as a result of cell permeabilisation. However DCA 2 mM caused a dramatic increase in fluorescence in a manner similar to Triton X-100, Figure 3.17B. Hence at this concentration, DCA can permeabilise the cell membrane in a detergent like manner but at 500 μM membrane integrity is not compromised at this time point.

A)

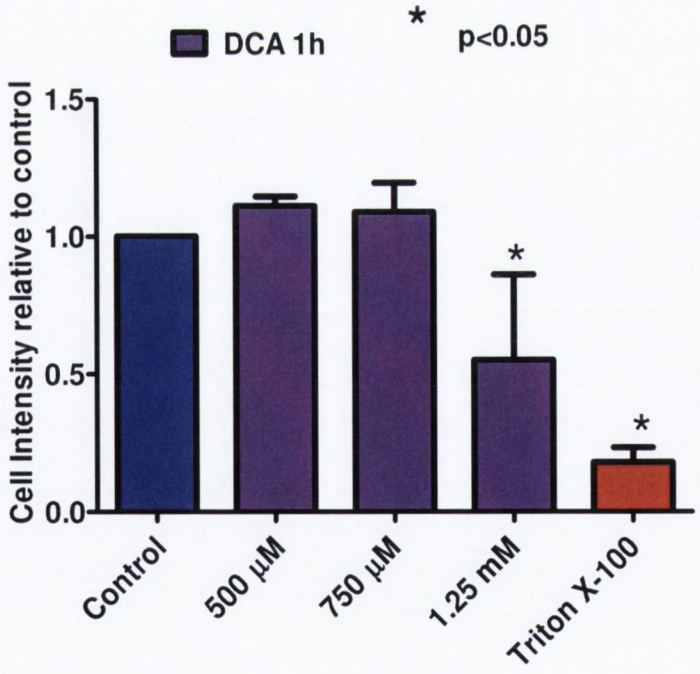

B)

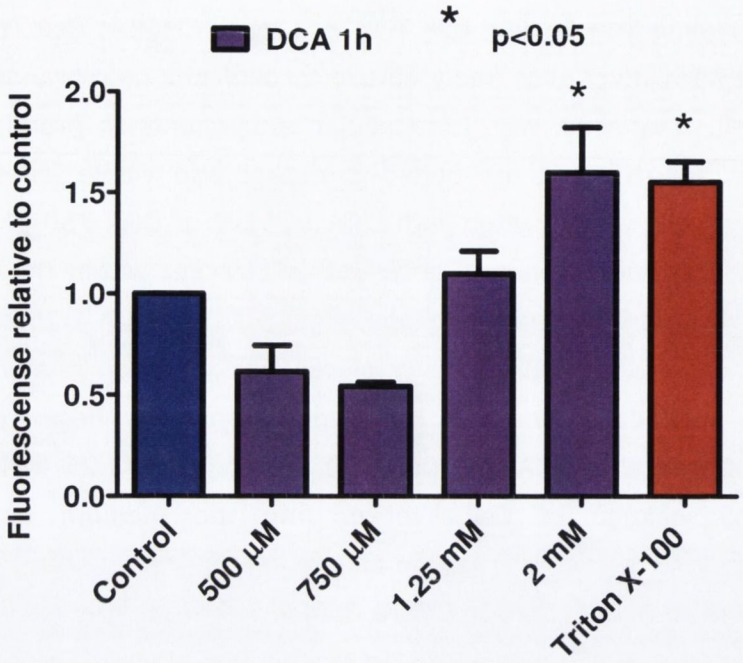

Figure 3.17 Leakage of cell tracker green, CMFDA from HET-1A cells after DCA treatment. *Cells pre-treated with Cell Tracker Green CMFDA (Molecular Probes, Invitrogen Life Sciences) were exposed to DCA 500 µM, 750 µM, 1.25 mM or Triton X-100 0.1% (v/v) for 1 h. A) Cells were visualized on the GE IN Cell 1000 and analysed as in Section 2.8.2.1. Values are expressed normalized to untreated control cells and are the mean ± SEM of three experiments, *p<0.05 as determined by a one-way ANOVA with Tukey post-hoc correction. B) Fluorescence intensity in the supernatants was measured using a fluorometer, Section 2.8.2.1. Values are expressed normalized to untreated control cells and are the mean ± SEM of three experiments, *p<0.05.*

3.3.4.3 BA toxicity screen

Having determined the hydrophobicity of our panel of compounds we then decided to examine the effects of this panel of BAs on the cell viability of the HET-1A cell line in order to investigate a correlation between cytotoxicity and hydrophobicity.

Having shown that BA induced cell death at 500 µM is mediated through an apoptotic signalling pathway whereas higher concentrations of BAs can lead to cell death through a detergency phenomenon; we decided to screen our panel of BAs at an initial concentration of 500 µM. Moreover, BAs can achieve this concentration *in vivo* and during UDCA treatment (Hess *et al.*, 2004; Stadler *et al.*, 1988) and the concentration effect curves we conducted with the natural BAs demonstrated that this concentration allowed for relative toxicity assessment of compounds that are moderately cytotoxic.

Cell viability in the esophageal HET-1A line was determined at an initial BA test concentration of 500 µM for all compounds in the set over 24 h. Where we observed a

significant effect on cell viability at 500 μM, the experiment was repeated at successively lower concentration in order to estimate an EC_{50} value. Concentration response curves were not calculated in cases where there was poor convergence using a monophasic sigmoid function. The 500 μM cell viability values were found to be most useful therefore for comparisons and they were consistent with EC_{50} values in the cases where these were estimated. Table 3.5 shows the effect on cell viability at 500 μM along with EC_{50} values where estimated.

Table 3.5 BAs physicochemical properties (R_{Mw}, HSA, polar surface area (PSA) and CMC). *The effect on cell viability relative to control in the HET-1A cell line after 24 h incubation is shown (n=3) along with an estimated EC_{50} value. Compounds were introduced in DMSO and cell viability was normalised to control DMSO at the same concentration.*

Compound Number and trivial name	R_{Mw}	Cell viability at 24 h 500 (μM)	EC_{50} (μM) (95% CI)
30 MeDCA	4.697	0.281	46 (30-69)
40 3OH,7βN_3	5.466	0.290	99 (65-147)
22 UDCA3βN_3	5.452	0.303	37 (30-44)
32 DCA3αN_3	5.402	0.307	71 (59-84)
33 DCA3βN_3	5.454	0.354	97 (72-129)
21 UDCA3αN_3	5.412	0.368	45 (28-70)
31 DCA-24NH_2	3.895	0.386	39 (32-49)
20 UDCA-24NH_2	4.54	0.397	161 (115-225)
23 3deoxyUDCA	5.304	0.399	30 (22-40)
4 DCA	4.023	0.412	257 (199-332)
3 LCA	5.27	0.417	25 (17-36)
5 CDCA	4.193	0.422	216 (134-346)
37 NCA3-acetate	5.638	0.472	366 (260-516)
34 LagoDCA	3.89	0.590	389 (251-601)
29 UDCA-24N_3	5.299	0.759	688 (206-1000)
36 NCA	4.468	0.769	nd
14 UDCA	3.35	0.788	1313 (997-1727)
25 BisnorUDCA	3.623	0.805	799
27 BisNorUDCACN	3.623	0.805	nd
41 UCA	3.011	0.808	nd
35 12-KetoLCA	3.66	0.818	nd
42 HCA	4.407	0.882	nd

Compound Number and trivial name	R_{Mw}	Cell viability at 24 h 500 (μM)	EC_{50} (μM) (95% CI)
24 Nor UDCA	3.395	0.888	Nd
39 3,7-diketone	3.266	0.935	Nd
26 UDCA24CN	4.938	0.940	Nd
19 MeUDCA	4.776	0.943	Nd
28 UDCA-24OH	5.032	0.975	Nd
11 CA	3.25	1.016	1075 (910-1270)
12 TCA	1.908	1.052	Nd
16 GUDCA	2.124	1.073	1002 (753-1333)
15 TUDCA	1.717	1.092	Nd
38 3,7,12-ketone	1.925	1.109	Nd
17 TDCA	2.529	1.113	1237
10 GCDCA	2.926	1.116	Nd
13 GCA	2.243	1.121	Nd
9 TCDCA	2.597	1.300	729
18 GDCA	2.926	1.148	Nd

Figure 3.18 shows MTT cell viability data for all compounds at 500 μM grouped as shown.

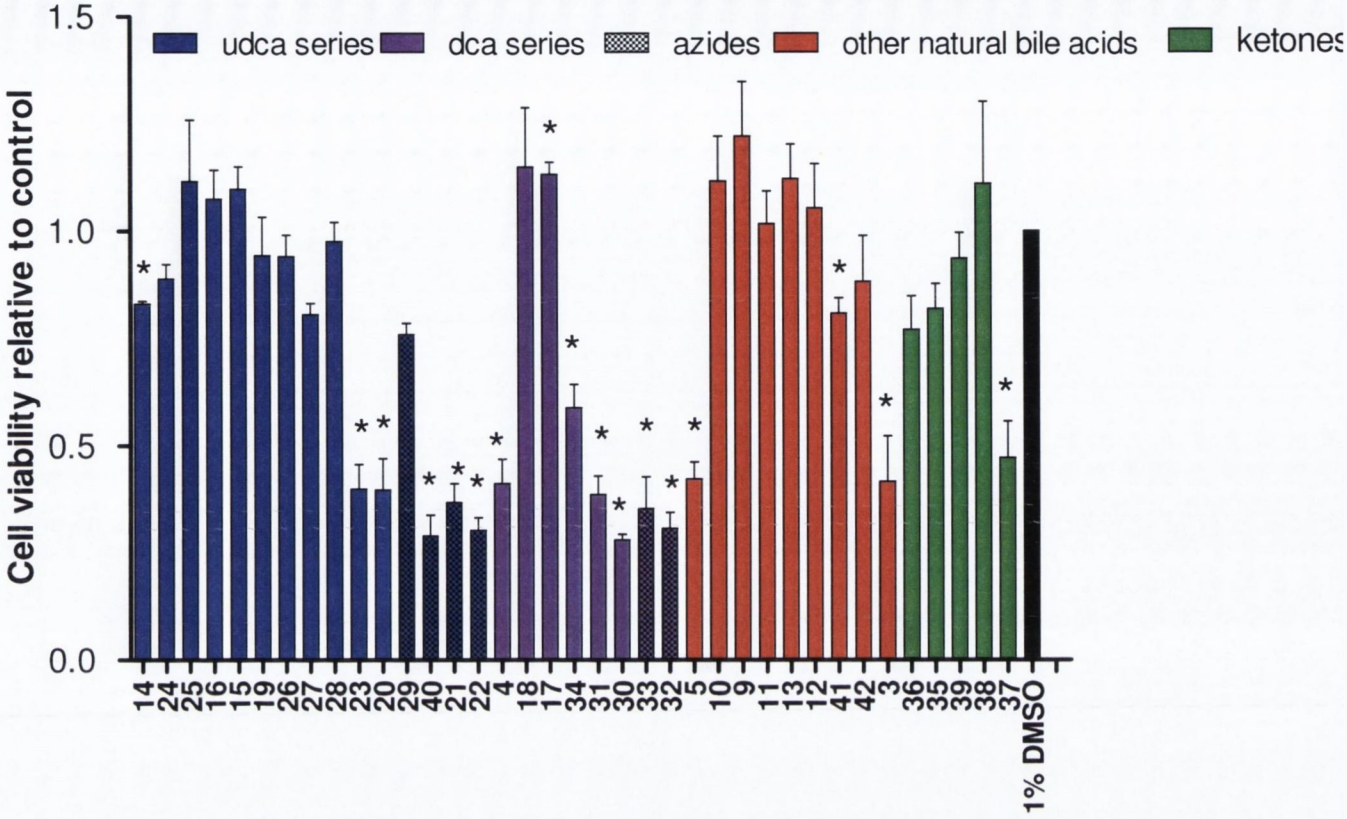

Figure 3.18 Cell viability of HET-1A cells in response to natural and synthetic BA derivatives classified as shown. *HET-1A cells were treated with various BAs for 24 h (500 μM) or PMA 1 μg/ml for 24 h. Cell viability was assessed in each case by the metabolism of the formazan salt, 3-(4, 5 dimethylthiazol-2-yl)-2,5 diphenyltetrazolium bromide (MTT) and is expressed relative to untreated control. Values represent the mean ± SEM of three experiments performed in triplicate, * $p<0.05$ as determined by a one sample t-test.*

These experiments allowed us to make a number of general structure-cytotoxicity observations. The glycine and taurine conjugates of CA, CDCA, DCA and UDCA were not cytotoxic at 500 μM. The lack of a BA transporter in the HET-1A cell line and the subsequent impermeability to ionised BA species most likely accounts for this. The conjugates did show a trend towards increased cell proliferation but this only achieved statistical significance in the case of TDCA. Three of these compounds did trigger cell death but only when the concentration was raised above ~1 mM. The EC_{50} of the conjugates and least toxic unconjugated BAs caused cell death at a similar concentration suggesting that at these high concentrations the mechanism of cell death was not structure specific for these compounds.

All of the ionisable azido compounds (**21**, **22**, **32**, **33**, **and 40**) were potently cytotoxic. The UDCA and DCA 3-azido analogues were significantly more toxic than the parent compounds. The 3α and 3β UDCA azides (**21**, **22**) were more potent than the DCA azides (**32**, **33**) with EC_{50} values of 45 μM and 37 μM respectively. The 7β–azido compound (**40**) was also cytotoxic (EC_{50} 99 μM) however the 24-azido UDCA derivative (**29**) was not toxic at 500 μM despite its high lipophilicity.

Indeed most of the neutral side chain UDCA analogues were not cytotoxic despite being highly hydrophobic. These included the UDCA alcohol (**28**), the UDCA nitrile (**26**) and bisnornitrile (**27**) and UDCA methyl ester (**19**).

The only exception to this rule was the UDCA amide (**20**) which was cytotoxic. Indeed both DCA and UDCA primary amides were markedly toxic (EC_{50} 39, 161 μM respectively) (**31**, **20**). In contrast, the DCA methyl ester (**30**) was more toxic than DCA itself (EC_{50} 46 μM) but the UDCA ester (**19**) was not more toxic than UDCA. The methyl ester was not acting as a prodrug for DCA in this context because it could be recovered unchanged from the medium at 24 h. The UDCA and DCA amide as well as the methyl esters were recovered unchanged from the medium.

The 3-deoxy UDCA compound (**23**) which had similar retention behaviour as LCA (an isomer of LCA) was highly toxic. Hence a 7β-OH is not a pre-requisite for a lack of toxicity. The nor and BisnorUDCA derivatives were not toxic (**24**, **25**).

Oxidation of the steroid secondary alcohols to a ketone was associated with a reduction in cytotoxicity. NCA (**36**) was less toxic than CDCA (**5**) and 12-keto LCA (**35**) was less toxic than DCA (**4**) for example. Esterification of NCA at the 3 position increased cytotoxicity to a significant extent (**37**). In fact while this was the most hydrophobic compound in the panel, it did not display the greatest toxicity having an EC_{50} of 366 μM, in the same range as LagoDCA (**34**).

3.3.5 Relationship between BA hydrophobicity and cell viability

A relationship between the hydrophobicity and toxicity of BAs has been speculated to exist for some time based mainly on the contrasting behaviour of LCA, DCA and CDCA and more polar di- and tri-hydroxy BAs such as UDCA and CA. In our study overall, the most polar compounds were in general the least cytotoxic with notable exceptions as outlined above. There was a significant linear relationship between R_{Mw} and cell viability at 24 h (r^2=0.6) in the total set of 37 compounds.

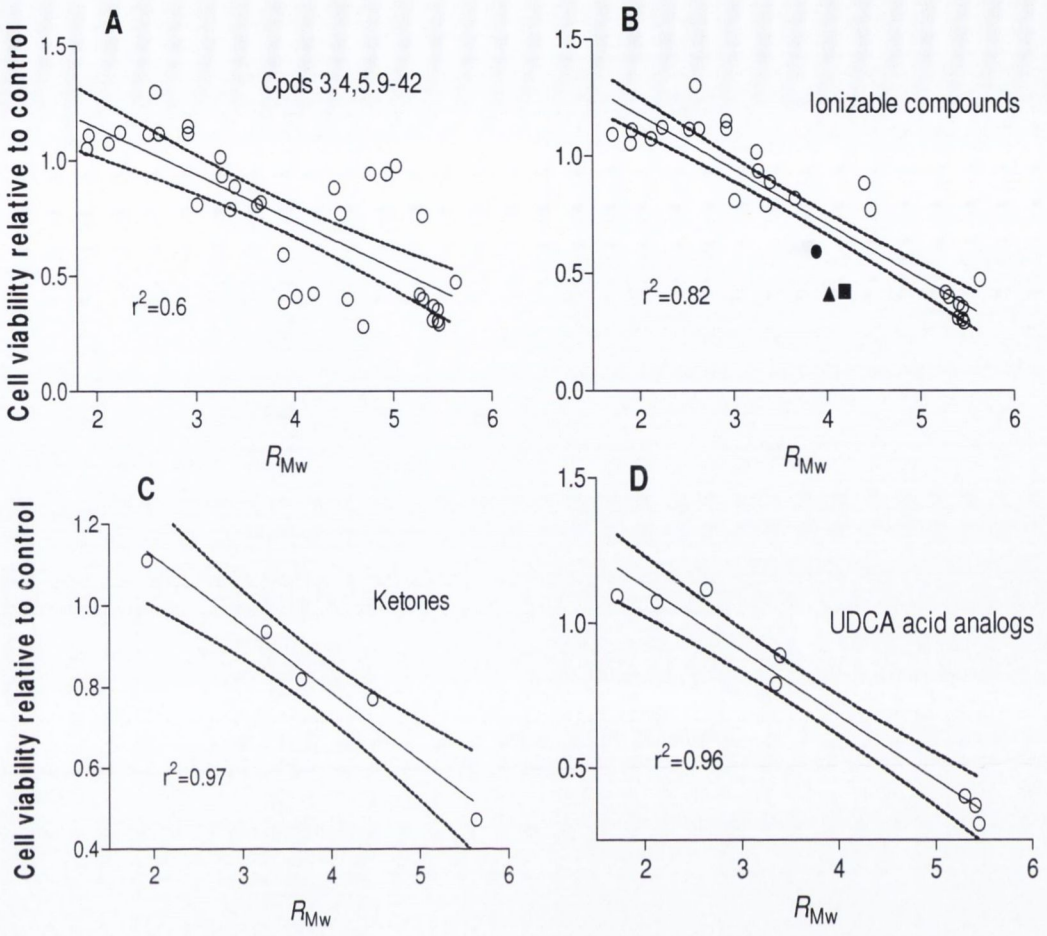

Figure 3.19 Linear regression lines showing 95% confidence bands for cell viability at 24 h in the HET-1A cell line and R_{Mw}. *The panels show,* ***A****: Linear regression for compounds* ***3, 4, 5, 9-42****;* ***B****: Linear regression for the ionisable (acidic) compounds* ***3, 4, 5, 9-18, 21-25, 32-42****; CDCA (■) DCA (▲) and LagoDCA(•) are highlighted;* ***C****: Linear regression for the ketones* ***35-39****;* ***D****: Linear regression for the UDCA analogues with an acidic side chain.*

A similar correlation level was achieved using the sparser EC_{50} values. The strength of the association was significantly increased when the neutral compounds were excluded (Figure 3.19B: r^2=0.82, n=29). This might be explained by differences in ionization between the neutral and acid compounds that overwhelm more subtle retention interactions. However, in the group of neutral compounds (n=8) there was a very weak association between R_{Mw} and cell viability (r^2=0.11). It is notable that in Figure 3.19B DCA, CDCA and LagoDCA are out of trend being significantly more toxic than predicted on the basis of R_{Mw}.

Excellent correlations were obtained for the ionisable UDCA group (r^2=0.96, n=8) and the ketone panel (r^2= 0.97, n=5) (Figure 3.19C and 3.19D); focussing in this way on

relatively homologous groups minimises confounding structural factors. There were no significant correlations between the *in silico* bulk hydrophobicity/polarity indices and effects on cell viability, consistent with the idea that relative BA hydrophobicity is a shape dependent property that is better predicted chromatographically.

3.4 Discussion

Experimental evidence identifies BAs as activators of various signalling pathways. However the exact interactions involved in initiating these signals remain unknown (Katona *et al.*, 2009). Many of the genomic actions of BAs can be accounted for by activation of FXR, a nuclear receptor for BAs (Makishima *et al.*, 1999; Parks *et al.*, 1999). More recently BAs have been found to act as agonists for the G protein-coupled receptor, TGR5 (Sato et al., 2008) which accounts for some of their non-genomic effects.

A specific binding target responsible for BA induced cell death remains elusive. BAs have also been shown to initiate signalling through membrane perturbations (Akare & Martinez, 2005; Jean-Louis *et al.*, 2006) indicating that some of their biological actions may not be due to specific protein interactions but rather are mediated by their physicochemical properties. This has lead to a general acceptance amongst researchers, that BA hydrophobicity is a determinant of cytotoxicity, exemplified by the toxicity associated with the hydrophobic LCA, CDCA and DCA and non-toxic effects of the relatively hydrophilic UDCA. Recent studies, particularly by Katona *et al*, using enantiomeric BAs have indicated that there are structural requirements for toxicity and hydrophobicity alone is not the sole determinant (Katona *et al.*, 2009).

BA hydrophobicity has not been correlated with cytotoxicity in the literature to date. Furthermore there is a dearth of information regarding BA toxicity SAR. Hence we decided to investigate the relationship between BA physicochemical characteristics and cell viability in an esophageal model, focusing on hydrophobicity.

In this work we aimed to assemble a panel of BA derivatives with a spectrum of physicochemical characteristics. The relative polarity of these compounds was initially evaluated using RPHPLC however we found that RPTLC retention extrapolated to zero organic modifier was a less ambiguous and more consistent measure of hydrophobicity. The effect of these compounds on cell viability of the HET-1A cell line was then determined using the MTT assay. We found that polarity as determined at pH7.4 was predictive of BA toxicity in our panel. Hence we are the first group to determine a direct correlation between BA hydrophobicity and toxicity. This correlation could prove to be a useful high throughput tool for cytotoxic BA discovery and development.

At present it is difficult to say whether the associations are due to a hidden common factor, such as membrane-perturbation effects or whether it is a reflection of a capacity to bind specifically to unidentified BA target proteins. Hence it is possible that a carboxylate group is required for binding to an unidentified target after which, increasing hydrophobicity increases efficacy. Correlations between hydrophobicity and

protein binding and potency are well known (Khatib *et al.*, 2007; Sarkar & Kellogg, 2010).

The toxicity of the UDCA amide could be accounted for by the fact that an amide is a classical bioisostere for COOH. Furthermore our correlation broke down for non-ionisable lipophilic BAs and it does not fully account for the toxicity associated with DCA, CDCA and LagoDCA.

A number of observations were made regarding BA toxicity SAR. For example azido substitution on the BA nucleus is associated with enhanced toxicity and the azide group may therefore be a useful design tool for BA-based cytotoxic agents. Simple DCA and UDCA amides also hold promise in this regard. However it is clear that only a much larger panel of compounds would allow for development of quantitative-SAR. Important compounds to include in such a panel would be CDCA, CA and LCA primary amides and azides. Indeed an LCA azide with an amide side chain would be predicted to be potently cytotoxic based on hydrophobicity and structural observations from our study. Other compounds of interest would be the chain shortened DCA and CDCA derivatives; methyl and ethyl esters of DCA, CDCA, UDCA and CA. Introduction of the amino functional group at various positions on the BA nucleus would be of interest due its hydrogen bonding ability. A classical hydrophobic group would be the fluoro group which would also make for an interesting series of compounds.

A number of BA based medicinal chemistry programmes are focussed on derivatising the natural BAs and increasing potency in terms of their cytotoxicity. In some ways this is paradoxical as the ability of the natural BAs to induce apoptosis which then leads to an apoptosis resistance is thought to be a mechanism by which BAs induce carcinogenesis. The development of resistance in response to a BA based cytotoxic agent would have to be investigated.

Furthermore little work has been done showing the specificity of these agents on cancer cells over normal cells. In this regard it would be important to elucidate the mechanism by which these agents induce apoptosis so that compounds specifically targeting proteins expressed in cancer cells could be developed. On the other hand prodrugs or methods for site specific delivery could be explored.

It would also be interesting to carry out this study in another cell line to determine if the correlation between hydrophobicity and cytotoxicity holds true across different cell lines. Indeed this correlation can only be interpreted with caution until the work has been validated in different cell models. An interesting model cell line to repeat this work in would be a hepatic cell line known to express a BA transporter. However before such work could be carried out it would be necessary to show that our derivatives bind to BA transporters.

The present work has also shown that esophageal cells are sensitive to BA induced injury and proliferation in the concentration range of 1 to 500 μM which is a pathological concentration and that cell death at <500 μM is mediated through intracellular signalling rather than through detergency. Direct changes in membrane integrity occur at DCA concentrations far in excess of that found in esophageal refluxate. Nehra *et al* have shown that peak BA concentrations in patients with Barrett's esophagus were in the 1 to 400 μM range (Nehra *et al.*, 1999). This work opens up the possibility for chemoprevention of esophageal adenocarcinoma in at risk patients through inhibition of specific molecular targets or antagonism of the secondary BAs.

In conclusion, in this work we have succeeding in demonstrating the relationship between BA toxicity and hydrophobicity. This represents the first direct correlation between BA toxicity and a hydrophobicity parameter that we are aware of. The correlation is strongest with acidic BAs and it was especially strong in structurally homologous subgroups. This could be a useful tool for development of cytotoxic BAs in esophageal cell lines. However the correlation must be interpreted with caution until it has been validated in other cell models.

4 CHAPTER FOUR

RESULTS

Modulation of the Glucocorticoid Receptor by UDCA and derivatives

Chapter IV

4.1 Introduction

4.1.1 Nuclear receptors

Nuclear receptors (NR) form the largest known family of eukaryotic transcriptional regulators (Renaud & Moras, 2000). They control a diverse range of physiological functions including development, growth, reproduction, cell differentiation, proliferation, apoptosis and metabolism (Renaud & Moras, 2000). Furthermore they are essential in the maintenance of homeostasis. All NRs share a highly conserved common structural organisation consisting of five to six domains depending upon the particular receptor. The DNA-binding domain (DBD) and the ligand binding domain (LBD) are the most highly conserved regions (Germain *et al.*, 2006; Heitzer *et al.*, 2007). By constructing a chimeric protein in which the estrogen receptor (ER) DBD was replaced with that of the GR, Green *et al* demonstrated that these domains can function independently of each other. This protein was able to bind to estradiol, the cognate ligand of the ER, but activated glucocorticoid (GC) responsive genes (Green *et al.*, 1988).

NR signalling is highly complex. It can be genomic or non-genomic and ligand-dependent or independent. NRs bind to sequence specific promoter elements on target genes as monomers, homodimers and sometimes as heterodimers with the retinoid X receptor (RXR) and thus modulate transcription by inducing gene activation and gene repression. NRs can themselves be the target of other signalling pathways that induce post-translational modifications in the receptor and subsequently affect their function (Germain *et al.*, 2006). Conversely the receptors can regulate other major cell signalling cascades. Forty-eight NRs are currently known out of which only 24 are liganded receptors (Germain *et al.*, 2006). Ligands for NRs include steroid and thyroid hormones, vitamins, eicosanoids, oxysterols and BAs which have been shown to bind to the FXR (Wang *et al.*, 1999). Different ligands and their corresponding receptors are shown in Figure 4.1. All ligands tend to be small and hydrophobic but other than this they all vary greatly in structure (Germain *et al.*, 2006).

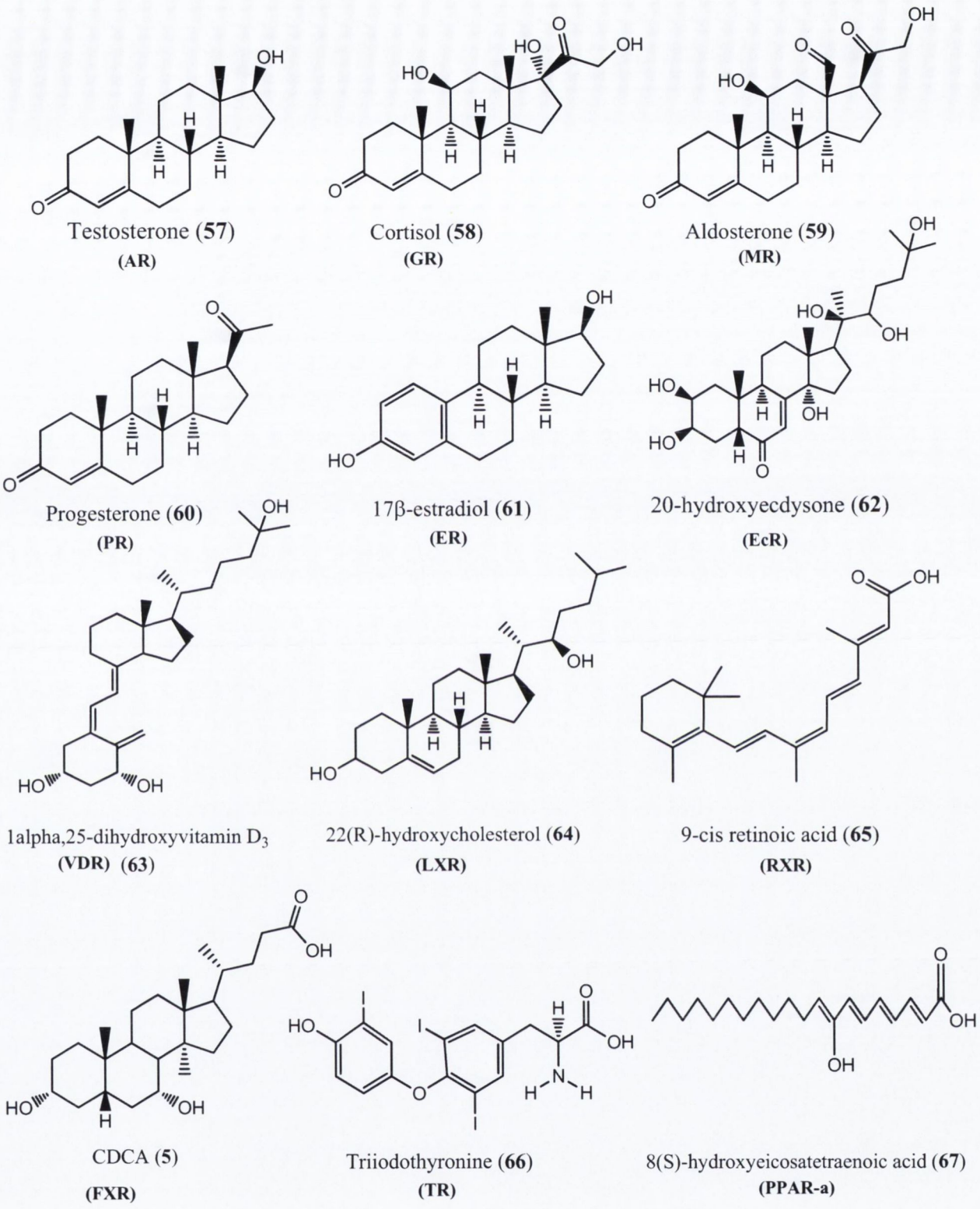

Figure 4.1 ***Structures of ligands and corresponding nuclear receptors.*** *AR=androgen receptor, MR=mineralocorticoid receptor, PR=progesterone receptor, ER=estrogen receptor, EcR=ecdysteroid nuclear receptor, VDR=Vitamin D receptor, LXR=liver X receptor, RXR=retinoid X receptor, FXR=farnesoid X receptor, TR=thyroid hormone receptor, PPAR=peroxisome proliferator activated receptor.*

In 1999 a unified nomenclature system was proposed for the NR family (Committee, 1999). The system is based on sequence alignment and phylogenetic tree construction connecting the 65 known NR genes in vertebrates, arthropods and nematodes. The human NR family is divided into six evolutionary conserved groups. The steroid hormone receptors and the steroid hormone receptor-like receptors form the NR subfamily 3 (NR3) (Beato & Klug, 2000). The steroid hormones which includes the estrogens, the progestins, androgens, GCs and mineralocorticoids (Beato & Klug, 2000) are produced in the gonads and adrenal glands in the mammals. NR3 consists of three groups A, B and C as shown in Table 4.1.

Table 4.1 ***Trivial and nomenclature names of the steroid hormone receptor family (NR3).***

Trivial Name	Nomenclature
ERα	NR3A1
ERβ	NR3A2
ERRα/ERR1 (estrogen related receptor)	NR3B1
ERRβ/ERR1	NR3B2
GR	NR3C1
MR	NR3C2
PR	NR3C3
AR	NR3C4

4.1.2 Structure and function of the GR

4.1.2.1 The GR gene

The structure of the human GR gene was elucidated in 1991 by Encio *et al* (Encio & Detera-Wadleigh, 1991). The gene is located in chromosome 5 and consists of 9 exons as shown in Figure 4.2A. Exon 1 represents the 5'-untranslated region, while exons 2–9 code for the protein and the 3'-untranslated regions (Encio & Detera-Wadleigh, 1991). Exon 1 is composed of several independent variants called 1A-1J, each of which contain its own transcriptional start site and unique promoters (Presul *et al.*, 2007; Turner *et al.*, 2006).

Analysis of the promoter region of the human GR reveals 15 unique binding sites for transcription factors (Yudt & Cidlowski, 2002). Two promoters known as promoters 1B and 1C exist in the region upstream of exon 1C. Promoter 1B contains a NF-κB binding site and promoter 1C an AP-2 site (Schaaf & Cidlowski, 2002). Further upstream, promoter 1A contains an interferon regulatory factor binding element and a sequence

resembling a GC responsive element (GRE) itself (Breslin, Geng & Vedeckis, 2001). Therefore although the GR is considered ubiquitous it is regulated by a variety of transcription factors binding to their response elements within its promoter regions (Yudt & Cidlowski, 2002). The varieties of promoters, transcription factor–binding sites, and transcriptional start sites are thought to account for the differences in gene expression of hGR throughout the body (Revollo & Cidlowski, 2009).

Similar to exon 1, exon 9 can also be alternatively spliced. Alternative splicing of exon 9 gives rise to the mRNA of the two best characterised hGR isoforms- GRα and GRβ (Revollo & Cidlowski, 2009). GRα mRNA (5.5 kb) contains exon 9α, whereas GRβ mRNA (4.3 kb) contains exon 9β (Schaaf & Cidlowski, 2002) , Figure 4.2B. A third hGR mRNA (7.0 kb) is also known to exist which contains the entire exon 9, including exon 9α, a 'J region', and exon 9β. This mRNA is most likely translated into hGRα (Breslin *et al.*, 2001).

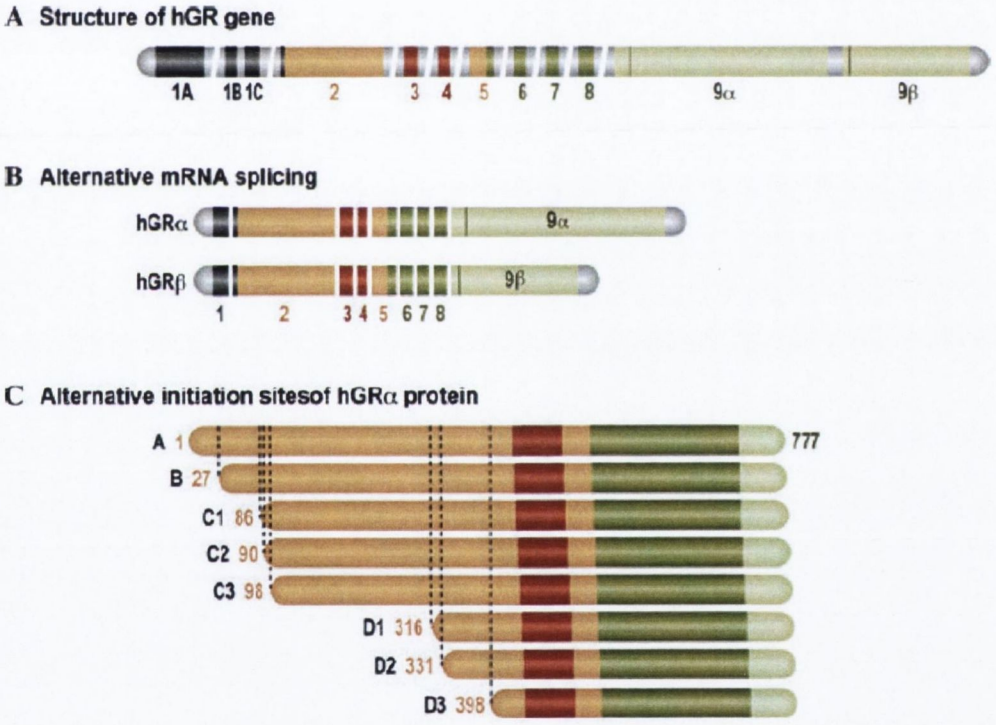

Figure 4.2 The human GR gene encodes for multiple isoforms. *A) The human GR gene is composed of nine exons. B) Alternative splicing of exon 9 gives rise to hGRα and hGRβ. C) Translation at different initiation sites can result in several more isoforms from each mRNA, image taken from (Revollo & Cidlowski, 2009).*

Several more GR isoforms are known to exist through alternative translation initiaton of the mature mRNA. This can occur when the ribosome skips an upstream initiation

codon starting translation from an alternative initiation site further downstream in the mRNA (Revollo & Cidlowski, 2009). These isoforms have shorter N-terminal regions as shown in Figure 4.2C. The human GRα and GRβ isoforms can each give rise to a further eight translational isoforms (Lu & Cidlowski, 2005). Lu *et al* have shown that these isoforms have unique tissue distribution patterns. Each isoform can undergo different post-translational modifications which further affect the function of the receptor (Lu & Cidlowski, 2006). Each GR isoform can display diverse patterns of trafficking from the cytosol to the nucleus. Furthermore the isoforms regulate a common but also a unique set of genes in the same cell type and so the authors propose that the unique GR isoform repertoire in cells determine the cell specific response to the GCs (Lu & Cidlowski, 2005).

Much work remains to be done in characterising these isoforms and human GRα and GRβ remain the most highly expressed isoforms. GRα is composed of 777 amino acids whereas GRβ is shorter with only 742 amino acids and is expressed to a lesser degree. GRα and GRβ are identical up to amino acid 727 after which the 15 carboxy-terminal amino acids in GRβ are unique and replace the carboxy-terminal 50 amino acids in GRα. The physiological relevance of GRβ remains unclear. To date it is thought that GRβ is transcriptionally inactive and is unable to bind agonists. However recent studies have shown that GRβ can bind mifepristone, a GC antagonist (Lewis-Tuffin *et al.*, 2007). This study showed that the presence of GRβ is sufficient to induce changes in gene expression and that in the presence of mifepristone these changes are inhibited. Higher expression of hGRβ has been associated with cardiovascular disease, as well as GC-resistant asthma, ulcerative colitis, and rheumatoid arthritis (Lewis-Tuffin & Cidlowski, 2006). The most physiologically relevant effect of GRβ however seems to be its negative regulation of GRα. Recent studies investigating this mechanism have shown that it is through the formation of GRα/β heterodimers which are incapable of binding co-activators as a ligand activated GRα homodimer would which mediates this attenuated GRα response (Oakley *et al.*, 1999).

4.1.2.2 GR protein

The domain structure of the human GRα protein, isoform A is shown in Figure 4.3.

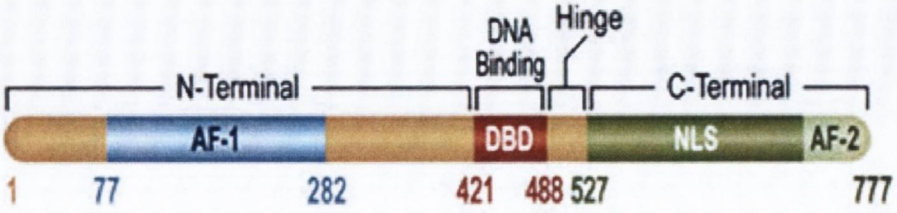

Figure 4.3 Domain structure of the human GRα protein, isoform A. *The GRα protein consists of three domains, an N terminal domain, a DBD and a ligand binding domain in the C-terminal region of the protein. Image taken from (Revollo & Cidlowski, 2009).*

GRα is a modular protein and is comprised of three major domains (Revollo & Cidlowski, 2009). The most N-terminal domain consists of amino acids 1–420. It is often referred to as the immunogenic domain, since human GR antibodies were initially raised against this region. The DNA-binding domain (DBD) of hGRα comprises amino acids 421–488, and its C-terminal LBD consists of amino acids 527–777 (Schaaf & Cidlowski, 2002).

The N-terminal domain contains the activation function-1 (AF-1) motif that physically interacts with basal transcriptional machinery such as the TATA box binding protein and RNA polymerase II to modulate gene activation (Kumar *et al.*, 2004). The AF-1 can act constitutively in the absence of the LBD and can stimulate transcription from simple promoters containing GREs (Kumar & Thompson, 2005). The AF-1 is rich in acidic amino residues. Studies have shown that the AF-1 region is mostly unstructured but acquires a folded functional conformation for example when the GR DBD is bound to GREs and AF1 binds other transcription factor proteins (Kumar & Thompson, 2005).

The DBD contains two zinc finger motifs and is essential for binding to DNA but also for receptor dimerisation and transrepression (Kumar & Thompson, 2005; Necela & Cidlowski, 2004; Revollo & Cidlowski, 2009). The DBD contains amino acids that contact specific bases in GRE sequences to provide site specificity for GR: DNA binding. These amino acids are in the first zinc finger whereas the second zinc finger stabilises the DBD: GRE interaction. Five amino acids in the second zinc finger region are referred to as the "D box". These play an important role in homodimerisation at the GRE (Kumar & Thompson, 2005).

The C-terminal domains contains the ligand binding motif, a nuclear localisation signal (NLS) and a second AF-2 motif (727-763) that is involved in interactions with various transcriptional regulatory factors (Kucera *et al.*, 2002; Revollo & Cidlowski, 2009). The AF2 functions in a ligand-dependent manner to fold so as to complete binding surfaces

for other proteins including co-activators and co-repressors (Kumar & Thompson, 2005). This region is also important for binding to the chaperone hsp90 (Necela & Cidlowski, 2004). In addition to these large domains there is a small flexible portion of the protein called the hinge region located between the DBD and the C-terminal domain which contains an additional NLS (Kumar & Thompson, 2005).

The GRα protein can also undergo post-translational modifications by phosphorylation, sumoylation and ubiquitination. Phosphorylation of the protein at serine residues 203, 211 and 226 leads to changes in its subcellular localisation (Revollo & Cidlowski, 2009) whereas ubiquitination at lysine 426 changes the cellular half life of the protein as it targets the receptor for proteasomal degradation (Duma, Jewell & Cidlowski, 2006). It is believed that such modifications can modify GR signalling. Phosphorylation of steroid receptors has been proposed as a potential mechanism for ligand independent activity. However the GR does not appear to respond to any such activation in the absence of a ligand (Weigel & Zhang, 1998). Ligand induced phosphorylation of the GR can occur (Bodwell *et al.*, 1998). It has been proposed by Defranco *et al* that the protein phosphatases type 1 and 2a regulate the nuclear-cytoplasmic distribution of the GR (DeFranco *et al.*, 1991). It has also been proposed that dephosphorylaton of the receptor might be required in the process of activation (Litwack, 1988; Reker *et al.*, 1987). The consequences of GR phosphorylation and dephosophorylation require much more investigation.

4.1.2.3 Mechanism of GR action

The unliganded GR is multimeric protein complex consisting of the GR polypeptide, a heat shock protein 90 (hsp90) heterocomplex which can consist of hsp90, hsp70, hsp56, hsp50 (Heitzer *et al.*, 2007; Necela & Cidlowski, 2004; Revollo & Cidlowski, 2009), a p23 subunit and one tetratricopeptide repeat protein (TPR) as shown in Figure 4.4.

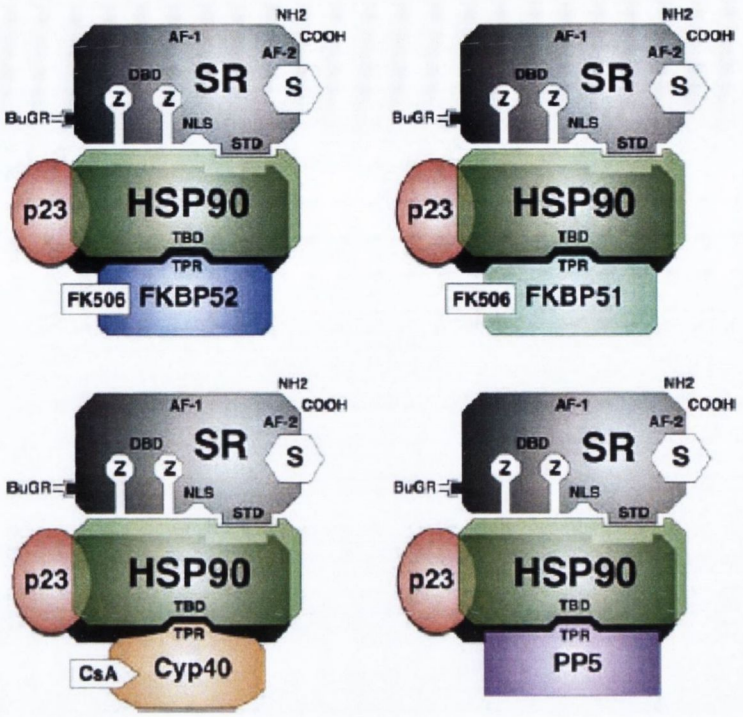

Figure 4.4 Four distinct steroid receptor complexes. *The unliganded GR is multimeric protein complex consisting of the GR polypeptide, a hsp90 heterocomplex ,a molecule of p23 and one TPR, image taken from (Heitzer et al., 2007).*

The p23 molecule is involved in stabilising the hormone binding conformation. The TPR proteins are the immunophilins, FKBP52, FKBP51, Cyp40 and PP5. These link with the receptor through the hsp90 complex. The associated TPR depends on the receptor subtype and the proteins are thought to modulate the activity of the receptor although they are not essential for its function (Heitzer *et al.*, 2007). Binding of GC agonists to the cytoplasmic GR induces this complex to dissociate, resulting in a conformational change that unmasks NLSs and results in rapid translocation of the GR to the nucleus (Dittmar *et al.*, 1997). Specific mechanisms suggested for translocation include the receptor first fusing with lysosomes and subsequently fusing with the nucleus or simply that the diameter of the nucelopore may be large enough to accommodate the activated receptor (Dittmar *et al.*, 1997). Upon ligand binding the receptor dimerises principally through the DBD but regions outside the DBD are also involved. Dimerisation precedes DNA binding as GR dimers have been shown to bind to GREs (Wrange, Eriksson & Perlmann, 1989).

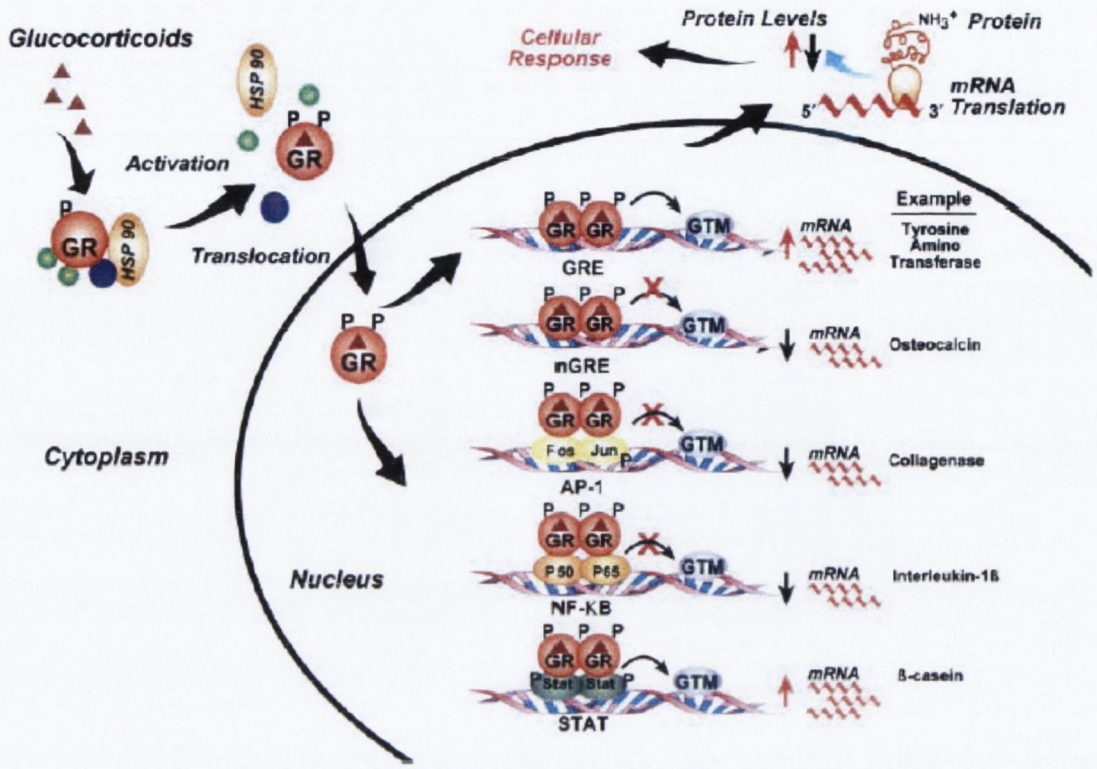

Figure 4.5 Mechanisms of GR action. *Ligand binding results in dissociation of GR from chaperones and translocation of the protein to the nucleus. The GR then binds as a dimer to GREs in target genes to activate transcription, to nGREs to inhibit transcription, and can also physically interact with the transcription factors AP-1, NF-κB and STAT family proteins to repress or enhance genes regulated by them. Example of genes regulated by the GR are shown on the right. GTM=general transcription machinery. Image taken from (Necela & Cidlowski, 2004).*

GREs are the DNA sequences to which GRα binds. The binding occurs in the major groove of the DNA through the central zinc finger of the DBD (Necela & Cidlowski, 2004). GREs are distributed in the proximal promoters of target genes but they differ in copy number, sequence, and location with respect to each other. These factors and other cellular influences contribute to the extent to which an individual gene is activated or repressed (Wieland, Schatt & Rusconi, 1990). GRα and DNA interactions can result in activation of genes through a variety of different mechanisms. If the GRE is in close proximity to the TATA-box then GRα can recruit key components of the basal transcription machinery including TATA box-binding protein (TBP), TBP-associated factors, and RNA polymerase II to the TATA-box itself. On the other hand, if the GRE is located at a distance to the TATA-box, then the GR can make use of co-activators to promote the recruitment of the basal transcription machinery to the

promoter elements (Revollo & Cidlowski, 2009; Rosenfeld & Glass, 2001). When the GR binds to GREs a conformational change is induced within the receptor which results in recruitment of several critical co-activator complexes. On top of their direct interactions with the transcription machinery, co-activators also affect local chromatin remodelling, through for example, histone acetylation and methylation, in order to induce nucleosomal rearrangement which enhances promoter accessibility (Heitzer *et al.*, 2007; Necela & Cidlowski, 2004; Ogryzko *et al.*, 1996; Onate *et al.*, 1995). Co-activators include the cAMP response element–binding protein (CREB)–binding protein/p300 and the p160 family of co-activators, designated steroid receptor co-activators (SRCs) which consists of SRC-1 (or NcoA1), SRC-2 (or TIF-2, GRIP1), and SRC-3 (or p/CIP,RAC3, ACTR, or AIB1) (Heitzer *et al.*, 2007; Necela & Cidlowski, 2004).

Co-repressors bind to nuclear receptors in the unliganded state and this interaction is believed to be stabilised by antagonists (Stevens *et al.*, 2003; Xu *et al.*, 2002). Recently co-repressors have also been identified as associating with both agonist and antagonist bound GR complexes (Wang *et al.*, 2004). Co-repressors have also been recently identified and include nuclear receptor Co-repressor (NCoR) and silencing mediator of retinoid and thyroid receptors (SMRT) (Horlein *et al.*, 1995). Co-repressors are thought to repress steroid receptor-mediated gene expression by interacting with histone deacetylases (HDACs), which promotes a closed chromatin structure and represses transcription (Glass & Rosenfeld, 2000; Heitzer *et al.*, 2007). Cells express a mixture of both co-activators and co-repressors and so it has been hypothesised by Wang *et al* that the agonist activity of GR complexes is modulated by the intracellular ratios of Co-repressor versus co-activator (Wang *et al.*, 2004).

Genes activated by GRα include interleukin-10, β-adrenergic receptor, interleukin-1 receptor antagonist and dual specificity protein phosphatise 1 (DUSP1), many of which have anti-inflammatory functions (Perretti & D'Acquisto, 2009). GCs also induce expression of the anti-inflammatory annexin A1 (lipocortin 1) but the mechanism by which they regulate annexin A1 has not been defined. Although it has been suggested that the mechanism may be indirect as the annexin A 1 promoter contains a partial consensus binding site that mediates responsiveness to IL-6 (Perretti & D'Acquisto, 2009).

GRα can also lead to a repression of genes by binding to negative GREs (nGRE). This process is often referred to as cis-repression. nGREs are similar to GREs but are located close to the DNA-binding sites of other transcription factors required to activate a particular gene (Revollo & Cidlowski, 2009). For example, the human FasL gene contains an nGRE adjacent to a nuclear factor-κB (NF-κB) site (Novac *et al.*, 2006). Binding of GRα to this nGRE prevents NF-κB binding leading to gene silencing.

4.1.2.4 GR protein-protein interactions

The majority of gene repression induced by GRα is mediated via direct protein interactions rather than through nGREs. These protein interactions have been characterised for the pro-inflammatory transcription factors NF-κB and AP-1. This method of repression is often referred to as trans-regulation or transrepression and is mediated through GR monomers (Zanchi *et al.*, 2010).

NF-κB is composed of subunits from the Rel family of proteins (p50, p52, p65, Rel B, and c-Rel). p50/p65 is the most common heterodimer combination. NF-κB is usually inactive, bound to IκB in the cytoplasm however inflammatory stimuli result in phosphorylation of IκB and its subsequent dissociation from NF-κB. NF-κB then translocates into the nucleus and activates transcription of genes involved in inflammatory processes. GRα can physically bind to p65 (Rel A) and repress the NF-κB-mediated transcription by preventing its association with its DNA-binding site. Even if NF-κB manages to reach its DNA binding site, binding of the GR to it can prevent the recruitment of the necessary transcription machinery (McKay & Cidlowski, 1998). Competition for the same co-activators can also result in repression. GRα has also been reported to inhibit NF-κB mediated phosphorylation of RNA polymerase II.

NF-κB regulates a large number of pro-inflammatory proteins. GRα induced NF-κB repression consequently leads to repression of a large number of pro-inflammatory genes including tumour necrosis factor α (TNFα), interleukin-1β, granulocyte monocyte colony stimulating factor, IL-6 and IL-8 and many others.

In a similar way GRα can bind and repress the transcriptional activity of the transcription factor AP-1. This interaction involves the GR DBD and the leucine zipper region of c-Jun, a subunit of the AP-1 protein (Schule *et al.*, 1990).

GRα can also directly interact with the STAT family of proteins to activate genes. The STAT proteins regulate expression of genes that influence growth, survival, and apoptosis. The GRα-STAT interaction can, in some instances, enhance STAT-mediated gene expression.

4.1.2.5 Non-genomic signalling

In general, significant changes in regulator protein concentration takes more than 30 min and it takes hours or days before changes on a cellular, tissue or organism level become evident (Stahn *et al.*, 2007). However some of the immunosuppressive effects of GCs occur too fast to be explained by effects on gene transcription. There is also increasing evidence that GCs are capable of non-genomic signalling events. One of the best examples of this is an inhibition in the production of the pro-inflammatory molecule, arachidonic acid through attenuation of the epidermal growth factor receptor pathway.

GRα has been shown to induce expression of lipocortin 1 (Goulding & Guyre, 1993; Perretti & D'Acquisto, 2009) but recently Croxtall *et al* demonstrated that ligand binding to GRα can lead to phosphorylation of lipocortin-1. Phosphorylated lipocortin 1 displaces the protein Grb2 from active EGF receptors decreasing EGF signalling which results in diminished activity of phospholipase A2. Phospholipase A2 catalyses the production of arachidonic acid, breakdown of which leads to production of prostaglandins. GRα signalling in this way can lead to a rapid decrease in prostaglandin production with the effect occurring within minutes (Croxtall, Choudhury & Flower, 2000; Revollo & Cidlowski, 2009; Schaaf & Cidlowski, 2002). Furthermore Solito *et al* showed that GC induced phosphorylation of lipocortin 1 results in its translocation to the membrane and that this is dependent on MAPK, phosphatidylinositol 3-kinase, and PKC pathways (Solito *et al.*, 2003).

Furthermore GCs can alter cell function by modifying cation transport through the plasma membrane and increasing proton leakage out of the mitochondria (Buttgereit *et al.*, 2004). Amsterdam *et al* have suggested that alteration in membrane potential is important in induction of cellular apoptosis by GCs (Amsterdam, Tajima & Sasson, 2002).

Hence the ligand activated GR can modulate gene expression by trans-activation through GREs, cis-repression through nGREs and trans-repression through protein-protein interactions.

4.1.3 GR Ligands

4.1.3.1 Cortisol-the endogenous GC

The adrenal cortex synthesises two classes of hormones, the corticosteroids which belong to the pregnane family of steroids and have 21 carbon atoms and the androgens which have 19. The corticosteroids consist of the GCs and the mineralocorticoids reflecting the receptors for which they have greatest affinity. Unlike BAs corticoids are relatively planar compared to BAs due to the trans fusion of the A/B ring (The A/B ring is cis fused in BAs). Cortisol (**58**) is the main endogenous GC in humans and aldosterone (**59**) is the predominant mineralocorticoid. Cortisol is secreted at an average daily rate of 10 mg/day with peripheral plasma concentration peaking in the morning at 16 μg/100 ml plasma.

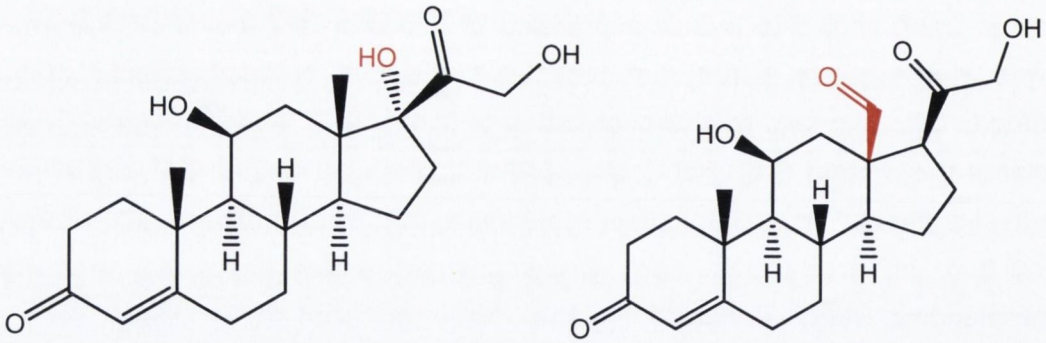

Figure 4.6 Structure and differences between cortisol and aldosterone

Cortisol is transported in the body as cortisone (**68**) and is found in plasma bound to carrier proteins. Cortisone undergoes reduction intracellularly by 11β-hydroxysteroid dehydrogenase 1 (11βHSD1) to cortisol establishing an equilibrium intracellularly as shown in Figure 4.7. Cortisol is pharmacologically referred to as hydrocortisone.

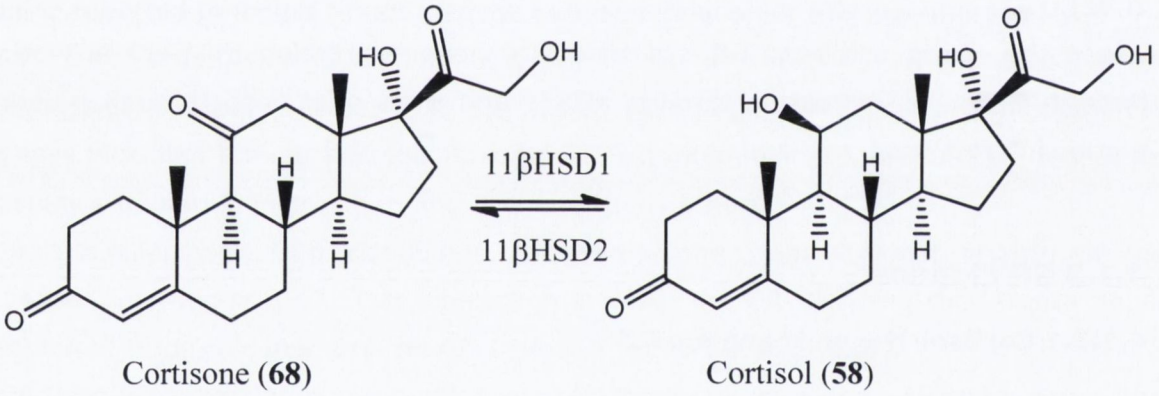

Figure 4.7 Cortisone exists in equilibrium with cortisol*. Intracellularly cortisol exists in equilibrium with cortisone. This equilibrium is maintained by the 11βHSD as shown.*

4.1.3.2 Physiological and pharmacological Effects of GCs

Cortisol is essential for life regulating transcription of a wide number of genes and hence affecting several physiological processes. Cortisol bound GR regulates transcription of an array of genes involved in glucose and lipid metabolism, bone turnover, lung maturation, and homeostasis of the immune, cardiovascular and central nervous system (Suino-Powell *et al.*, 2008). Cortisol counteracts insulin inducing a decrease in the uptake and utilisation of glucose and an increase in gluconeogenesis resulting in hyperglycaemia. This leads to increased glycogen storage in response to increased insulin secretion as a result of the hyperglycaemia. Effects on protein

include decreased protein synthesis and increased protein breakdown especially in muscle. There are two principal effects of GCs on lipid metabolism. One is the dramatic redistribution of body fat which occurs in excessive GC production in a disease called Cushing's syndrome. The redistribution is predominantly seen in the back of the neck and face. The other is the permissive facilitation of the effect of other agents such as growth hormone which can induce lipolysis in adipocytes resulting in an increase in free fatty acid concentration. It also acts as an anti-diuretic agent and can control mood, behaviour and excitability. It is also essential in control of the circadian rhythm.

In addition to these effects, cortisol can prevent or suppress all types of inflammatory reactions in response to multiple events including radiant, mechanical, chemical, infectious and immunological stimuli. This suppression of inflammation is of huge clinical utility and has made GCs one of the most prescribed clinical agents. When given therapeutically, GCs can inhibit both the early and the late manifestations of inflammation which include wound healing and repair and also the proliferative reactions which are seen in chronic inflammation. The anti-inflammatory action of GCs on inflammatory cells and on the mediators of inflammation and immune responses are outlined in Table 4.3.

Table 4.2 Anti-inflammatory actions of GCs, adapted from (H.P. Rang, 1999).

Actions on Inflammatory Cells	Actions on mediators of inflammation
Decreased egress of neutrophils from blood vessels and reduced activity of neutrophils and macrophages due to decreased transcription of genes for cell adhesion factors	Decreased production of prostanoids owing to decreased expression of cyclooxygenase-2
Decreased activity of T-helper cells and reduced clonal proliferation of T cells, due to decreased transcription of the genes for IL-2 and its receptor	Decreased production of cytokines-IL-1, IL-2, IL-3, IL-4, IL-5, IL-6, IL-8, TNF-α, cell adhesion factors and granulocyte-macrophage colony stimulating factor
Promotion of apoptosis of T-lymphocytes and eosinophils	Reduction in the concentration of complement components in the plasma
Decreased fibroblast function and less production of collagen and glycosaminoglycans	Decreased generation of induced nitric oxide
Reduced function of osteoblasts and increased activity of osteoclasts, thus a decrease in bone resorption.	Decreased histamine release from basophils
	Decreased IgG production

4.1.3.3 Synthetic GCs

Physiological GCs in pharmacological concentrations can have significant mineralocorticoid activity. This results in an electrolyte imbalance and significant retention of sodium and water. Chemical modifications to cortisol have generated derivatives with greater separation of GC and mineralocorticoid activity and have provided much information on the SAR of GC activity, Figure 4.8.

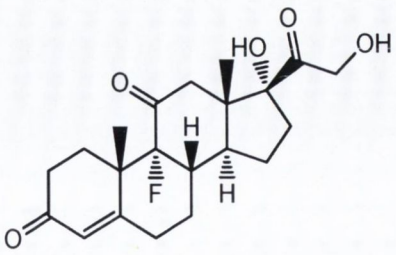

Fludrocortisone (**69**)

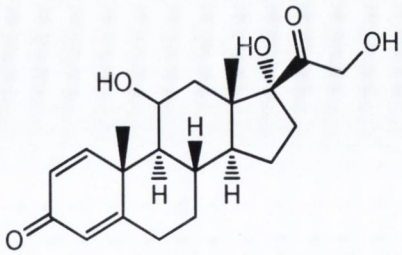

Prednisolone (**70**)

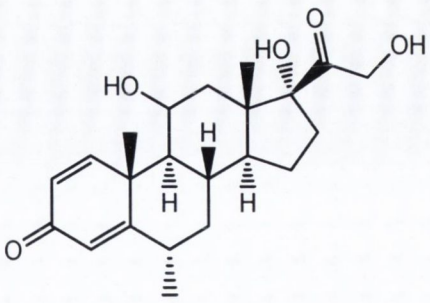

Methylprednisolone (**71**)

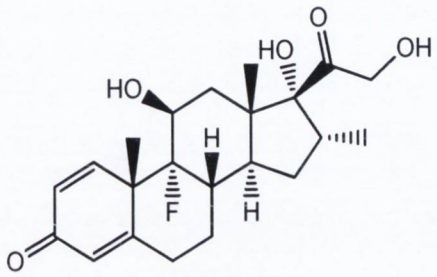

Dexamethasone (**72**)

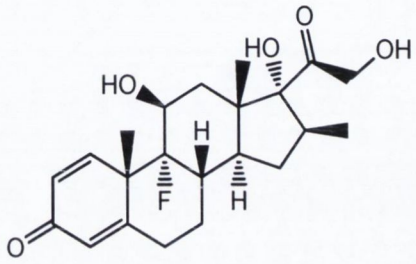

Betamethasone (**73**)

Figure 4.8 Synthetic GCs in clinical use. *Modifications to cortisol have generated derivatives with greater separation of GC and mineralocorticoid activity. Fludrocortisone is indicated for the treatment of Addison's disease whereas prednisolone, methylprednisolone, dexamethasone and betamethasone are used for their anti-inflammatory effects.*

It was recognised early on that a carbonyl group at C-3, a double bond between carbons 4 and 5, an oxygen (C=O or β-OH) at C-11 and a β-ketol side chain at position 17 are required for good GC activity. Synthesis of analogs containing additional groups at other positions on the basic steroid structure produced a variety of new derivatives some of which are shown in Figure 4.8. Addition of a fluorine group in the 9α position produced the derivative fludrocortisone (**69**) which has 11 fold GR activity but 800 fold mineralocorticoid receptor (MR) activity in comparison to the endogenous cortisol. Hence although this derivative is not useful for treatment of inflammation due to its profound effect on sodium and water retention it is used in the treatment of Addison's disease for mineralocorticoid replacement therapy as these patients have adrenocortical insufficiency. The Δ-corticoids prednisone and prednisolone (**70**) are 1-dehydro derivatives of cortisone and cortisol respectively. They are more commonly known as Δ^1-corticoids due to the extra double bond between positions 1 and 2. The Δ^1-corticoids have 4 fold GR activity and only 0.8 MR activity of cortisol. The double bond at position 1 changes the geometry of the A ring

as it changes from a chair conformation to a flattened boat. Prednisolone and its 6α-methyl analogue (**71**) are widely used for treatment of inflammatory conditions. The structure of dexamethsone (**72**) combines the 9α-fluoro of fludrocortisone and the double bond between carbons 1 and 2 with an additional α-methyl group at position 16. Betamethasone (**73**) differs only from dexamethasone with regard to the β configuration of the 16-methyl group. These drugs are very potent with 30 fold GR activity in comparison to cortisol but have minimal activity on the MR.

These derivatives, their esters and salts are widely used in clinical medicine for treatment in a range of disease states. They are used topically for treatment of inflammatory conditions of the skin. They are also used topically and systemically for treatment and management of ulcerative colitis and Crohn's disease. They are the mainstay of treatment for asthma principally administered by inhalation but also used systemically in the treatment of severe acute asthma. They are indicated in the treatment of hypersensitivity reactions such as angioedema of the upper respiratory tract and anaphylactic shock. GCs are also useful in conditions such as autoimmune hepatitis, rheumatoid arthritis, sarcoidosis and systemic lupus erythematosus.

In recent years a role for GCs in oncology and malignancy has also emerged. Dexamethasone (**72**) and betamethasone (**73**) are used in the management of raised intracranial pressure or cerebral oedema that occurs as a result of malignancy and in the management of emesis. Furthermore prednisolone (**70**) for example has a marked antitumour effect in haematological malignancies such as acute lymphoblastic leukaemia, Hodgkin's disease and non-hodgkin lymphomas. This is due to the efficient cytolytic effect of GCs on cells of the lymphoid region (Banciu *et al.*, 2008b; Schiffelers *et al.*, 2005). There are indications that GCs have effects on solid tumour growth as well due to their suppressive effects on angiogenesis (Banciu *et al.*, 2008a; Banciu *et al.*, 2006). However the effects of GCs on apoptosis remain controversial. Herr *et al* have shown that dexamethasone induced a strong anti-apoptotic effect in lung carcinoma cell lines and that it prevented cancer therapy-induced tumour reduction and apoptosis. This is due to inhibition of key molecules of the extrinsic and intrinsic apoptotic pathway resulting in a blockade of caspase activity (Herr *et al.*, 2003).

Interestingly Forster *et al* have shown that GCs can protect renal mesangial cells of the rat from stress factor induced apoptosis (Forster *et al.*, 2010). Hence the effects of GCs on apoptosis and inhibition of apoptosis in response to various stimuli requires much further investigation.

4.1.3.4 Side effects of GCs

Despite the wide range of indications for GCs their chronic use in therapy is limited by the large number of debilitating side effects they commonly induce. These side effects include a tendency towards hyperglycaemia which can induce diabetes. Furthermore overactivation of osteoclasts results in a breakdown of bone which can lead to osteoporosis particularly in the elderly. High doses of GCs can result in a redistribution of body fat due to effects on lipid metabolism particularly to the face and abdomen. Cushing's syndrome in which there is excessive production of GCs is characterised by a moon face and striae for example.

Systemic GCs have also been linked to psychiatric reactions including euphoria, nightmares, insomnia, irritability, mood lability, aggravation of epilepsy and psychotic reactions. They can induce musculoskeletal weakness due to effects on protein metabolism and also have profound effects on the endocrine system. These include menstrual irregularities, weight gain and increased appetite. Their effects on the immune system result in an increased susceptibility to infection. They can have ophthalmic side effects, the most severe and common of which is glaucoma. These and other common side effects are shown in Figure 4.9.

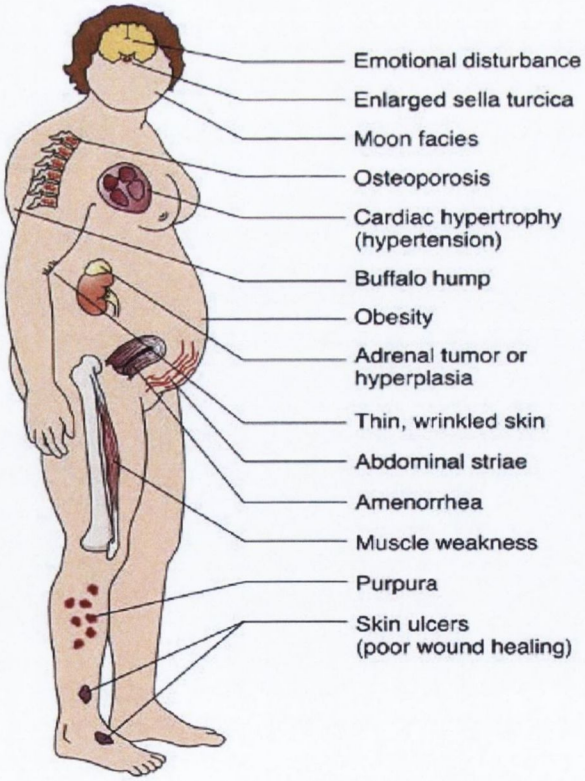

Figure 4.9 Side effects of GCs. *GCs cause a large number of side effects including diabetes, obesity, osteoporosis and psychotic reactions. Taken from* http://www.health-res.com/EX/08-04-08/cushings-syndrome2.jpgz

4.1.4 Crystal Structure of GR-LBD

Although GCs have been used clinically for several decades now, the crystal structure of the GR ligand binding domain remained elusive because of purification difficulties relating to the solubility of the protein (Necela & Cidlowski, 2003). It was only in 2002 that Bledsoe *et al* managed to crystallise the GR-LBD in a ternary complex with dexamethasone (**72**) and the LXXLL motif of the co-activator peptide, transcriptional intermediary factor 2 (TIF2) (Bledsoe *et al.*, 2002). TIF2 is also known as steroid receptor co-activator 2. The Leu-Xaa-Xaa-Leu-Leu (LXXLL) motif, originally observed in cofactor proteins that interact with hormone-activated nuclear receptors is necessary and sufficient to mediate the binding of these proteins to liganded nuclear receptors (Heery *et al.*, 1997; Plevin, Mills & Ikura, 2005).

Bledsoe *et al* achieved the crystallisation through a single point mutation in residue 602 of the LBD of the GR which had no effect on GR function. The structure was found to consist of 11 α-helices and 4 β-strands folded into a three layer helical sandwich. This is similar to other NRs, however the GR was found to contain a unique dimerisation interface that involves the formation of a central hydrophobic intermolecular β sheet (Necela & Cidlowski, 2003). The structure also revealed the presence of a unique steroid binding pocket which is absent from the ER, PR and AR. This difference arises in helix 6 and 7 as the sequences of the helices in the GR are different compared to the ER, PR and AR. Bledsoe *et al* propose that this pocket may allow for selective binding of GCs which have larger substituents at the C-17 α position than other steroids and its absence in the ER, PR and AR might explain their inability to bind GCs (Bledsoe *et al.*, 2002; Necela & Cidlowski, 2003).

Elucidation of the GR-LBD structure bound to the agonist dexamethasone (**72**) was soon followed by that of the LBD in an antagonist conformation bound to RU-486 also known as mifepristone (**74**), Figure 4.10 (Kauppi *et al.*, 2003). During the past decade, a large number of promising therapeutic applications of selective GR antagonists have been investigated. These include treatments of Cushing's syndrome, psychotic depression, diabetes, obesity, Alzheimer's disease, neuropathic pain, drug abuse, and glaucoma (Schoch *et al.*, 2010).

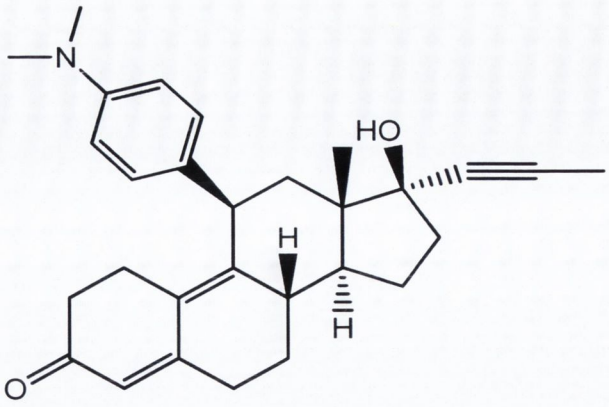

Mifepristone (**74**)

Figure 4.10 Structure of the GR antagonist, mifepristone. *GR antagonists have potential therapeutic value for treatment of Cushing's syndrome, diabetes and obesity.*

Similar to the dexamethasone bound structure the LBD adopts a helical bundle containing a cavity for binding of the ligand. However in the dexamethasone bound structure this cavity is completely closed. The C-3 ketone from the A-ring hydrogen bonds with the 570 and 611 residues which seals one side of the pocket along helices 3 and 7. The other side of the pocket is sealed by helix H12 (or the AF-2 helix), which makes direct contact with the C-11 hydroxyl and the C-18 methyl of the bound steroid. These interactions with dexamethasone lock the AF-2 helix into the active conformation that is able to bind the LXXLL motif of TIF2. However in mifepristone the presence of the dimethyl amino phenyl moiety clashes with the AF-2 agonist conformation and pushes it out of its active conformation. Thus it cannot bind to the TIF2 co-activator peptide and hence is not transcriptionally active (Schoch *et al.*, 2010; Suino-Powell *et al.*, 2008).

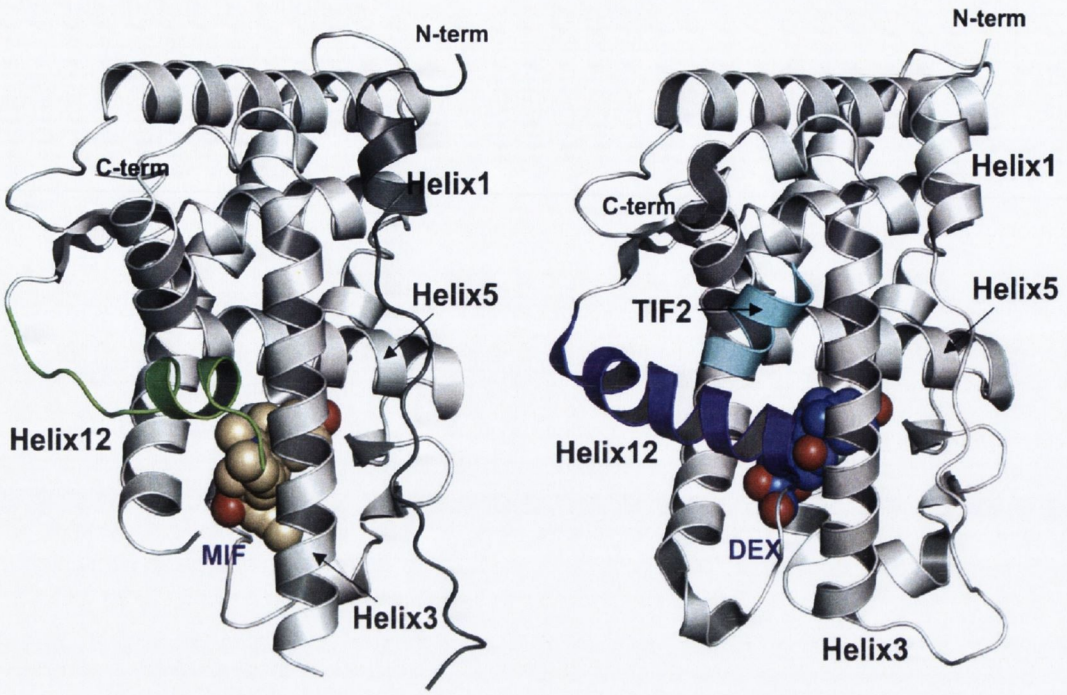

Figure 4.11 Helix 12 conformational changes in GR/mifepristone and GR/dexamethasone complexes. *The dimethyl amino phenyl group in mifepristone pushes helix 12 (AF-2 helix) out of its active conformation and does not allow an interaction with TIF2. The N-terminal regions (residues 527–553) are coloured dark gray, TIF2 and the helix 12 region of GR-LBD (residues 750–767) are highlighted and coloured differently, taken from (Schoch et al., 2010).*

Mifepristone has been shown to have partial agonist activity in certain cell types (Zhang, Jonklaas & Danielsen, 2007), which requires co-activator binding. GST pull down assays, however, have shown that the GR-mifepristone complex is not able to bind to the co-activators, TIF2 or SRC1 (He, Szapary & Simons, 2002; Stevens *et al.*, 2003). The mifepristone concentration in these experiments ranged from 100 nM to 1 µM. Other glucocorticoid antagonists such Dex-21-mesylate and Dex-oxetanone (Dex-Ox) on the other hand were able to bind to TIF2 (He *et al.*, 2002). Schoch *et al* recently reported the crystal structure of a ternary complex of the GR-LBD with mifepristone and presented a conformation intermediate between the active antagonist and agonist conformation in Figure 4.11. In this conformation helix 12 adopts an intermediate position which may still allow the GR mifepristone complex to recruit co-activators and display partial agonism (Schoch *et al.*, 2010).

4.1.4.1 Deacetylcortivazol doubles the size of the GR ligand binding pocket

The crystal structures of mifepristone and dexamethasone however failed to account for the binding of a large number of steroidal and non-steroidal ligands. The most

puzzling case was deacetylcortivazol (**75**), Figure 4.12, which is 40-fold more potent than dexamethasone but surprisingly the compound includes a phenylpyrazole group in place of the critical ketone at C-3. The structure of the GR LBD bound to both dexamethasone and mifepristone does not account for this as there is not enough space in the ligand binding cavity to accommodate the phenylpyrazole moiety (Suino-Powell *et al.*, 2008).

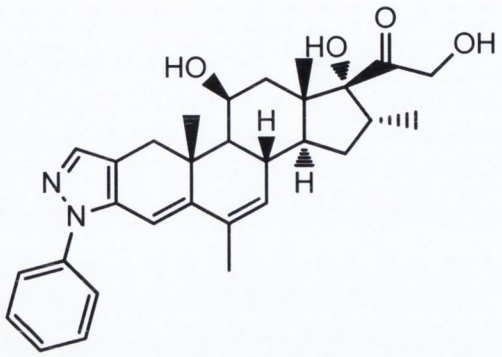

Deacetylcortivazol (**75**)

Figure 4.12 Structure of the potent GR agonist, deacetylcortivazol (75). *The structure of the GR LBD bound to dexamethasone and mifepristone do not account for the binding of the potent GR agonist deacetylcortivazol (**75**) which has a large phenylpyrazole moiety.*

Suino-Powell *et al* determined the crystal structure of the GR-LBD bound to deacetylcortivazol and revealed that the GR ligand binding pocket can expand to accommodate deacetylcortivazol in which the phenylpyrazole ring extends into a new channel (Suino-Powell *et al.*, 2008) but can still leave the AF-2 helix in the active conformation, Figure 4.13. This channel has recently been exploited by Biggadike *et al* in the design of novel GC ligands containing an indazole amide structure (Biggadike *et al.*, 2009).

A)

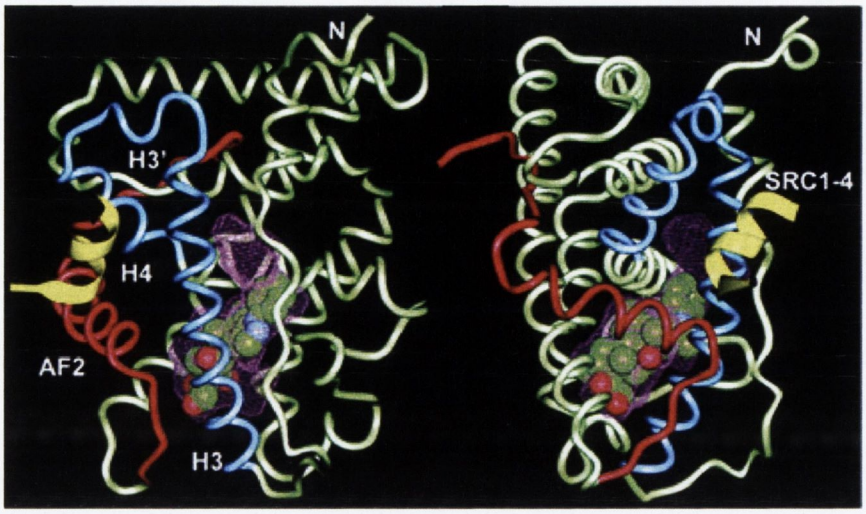

B)

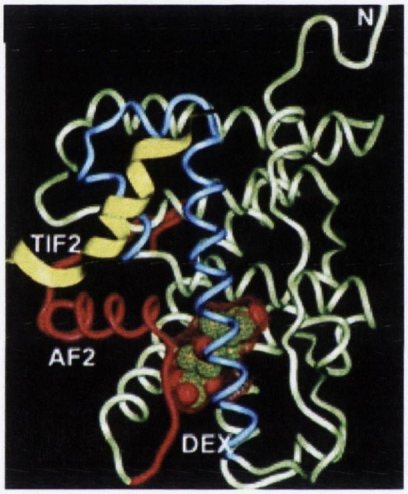

Figure 4.13 Crystal structure of GR/DAC/SRC1-4 complex. *A) Two different views of the crystal structure are shown. The DAC-biding surface is shown as a pink surface, the SRC1-4 peptide is in yellow and the bound DAC is shown in a space filling representation with carbon and oxygen atoms in green and red respectively. B) The GR/Dex/TIF2 complex is shown for comparison. Image taken from (Suino-Powell et al., 2008).*

Suino-Powell *et al* also highlight in this study that despite different co-activator motifs and ligands, the co-activator binding site in the GR/DAC/SRC1-4 complex is nearly identical to that of the GR/DEX/TIF2 complex, and the SRC1-4 helix adopts the same binding mode as the TIF2 motif, Figure 4.14 (Suino-Powell *et al.*, 2008).

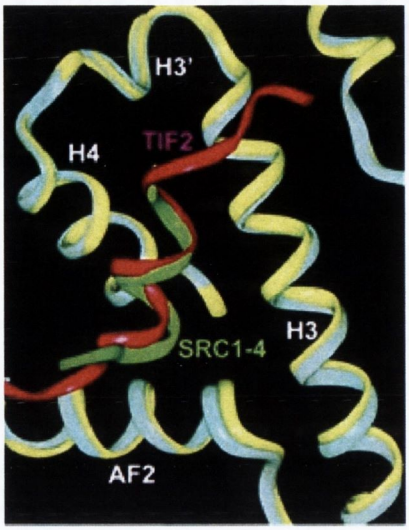

Figure 4.14 ***Structural comparison of co-activator binding.*** *Structural comparison between the DAC (cyan) and dexamethasone bound structures (yellow). The SRC1-4 and TIF2 helices are shown in green and red respectively. Image taken from (Suino-Powell et al., 2008).*

Crystal structures of the GR bound to fluticasone furoate (Biggadike *et al.*, 2008) and a non-steroidal glucocorticoid agonist have also been published recently (Madauss *et al.*, 2008). The fluticasone furoate structure reveals how the ligand can extend the GC bind pocket in the opposite direction to deacetylcortivazol, Figure 4.15. The non-steroidal ligand uses both these opportunities for pocket extension (Madauss *et al.*, 2008).

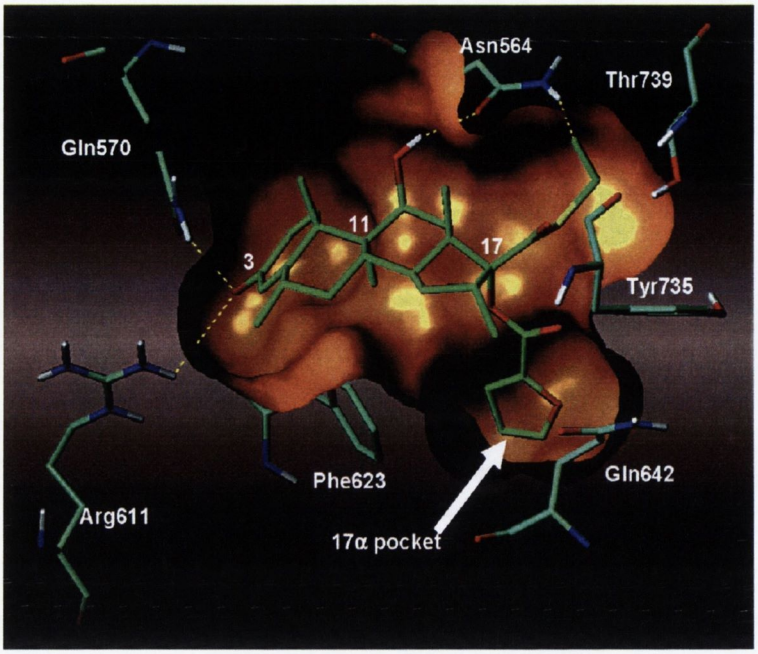

Figure 4.15 ***Crystal structure of GR LBD/TIF2 bound to fluticasone furoate.*** *Fluticasone furoate extends the GC pocket in the opposite direction to deacetylcortivazol as seen by the 17α pocket.*

4.1.5 Dissociated Steroids

In order to address the number of side effects induced by the current clinically used GCs a great deal of research in recent years has focused on the design of GCs that exhibit similar anti-inflammatory potency to conventional agents but have reduced side effects. This concept arose from a study which was done with GR mutants that could not transactivate GREs but could still transrepress AP-1 and NF-κB (Heck *et al.*, 1994; Tao, Williams-Skipp & Scheinman, 2001; Yang-Yen *et al.*, 1990). Replacement of alanine 458 with threonine allows transrepression and prevents dimerisation. This mutation yields mice that are defective in dexamethasone induced GRE-dependent transcription and endogenous TAT gene expression yet are competent at repression of AP-1 dependent and classic inflammatory genes (Reichardt *et al.*, 1998; Reichardt *et al.*, 2001). Furthermore Wu *et al* have demonstrated GR mutants that cannot bind co-activators or transactivate but can still transrepress NF-κB (Wu *et al.*, 2004).

There is a general consensus that transactivation is responsible for the side effects of steroids whereas the anti-inflammatory action of steroids predominantly arises from transrepression. The studies with GR_{dim} mutants suggest the potential of designing GR ligands that would maintain anti-inflammatory properties associated with transrepression but reduce the side effects associated with transactivation (Xiao *et al.*,

2010). Rosen *et al* provide definitions for different types of GR ligands that have been designed in recent years (Rosen & Miner, 2005). They divide these compounds into four principal types:

- Selective GR modulator and selective GR agonists-compounds with an improved therapeutic index *in vivo* achieved by various mechanisms
- Gene selective compounds-compounds that act on the receptor to alter gene expression in a gene or promoter specific fashion but the resulting profile differs from that of conventional GCs
- Dissociated steroids/compounds-steroids or non-steroidal compounds that fail to globally activate gene expression but still significantly repress transcription
- Soft steroids/GCs-corticosteroids that act at or near the site of administration but are inactivated by enzymes, thereby reducing systemic exposure and activity.

Out of these compounds the greatest research efforts have been invested in the design of dissociated compounds. Vayssiere *et al* described a first generation of dissociated steroids (Vayssiere *et al.*, 1997). Following the screening of a GC library they identified three compounds that displayed dissociated behaviour. These were RU24782, RU24858, and RU40066. The compounds had residual transactivation activity (between 9% and 35% of dexamethasone) but retained a strong transrepressive activity on AP-1 (De Bosscher, 2010; Vayssiere *et al.*, 1997). The most promising of these compounds was RU24858, Figure 4.16.

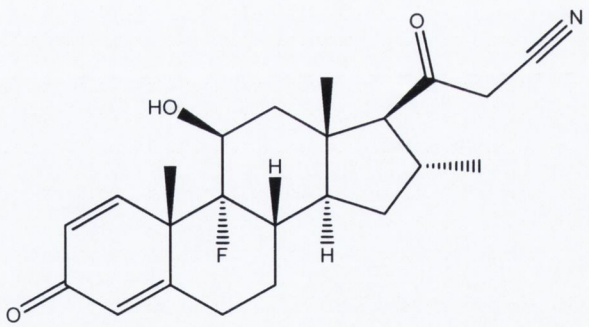

RU24858

Figure 4.16 Structure of the dissociated steroid, RU24858. *Dissociated steroids are compounds that fail to globally activate gene expression but still significantly repress transcription.*

However subsequent work by Belvisi *et al* showed that these compounds displayed the same side effects *in vivo* (Belvisi *et al.*, 2001b). An animal model of lung oedema was

used and although the same efficacy in anti-inflammatory activity was achieved animals still lost body weight and developed ostopenia of the femur, although to a lesser degree (De Bosscher, 2010). Hence *in vitro* separation of transrepression from transactivation does not necessarily result in improved therapeutic ratio *in vivo*. Rosen *et al* comment that it is unclear whether this failure is due to the fact that the compounds that were dissociated *in vitro* were fully activating *in vivo* or whether the sole ability to transrepress was sufficient to induce side effects as well as attenuate inflammation (Rosen & Miner, 2005). Interestingly however, compounds which have shown strong activation and weak repression are unable to suppress inflammation (Rosen & Miner, 2005).

Research in the area remains intensive with Xiao *et al* recently synthesising a novel set of dissociated compounds based on the hexahydroimidazol[1,5b]isoquinoline scaffold (Xiao *et al.*, 2010). This study shows differential regulation across one or two genes but does not demonstrate that the compounds are dissociated on all GC target genes. A similar trend is seen in most medicinal chemistry programmes investigating dissociated steroids.

The actual utility of a truly dissociated compound is a matter of much debate. Although activation of genes is responsible for side effects, activation of anti-inflammatory genes is also central to attenuation of inflammation. Nevertheless the compounds provide a useful mechanistic insight into GR function.

Wang *et al* evaluated a series of fifteen arylpyrazole compounds possessing high affinity for the GR (van der Laan & Meijer, 2008; Wang *et al.*, 2006). Subtle differences in the ligand structure resulted in different biological effects reflected in variations in cell proliferation and differentiation. All the compounds induced GR translocation but displayed differential gene expression profiles. Furthermore the compounds induced differential promoter occupancy of the GR as determined by chromatin immunoprecipitation assays. Wang *et al* suggest that the receptor conformation induced by a particular ligand may promote binding to only a subset of the occupied sites.

In the same vein, Discovery research pharmaceuticals recently described a benzylidene compound, LGD-5552 for use in inflammatory disorders including arthritis and multiple sclerosis models. The compound showed differential gene expression to prednisolone and suppressed inflammation without inducing side effects of GCs in both acute and chronic models of inflammation and side effects (Lopez *et al.*, 2008). Lopez *et al* suggest that LGD-5552 is different from conventional GCs due to an alteration in the outer receptor structure when bound in the LBD resulting in a change in the ability of the protein to interact with co-activators and Co-repressors which results in differential gene expression. A similar compound AL-438 developed by Coghlan *et al*

displayed similar biological properties and exhibited significantly different interactions with co-activators (Coghlan *et al.*, 2003).

Recent work by Ronacher *et al* also support the idea that different ligands induce differential interactions of the GR with the co-activators GRIP-1 and SRC-1 and Co-repressors like NCoR and SMRT (Ronacher *et al.*, 2009)

Ray *et al* suggest that these partial agonist ligands induce a conformational change in the GR into a partial transactivating transcription factor. The structure of RU24858 differs from conventional GCs in the D ring which suggests that this part of the molecule is involved in interactions with the GR which convey the activation signal. This study identifies the Tyr 735 as important for ligand binding and ligand dependent transactivation. Mutation of Tyr 735 to phenylalanine results in an unchanged ligand binding affinity and transrepressive effect but decreases activation potential. Mutation to a valine residue results in a minimal decrease in ligand binding affinity, no change in transrepression, but induces similar changes in transactivation as the phenylalanine mutant. Mutation to serine however decreases ligand binding affinity slightly, does not affect transrepression but has a marked effect on transactivation. The authors conclude that the hydrophobic benzene ring of tyrosine contributes to ligand binding, and the tyrosine hydroxyl side chain contributes to transactivation (Ray *et al.*, 1999).

Hence Tyr 735 is an important amino acid for determining for determining the final GR conformation after ligand binding, and subsequent recruitment of co-activators and co-repressors (Stevens *et al.*, 2003).

4.1.6 UDCA and the GR

UDCA (**14**), a tertiary BA is clinically used for the treatment of a number of hepatic diseases and has a history of minimal adverse effects. UDCA has demonstrated an anti-apoptotic cytoprotective action in hepatic (Amaral *et al.*, 2009a; Azzaroli *et al.*, 2002) as well as non-hepatic cell lines (Fimognari *et al.*, 2009; Rodrigues *et al.*, 1999). Furthermore UDCA has the ability to inhibit apoptosis induced by the cytotoxic BAs, DCA (**4**) and CDCA (**5**) (Benz et al., 2000; Im & Martinez, 2004; Silva et al., 2001), both of which have been implicated in the pathogenesis of hepatic and intestinal diseases (Hofmann, 1999; Thompson, 1996). The chemopreventative potential of UDCA has been demonstrated in patients with ulcerative colitis and cholestatic diseases who display lower rates of colorectal dysplasia (Tung *et al.*, 2001). The cytoprotective and chemopreventative effects of UDCA are thought to lie in its ability to modulate the immune system. Indeed its clinical use in hepatic inflammatory conditions infers that it has immunomodulatory properties.

UDCA has been suggested to act as an immunomodulator for the immune system (Yoshikawa *et al.*, 1992). UDCA suppressed the production of IgM, IgG and IgA induced by Staphylococcus aureus Cowan I in peripheral blood mononuclear cells derived from healthy subjects and patients with PBC and also in human B lymphoma cell lines. Concanavalin A induced IL-2 and IL-4 were also suppressed as was concanavalin-A induced thymocyte proliferation. Similar findings have been reported in other studies where UDCA treatment has been shown to reduce the serum level of IgM class AMA antibodies (Poupon *et al.*, 1991) and IgG antibodies to pyruvate dehydrogenase (Kisand *et al.*, 1996) in patient groups with PBC. In cholestasis the major histocompatibility complex (MHC) class I and class II molecules are overexpressed in hepatocytes and biliary epithelia, respectively (Innes et al., 1988). Inappropriate expression of MHC class I on hepatocytes may lead to their recognition and subsequent destruction by cytotoxic T lymphocytes. Calmus *et al* have reported that both cyclosporine and corticosteroids were unable to suppress MHC class I overexpression (Calmus *et al.*, 1992). It is thought that in PBC MHC class I overexpression is a result of the effect of BAs on MHC class I transcriptional activity through activation of PKC and PKA (Hillaire *et al.*, 1994). Unlike cyclosporin and corticosteroids UDCA has been shown to decrease the hepatocellular and biliary expression of both MHC class I and class II molecules (Calmus *et al.*, 1990; Terasaki *et al.*, 1991), respectively in patients with PBC. This suggests that UDCA might reduce the T-cell mediated hepatocellular damage. Furthermore, in PBC patients UDCA therapy has been reported to correct the defective natural killer (NK) cell activity by inhibiting prostaglandin E2 production (Nishigaki *et al.*, 1996). Furthermore Ikegami *et al* demonstrated that UDCA has a suppressive effect at the transcriptional level on Phospholipase A_2 IIA (PLA_2IIA) in hepatocytes, similar to many glucocorticoids (GCs) (Ikegami *et al.*, 2005).

UDCA's modulation of the immune system shows similarities with GC mediated immunomodulation (Amaral *et al.*, 2009c). Indeed much work over the last two decades indicates that UDCA's immunomodulatory and potentially its cytoprotective and chemopreventative effects are mediated via a GR pathway.

UDCA has been shown to induce translocation of the GR in primary rat hepatocytes (Weitzel *et al.*, 2005), Chinese hamster ovary cells (CHO) (Tanaka & Makino, 1992; Tanaka *et al.*, 1996) and COS cells which are derived from the kidney of the African green monkey (Miura *et al.*, 2001). There are conflicting reports regarding UDCAs activation of the GR as some studies have shown that UDCA can induce transactivation of the GR (Tanaka *et al.*, 1996; Weitzel *et al.*, 2005) but others have been unable to demonstrate this effect (Miura *et al.*, 2001; Sola *et al.*, 2005).

A physical interaction with the GR has not been demonstrated to date but the ligand binding domain (LBD) of the GR seems essential for UDCA's actions. UDCA requires the GR-LBD to induce GR nuclear translocation and for its subsequent biological effects (Miura *et al.*, 2001; Sola *et al.*, 2005; Sola *et al.*, 2004). Using a series of GR mutants, Miura *et al* showed that UDCA influences a broader region of the LBD than dexamethasone. They found that GR deletion mutants (1-765, 1-750, 1-740) did not translocate to the nucleus in response to dexamethasone but did in response to UDCA (Miura *et al.*, 2001). On the other hand GR-mutant (1-730) was unresponsive to UDCA. This observation was later confirmed by Sola *et al* who identified this specific carboxy terminal region of the LBD as essential for translocation and UDCAs cytoprotective effect on TGFβ1 induced apoptosis (Sola *et al.*, 2005). The authors suggest that the reason for this is that this mutant lacks Tyr 735 of the steroid binding pocket, which is necessary for hydrophobic contact between ligands and the GR (Stevens *et al.*, 2003). These studies clearly indicate that UDCA acts on a distinct region of the LBD compared to dexamethasone.

Sola *et al* used siRNA technology and GR mutants to confirm that UDCA significantly reduces TGFβ1–induced apoptosis of primary rat hepatocytes through a GR-dependent pathway (Sola *et al.*, 2005). Again the LBD was identified as critical for the inhibition of apoptosis. Recently Byrne *et al* have showed that siRNA knockdown of the GR inhibits UDCA's cytoprotective effects on the golgi apparatus (Byrne *et al.*, 2010). This study will be discussed in greater detail in Chapter 5. In the same vein GR knockdown attenuates UDCAs inhibitory effects on PLA_2IIA (Ikegami *et al.*, 2005).

Furthermore Miura *et al* demonstrated that UDCA can suppress NF-κB and that this repression occurs via activation of the GR (Miura *et al.*, 2001). They proposed that UDCA could be a prototype for the development of a novel GR modulator.

4.1.7 Inflammation in Esophageal Cancer

Bile and acid exposure can lead to chronic inflammation in the esophagus (Abdel-Latif *et al.*, 2009a).

If this inflammation persists then it can lead to release of pro-inflammatory mediators including cytokines, chemokines, prostaglandins (PGs), and reactive oxygen/nitrogen species which can promote cell growth, invasion, mutagenesis and essentially carcinogenesis. Such inflammatory mediators have been shown to support transformation, initiation and progression of tumour development (Coussens & Werb, 2002).

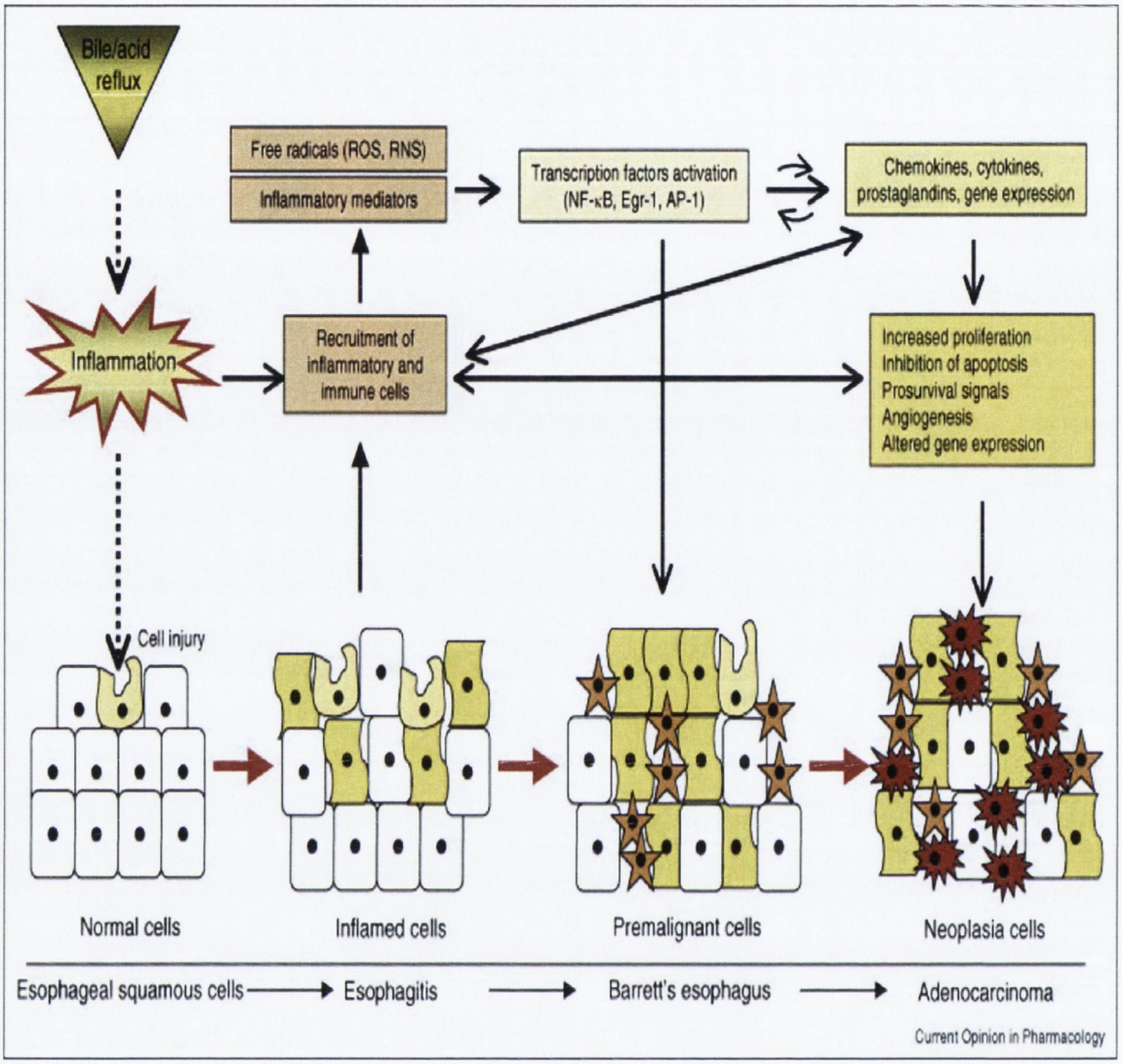

Figure 4.17 Proposed mechanism of inflammation in the development of esophagitis, Barrett's esophagus and adenocarcinoma of the esophagus. *Recruitment of inflammatory and immune cells in esophagitis can lead to activation of the transcription factors NF-κB, AP-1 and Egr-1. These transcription factors can ultimately alter gene expression resulting in increased proliferation and angiogenesis leading to neoplasia, taken from (Abdel-Latif et al., 2009a).*

The transcription factors NF-κB, AP-1 and early growth response gene-1 (Egr-1) are thought to be the key inflammatory players in mediating chronic inflammation of the esophagus (Abdel-Latif *et al.*, 2009a). These transcription factors can increase the transcription of genes involved in immunity, proliferation, and prevention of apoptosis (Hsu *et al.*, 2000; McMahon & Monroe, 1996). Altered gene expression can also switch on pro-survival signals resulting in angiogenesis and development of full-blown carcinoma, Figure 4.17.

4.2 Aims and Objectives

The extensive clinical usage of UDCA in hepatic inflammatory conditions, its history of minimal side effects and furthermore the recent studies showing that it can induce GR translocation and suppress NF-κB indicate that UDCA would be an excellent prototype for development of a novel GR modulator. BA reflux has been linked to inflammation in the esophagus and considering that UDCA has been shown to antagonise the actions of secondary toxic BAs, we felt that a GR modulator based on UDCA could have potential use in attenuating BA induced inflammation. We also hypothesised that in the long term the chemopreventative effects of UDCA in colon cancer might be extended to esophageal cancer. We aimed to synthesise compounds based on the UDCA structure with increased potency and efficacy that could serve as useful tools for further characterising UDCA's effects on the GR and elucidating its mechanism of action as a cytoprotective and chemopreventative agent.

Hence the specific aims and objectives of this study were to:

1) Determine if UDCA could induce GR translocation in an esophageal cell line.

2) If so, to synthesise a series of UDCA analogues with a view to making a more potent GR modulator.

3) To screen these analogues in a high content assay for GR translocation.

4) To determine if compounds found to modulate GR translocation could bind to the GR, induce GR activation and suppress NF-κB activity.

4.3 Results

4.3.1 UDCA induces GR translocation

Our first aim was to establish if UDCA could induce translocation of the GR to the nucleus in an esophageal cell line. We initially decided to use an adenoviral vector delivery system to overexpress the GR in our cell model.

4.3.1.1 Ad-A-Gene GR Assay

Adenoviruses are a family of DNA viruses that are used as a vehicle for the delivery of genes into cultured cells. A series of replication defective recombinant adenoviral preparations containing a gene encoding a protein target fused to an Enhanced Green Fluorescent Protein (EGFP) called Ad-a-gene vectors were provided by GE Healthcare. We used a replication defective recombinant adenoviral preparation containing the GR gene encoding a protein fused to an EGFP. These initial investigations were done using the esophageal cancer cell line, the SKGT-4. High content analysis of acquired images revealed that UDCA could induce translocation of the GR to the nucleus, Figure 4.18. This was similar to the GC, dexamethasone (**72**) shown here as an increase in the intensity of the GR within the nucleus.

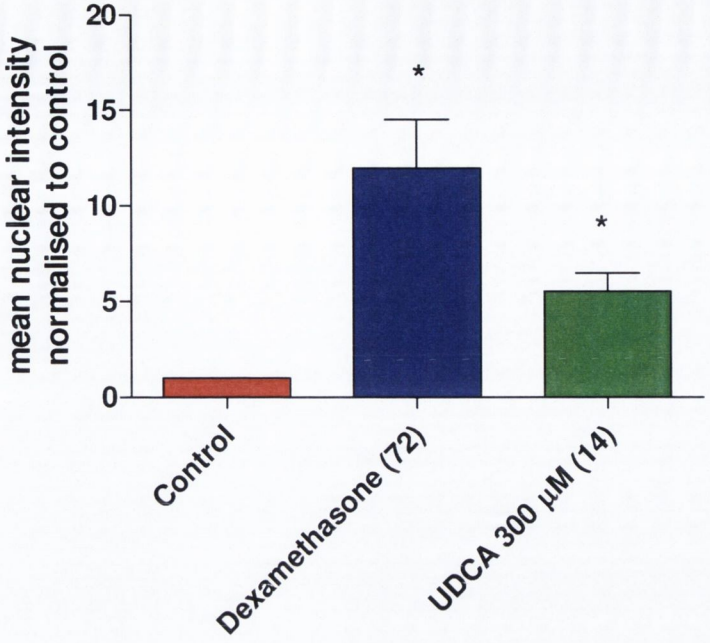

Figure 4.18 UDCA induces translocation of the GR in SKGT-4 cells. *The SKGT-4 cell line was transiently transfected with EGFP-GR and then left untreated or treated with dexamethasone 50 nM or UDCA 300 µM for 2 h, Section 2.15. Cells were fixed in formaldehyde 2% for 10 min and stained for the nuclei with Hoechst. GR translocation was measured using the Investigator software package. Analysis was based on the mean nuclear intensity normalised to untreated control. Values are expressed as the mean ± SEM of three experiments performed in duplicate, * p< 0.05 relative to control, as determined by one-way ANOVA and Dunnett's post-hoc correction.*

4.3.1.2 Immunofluorescence Assay

Before further screening using the Ad-A-Gene assay could be carried out the manufacturer stopped producing these constructs. Hence using an antibody, we decided to develop an immunofluorescence GR translocation assay, Section 2.9. In some ways this assay was preferable to the Ad-A-gene assay as it did not rely on overexpression of the GR but rather reflected translocation of endogenous GR in the cell line. However the staining procedure introduced a series of extra steps which made the assay more laborious. This assay was developed by another PhD student using a number of different esophageal cell lines including the HET-1A, QH and SKGT-4 cell lines. We decided to continue to use the SKGT-4 cell line for our studies as the assay displayed the greatest range using this cell line and dexamethasone as a positive control. The analysis was carried out using the GE Investigator software package. Hoechst staining enabled the software package to detect cell nuclei. Cells

were stained with phalloidin for the actin cytoskeleton which defined the cell boundary and allowed for cell segmentation if necessary.

The intensity of the GR within the nucleus and cytoplasm was determined using an algorithm providing multi-parametric information on each of the channels. The optimisation of the analysis was carried out using vehicle treated cells as negative control and dexamethasone treated cells as positive control.

Using this antibody assay we similarly found that UDCA could induce translocation of the endogenous GR from the cytoplasm to the nucleus.

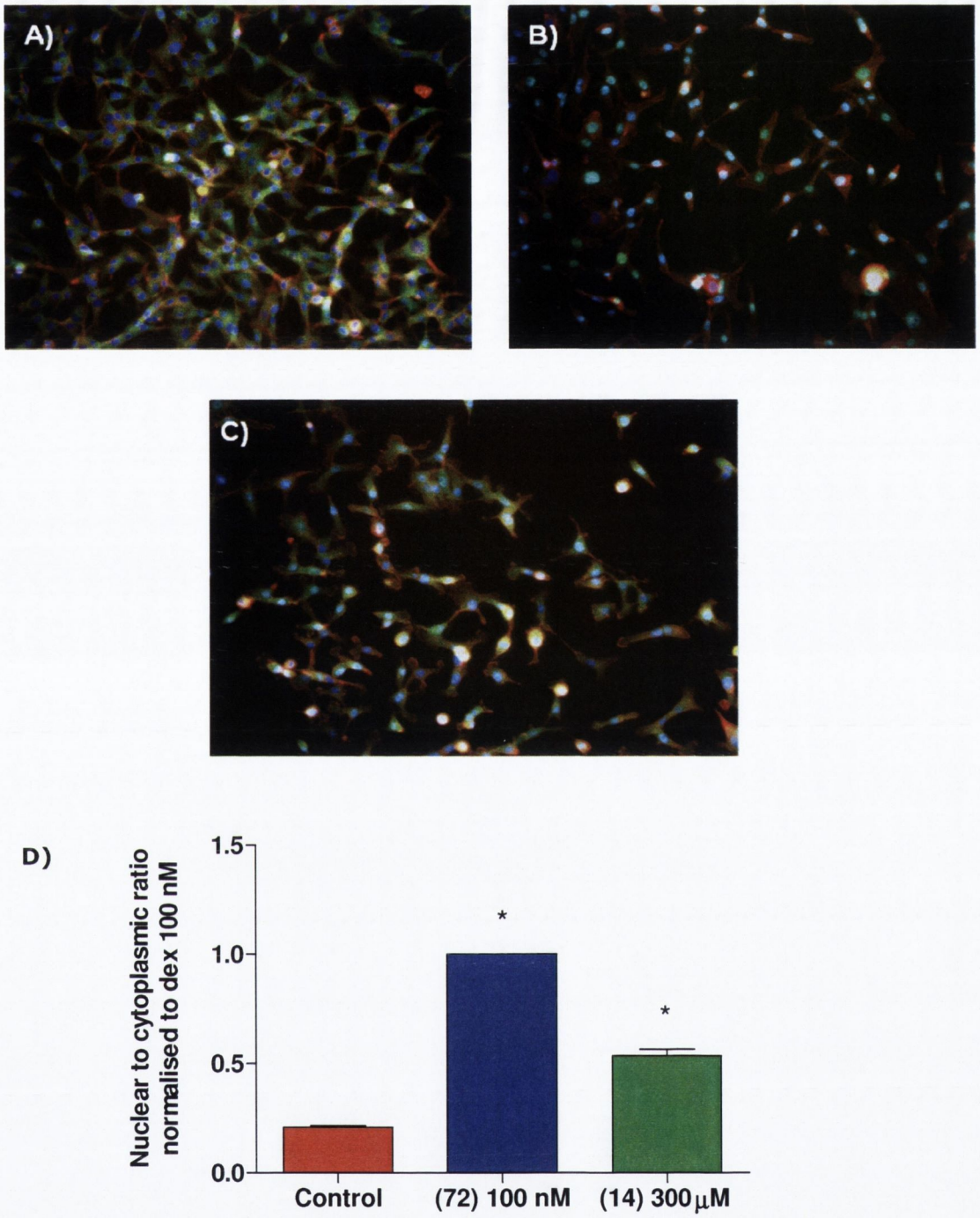

Figure 4.19 UDCA induces translocation of the GR. *SKGT-4 cells were A) untreated or B) treated with dexamethasone 100 nM or C) UDCA 300 μM for 4 h. Cells were fixed with paraformaldehyde 4% in PBS after 4 h. The GR was identified using a mouse monoclonal GR antibody (green) and cells were stained with Hoechst (blue) and phalloidin (red) to identify the nucleus and actin cytoskeleton. Cells were imaged using the GE In cell Analyser 1000. Original magnification, x10. D) Cells were analysed using the Investigator software package, Section 2.9.1. Values are normalised to nuclear to cytoplasmic ratio of dexamethasone 100 nM and are expressed as the mean*

*± SEM of two experiments performed in triplicate, * p< 0.05 relative to control, as determined by one-way ANOVA followed by Dunnett's post-hoc correction.*

Having carried out these proof of principle experiments showing that UDCA can induce translocation of endogenous GR in our esophageal model, we then went on to synthesise a panel of UDCA analogues.

4.3.2 Chemistry

4.3.2.1 Panel of compounds screened for GR translocation

Various studies have shown that the BA nucleus is an important structural determinant of activity against different nuclear and membrane receptors (Pellicciari *et al.*, 2004). For example Wang *et al* showed that the BA nucleus determined binding to the farnesoid X receptor (FXR) with LCA (3α-OH), CDCA and DCA showing FXR activity and UDCA showing none (Wang *et al.*, 1999). Similarly it was recently found that BA alcohols of the CDCA family showed most activity for the TGR-5 receptor (Iguchi *et al.*, 2009). Hence we decided to assemble a panel of compounds with modifications at the side chain of UDCA keeping in mind that subtle changes in the nucleus could result in dramatic changes in activity. Another reason for screening side chain derivatives is that natural BAs principally occur conjugated to taurine and glycine in the body (Maitra & Mukhopadhyay, 2004). Side chain modification produces derivatives which are not amenable to conjugation and hence would not be expected to exert different physicochemical and biological effects *in vivo*.

The amide derivatives in Scheme 4.1 and the series of UDCA derivatives in Table 4.3 were screened for their ability to induce GR translocation. We primarily focussed on the 24 position but also included the ketone series which had modifications at the 3, 7 and 12 positions. The synthesis of the derivatives in Table 4.3 has been described in Chapter 3.

Table 4.3 Panel of UDCA derivatives screened for GR translocation. *A panel of UDCA derivatives with modifications at the 24 position was assembled for screening in the GR assay along with the UDCA amides in Scheme 4.1. A series of oxo derivatives was also included in the panel.*

Nitriles/Alcohol	Acids	Esters	Oxo derivatives
24-Nitrile (**26**)	norUDCA (**24**)	MethylUDCA (**19**)	NCA (**36**)
UDCA Nornitrile (**55**)	BisNorUDCA (**25**)	Benzylester (**43**)	12-keto LCA (**35**)
UDCA bisnornitrile (**27**)			3,7-diketo acid (**39**)
UDCA alcohol (**28**)			3,7,12-triketo acid (**38**)

4.3.2.2 Synthesis of UDCA Amides

The preparation of UDCA amide derivatives is shown in Scheme 4.1. Briefly the 3- and 7-hydroxy groups of UDCA (**14**) were formyl protected followed by conversion to the acid chloride (**76**) using a thionyl chloride reflux. The amide was then prepared by reacting the acid chloride with the respective amine in dichloromethane with triethylamine as a base to neutralise the HCl formed during the reaction. Subsequent deprotection by hydrolysis using sodium methoxide in methanol afforded the UDCA amide derivatives shown in Scheme 4.1.

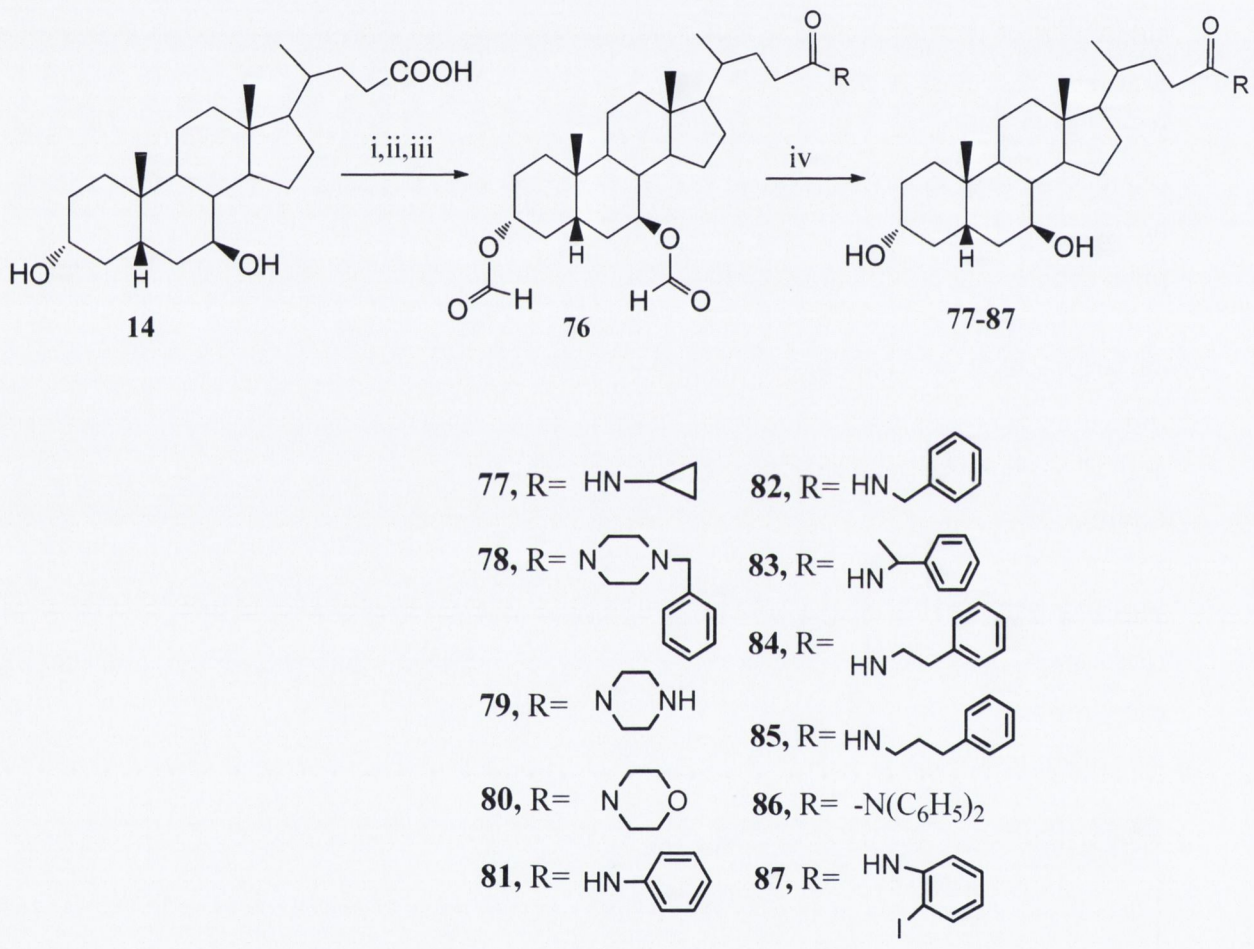

(i) Formic acid/perchloric acid, 47 °C, 3 h; (ii) thionyl chloride, reflux, 2 h; (iii) RNH_2, NEt_3, DCM, RT, 16-24 h; (iv) NaOMe/MeOH, reflux, 2 h.

Scheme 4.1 Synthesis of UDCA amides

4.3.3 BA derivatives induce translocation of the GR

The UDCA derivatives in Scheme 4.1 and Table 4.3 were tested in a high content screening assay for their ability to induce translocation. These derivatives were initially tested at a concentration of 300 μM for 4 h to investigate their effects on the GR.

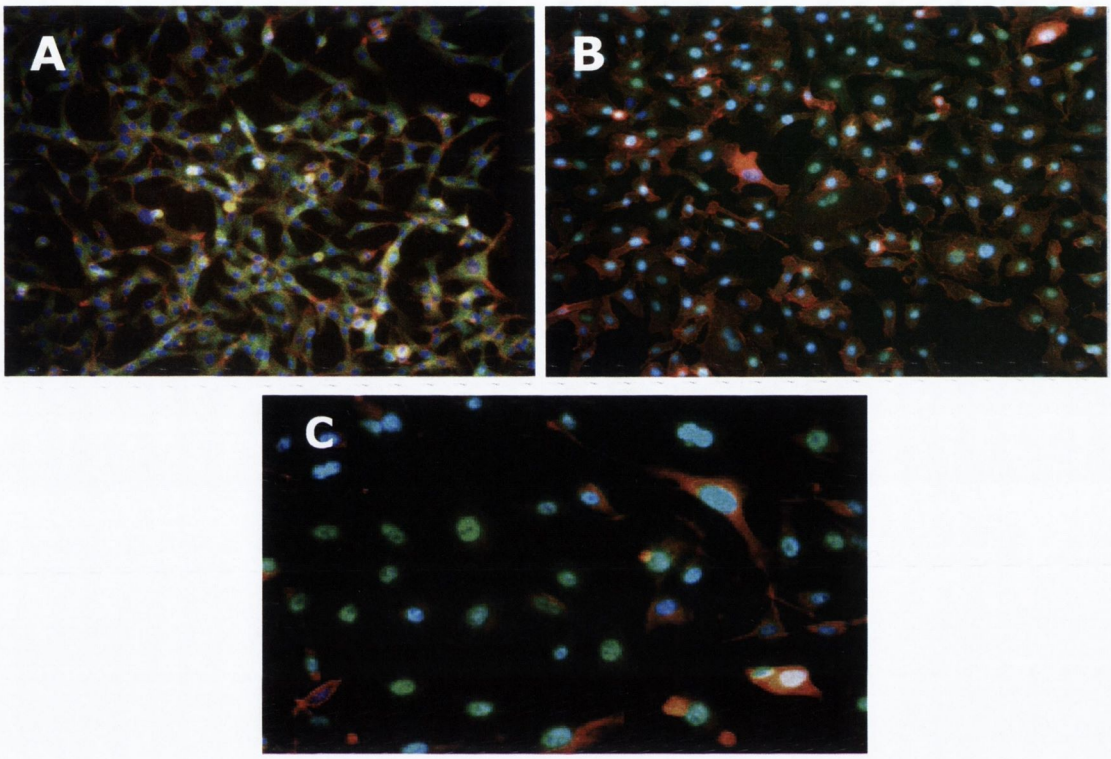

Figure 4.20 UDCA derivatives induce GR translocation. *SKGT-4 cells were A) treated with DMSO 1% or treated with B) CPA 300 μM (**77**) C) **79** 300 μM. Cells were fixed, stained and visualised as described in Figure 4.19. Original magnification, x10.*

It was clear from the images acquired, that the derivatives synthesised were able to induce GR translocation with greater efficacy than UDCA. Representative images are shown in Figure 4.20. Analysis of these images using the GE Investigator package gave the following results, Figure 4.21.

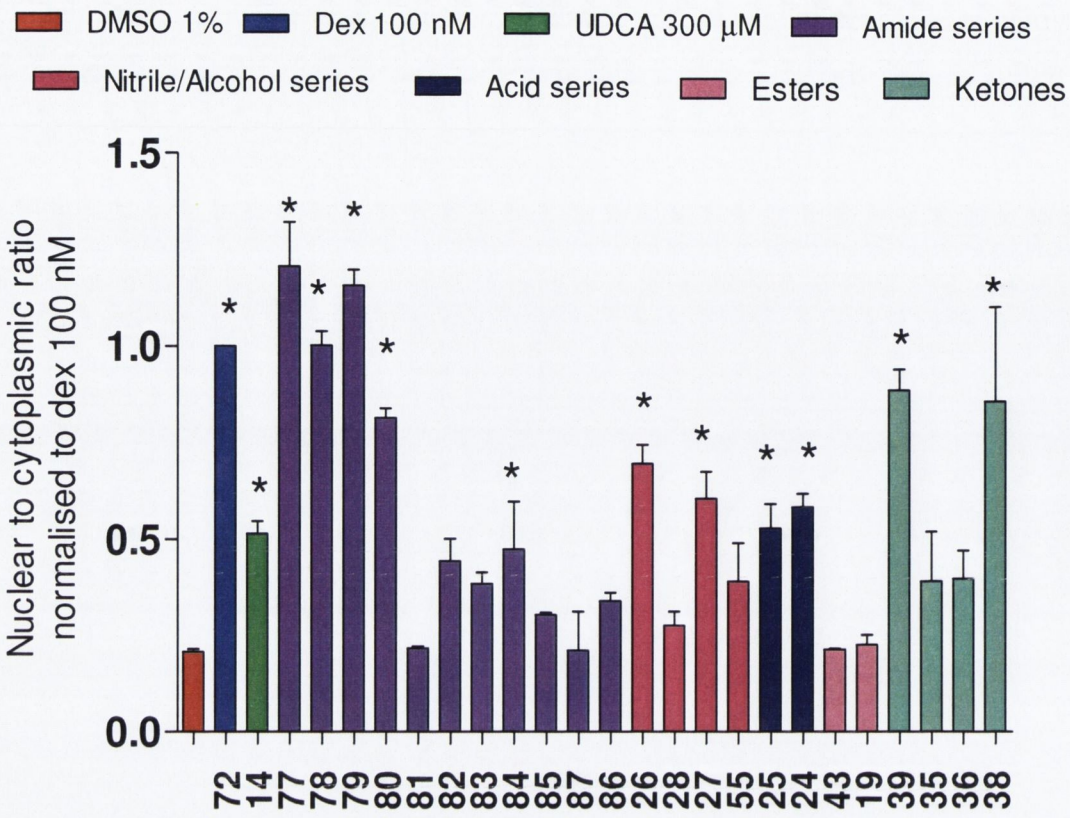

Figure 4.21 Analysis of GR translocation induced by UDCA derivatives. *SKGT-4 cells were treated with DMSO 1% as vehicle control treated with dexamethasone (**72**) 100 nM as a positive control, UDCA 300 µM (**14**) and A) amide derivatives B) nitrile derivatives C) norUDCA and BisNorUDCA D) ester derivatives and E) ketone derivatives. All BA derivatives were tested at 300 µM. After 4 h cells were fixed, stained, visualised and analysed as described, Figure 4.19. Values are normalised to nuclear to cytoplasmic ratio of dexamethasone 100 nM and are expressed as the mean ± SEM of two experiments performed in triplicate, *p< 0.05 relative to vehicle control as determined by one-way ANOVA and Dunnett's post-hoc correction.*

Six-point concentration effect curves were performed for those derivatives which showed increased translocation efficacy to UDCA. Concentration effect curves for CPA (**77**) and **78** are shown in Figure 4.22 as representative examples. EC_{50} values were generated in GraphPad Prism 5 and are shown in Table 4.4.

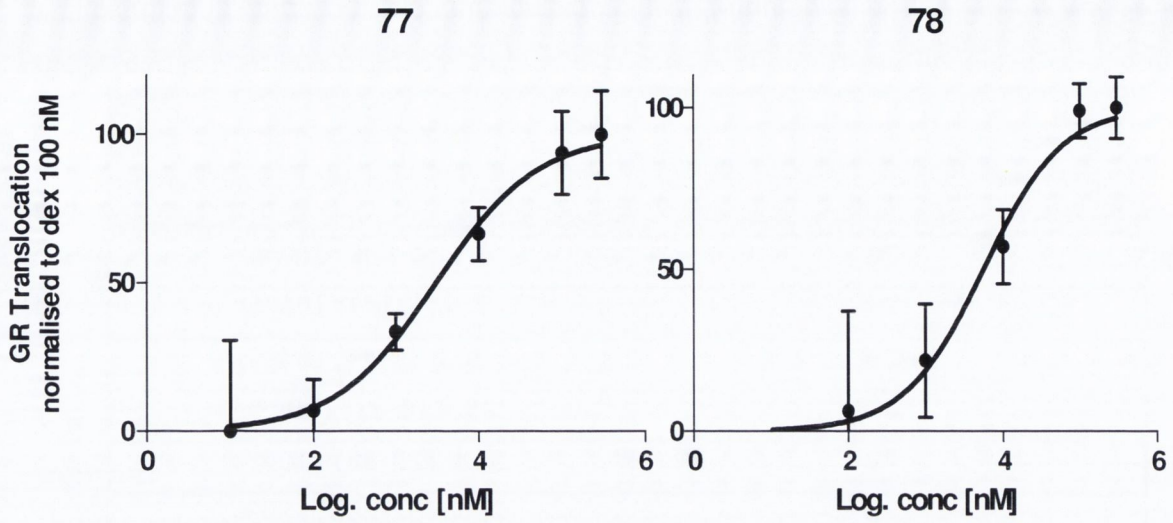

Figure 4.22 Concentration-effect curves for CPA (77) and benzypiperazinamde (78). *SKGT-4 cells were treated with DMSO 1% as vehicle control or indicated concentrations of CPA (**77**) or benzylpiperazine amide derivatives of UDCA (**78**). Values are normalised to nuclear to cytoplasmic ratio of dexamethasone 100 nM and are expressed as the mean ± SEM of two experiments performed in triplicate. Concentration effect curves were generated using non-linear regression models in GraphPad Prism 5.*

Table 4.4 EC_{50} values for GR translocation of UDCA derivatives. *EC_{50} values for translocation after 4 h of treatment were determined from six point concentration-effect curves generated using non-linear regression models in GraphPad Prism 5.*

Compound	EC_{50} (μM, 95% CI) (% efficacy of dexamethasone 100 nM at maximum)
78	5.6 (1-25) (100%)
77	7.4 (1-14) (100%)
39	20.8 (9-44) (84%)
80	25.3 (6-31) (100%)
79	50.8 (29-88) (100%)
25	99.7 (51-203) (59%)
38	104.0 (45-152) (81%)
24	105.3 (54-201) (58%)
82	109.5 (60-221) (49%)
83	123.5 (57-191) (49%)
84	109.0 (42-168) (53%)
27	130.0 (25-181) (59%)
26	100.1 (44-168) (70%)
14	298.7 (151-432) (54%)

The amide series produced the most potent and efficacious compounds. In particular, the cyclopropyl derivative (CPA, **77**) and the piperazine (**78**, **79**) and morpholine derivatives (**80**), had similar efficacy to dexamethasone 100 nM. **78** and **77** were the most potent compounds with EC_{50} values of 5.6 μM and 7.3 μM respectively. Removal of the benzyl group on the piperazine ring in **79** maintained GR translocation efficacy but reduced potency by ten-fold (50.8 μM). The anilinamide (**81**) did not induce translocation but the benzylamide (**82**), alpha-methylbenzylamide (**83**) and phenethylamide (**84**) showed equal efficacy to UDCA with increased potency of translocation, 109.5 μM, 123.5 μM and 109.0 μM respectively, although the confidence intervals were wide. Lengthening out the side chain further by one carbon produced an inactive compound (**85**).

Shortening the side chain but maintaining the acid functionality resulted in compounds with equal efficacy to UDCA but enhanced potency, norUDCA (**24**) (EC_{50} of 105 μM) and BisNorUDCA (**25**) (EC_{50} of 99.7 μM). The UDCA alcohol (**28**) did not induce

translocation but conversion of UDCA to a 24-nitrile (**26**) enhanced potency (EC_{50} of 100 μM, 70%). The bisnornitrile (**27**) (EC_{50} of 130 μM, 59%) showed similar efficacy and potency to **26** although the nornitrile (**55**) did not induce significant translocation. UDCA esters (**19**, **43**) did not induce GR translocation. These lipophilic compounds were expected to possess increased cell permeability and their lack of activity was surprising.

Oxidation to a 7-ketone in NCA (**36**) abrogated activity. However, interestingly the 3, 7 diketo acid (**39**) and the triketo acid (**38**), particularly the former showed excellent activity and potency. The 12-keto DCA did not induce translocation of the GR.

4.3.4 UDCA derivatives induce translocation in a time dependent manner

We next wanted to examine the rate at which UDCA derivatives induce translocation of the GR. The time course of a ligand-dependent protein event, such as GR translocation, is a function of the affinity of the ligand for the protein and the ligand concentration. Therefore dexamethasone 100 nM induced significant and maximum translocation of the GR at 30 min consistent with reported values, whereas at 100 pM the translocation is slower, only reaching significance at 120 min, Figure 4.23.

Pre-treatment of SKGT-4 cells with cycloheximide, an inhibitor of protein biosynthesis, did not affect CPA (**77**) induced GR translocation, Figure 4.24. Cycloheximide did not induce translocation of the GR by itself. Hence although induction of GR translocation through secondary signals cannot be ruled out these experiments indicate that CPA induced GR translocation occurs independent of protein translation and in a similar time frame to dexamethasone albeit at a lower rate.

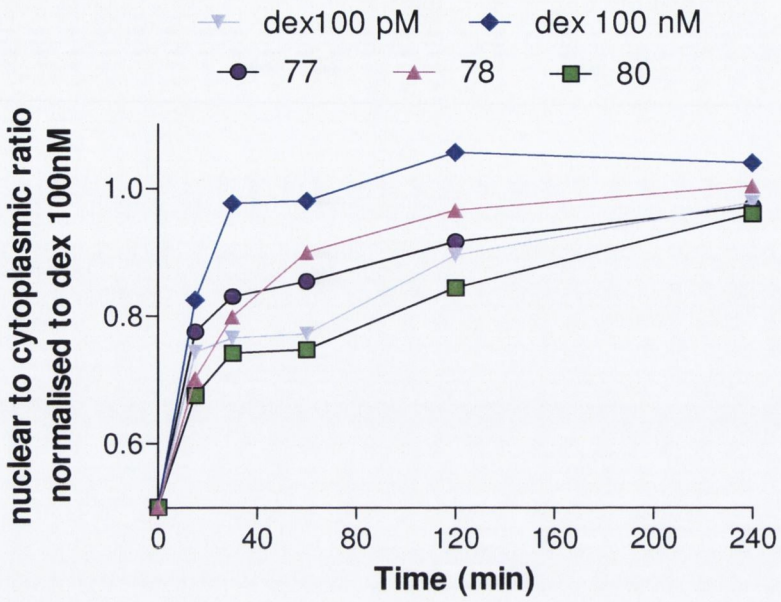

Figure 4.23 UDCA derivatives show similar translocation kinetics to dexamethasone. *SKGT-4 cells were treated with UDCA derivatives 100 μM or dexamethasone 100 pM and 100 nM for 15 min, 30 min, 60 min, 120 min or 240 min. Cells were fixed, stained and analysed for GR translocation as described in Figure 4.19. Values are normalised to nuclear to cytoplasmic ratio of dexamethasone 100 nM and are expressed as the mean ± SEM of two experiments performed in triplicate, *p<0.05 relative to DMSO 1% for* ***77*** *(120 min, 240 min),* ***80*** *(240 min),* ***78*** *(60, 120, 240 min), dexamethasone 100 pM (120 min, 240 min), dexamethasone 100 nM (30 min, 60 min, 120 min, 240 min).*

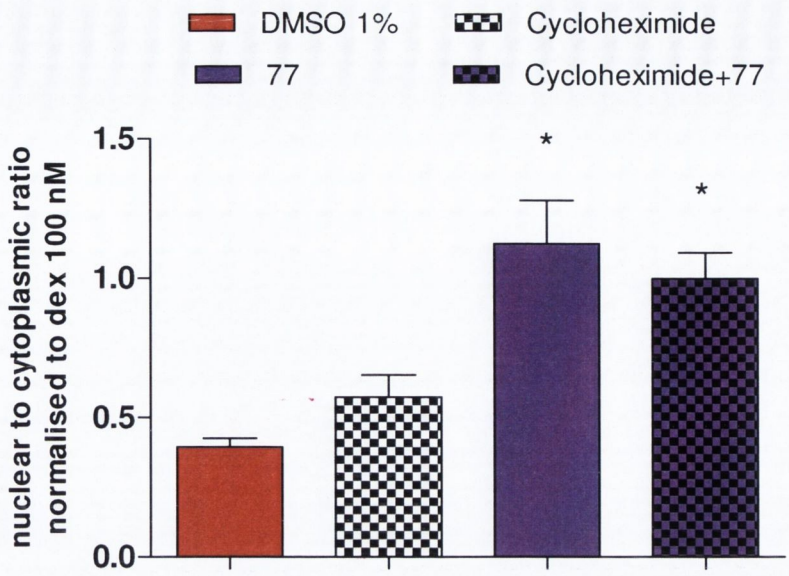

Figure 4.24 Cycloheximide does not inhibit CPA induced GR translocation. *SKGT-4 cells were treated with cycloheximide 2 μg/ml for 2 h. Cells were then co-treated with cycloheximide 2 μg/ml and CPA (**77**) 100 μM for a further 4 h. Cells were fixed, stained and analysed as described, Figure 4.19. Values are normalised to nuclear to cytoplasmic ratio of dexamethasone 100 nM and are expressed as the mean ± SEM of two experiments performed in triplicate, *p< 0.05 relative to DMSO 1% as determined by one-way ANOVA and Dunnett's post hoc correction.*

4.3.5 Amide derivatives of DCA and CDCA do not induce GR translocation

Having shown that UDCA amides were excellent inducers of GR translocation we wanted to investigate whether amide derivatives of other BAs could similarly induce translocation of the GR in order to determine whether GR translocation was dependent on the side chain or the core BA structure. In order to do this the cyclopropyl and benzylpiperazine derivatives of DCA (**4**) and UDCA's epimer CDCA (**5**) were synthesised as gifts from Mr. Ferenc Majer, Figure 4.25. These derivatives were screened for GR translocation at a concentration of 10 μM, the EC_{50} of translocation for **77** and **78**.

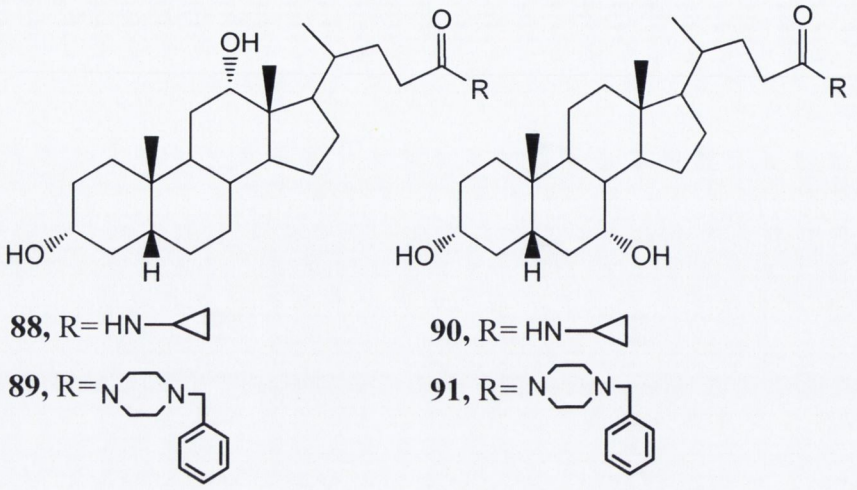

Figure 4.25 DCA and CDCA amides. *DCA and CDCA amides were synthesised in order to determine if GR translocation was dependent on the side chain or the core BA structure.*

It was found that the DCA and CDCA amides were unable to induce translocation indicating that this ability is restricted to specific amides with the UDCA core nucleus.

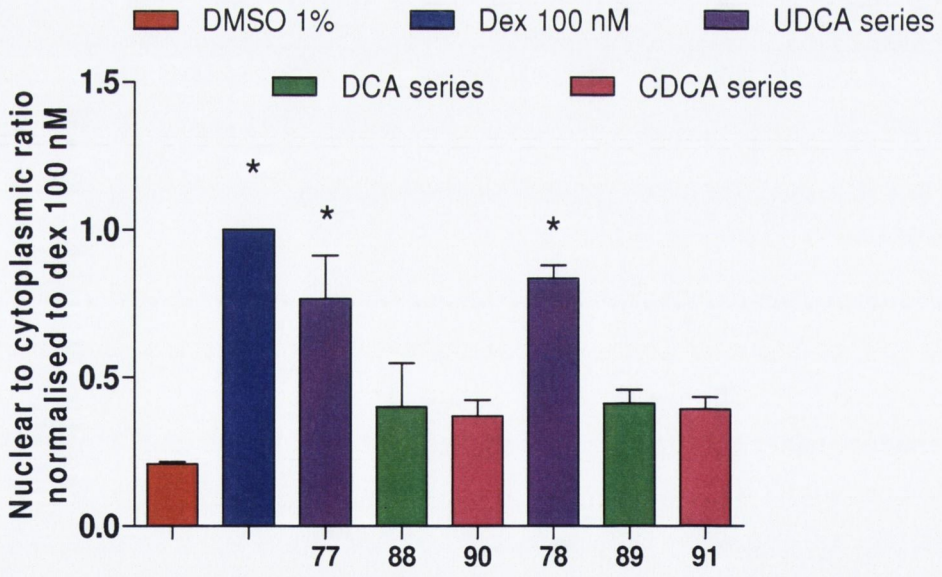

Figure 4.26 DCA and CDCA amides do not induce GR translocation. *SKGT-4 cells were treated with 1% DMSO, dexamethasone 100 nM as a positive control or cyclopropyl and benzylpiperazine amide derivatives of UDCA (**77**, **78**), DCA (**88**, **89**) and CDCA (**90**, **91**) at a concentration of 10 μM. This concentration was chosen as higher concentrations of the DCA and CDCA derivates were cytotoxic. Cells were fixed, stained and analysed for GR translocation as described, Figure 4.19. Values are*

*normalised to nuclear to cytoplasmic ratio of dexamethasone 100 nM and are expressed as the mean ± SEM of two experiments performed in triplicate, * $p < 0.05$ as determined by one-way ANOVA and Dunnett's post-hoc correction.*

4.3.6 Can UDCA and derivatives bind to the GR?

A physical interaction between UDCA and the GR has not been demonstrated to date. Evidence suggests that UDCA does not bind to the GR at the classical GC binding site. Weitzel *et al* showed that incubation of radiolabelled UDCA with the GR binding site expressed in a GR fusion protein yielded no specific binding of UDCA to the GR. Similarly Tanaka *et al* showed that UDCA did not displace tritiated dexamethasone from the GR binding site and also that specific binding of specially formulated tritiated UDCA to GR could not be detected in CHOpMTGR cells (Miura *et al.*, 2001; Weitzel *et al.*, 2005).

The curved L-shape of BAs is very different to the planar structure of conventional GCs and hence we decided to investigate, in silico, if it would be possible to dock UDCA into the GR LBD. Using the crystal structure of the GR bound to deacylcortivazol (**75**) we found that UDCA could be accommodated into the pocket with the carboxylic group extending out into the channel which accommodates the phenylpyrazole group of deacylcortivazol but still allowing for interaction of AF-2 with the co-activator peptide shown. Hence the molecule could be fitted into the LBD with the D ring in the position that the A ring of deacylcortivazol occupies.

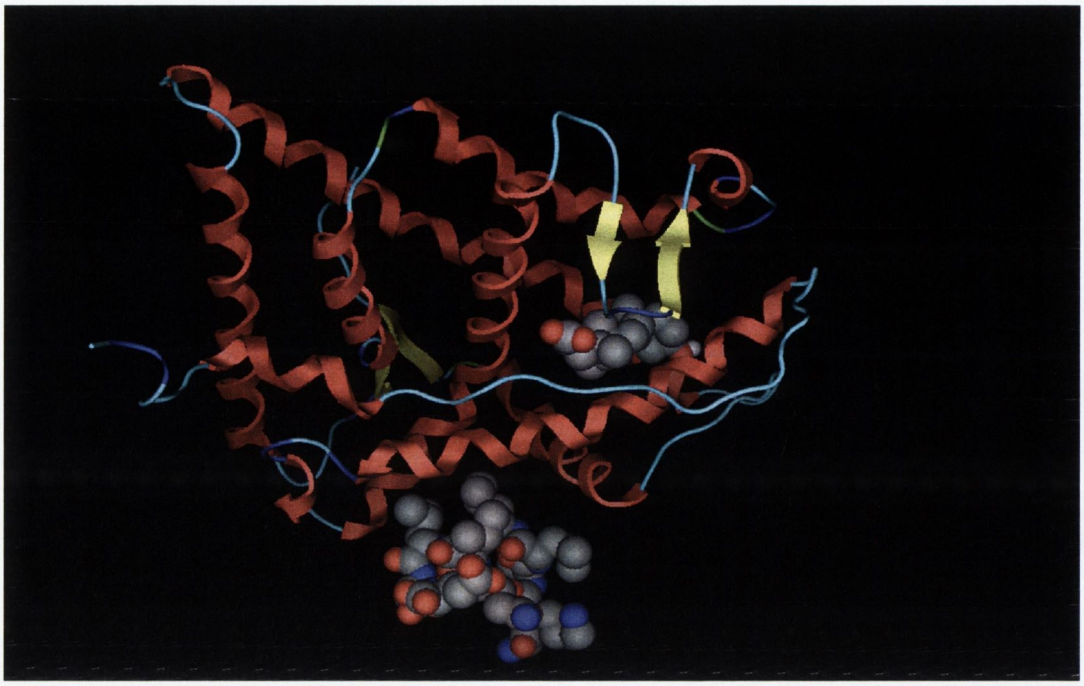

Figure 4.27 Docking UDCA into the GR. *This was visualised in MOE. The X-ray crystal structure was obtained from (Suino-Powell et al., 2008). UDCA and the co-activator peptide, SRC1-4, are shown as a space filling model.*

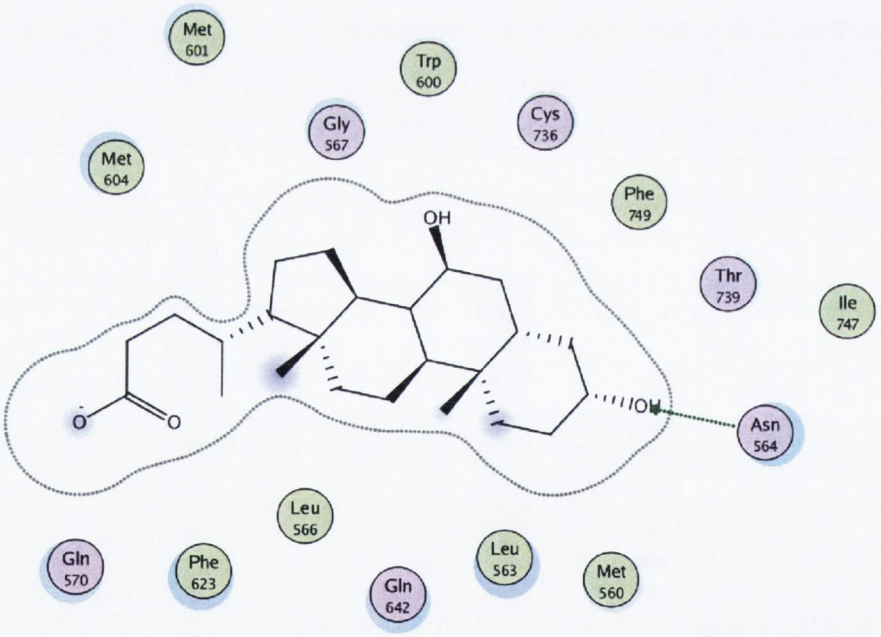

Figure 4.28 Potential interactions of UDCA with the GR LBD. *Generated using MOE.*

In dexamethasone (**72**) the 3 carbonyl oxygen on the A ring hydrogen bonds to the amide group of Gln570 (Onnis *et al.*, 2010). In deacetylcortivazol (**75**) the

phenylpyrazole in involved in the same interactions. Figure 4.28, shows that the carboxyl group on the acid side chain can potentially interact with Gln570 (Suino-Powell *et al.*, 2008).

The D ring of dexamethasone and deacetylcortivazol are the same. The 17-β-hydroxyl group interacts with Gln642 while the 21-carbonyl hydrogen with Thr739. The 11-hydroxyl in the C ring and the 24-hydroxyl in the D ring can interact with Asn654. This latter interaction can be seen with the 3α-hydroxyl of UDCA.

However, when a commercial radioligand binding assay was carried out it was found that neither UDCA or a selection of our derivatives at the indicated concentration could displace radiolabelled tritiated dexamethasone (3 nM [^{3}H] Dexamethasone) from the GR LBD, Table 4.5. The significance criteria was greater than 50% inhibition in radioactivity of the receptor-ligand complex, a decrease in activity indicating displacement of tritiated dexamethasone.

Table 4.5 Radioligand Competition Binding Assay. *A competition binding experiment was carried out in order to determine if UDCA and derivatives could displace dexamethasone from the GC binding site, section 2.16.*

Compound	Concentration	% Inhibition Radioactivity
24	10 μM	-10
55	10 μM	3
84	10 μM	23
36	10 μM	-2
39	10 μM	6
40	10 μM	18
CPA (**77**)	10 μM	17
UDCA (**14**)	50 μM	14
UDCA (**14**)	10 μM	2
Dexamethasone (**72**)	10 μM	Nonspecific binding control

The competition binding experiment indicates that UDCA and derivatives do not bind to the classical GR LBD used by conventional GCs, deacylcortivazol and indeed all dissociated compounds designed to date. This indicated that the UDCA derivatives may be inducing translocation secondary to another signalling event. However we did feel that the high efficacy of translocation and furthermore the similarity in

translocation kinetics to dexamethasone would not be possible without direct interaction with the GR. Hence we decided to carry out a time resolved fluorescence energy transfer (TR-FRET) assay, Section 2.17. In this assay a GR LBD is tagged with a glutathione-S-transferase (GST) to which a terbium-labelled anti-GST antibody (Tb-anti-GST Ab) binds. Binding of agonist to the nuclear receptor causes a conformational change in the LBD of the GR which results in recruitment of the co-activator peptide, a fluorescein labelled steroid receptor co-activator-1 peptide (Fl-SRC-1). When the terbium label on the anti-GST antibody is excited at 340 nm, energy is transferred to the fluorescein label on the co-activator peptide and detected as emission at 520 nm. Energy transfer can only take place however if the GR LBD and the co-activator peptide are brought in close proximity to each other which will only occur due to a conformational change in the GR LBD.

This assay showed that the CPA (**77**) derivative is capable of co-activator recruitment meaning that the derivative induces a conformational change in the LBD of the GR resulting in a FRET reaction between a terbium-GST tag and steroid receptor co-activator-1 with a fluorescein tag, Figure 4.29.

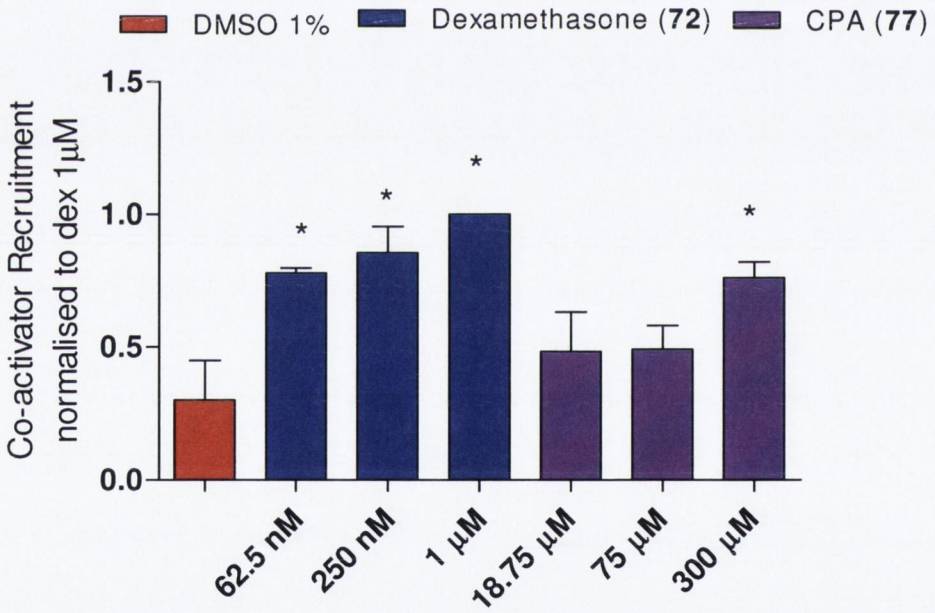

***Figure 4.29 GR FRET Co-activator recruitment assay**. A Lanthascreen™ TR-FRET Glucocorticoid Receptor Co-activator Assay kit was used to determine if the UDCA derivatives were capable of co-activator recruitment, Section 2.17. Dexamethasone and CPA (**77**) were incubated at room temperature for 3 h the indicated concentrations with a GST-tagged GR-LBD and a mixture of the fluorescein labelled co-activator peptide and the terbium labelled anti-GST antibody. Values represent the*

*mean ± SEM of three experiments performed in duplicate, normalised to positive control, dexamethasone 1μM, * p< 0.05 relative to control as determined by one-way ANOVA and Dunnett's post hoc correction.*

However we did find that the UDCA itself had no effect on co-activator recruitment even at very high concentrations, Figure 4.30. This is consistent with previous work by Miura *et al* which failed to show an interaction between UDCA and the co-activator TIF-2 (Miura *et al.*, 2001). The CDCA and DCA cyclopropyl derivatives (**88, 90**) could not induce this conformational change again underlying the importance of a UDCA nucleus for a GR interaction.

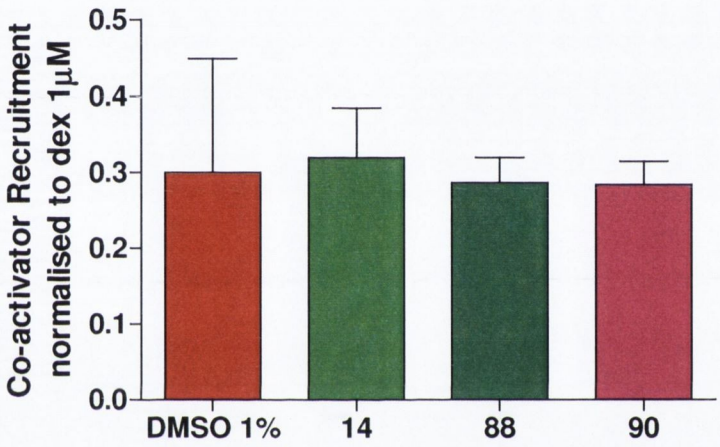

Figure 4.30 Co-activator Recruitment Assay. *A Lanthascreen™ TR-FRET GR Co-activator Assay kit was used to determine if UDCA (**14**), **88** or **90** (300 μM) derivatives were capable of co-activator recruitment. Values represent the mean ± SEM of three experiments performed in duplicate, normalised to positive control, dexamethasone 1μM.*

4.3.7 UDCA derivatives can induce transactivation and transrepression

The co-activator recruitment assay indicated that CPA (**77**) could induce a conformational change in the LBD, possibly by binding to an as yet unknown pocket of the GR LBD. We therefore wanted to investigate if CPA could induce transactivation of GREs. Using a gene reporter assay we found that CPA treatment of transiently transfected SKGT-4 cells with a GRE-firefly luciferase construct induced GRE transactivation in a concentration dependent manner, Figure 4.31. Hence CPA treatment induces a conformational change in the GR so that it can bind to GRE sequences and thereby alter gene expression.

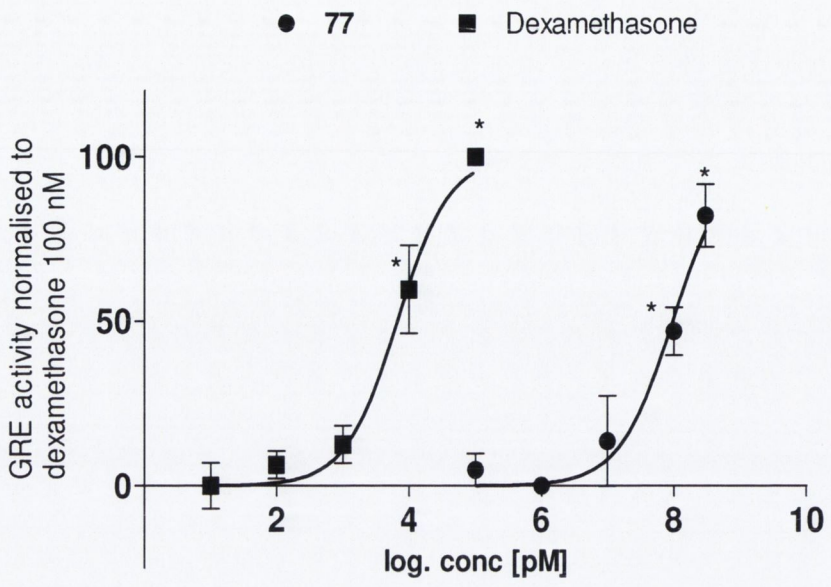

Figure 4.31 UDCA derivatives transactivate the GR. *SKGT-4 cells were transiently transfected with a mixture of an inducible GC responsive F.luc reporter and constitutively expressing Renilla construct (40:1), Section 2.13. Cells were treated with increasing concentrations of dexamethasone or CPA (**77**) for 16 h. Cells were then lysed and assayed for luciferase activity. F.luc activity was normalised to the internal vector control, R.luc to control for transfection efficiency. Values are expressed as the mean ± SEM of three experiments performed in duplicate, normalised to dexamethasone 100 nM.*

This experiment showed that CPA (**77**) is capable of inducing GRE transactivation in a concentration dependent manner with an EC_{50} of 124 μM. UDCA could only induce weak transactivation which was only significant at high concentrations (500 μM), Figure 4.32.

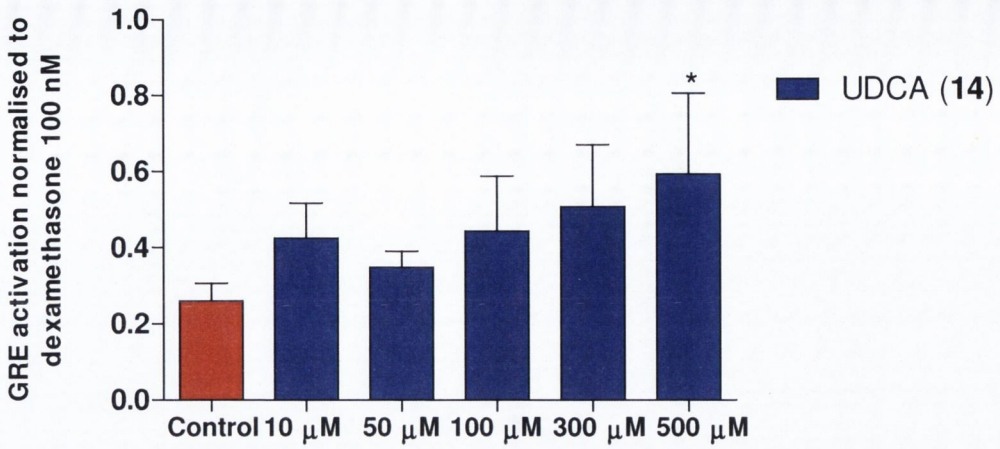

Figure 4.32 UDCA induces weak transactivation of the GR. *SKGT-4 cells were transiently transfected with a mixture of an inducible GC responsive F.luc reporter and constitutively expressing Renilla construct (40:1), Section 2.13. Cells were treated with increasing concentrations of UDCA for 16 h. Cells were then lysed and assayed for luciferase activity. F.luc activity was normalised to the internal vector control, R.luc to control for transfection efficiency. Values are expressed as the mean ± SEM of three experiments performed in duplicate, normalised to dexamethasone 100 nM. * $p < 0.05$ relative to untreated control as determined by one-way ANOVA and Dunnett's post hoc correction.*

Furthermore CPA was capable of transrepression decreasing TNF-α induced NF-κB activity (with an EC_{50} of 17 μM), Figure 4.33. This experiment was carried out in the HEK-293 cell line as attempts to do it in the SKGT-4 cell line were not successful. At the time that this experiment was performed we did not have access to a R.luc construct and so we had to normalise to β-gal activity. However the metabolism of the SKGT-4 cell line was slow and hence the ONPG production only occurred over long incubation times and never reached the linear range of the assay. Hence we used the HEK-293 cell line to as a proof of concept experiment to investigate if UDCA derivatives could suppress NF-κB activity.

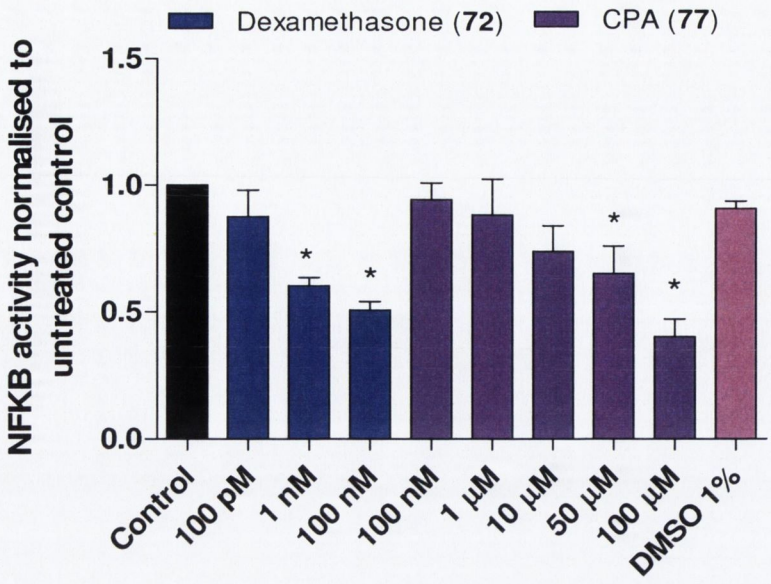

Figure 4.33 UDCA derivatives decrease NF-κB activity. *HEK-293 cells were transiently transfected with an inducible NFKB responsive F.luc reporter gene construct and a constitutively expressing β-galactosidase construct, Section 2.12. After 24 h the cells were treated with TNF-α 10 ng/µl alone or with TNF-α 10 ng/µl and varying concentrations of dexamethasone or CPA (**77**). After 16 h the cells were lysed and the lysates assayed for F.luc activity. Firefly luciferase activity was normalised to β-galactosidase activity to control for transfection efficiency. Values are expressed as the mean ± SEM of three experiments performed in duplicate, normalised to untreated control, * $p < 0.05$ relative to untreated control as determined by one-way ANOVA and Dunnett's post hoc correction.*

Taken together this data suggests that the derivative can bind to a non-classical site in the LBD of the GR and then proceed to induce transactivation of GC response elements and transrepression of pro-inflammatory cytokines. The binding is dependent on the BA nucleus and is specific to the UDCA ring.

4.3.8 Pharmacological Inhibitor Screen of CPA induced GR translocation

In order to investigate if GR translocation was occurring secondary to BA induced activation of other cellular pathways we decided to carry out a preliminary screen using a series of inhibitors. If pre-treatment with any of the inhibitors reduced or augmented CPA induced GR translocation then this could reveal the pathway or protein through which the derivative works.

***Table 4.6 Panel of Inhibitors**. A panel of inhibitors was assembled to investigate if GR translocation was occurring secondary to activation of other cellular pathways.*

Compound	Function
Geldenamycin	Hsp90 inhibitor
Rapamycin	FKBP52 inhibitor
Cyclosporin A	Calcineurin (Protein phosphatase 2B) Inhibitor
PD98059	ERK inhibitor
SB203580	p38 inhibitor (MAPK family)
GO6976	Conventional PKC inhibitor
Rottlerin	PKCδ inhibitor
Bisindolylmaleimide	PKC inhibitor
H89	MSK-1/PKA inhibitor
Primaquine	Inhibitor of endocytosis and recycling
Mifepristone	GR antagonist

We initially examined the effect of the inhibitors by themselves on GR translocation, Figure 4.34.

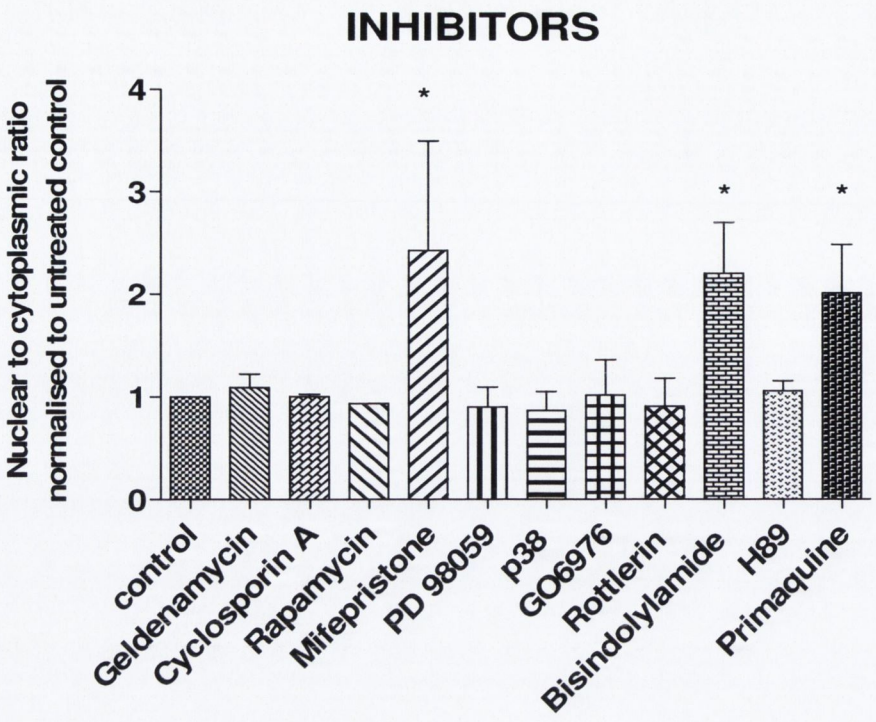

Figure 4.34 Analysis of GR translocation induced by a panel of inhibitors. *SKGT-4 cells were treated with 1% DMSO as control, geldenamycin 500 nM, cyclosporine A 100 nM, rapamycin 100 nM, mifepristone 100 nM, PD98059 10 μM, SB203580 10 μM, GO6970 1 μM, rottlerin 5 μM, bisindolylmaleimide 1 μM, H89 500 nM, primaquine 300 μM as shown for 4 h. Cells were fixed, stained, visualised and analysed in the usual way as described. Values are normalised to nuclear to cytoplasmic ratio of untreated control and are expressed as the mean ± SEM of two experiments performed in triplicate, * $p < 0.05$ relative to untreated control as determined by one-way ANOVA and Dunnett's post hoc correction.*

As mifepristone (**74**), bisindolylmaleimide and primaquine induced GR translocation by themselves these inhibitors were not included in the panel. Pre-treatment with the inhibitors for 30 min followed by treatment with CPA, UDCA or dexamethasone showed that out of the inhibitors selected only geldenamycin and rottlerin pre-treatment showed a decrease in translocation induced, Figure 4.35.

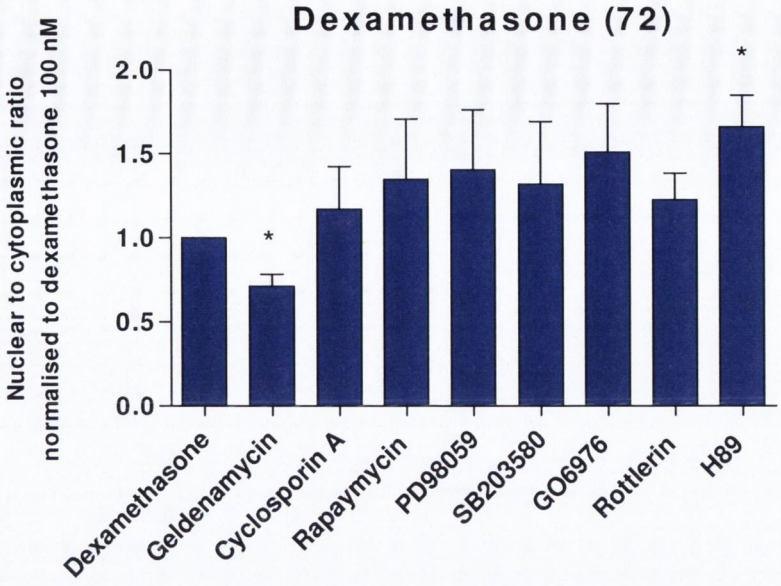
Dexamethasone (72)
Nuclear to cytoplasmic ratio
normalised to dexamethasone 100 nM
2.0
1.5
1.0
0.5
0.0
*
*
Dexamethasone
Geldenamycin
Cyclosporin A
Rapaymycin
PD98059
SB203580
GO6976
Rottlerin
H89

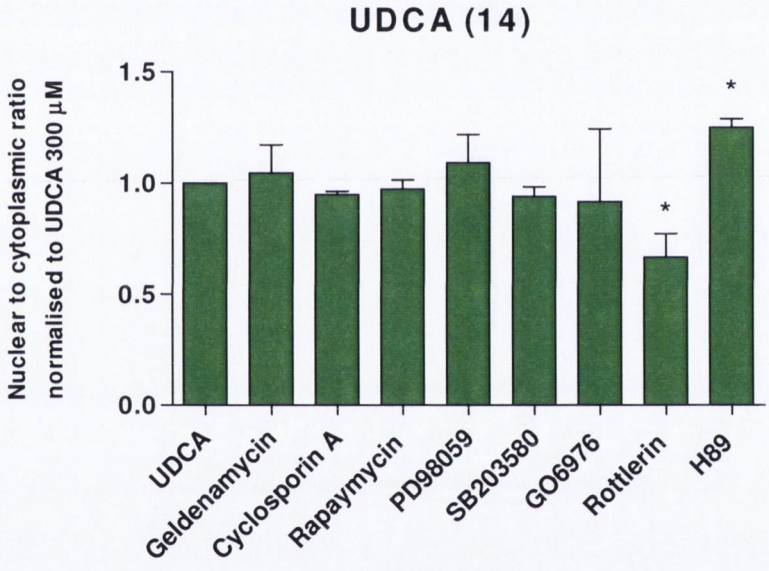
UDCA (14)
Nuclear to cytoplasmic ratio
normalised to UDCA 300 µM
1.5
1.0
0.5
0.0
*
*
UDCA
Geldenamycin
Cyclosporin A
Rapaymycin
PD98059
SB203580
GO6976
Rottlerin
H89

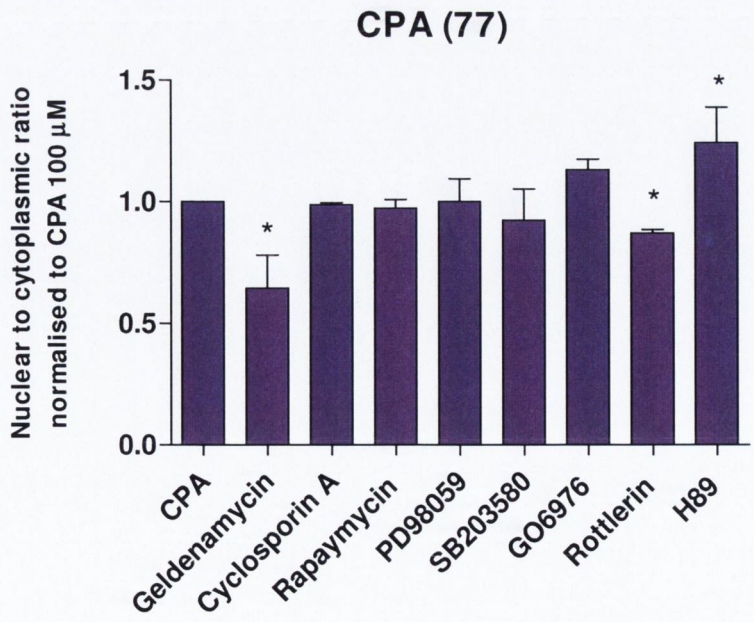
CPA (77)
Nuclear to cytoplasmic ratio
normalised to CPA 100 µM
1.5
1.0
0.5
0.0
*
*
*
CPA
Geldenamycin
Cyclosporin A
Rapaymycin
PD98059
SB203580
GO6976
Rottlerin
H89

Figure 4.35 Effect of inhibitors on dexamethasone, UDCA and CPA induced GR translocation. *SKGT-4 cells were treated with 1% DMSO as control, Geldenamycin 500 nM, Cyclosporin A 100 nM, Rapamycin 100 nM, PD98059 10 μM, SB203580 10 μM, GO6970 1 μM, Rottlerin 5 μM or H89 500 nM for 30 min prior to co-treatment with CPA 100 μM, UDCA 300 μM or dexamethasone 100 nM for a further 4 h as indicated. Cells were fixed, stained, visualised and analysed as described, Figure 4.19. Values are normalised to nuclear to cytoplasmic ratio of dexamethasone, UDCA or CPA as indicated and are expressed as the mean ± SEM of two experiments performed in triplicate, * $p < 0.05$ relative to dexamethasone, UDCA or CPA as determined by one way ANOVA and Dunnett's post hoc correction.*

Furthermore treatment with Geldenamycin is cytotoxic and so the reduction in nuclear to cytoplasmic ratio may be as a result of cell death, particularly as dexamethasone induced translocation is also reduced. Pre-treatment with Rottlerin only causes a decrease in translocation with CPA and UDCA. Unfortunately the selectivity of Rottlerin as an inhibitor of PKCδ has been called into question (Soltoff, 2007). Although it has been used in several studies for this purpose it has been shown to block activity of other kinases and non-kinase proteins (Soltoff, 2007). BAs have been shown to induce translocation of PKCδ (Shah *et al.*, 2005) and hence this inhibition of GR induced translocation could potentially be interesting. However due to the fact that Rottlerin may have multiple targets more studies would be required to verify these effects.
H89 treatment caused an increase in translocation induced by CPA, UDCA and dexamethasone. H89 inhibits both mitogen and stress activated protein kinase 1 (MSK1) and PKA. This is consistent with recent studies that have shown that combination of GCs and MSK1 inhibitors have an additive effect on repression of pro-inflammatory gene expression (Beck *et al.*, 2009). CPA and UDCA seem to share this additive effect but further work is required to investigate these effects more thoroughly.

4.3.9 TCA induces GR translocation

It was found during the course of our screening work for GR translocation that TCA (**12**) was a potent inducer of GR translocation with an EC_{50} in the same range as that of the most potent amides and the same efficacy as dexamethasone, Figure 4.37A. A time course experiment showed a similar time profile to dexamethasone, Figure 4.37B.

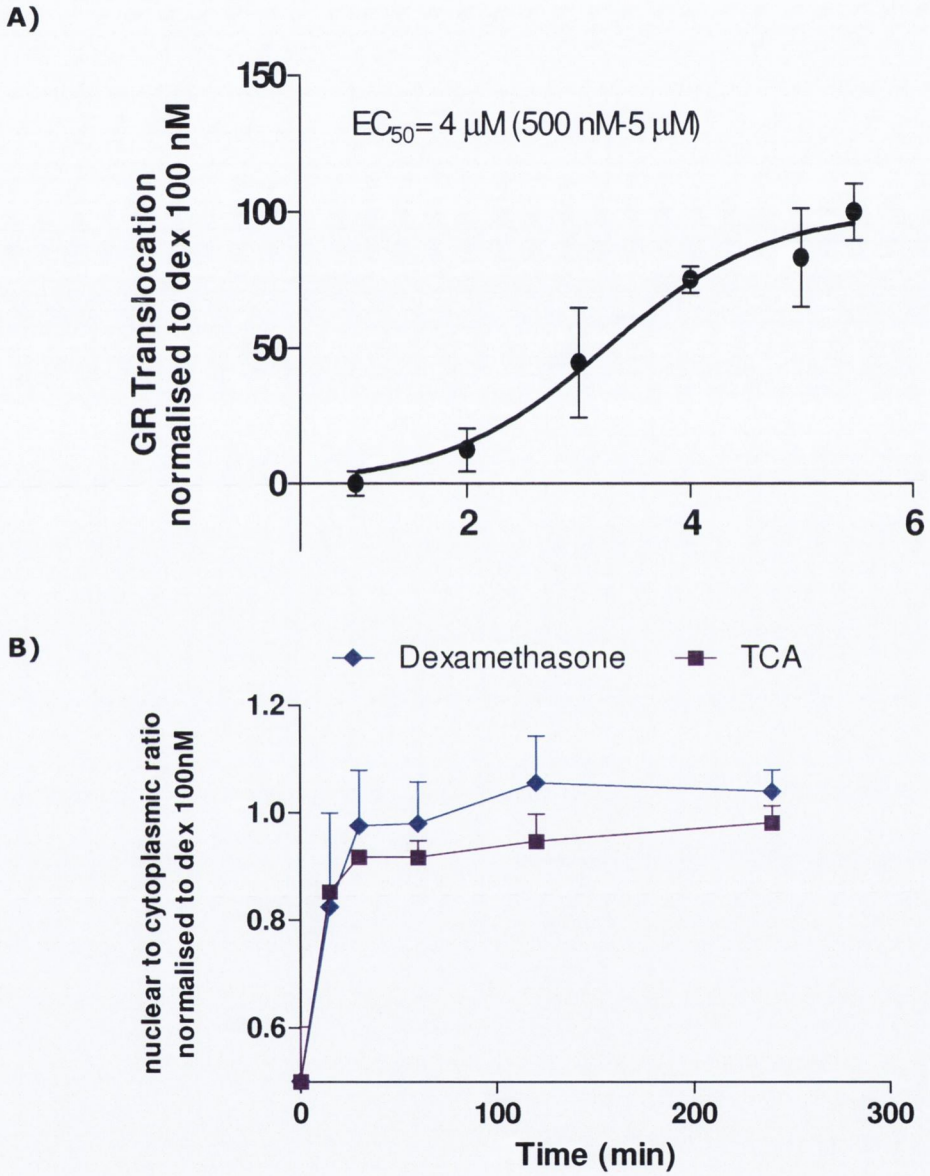

Figure 4.36 TCA is a potent inducer of GR translocation. A) *SKGT-4 cells were treated with indicated concentrations of TCA. Values are normalised to nuclear to cytoplasmic ratio of dexamethasone 100 nM and expressed as the mean ± SEM of two experiments performed in triplicate. Concentration effect curves were generated using non-linear regression models in Graph Pad Prism 5.* ***B)*** *SKGT-4 cells were treated with TCA 100 µM or dexamethasone 100 nM for 15 min, 30 min, 60 min, 120 min or*

240 min. Cells were fixed, stained and analysed for GR translocation as described in Section 2.9. Values are normalised to nuclear to cytoplasmic ratio of dexamethasone 100 nM and are expressed as the mean ± SEM of two experiments performed in triplicate, $p < 0.05$ relative to control for Dexamethasone 100nM (30 min, 60 min, 120 min, 240 min) and TCA (30 min, 60 min, 120 min, 240 min).

This observation is interesting for a variety of reasons. TCA is one of the predominant BAs present in human bile. Despite this no study has ever suggested an anti-inflammatory role for TCA. Indeed CA and its conjugates are generally regarded as inert BAs.

Furthermore the mechanism of this translocation is also interesting as it is not known whether a BA transporter is present in the SKGT-4 cell line. In the absence of a transporter the BA would not be permeable and hence the effect would be assumed to be cell surface mediated. This may be explained by a recently found membrane bound GC receptor (mGR). Bartholome *et al* demonstrated the existence of mGR on monocytes and B cells obtained from blood donors using high-sensitivity immunofluorescent staining (Bartholome *et al.*, 2004). This technique uses antibody conjugated magneto-fluorescent particles and so increases fluorescence intensity by 1000 fold allowing these molecules to be visualised. Interestingly over-expression of cytosolic GR does not lead to an increase in the expression of mGR and so it is believed that it is not cytosolic GR that has been transported to the cell surface. Hence it has been suggested that mGR is a variant of cytosolic GR but its origin, mechanism of action and function even remain unknown.

4.4 Discussion

Developing novel anti-inflammatory agents with high affinity for the GR but lacking the side effect profile of conventional GCs has been the focus of much research over the past few decades (Ali *et al.*, 2008; Barker *et al.*, 2006; Barnes, 1998; Newton & Holden, 2007; Regan *et al.*, 2006). UDCA's excellent safety profile during its clinical use for hepatic inflammatory diseases coupled with recent studies showing its ability to induce GR translocation make it an excellent candidate for such an anti-inflammatory agent (Angulo & Lindor, 1998; Miura *et al.*, 2001; Tanaka *et al.*, 1996). However, the concentrations at which UDCA causes translocation of the GR and immunosuppression *in vitro* are high (Miura *et al.*, 2001; Sola *et al.*, 2005; Sola *et al.*, 2004; Weitzel *et al.*, 2005). In this study we report an EC_{50} of 300 μM for GR translocation after 4 hours of UDCA treatment. Although UDCA concentrations in the liver and bile duct are much elevated during UDCA therapy (Setchell *et al.*, 1997) such high concentrations are never reached in blood serum (Ewerth *et al.*, 1985) thus limiting UDCA's therapeutic utility as an anti-inflammatory agent to specific organs.

Additionally, UDCA's potency makes studying its biological effects challenging. UDCA's mechanism of action in the treatment of hepatic diseases remains unknown. Although it can cause translocation of the GR from the cytoplasm to the nucleus in multiple cell systems (Miura *et al.*, 2001; Sola *et al.*, 2005; Tanaka *et al.*, 1996), studies are conflicted over its ability to activate GRE's, (Miura *et al.*, 2001; Sola *et al.*, 2005; Tanaka *et al.*, 1996; Weitzel *et al.*, 2005) and a physical interaction between UDCA and the GR has yet to be demonstrated.

Thus, our decision to make UDCA derivatives was driven by the desire to produce analogs with increased potency and efficacy which could serve as useful tools for further characterising UDCA's mechanism of action and understanding its interactions with the GR. We also felt that UDCA's cytoprotective and chemopreventative effects in colon cancer were a good basis for selecting it as a lead molecule for synthesis of anti-inflammatory agents targeting esophageal inflammatory disorders which can progress to esophageal adenocarcinoma (Fitzgerald *et al.*, 2002; Fitzgerald *et al.*, 2001).

Although a greater number of compounds are required to develop comprehensive structure activity relationships for GR translocation, there are definite patterns in the panel of compounds produced so far. Shortening of the acid side chain produces compounds of equal efficacy but increased potency as does replacing the acid with a nitrile. Amidation of the acid side chain increases efficacy and potency in general. Interestingly esterification (**19**, **43**) abolished activity as did reduction to the alcohol (**28**). This indicates that increasing lipophilicity and hence cell penetration does not result in increased GR translocation. The mono oxo- derivatives had reduced translocation efficacy compared to UDCA but the diketo (**39**) and triketo (**38**)

compounds were potent inducers of translocation. Out of the derivatives synthesised the amide series was found to be the best with the cyclopropyl (**77**) and benzylpiperazine amide (**78**) derivatives of UDCA having the greatest potency. The next series of compounds to be synthesised could include the cyclopropyl and piperazine derivatives of the diketo compound (**39**) and also of norUDCA (**24**) and BisNorUDCA (**25**). It would also be important to tease out the optimal structure of the amide side chain through synthesis of a large number of amide derivatives.

We found that the GR translocation was specific to the UDCA nucleus as both the cyclopropyl and benzylpiperazine derivatives of DCA and CDCA did not induce translocation (**88-91**). This is of significance as it confirms the importance of the UDCA nucleus and β orientation at the 7 position. The abrogation of translocation in the 7-keto derivative (**36**) supports this but the activity of the di- and triketo derivatives is somewhat contradictory of these observations. One must assume that the shape of these oxo- derivatives allows for interaction with the GR in a way that is not possible in the presence of a 3α-OH group. Hence manipulation of the 3-position would also be important in a future series of compounds.

The compounds tested here were not toxic during the time frame of any of the assays. Interestingly however the cyclopropyl and benzylpiperazine derivatives of DCA and CDCA were very toxic (**88-91**). This is an interesting observation in the light of our findings in Chapter 3 and of interest as structurally similar piperazine derivatives of DCA and LCA have been recently described by El Kihel *et al*, Figure 3.1 (El Kihel *et al.*, 2008) with the most potent compound having an LD_{50} of 8.5 μM in cytotoxicity assays. It would be interesting to test these derivatives in such assays as they could potentially be exploited for their cytocidal effects.

Previous authors have suggested that UDCA may interact with the cell membrane and set up a series of cytoplasmic events through secondary signals, one of which may be GR activation (Miura *et al.*, 2001; Sola *et al.*, 2004). Although we cannot rule out that the derivatives induce translocation due to secondary signals the higher log P of the amide derivatives would certainly result in diffusion through the cell membrane and allow for interaction with the GR. Furthermore translocation is induced independent of protein biosynthesis and although the derivatives display a slower rate of translocation to dexamethasone 100 nM which reaches maximal translocation at 30 minutes this is probably due to their weaker affinity for the GR as dexamethasone 100 pM displays a slower profile as well.

CPA was able to recruit steroid receptor co-activator 1-4 in a FRET assay and could induce transactivation of GRE's in a sigmoidal fashion, with an EC_{50} of 124 μM. Furthermore the derivative could induce transrepression of TNF-α stimulated NF-κB showing the same efficacy as dexamethasone 100 nM.

Puzzlingly however, we found that UDCA and none of our derivatives were able to displace tritiated dexamethasone from the GR binding site. GR activation can be regarded as consisting of two principal steps. In the first step, a conformational change in cytoplasmic GR exposes a nuclear localisation signal which results in nuclear translocation. In the second step binding of the GR to GREs allows for recruitment of co-activators to the AF-1 and AF-2 helix domains. The LXXLL motif of co-activators can only bind to helix 12 however if it has been locked into the active conformation. It is generally thought that ligand binding is essential for both steps to occur.

Pariante *et al*, however, demonstrated that the tricyclic antidepressant desipramine could induce translocation of the GR from the cytoplasm to the nucleus (Pariante *et al.*, 1997). Similar to CPA, desipramine could not displace dexamethasone from the GR binding pocket in a radioligand competition binding experiment. The authors suggest that the compound may be binding to hsp90 complex resulting in dissociation from the GR and subsequent translocation. In this study we found that pre-treatment of the SKGT-4 cell line with the hsp90 inhibitor did decrease CPA induce GR translocation but this was seen in dexamethasone as well and because geldenamycin is potently cytotoxic it is hard to derive conclusive information from the experiment. FKBP52 is another chaperone protein bound to the GR, Figure 4.4. Therefore we investigated the effect of the FKBP52 inhibitor, rapamycin, but found there was no effect on CPA induced GR translocation.

Crucially however desipramine differs from CPA in its inability to induce activation of the GR alone, although it does potentiate dexamethasone mediated GR transcription. In the case of CPA even if we consider that nuclear translocation of the GR is occurring independent of direct ligand binding, it is hard to account for the second step in GR activation which requires helix 12 to be in an active conformation for recruitment of co-activators. Nuclear translocation of the GR is not sufficient to induce this conformational change in helix 12 as antagonists such as mifepristone also induce GR translocation (Pariante *et al.*, 2001). CPA seems to induce this active conformation as it resulted in co-activator recruitment in a TR-FRET assay, albeit at high concentration (300 μM). It is hard to understand how this active conformation could be induced without direct binding of a ligand. Binding could potentially be occurring at an unknown binding pocket in the GR LBD. CPA could be binding to helix 12 itself stabilising it in an active conformation. Further structural analysis is required to confirm such a theory. An isotopically labelled GR LBD domain could be used for mapping the interactions of the ligand with the LBD. Microcalorimetry and surface plasma resonance studies with the GR LBD could also be carried out to determine the dissociation constant of the derivative.

Another potential mechanism of CPA effects could involve inhibition of the enzyme 11βHSD, Figure 4.7. 11βHSD1 and 11βHSD2 maintain an equilibrium between cortisone and cortisol. Interestingly BAs, including CDCA and UDCA have been shown to bind to and inhibit rat microsomal 11βHSD1 with a *K*i of 15 μM and 200 μM respectively (Maeda *et al.*, 2010). Stauffer *et al*, showed that CDCA and DCA can inhibit 11βHSD2 (Stauffer *et al.*, 2002). The authors also demonstrated that inhibition of 11βHSD2 by DCA and CDCA resulted in translocation and activation of the MR in response to low concentrations of cortisol (Stauffer *et al.*, 2002). It would be interesting to investigate if CPA could inhibit 11 βHSD1 which would provide an elegant explanation for its effects on GR translocation, transactivation and transrepression.

In this work a pharmacological inhibitor screen was also conducted to investigate other cellular pathways which may be involved in CPA induced GR translocation. The work was only preliminary, however, there is string indication that PKCδ may be involved as pre-treatment with the PKCδ inhibitor rottlerin resulted in a decrease in CPA induced translocation. This was interesting as BAs have been shown to activate various PKC isoforms (Rao et al., 1997). Rottlerin however is an non-specific inhibitor and therefore this effect should be validated using a siRNA for PKCδ.

Another interesting observation made during these investigations was the ability of TCA to induce GR translocation. The SKGT-4 cell line is not known to have BA transporters and hence TCA would not be expected to be membrane permeable and to bind to the GR. It is possible that TCA is binding to a mGR however further experimental work would be required to verify this. It would be interesting to investigate if CPA could still induce GR translocation is passive diffusion was blocked. This might indicate that the mechanism of BA induced translocation is mGR dependent.

To date all known GR modulators, including dissociated steroids have only shown binding to the classical GC binding site (Barker *et al.*, 2006; Belvisi *et al.*, 2001a; Newton & Holden, 2007; Regan *et al.*, 2006). Regardless of the mechanism of action of CPA and the other derivatives presented here, the compounds represent a novel mechanism for GR activation.

A new mechanism of action for GR activation could result in novel anti-inflammatory compounds. Our lead compound shows the same selectivity for transrepression over transactivation as dexamethasone and hence cannot be classified as a dissociated steroid. Further development could separate these effects. However in the context of the ongoing debate regarding dissociated steroids the gene expression profile of these compounds would determine their real clinical utility and side effect profile. The fact

that the derivatives are based on a compound which has minimal history of side effects would support their potential use as gene selective compounds.

5 CHAPTER FIVE

RESULTS

Bile acid interactions with the secretory pathway-implications for carcinogenesis

Chapter V

5.1 Introduction

The ability of a cell to evade cell death through classical apoptosis pathways is regarded as one of the hallmarks of cancer. Consequently, in recent years researchers have focussed on alternative apoptotic and non-apoptotic pathways as potential targets of pharmacological therapies to contribute to tumour cell demise (Wlodkowic *et al.*, 2009). In particular it has been shown that components of the secretory pathway such as the endoplasmic reticulum (ER) and Golgi apparatus are involved in sensing cellular stress and initiating cell death pathways (Maag, Hicks & Machamer, 2003; Wlodkowic *et al.*, 2009). Moreover, it has also become apparent in recent years that activation of stress in these organelles, particularly in the ER, is a common manifestation of many tumours and it is now believed that an ER stress response plays a critical role in tumour cell development and in the ability of a tumour cell to metastasise (Healy *et al.*, 2009; Lee & Hendershot, 2006). This chapter is focused on investigating the effects of BAs on the secretory pathway focussing initially on the Golgi apparatus and then moving towards the ER.

5.1.1 Structure and Function of the Golgi apparatus

The Golgi is typically located in the juxtanuclear region of the cell around the centrosome. It is composed of a ribbon like system of membranes that are closely apposed and aligned in parallel to form stacks, Figure 5.1 (Shorter & Warren, 2002). It is composed of three main compartments: the cis-, medial and trans-Golgi, the cis Golgi being the face closest to the ER. The compartments consist of membranous stacks of flat disc-shaped cisternae and tubulovesicular networks found on either face of the Golgi stack, the cis-Golgi network (CGN) and the trans-Golgi network (TGN). The Golgi architecture is conserved through eukaryotic evolution and is present even in the most primitive of eukaryotes, the Giardia lamblia (Shorter & Warren, 2002).
Studies by Shorter *et al* investigated the mechanism of Golgi stacking and revealed that Golgi stacking occurs through a cisternal tethering reaction involving the proteins p115, giantin and GM130 (Shorter & Warren, 1999). GM130 is a peripheral cytoplasmic protein that is tightly bound to Golgi membranes. The protein is predominantly located in the CGN and has shown overlap with the CGN marker, syntaxin5. It is particularly important in maintaining cis-Golgi structure (Nakamura *et al.*, 1995). The peripheral membrane proteins GRASP65 and GRASP55 are found in the cis and medial Golgi and also play an integral role in the cisternal stacking interactions (Shorter *et al.*, 1999).

Membrane tubules are also a predominant feature of the Golgi although the exact role of these is still somewhat unclear. They are potentially involved in the recycling of resident Golgi proteins back to the ER (Cole *et al.*, 1998; Glick, 2000).

The Golgi occupies a central position in the secretory pathway as it receives polypeptides from the ER and acts to post-translationally process and ultimately transport and sort cargo to their final destinations (Shorter & Warren, 2002). Specifically the CGN functions to receive the biosynthetic output from the ER whereas the TGN sorts completed post-translationally modified products. Enzymes in the Golgi including glycosyltransferases conjugate proteins with diverse patterns of glycans.

The Golgi also serves as the major site of sphingolipid biosynthesis within the cell acting as a buffer between the glycerolipid-rich ER and the sterol/sphingolipid-rich plasma membrane (Holthuis *et al.*, 2001).

.

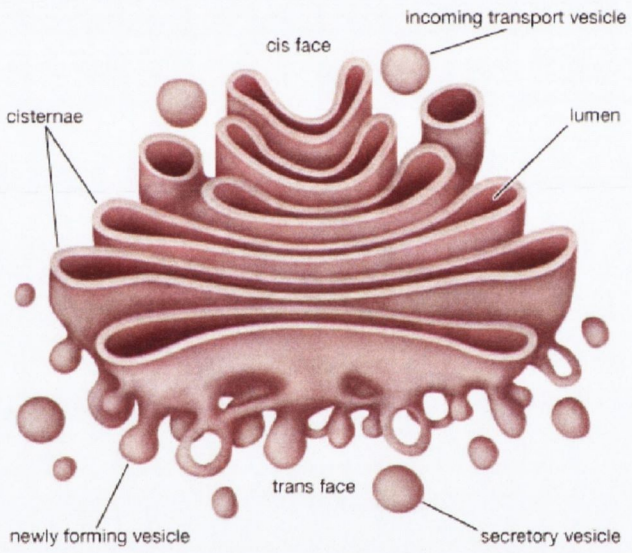

Figure 5.1 Structure of the Golgi apparatus. *The Golgi apparatus is composed of a ribbon like system of membranous stacks of flat disc-shaped cisternae. Cargo enters the Golgi at the cis face and then travels through the medial Golgi to the TGN.*

5.1.1.1 Trafficking to, through and from the Golgi

Following synthesis in the ER, newly formed proteins are initially packaged into coat protein II (COPII)-coated vesicles at the transitional ER, which is a specialised site in the ER that lacks bound ribosomes. These proteins then enter an intermediate compartment referred to as the ER-Golgi intermediate compartment and these clusters translocate to the Golgi, potentially along the microtubule networks to form the CGN (Glick, 2000).

There are conflicting opinions on movement of cargo through the Golgi itself. In the stable compartment model it is proposed that COPI vesicles carry the secretory cargo forward but exclude the resident Golgi proteins. In the cisternal maturation model it is proposed that entire cisternae carry the secretory cargo forward and the COPI vesicles move back through the Golgi recycling resident Golgi proteins to younger cisternae (Glick, 2000). Convincing evidence exists for both models opening up the possibility that there are multiple mechanisms of transport through the Golgi. Either way, when the cargo reaches the TGN there are several types of transport carriers formed (Mellman & Simons, 1992). These include clathrin-coated vesicles which deliver protein to the endosomal/lysosomal and vacuolar compartments.

These carriers are dissociated from the TGN by a controlled process termed membrane fission. Once cargo accumulates at the TGN, a G protein coupled receptor (GPCR) activates a trimeric G protein at the TGN resulting in the activation of PKCη and recruitment and phosphorylation of PKD. PKD can then activate downstream targets to control membrane carrier fission (Bard & Malhotra, 2006).

5.1.1.2 Golgi Fragmentation

There is a general consensus in the literature, that during cell division the Golgi undergoes dramatic structural changes involving fragmentation and dispersal (Colanzi, Suetterlin & Malhotra, 2003a). However, opinion is greatly divided amongst the leading investigators in the field about the specific fate of Golgi membranes. Certain investigators believe that the Golgi proteins fuse with the ER during mitosis (Zaal *et al.*, 1999), others that the Golgi fragments into small vesicles (Jesch *et al.*, 2001), yet others believe that the Golgi disassembles into bigger tubular-reticular elements (Shima *et al.*, 1997).

Most investigators however agree that in late prophase the Golgi stacks break down into smaller membranes and that during pro-metaphase and early anaphase these membranes undergo further fragmentation (Colanzi *et al.*, 2003a). The Golgi then reassembles during telophase (Gonatas, Stieber & Gonatas, 2006). The three enzymes that have been identified to mediate this conversion are the mitogen-activated protein kinase (MAPK) kinase 1 (MEK1), polo-like kinase 1 and Cdc2 kinase, Figure 5.2.

MEK1 is found on Golgi membranes during late prophase but is absent from the smaller fragments found during pro-metaphase and anaphase. Colanzi *et al* propose that MEK1 phosphorylation of GRASP55 in prophase may be responsible for the disassembly of the Golgi (Colanzi, Sutterlin & Malhotra, 2003b). Cdc2 kinase is required for the second step in the conversion to small fragments. The Golgi protein GM130 is known to bind to the COP1-vesicle associated protein p115 which tethers COP1 vesicles to the Golgi cisternae. However *in vitro* studies have shown that Cdc2

kinase can phosphorylate GM130 decreasing its interaction with p115 and resulting in the formation of vesicles (Colanzi *et al.*, 2003a; Lowe *et al.*, 1998).

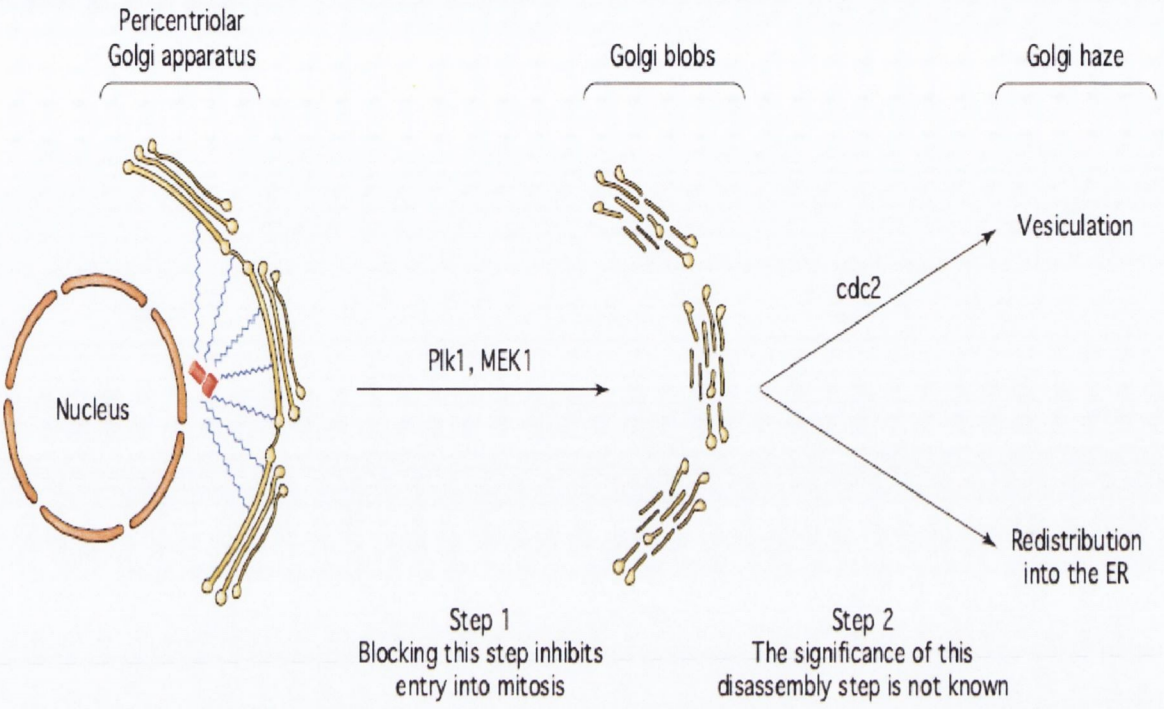

Figure 5.2 Proposed mechanism of Golgi fragmentation during mitosis. *MEK1 and Plk1 are involved in disassembly of Golgi stacks to smaller membranous structures or blobs in the first stage of Golgi fragmentation during mitosis. Cdc2 kinase is then responsible for further breakdown to smaller fragments, image taken from (Colanzi et al., 2003a).*

The Golgi also fragments during apoptosis and in this case it is thought that the fragmentation involves the activation of caspases which can cleave the Golgi-associated matrix proteins. These proteins include Golgin 160 which is important in maintaining structural integrity of the Golgi (Mancini *et al.*, 2000). The stacking protein GRASP65 is a substrate of the executioner caspase-3. Lane *et al* demonstrated that expression of a mutant caspase-resistant form of GRASP65 partially preserved Golgi structure and inhibited Golgi fragmentation in apoptotic cells (Lane *et al.*, 2002). Pharmacological agents can also cause Golgi fragmentation and different agents can induce distinct Golgi morphologies. For example okadaic acid, a protein phosphatase inhibitor, causes the Golgi cluster to resemble that in mitotic cells. The fungal metabolite brefeldin A (**92**), Figure 5.3, induces vesiculation of the Golgi causing it to fuse with the ER. On the other hand nocodazole, a microtubule depolymerising drug breaks the Golgi into shortened cisternae (Fan *et al.*, 2008). The marine product

iliminaquinone has also been shown to induce Golgi fragmentation (Diaz Anel & Malhotra, 2005).

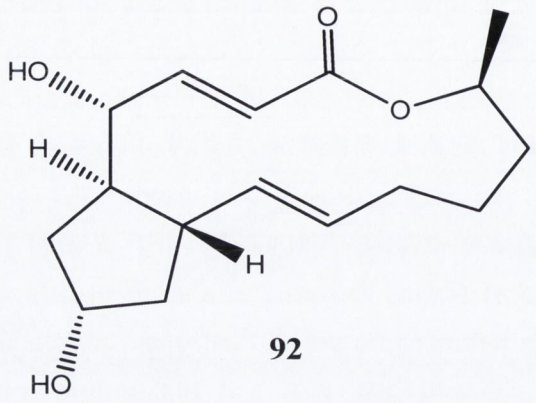

92

Figure 5.3 Structure of the fungal metabolite brefeldin A. *Brefeldin A induces vesiculation of the Golgi apparatus causing it to fuse with the ER.*

5.1.2 Golgi fragmentation and disease

Fragmentation of the Golgi apparatus is now recognised as a central feature of a number of diseases, principally neurodegenerative diseases. Golgi fragmentation was first observed in sporadic amyotrophic lateral sclerosis (sALS) in which the normal network of the Golgi of spinal cord motor neurons was replaced by numerous disconnected elements. The fragmentation is not occurring as a result of apoptosis as Golgi fragmentation has been observed in non-apoptotic neurons (Gonatas *et al.*, 2006). Furthermore the morphology of the Golgi resembled shorter cisternae as opposed to the clusters of vesicles seen during apoptosis in these cells (Gonatas *et al.*, 2006).

Golgi fragmentation has also been observed in Alzheimer's disease (Nakagomi *et al.*, 2008; Sun *et al.*, 2008) and in Creutzfeldt-Jacob disease (Gonatas *et al.*, 2006). Gonatas *et al* comment that neuronal Golgi fragmentation is an early and irreversible lesion in neurodegeneration and that it leads to a compromise in the secretory function of these cells (Gonatas *et al.*, 2006).

Although the mechanism of fragmentation remains to be clarified, it is thought that interaction between mutant proteins, and the proteins involved in maintenance of the structure of the Golgi might disrupt its structure and function. Sun *et al* recently revealed a major role for Cdk5 in Golgi fragmentation following beta-amyloid and glutamate stimulation of neuronal cells and primary neurons (Sun *et al.*, 2008).

Golgi fragmentation has also been observed in growth hormone disorders where patients express a mutant form of growth hormone lacking amino acids 32-71 resulting in misfolding of the protein. Transfection of COS-7 cells with this mutant protein resulted in Golgi fragmentation with Golgi markers β-cop, membrin and 58k highly dispersed in these cells. Golgi morphology was intact in cells expressing wild type growth hormone. The microtubule organising centres of the mutant cells were also disrupted as was the trafficking of the two secretory proteins prolactin and secreted alkaline phosphatase (Graves *et al.*, 2001).

5.1.3 Golgi fragmentation and cancer

Glycosyltransferase enzymes in the Golgi apparatus modify O- and N-linked carbohydrate chains on glycoproteins and glycolipids. These terminal oligosaccharide units expressed on proteins and lipids confer highly specific recognition capabilities to these molecules. At a cellular level, variation in the terminal oligosaccharide units can alter differentiation, proliferation and promote neoplastic progression (Byrne *et al.*, 2010).

Abnormal glycosylation of cellular glyco-conjugates is a common phenotypic change in many human tumours including leukaemia and neuroblastoma tumour gangliosides (Ladisch *et al.*, 1989; Petrini *et al.*, 1989). Aberrant glycosylation patterns are found in tissue from inflammatory bowel disease and colon cancer patients (Campbell, Yu & Rhodes, 2001; Rivinoja *et al.*, 2006). DNA hypermethylation has also been proposed to silence the activity of glycosyltransferases leading to abnormal glycosylation and expression of cancer associated carbohydrate antigens (Kawamura *et al.*, 2008). Disruption of N-linked glycosylation can lead to over-expression of the carbohydrate antigens sialyl Lewis a and sialyl Lewis x which are found in many tumours including pancreatic and gastric tumours (Peracaula et al., 2005; Varki et al., 1999). The expression level of these antigens correlates with the metastatic potential of the tumours (Peracaula *et al.*, 2005).

Stieber *et al* demonstrated that Golgi fragmentation is associated with disruptions in the secretory pathway as measured by decreased expression of the cell surface glycocprotein CD4 (Stieber *et al.*, 2004). Another study by Kellokumpu *et al* showed that Golgi fragmentation in the MCF-7 breast tumour cell line is associated with abnormally glycosylated proteins. Constitutive Golgi fragmentation has also been observed in a number of colon cancer cell lines such as the SW480, Caco-2, HT-29 and T-84 (Kellokumpu, Sormunen & Kellokumpu, 2002). Therefore, as the Golgi is inherently involved in post-translational modifications and glycosylation it is reasonable to assume that disruption of its architecture could lead to aberrant

secretion of proteins and abnormal cell signalling ultimately contributing to carcinogenesis.

5.1.4 The ER stress response

Secretory proteins intended are initially processed through the ER as it provides an optimal and unique environment for protein folding, assembly and disulfide bond formation (Wu & Kaufman, 2006). These proteins then traffic to the Golgi where they can undergo post-translational modifications. Insults including nutrient deprivation, alterations in the oxidation-reduction balance, changes in calcium concentration and failure of post-translational modifications can lead to protein misfolding in the ER (Wu & Kaufman, 2006). Accumulation of these misfolded/unfolded proteins leads to an ER stress response more commonly referred to as an unfolded protein response (UPR).
The three main pathways of ER stress are the PKR-like ER protein kinase/pancreatic eIF2α (eukaryotic translation initiation factor 2, a subunit) kinase (PERK/PEK) pathway; the activating transcription factor 6 (ATF6) pathway and the inositol-requiring enzyme 1 (IRE1) pathway, Figure 5.4.

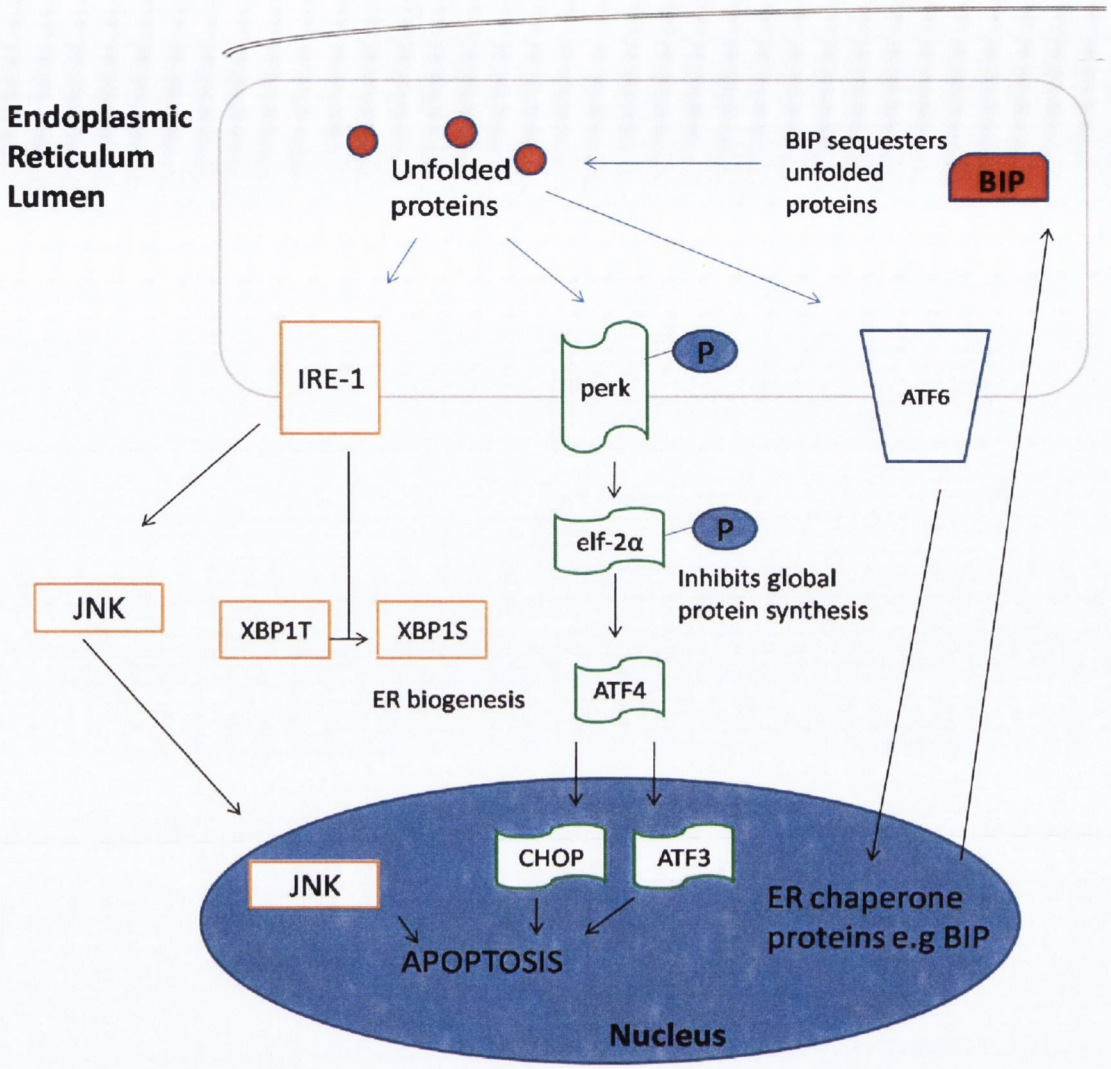

Figure 5.4 Pathways of ER stress/UPR. *The three main pathways of ER stress are the PKR-like ER protein kinase/pancreatic eIF2α (eukaryotic translation initiation factor 2, a subunit) kinase (PERK/PEK) pathway; the activating transcription factor 6 (ATF6) pathway and the inositol-requiring enzyme 1 (IRE1) pathway. The overall aim of the UPR is to reduce the burden on the ER and to remove unfolded proteins from the cell. If the response fails to reduce ER burden then apoptosis is triggered. CHOP, ATF3 and JNK are thought to be involved in inducing apoptosis. Adapted from (Cunha et al., 2008).*

In a pre stress state these ER proteins are maintained in a soluble form mainly bound to Bip/GRP78 which is the most highly expressed ER resident protein. Bip dissociates from these proteins to sequester unfolded proteins in the ER lumen allowing PERK, ATF6 and IRE-1 to initiate ER stress cascades. Active IRE-1 splices *XBP1* (X-box binding protein 1) mRNA which can then induce genes involved in ER expansion and biogenesis (Lee *et al.*, 2005) and degradation of misfolded proteins (Wu & Kaufman,

2006). Overexpression of XBP-1 leads to upregulation of genes encoding proteins of multiple compartments of the secretory pathway including the Golgi (Okunade *et al.*, 2007). ATF6 induces transcription of ER chaperone proteins such as Bip. PERK on the other hand phosphorylates the eukaryotic translation initiation factor eIF2 α which results in an overall inhibition of global protein synthesis. However translation of selected proteins such as ATF4 (Cunha *et al.*, 2008) and PKC η (Raveh-Amit *et al.*, 2009) is facilitated. ATF4 can then increase expression of downstream C/EBP homologous protein (CHOP/GADD153/ DDIT3) and ATF3.

The overall aim of the UPR response is to reduce the burden on the ER but if the response fails then apoptosis is triggered (Banhegyi *et al.*, 2007; Cunha *et al.*, 2008; Wu & Kaufman, 2006). During physiological ER stress, survival pathway activation outweighs death pathway activation, whereas during chronic unresolvable ER stress conditions, death pathway activation dominates that of survival pathways (Ishigaki *et al.*, 2010).

CHOP and ATF3 are thought to be activated during the ER stress response as a means of inducing apoptosis when the rest of the ER machinery fails to adequately deal with the stress imposed. CHOP alters the balance between pro-survival and pro-apoptotic Bcl-2 family members thus promoting apoptosis through the mitochondrial pathway (Healy *et al.*, 2009; McCullough *et al.*, 2001). CHOP has also been reported to cause upregulation of TRAIL death receptors in human carcinoma cells (Yamaguchi & Wang, 2004).

5.1.5 Role of ER stress in Cancer

The tumour microenvironment is exposed to a variety of stressful conditions; these include hypoxia caused by poor vascularisation and nutrient deprivation. Such conditions can lead to activation of the UPR (Wlodkowic *et al.*, 2009). In recent years evidence has emerged that the ER stress response could be important for the growth and development of tumours. Activation of the UPR has been shown in many cancers with increased expression of UPR target genes in human tumour samples (Healy *et al.*, 2009; Wlodkowic *et al.*, 2009). For example, Bip levels have been reported to be increased in various cancer types including prostate, breast and gastric cancers (Dong *et al.*, 2004; Fernandez *et al.*, 2000; Lee, 2007; Zheng *et al.*, 2008). This increased expression has been observed in both cancer cell lines as well as in ex vivo human primary and animal model tissues (Healy *et al.*, 2009). Bip has also been implicated in tumour cell proliferation as high expression levels in a range of glioma cells correlate with higher rates of proliferation whereas siRNA-mediated down-regulation of Bip decreased glioma cell proliferation rate (Pyrko *et al.*, 2007). Bip has also been shown

to play a role in angiogenesis (Healy *et al.*, 2009; Virrey *et al.*, 2008) and to protect from doxorubicin induced apoptosis by suppressing apoptotic pathways (Reddy *et al.*, 2003). Bip can inhibit apoptosis by inhibiting the activity of caspase-7, and by acting as a Ca^{2+}-binding protein to preserve ER Ca^{2+} homeostasis (Reddy *et al.*, 2003).

PERK has also been suggested to play a role as a survival factor for tumour cells under stress conditions (Ranganathan *et al.*, 2006). For example, Koumenis *et al* used a HT29 colorectal carcinoma cell line expressing a kinase dead PERK, which acted as a dominant-negative mutant inhibiting the phosphorylation of eIF2α. These cells exhibited lower survival rates in hypoxic conditions compared to wild type cells (Koumenis *et al.*, 2002).

Other mediators of the UPR implicated in various aspects of cancer progression are summarised in Table 5.1.

Table 5.1 The UPR and cancer. *Increased expression of UPR target genes has been shown to be associated with characteristics of many human cancers including gastric cancers. Table adapted from (Healy et al., 2009).*

	Bip	IRE1/XBP-1	PERK/eIF-2α
Increased proliferation	+	+	+
Evasion of apoptosis	+		
Angiogenesis	+	+	+
Metastasis	+		
Resistance to chemotherapy	+	+	+

5.1.6 BAs and Cancer

The ability of BAs to act as tumour promoters was first proposed by Cook in 1940 based on the induction of tumours in mice when injected with DCA (Bernstein *et al.*, 2005). Since this time, a number of *in vitro*, *in vivo* and clinical studies have demonstrated the tumour promoting properties of BAs, particularly in colon carcinogenesis. These include activation of carcinogenic cascades *in vitro*, promotion of tumour formation in rats (Narisawa *et al.*, 1974; Reddy *et al.*, 1977) and increased concentrations of fecal BAs in patients with colorectal cancer (de Kok *et al.*, 1999; Stadler *et al.*, 1988; Tong *et al.*, 2008). Based on evidence of their DNA damaging effects and mutagenicity, the secondary BAs, DCA and LCA, are most likely to be

implicated in colon carcinogenesis (Bernstein *et al.*, 2005; Hill, 1990; Nagengast, Grubben & van Munster, 1995) although other BAs, in particular CDCA have been shown to play a role (Tong *et al.*, 2008).

BAs are known to induce apoptosis but it is thought that continual exposure of cells to BAs can lead to apoptosis resistance (Yui *et al.*, 2009) allowing for selective growth of cells resistant to BA-induced apoptosis. In a rat model, repeated feeding of a diet containing 0.2% cholic acid resulted in the development of increased resistance to apoptosis of the colon crypt cells (Magnuson, Shirtliff & Bird, 1994). Furthermore, repeated long-term exposure of a human colonic epithelial cell line to sublethal concentrations of DCA selected for cells that are resistant to DCA induced apoptosis. BAs have also been shown to activate cell survival pathways, for example the NF-κB pathway (Bernstein *et al.*, 2009). These pathways contribute to stable apoptosis resistance that characterises cell lines persistently exposed to DCA (Crowley-Weber *et al.*, 2002). In this study Crowley-Weber *et al* cultured HCT116 cells in the presence of increasing concentrations of DCA and the resulting apoptosis resistant cell lines were able to grow in concentrations of DCA up to 500 μM.

In recent years it has also emerged that BAs can alter the expression of UPR genes. DCA and GCDCA increase expression of ER stress proteins Bip and CHOP in hepatocytes (Tsuchiya *et al.*, 2006) and also in colonic cancer cell lines (Bernstein *et al.*, 1999; Scott *et al.*, 2005). DCA has also been shown to induce apoptosis in colon cancer cell lines via a CHOP dependent process (Qiao *et al.*, 2002; Scott *et al.*, 2005). A number of studies have recently been done with GCDCA showing that CHOP is involved in GCDCA mediated apoptosis in hepatocyte cell lines and furthermore that a deficiency in CHOP can attenuate GCDCA induced cell death (Iizaka *et al.*, 2007; Tamaki *et al.*, 2008).

5.2 Aims and Objectives

Taking into account the carcinogenic effects of DCA and the evidence that it can increase the UPR in hepatocytes and colonic cell lines we hypothesised that BA induced carcinogenesis could, at least in part, be mediated via the secretory pathway. We decided to conduct a series of studies examining the effects of BAs on the secretory pathway especially focussing on Golgi structure and function and also investigating markers associated with ER stress. As UDCA has been shown to act as a chemopreventative agent we were also interested in examining the potential of UDCA and our UDCA analogues to inhibit effects on the structure/function of these organelles.

This work was initially carried out in a colon cancer cell line as observations had been previously made in our group indicating the DCA could induced Golgi fragmentation in the HCT116 cell line. The work was then adapted to an esophageal model. The specific aims of this chapter were to:

1. Investigate the effect of BAs on the Golgi morphology in colon and esophageal cell lines.

2. To demonstrate a functional consequence of BA mediated alterations to Golgi structure in colonic and esophageal cells.

3. To screen our panel of BA derivatives as potential inhibitors of BA-induced Golgi fragmentation.

4. To determine the effect of natural BAs on ER stress.

5.3 Results

5.3.1 Colon cancer Model

5.3.1.1 DCA induces Golgi fragmentation

A series of studies in our laboratory investigating the effect of BAs in colon cancer pathogenesis revealed that DCA could induce fragmentation of the Golgi. This work was done in the HCT116, colon cancer cell line (Byrne *et al.*, 2010). Although pharmacological agents have previously been shown to induce Golgi fragmentation, DCA is the first physiological molecule shown to do this, Figure 5.5B. Brefeldin A was used in these experiments as a positive control for Golgi fragmentation, Figure 5.5C.

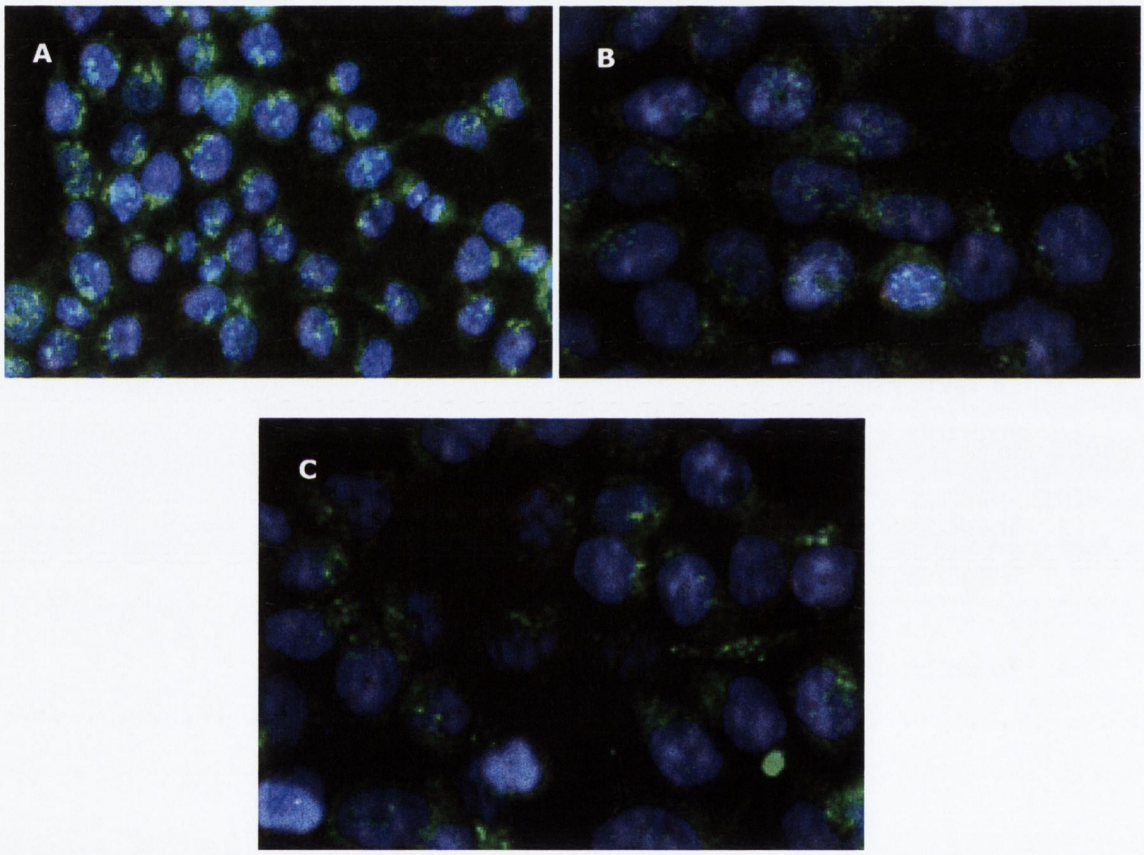

Figure 5.5 DCA induces Golgi fragmentation in the HCT116 cell line. *HCT116 cells were A) untreated or B) treated with DCA 300 μM or C) treated with brefeldin A 1 μg/ml as a positive control for Golgi fragmentation. After 6 h cells were fixed with paraformaldehyde 4% in PBS. The Golgi was identified using a rabbit polyclonal GM130 antibody (green) and cells were stained with hoecsht (blue) to identify the nucleus. Cells were imaged using the GE In cell Analyser 1000. Original magnification, x20. Images are representative of n=3 experiments.*

Although DCA is a cytotoxic BA, this concentration is not toxic to this cell line during the 6 h time frame of the experiment. Byrne *et al* have demonstrated that this fragmentation occurs via activation of the membrane fission process which involves activation of PKCη and phosphorylation of PKD (Byrne *et al.*, 2010). Hyperactivation of PKD results in formation of transport carriers at the TGN until it is reduced to small vesicles.

5.3.1.2 The functional significance of Golgi fragmentation

As described, the Golgi is an integral organelle involved in transporting and processing proteins and lipids from the ER. Hence disruption of its architecture by DCA could potentially lead to alterations in normal protein processing and aberrant secretion of proteins. In order to determine the effects of DCA on the secretory capacity of the HCT116 cell line we decided to carry out a Gaussia luciferase (G.luc) secretory assay, Figure 5.6. The G.luc assay is an assay recently developed by Badr *et al* (Badr *et al.*, 2007). G.luc is a luciferase obtained from the marine copepod Gaussia princeps which when expressed in cells is secreted into the extracellular medium. The assay involves transfection of a reporter gene constitutively expressing G.luc and measuring secretion of the G.luc protein using a coelenterazine substrate. Reduction of coelenterazine to coelenteramide results in release of energy in the form of a luminescent signal.

Traditional techniques for measuring trafficking through the secretory pathway include use of radioactively labelled endogenous glycoproteins and measurement of secreted alkaline phosphatase (SEAP) activity. The G.luc assay is simpler than the former and has been shown to be 20,000 fold more sensitive than the SEAP assay (Badr *et al.*, 2007).

Hence DCA treatment leads to Golgi fragmentation and disruption in the secretory capacity which may be an explanation of its role in colon carcinogenesis. This hypothesis is supported by the fact that Byrne *et al* observed Golgi fragmentation in biopsies of patients with ulcerative colitis and colon cancer. Patients with colorectal adenomas have been shown to have increased blood and fecal levels of the secondary BAs, in particular DCA (Bayerdorffer *et al.*, 1994; Bayerdorffer *et al.*, 1995).

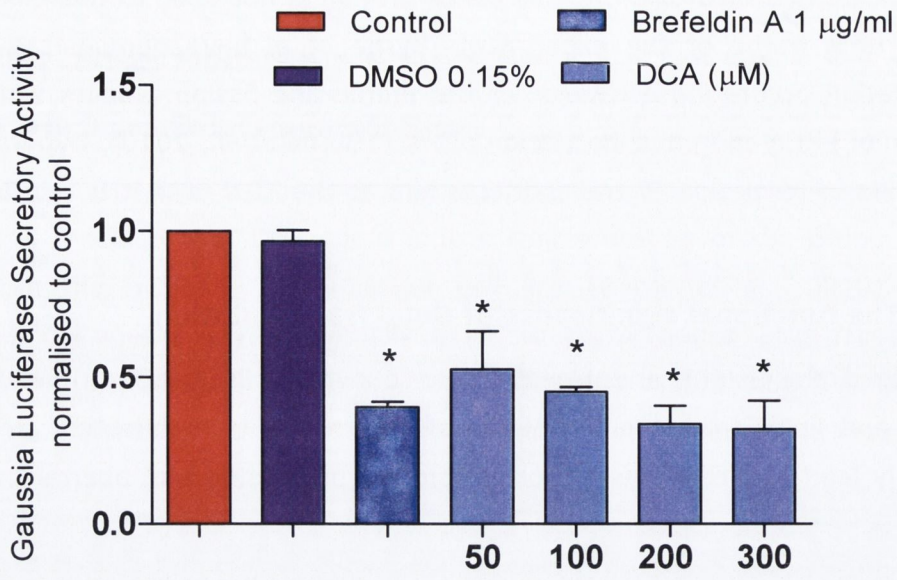

Figure 5.6 DCA decreases the secretory capacity of HCT116 cells. *HCT116 cells were transiently transfected with a mixture of a constitutively expressing G.luc construct and a constitutively expressing firefly luciferase construct (1:1), Section 2.14. Cells were left untreated or treated with DMSO 0.15 %, brefeldin A 1 μg/ml or increasing concentrations of DCA (**4**) as shown. G.luc activity was normalised to firefly luciferase and protein content to act as internal controls to control for transfection efficiency and cell death. Values are expressed as the mean ± SEM of three experiments performed in triplicate, normalised to untreated control, *p< 0.05 as determined by one-way ANOVA and Dunnett's post hoc correction.*

5.3.1.3 UDCA inhibits DCA induced Golgi fragmentation

As UDCA has been shown to antagonise a number of the adverse biological effects mediated by DCA, we decided to investigate whether UDCA could inhibit DCA induced Golgi fragmentation. In order to do this the HCT116 cell line was pre-treated with UDCA prior to DCA treatment. Interestingly it was found that UDCA pre-treatment lead to an inhibition in DCA induced Golgi fragmentation.

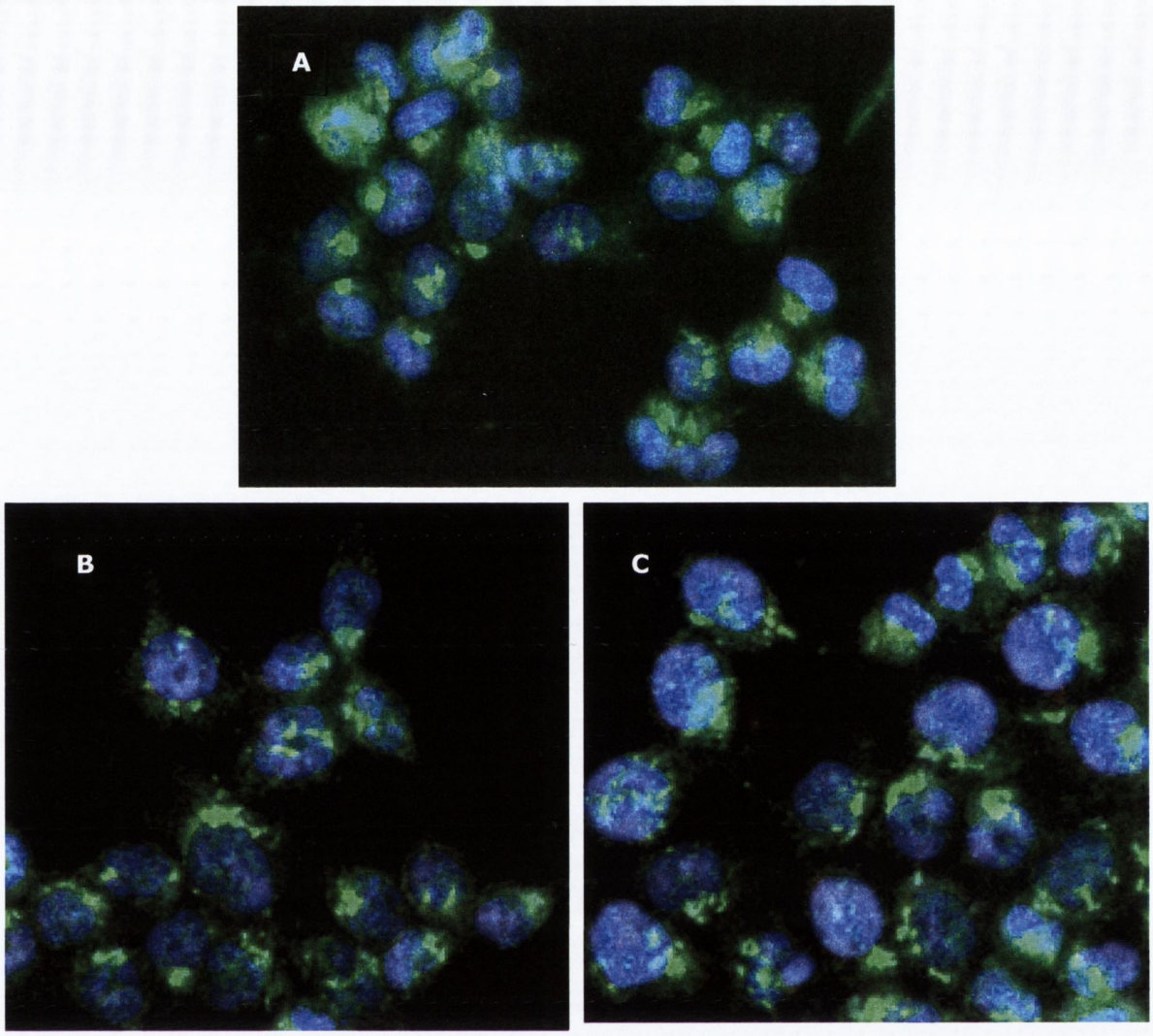

Figure 5.7 UDCA inhibits DCA induced Golgi fragmentation. *HCT116 cells were A) untreated or treated with B) UDCA 300 μM for 24 h or C) UDCA 300 μM for 18 h and then co-treated with UDCA 300 μM and DCA 300 μM for a further 6 h. After the DCA treatment the cells were fixed with paraformaldehyde 4% in PBS. The Golgi was identified using a rabbit GM130 antibody (green) and cells were stained with Hoechst (blue) to identify the nucleus. Cells were imaged using the GE In cell Analyser 1000. Original magnification, x20. Images are representative of n=3 experiments.*

UDCAs inhibition of DCA induced Golgi fragmentation could be a potential explanation for UDCA's mechanism of action as a potential chemopreventative agent in colon cancer.

5.3.1.4 Does UDCA inhibit DCA induced Golgi fragmentation via the GR?

As many of UDCAs biological effects including its cytoprotective effects have been shown to be mediated via the GR we decided to investigate whether UDCAs inhibition of DCA induced Golgi fragmentation was GR dependent. In order to do this we decided

to inhibit GR transcriptional activity using the GR antagonist, mifepristone. When cells were treated with mifepristone and UDCA prior to DCA treatment it was found that UDCA could no longer inhibit DCA induced Golgi fragmentation and the Golgi remained fragmented, Figure 5.8. Mifepristone itself was found to have no effect on the Golgi.

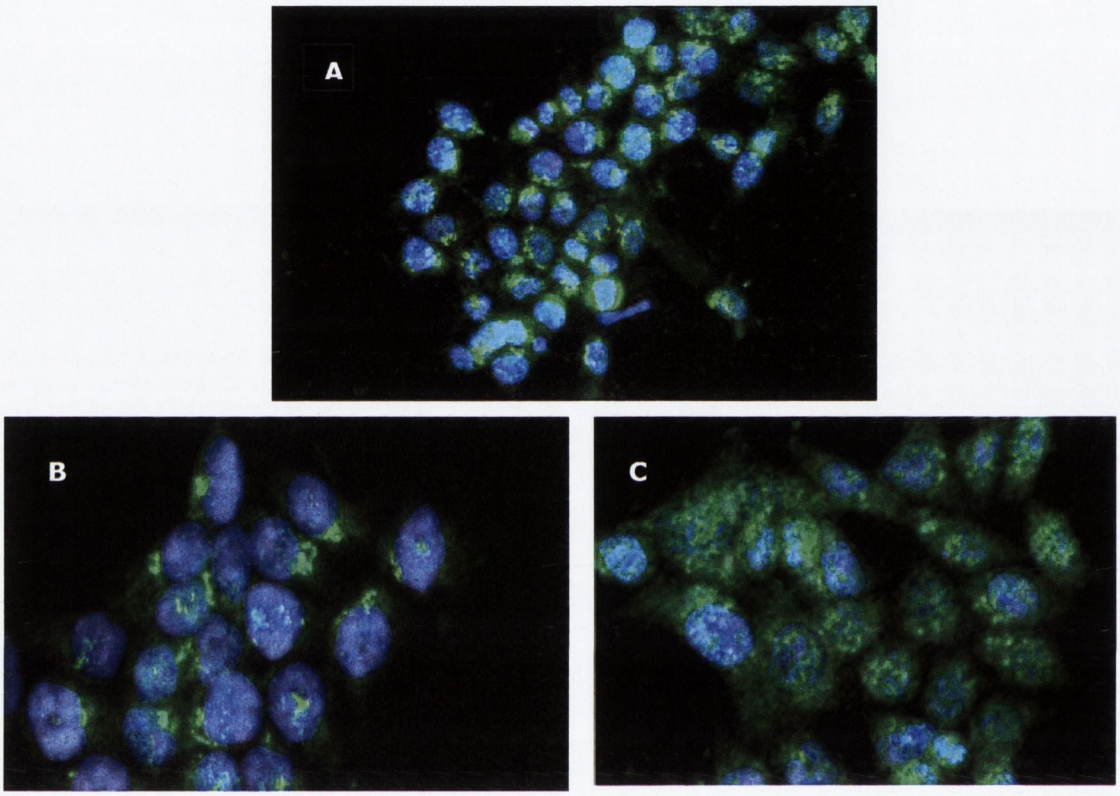

Figure 5.8 UDCA acts via the GR to inhibit DCA induced Golgi fragmentation. *HCT116 cells were A) untreated or treated with B) mifepristone 100 nM for 26 h or C) Mifepristone 100 nM for 2 h then, mifepristone 100 nM and UDCA 300 μM for 18 h and then mifepristone 100 nM , UDCA 300 μM and DCA 300 μM for a further 6 h. After the DCA treatment the cells were fixed, stained and visualised as described in Figure 5.5. Original magnification, x10 (A), x20(B,C). Images are representative of n=3 experiments.*

We decided to quantify Golgi fragmentation by High Content Analysis using the GE investigator software package. Six fields of view per well were acquired using a 20 × objective in duplicate wells for n=3 experiments. The Investigator software package provides an algorithm which allows for detection of objects within a cell. The multi-target analysis algorithm was optimised to detect objects or Golgi fragments within a cell using untreated cells with intact Golgi as negative control and brefeldin A treated cells with fragmented Golgi as a positive control. The "object mean area" parameter

was used to classify cells as having intact Golgi (object mean area > 0.5 μM) or fragmented Golgi (object mean area < 0.5 μM). Three hundred cells were analysed per treatment group. Figure 5.9 provides an example of cellular analysis with the HET-1A cell line.

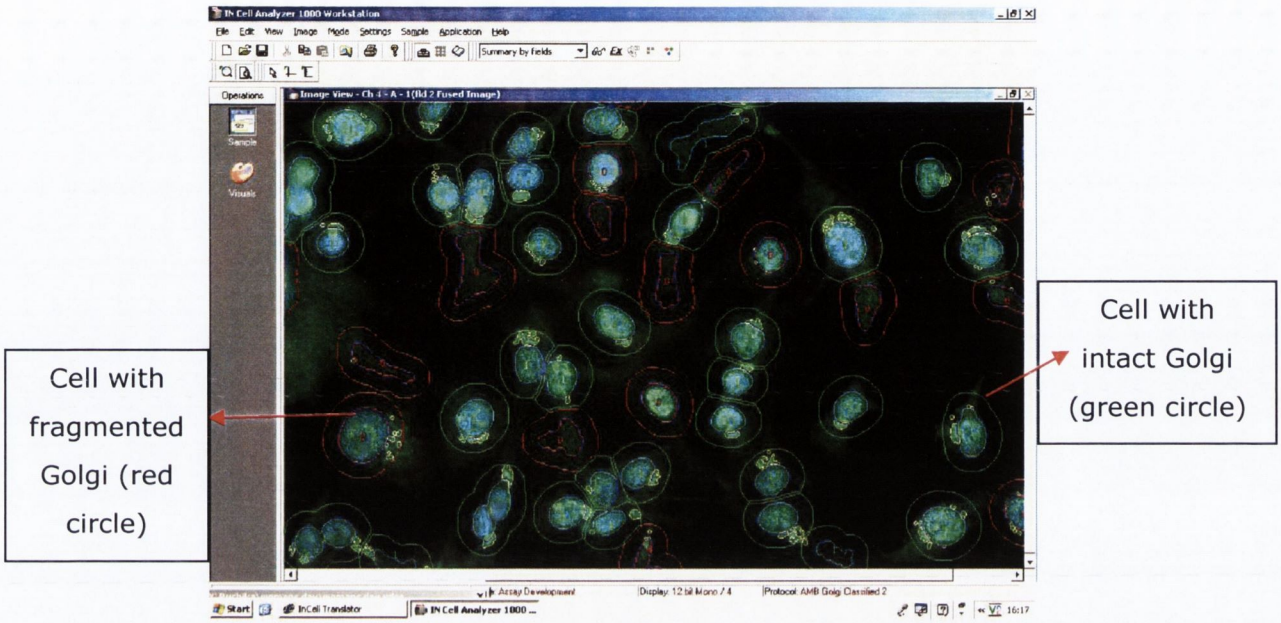

Figure 5.9 Cellular analysis for Golgi fragmentation. *The GE investigator software package was used to quantify Golgi fragmentation. The multi-target analysis algorithm was optimised to detect objects or Golgi fragments within a cell using untreated cells with intact Golgi as negative control and brefeldin A treated cells with fragmented Golgi as a positive control. Cells with intact Golgi are circled in green and those with fragmented Golgi are circled in red. Three hundred cells were analysed per treatment group.*

Using this algorithm the following results were obtained which confirmed our previous observations, Figures 5.7, 5.8. Mifepristone itself had no effect on Golgi fragmentation. Mifepristone did not inhibit DCA induced fragmentation but mifepristone pre-treatment abrogated UDCAs protective effect on the Golgi.

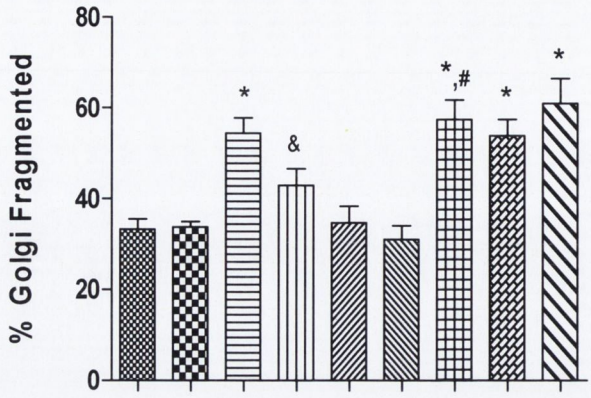

UDCA 300 µM	-	+	-	+	-	+	+	-	-
DCA 300 µM	-	-	+	+	-	-	+	+	-
Mifepristone 100 nM	-	-	-	-	+	+	+	+	-
Brefeldin A 1 µg/ml	-	-	-	-	-	-	-	-	+

Figure 5.10 Analysis of Golgi fragmentation. *HCT116 cells were treated as indicated. After the DCA treatment the cells were fixed, stained and visualised as described in Figure 5.5. Cells were analysed as described using the Investigator software package and a multi-target analysis algorithm. Original magnification, x20. Values represent the mean ± SEM of n=3 experiments, *p< 0.05 relative to control, & p<0.05 relative to DCA 300 µM and # p< 0.05 relative to UDCA 300 µM pre-treatment and DCA 300 µM as determined by one-way ANOVA and Tukey post-hoc correction.*

This experiment was carried out in parallel with an experiment using siRNA to the GR. The results of this experiment can be seen in Appendix 3 in the publication of Byrne *et al* (Byrne *et al.*, 2010).

5.3.2 Adapting the Golgi assay to an esophageal model

As the primary focus of our grant is investigating the role that BAs have to play in esophageal cancer progression, we investigated if DCA induced Golgi fragmentation in these cells in a similar fashion. Using similar assay conditions we found that DCA could induce Golgi fragmentation in the HET-1A cell line, Figure 5.11.

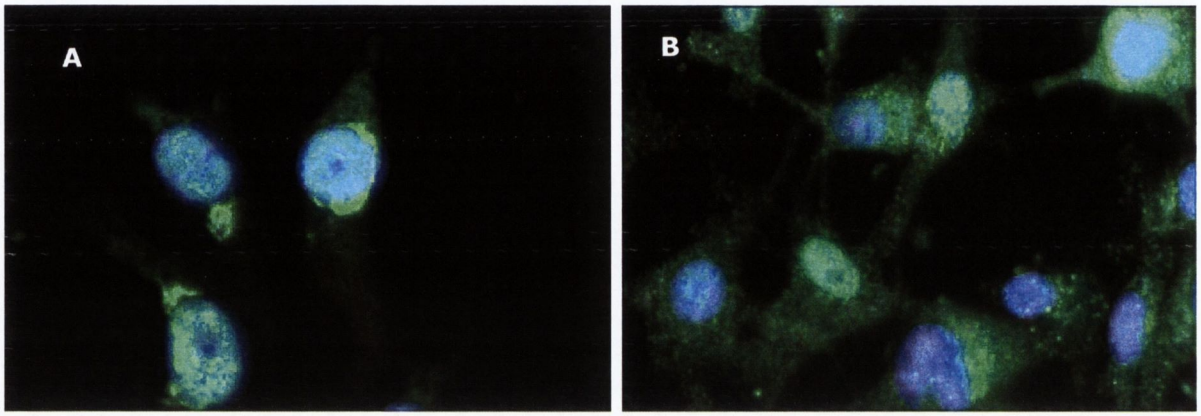

Figure 5.11 DCA induces Golgi fragmentation in the HET-1A cell line. *HET-1A cells were A) untreated or B) treated with DCA 300 μM. After 6 h cells were fixed, stained and visualised as described in Section 5.5. Original magnification, x40. Images are representative of n=3 experiments.*

This was repeated at lower concentrations of DCA and it was found that DCA induced Golgi fragmentation following a concentration dependent trend, however this only reached significance at 300 μM. Analysis was carried out as previously described using the multi-target analysis algorithm. Rather than expressing the results in terms of number of cells with fragmented Golgi we decided to express them in terms of mean Golgi area as we felt that this gave more reproducible results as the basal level of cells with Golgi fragmentation was variable depending on their stage in the cell cycle.

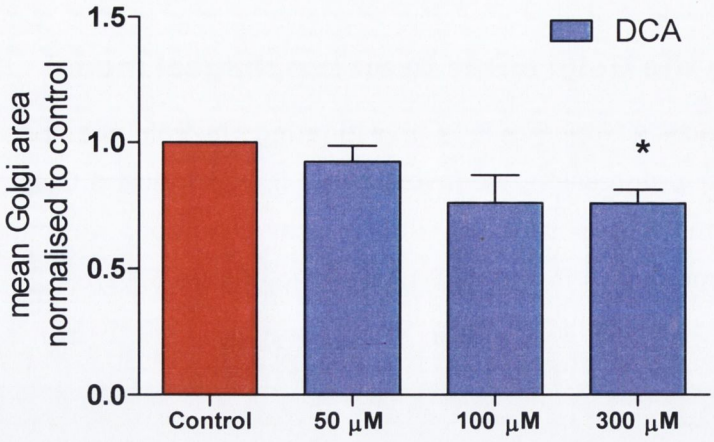

Figure 5.12 Analysis of DCA induced Golgi fragmentation. *HET-1A cells were untreated or treated with varying concentrations of DCA as indicated. After 6 h cells were fixed, stained and visualised as described in Figure 5.5. Original magnification, x20. The acquired images were analysed using the multi-target analysis algorithm on the GE Investigator software package. Values are expressed as mean Golgi area normalised to control and represent the mean ± SEM of n=3 experiments, *p< 0.05 relative to untreated control.*

5.3.2.1 Secretory Assay in the HET-1A and QH cell line

The secretory assay was repeated in the HET-1A cell line and also in the QH cell line, Figure 5.13. It was decided to conduct the assay at 1 h and 6 h time points as time course experiments by other members in the group showed that Golgi fragmentation can occur within 1 h of DCA treatment.

DMSO 0.15% had no effect on secretory capacity of the cells. DCA decreased the secretory capacity of both cell lines. Interestingly, the secretory capacity of the QH cell line was more sensitive to DCA. DCA 50 μM was found to induce significant changes in secretion at the 1 h and 6 h time point in the QH cells whereas there was no effect on secretion up to 200 μM at the 6 h time point in the HET-1A cell line.

A)

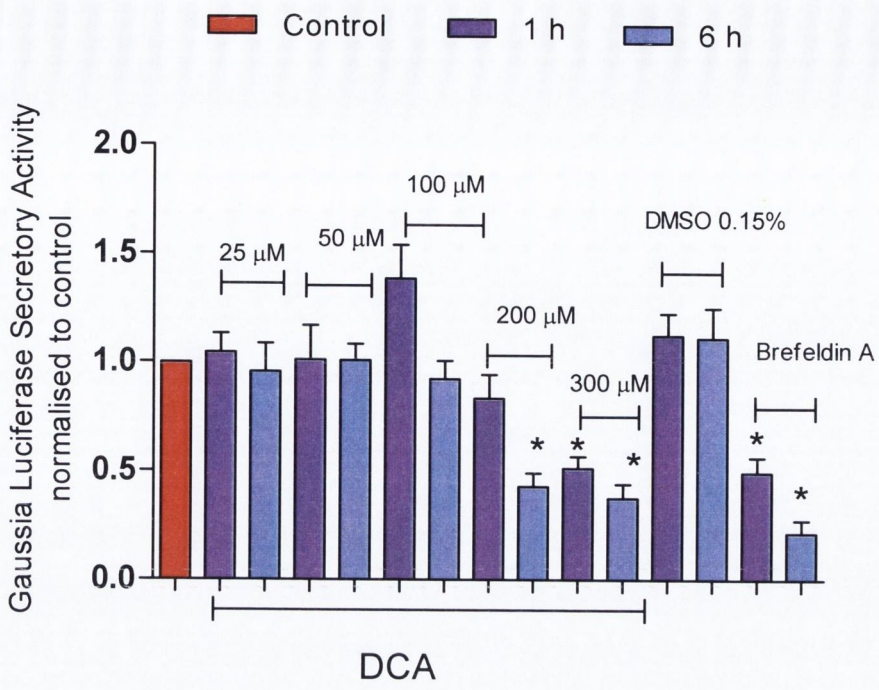
Control
1 h
6 h
Gaussia Luciferase Secretory Activity normalised to control
2.0
1.5
1.0
0.5
0.0
25 μM
50 μM
100 μM
200 μM
300 μM
DMSO 0.15%
Brefeldin A
DCA

B)

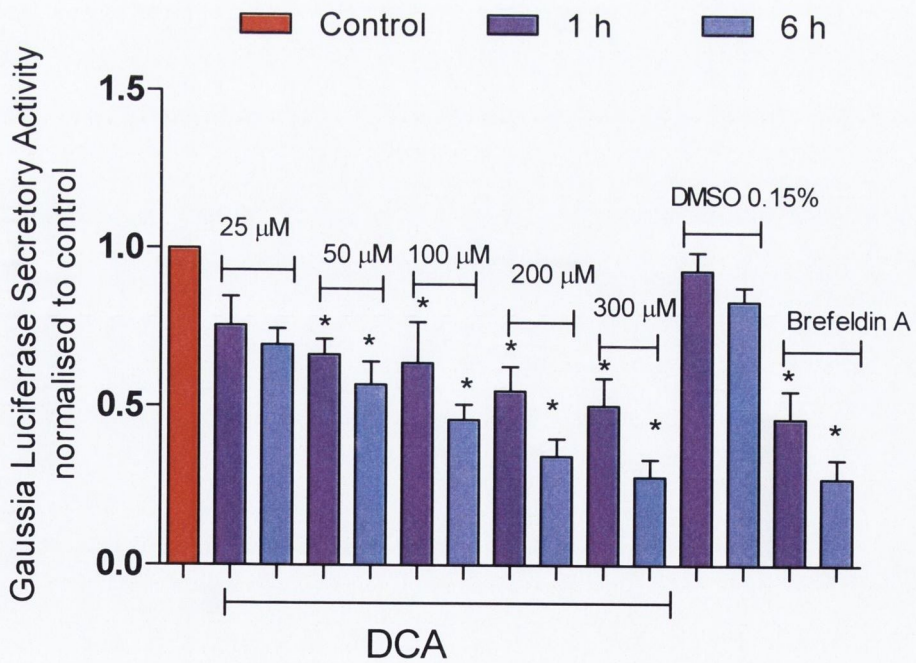
Control
1 h
6 h
Gaussia Luciferase Secretory Activity normalised to control
1.5
1.0
0.5
0.0
25 μM
50 μM
100 μM
200 μM
300 μM
DMSO 0.15%
Brefeldin A
DCA

Figure 5.13 DCA decreases the secretory capacity of HET-1A and QH-tert cell lines. A) *HET-1A cells or* ***B)*** *QH cells were transiently transfected with a mixture of a constitutively expressing G.luc construct and a constitutively expressing F.luc construct (1:1) as described in Section 2.14. Cells were left untreated or treated with DMSO 0.15 %, brefeldin A 1 µg/ml or increasing concentrations of DCA as shown. G.luc activity was normalised to F.luc and protein content to act as internal controls to control for transfection efficiency and cell death. Values are expressed as the mean ± SEM of three experiments performed in triplicate, normalised to untreated control, *p< 0.05 as determined by one-way ANOVA and Dunnett's post hoc correction.*

5.3.3 Can other natural BAs induce Golgi fragmentation?

We decided to investigate whether the ability to induce Golgi fragmentation was unique to DCA or whether other BAs shared this property. In order to do this we conducted a screen of a panel of 13 natural BAs including UDCA, CA and CDCA and their glycine and taurine conjugates, Figure 5.14. The glycine and taurine conjugates of DCA and LCA were also included in the panel. All BAs were screened initially at 300 µM as this concentration of any of the BAs does not lead to apoptosis in the 6 hr time frame used during the experiment and falls within the concentration range of BAs found in the esophagus during esophagitis and Barrett's metaplasia (Nehra *et al.*, 1999). LCA was tested at 25 µM as higher concentrations were cytotoxic.

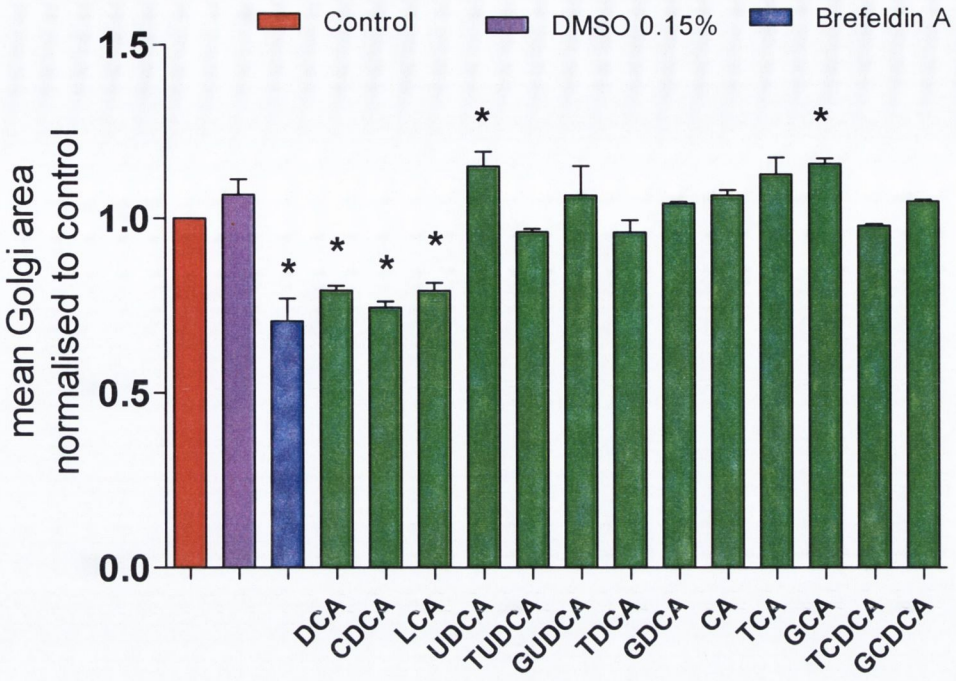

Figure 5.14 BA screen for Golgi fragmentation. *HET-1A cells were left untreated or treated with DMSO 0.15%, brefeldin A 1 μg/ml or BAs at 300μM or LCA 25μM for 6 h. Cells were fixed and stained as described in Figure 5.5. Images were acquired using the GE In Cell Analyser 1000 and quantified using the Investigator software package, original magnification 20×. Data are represented as mean ± SEM, normalised to untreated control for n=3 experiments, * p<0.05 relative to untreated control as determined by one-way ANOVA and Dunnett's post-hoc correction.*

High content analysis of the acquired images revealed that of the panel of thirteen BAs studied, CDCA and LCA were the only other BAs (apart from DCA) capable of inducing Golgi fragmentation represented here as a decrease in the mean Golgi area, Figure 5.14. These three BAs decreased mean Golgi area to the same extent. CDCA could significantly decrease the mean Golgi area at 100 μM, figure 5.15. Lower concentrations of LCA did not have any effect on the Golgi. UDCA and GCA had a significantly higher mean Golgi area than control. This might be as a result of less cells undergoing mitosis in these populations.

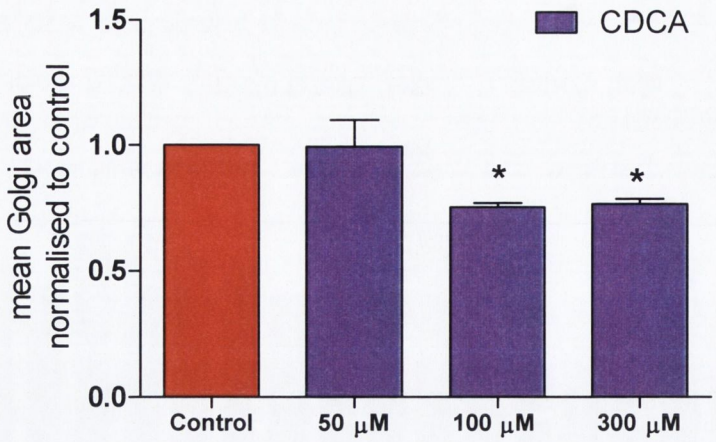

Figure 5.15 CDCA induces Golgi fragmentation in a concentration dependent manner. *HET-1A cells were untreated or treated with varying concentrations of CDCA as indicated. After 6 h cells were fixed, stained and visualised as described in Figure 5.5. Cells were imaged using the GE In cell Analyser 1000. Original magnification, x20. The acquired images were analysed using the multi-target analysis algorithm on the GE Investigator software package. Values are expressed as mean Golgi area normalised to control and represent the mean ± SEM of n=3 experiments, *p< 0.05 relative to untreated control as determined by one-way ANOVA and Dunnett's post-hoc correction.*

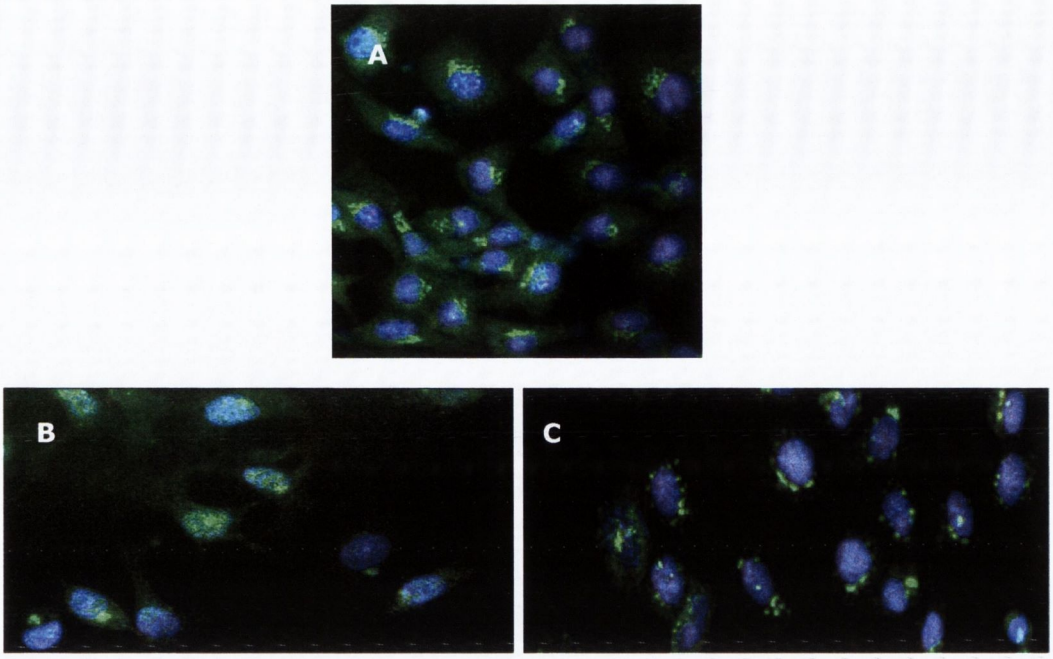

Figure 5.16 CDCA and LCA induce Golgi fragmentation. *HET-1A cells were A) untreated or treated with B) CDCA 300 μM or C) LCA 25 μM. After 6 h cells were fixed with paraformaldehyde 4% in PBS. The Golgi was identified using a rabbit monoclonal GM130 antibody (green) and cells were stained with Hoechst (blue) to identify the nucleus. Cells were imaged using the GE In cell Analyser 1000. Original magnification, x20. Images are representative of n=3 experiments.*

Treatment of HET-1A cells with UDCA, CA and their glycine and taurine conjugates had no effect on mean Golgi area. In Chapter 3 we demonstrated that the taurine and glycine conjugates of DCA and CDCA do not decrease cell viability of HET-1A cells unlike the parent BAs. Similarly the taurine and glycine conjugates of both DCA and CDCA did not induce fragmentation of the Golgi.

5.3.4 Can other BAs protect against DCA induced Golgi fragmentation in oesophageal cells?

UDCA pre-treatment inhibited DCA induced Golgi fragmentation in the HET-1A cell line in a similar manner to the HCT116 cell line.

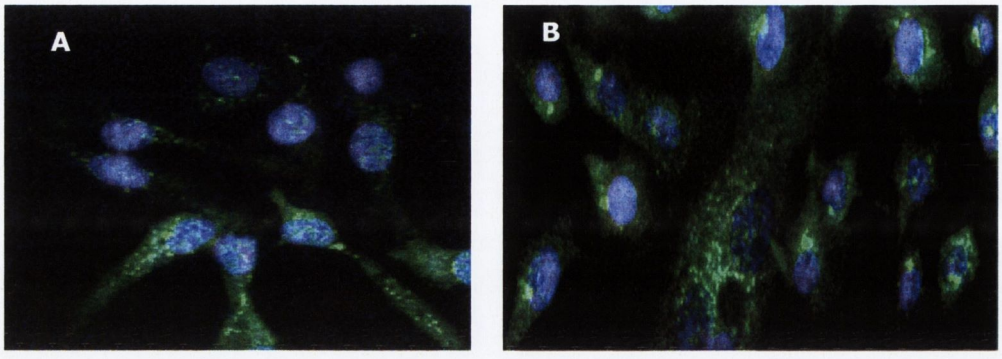

Figure 5.17 UDCA inhibits DCA induced Golgi fragmentation. *HET-1A cells were treated with A) DCA 300 μM for 6 h or B) UDCA 300 μM for 18 h and then co-treated with UDCA 300 μM and DCA 300 μM for a further 6 h. After the DCA treatment the cells were fixed and stained as described in Figure 5.5. Cells were imaged using the GE In cell Analyser 1000. Original magnification, x20. Images are representative of n=3 experiments.*

Based on results described in Chapter 4 which demonstrated that UDCA and its derivatives could induce translocation of the GR from the cytoplasm to the nucleus and our finding that UDCA inhibits DCA induced fragmentation via the GR, we decided to screen a panel of our compounds which were potent inducers of GR translocation. We also decided to screen the other natural BAs for potential protective effects on the Golgi (**9-13**, **15-18**). High content analysis revealed that GUDCA was the only other BA which could inhibit DCA induced Golgi fragmentation, Figure 5.18.

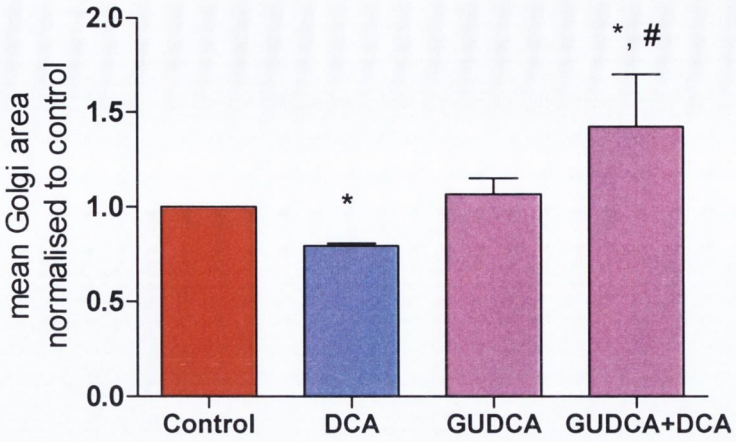

Figure 5.18 GUDCA inhibits DCA induced Golgi fragmentation. *HET-1A cells were treated with GUDCA 300 μM for 18 h and then co-treated with GUDCA 300 μM and DCA 300 μM for a further 6 h. After the DCA treatment the cells were fixed and stained as described in Figure 5.5. Cells were imaged using the GE In cell Analyser 1000. Original magnification, x20. Values are expressed as mean Golgi area normalised to control and represent the mean ± SEM of n=3 experiments, *p< 0.05 relative to untreated control, # p< 0.05 relative to DCA 300 μM as determined by one way ANOVA and Tukey post-hoc correction.*

We have already shown that UDCA acts via the GR to inhibit DCA induced Golgi fragmentation. However, despite GUDCAs protective effect on the Golgi it did not significantly induce translocation of the GR in the SKGT-4 cell, Figure 5.19.

In the same way we found that a selection of our BA derivatives which were potent activators of the GR, for example, CPA (**77**) were unable to significantly protect against DCA induced Golgi fragmentation, Figure 5.20.

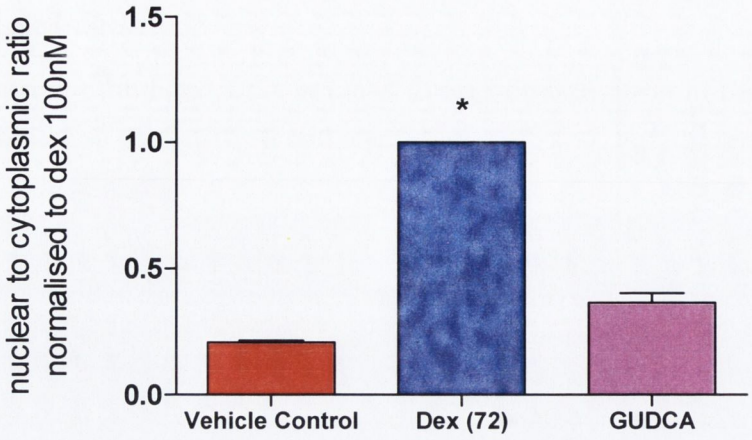

Figure 5.19 GUDCA does not induce GR translocation. *SKGT-4 cells were treated with DMSO 1% as vehicle control, treated with dexamethasone 100 nM as a positive control or GUDCA 300 μM. After 4 h cells were fixed, stained, visualised and analysed as described. Values are normalised to nuclear to cytoplasmic ratio of dexamethasone 100 nM and are expressed as the mean ± SEM of two experiments performed in triplicate, * $p < 0.05$ relative to vehicle control as determined by one-way ANOVA and Dunnett's post-hoc correction.*

A)

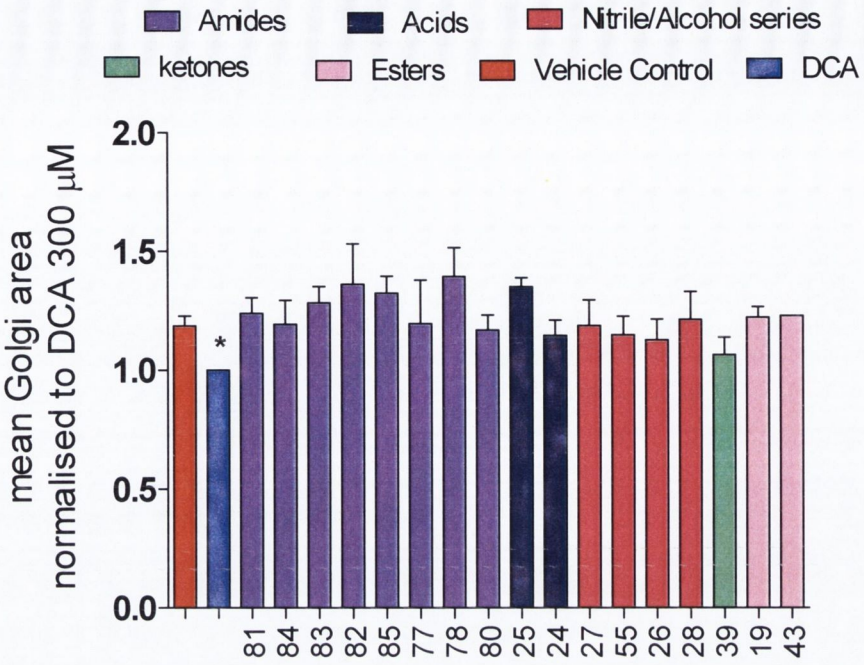
Amides
Acids
Nitrile/Alcohol series
ketones
Esters
Vehicle Control
DCA
mean Golgi area normalised to DCA 300 μM
2.0
1.5
1.0
0.5
0.0
*
81
84
83
82
85
77
78
80
25
24
27
55
26
28
39
19
43

B)

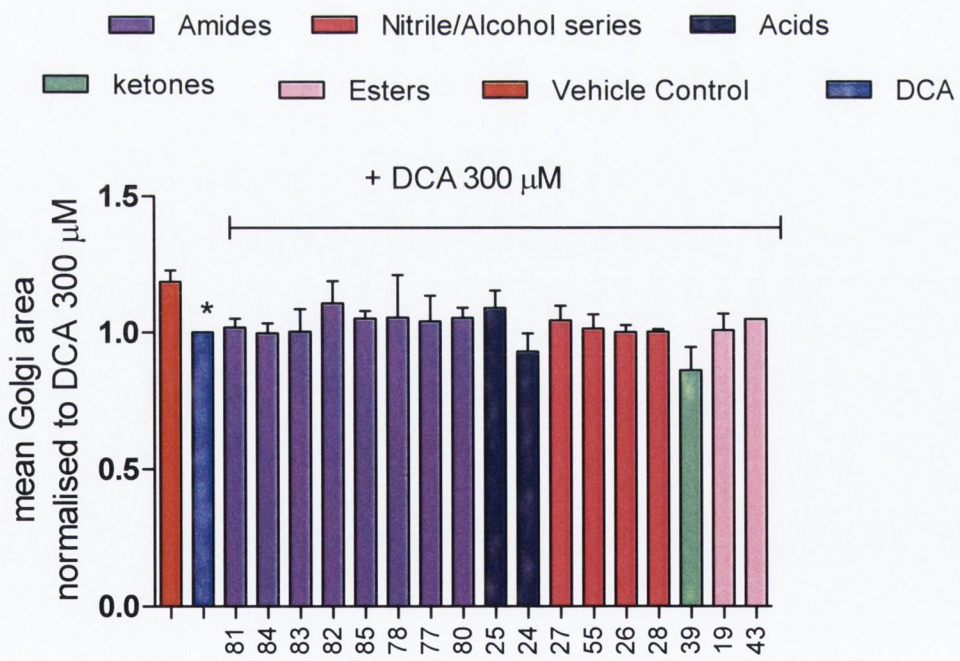
Amides
Nitrile/Alcohol series
Acids
ketones
Esters
Vehicle Control
DCA
+ DCA 300 μM
mean Golgi area normalised to DCA 300 μM
1.5
1.0
0.5
0.0
*
81
84
83
82
85
78
77
80
25
24
27
55
26
28
39
19
43

Figure 5.20 UDCA derivatives do not inhibit DCA induced Golgi fragmentation. *HET-1A cells were A) treated with BA derivatives (300 μM) for 24 h or B) treated with BA derivatives (300 μM) for 18 h and then co-treated with DCA 300 μM for a further 6 h. After the DCA treatment the cells were fixed, stained and visualised as described in Figure 5.5. Original magnification, x20. Values are expressed as mean Golgi area normalised to DCA 300 μM and represent the mean ± SEM of n=3 experiments in duplicate, * p< 0.05 relative to vehicle control as determined by one-way ANOVA and Dunnett's post-hoc correction.*

Hence, although UDCA acts via the GR to inhibit DCA induced fragmentation derivatives with increased potency for GR translocation did not significantly inhibit Golgi fragmentation. This indicates that UDCA only partly acts via the GR in preventing fragmentation but also inhibits DCA induced fragmentation via other pathways which our current panel of compounds do not affect.

5.3.5 Do BAs affect other components of the secretory pathway?

Ongoing work in our laboratory has shown that there are multiple downstream effects of Golgi fragmentation. These include defects in the secretory pathway as outlined and effects on glycosylation pattern.

Failure of post-translational modification is one of the insults that can lead to the activation of the ER stress (Wu & Kaufman, 2006). Hence we wanted to investigate the effects of BAs on the UPR. We decided to screen the panel of 13 natural BAs to investigate effects on three different markers of the UPR: Bip, CHOP, ATF3, Figure 5.21. All BAs were initially tested at 300 μM. We found that BAs that induced fragmentation of the Golgi were capable of inducing an ER stress response to a significant extent.

A)

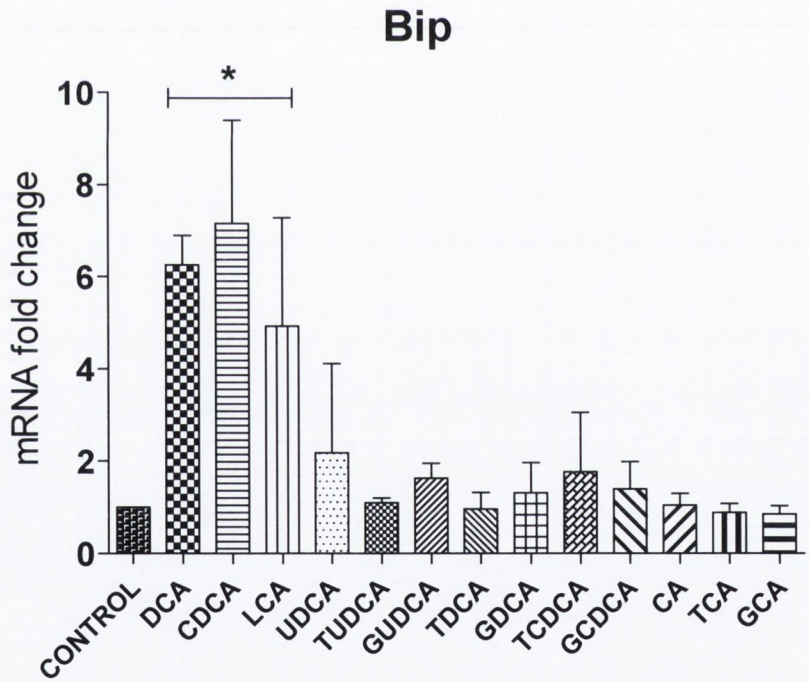

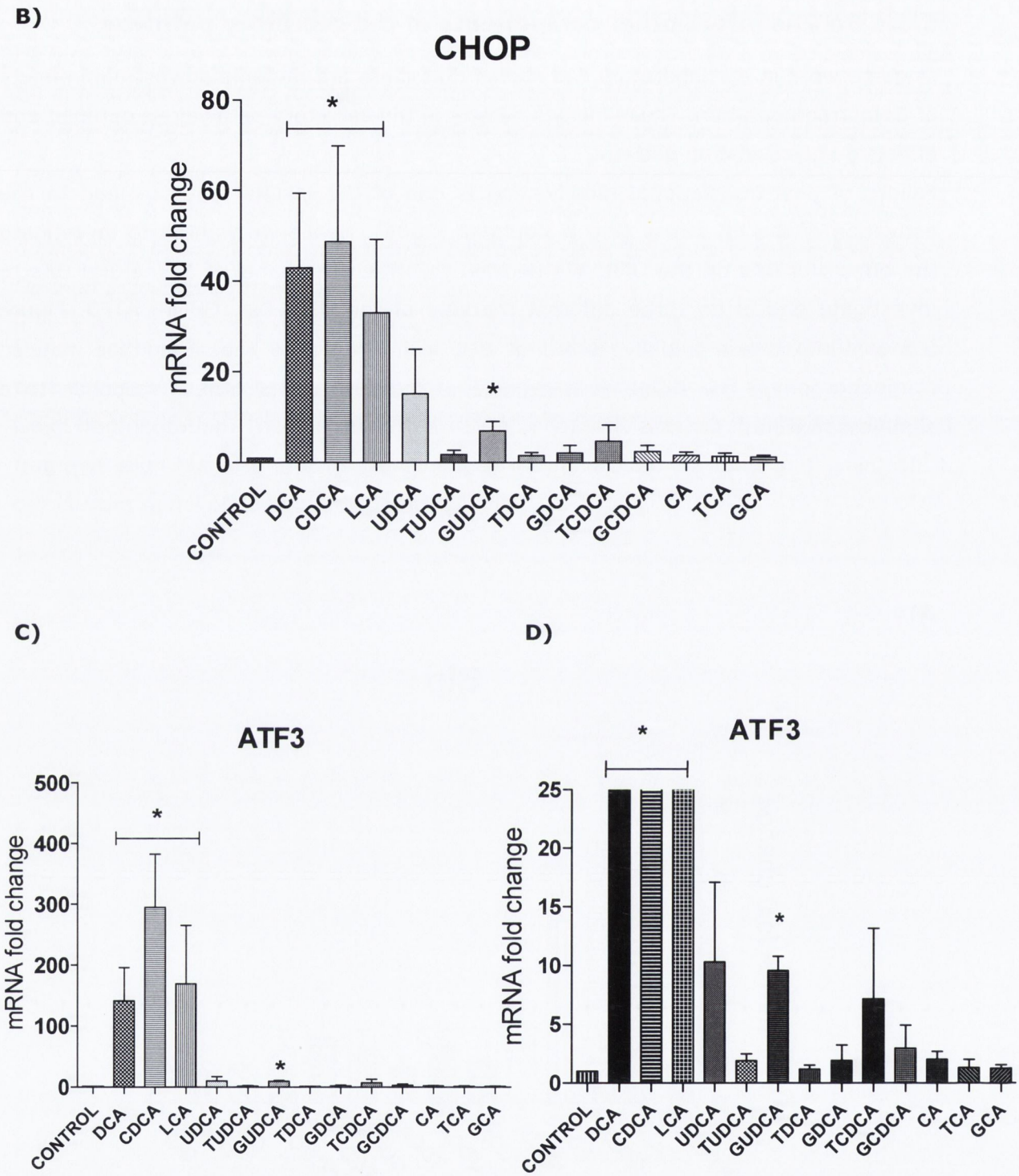

Figure 5.21 DCA, CDCA and LCA increase expression of BIP, CHOP and ATF3. *HET-1A cells were treated with medium or various BAs (300μM) or LCA (25μM) for 6 h. BIP, CHOP and ATF3 mRNA was measured by real-time PCR using GAPDH as denominator control gene. Panel C and D show the same data on different scales. Values represent the mean ± SEM for n=3 experiments, * $p<0.05$ relative to untreated control as determined by a one sample t-test based on delta Ct values.*

DCA, CDCA and LCA increased expression of Bip by 6 fold. There was a large increase in the levels of CHOP and ATF3 with CHOP being increased by these BAs, 40-60 fold, ATF3 expression increasing by 100 fold, following treatment with DCA and LCA. CDCA was found to be the most potent inducer of ATF3, increasing gene expression by ~300 fold. CA or its conjugates did not have any effect on the expression of any of the ER stress response genes. UDCA and both its conjugates increased levels of CHOP and ATF3 (10-15 fold) although this was only significant in the case of GUDCA. None of the other BAs had any effect on gene expression. A number of studies have recently shown that CHOP is involved in GCDCA mediated apoptosis in hepatocyte cell lines and furthermore that a deficiency in CHOP can attenuate GCDCA induced cell death (Iizaka *et al.*, 2007; Tamaki *et al.*, 2008). Interestingly GCDCA had no effect on the levels of Bip, CHOP or ATF3 in our cell model. Indeed the glyco and tauro conjugated forms of DCA and CDCA had no effect on any of the ER stress proteins.

This is consistent with animal models and human studies which suggest that at neutral pH, unconjugated BAs have a greater role to play in esophageal mucosal injury whereas the conjugated forms are more injurious at lower pH (Vaezi, Singh & Richter, 1995)

We also investigated the effect of DCA, CDCA and LCA on XBP-1, Figure 5.23. Unlike the other markers of ER stress, DCA, CDCA and LCA were found to have no effect on the levels of XBP-1. This is of interest as under expression of XBP-1 has been linked with defects in the structural integrity of the ER. Also, Lee *et al* report that it is necessary for the full biogenesis of the secretory machinery in exocrine cells.

Lower concentrations of DCA and CDCA (50 μM and 100 μM) also significantly increased levels of CHOP and ATF3 although the concentration effect profile for both DCA and CDCA was not a typical pharmacological one, Figure 5.24. Lower concentrations did not have a significant effect on Bip expression.

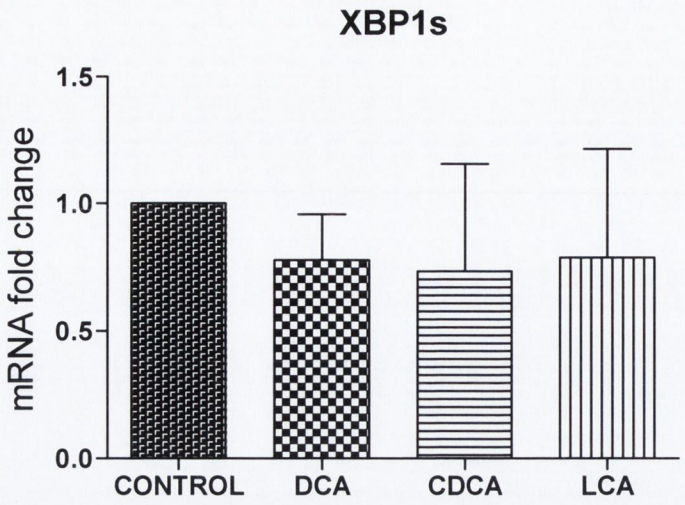

Figure 5.22 DCA, CDCA and LCA do not effect levels of XBP1s. *HET-1A cells were treated with DCA (300μM), CDCA (300μM) and LCA (25μM) for 6 h and XBP1s mRNA was measured by real-time PCR using GAPDH as denominator control gene. Values represent the mean ± SEM for n=3 experiments, * p<0.05 relative to untreated control.*

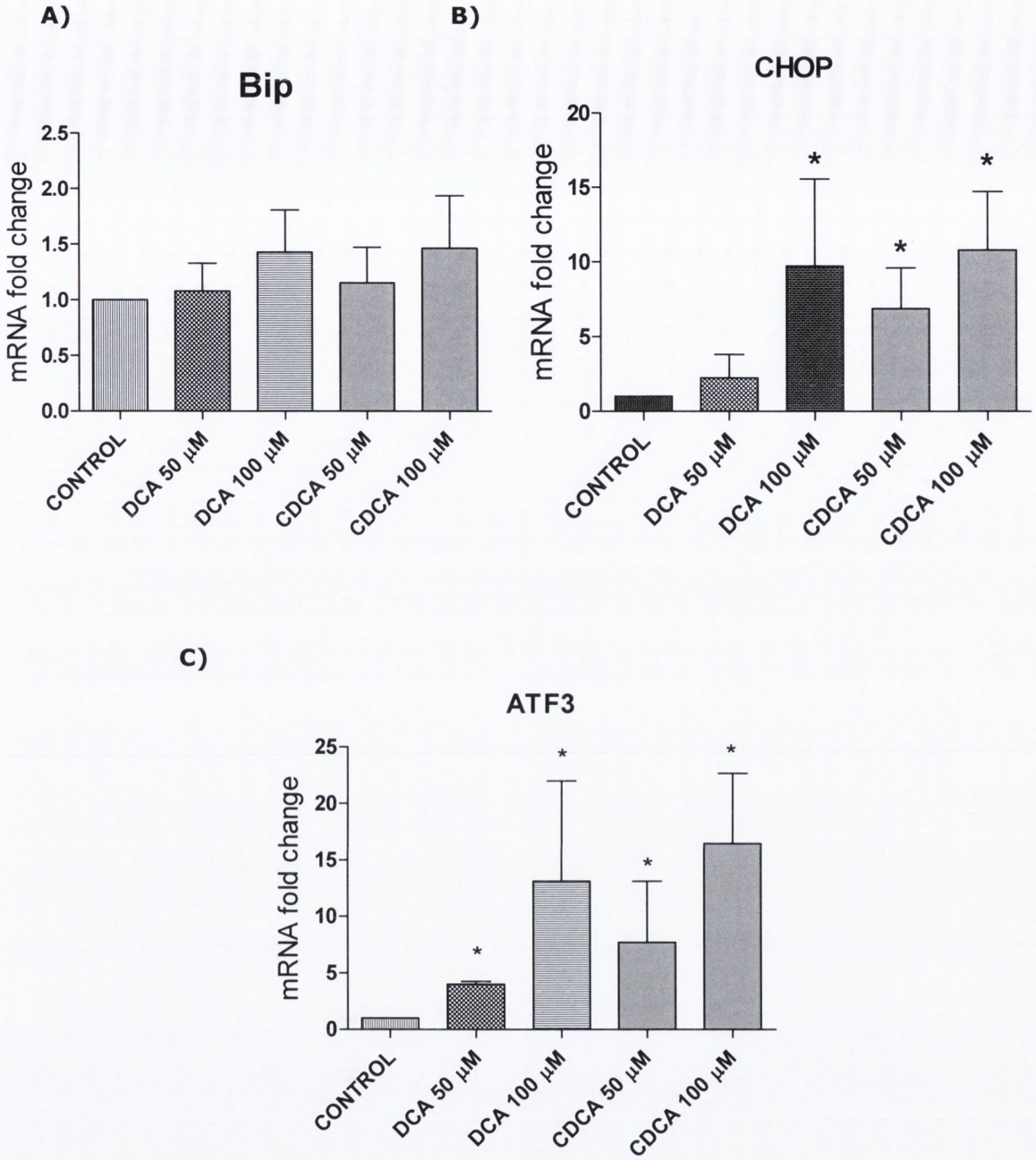

Figure 5.23 DCA, CDCA and LCA increase CHOP and ATF3 expression in a concentration dependent manner. *HET-1A cells were treated with varying concentrations of DCA and CDCA for 6 h. For A) B) and C) BIP, CHOP and ATF3 mRNA was measured by real-time PCR using GAPDH as denominator control gene. Values represent the mean ± SEM for n=3 experiments, * $p<0.05$ relative to untreated control as determined by a one sample t-test based on delta Ct values.*

5.3.6 Salubrinal, an inhibitor of ER stress, inhibits BA induced Golgi fragmentation

Having demonstrated that DCA, CDCA and LCA can induce both Golgi fragmentation and an ER stress response we wanted to investigate if there is a link between these two phenomena. Salubrinal, is an inhibitor of ER stress (Nakka, Gusain & Raghubir, 2010; Sequeira *et al.*, 2009). It inhibits ER stress by inhibiting GADD34-phosphatase which dephosphorylates eIF-2α. Maintaining eIF-2α in a phosphorylated state maintains an inhibition of global protein synthesis and thus decreasing the demand on the ER. Pre-treatment with salubrinal 50 μM prior to LCA, DCA and CDCA treatment resulted in a decrease in BA induced Golgi fragmentation. Salubrinal itself had no effect on the integrity of the Golgi. The fact that inhibition of ER stress, in turn, inhibits Golgi fragmentation may indicate that the Golgi is fragmenting in response to the cellular stress imposed by these toxic BAs.

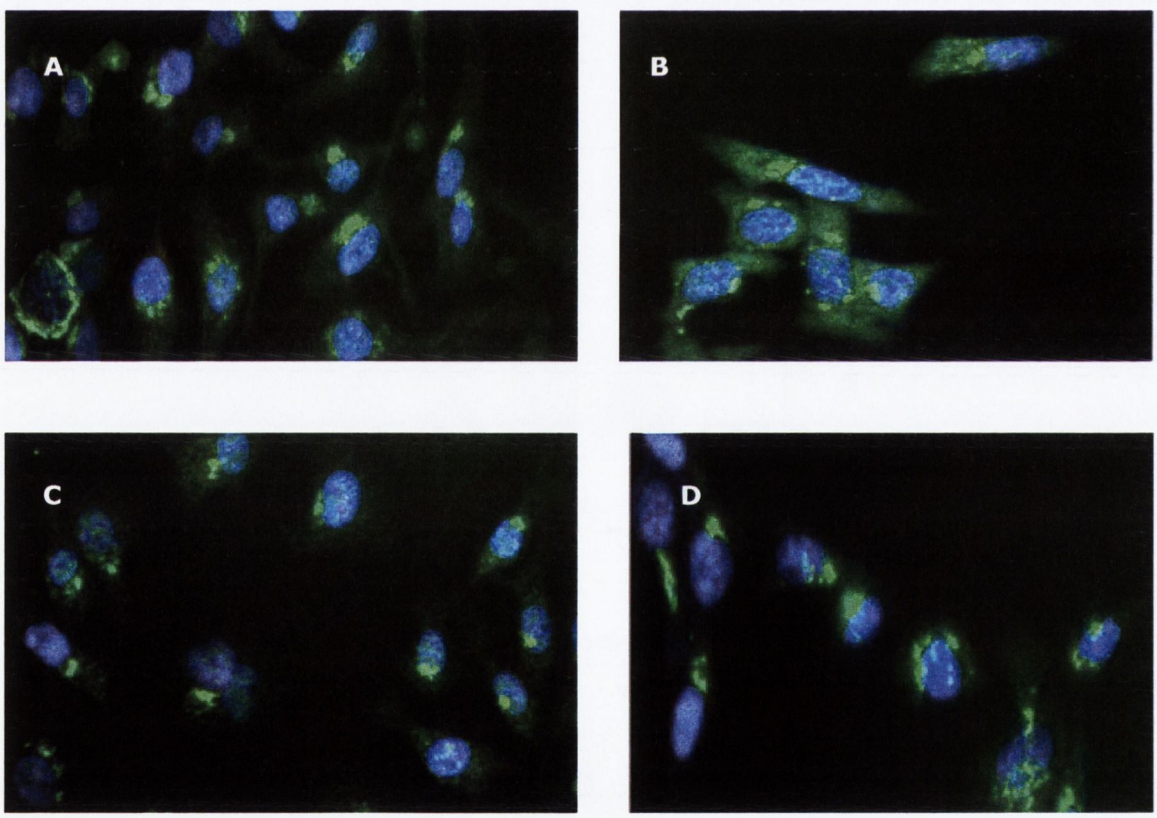

Figure 5.24 Salubrinal inhibits BA induced Golgi Fragmentation. *HET-1A cells were pre-treated with A) salubrinal 50μM for 24 h or pre-treated with salubrinal 50 μM for 18 h and then co-treated with salubrinal 50 μM and B) DCA 300 μM or C) CDCA 300 μM or D) LCA 25 μM for a further 6 h. Cells were fixed, stained and images acquired using InCell-1000, original magnification, ×20.*

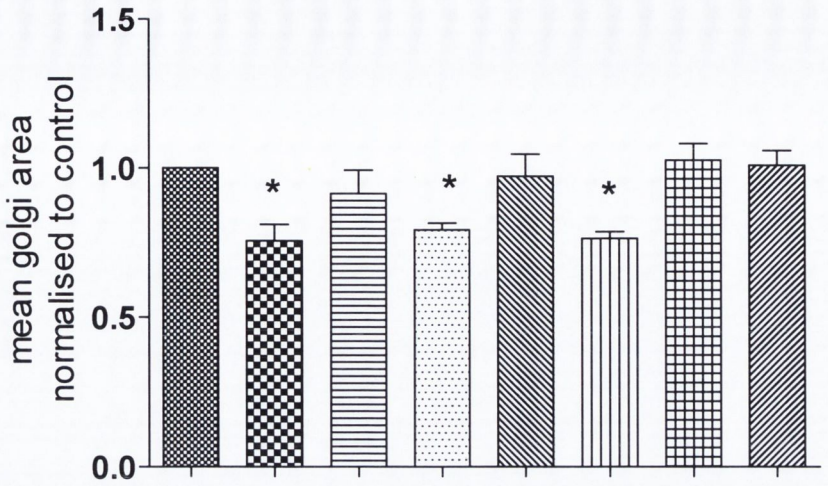

Salubrinal 50 µM	-	-	+	-	+	-	+	+
DCA 300 µM	-	+	+	-	-	-	-	-
LCA 25 µM	-	-	-	+	+	-	-	-
CDCA 300 µM	-	-	-	-	-	+	+	-
Vehicle Control	+	-	-	-	-	-	-	-

Figure 5.25 Analysis of salubrinal pre-treatment. *HET-1A cells were treated as indicated. Cells were fixed, stained and images acquired using the GE In Cell Analyser 1000, original magnification 20× and quantified using the Investigator software package. Data are represented as mean ± SEM, normalised to vehicle control for n=3 experiments,* $p<0.05$ as determined by one way ANOVA and Dunnett's post-hoc correction.*

5.4 Discussion

In this study we showed that DCA can induce Golgi fragmentation in a colon cancer cell line and that this effect can be inhibited by UDCA in a GR dependent mechanism. Using an esophageal cell model we then went on to demonstrate that UDCA can inhibit DCA induced Golgi fragmentation. In these cells the inhibition of DCA induced Golgi by UDCA may at least in part explain its chemopreventative role in colon cancer and it opens up the possibility for its use in chemoprevention of esophageal cancer.

As UDCA inhibition of DCA induced Golgi fragmentation is mediated via the GR we screened a panel of our BA derivatives that demonstrated good potency for GR translocation, for their protective effects on the Golgi. The panel of compounds did not share UDCAs property of inhibiting DCA induced Golgi fragmentation.

Furthermore GUDCA significantly inhibited DCA induced golgi fragmentation however this BA could not induce GR translocation. This strongly indicates that although UDCA inhibits DCA induced golgi fragmentation via the GR other mechanisms must also be involved. It would be interesting to investigate if GUDCAs protective effect could be abrogated with mifepristone treatment however the fact that it is not induce GR translocation indicates that it is acting through another mechanism.

DCA, CDCA and LCA were found to be potent inducers of the UPR, increasing levels of Bip, CHOP and ATF3 mRNA. BAs have been shown to induce apoptosis through the ER stress pathway however, induction of the ER stress response by the toxic BAs resulted in activation of both pro-survival (Bip) and pro-apoptotic (CHOP, ATF3) genes.

Studies have shown that continual exposure of cells to BAs can lead to an apoptosis resistance (Yui *et al.*, 2009) allowing for selective growth of cells resistant to BA-induced apoptosis. Crowley-Weber *et al* carried out molecular characterisation of a BA apoptosis resistant colon cancer cell line and found that a number of genes that may play a role in early stage carcinogenesis were up-regulated in this cell line. Interestingly one of these genes was Bip. Hence taking our work here and previous studies into account we hypothesise that increased levels of Bip could contribute to proliferation and tumourigenesis in these apoptosis-resistant populations(Crowley-Weber et al., 2002).

It would be interesting to investigate the effect of BAs on other pro-survival ER stress proteins such as eif-2α to add weight to this argument.

A new gene, apoptosis antagonizing transcription factor (AATF) has also recently been identified which has been shown to be part of the UPR. AATF has previously been shown to have a function in DNA damage response and can promote cell proliferation through transcriptional regulation of prosurvival factors such as p53 (Bruno *et al.*, 2006; Bruno *et al.*, 2008). Recently Ishigaki *et al* demonstrated that AATF is induced by PERK signalling and can transcriptionally activate the AKT1 gene (Ishigaki *et al.*,

2010). Akt is a serine/threonine protein kinase that has an important function in inhibition of apoptosis and has been shown to play a critical role in controlling cell survival by resisting ER stress-induced cell death signalling (Hu *et al.*, 2004). The exact mechanisms involved remain to be clarified. It would be interesting to investigate the effect of BAs on the expression of AATF and of Akt in our esophageal model.

Analogous to the ER response, the Golgi also fragments only on exposure to sublethal concentrations of the toxic BAs DCA, CDCA and LCA. The idea of the Golgi as a sensor of stress is a relatively new concept although it has now become recognised that most cell organelles might have a capacity to sense stress (Hicks & Machamer, 2005; Maag *et al.*, 2003; Wlodkowic *et al.*, 2009). Hicks and Machamer comment that although there are no documented Golgi specific stress inducers, potential inducers would include disruption of ER protein modifications or folding (Hicks & Machamer, 2005). They further suggest that morphological changes in the Golgi cisternal structure, including unstacking or swelling, could also transduce a stress signal by itself. Hence an ER stress could lead to a Golgi stress resulting in Golgi fragmentation. Conversely Golgi fragmentation which would be expected to result in abnormally glycosylated proteins, could further amplify the UPR.

Either way induction of Golgi fragmentation by the toxic BAs results in a disruption in secretion as demonstrated using DCA. Secreted proteins include cytokines, chemokines, hormones, digestive enzymes, antibodies as well as structural components of the extra-cellular space (Chen *et al.*, 2005). Such proteins carry out fundamental biological functions and provide the main mechanism for intercellular communication (Anelli & Sitia, 2008). It is therefore essential that the secretory pathway processes these proteins so that they can attain the correct conformation allowing for ligand-receptor interaction and correct transmission of signalling (Anelli & Sitia, 2008). Defects in vesicular secretion have also been shown to cause defective cellular migration (Cortopassi *et al.*, 2006). Hence it is reasonable to suggest that the disruption of the secretory pathway by DCA could lead to disruptions in secretion of these proteins resulting in abnormal cell signalling.

Also, ongoing work in our group has demonstrated aberrant glycosylation patterns in esophageal cells upon DCA exposure which could induce characteristics associated with the carcinogenic process. Altered glycosylation of the surfaces of secreted proteins of tumour cells is a common phenotypic change associated with many tumours including leukaemia, neuroblastoma tumour gangliosides and pancreatic cancer (Ladisch *et al.*, 1989; Petrini *et al.*, 1989; Wu *et al.*, 2009). Aberrant glycosylation in glycoproteins and glycosphingolipids of tumour cells has been implicated in defining the stage, direction and fate of tumour progression (Hakomori,

1996). In particular altered glycosylation patterns have been linked to the invasiveness and metastatic potential of a tumour (Hakomori, 1996). This has been reflected in decreased patient survival rate (Hakomori, 2001). Activation of abnormal glycosylation pathways can lead to the formation of Tn and sialyl-Tn antigen which blocks regular carbohydrate chain elongation. Sialyl-Tn antigen is rarely expressed in normal tissues but is aberrantly expressed in colorectal, lung, breast and other cancer (Pinho *et al.*, 2007). Other common types of aberrant glycosylation patterns include expression of sialyl Lewis a and sialyl Lewis x antigens (Hakomori, 2001). Promiscuous O-glycosylation is also seen which results in peptide conformational changes (Hakomori, 1996). Altered glycosylation patterns are able to modulate different malignant phenotypes. Decreased intertumour cell adhesion is commonly seen which results in increased motility of tumour cells increasing metastatic potential (Hakomori, 1996). Altered sialyl-Tn antigen has also been shown to decrease cell-cell aggregation and increased extracellular matrix adhesion, migration and invasion in gastric carcinoma cells (Pinho *et al.*, 2007).

Byrne *et al* demonstrated that after 6 h of DCA treatment removal of the BA resulted in reformation of the Golgi. This indicates that a fragmented Golgi architecture does not mean that the cells are apoptotic as apoptosis is an irreversible process (Byrne *et al.*, 2010). However both the UPR and Golgi are only affected by those BAs which have previously been shown to be cytotoxic in this cell line in Chapter 3, albeit after a longer exposure time. Gonatas *et al* suggest that Golgi fragmentation is a stress response which can trigger apoptosis (Gonatas *et al.*, 2006). Our work here substantiates this idea, particularly as inhibition of cellular ER stress by salubrinal inhibited BA induced Golgi fragmentation. Mancini *et al* propose that the Golgi transduces pro-apoptotic signals through local caspases which can then regulate local effectors (Mancini *et al.*, 2000). Interestingly, the Golgi-disrupting agent brefeldin A has also been shown to induce apoptosis in human follicular lymphoma cell lines (Wlodkowic, Skommer & Pelkonen, 2007). It would be interesting to investigate if higher concentrations of brefeldin A were cytotoxic in the HET-1A cell line.

On the other hand Sodeman *et al* have demonstrated that brefeldin A inhibits BA induced translocation of the death receptor Fas, to the cell membrane which results in an attenuation in BA induced apoptosis in McNtcp.24 cells, an hepatocyte-derived cell line that stably expresses the sodium-dependent taurocholate-cotransporting polypeptide (Sodeman *et al.*, 2000). This indicates that Golgi fragmentation can protect against BA apoptosis due to abnormal trafficking of Fas. However DCA, CDCA and LCA have been shown to induce Fas translocation to the membrane in hepatocytes, in a similar time frame to induction of Golgi fragmentation in our cell line indicating that Golgi disruption by these agents does not inhibit Fas translocation.

Interestingly, Golgi fragmentation in neuronal diseases has been shown to occur in non-apoptotic cells (Gonatas *et al.*, 2006) and therefore more studies are required to address the question of whether Golgi fragmentation is an apoptosis independent event or whether it is a precursor to apoptosis.

It would have been interesting to investigate a correlation between toxicity and Golgi fragmentation in our synthetic panel of compounds. Unfortunately when cells were treated with these derivatives at 300 μM and stained for Golgi morphology the number of non-apoptotic cells remaining were too few to draw any conclusions. It would be interesting to carry out concentration effect curves for these compounds to determine if sub-lethal concentrations of these derivatives also induce Golgi fragmentation.

Although BA induced Golgi fragmentation is reversible it is reasonable to propose that this reversal would not be maintained on a continual exposure to BAs and that BA apoptosis resistant population might have a constitutively fragmented Golgi architecture. Indeed there are a number of colon cancer cell lines with constitutively fragmented Golgi including the SW480, Caco-2, HT-29 and T-84 colon cancer cell lines (Kellokumpu *et al.*, 2002). Furthermore Golgi fragmentation has been observed in ulcerative colitis and colorectal cancer patients (Byrne *et al.*, 2010). Altered secretion and glycosylation patterns in such cells would be expected to contribute to carcinogenesis.

BAs induce an ER stress response which leads to increased levels of Bip which could contribute to proliferation and tumourigenesis in BA apoptosis resistant populations. However multiple proteins are also activated downstream of ER stress, including NF-κB which has been implicated in esophageal carcinogenesis (Hung *et al.*, 2004; Pahl & Baeuerle, 1997; Waris, Tardif & Siddiqui, 2002). Hung *et al* recently demonstrated that induction of ER stress by tunicamycin resulted in translocation of NF-κB from the cytoplasm to the nucleus (Hung *et al.*, 2004). BAs have previously been shown to transcriptionally activate NF-κB in colon and esophageal cells (Duggan *et al.*, 2010; Jenkins *et al.*, 2004; Shah *et al.*, 2006a; Shah *et al.*, 2006b). NF-κB has been implicated in the pathogenesis of esophageal cancer and has been shown to block apoptosis, mediate tumour cell proliferation and induce resistance to chemotherapeutic drugs (Abdel-Latif, Kelleher & Reynolds, 2009b). As NF-κB is a pro-inflammatory transcription factor it can regulate the transcriptional activity of a number of genes, including COX-2. Interestingly Hung *et al* also demonstrated that ER stress can lead to increased expression of COX-2 in a NF-κB dependent fashion. BAs have been shown to increase COX-2 expression in esophageal cell lines (Looby *et al.*, 2009), the implications of which have been discussed in Chapter 1.

In Chapter 4 we demonstrated that UDCA can inhibit NF-κB activity. It would be interesting to investigate if this inhibition is secondary to inhibition of ER stress.

Indeed if UDCA was shown to inhibit BA induced ER stress this might provide another mechanism by which it inhibits golgi fragmentation and may account for GUDCAs effect. This is particularly pertinent as TUDCA has been shown to inhibit ER stress in response to advanced glycation end products (Chen et al., 2008).

Hence we propose that BAs induce ER stress which leads to Golgi fragmentation resulting in abnormal glycosylation and secretion. Simultaneous activation of pathways downstream of ER stress such as the NF-κB pathway can also contribute to this cancer progression.

In conclusion, in this work we demonstrate that the BAs DCA, CDCA and LCA affect the secretory pathway of HET-1A cells which manifests as an ER stress response and Golgi fragmentation. The UPR and Golgi are only affected by those BAs which have previously been shown to be cytotoxic in this cell line. We propose that these changes induced by BAs on the secretory pathway contribute to the development of carcinogenesis by BAs.

CHAPTER SIX

GENERAL DISCUSSION

Traditionally BAs are known for their ability to act as solubilising agents in the gut, where they aid in the absorption of dietary lipids through the formation of mixed micelles (Hofmann, 1999). However the identification of BAs as ligands of the FXR has lead to the realisation that these molecules have a much greater spectrum of biological effects (Parks *et al.*, 1999).

BAs can regulate lipid and glucose homeostasis through activation of the nuclear receptor, FXR and the G-protein coupled receptor, TGR5 (Claudel *et al.*, 2005; Fiorucci *et al.*, 2009; Lefebvre *et al.*, 2009; Pellicciari, Costantino & Fiorucci, 2005). They can also activate a variety of signalling pathways including apoptotic, inflammatory and carcinogenic cascades. On the other hand certain BAs have been shown to have profound anti-inflammatory effects (Yasukawa, Iida & Fujimoto, 2009). Recently BAs found in human cerebrospinal fluid have been shown to activate the Liver X receptor (Ogundare *et al.*, 2010). Activation of this receptor can reduce symptoms of Alzheimer's disease.

This renaissance in BA biology has simultaneously led to the development of a variety of medicinal chemistry programmes with different therapeutic targets but all using BAs as lead structures. BA derivatives with increased efficacy and potency for FXR and TGR5 have been generated which hold great promise for the treatment of metabolic disorders. The peculiar effects of BAs on cell viability have been exploited for the design of selective cytocidal agents for treatment of various cancers (El Kihel *et al.*, 2008). BA derivatives have also been screened with much success for anti-microbial and anti-fungal properties (Aher *et al.*, 2009; Vatmurge *et al.*, 2008). Recently BA derivatives have also been shown to be inhibitors of carbonic anhydrase, opening up the possibility for their use in the treatment of glaucoma (Bulbul *et al.*, 2002).

Our interest in BAs initially arose from the recent studies showing that the BA UDCA could induce translocation of the GR (Miura *et al.*, 2001; Weitzel *et al.*, 2005). Glucocorticoids such as dexamethasone and prednisolone are amongst the most highly prescribed drugs due to their profound anti-inflammatory effect but their chronic use is limited due to extensive side effects. Taking into account UDCAs excellent safety profile during its clinical use for hepatic inflammatory conditions coupled with the recent studies showing its effects on the GR we felt that it would make an excellent candidate for developing a novel anti-inflammatory agent (Angulo & Lindor, 1998; Miura *et al.*, 2001; Tanaka *et al.*, 1996).

The concentrations at which UDCA causes translocation of the GR and immunosuppression are very high (Miura *et al.*, 2001; Sola *et al.*, 2005; Sola *et al.*, 2004; Weitzel *et al.*, 2005). The enterohepatic recycling of UDCA means that these high concentrations are only reached in the liver and bile duct during UDCA therapy (Setchell *et al.*, 1997) but concentrations in the blood serum remain low (Ewerth *et*

al., 1985). Thus our decision to make UDCA derivatives was driven by the desire to produce analogs with increased potency and efficacy for GR translocation which would also serve as useful tools for further characterising UDCA's mechanism of action and understanding its interactions with the GR. We carried this work out in an esophageal model with the hope of finding a novel agent which could target esophageal anti-inflammatory disorders. Esophageal inflammation has been linked to the pathogenesis of esophageal adenocarcinoma (Fitzgerald *et al.*, 2002; Fitzgerald *et al.*, 2001).

This work has led to the discovery of a series of UDCA derivatives which can induce GR translocation with increased efficacy and potency to UDCA. A series of structure activity relationships for GR translocation have emerged as a result of this study which can now be used for synthesis of a larger compound library. Furthermore we have shown that one of the more potent derivatives, CPA (**77**) is capable of activating the GR and inducing transrepression of TNF-α stimulated NF-κB activity. We found that this effect was determined by the BA nucleus as both DCA and CDCA amides (**88-91**) could not induce GR translocation. Crucially we found that this derivative, in a similar vein to UDCA, is not able to displace dexamethasone from the GR LBD. CPA is however able to induce a conformational change in the GR LBD allowing for recruitment of co-activators. The manner in which these derivatives interact with the GR is not known although potential mechanisms have been proposed in Chapter 4. CPA represents a novel mode of action for a GR modulator as all known GR modulators bind to the conventional glucocorticoid binding site in the LBD. Mechanistic studies into the binding mode of these molecules could lead to a new class of anti-inflammatory agents.

We were also interested in the chemopreventative effects of UDCA in colon cancer and in the potential of translating this to esophageal cancer. BAs have been much implicated in the pathogenesis of colon and esophageal cancer (Bernstein *et al.*, 2005; Debruyne *et al.*, 2001) in particular the toxic BAs DCA, CDCA and LCA. This work specifically looked at BA mediated modulation of the secretory pathway and its potential involvement in esophageal cancer progression. In Chapter 5 we showed that the BAs DCA, CDCA and LCA are capable of inducing Golgi fragmentation. The Golgi apparatus plays an essential role in the post-translational modification of proteins and hence we believe that disruptions to its architecture by these BAs could be the means by which they induce carcinogenesis. We also demonstrated that UDCA was capable of inhibiting Golgi fragmentation via the GR. Interestingly, our BA derivatives, with increased potency for GR translocation were unable to significantly protect against DCA induced Golgi fragmentation indicating that other mechanisms are also involved in UDCAs inhibition of Golgi fragmentation. We went on to demonstrate that these BAs were capable of inducing ER stress and that inhibition of this stress lead to a

reduction in BA induced Golgi fragmentation. Therefore it is possible that Golgi fragmentation is a sensor of BA induced stress. TUDCA has previously been shown to inhibit ER stress (Chen *et al.*, 2008), hence UDCA may be inhibiting Golgi fragmentation in a similar manner in our model. This observation would be interesting to explore further. The work here demonstrates that BAs can increase expression of markers of ER stress which have been implicated in cancer progression. Continual exposure to BAs is known to induce apoptosis resistance and so increased levels of these ER stress proteins coupled with a disrupted Golgi architecture in an apoptosis resistant population would be expected to lead to abnormal cell signalling and carcinogenesis.

As mentioned novel cytotoxic agents have been developed using BAs as lead molecules. These studies have exploited the known cytotoxicity of the BAs, DCA, CDCA and LCA. These BAs are considered to be cytotoxic due to their relative hydrophobicity compared to other BAs such as UDCA which are relatively hydrophilic. During the course of our work on the GR we discovered that manipulation of the BA side chain produced derivatives with high hydrophobicity which were not cytotoxic. There is a general consensus in the literature that BA hydrophobicity is a determinant of cytotoxicity but few studies have been done correlating these two characteristics. We augmented our panel of BA derivatives through synthesis and from generous donations allowing us to assemble a panel of BA derivatives with a range of polarities. We determined relative polarity by developing a RPTLC approach and correlated this with cell viability using MTT assays.

This work demonstrated a relationship between hydrophobicity and cytotoxicity with a correlation of 0.6 which increased to 0.82 when only ionisable acidic compounds were considered. This opens up the possibility for using RPLTLC as a predictor of BA cytotoxicity. However hydrophobic BA derivatives are not necessarily toxic indicating that hydrophobicity alone does not govern cytotoxicity emphasising the need for specific structural requirements.

This thesis has answered interesting questions with regard to BA effects and mechanism but has also posed a great deal more questions which need to be addressed in the future. The correlation between hydrophobicity and toxicity needs to be explored in other cell lines. Differences in toxicity patterns of these derivatives across various cell lines could establish interesting model systems to explore differences in protein targeting of the compounds allowing for elucidation of mechanisms. A number of derivatives should be developed further in particular the azide derivatives with a view to honing down on SAR and rationally designing BA based cytotoxic agents.

The study in Chapter 4 has probably posed the biggest question in this work. The binding mode of the UDCA amides to the GR needs to be investigated using various structural biology and biophysical techniques. It is first of all important to validate if these derivatives bind to the GR using an isothermal titration calorimetry approach. This is based on the idea that a binding event is accompanied by a change in the free energy of the system. A number of GR mutants could then be developed in order to characterise the specific binding site. An isotopically labelled GR would allow for identification of protein-ligand interactions potentially through NMR, although the size of the GR protein may prove a limitation. Another approach would synthesis of a biotinylated GR derivative which could then be attached on to beads and potential proteins that the compound is interacting with could be isolated and identified through the use of affinity chromatography and mass spectroscopy. Work also needs to be done to investigate TCAs mechanism of inducing GR translocation.

Our investigations in to the golgi apparatus also need to be followed up studies which further elucidate the mechanism by which GUDCA inhibits golgi fragmentation. It is also important to study the mechanism of golgi fragmentation downstream of ER stress in greater detail. It would also be interesting to see if inhibiting BA induced ER stress leads to a decrease in pro cancerous transcription factors such as AP-1 and NF-κB.

BAs have been described as regulators of diverse cellular functions. We have combined a medicinal chemistry and cellular biology approach to explore the effect of a panel of BAs on three different biological phenomena. These studies have made interesting conclusions regarding the anti-inflammatory, cytotoxic and carcinogenic behaviour of these enigmatic substances. The thesis underlines the importance of chemical structure in understanding the vast biological effects of these molecules. It has also laid a strong foundation for the development of BA based drug discovery programmes which can potentially lead to novel cytocidal and novel anti-inflammatory agents.

CHAPTER SEVEN

EXPERIMENTAL

Uncorrected melting points were obtained using a Stuart® melting point SMP11 melting point apparatus. Spectra were obtained using a Perking Elmer 205 FT Infrared Paragon 1000 spectrometer. Band positions are given in cm^{-1}. Solid samples were obtained by KBr disk; oils were analyzed as neat films on NaCl plates. ^{1}H and ^{13}C spectra were recorded at 27 °C on a Bruker Advance II 600 MHz spectrometer (600.13 MHz ^{1}H, 150.91 MHz ^{13}C) and Bruker DPX 400MHz FT NMR spectrometer (400.13 MHz ^{1}H, 100.16 MHz ^{13}C), in either $CDCl_3$ or CD_3OD, (tetramethylsilane as internal standard).

For $CDCl_3$, ^{1}H-NMR spectra were assigned relative to the TMS peak at 0.00 δ and ^{13}CNMR spectra were assigned relative to the middle CDCl3 triplet at 77.00 ppm. For CD_3OD, ^{1}H and ^{13}C-NMR spectra were assigned relative to the centre peaks of the CD_3OD multiplets at 3.30 δ and 49.00 ppm respectively. High resolution mass spectrometry (HRMS) was performed on a Micromass mass spectrophotometer (EI mode) at the Department of Chemistry, Trinity College. HPLC was performed on a reverse phase 250 mm x 4.6 mm Waters Spherisorb ODS-2, 5 μm column using a Waters Alliance 2695 chromatograph equipped with an autosampler, column oven and dual wavelength detector. TLC was performed on silica gel Merck F-254 plates. Compounds were visually detected by absorbance at 254 nm and/or vanillin staining.

The ^{1}H NMR spectra of BAs are very complex due to the large number of overlapping aliphatic peaks which appear between 1.0 to 2.0 ppm. As a result the characterisation of the ^{1}H NMR spectra of compounds in this thesis only contains assignments for those compounds which are unambiguously assignable and are affected by the chemical modifications made. This is in keeping with convention and published literature.

24-Benzyl 3α, 7β-dihydroxy-5β-cholanoate (43)

3α,7β-Dihydroxy-5β-cholan-24-oic acid (UDCA, **14**) (1.178 g, 3 mmol) was added to a mixture of benzyl bromide (393 μl, 3 mmol) and cesium carbonate (2.93 g, 9 mmol) in N,N-dimethylformamide (10 ml). The mixture was stirred at room temperature and monitored by TLC for disappearance of the acid. After 16 h the reaction mixture was filtered to remove the cesium carbonate salt. The filtrate was collected and partitioned between diethyl ether and water. The organic layer was washed with NaOH (2 × 20 ml) and water (2 × 20 ml), dried ($MgSO_4$) and the solvent removed *in vacuo* to afford the benzyl ester as a white, odourless, solid (1.2 g, 85%).

^{1}H-NMR δ ($CDCl_3$): 0.65 (3-H, s, 18-CH_3), 0.94 (3-H, d, J=6.52 Hz, 21-CH_3), 0.95 (3-H, s, 19-CH_3), 3.60 (2-H, m, 3 β-H, 7 α-H), 5.12 (2-H, s, benzylic CH_2), 7.37 (5-H, m, Aromatic-CH). ^{13}C-NMR ppm ($CDCl_3$): 12.7 (CH_3), 19.1 (CH_3), 22.6 (CH_2), 24.0 (CH_3), 28.1 (CH_2), 29.7 (CH_2), 31.3 (CH_2), 32.2 (CH_2), 32.4 (CH_2), 35.3 (CH_2), 36.1 (CH),

36.7 (CH_2), 38.2 (CH_2), 38.7 (CH_2), 40.1 (CH), 41.6 (CH_2), 44.4 (CH), 44.8 (CH), 44.9, 56.6 (CH), 57.8 (CH), 66.1 (Benzyl-C, CH_2), 71.9 (3-C, 7-C, CH), 128.1, 129.8, 130.4 (Aromatic-C, CH), 175.1 (C=O). HRMS: Found: $(M\text{-}Na)^+$ =505.3309. IR_{vmax} (KBr): 1717 (ester carbonyl), 2859, 2922, 3030 cm^{-1}. mp: 134-136 °C.

24-Methyl 3α, 7β-dihydroxy-5β-cholanoate (19)

Dry methanol (10 ml) was added to 3α, 7β-Dihydroxy-5β-cholan-24-oic acid (UDCA, **14**) (1 g, 2.6 mmol) at 0 °C. Acetyl chloride (0.5 ml) was added drop wise to the mixture. When the addition was complete the reaction mixture was allowed to warm to room temperature. The reaction was monitored by TLC for the formation of methyl ester and disappearance of acid. After 3 h the methanol was removed *in vacuo* and the residue dissolved in ethyl acetate (20 ml). This was partitioned with $NaHCO_3$ (2 × 10 ml) and water (2 × 10 ml). The organic layer was collected and dried ($MgSO_4$) and evaporation of solvent gave the methyl ester as a white, odourless, solid (0.92 g, 88%).

^{1}H-NMR δ ($CDCl_3$): 0.68 (3H, s, 18-CH_3), 0.93 (3-H, d, J=6.52 Hz, 21-CH_3) , 0.95 (3-H, s, 19-CH_3), 3.60 (2-H, m, 3 β-H, 7 α-H), 3.67 (3-H,s,-OCH_3).^{13}C-NMR ppm ($CDCl_3$): 12.9 (CH_3), 19.0 (CH_3), 22.5 (CH_2), 24.0 (CH_3), 28.0 (CH_2), 29.8 (CH_2), 31.1 (CH_2), 32.2 (CH_2), 32.5 (CH_2), 35.3 (CH_2), 36.1 (CH), 36.9 (CH_2), 38.1 (CH_2), 38.9 (CH_2), 40.9 (CH), 41.7 (CH_2), 44.1 (CH), 44.7 (CH), 44.9, 51.1 ($O\underline{C}H_3$), 56.6 (CH), 57.8 (CH), 71.9 (3-C, 7-C, CH), 175.1 (C=O). HRMS: Found: $(M\text{-}Na)^+$= 429.2993. IR_{vmax} (KBr): 1741 (ester carbonyl), 2864, 2937 cm^{-1}. mp: 170-175 °C. literature mp: 58.4-58.6 °C (Huang *et al.*, 2009).

24-Methyl 3α, 7α-dihydroxy-5β-cholanoate (44)

Dry methanol (10 ml) was added to 3α, 7α-dihydroxy-5β-cholan-24-oic acid (CDCA, **5**) (1 g, 2.6 mmol) at 0 °C. Acetyl chloride (0.5 ml) was added drop wise to the mixture. When the addition was complete the reaction mixture was allowed to warm to room temperature. The reaction was monitored by TLC for the formation of methyl ester and disappearance of acid. After 3 h the methanol was removed *in vacuo* and the residue was dissolved in ethyl acetate (20 ml). This was partitioned with $NaHCO_3$ (2 × 10 ml) and water (2 × 10 ml). The organic layer was collected and dried ($MgSO_4$) and the solvent removed to give the methyl ester as a white, odourless, solid (0.98 g, 94%).

^{1}H-NMR δ ($CDCl_3$): 0.68 (3H, s, 18-CH_3), 0.93 (3-H, d, J=6.52 Hz, 21-CH_3), 0.95 (3-H, s, 19-CH_3) 3.44 (1-H, m, 3α-H), 3.83 (1-H, s, 7 α-H), 3.67 (3-H, s, -OCH_3). ^{13}C-NMR ppm ($CDCl_3$): 12.9 (CH_3), 19.2 (CH_3), 22.4 (CH_2), 24.0 (CH_3), 28.3 (CH_2), 29.8 (CH_2),

31.1 (CH_2), 32.4 (CH_2), 32.5 (CH_2), 35.3 (CH_2), 36.3 (CH), 36.9 (CH_2), 38.1 (CH_2), 38.9 (CH_2), 40.9 (CH), 41.7 (CH_2), 44.1 (CH), 44.7 (CH), 44.9, 51 (-C=O<u>C</u>H_3), 56.3 (CH), 57.4 (CH), 68.1 (7-C, CH), 71.9 (3-C, CH), 175.0 (C=O). IR_{vmax} (KBr): 1741 (ester carbonyl), 2864, 2937 cm^{-1}. mp: 171-172 °C. literature mp: 85.2-86.0 °C (Huang *et al.*, 2009).

24-Benzyl 3α, 7α-dihydroxy-5β-cholanoate (52)

CDCA (**5**) (4.7g, 12 mmol) was added to a mixture of benzyl bromide (1.6 ml, 13 mmol) and cesium carbonate (12 g, 36 mmol) in N,N-dimethylformamide (40 ml). The mixture was stirred at room temperature and monitored by TLC for disappearance of the acid. After 16 h the reaction mixture was filtered to remove the cesium carbonate salt. The filtrate was collected and partitioned between diethyl ether and water. The organic layer was washed with NaOH (2 × 30 ml) and water (2 × 30 ml), dried ($MgSO_4$) and the solvent removed to afford the benzyl ester as a white, odourless, solid (5.02 g, 87%).

^{1}H-NMR δ ($CDCl_3$): 0.64 (3-H, s, 18-CH_3), 0.89 (3-H, s, 19-CH_3), 0.90 (3-H, d, J=6.53 Hz, 21-CH_3), 3.44 (1-H, m, 3α-H), 3.83 (1-H, s, 7 α-H), 5.10 (2-H, s, benzylic CH_2), 7.35 (5-H, m, Aromatic-CH). ^{13}C-NMR ppm ($CDCl_3$): 12.8 (CH_3), 19.2 (CH_3), 22.1 (CH_2), 24.2 (CH_3), 28.3 (CH_2), 29.7 (CH_2), 31.2 (CH_2), 32.4 (CH_2), 32.5 (CH_2), 35.3 (CH_2), 36.1 (CH), 36.9 (CH_2), 38.1 (CH_2), 38.9 (CH_2), 40.9 (CH), 41.7 (CH_2), 44.0 (CH), 44.7 (CH), 44.9 (13-C), 56.7 (CH), 57.7 (CH), 66.2 (benzyl-C, CH_2), 68.0 (7-C, CH), 71.9 (3-C, CH), 128.1, 129.3, 130.4 (Aromatic-C, CH), 174.2 (C=O). mp: 139-143 °C (Huang *et al.*, 2009).

24-Benzyl 3α-acetoxy-7α-hydroxy-5 β-cholanoate (49)

The benzyl CDCA ester (**52**) (770 mg, 1.5 mmol) was dissolved in DCM (5 ml) at 0 °C. Acetic anhydride (1 ml) and dry pyridine (2 ml) were added to this mixture, warmed to room temperature and stirred for 16 h. After 16 h methanol (0.5 ml) was added to stop the reaction and the mixture was washed with water (2 × 5 ml), HCl (2 × 5 ml) and $NaHCO_3$ (1 × 5 ml). The organic layer was collected and dried ($MgSO_4$). TLC analysis revealed a mixture of products (90% monoacetoxy, 10% diacetoxy). Column chromatography of the mixture with gradient elution (hexane-1:2 ethyl acetate: hexane) afforded the pure monoacetate (524 mg, 66%) as a white odourless solid which was recrystallised from ethanol (460 mg, 53%). Subsequent reactions were carried out on a larger scale. The solid collected after partitioning was recrystallised from ethanol seeding with the crystals collected from the small scale reaction above. Yields ranging from 75-85% were achieved.

^{1}H-NMR δ ($CDCl_3$): 0.65 (3-H, s, 18-CH_3), 0.93 (6-H, m, 19-CH_3, 21-CH_3), 2.02 (3-H, s, 3-OCH_3), 3.86 (1-H, s, 7 β-H), 4.59 (1-H, s, 3 β-H), 5.13 (2-H, dd, J_1=12.04 Hz, J_2=2.51 Hz, J_3=12.55 Hz, benzylic-CH_2), 7.37 (5-H, m, Aromatic-CH). ^{13}C-NMR ppm ($CDCl_3$): 12.8 (CH_3), 19.4 (CH_3), 21.1 (3-OC=O<u>C</u>H_3), 22.5 (CH_2), 24.0 (CH_3), 28.0 (CH_2), 29.8 (CH_2), 31.1 (CH_2), 32.3 (CH_2), 32.5 (CH_2), 35.3 (CH_2), 36.1 (CH), 36.5 (CH_2), 38.2 (CH_2), 38.9 (CH_2), 40.7 (CH), 41.6 (CH_2), 44.0 (CH), 44.7 (CH), 44.9 (13-C), 56.5 (CH), 57.9 (CH), 66.0 (benzyl-C, CH_2), 68.2 (7-C, CH), 75.4 (3-C, CH), 128.2, 129.3, 130.0 (Aromatic-C, CH), 170.1 (3-O<u>C</u>=OCH_3), 175.4 (<u>C</u>=OOC_7H_7). HRMS: Found (M-Na) $^{+}$ =547.3399. IR_{vmax} (KBr): 1734, 2814, 2957, 3045 cm^{-1}. mp: 184-187 °C.

24-Methyl 3 α-acetoxy-7α-hydroxy-5 β-cholanoate (45)

The methyl CDCA ester (**44**) (0.7 mg, 1.7 mmol) was dissolved in DCM (5 ml) at 0 °C. Acetic anhydride (1 ml) and dry pyridine (2 ml) were added to this, the mixture warmed to room temperature and stirred for 16 h. After 16 h methanol (0.5 ml) was added to stop the reaction and the mixture was washed with water (2 × 5ml), HCl (2 × 5ml) and $NaHCO_3$ (1 × 5 ml). The organic layer was collected and dried ($MgSO_4$). TLC analysis revealed a mixture of products (90% monoacetoxy, 10% diacetoxy). Column chromatography of the mixture with gradient elution (hexane-1:2 ethyl acetate: hexane) afforded the pure monoacetate (0.495 g, 65%) as a white odourless solid which was recrystallised from ethanol (0.38 g, 51%). Subsequent reactions were carried out on a larger scale. The solid collected after partitioning was recrystallised from ethanol seeding with the crystals collected from the small scale reaction above. Yields ranging from 75-85% were achieved.

^{1}H-NMR δ ($CDCl_3$): 0.65 (3-H, s, 18-CH_3), 0.93 (6-H, m, 19-CH_3, 21-CH_3), 2.02 (3-H, s, 3-OCH_3), 3.65 (3-H, s, 24-CH_3,), 3.87 (1-H, s, 7 β-H), 4.59 (1-H, s, 3 β-H). ^{13}C-NMR ppm ($CDCl_3$): 12.6 (CH_3), 19.1 (CH_3), 21.0 (3-OC=O<u>C</u>H3), 22.5 (CH_2), 24.2 (CH_3), 28.1 (CH_2), 29.8 (CH_2), 31.1 (CH_2), 32.3 (CH_2), 32.7 (CH_2), 35.3 (CH_2), 36.0 (CH), 36.9 (CH_2), 38.1 (CH_2), 38.9 (CH_2), 40.9 (CH), 41.8 (CH_2), 44.1 (CH), 44.7 (CH), 44.9 (13-C), 51.1 (O<u>C</u>H_3), 56.6 (CH), 57.8 (CH), 68.1 (7-C, CH), 71.1 (3-C, CH), 170.0 (3-O<u>C</u>=OCH_3), 175.3 (<u>C</u>=OCH_3). mp: 145-148 °C. literature mp: 79.5-80 °C (Mukhopadhyay & Maitra, 2004).

3 α-hydroxy-7β-azido-5 β-cholan-24-oic acid (40)

Methyl monoacetate (**45**) (2.09 g, 4.66 mmol) was dissolved in dry pyridine (20 ml) and cooled to 0 °C. To this methane sulfonyl chloride (1.92 ml, 24.8 mmol) was added drop wise. The mixture was allowed to warm to room temperature and then the

reaction was left overnight (16 h). A clear dark solution had formed. TLC analysis showed formation of two products one with a lower Rf of 0.4 compared to 0.6 of the starting material and one with an Rf of 0.8 (mobile phase ethyl acetate: hexane (1:2)). The dark solution was dripped into cold water and then extracted with ethyl acetate (2 × 20ml). The organic layers were combined and washed with HCl (6 × 15 ml) to neutralize the pyridine. The organic layer was retrieved, dried ($MgSO_4$) and the solvent removed *in vacuo* to yield an orange residue. Column chromatography of the mixture with gradient elution (hexane-1:2 ethyl acetate: hexane) gave a white product (1.54 g, 63%). The mesylate was the spot with lower Rf. The mesylate (1.4 g, 2.7 mmol) was dissolved in DMSO (10 ml). This solution was then saturated with sodium azide and the mixture left at room temperature for 7 days. TLC analysis revealed formation of the azide with some remaining starting material. The mixture was partitioned between ethyl acetate and water. The organic layer was retrieved and dried ($MgSO_4$). Column chromatography of the residue eluting with ethyl acetate: hexane (1:4) afforded a white odourless solid (0.9039 g, 72%). The protected azide (800 mg, 1.7 mmol) was dissolved in methanol/NaOH (20 ml, pH 14) and stirred for 16 h at room temperature. The solvent was removed by evaporation and the remaining water solution was acidified with HCl to pH 1. This was then partitioned between ethyl acetate and water to yield a residue containing azide acid as the main product with contamination form partially hydrolysed compounds and benzyl alcohol. Column chromatography using gradient elution (ethyl acetate: DCM (1:1) to methanol) afforded the pure azide acid from the methanol fractions (367 mg, 52%). ^{1}H-NMR δ (CD_3OD): 0.69 (3H, s, 18-CH_3), 0.94 (3-H, d, J=6.52 Hz, 21-CH_3), 0.95 (3-H, s, 19-CH_3), 3.05 (1-H, m, 7 α-H), 3.64 (1-H, m, 3 β-H). ^{13}C-NMR ppm (CD_3OD): 13.0 (CH_3), 18.9 (CH_3), 22.4 (CH_2), 24.1 (CH_3), 28.1 (CH_2), 29.7 (CH_2), 31.0 (CH_2), 32.1 (CH_2), 32.4 (CH_2), 35.3 (CH_2), 36.2 (CH), 36.9 (CH_2), 38.0 (CH_2), 38.9 (CH_2), 40.5 (CH), 41.7 (CH_2), 44.2 (CH), 44.6 (CH), 44.9 (13-C), 56.5 (CH), 57.8 (CH), 61.0 (7-C, CH), 71.1 (3-C, CH), 178.0 (-O=C̲OH). HRMS: Found $(M-Na)^+$ =440.2889. IR_{vmax} (KBr): 1702 (C=O), 2867, 2932, 3429cm^{-1}. mp: 58-60 °C.

24-Benzyl 3 α-acetoxy-7-keto-5 β-cholanoate (50)

24-Benzyl 3 α-acetoxy-7α-hydroxy-5 β-cholanoate (**49**) (1 g, 1.9 mmol) was dissolved in DCM (10 ml). To this pyridinium chlorochromate (0.412 g, 1.9 mmol) was added and the reaction was left to stir for 16 h. After 16 h the brown solution of DCM was pushed through a small plug of silica to remove the reduced PCC. Ether (5 × 10 ml) was added to the flask until the brown PCC residue crumbled up. These ether washings were added to the plug of silica. The compound was then eluted with ethyl

acetate. The organic fractions were combined and the solvent removed to give a white odourless solid (1 g, 99%).

^{1}H-NMR δ ($CDCl_3$): 0.64 (3H, s, 18-CH_3), 0.93 (6-H, m, 19-CH_3, 21-CH_3), 2.01 (3-H, s, 3-OCH_3), 4.70 (1-H, m, 3 β-H), 5.12 (2-H, dd, dd, J_1=12.04 Hz, J_2=2.51 Hz, J_3=12.55 Hz, benzylic-CH_2), 7.37 (5-H, m, Aromatic-CH).^{13}C-NMR ppm ($CDCl_3$): 12.9 (CH_3), 18.9 (CH_3), 21.1 (3-OC=O$\underline{C}H_3$), 22.5 (CH_2), 24.0 (CH_3), 28.0 (CH_2), 29.8 (CH_2), 31.1 (CH_2), 32.2 (CH_2), 32.5 (CH_2), 35.3 (CH_2), 36.1 (CH), 36.9 (CH_2), 38.1 (CH_2), 38.9 (CH_2), 40.9 (CH), 41.7 (CH_2), 44.1 (CH), 44.7 (CH), 44.9 (13-C), 56.6 (CH), 57.7 (CH), 66.1 (benzyl-C, CH), 75.2 (3-C, CH), 128.1, 129.2, 130.4 (Aromatic-C, CH), 170.1 (3-O$\underline{C}$=OCH_3), 175.0 ($\underline{C}$=OOC_7H_7), 212.2 (7-$\underline{C}$=O). HRMS: Found (M-Na) $^{+}$ = 545.3243. IR_{vmax} (KBr): 1722, 2798, 2937, 3105 cm^{-1}. mp: 161-166 ^{o}C.

3 α-hydroxy-7-keto-5 β-cholan-24-oic acid (36)

The protected ketone (**50**) (800 mg, 1.5 mmol) was dissolved in methanol/NaOH (pH 14) and the reaction left to stir for 16 h. After 16 h, the methanol was removed *in vacuo* and the remaining solution acidified with HCl (pH 1). The precipitated acid was then extracted with ethyl acetate (2 × 20 ml). The solvent was removed to give a yellow residue. Column chromatography using gradient elution (ethyl acetate: dichloromethane 1:1 to methanol) afforded the keto acid in the methanol fractions (339 mg, 58%).

^{1}H-NMR δ (CD_3OD): 0.73 (3H, s, 18-CH_3), 0.97 (3-H, d, J=6.54 Hz, 21-CH_3), 1.25 (3-H, s, 19-CH_3), 3.5010 (1-H, m, 3 β-H). ^{13}C-NMR ppm (CD_3OD): 12.7 (CH_3), 19.0 (CH_3), 22.5 (CH_2), 24.0 (CH_3), 28.0 (CH_2), 29.8 (CH_2), 31.1 (CH_2), 32.2 (CH_2), 32.5 (CH_2), 35.5 (CH_2), 36.1 (CH), 36.7 (CH_2), 38.1 (CH_2), 38.9 (CH_2), 40.9 (CH), 41.7 (CH_2), 44.1 (CH), 44.7 (CH), 44.9 (13-C), 56.4 (CH), 57.8 (CH), 70.1 (3-C, CH), 176.3 (-O=COH), 215.4 (7-C). HRMS: Found (M-Na) $^{+}$= 413.2668. IR_{vmax} (KBr): 1703 (C=O), 2942, 3430 cm^{-1} mp: 190-196 ^{o}C, literature mp: 198-201 ^{o}C (Ishida & Kikuchi, 1967).

3 α-acetoxy-7-keto-5 β-cholan-24-oic acid (37)

The protected ketone (**50**) (400 mg, 0.75 mmol) was dissolved in ethyl acetate. Palladium on carbon was added to this and the compound was reduced with hydrogen for 8 h. The mixture was filtered through silica to remove the palladium. The silica was washed with methanol to elute the acid. The solvent was removed to produce a white odourless compound (300 mg, 92%).

^{1}H-NMR δ (CD_3OD): 0.73 (3H, s, 18-CH_3), 1.00 (3-H, d, J=6.52 Hz, 21-CH_3), 1.28 (3-H, s, 19-CH3), 2.01 (3-H, s, 3-OCH_3), 3.08, 4.69 (1-H, m, 3 β-H). ^{13}C-NMR ppm

(CD_3OD): 13.0 (CH_3), 19.1 (CH_3), 21.1 (3-OC=O$\underline{C}H_3$), 22.5 (CH_2), 24.2 (CH_3), 28.1 (CH_2), 29.5 (CH_2), 31.3 (CH_2), 32.2 (CH_2), 32.7 (CH_2), 35.4 (CH_2), 36.1 (CH), 36.6 (CH_2), 38.1 (CH_2), 38.7 (CH_2), 40.9 (CH), 41.2 (CH_2), 44.1 (CH), 44.7 (CH), 44.9 (13-C), 56.4 (CH), 57.7 (CH), 75.3 (3-C, CH), 170.4 (3-O$\underline{C}$=OCH_3), 215.0 (7-$\underline{C}$=O). HRMS: Found $(M\text{-}Na)^+$ = 455.2770. IR_{vmax} (KBr): 1705 (7-C=O), 1738 (3-O$\underline{C}$=O$\underline{C}H_3$), 2870, 2937, 3425 cm^{-1}. mp: 157-160 °C (Snopek *et al.*, 1988).

24-Benzyl 3 α-hydroxy-7-keto-5 β-cholanoate (51)

The protected ketone (**50**) (400 mg, 0.75 mmol) was dissolved in methanol/$NaHCO_3$ (pH 10). This was left overnight. The mild basic conditions resulted in selective removal of the acetate group monitored by TLC analysis. The methanol was removed *in vacuo*. The residue was extracted with ethyl acetate (2 × 20 ml). This was then washed with HCl and water to neutrality. The organic layer was dried ($MgSO_4$) and the solvent removed to leave a residue. The titled product was obtained after chromatographic elution with (ethyl acetate: hexane 1:1).

^{1}H-NMR δ (CD_3OD): 0.68 (3H, s, 18-CH_3), 0.72 (3-H, s, 19-CH_3), 0.98 (3-H, d, J= 6.53 Hz, 21-CH_3), 3.01, 3.37 (1-H, m, 3 β-H), 5.12 (2-H, dd, J_1=12.04 Hz, J_2=2.51 Hz, J_3=12.55 Hz, benzylic-CH_2), 7.37 (5-H, m, Aromatic= CH). ^{13}C-NMR ppm (CD_3OD): 12.8 (CH_3), 18.9 (CH_3), 22.4 (CH_2), 24.0 (CH_3), 28.2 (CH_2), 29.8 (CH_2), 31.1 (CH_2), 32.2 (CH_2), 32.5 (CH_2), 35.5 (CH_2), 36.3 (CH), 36.9 (CH_2), 38.1 (CH_2), 38.5 (CH_2), 40.9 (CH), 41.7 (CH_2), 44.1 (CH), 44.5 (CH), 44.9 (13-C), 57.0 (CH), 57.5 (CH), 66.1 (benzyl-C, CH_2), 71.2 (3-C, CH), 128.1, 129.0, 130.2 (Aromatic-C, CH), 175.0 ($\underline{C}$=OOC_7H_7), 215.1 (7-$\underline{C}$=O). HRMS: Found $(M\text{-}Na)^+$ = 503.3137. IR_{vmax} (KBr): 1709 (7-C=O), 1738 (ester carbonyl), 2870, 2937, 3425 cm^{-1}. mp: 30-35 °C.

3, 7-Diketo-5 β-cholan-24-oic acid (39)

The benzyl CDCA ester (**52**) (1.5 g, 3 mmol) was dissolved in DCM and pyridinium chlorochromate (1.684 g, 7.8 mmol) was added to this. The reaction was left to stir at room temperature for 16 h. After 16 h the brown solution of DCM was pushed through a small plug of silica to remove the reduced PCC. Ether (5 × 10 ml) was added to the flask until the brown PCC residue crumbled up. These ether washings were added to the plug of silica. The compound was then eluted with ethyl acetate. The organic fractions were combined and the solvent removed to give a white odourless solid (1.3 g, 92%). The protected ketone (500 mg, 1 mmol) was dissolved in ethyl acetate. Palladium on carbon was added to this and the compound was reduced with hydrogen for 8 h. The mixture was filtered through silica to remove the palladium. The silica was

washed with methanol to elute the acid. The solvent was removed to produce a white odourless compound (382 mg, 94%).

^{1}H-NMR δ (CD_3OD): 0.77 (3H, s, 18-CH_3), 0.99 (3-H, d, J=6.52 Hz, 21-CH3), 1.36 (3H, s, 19-CH_3). ^{13}C-NMR ppm (CD_3OD): 12.9 (CH_3), 19.1 (CH_3), 22.5 (CH_2), 24.0 (CH_3), 28.0 (CH_2), 29.8 (CH_2), 31.1 (CH_2), 32.2 (CH_2), 32.5 (CH_2), 35.3 (CH_2), 36.1 (CH), 36.9 (CH_2), 38.2 (CH_2), 38.9 (CH_2), 40.8 (CH), 41.5 (CH_2), 44.1 (CH), 44.6 (CH), 44.9 (13-C), 56.5 (CH), 57.8 (CH), 176.2 (O=COH), 212.0 (7-C=O), 215.1 (3-C=O). HRMS: Found $(M-Na)^+$ = 411.2511. IR_{vmax} (KBr): 1436, 1710, 2960, 3473 cm^{-1}. mp: 152-154 °C, literature mp: 152-154 °C (Kitahara & Sato, 1964).

3α, 7β -diformyloxy-5 β-cholan-24-oic acid (54)

UDCA (**14**) (5 g, 12 mmol) was dissolved in formic acid (96%). Perchloric acid (0.5 ml) was added to this drop wise and the reaction was stirred for 3 h at 47-50 °C. After 3 h the temperature was reduced to 40 °C and acetic anhydride was added drop wise to the reaction mixture until bubbles were produced (approx. 10 ml, over 10 min). This was then left to stir for another 10 min. The mixture was cooled to room temperature and added to 100 ml water. The precipitated acid was collected through Buchner filtration and then dissolved in diethyl ether. The organic fraction was successively washed with NaCl solution (20%) and water to neutrality. The diethyl ether was dried ($MgSO_4$) and the solvent removed *in vacuo* to yield a white solid (5.44 g, 96%). This was then recrystallised from hot ethanol to give white needle like crystals (4.896 g, 90%).

^{1}H-NMR δ (CD_3OD): 0.70 (3-H, s, 18-CH_3), 0.93 (3-H, d, J=6.02 Hz, 21-CH_3), 1.00 (3-H, s, 19-CH_3), 4.83-4.95 (2-H, m, 3-β H, 7-α H), 8.03 (2-H, s, OCOH). ^{13}C-NMR ppm (CD_3OD): 12.7 (CH_3), 19.0 (CH_3), 22.4 (CH_2), 24.0 (CH_3), 28.0 (CH_2), 29.8 (CH_2), 31.0 (CH_2), 32.5 (CH_2), 32.5 (CH_2), 35.5 (CH_2), 36.1 (CH), 36.9 (CH_2), 38.1 (CH_2), 38.9 (CH_2), 40.9 (CH), 41.5 (CH_2), 44.1 (CH), 44.7 (CH), 44.9 (13-C), 56.6 (CH), 57.8 (CH), 79.1 (3-C, 7-C, CH), 161.5, 162.0 (-OC=OH), 180.4 (24-C=OOH). mp: 145-148 °C, literature mp: 170-171 °C (Babu & Maitra, 2005).

3α, 7β -diformyloxy-5 β-cholan-23-nitrile (93)

The reaction was carried out in a round bottomed flask with an air condenser fitted with a moisture trap. Formyl protected UDCA (**54**) (5.06 g, 12.9 mmol) was stirred in trifluoroacetic acid (4 ml) and trifluoroacetic anhydride (1 ml) at 0-5 °C until dissolution was complete. Sodium nitrite (0.786 g) was then added in small portions, waiting for the salt to react between additions. After addition the mixture was stirred at 0-5 °C for 1 h. The mixture was then warmed to 38-40 °C and left to stir for another 2 h. The brown solution was cooled to room temperature and added to a

mixture of water/ 1M NaOH (100 ml each). The nornitrile was extracted with ethyl acetate and washed with NaOH (4 × 20 ml) and water to neutrality. The ethyl acetate was dried ($MgSO_4$) and removed by evaporation to yield an off white solid. The compound was characterised in the next step as washing with NaOH yielded a mixture of hydrolysis products.

3α, 7β -dihydroxy-24-nor-5β-cholane-23-nitrile (55)

Sodium (1 g) was added to methanol (50 ml) to form an excess of sodium methoxide. The formyl nitrile (**93**) obtained in the above reaction was added to this solution and refluxed for 2 h. After 2 h the reaction was cooled to room temperature and added to water (100 ml). The nornitrile was extracted with ethyl acetate. The organic layer was then washed with water (3 × 20 ml) and dried ($MgSO_4$). The solvent was removed by evaporation to yield a yellow solid (4.39 g, 95%).

^{1}H-NMR δ ($CDCl_3$): 0.72 (3-H, s, 18-CH_3), 0.97 (3-H, s, 19-CH_3), 1.18 (3-H, d, J=6.02 Hz, 21-CH_3), 2.24 (1-H, m, 22-α (β) CH_2), 2.36 (1-H, m, 22-α (β) CH_2), 3.61 (2-H, m, 3- β H, 7-α H). ^{13}C-NMR ppm ($CDCl_3$): 12.5 (CH_3), 19.1 (CH_3), 22.5 (CH_2), 24.0 (CH_3), 28.0 (CH_2), 29.8 (CH_2), 31.1 (CH_2), 32.5 (CH_2), 35.5 (CH_2), 36.1 (CH), 36.5 (CH_2), 38.1 (CH_2), 38.5 (CH_2), 40.9 (CH), 41.7 (CH_2), 44.1 (CH), 44.7 (CH), 44.9 (13-C), 56.6 (CH), 57.8 (CH), 71.5 (3-C,7-C, CH), 118.6 (-C≡N). HRMS: Found: $(M-H)^-$= 358.2746. IR_{vmax} (KBr): 2243, 3026, 3452 (nitrile peak) cm^{-1}. mp: 215-217 °C, literature mp: 232-233.5 °C (Schteingart & Hofmann, 1988).

3α, 7β -dihydroxy-24-nor-5β-cholane-23-oic acid (24)

3α, 7β -dihydroxy-24-nor-5β-cholane-23-nitrile (**55**) (4 g, 11.1 mmol) was refluxed with 10% KOH in 50 ml ethanol: water (1:1) for 96 h. The ethanol was evaporated and the solution was extracted with diethyl ether until TLC examination showed no more basic compounds in the organic layer. The aqueous layer was then acidified with 6M HCl and the norbile acid was extracted with ethyl acetate (3 × 20 ml). The combined organic layers were then washed with 20% NaCl to neutrality, dried ($MgSO_4$) and evaporated which after column chromatography with ethyl acetate: hexane 4:1 produced a white solid (3.318 g, 79%).

^{1}H-NMR δ (CD_3OD): 0.77 (3-H, s, 18-CH_3), 0.98 (3-H, s, 19-CH_3), 1.02 (3-H, d, J=5.53 Hz, 21-CH_3,), 2.06 (1-H, m, 22α(β)-C), 2.39 (1-H, m, 22α (β)-C), 3.50 (2-H,m, 3- β H, 7-α H). ^{13}C-NMR ppm (CD_3OD): 12.8 (CH_3), 19.1 (CH_3), 22.4 (CH_2), 24.1 (CH_3), 28.0 (CH_2), 29.8 (CH_2), 31.1 (CH_2), 32.5 (CH_2), 35.3 (CH_2), 36.1 (CH), 36.9 (CH_2), 38.1 (CH_2), 38.5 (CH_2), 40.9 (CH), 41.7 (CH_2), 44.5 (CH), 44.7 (CH), 44.9 (13-C), 56.5 (CH), 57.8 (CH), 71.1 (3-C, 7-C, CH), 182.3 (23-C=OOH). HRMS: Found (M-

H)$^-$ =377.2692. IR_{vmax} (KBr): 1708, 3021, 3320 cm^{-1}. mp: 250-253 °C, literature mp: 248-250 °C (Schteingart & Hofmann, 1988).

3α, 7β -diformyloxy-5 β-cholan-23-oic acid (94)

3α, 7β -dihydroxy-24-nor-5β-cholane-23-oic acid (**24**) (3.2 g, 8.4 mmol) was dissolved in formic acid (96%). To this perchloric acid (0.5 ml) was added drop wise and the reaction was stirred for 3 h at 47-50 °C. After 3 h the temperature was reduced to 40 °C and acetic anhydride was added drop wise to the reaction mixture until bubbles were produced (approx. 10 ml, over 10 min). This was then left to stir for another 10 min. The mixture was cooled to room temperature and added to 100 ml water. The precipitated acid was collected through Buchner filtration and then dissolved in diethyl ether. The organic fraction was successively washed with sodium chloride (20%) and water to neutrality. The diethyl ether was dried ($MgSO_4$) and the solvent removed to yield a white solid (3.6 g, 98%).

^{1}H-NMR δ ($CDCl_3$): 0.77 (3-H, s, 18-CH_3), 0.98 (3-H, s, 19-CH_3), 1.02 (3-H, d, J=5.53 Hz, 21-CH_3,), 4.83, 4.95 (2-H, m, 3-β H, 7-α H), 8.03 (2-H, s, OCO<u>H</u>) ^{13}C-NMR ppm ($CDCl_3$): 12.7 (CH_3), 19.2 (CH_3), 22.4 (CH_2), 24.1 (CH_3), 28.2 (CH_2), 29.0 (CH_2), 31.0 (CH_2), 32.5 (CH_2), 35.3 (CH_2), 36.1 (CH), 36.9 (CH_2), 38.5 (CH_2), 38.8 (CH_2), 40.9 (CH), 41.5 (CH_2), 44.1 (CH), 44.7 (CH), 44.9 (13-C), 56.6 (CH), 57.7 (CH), 79.1 (3-C, 7-C, CH), 161.5, 162.7 (-O<u>C</u>=OH), 180.1 (23-<u>C</u>=OOH).

3α, 7β -diformyloxy-5 β-cholan-22-nitrile (95)

The reaction was carried out in a round bottomed flask with an air condenser fitted with a moisture trap. Formyl protected norUDCA (**94**) (3.5 g, 8 mmol) was stirred in trifluoroacetic acid (4 ml) and trifluoroacetic anhydride (1 ml) at 0-5 °C until dissolution was complete. Sodium nitrite (0.786 g) was then added in small portions, waiting for the salt to react between additions. After addition the mixture was stirred at 0-5 °C for 1 h. The mixture was then warmed to 38-40 °C and left to stir for another 2 h. The brown solution was cooled to room temperature and added to a mixture of water/ 1M NaOH (100 ml each). The bisnornitrile was extracted with ethyl acetate and washed with NaOH (4 × 20 ml) and water to neutrality. The ethyl acetate was dried ($MgSO_4$) and removed by evaporation to yield an off white solid. The compound was characterised in the next step as washing with NaOH yielded a mixture of hydrolysis products.

3α, 7β -dihydroxy-24-bisnor-5β-cholane-22-nitrile (27)

Sodium (1 g) was added to methanol (50 ml) to form an excess of sodium methoxide. The formyl bisnornitrile (**95**) obtained in the above reaction was added to this solution and refluxed for 2 h. After 2 h the reaction was cooled to room temperature and added to water (100 ml). The bisnornitrile was extracted with ethyl acetate. The organic layer was then washed with water (3 × 20 ml) and dried ($MgSO_4$). The solvent was removed by evaporation to yield a yellow solid (2.6 g, 94%).

^{1}H-NMR δ ($CDCl_3$): 0.75 (3-H, s, 18-CH_3), 0.99 (3-H, s, 19-CH_3), 1.34 (3-H, d, J=7.02 Hz, 21-CH_3,), 2.81 (1-H, m, 20-CH), 3.48 (2-H, m, 3- β H, 7-α H). ^{13}C-NMR ppm ($CDCl_3$): 12.7 (CH_3), 19.2 (CH_3), 22.4 (CH_2), 24.2 (CH_3), 28.1 (CH_2), 29.9 (CH_2), 31.1 (CH_2), 35.3 (CH_2), 36.1 (CH), 36.9 (CH_2), 38.1 (CH_2), 38.9 (CH_2), 40.9 (CH), 41.7 (CH_2), 44.5 (CH), 44.7 (CH), 44.9 (13-C), 56.5 (CH), 57.8 (CH), 71.5 (3-C, 7-C, CH), 124.5 (-C≡N). HRMS: Found $(M-H)^-$ =344.2590. IR_{vmax} (KBr): 2238 (nitrile peak), 3054, 3326 cm^{-1}. mp: 75-78 °C.

3α, 7β -dihydroxy-24-nor-5β-cholane-22-oic acid (25)

3α, 7β -dihydroxy-24-nor-5β-cholane-23-nitrile (**27**) (2.5 g, 7.2 mmol) was refluxed with 10% KOH in 50ml ethanol: water (1:1) for 96 h. The ethanol was evaporated and the solution extracted with diethyl ether until TLC examination showed no more basic compounds in the organic layer. The aqueous layer was then acidified with 6M HCl and the bisnorbile acid was extracted with ethyl acetate (3 × 20 ml). The combined organic layers were then washed with 20% NaCl to neutrality, dried ($MgSO_4$) and evaporated to give bisnorUDCA which after column chromatography with ethyl acetate: hexane 4:1 presented as a white solid (1.86 g, 72%).

^{1}H-NMR δ (CD_3OD): 0.76 (3-H, s, 18-CH_3), 0.98 (3-H, s, 19-CH_3), 1.02 (3-H, d, J=7.03 Hz, 21-CH_3,), 2.22, 3.50 (2-H, m, 3- β H, 7-α H). ^{13}C-NMR ppm (CD_3OD): 12.8 (CH_3), 19.0 (CH_3), 22.5 (CH_2), 24.0 (CH_3), 28.0 (CH_2), 29.8 (CH_2), 31.5 (CH_2), 35.3 (CH_2), 36.1 (CH), 36.5 (CH_2), 38.1 (CH_2), 38.9 (CH_2), 40.9 (CH), 41.7 (CH_2), 44.5 (CH), 44.7 (CH), 44.9 (13-C), 56.6 (CH), 57.5 (CH), 71.1 (3-C, 7-C, CH), 182.2 (22-C=OOH). HRMS: Found: $(M-H)^-$= 363.2538. IR_{vmax} (KBr): 1708 cm^{-1} (C=O). mp: 88-90 °C, literature mp: 177-180 °C (Batta *et al.*, 1999).

3α,7β -diformyloxy-5 β-cholan-24-oyl chloride (76)

3α, 7β-diformyloxy-5 β-cholan-24-oic acid (**54**) was (1 g, 2 mmol) was dissolved in thionyl chloride (5 ml) and refluxed at 90 °C for 2 h. After 1 h the reaction was cooled to room temperature and the thionyl chloride was removed *in vacuo*, to leave a sticky solid which was the acid chloride (1 g, 97%).

^{1}H-NMR δ ($CDCl_3$): 0.70 (3-H, s, 18-CH_3), 0.93 (3-H, d, J=6.52 Hz, 21-CH_3), 1.00 (3-H, s, 19-CH_3), 4.95 (2-H, m, 3-β H, 7-α H), 8.03 (2-H, s, OCOH). ^{13}C-NMR ppm

($CDCl_3$): 12.9 (CH_3), 19.0 (CH_3), 22.4 (CH_2), 24.0 (CH_3), 28.0 (CH_2), 29.8 (CH_2), 31.2 (CH_2), 32.2 (CH_2), 32.5 (CH_2), 35.3 (CH_2), 36.1 (CH), 36.9 (CH_2), 38.1 (CH_2), 38.9 (CH_2), 40.9 (CH), 41.7 (CH_2), 44.1 (CH), 44.7 (CH), 44.9 (13-C), 56.6 (CH), 57.8 (CH), 79.1 (3-C, 7-C, CH), 161.0 (-O<u>C</u>=OH), 162.5 (-O<u>C</u>=OH), 172.1 (24-<u>C</u>=OCl).

3α, 7β, 24-Trihydroxy-5 β-cholane (28)

UDCA (**14**) (2 g, 5 mmol) was dissolved in dry THF (20 ml) and added drop wise to a solution of lithium aluminium hydride (0.39 g, 10 mmol) in dry THF in a 2-neck round bottomed flask under inert atmosphere conditions. The reaction mixture was refluxed for 3 h at 70 °C. After 3 h water was added to quench the reaction. The aluminium salts were removed by filtration through a cellite column. The alcohol was then extracted with ethyl acetate and the organic layer washed with (3 × 20 ml HCl) and water (3 × 20 ml) and dried over ($MgSO_4$). The solvent was removed *in vacuo* to yield a white odourless solid (1.7 g, 89%).

^{1}H-NMR δ ($CDCl_3$): 0.70 (3H, s, 18-CH_3), 0.95 (6-H, m, 19- CH_3, 21-CH_3), 3.63 (4-H, m, 3 -β H, 7-α H, 23-C<u>H</u>$_2$). ^{13}C-NMR ppm ($CDCl_3$): 12.6 (CH_3), 18.7 (CH_3), 22.3 (CH_2), 24.0 (CH_3), 25.2 (CH_2), 25.5 (CH_2), 28.0 (CH_2), 29.8 (CH_2), 31.1 (CH_2), 35.3 (CH_2), 36.1 (CH), 36.4 (CH_2), 38.1 (CH_2), 38.9 (CH_2), 40.3 (CH), 41.7 (CH_2), 44.1 (CH), 44.7 (CH), 44.8 (13-C), 56.2 (CH), 57.8 (CH), 63.1 (24-C, CH_2), 71.2 (3-C, 7-C, CH). IR_{vmax} (KBr): 2864, 2927, 3338.27 cm^{-1}. mp: 152 °C, literature mp: 163-164 °C (Kihira *et al.*, 1990).

24-Cyclopropyl-3α, 7β-diformyloxy-5 β-cholanamide (96)

3α, 7β-diformyloxy-5 β-cholan-24-oyl chloride (**76**) (1 g, 1.9 mmol) was dissolved in dry DCM (10 ml). Cyclopropylamine (131 µL, 1.9 mmol) and triethylamine (244 µL, 1.9 mmol) were added on ice. The reaction mixture was allowed to warm to room temperature and stirred monitoring for disappearance of the starting material by TLC. After 24 h the solvent was removed *in vacuo*. The residue was dissolved in ethyl acetate (20 ml) and washed with HCl (3 × 20 ml) for removal of unreacted amines, water (2 × 20 ml) and brine solution (2 × 20 ml). The organic layer was dried and evaporation of solvent gave the cyclopropylamide after chromatographic elution (Hexane: ethyl acetate 1:1) (0.72 g, 76%).

^{1}H-NMR δ ($CDCl_3$): 0.68 (3-H, s, 18-CH_3), 0.91 (3-H, d, J=6.52 Hz, 21-CH_3), 0.99 (3-H, s, 19-CH_3), 2.70 (1-H, m, 25-CH) 4.83, 4.95 (2-H, m, 3-β H, 7-α H), 5.62 (1-H, broad, -N<u>H</u>), 8.03 (2-H, s, OCO<u>H</u>). ^{13}C-NMR ppm ($CDCl_3$): 5.1 (26-C, 27-C, CH_2), 12.9 (CH_3), 19.0 (CH_3), 22.5 (CH_2), 24.0 (CH_3), 25.2 (CH_2), 25.5 (CH_2), 28.0 (CH_2), 29.8 (CH_2), 31.6 (CH_2), 35.6 (CH_2), 36.1 (CH), 36.9 (CH_2), 38.6 (CH_2), 38.9 (CH_2), 40.9

(CH), 41.8 (CH_2), 44.1 (CH), 44.7 (CH), 44.8 (13-C), 56.6 (CH), 57.8 (CH), 79.1 (3-C, 7-C, CH), 161.2 (-O<u>C</u>=OH), 162.4 (-O<u>C</u>=OH), 175.0 (24-<u>C</u>=ONH).

24-Cyclopropyl-3α, 7β -dihydroxy-5 β-cholanamide (77)

Sodium (0.1 g) was added to hplc grade methanol (10 ml) to form an excess of sodium methoxide. The formyl cyclopropylamide (**96**) (0.5 g, 1 mmol) obtained in the above reaction was added to this solution and refluxed for 2 h. After 2 h the reaction was cooled to room temperature and added to water (100 ml). The amide was extracted with ethyl acetate. The organic layer was then washed with water (3 × 20 ml) and dried ($MgSO_4$). The solvent was removed *in vacuo* and after chromatographic elution with ethyl acetate afforded a white solid (0.4 g, 92%).

^{1}H-NMR δ (CD_3OD): 0.49 (2-H, m, 26-CH_2(27)), 0.65 (3-H, s, 18-CH_3), 0.92 (3-H, d, J=6.52 Hz, 21-CH_3,), 0.97 (3-H, s, 19-CH_3), 2.75 (1-H, m, 25-CH) 3.61 (2-H, m, 3-β H, 7-α H), 5.32 (1-H, broad, -N<u>H</u>). ^{13}C-NMR ppm (CD_3OD): 8.4 (26-C, 27-C, CH_2), 12.4 (CH_3), 18.8 (CH_3), 22.4 (CH_2), 24.0 (CH_3), 25.2 (CH_2), 25.5 (CH_2), 28.0 (CH_2), 29.8 (CH_2), 31.1 (CH_2), 35.3 (CH_2), 36.5 (CH), 36.9 (CH_2), 38.1 (CH_2), 38.8 (CH_2), 40.9 (CH), 41.7 (CH_2), 44.1 (CH), 44.6 (CH), 44.9 (13-C), 56.5 (CH), 57.8 (CH) 24.1 (25-C, CH), 71.1 (3-C, 7-C), 175.2 (24-<u>C</u>=ONH). HRMS: Found $(M\text{-}Na)^+$ =454.3297. Elemental Analysis- Required C75.13 H 10.51 N 3.24 Obtained C 74.17 H 10.53 N 3.24. IR_{vmax} (KBr): 1717, 2864, 2922, 3234, 3501 cm^{-1}. mp: 124 °C

24-Diphenyl-3α, 7β-diformyloxy-5 β-cholanamide (97)

3α, 7β -diformyloxy-5 β-cholan-24-oyl chloride (**76**) (1 g, 1.9 mmol) was dissolved in dry DCM (10 ml). Diphenylamine (0.321 g, 1.9 mmol) and triethylamine (244 µL, 1.9 mmol) were added on ice. The reaction mixture was allowed to warm to room temperature and stirred monitoring for disappearance of the starting material by TLC. After 48 h the solvent was removed *in vacuo*. The residue was dissolved in ethyl acetate (20 ml) and washed with HCl (3 × 20 ml) for removal of unreacted amines, water (2 × 20 ml) and brine solution (2 × 20 ml). The organic layer was dried and the solvent removed by evaporation to produce the diphenylamide after column chromatography (Hexane: ethyl acetate 1:1). (0.9 g, 80%).

^{1}H-NMR δ ($CDCl_3$): 0.67 (3-H, s, 18-CH_3), 0.7990 (3-H, d, J=5.52 Hz, 21-CH_3,), 1.00 (3-H, s, 19-CH_3), 4.88 (2-H, m, 3-β H, 7-α H), 7.11 (10-H, m, Aromatic-CH) 8.03 (2-H, s, OCO<u>H</u>). ^{13}C-NMR ppm ($CDCl_3$): 12.9 (CH_3), 19.0 (CH_3), 22.5 (CH_2), 24.0 (CH_3), 25.2 (CH_2), 25.5 (CH_2), 28.0 (CH_2), 29.8 (CH_2), 31.1 (CH_2), 35.3 (CH_2), 36. (CH), 36.9 (CH_2), 38.1 (CH_2), 38.9 (CH_2), 40.9 (CH), 41.5 (CH_2), 44.1 (CH), 44.7 (CH), 44.9

(13-C), 56.6 (CH), 57.8 (CH), 79.1 (3-C, 7-C, CH), 125-128 (Aromatic-C, CH), 142.1 (Aromatic-C), 161.0 (-O<u>C</u>=OH), 162.1 (-O<u>C</u>=OH), 171.1 (24-<u>C</u>=ONH).

24-Diphenyl-3α, 7β-hydroxy-5 β-cholanamide (86)

Sodium (0.1 g) was added to hplc grade methanol (10 ml) to form an excess of sodium methoxide. The formyl diphenylamide (**97**) (0.8 g, 1.3 mmol) obtained in the above reaction was added to this solution and refluxed for 2 h. After 2 h the reaction was cooled to room temperature and added to water (100 ml). The amide was extracted with ethyl acetate. The organic layer was then washed with water (3 × 20 ml) and dried ($MgSO_4$). The solvent was removed *in vacuo* and after chromatographic elution with ethyl acetate afforded a white solid (0.54 g, 76%).

^{1}H-NMR δ (CD_3OD): 0.65 (3-H, s, 18-CH_3), 0.77 (3-H, d, J=5.52 Hz, 21-CH_3,), 1.02 (3-H, s, 19-CH_3), 3.62 (2-H, m, 3-β H, 7-α H), 7.11 (10-H, m, Aromatic-CH). ^{13}C-NMR ppm (CD_3OD): 12.9 (CH_3), 19.0 (CH_3), 22.5 (CH_2), 24.1 (CH_3), 25.2 (CH_2), 25.5 (CH_2), 28.8 (CH_2), 29.8 (CH_2), 31.1 (CH_2), 35.2 (CH_2), 36.3 (CH), 36.9 (CH_2), 38.4 (CH_2), 38.9 (CH_2), 40.9 (CH), 41.7 (CH_2), 44.1 (CH), 44.7 (CH), 44.9 (13-C), 56.6 (CH), 57.8 (CH), 71.1 (3-C, 7-C), 125.7 (Aromatic-C, CH), 142.1 (Aromatic-C), 171.0 (24-<u>C</u>=ONH). HRMS: Found (M-Na) $^+$ = 566.3621. IR_{vmax} (KBr): 1720 (C=O), 2948, 3423 cm^{-1}. mp: 102-104 ^oC.

24-Phenylethyl-3α, 7β-diformyloxy-5 β-cholanamide (98)

3α, 7β -diformyloxy-5 β-cholan-24-oyl chloride (**76**) (1 g, 1.9 mmol) was dissolved in dry DCM (10 ml). Phenethylamine (240 µL, 1.9 mmol) and triethylamine (244 µL, 1.9 mmol) were added on ice. The reaction mixture was allowed to warm to room temperature and stirred monitoring for disappearance of the starting material by TLC. After 16 h the solvent was removed *in vacuo*. The residue was dissolved in ethyl acetate (20 ml) and washed with HCl (3 × 20 ml) for removal of unreacted amines, water (2 × 20 ml) and brine solution (2 × 20 ml). The organic layer was dried and the solvent removed *in vacuo* which gave the phenethylamide after column chromatography (Hexane: ethyl acetate 1:1) (0.97 g, 93%).

^{1}H-NMR δ ($CDCl_3$): 0.69 (3-H, s, 18-CH_3), 0.92 (3-H, d, J= 6.53 Hz, 21-CH_3), 0.97 (3-H, s, 19-CH_3,), 2.86 (2-H, t, J=6.78 Hz , 26-CH_2,), 3.55 (2-H, dd, J_1=6.03 Hz, J_2=6.77 Hz, 25-CH_2), 4.88 (2-H, m, 3-β H, 7-α H), 7.11 (5-H, m, Aromatic-CH), 8.03 (2-H, s, OCO<u>H</u>). ^{13}C-NMR ppm ($CDCl_3$): 12.6 (CH_3), 19.1 (CH_3), 22.5 (CH_2), 24.0 (CH_3), 25.2 (CH_2), 25.5 (CH_2), 28.5 (CH_2), 29.8 (CH_2), 31.1 (CH_2), 35.5 (CH_2), 36.1 (CH), 36.3 (26-C, CH_2), 36.9 (CH_2), 38.1 (CH_2), 38.9 (CH_2), 39.1 (25-C, CH_2), 40.9 (CH), 41.7

(CH_2), 44.1 (CH), 44.7 (CH), 44.9 (13-C), 56.6 (CH), 57.8 (CH), 79.2 (3-C, 7-C, CH), 126.1 (Aromatic para-C, CH), 129.4 (Aromatic, ortho and meta-C, CH), 139.0 (Aromatic-C, CH) 161.5 (-O<u>C</u>=OH), 162.5 (-O<u>C</u>=OH), 171.4 (24-<u>C</u>=ONH).

24-Phenylethyl-3α, 7β-dihydroxy-5 β-cholanamide (84)

Sodium (0.1 g) was added to hplc grade methanol (10 ml) to form an excess of sodium methoxide. The formyl phenethylamide (**98**) (0.83 g, 1.5 mmol) obtained in the above reaction was added to this solution and refluxed for 2 h. After 2 h the reaction was cooled to room temperature and added to water (100 ml). The amide was extracted with ethyl acetate. The organic layer was then washed with water (3 × 20 ml) and dried ($MgSO_4$). The solvent was removed *in vacuo* and after chromatographic elution with ethyl acetate afforded a white solid (0.67 g, 90%).
^{1}H-NMR δ (CD_3OD): 0.65 (3-H, s, 18-CH_3), 0.92 (3-H, d, J= 6.53 Hz, 21-CH_3), 0.97 (3-H, s, 19-CH_3,), 2.83 (2-H, t, J=6.78 Hz, 26-CH_2,), 3.51 (2-H, q, J_1=6.03 Hz, J_2= 6.77 Hz, 25-CH_2,) 3.62 (2-H, m, 3-β H, 7-α H), 7.12 (5-H, m, Aromatic-CH). ^{13}C-NMR ppm (CD_3OD): 12.8 (CH_3), 19.0 (CH_3), 22.4 (CH_2), 24.0 (CH_3), 25.2 (CH_2), 25.5 (CH_2), 28.0 (CH_2), 29.8 (CH_2), 31.1 (CH_2), 35.3 (CH_2), 36.1 (CH), 36.5 (26-C), 36.9 (CH_2), 38.2 (CH_2), 38.9 (CH_2), 39.2 (25-C), 40.3 (CH), 41.7 (CH_2), 44.1 (CH), 44.7 (CH), 44.9 (13-C), 56.6 (CH), 57.8 (CH), 71.2 (3-C, 7-C), 126.2 (Aromatic para-C, CH), 128.1, (Aromatic ortho and meta-C, CH), 140.4 (Aromatic-C), 171.0 (24-<u>C</u>=ONH). HRMS: Found $(M\text{-}Na)^+$ = 518.3265. Elemental analysis-required C 77.53, H 9.96, N 2.83 Found C 77.30 H 9.89 N 2.83. IR_{vmax} (KBr): 1551, 1647, 2863, 3927, 3086, 3319 cm^{-1}. mp: 100-103 °C.

24-Anilin-3α, 7β-diformyloxy-5 β-cholanamide (99)

3α, 7β -diformyloxy-5 β-cholan-24-oyl (**76**) (1 g, 1.9 mmol) was dissolved in dry DCM (10 ml). Aniline (173 µL, 1.9 mmol) and triethylamine (244 µL, 1.9 mmol) were added on ice. The reaction mixture was allowed to warm to room temperature and stirred monitoring for disappearance of the starting material by TLC. After 16 h the solvent was removed *in vacuo*. The residue was dissolved in ethyl acetate (20 ml) and washed with HCl (3 × 20 ml) for removal of unreacted amines, water (2 × 20 ml) and brine solution (2 × 20 ml). The organic layer was dried and the solvent removed *in vacuo* which gave the anilinamide on column chromatography (Hexane: ethyl acetate 1:1) (0.944 g, 95%).
^{1}H-NMR δ ($CDCl_3$): 0.74 (3-H, s, 18-CH_3), 0.98 (3-H, s, 19-CH_3), 1.03 (3-H, d, J=6.52 Hz, 21-CH_3), 4.88 (2-H, m, 3-β H, 7-α H), 7.09 (1-H, t, J_1=7.53 Hz, J_2=7.02 Hz

Aromatic para-H) , 7.31 (2-H, t, J=7.53 Hz, J2=8.53 Hz, Aromatic meta-H) 7.54 (2-H, d, J=8.53 Hz , Aromatic ortho-H) , 8.03 (2-H, s, OCOH). ^{13}C-NMR ppm ($CDCl_3$): 12.6 (CH_3), 19.1 (CH_3), 22.3 (CH_2), 24.1 (CH_3), 25.1 (CH_2), 25.7 (CH_2), 28.1 (CH_2), 29.8 (CH_2), 31.1 (CH_2), 35.3 (CH_2), 36.1 (CH), 36.9 (CH_2), 38.1 (CH_2), 38.9 (CH_2), 40.9 (CH), 41.8 (CH_2), 44.1 (CH), 44.7 (CH), 44.9 (13-C), 56.6 (CH), 57.4 (CH), 79.1 (3-C, 7-C, CH), 120.5 (Aromatic ortho carbon, CH), 124.3 (Aromatic para-C, CH), 129.1 (Aromatic meta-C, CH), 140.0 (Aromatic-C) 161.2 (-OC=OH), 162 (-OC=OH), 171 (24-C=ONH).

24-Anilin-3α, 7β-dihydroxy-5 β-cholanamide (81)

Sodium (0.1 g) was added to hplc grade methanol (10 ml) to form an excess of sodium methoxide. The formyl anilinamide (**99**) (0.85 g, 1.6 mmol) obtained in the above reaction was added to this solution and refluxed for 2 h. After 2 h the reaction was cooled to room temperature and added to water (100 ml). The amide was extracted with ethyl acetate. The organic layer was then washed with water (3 × 20 ml) and dried ($MgSO_4$). The solvent was removed *in vacuo* and after chromatographic elution with ethyl acetate afforded a white solid (0.7 g, 93%).

^{1}H-NMR δ (CD_3OD): 0.74 (3-H, s, 18-CH_3), 0.97 (3-H, s, 19-CH_3), 1.04 (3-H, d, J=6.53 Hz, 21-CH_3,), 3.51 (2-H, m, 3-β H, 7-α H), 7.12 (1-H, t, J1=7.53 Hz, J2=7.02 Hz Aromatic para H) , 7.29 (2-H, t, J=7.53 Hz, J2=8.53 Aromatic meta-H) 7.63 (2-H, d, J= 8.53 Hz, Aromatic ortho H). ^{13}C-NMR ppm (CD_3OD): 12.4 (CH_3), 19.1 (CH_3), 22.2 (CH_2), 24.4 (CH_3), 25.2 (CH_2), 25.5 (CH_2), 28.0 (CH_2), 29.8 (CH_2), 31.1 (CH_2), 35.3 (CH_2), 36.1 (CH), 36.5 (CH_2), 38.4 (CH_2), 38.9 (CH_2), 40.9 (CH), 41.7 (CH_2), 44.1 (CH), 44.7 (CH), 44.9 (13-C), 56.4 (CH), 57.9 (CH), 71.1 (3-C, 7-C, CH), 120.8 (Aromatic ortho-C, CH), 125.3 (Aromatic para-C), 129.0 (Aromatic meta-C), 140.5 (Aromatic-C) ,171.2 (24-C=ONH). HRMS: Found $(M\text{-}Na)^+$ = 490.3297. Elemental Analysis- Required C77.04 H 9.7 N 2.98 Obtained C 76.95 H 9.84 N 2.96. IR_{vmax} (KBr): 1660, 1706, 1794, 1860, 1934, 2922, 3262cm^{-1}. mp: 210-212 °C.

24-α-methylbenzyl-3α, 7β-diformyloxy-5 β-cholanamide (100)

3α, 7β -diformyloxy-5 β-cholan-24-oyl chloride (**76**) (1 g, 1.9 mmol) was dissolved in dry DCM (10 ml). Alphamethylbenzylamine (247 µL, 1.9 mmol) and triethylamine (244 µL, 1.9 mmol) were added on ice. The reaction mixture was allowed to warm to room temperature and stirred monitoring for disappearance of the starting material by TLC. After 16 h the solvent was removed. The residue was dissolved in ethyl acetate (20 ml) and washed with HCl (3 × 20 ml) for removal of unreacted amines, water (2x20 ml) and brine solution (2 × 20 ml). The organic layer was dried and the solvent

removed *in vacuo* which gave the title compound after column chromatography (Hexane: ethyl acetate 1:1) (0.75 g, 72%).

^{1}H-NMR δ ($CDCl_3$): 0.68 (3-H, s, 19-CH_3), 0.94 (3-H, d, J= 6.02 Hz, 21-CH_3), 1.00 (3-H, s, 18-CH_3), 1.49 (3-H, m, 26-CH_3,) 4.81 (2-H, m, 3-β H, 7-α H), 5.14 (1-H, m, 25-H), 7.33 (5-H, m, Aromatic-CH), 8.00 (2-H, s, OCO<u>H</u>). ^{13}C-NMR ppm ($CDCl_3$): 12.8 (CH_3), 19.0 (CH_3), 22.0 (26-C), 22.5 (CH_2), 24.0 (CH_3), 28.0 (CH_2), 29.8 (CH_2), 31.8 (CH_2), 35.3 (CH_2), 36.1 (CH), 36.8 (CH_2), 38.1 (CH_2), 38.9 (CH_2), 40.9 (CH), 41.7 (CH_2), 44.1 (CH), 44.7 (CH), 44.8 (13-C), 48.1 (25-CH), 56.6 (CH), 57.8 (CH), 73.2 (3-C, 7-C), 125-130 (Aromatic-C, CH and C), 161.8 (-O<u>C</u>=OH) ,162.5 (-O<u>C</u>=OH), 173.4 (24-<u>C</u>=ONH).

24-α-methylbenzyl-3α, 7β-dihydroxy-5 β-cholanamide (83)

Sodium (0.1 g) was added to hplc grade methanol (10 ml) to form an excess of sodium methoxide. The formyl alphamethylbenzylamide (**100**) (0.5 g, 0.9 mmol) obtained in the above reaction was added to this solution and refluxed for 2 h. After 2 h the reaction was cooled to room temperature and added to water (100 ml). The amide was extracted with ethyl acetate. The organic layer was then washed with water (3 × 20 ml) and dried ($MgSO_4$). The solvent was removed in vacuo and after chromatographic elution with ethyl acetate afforded a white solid (0.4 g, 91%).

^{1}H-NMR δ (CD_3OD): 0.70 (3-H, s, 19-CH_3), 0.96 (3-H, d, J=6.02 Hz, 21-CH_3), 1.00 (3-H, s, 18-CH_3), 1.51 (3-H, m , 26-CH_3,) 3.52 (2-H, m, 3-β H, 7-α H), 5.13 (1-H, m, 25-CH), 7.33 (5-H, m, Aromatics-CH). ^{13}C-NMR ppm (CD_3OD): 12.6 (CH_3), 19.1 (CH_3), 21.3 (26-C, CH_3), 22.5 (CH_2), 24.0 (CH_3), 28.0 (CH_2), 29.8 (CH_2), 31.1 (CH_2), 32.2 (CH_2), 32.5 (CH_2), 35.5 (CH_2), 36.1 (CH), 36.9 (CH_2), 38.1 (CH_2), 38.9 (CH_2), 40.9 (CH), 41.7 (CH_2), 44.1 (CH), 44.7 (CH), 44.9 (13-C), 48.5 (25-C, CH), 56.5 (CH), 57.4 (CH), 71.1 (3-C, 7-C, CH), 125.0-130.1 (Aromatic-C, CH), 173.4 (24-<u>C</u>=ONH). HRMS: Found $(M\text{-}Na)^+$ = 518.3591. Elemental Analysis- Required C 77.53 H 9.96 N 2.83 Obtained C 76.35 H 10.05 N 2.82. IR_{vmax} (KBr): 1547, 1651, 1706, 2865, 2942, 3320 cm^{-1}. mp: 118-120 °C.

24-Benzyl-3α, 7β-diformyloxy-5 β-cholanamide (101)

3α, 7β -diformyloxy-5 β-cholan-24-oyl chloride (**76**) (1 g, 1.9 mmol) was dissolved in dry DCM (10 ml). Benzylamine (207 µL, 1.9 mmol) and triethylamine (244 µL, 1.9 mmol) were added on ice. The reaction mixture was allowed to warm to room temperature and stirred monitoring for disappearance of the starting material by TLC. After 16 h the solvent was removed *in vacuo*. The residue was dissolved in ethyl acetate (20 ml) and washed with HCl (3 × 20 ml) for removal of unreacted amines,

water (2 × 20 ml) and brine solution (2 × 20 ml). The organic layer was dried and the solvent removed which gave the title compound after column chromatography (Hexane: ethyl acetate 1:1) (0.80 g, 78.4%).

^{1}H-NMR δ ($CDCl_3$): 0.68 (3-H, s, 18-CH_3), 0.94 (6-H, m, 19-CH_3, 21-CH_3), 4.36 (2-H, d, J= 6.04 Hz, 25-CH_2), 4.81 (2-H, m, 3-β H, 7-α H), 7.27 (5-H, m, Aromatic-CH) 8.00 (2-H, s, OCO<u>H</u>). ^{13}C-NMR ppm ($CDCl_3$): 12.5 (CH_3), 19.1 (CH_3), 22.2 (CH_2), 24.0 (CH_3), 28.0 (CH_2), 29.5 (CH_2), 31.1 (CH_2), 32.2 (CH_2), 32.5 (CH_2), 35.3 (CH_2), 36.1 (CH), 36.9 (CH_2), 38.2 (CH_2), 38.9 (CH_2), 40.9 (CH), 41.7 (CH_2), 44.1 (CH), 44.5 (CH), 44.9 (13-C), 45.1 (25-C, CH_2), 56.6 (CH), 57.8 (CH) 73 (3-C, 7-C, CH), 122.0, 123.1, 124.2 (Aromatic-CH), 140.1 (Aromatic-C), 161.4 (-O<u>C</u>=OH), 162.5 (-O<u>C</u>=OH), 173.3 (24-<u>C</u>=ONH).

24-Benzyl-3α, 7β-hydroxy-5 β-cholanamide (82)

Sodium (0.1 g) was added to hplc grade methanol (10 ml) to form an excess of sodium methoxide. **101** (0.65 g, 1.2 mmol) obtained in the above reaction was added to this solution and refluxed for 2 h. After 2 h the reaction was cooled to room temperature and added to water (100 ml). The amide was extracted with ethyl acetate. The organic layer was then washed with water (3 × 20 ml) and dried ($MgSO_4$). The solvent was removed *in vacuo* and after chromatographic elution with ethyl acetate afforded a white solid (0.4 g, 70%).

^{1}H-NMR δ (CD_3OD): 0.71 (3-H, s, 18-CH_3), 0.98 (6-H, m, 19-CH_3, 21-CH_3), 3.50 (2-H, m, 3-β H, 7-α H), 4.36 (2-H, d, J=6.04 Hz, 25-CH_2), 7.21 (5-H, m, Aromatic-CH). ^{13}C-NMR ppm (CD_3OD): 12.7 (CH_3), 19.1 (CH_3), 22.2 (CH_2), 24.0 (CH_3), 28.0 (CH_2), 29.8 (CH_2), 31.1 (CH_2), 32.2 (CH_2), 32.5 (CH_2), 35.2 (CH_2), 36.1 (CH), 36.9 (CH_2), 38.1 (CH_2), 38.4 (CH_2), 40.5 (CH), 41.7 (CH_2), 44.1 (CH), 44.2 (CH), 44.9 (13-C), 45.3 (25-C, CH_2), 56.5 (CH), 57.9 (CH), 71.2 (3-C, 7-C, CH), 122.1, 123.4, 124.1 (Aromatic-CH), 140.0 (Aromatic-C), 173.1 (24-<u>C</u>=ONH). HRMS: Found $(M\text{-}Na)^{+}$ = 504.3460. IR_{vmax} (KBr): 1151, 1651, 1706, 2241, 2862, 3087, 3311 cm^{-1}. mp: 100-102 °C (Fini *et al.*, 1990).

24-Phenylpropyl-3α, 7β-diformyloxy-5 β-cholanamide (102)

3α, 7β -diformyloxy-5 β-cholan-24-oyl chloride (**76**) (1 g, 1.9 mmol) was dissolved in dry DCM (10 ml). Phenylpropylamine (271 µL, 1.9 mmol) and triethylamine (244 µL, 1.9 mmol) were added on ice. The reaction mixture was allowed to warm to room temperature and stirred monitoring for disappearance of the starting material by TLC. After 16 h the solvent was removed *in vacuo*. The residue was dissolved in ethyl acetate (20 ml) and washed with HCl (3 × 20 ml) for removal of unreacted amines, water (2 × 20 ml) and brine solution (2 × 20 ml). The organic layer was dried and the

solvent removed to give the phenylpropylamide after column chromatography (Hexane: ethyl acetate 1:1) (0.70 g, 66%).

^{1}H-NMR δ ($CDCl_3$): 0.69 (3-H, s, 18-CH_3), 0.95 (3-H, d, J=6.52 Hz, 21-CH_3), 0.97 (3-H, s, 21-CH_3,), 2.68 (2-H, t, J_1=7.78 Hz , J_2=7.28 Hz, 27-CH_2), 3.3474 (2-H, dd, J_1= 7.02 Hz, J_2=6.03 Hz, 25-CH_2), 4.81 (2-H, m, 3-β H, 7-α H), 7.21-7.43 (5-H, m, Aromatic-CH), 8.00 (2-H, s, OCOH). ^{13}C-NMR ppm ($CDCl_3$): 12.6 (CH_3), 19.0 (CH_3), 22.3 (CH_2), 24.0 (CH_3), 28.0 (CH_2), 29.8 (CH_2), 31.1 (CH_2), 32.2 (CH_2), 32.5 (CH_2), 34.0 (26-C, 27-C, CH_2), 35.3 (CH_2), 36.1 (CH), 36.8 (CH_2), 38.1 (CH_2), 38.9 (CH_2), 39 (25-C, CH_2), 40.5 (CH), 41.7 (CH_2), 44.1 (CH), 44.4 (CH), 44.8 (13-C), 56.4 (CH), 57.9 (CH) , 73.5 (3-C, 7-C, CH), 126.1 (Aromatic meta-C), 129.0 (Aromatic ortho-C, para-C, CH), 141.1 (Aromatic-C) 161.1 (-OC=OH), 162.3 (-OC=OH), 174.5 (24-C=ONH).

24-Phenpropyl-3α, 7β-dihydroxy-5 β-cholanamide (85)

Sodium (0.1 g) was added to hplc grade methanol (10 ml) to form an excess of sodium methoxide. **102** (0.5 g, 0.8 mmol) obtained in the above reaction was added to this solution and refluxed for 2 h. After 2 h the reaction was cooled to room temperature and added to water (100 ml). The amide was extracted with ethyl acetate. The organic layer was then washed with water (3 × 20 ml) and dried ($MgSO_4$). The solvent was removed *in vacuo* and after chromatographic elution with ethyl acetate afforded a white solid (0.35 g, 87.5%).

^{1}H-NMR δ ($CDCl_3$): 0.69 (3-H, s, 18-CH_3), 0.95 (3-H, d, J=6.52 Hz, 21-CH_3) 0.97 (3-H, s, 21-CH_3), 2.68 (2-H, t, J_1=7.78 Hz , J_2= 7.28 Hz , 27-CH_2) 3.3465 (2-H, dd, J_1= 7.02 Hz, J_2=6.03 Hz, 25-CH_2), 4.54 (2-H, m, 3-β H, 7-α H), 7.22-7.41 (5-H, m, Aromatic-CH). ^{13}C-NMR ppm ($CDCl_3$): 12.4 (CH_3), 19.1 (CH_3), 22.3 (CH_2), 24.0 (CH_3), 28.0 (CH_2), 29.8 (CH_2), 31.1 (CH_2), 32.2 (CH_2), 32.5 (CH_2), 34.1 (26-C, 27-C), 35.3 (CH_2), 36.5 (CH), 36.9 (CH_2), 38.1 (CH_2), 38.9 (CH_2), 40.0 (25-C), 40.9 (CH), 41.7 (CH_2), 44.1 (CH), 44.7 (CH), 44.9 (13-C), 56.6 (CH), 57.8 (CH), 71.1 (3-C, 7-C), 126.1 (Aromatic meta-C, CH), 128.0 (Aromatic ortho and para-C, CH), 141.5 (Aromatic-C), 174.3 (24-C=ONH). HRMS: Found (M-Na) $^{+}$ = 532.3767. Elemental Analysis- Required C 77.75 H 10.08 N 2.75 Obtained C 77.27 H 9.98 N 2.75. IR_{vmax} (KBr): 1154, 1648, 2803, 3026, 3085, 3310 cm^{-1}. mp: 86-88 ^{o}C.

24-Morpholine-3α, 7β-diformyloxy-5 β-cholanamide (103)

3α, 7β -diformyloxy-5 β-cholan-24-oyl chloride (**76**) (1 g, 1.9 mmol) was dissolved in dry DCM (10 ml). Morpholine (167 µL, 1.9 mmol) and triethylamine (244 µL, 1.9 mmol) were added on ice. The reaction mixture was allowed to warm to room temperature and stirred monitoring for disappearance of the starting material by TLC.

After 16 h the solvent was removed *in vacuo*. The residue was dissolved in ethyl acetate (20 ml) and washed with HCl (3 × 20 ml) for removal of unreacted amines, water (2 × 20 ml) and brine solution (2 × 20 ml). The organic layer was dried and the solvent removed *in vacuo* which gave the morpholinamide after chromatographic elution (Hexane: ethyl acetate 1:1) (0.933 g, 95%).

^{1}H-NMR δ ($CDCl_3$): 0.69 (3-H, s, 18-CH_3), 0.97 (3-H, s, 19-CH_3) 1.00 (3-H ,d, J=6.52 Hz,21-CH_3), 3.53 (4-H, m, morpholine-CH_2), 3.71 (4-H, m, morpholine-CH_2), 4.81 (2-H, m, 3-β H, 7-α H), 8.00 (2-H, s, OCOH). ^{13}C-NMR ppm ($CDCl_3$): 12.5 (CH_3), 18.8 (CH_3), 22.5 (CH_2), 24.0 (CH_3), 28.0 (CH_2), 29.8 (CH_2), 31.1 (CH_2), 32.2 (CH_2), 32.5 (CH_2), 35.3 (CH_2), 36.1 (CH), 36.7 (CH_2), 38.8 (CH_2), 40.0 (CH_2), 40.9 (CH), 41.7 (CH_2), 42.1 (morpholine-C CH_2), 44.0 (CH), 44.7 (CH), 44.9 (13-C), 46.6 (morpholine-C CH_2), 56.4 (CH), 57.8 (CH), 66(morpholine-C CH_2), 73.1 (3-C, 7-C, CH), 161.2 (-OC=OH), 162.1 (-OC=OH), 175.0 (24-C=ONH).

24-Morpholine-3α, 7β-dihydroxy-5 β-cholanamide (80)

Sodium (0.1 g) was added to hplc grade methanol (10 ml) to form an excess of sodium methoxide. The formyl morpholinamide (**103**) (0.7 g, 1.3 mmol) obtained in the above reaction was added to this solution and refluxed for 2 h. After 2 h the reaction was cooled to room temperature and added to water (100 ml). The amide was extracted with ethyl acetate. The organic layer was then washed with water (3 × 20 ml) and dried ($MgSO_4$). The solvent was removed and chromatographic elution with ethyl acetate afforded a white solid (0.5 g, 86%).

^{1}H-NMR δ (CD_3OD): 0.74 (3-H, s, 18-CH_3), 0.98 (3-H, s, 19-CH_3), 1.00 (3-H, d, J=6.52 Hz 21-CH_3), 3.51 (4-H, m, morpholine-CH_2, 2-H, m, 3-β H, 7-α H), 3.74 (4-H, m, morpholine-CH_2). ^{13}C-NMR ppm (CD_3OD): 12.9 (CH_3), 18.8 (CH_3), 22.5 (CH_2), 24.0 (CH_3), 28.0 (CH_2), 29.8 (CH_2), 31.1 (CH_2), 32.2 (CH_2), 32.5 (CH_2), 35.3 (CH_2), 36.1 (CH), 36.7 (CH_2), 38.8 (CH_2), 40.4 (CH_2), 40.9 (CH), 41.7 (CH_2), 42.1 (morpholine-C CH_2), 44.0 (CH), 44.7 (CH), 44.9 (13-C), 46.6 (morpholine-C CH_2), 56.4 (CH), 57.8 (CH), 66 (morpholine-C CH_2), 73.1 (3-C, 7-C, CH), 175.0 (24-C=ONH). HRMS: Found $(M\text{-}Na)^+$ = 462.3583. IR_{vmax} (KBr): 1445, 1625, 2860, 2926, 3399 cm^{-1}. mp: 72-73 °C (Bellini *et al.*, 1983).

24-(2)-Iodoaniline-3α, 7β-diformyloxy-5 β-cholanamide (104)

3α, 7β -diformyloxy-5 β-cholan-24-oyl chloride (**76**) (1 g, 1.9 mmol) was dissolved in dry DCM (10 ml). 2-iodoaniline (0.416 g, 1.9 mmol) and triethylamine (244 µL, 1.9 mmol) were added on ice. The reaction mixture was allowed to warm to room temperature and stirred monitoring for disappearance of the starting material by TLC. After 16 h the solvent was removed *in vacuo*. The residue was dissolved in ethyl

acetate (20 ml) and washed with HCl (3 × 20 ml) for removal of unreacted amines, water (2 × 20 ml) and brine solution (2 × 20 ml). The organic layer was dried and the solvent removed *in vacuo* which gave the iodoanilinamide on column chromatography (Hexane: ethyl acetate 1:1) (0.9 g, 73%).

^{1}H-NMR δ ($CDCl_3$): 0.70(3-H, s, 18-CH_3), 0.96 (3-H, s, 19-CH_3), 1.0122 (3-H, d, J= 6.52 Hz, 21-CH_3), 4.78 (2-H, m, 3-β H, 7-α H), 6.548 (1-H, m, meta-H), 7.321 (1-H, m, Aromatic para-H) , 7.6613 (1-H, d, J= 7.53 Hz, Aromatic meta-H), 8.0019 (2-H, s, OCOH), 8.25 (1-H, m , Aromatic ortho-H). ^{13}C-NMR ppm ($CDCl_3$): 12.9 (CH_3), 19.2 (CH_3), 22.3 (CH_2), 24.5 (CH_3), 28.1 (CH_2), 29.5 (CH_2), 31.1 (CH_2), 32.2 (CH_2), 32.5 (CH_2), 35.3 (CH_2), 36.1 (CH), 36.9 (CH_2), 38.1 (CH_2), 38.9 (CH_2), 40.9 (CH), 41.7 (CH_2), 44.1 (CH), 44.7 (CH), 44.9 (13-C), 56.6 (CH), 57.8 (CH), 73.1 (3-C, 7-C, CH), 90.1 (C-I), 123.2 (Aromatic ortho-C, CH), 125.1 (Aromatic meta-C), 129.0 (Aromatic para-C), 140.3 (Aromatic-C) 161.1 (-OC=OH), 162.2 (-OC=OH), 175.1 (24-C=ONH).

24-(2)-Iodoaniline-3α, 7β-dihydroxy-5 β-cholanamide (87)

Sodium (0.1 g) was added to hplc grade methanol (10 ml) to form an excess of sodium methoxide. **104** (0.8 g, 1.2 mmol) obtained in the above reaction was added to this solution and refluxed for 2 h. After 2 h the reaction was cooled to room temperature and added to water (100 ml). The amide was extracted with ethyl acetate. The organic layer was then washed with water (3 × 20 ml) and dried ($MgSO_4$). The solvent was removed *in vacuo* and after chromatographic elution with ethyl acetate afforded a white solid (0.45 g, 63%).

^{1}H-NMR δ (CD_3OD): 0.72 (3-H, s, 18-CH_3), 0.94 (3-H, s, 19-CH_3), 1.01 (3-H, d, J= 6.52 Hz, 21-CH_3), 3.53 (2-H, m, 3-β H, 7-α H), 6.62 (1-H, m, meta-H), 7.31 (1-H, m , Aromatic para-H) , 7.70 (1-H, d, J=7.53 Hz , Aromatic meta-H) , 8.21 (1-H, m, Aromatic ortho-H). ^{13}C-NMR ppm (CD_3OD): 12.8 (CH_3), 19.0 (CH_3), 22.5 (CH_2), 24.0 (CH_3), 28.0 (CH_2), 29.8 (CH_2), 31.1 (CH_2), 32.3 (CH_2), 32.5 (CH_2), 35.3 (CH_2), 36.1 (CH), 36.9 (CH_2), 38.1 (CH_2), 38.9 (CH_2), 40.9 (CH), 41.7 (CH_2), 44.1 (CH), 44.7 (CH), 44.8 (13-C), 56.6 (CH), 57.8 (CH), 71.0 (3-C, 7-C, CH), 90.0 (C-I), 124.2 (Aromatic ortho-C, CH) 125.4 (Aromatic meta-C, CH), 129.0 (Aromatic para-C, CH), 140.1 (Aromatic-C), 173.4 (24-C=ONH). HRMS: Found (M-Na) $^+$= 616.2264. IR_{vmax} (KBr): 1583, 1670, 2863, 2932, 3383 cm^{-1}. mp: 135-137 °C.

24-Piperazine-3α, 7β-diformyloxy-5 β-cholanamide (105)

3α, 7β -diformyloxy-5 β-cholan-24-oyl chloride (**76**) (1 g, 1.9 mmol) was dissolved in dry DCM (10 ml). 1-BOC piperazine (0.354 g, 1.9 mmol) and triethylamine (244 µL, 1.9 mmol) were added on ice. The reaction mixture was allowed to warm to room

temperature and stirred monitoring for disappearance of the starting material by TLC. After 16 h the solvent was removed *in vacuo*. The residue was dissolved in ethyl acetate (20 ml) and washed with HCl (3 × 20 ml) for removal of unreacted amines, water (2 × 20 ml) and brine solution (2 × 20 ml). The organic layer was dried and the solvent removed *in vacuo* which gave the piperazinamide on column chromatography (Hexane: ethyl acetate 1:1) (0.8 g, 68%).

^{1}H-NMR δ ($CDCl_3$): 0.70 (3-H, s, 18-CH_3), 0.96 (6-H, m, 19-CH_3), 1.49 (9-H, m, BOC group), 3.41-3.60 (8-H, m, piperazine-H), 4.80 (2-H, m, 3-β H, 7-α H) 8.00 (2-H, s, OCOH). ^{13}C-NMR ppm ($CDCl_3$): 12.6 (CH_3), 18.9 (CH_3), 22.5 (CH_2), 24.0 (CH_3), 26.1 (BOC group carbons), 28.0 (CH_2), 29.8 (CH_2), 31.1 (CH_2), 32.1 (CH_2), 32.5 (CH_2), 35.3 (CH_2), 36.1 (CH), 36.9 (CH_2), 38.1 (CH_2), 38.9 (CH_2), 39.2 (piperazine-C, CH_2), 40.9 (CH), 41.7 (CH_2), 44.5 (CH), 44.7 (CH), 44.9 (13-C), 45.2 (piperazine ring-C, CH_2), 56.6 (CH), 57.4 (CH), 71.1 (3-C, 7-C, CH), 80.0 (C-O), 161.1(-OC=OH), 162.3 (-OC=OH), 175.2 (24-C=ONH).

24-Piperazine-3α, 7β-dihydroxy-5 β-cholanamide (79)

Sodium (0.1 g) was added to hplc grade methanol (10 ml) to form an excess of sodium methoxide. **105** (0.6 g, 0.9 mmol) obtained in the above reaction was added to this solution and refluxed for 2 h. After 2 h the reaction was cooled to room temperature and added to water (100 ml). The amide was extracted with ethyl acetate. The organic layer was then washed with water (3 × 20 ml) and dried ($MgSO_4$). The solvent was removed *in vacuo* and after chromatographic elution with ethyl acetate afforded a white solid (0.35 g, 64%).

^{1}H-NMR δ (CD_3OD): 0.72 (3-H, s, 18-CH_3), 0.95 (6-H, m, 19-CH_3), 1.50 (9-H, m, BOC group), 3.41-3.60 (8-H, m, piperazine-H), 3.51 (2-H, m, 3-β H, 7-α H). ^{13}C-NMR ppm (CD_3OD): 12.6 (CH_3), 19.1 (CH_3), 22.5 (CH_2), 24.0 (CH_3), 26.1 (BOC group, CH_3), 28.2 (CH_2), 29.6 (CH_2), 31.1 (CH_2), 32.1 (CH_2), 32.5 (CH_2), 35.3 (CH_2), 36.1 (CH), 36.9 (CH_2), 38.1 (CH_2), 38.9 (CH_2), 39.2 (piperazine-C, CH_2), 40.9 (CH), 41.7 (CH_2), 44.3 (CH), 44.7 (CH), 44.9 (13-C), 45.1 (piperazine-C, CH_2), 56.6 (CH), 57.8 (CH), 71.2 (3-C, 7-C, CH), 80.4 (C-O), 175.2 (24-C=ONH). HRMS: Found $(M\text{-}Na)^{+}$ = 583.4097. IR_{vmax} (KBr): 1574, 1654, 1637, 1698, 1705, 1773, 2865, 2937, 3432 cm^{-1}. mp: 125-128 °C.

The BOC piperazinamide (0.25 g) was dissolved in methanol and trifluoroacetic acid (5eq) was added till the BOC group disappeared on monitoring by TLC. The methanol was evaporated to leave the solid product in 98% yield.

24-Benzylpiperazine-3α, 7β-diformyloxy-5 β-cholanamide (106)

3α, 7β -diformyloxy-5 β-cholan-24-oyl chloride (**76**) (1 g, 1.9 mmol) was dissolved in dry DCM (10 ml). Benzylpiperazine (0.334 g, 1.9 mmol) and triethylamine (244 µL, 1.9 mmol) were added on ice. The reaction mixture was allowed to warm to room temperature and stirred monitoring for disappearance of the starting material by TLC. After 16 h the solvent was removed *in vacuo*. The residue was dissolved in ethyl acetate (20 ml) and washed with HCl (3 × 20 ml) for removal of unreacted amines, water (2 × 20 ml) and brine solution (2 × 20 ml). The organic layer was dried and the solvent removed *in vacuo* which gave the benzylpiperazinamide after column chromatography (Hexane: ethyl acetate 1:1) (0.9 g, 79%).

^{1}H-NMR δ ($CDCl_3$): 0.70 (3-H, s, 18-CH_3), 0.96 (6-H, m, 19-CH_3), 3.41-3.60 (8-H, m, piperazine-H, CH_2) , 4.87 (2-H, m, 3-β H, 7-α H) 5.585 (2-H, m, benzyl CH_2) 7.758 (Aromatic-C, CH), 8.0019 (2-H, s, OCO<u>H</u>). ^{13}C-NMR ppm ($CDCl_3$): 12.8 (CH_3), 19.0 (CH_3), 22.5 (CH_2), 24.0 (CH_3), 28.4 (CH_2), 29.8 (CH_2), 31.1 (CH_2), 32.2 (CH_2), 32.5 (CH_2), 35.2 (CH_2), 36.1 (CH), 36.9 (CH_2), 38.1 (CH_2), 38.5 (CH_2), 40.9 (CH), 41.7 (CH_2), 44.1 (CH), 44.7 (CH), 44.9 (13-C), 39 (piperazine-C, CH_2), 45 (piperazine-C, CH_2), 56.6 (CH), 57.8 (CH), 71.1 (3-C, 7-C, CH), 80.2 (C-O), 130.1 (Aromatic-C, CH), 161.1 (-O<u>C</u>=OH), 162.2 (-O<u>C</u>=OH), 175.5 (24-<u>C</u>=ONH).

24-Benzylpiperazine-3α, 7β-dihydroxy-5 β-cholanamide (78)

Sodium (0.1 g) was added to hplc grade methanol (10 ml) to form an excess of sodium methoxide. **106** (0.7 g, 1.15 mmol) obtained in the above reaction was added to this solution and refluxed for 2 h. After 2 h the reaction was cooled to room temperature and added to water (100 ml). The amide was extracted with ethyl acetate. The organic layer was then washed with water (3 × 20 ml) and dried ($MgSO_4$). The solvent was removed *in vacuo* and after chromatographic elution with ethyl acetate afforded a white solid (0.5 g, 79%).

^{1}H-NMR δ (CD_3OD): 0.70 (3-H, s, 18-CH_3), 0.95 (6-H, m, 19-CH_3, 21-CH_3), 3.41-3.60 (8-H, m, piperazine-H, CH_2), 3.52 (2-H, m, 3-β H, 7-α H). ^{13}C-NMR ppm (CD_3OD): 12.9 (CH_3), 19.0 (CH_3), 22.5 (CH_2), 24.0 (CH_3), 28.0 (CH_2), 29.8 (CH_2), 31.1 (CH_2), 32.2 (CH_2), 32.5 (CH_2), 35.1 (CH_2), 36.1 (CH), 36.8 (CH_2), 38.1 (CH_2), 38.9 (CH_2), 39.2 (piperazine-C, CH_2), 40.9 (CH), 41.7 (CH_2), 44.2 (CH), 44.7 (CH), 44.9 (13-C), 45.3 (piperazine-C, CH_2), 56.6 (CH), 57.8 (CH), 71.1 (3-C, 7-C, CH), 80.3 (C-O), 130.2 (Aromatic-C, CH), 175.5 (24-<u>C</u>=ONH). HRMS: Found (M-Na) $^{+}$ = 573.4097. IR_{vmax} (KBr): 1634, 1710, 2497, 2603, 2875, 3947, 3417 cm^{-1}. mp: 74-76 °C.

24-Azido-3α, 7β -dihydroxy-5 β-cholane (29)

3α, 7β, 24 -trihydroxy-5 β-cholane (**28**) (0.2 g, 0.54 mmol) was dissolved in dry pyridine (4 ml) at 0 °C followed by the addition of methane sulfonyl chloride (63 µl,

8.1 mmol). After 20 min the reaction was quenched by adding crushed ice and the compound was extracted with ethyl acetate (2 x 10 ml). The organic layer was washed with cold water (2 x 20 ml), cold HCl (2 x 20 ml) and dried ($MgSO_4$) to afford a white solid. TLC of this product revealed starting material and a new product spot. Chromatographic elution with ethyl acetate afforded a white solid (**48**) (0.143 g, 58%). The product was dissolved in DMPU and treated with an excess of NaN_3 at 50 °C for two days. The title compound was obtained by partitioning between ethyl acetate and water, followed by successive acid and base wash, evaporation and flash chromatography (0.106 g, 84%).

^{1}H-NMR δ (CD_3OD): 0.70 (3-H, s, 18-CH_3), 0.99 (6-H, m, 19-CH_3, 21-CH_3), 3.26 (2-H, m, 23-CH_2), 3.51 (2-H, m, 3-β H, 7-α H). ^{13}C-NMR ppm (CD_3OD): 12.6 (CH_3), 18.9 (CH_3), 22.2 (CH_2), 24.2 (CH_3), 28.1 (CH_2), 29.7 (CH_2), 31.2 (CH_2), 32.4 (CH_2), 32.6 (CH_2), 35.3 (CH_2), 36.1 (CH), 36.9 (CH_2), 38.1 (CH_2), 38.9 (CH_2), 40.9 (CH), 41.7 (CH_2), 44.1 (CH), 44.5 (CH), 44.9 (13-C), 51.1 (23-C, CH_2), 56.6 (CH), 57.8 (CH), 71.2 (3-C, 7-C, CH). HRMS: Found $(M\text{-}Na)^+$ = 426.3096. IR_{vmax} (KBr): 1453, 2094, 2864, 2932, 3369 cm^{-1}. mp: 95-97 °C.

3α, 7β -dihydroxy-5 β-cholan-24-nitrile (26)

UDCA (**14**) (2.00 g, 4.8 mmol) was dissolved in DCM (20 ml). Pyridine (245 µl, 3 mmol), BOC_2O (1.4 g, 6.48 mmol) and ammonium bicarbonate (0.47 g, 6 mmol) were added to this mixture and stirred at room temperature for 24 h. After 24 h the solvent was removed by evaporation and redissolved in ethyl acetate for work up. The mixture was washed with water (2 × 20 ml), HCl (2 × 20 ml) and dried ($MgSO_4$) to afford a white solid (**56**) (1.16 g, 57%). The formyl UDCA amide (0.42 g, 0.9 mmol) was dissolved in dry THF (10 ml) at 0 °C. Pyridine (150 µl, 1.9 mmol) and trifluoroacetic anhydride (270 µl, 1.9 mmol) were added to this mixture. After completion of the reaction as monitored by TLC (10 h) the solvent was removed *in vacuo* and redissolved in ethyl acetate (20 ml) and washed with HCl (3 × 20 ml) and water to neutrality. Chromatographic elution with ethyl acetate: hexane (1:1) afforded a white solid. Sodium (0.2 g) was added to methanol (10 ml) to form an excess of sodium methoxide. The formyl nitrile obtained in the above reaction was added to this solution and refluxed for 2 h. After 2 h the reaction was cooled to room temperature and added to water (20 ml). The nitrile was extracted with ethyl acetate. The organic layer was then washed with water (3 × 20 ml) and dried ($MgSO_4$). The solvent was removed *in vacuo* to yield a white solid (0.3 g, 78%).

^{1}H-NMR δ (CD_3OD) 0.75 (3-H, s, 18-CH_3), 0.98 (3-H, s, 19-CH_3), 1.00 (3-H, d, J=6.02 Hz, 21-CH_3), 2.84 (1-H, m, 20-CH), 3.50 (2-H, m, 3- β H, 7-α H). ^{13}C-NMR ppm (CD_3OD) 12.9 (CH_3), 19.0 (CH_3), 22.5 (CH_2), 24.0 (CH_3), 28.0 (CH_2), 29.8 (CH_2), 31.1

(CH_2), 32.2 (CH_2), 32.2 (CH_2), 35.3 (CH_2), 36.1 (CH), 36.8 (CH_2), 38.1 (CH_2), 38.7 (CH_2), 40.9 (CH), 41.7 (CH_2), 44.1 (CH), 44.7 (CH), 44.9 (13-C), 56.6 (CH), 57.8 (CH), 71.3 (3-C, 7-C, CH), 124.5 (C≡N, 22-C). HRMS: Found (M-Na) $^{+}$=396.2867. IR_{vmax} (KBr): 1429, 1453, 1638, 2243 (nitrile peak), 2855, 2934, 3468 cm^{-1}. mp: 126-128 ^{o}C.

BIBLIOGRAPHY

A. Roda, A.M., M. A. Angellotti,t and A. Finit. 1990. Bile acid structure-activity relationship: evaluation of bile acid lipophilicity using I-octanol/water partition coefficient and reverse phase HPLC. *Journal of Lipid Research* **31:**1433-1443

Abdel-Latif, M.M., Duggan, S., Reynolds, J.V., Kelleher, D. 2009a. Inflammation and esophageal carcinogenesis. *Curr Opin Pharmacol* **9:**396-404

Abdel-Latif, M.M., Kelleher, D., Reynolds, J.V. 2009b. Potential role of NF-kappaB in esophageal adenocarcinoma: as an emerging molecular target. *J Surg Res* **153:**172-80

Aher, N.G., Pore, V.S., Mishra, N.N., Shukla, P.K., Gonnade, R.G. 2009. Design and synthesis of bile acid-based amino sterols as antimicrobial agents. *Bioorg Med Chem Lett* **19:**5411-4

Ahmadian, S., Barar, J., Saei, A.A., Fakhree, M.A., Omidi, Y. 2009. Cellular toxicity of nanogenomedicine in MCF-7 cell line: MTT assay. *J Vis Exp*

Akare, S., Martinez, J.D. 2005. Bile acid induces hydrophobicity-dependent membrane alterations. *Biochim Biophys Acta* **1735:**59-67

Alberts, B., Johnson, A., Lewis, J., Raff, M., Roberts, K., Walter, P. 2008. Molecular Biology of the Cell. Garland Science, Taylor and Francis Group, New York

Alberts, D.S., Martinez, M.E., Hess, L.M., Einspahr, J.G., Green, S.B., Bhattacharyya, A.K., Guillen, J., Krutzsch, M., Batta, A.K., Salen, G., Fales, L., Koonce, K., Parish, D., Clouser, M., Roe, D., Lance, P. 2005. Phase III trial of ursodeoxycholic acid to prevent colorectal adenoma recurrence. *J Natl Cancer Inst* **97:**846-53

Aldini, R., Roda, A., Labate, A.M., Cappelleri, G., Roda, E., Barbara, L. 1982. Hepatic bile acid uptake: effect of conjugation, hydroxyl and keto groups, and albumin binding. *J Lipid Res* **23:**1167-73

Ali, A., Balkovec, J.M., Greenlee, M., Hammond, M.L., Rouen, G., Taylor, G., Einstein, M., Ge, L., Harris, G., Kelly, T.M., Mazur, P., Pandit, S., Santoro, J., Sitlani, A., Wang, C., Williamson, J., Forrest, M.J., Carballo-Jane, E., Luell, S., Lowitz, K., Visco, D. 2008. Discovery of betamethasone 17alpha-carbamates as dissociated glucocorticoid receptor modulators in the rat. *Bioorg Med Chem* **16:**7535-42

Altorki, N., Schwartz, G.K., Blundell, M., Davis, B.M., Kelsen, D.P., Albino, A.P. 1993. Characterization of cell lines established from human gastric-esophageal adenocarcinomas. Biologic phenotype and invasion potential. *Cancer* **72:**649-57

Amaral, J.D., Castro, R.E., Sola, S., Steer, C.J., Rodrigues, C.M. 2007. p53 is a key molecular target of ursodeoxycholic acid in regulating apoptosis. *J Biol Chem* **282:**34250-9

Amaral, J.D., Castro, R.E., Steer, C.J., Rodrigues, C.M. 2009a. p53 and the regulation of hepatocyte apoptosis: implications for disease pathogenesis. *Trends Mol Med* **15:**531-41

Amaral, J.D., Correia, A.R., Steer, C.J., Gomes, C.M., Rodrigues, C.M. 2009b. No evidence of direct binding between ursodeoxycholic acid and the p53 DNA-binding domain. *Biosci Rep*

Amaral, J.D., Viana, R.J., Ramalho, R.M., Steer, C.J., Rodrigues, C.M. 2009c. Bile acids: regulation of apoptosis by ursodeoxycholic acid. *J Lipid Res* **50:**1721-34

Amsterdam, A., Tajima, K., Sasson, R. 2002. Cell-specific regulation of apoptosis by glucocorticoids: implication to their anti-inflammatory action. *Biochem Pharmacol* **64:**843-50

Anderson, I.G., Haslewood, G.A. 1964. Comparative studies of 'bile salts'. 20. Bile salts of the coelacanth, Latimeria chalumnae Smith. *Biochem J* **93:**34-9

Anelli, T., Sitia, R. 2008. Protein quality control in the early secretory pathway. *EMBO J* **27:**315-27

Angulo, P., Lindor, K.D. 1998. Management of primary biliary cirrhosis and autoimmune cholangitis. *Clin Liver Dis* **2:**333-51, ix

Araki Y, F.Y., Andoh A, Nakamura F, Shimada M, Takaya H, Bamba T. 2001. Hydrophilic and hydrophobic bile acids exhibit different cytotoxicities through cytolysis, interleukin-8 synthesis and apoptosis in the intestinal epithelial cell lines. IEC-6 and Caco-2 cells. *Scand J Gastroenterol* **36:**533-9

Arenzana-Seisdedos, F., Fernandez, B., Dominguez, I., Jacque, J.M., Thomas, D., Diaz-Meco, M.T., Moscat, J., Virelizier, J.L. 1993. Phosphatidylcholine hydrolysis activates NF-kappa B and increases human immunodeficiency virus replication in human monocytes and T lymphocytes. *J Virol* **67:**6596-604

Armstrong, M.J., Carey, M.C. 1982. The hydrophobic-hydrophilic balance of bile salts. Inverse correlation between reverse-phase high performance liquid chromatographic mobilities and micellar cholesterol-solubilizing capacities. *J Lipid Res* **23:**70-80

Asamoto, Y., Tazuma, S., Ochi, H., Chayama, K., Suzuki, H. 2001. Bile-salt hydrophobicity is a key factor regulating rat liver plasma-membrane communication: relation to bilayer structure, fluidity and transporter expression and function. *Biochem J* **359:**605-10

Attili, A.F., Angelico, M., Cantafora, A., Alvaro, D., Capocaccia, L. 1986. Bile acid-induced liver toxicity: relation to the hydrophobic-hydrophilic balance of bile acids. *Med Hypotheses* **19:**57-69

Attwood, S.E., Smyrk, T.C., DeMeester, T.R., Mirvish, S.S., Stein, H.J., Hinder, R.A. 1992. Duodenoesophageal reflux and the development of esophageal adenocarcinoma in rats. *Surgery* **111:**503-510

Avissar NE, T.L., Hu Y, Watson TJ, Jones C, Raymond DP, Matousek A, Peters JH. 2009. Bile acid alone or in combination with acid, induces CDX2 expression through activation of the epidermal growth factor receptor. *Journal of Gastrointestinal Surgery* **13:**212-222

Azzaroli, F., Mehal, W., Soroka, C.J., Wang, L., Lee, J., Crispe, N., Boyer, J.L. 2002. Ursodeoxycholic acid diminishes Fas-ligand-induced apoptosis in mouse hepatocytes. *Hepatology* **36:**49-54

Babu, P., Maitra, U. 2005. Synthesis and in vitro cholesterol dissolution by 23- and 24-phosphonobile acids. *Steroids* **70:**681-9

Badr, C.E., Hewett, J.W., Breakefield, X.O., Tannous, B.A. 2007. A highly sensitive assay for monitoring the secretory pathway and ER stress. *PLoS One* **2:**e571

Banciu, M., Metselaar, J.M., Schiffelers, R.M., Storm, G. 2008a. Liposomal glucocorticoids as tumor-targeted anti-angiogenic nanomedicine in B16 melanoma-bearing mice. *J Steroid Biochem Mol Biol* **111:**101-10

Banciu, M., Schiffelers, R.M., Fens, M.H., Metselaar, J.M., Storm, G. 2006. Anti-angiogenic effects of liposomal prednisolone phosphate on B16 melanoma in mice. *J Control Release* **113:**1-8

Banciu, M., Schiffelers, R.M., Metselaar, J.M., Storm, G. 2008b. Utility of targeted glucocorticoids in cancer therapy. *J Liposome Res* **18:**47-57

Banhegyi, G., Baumeister, P., Benedetti, A., Dong, D., Fu, Y., Lee, A.S., Li, J., Mao, C., Margittai, E., Ni, M., Paschen, W., Piccirella, S., Senesi, S., Sitia, R., Wang, M., Yang, W. 2007. Endoplasmic reticulum stress. *Ann N Y Acad Sci* **1113:**58-71

Baniecki, M.L., Wirth, D.F., Clardy, J. 2007. High-throughput Plasmodium falciparum growth assay for malaria drug discovery. *Antimicrob Agents Chemother* **51:**716-23

Bard, F., Malhotra, V. 2006. The formation of TGN-to-plasma-membrane transport carriers. *Annu Rev Cell Dev Biol* **22:**439-55

Barker, M., Clackers, M., Copley, R., Demaine, D.A., Humphreys, D., Inglis, G.G., Johnston, M.J., Jones, H.T., Haase, M.V., House, D., Loiseau, R., Nisbet, L., Pacquet, F., Skone, P.A., Shanahan, S.E., Tape, D., Vinader, V.M., Washington, M., Uings, I., Upton, R., McLay, I.M., Macdonald, S.J. 2006. Dissociated nonsteroidal glucocorticoid receptor modulators; discovery of the agonist trigger in a tetrahydronaphthalene-benzoxazine series. *J Med Chem* **49:**4216-31

Barnes, D., Talenti, D., Cammell, G., Goormastic, M., Farquhar, L., Henderson, M., Vogt, D., Mayes, J., Westveer, M.K., Carey, W. 1997. A randomized clinical trial of ursodeoxycholic acid as adjuvant treatment to prevent liver transplant rejection. *Hepatology* **26:**853-7

Barnes, P.J. 1998. Anti-inflammatory actions of glucocorticoids: molecular mechanisms. *Clin Sci (Lond)* **94:**557-72

Bartholome, B., Spies, C.M., Gaber, T., Schuchmann, S., Berki, T., Kunkel, D., Bienert, M., Radbruch, A., Burmester, G.R., Lauster, R., Scheffold, A., Buttgereit, F. 2004. Membrane glucocorticoid receptors (mGCR) are expressed in normal human peripheral blood mononuclear cells and up-regulated after in vitro stimulation and in patients with rheumatoid arthritis. *FASEB J* **18:**70-80

Batta, A.K., Datta, S.C., Tint, G.S., Alberts, D.S., Earnest, D.L., Salen, G. 1999. A convenient synthesis of dinorbile acids: oxidative hydrolysis of norbile acid nitriles. *Steroids* **64:**780-4

Bayerdorffer, E., Mannes, G.A., Ochsenkuhn, T., Dirschedl, P., Paumgartner, G. 1994. Variation of serum bile acids in patients with colorectal adenomas during a one-year follow-up. *Digestion* **55:**121-9

Bayerdorffer, E., Mannes, G.A., Ochsenkuhn, T., Dirschedl, P., Wiebecke, B., Paumgartner, G. 1995. Unconjugated secondary bile acids in the serum of patients with colorectal adenomas. *Gut* **36:**268-73

Beato, M., Klug, J. 2000. Steroid hormone receptors: an update. *Hum Reprod Update* **6:**225-36

Bechalany, A.T.-K., A.; El Tayar, N.; Testa, B. 1991. Measurement of lipophilicity indices by reversed-phase high performance liquid chromatography: comparison of two stationary phases and various eluents. *Journal of Chromatography* **541:**221-229

Beck, I.M., Berghe, W.V., Gerlo, S., Bougarne, N., Vermeulen, L., De Bosscher, K., Haegeman, G. 2009. Glucocorticoids and mitogen- and stress-activated protein kinase 1 inhibitors: possible partners in the combat against inflammation. *Biochem Pharmacol* **77:**1194-205

Beers, M.H. 2004. The Merck manual of medical information. Simon & Schuster, New York, London

Begley, M., Gahan, C.G., Hill, C. 2005. The interaction between bacteria and bile. *FEMS Microbiol Rev* **29:**625-51

Bellini, A.M., Quaglio, M.P., Guarneri, M., Cavazzini, G. 1983. Cheno and ursodeoxycholic acids derivatives (Part II). Antimicrobial activity of cholane compounds. *European Journal of Medicinal Chemistry* **18:**191-5

Belvisi, M.G., Brown, T.J., Wicks, S., Foster, M.L. 2001a. New Glucocorticosteroids with an improved therapeutic ratio? *Pulm Pharmacol Ther* **14:**221-7

Belvisi, M.G., Wicks, S.L., Battram, C.H., Bottoms, S.E., Redford, J.E., Woodman, P., Brown, T.J., Webber, S.E., Foster, M.L. 2001b. Therapeutic benefit of a dissociated glucocorticoid and the relevance of in vitro separation of transrepression from transactivation activity. *J Immunol* **166:**1975-82

Bennett, M., Macdonald, K., Chan, S.W., Luzio, J.P., Simari, R., Weissberg, P. 1998. Cell surface trafficking of Fas: a rapid mechanism of p53-mediated apoptosis. *Science* **282:**290-3

Benz, C., Angermuller, S., Otto, G., Sauer, P., Stremmel, W., Stiehl, A. 2000. Effect of tauroursodeoxycholic acid on bile acid-induced apoptosis in primary human hepatocytes. *Eur J Clin Invest* **30:**203-9

Bernstein, H., Bernstein, C., Payne, C.M., Dvorak, K. 2009. Bile acids as endogenous etiologic agents in gastrointestinal cancer. *World J Gastroenterol* **15:**3329-40

Bernstein, H., Bernstein, C., Payne, C.M., Dvorakova, K., Garewal, H. 2005. Bile acids as carcinogens in human gastrointestinal cancers. *Mutat Res* **589:**47-65

Bernstein, H., Payne, C.M., Bernstein, C., Schneider, J., Beard, S.E., Crowley, C.L. 1999. Activation of the promoters of genes associated with DNA damage, oxidative stress, ER stress and protein malfolding by the bile salt, deoxycholate. *Toxicol Lett* **108:**37-46

Beuers, U., Nathanson, M.H., Boyer, J.L. 1993. Effects of tauroursodeoxycholic acid on cytosolic Ca2+ signals in isolated rat hepatocytes. *Gastroenterology* **104:**604-12

Beuers, U., Spengler, U., Zwiebel, F.M., Pauletzki, J., Fischer, S., Paumgartner, G. 1992. Effect of ursodeoxycholic acid on the kinetics of the major hydrophobic bile acids in health and in chronic cholestatic liver disease. *Hepatology* **15:**603-8

Beuers, U., Throckmorton, D.C., Anderson, M.S., Isales, C.M., Thasler, W., Kullak-Ublick, G.A., Sauter, G., Koebe, H.G., Paumgartner, G., Boyer, J.L. 1996. Tauroursodeoxycholic acid activates protein kinase C in isolated rat hepatocytes. *Gastroenterology* **110:**1553-63

Biggadike, K., Bledsoe, R.K., Coe, D.M., Cooper, T.W., House, D., Iannone, M.A., Macdonald, S.J., Madauss, K.P., McLay, I.M., Shipley, T.J., Taylor, S.J., Tran, T.B., Uings, I.J., Weller, V., Williams, S.P. 2009. Design and x-ray crystal structures of high-potency nonsteroidal glucocorticoid agonists exploiting a novel binding site on the receptor. *Proc Natl Acad Sci U S A* **106:**18114-9

Biggadike, K., Bledsoe, R.K., Hassell, A.M., Kirk, B.E., McLay, I.M., Shewchuk, L.M., Stewart, E.L. 2008. X-ray crystal structure of the novel enhanced-affinity

glucocorticoid agonist fluticasone furoate in the glucocorticoid receptor-ligand binding domain. *J Med Chem* **51:**3349-52

Billington, D., Evans, C.E., Godfrey, P.P., Coleman, R. 1980. Effects of bile salts on the plasma membranes of isolated rat hepatocytes. *Biochem J* **188:**321-7

Bledsoe, R.K., Montana, V.G., Stanley, T.B., Delves, C.J., Apolito, C.J., McKee, D.D., Consler, T.G., Parks, D.J., Stewart, E.L., Willson, T.M., Lambert, M.H., Moore, J.T., Pearce, K.H., Xu, H.E. 2002. Crystal structure of the glucocorticoid receptor ligand binding domain reveals a novel mode of receptor dimerization and coactivator recognition. *Cell* **110:**93-105

Bodwell, J.E., Webster, J.C., Jewell, C.M., Cidlowski, J.A., Hu, J.M., Munck, A. 1998. Glucocorticoid receptor phosphorylation: overview, function and cell cycle-dependence. *J Steroid Biochem Mol Biol* **65:**91-9

Breslin, M.B., Geng, C.D., Vedeckis, W.V. 2001. Multiple promoters exist in the human GR gene, one of which is activated by glucocorticoids. *Mol Endocrinol* **15:**1381-95

Bruno, T., De Nicola, F., Iezzi, S., Lecis, D., D'Angelo, C., Di Padova, M., Corbi, N., Dimiziani, L., Zannini, L., Jekimovs, C., Scarsella, M., Porrello, A., Chersi, A., Crescenzi, M., Leonetti, C., Khanna, K.K., Soddu, S., Floridi, A., Passananti, C., Delia, D., Fanciulli, M. 2006. Che-1 phosphorylation by ATM/ATR and Chk2 kinases activates p53 transcription and the G2/M checkpoint. *Cancer Cell* **10:**473-86

Bruno, T., Iezzi, S., De Nicola, F., Di Padova, M., Desantis, A., Scarsella, M., Di Certo, M.G., Leonetti, C., Floridi, A., Passananti, C., Fanciulli, M. 2008. Che-1 activates XIAP expression in response to DNA damage. *Cell Death Differ* **15:**515-20

Bulbul, M., Saracoglu, N., Kufrevioglu, O.I., Ciftci, M. 2002. Bile acid derivatives of 5-amino-1,3,4-thiadiazole-2-sulfonamide as new carbonic anhydrase inhibitors: synthesis and investigation of inhibition effects. *Bioorg Med Chem* **10:**2561-7

Buttar, N.S., Wang, K.K., Anderson, M.A., Dierkhising, R.A., Pacifico, R.J., Krishnadath, K.K., Lutzke, L.S. 2002. The effect of selective cyclooxygenase-2 inhibition in Barrett's esophagus epithelium: an in vitro study. *J Natl Cancer Inst* **94:**422-9

Buttgereit, F., Straub, R.H., Wehling, M., Burmester, G.R. 2004. Glucocorticoids in the treatment of rheumatic diseases: an update on the mechanisms of action. *Arthritis Rheum* **50:**3408-17

Byrne, A.M., Foran, E., Sharma, R., Davies, A., Mahon, C., O'Sullivan, J., O'Donoghue, D., Kelleher, D., Long, A. 2010. Bile acids modulate the Golgi membrane fission

process via a protein kinase C{eta} and protein kinase D-dependent pathway in colonic epithelial cells. *Carcinogenesis*

Calmus, Y., Arvieux, C., Gane, P., Boucher, E., Nordlinger, B., Rouger, P., Poupon, R. 1992. Cholestasis induces major histocompatibility complex class I expression in hepatocytes. *Gastroenterology* **102:**1371-7

Calmus, Y., Gane, P., Rouger, P., Poupon, R. 1990. Hepatic expression of class I and class II major histocompatibility complex molecules in primary biliary cirrhosis: effect of ursodeoxycholic acid. *Hepatology* **11:**12-5

Cameron, A.J. 1997. Epidemiology of columnar-lined esophagus and adenocarcinoma. *Gastroenterol Clin North Am* **26:**487-94

Campbell, B.J., Yu, L.G., Rhodes, J.M. 2001. Altered glycosylation in inflammatory bowel disease: a possible role in cancer development. *Glycoconj J* **18:**851-8

Carey, M. 1983. Measurement of the physical-chemical properties of bile salt solutions. *In:* Bile Acids in Gastroenterology. L. Barbara, A.F. Hofmann, E. Roda, and R.H. Dowling, editors. pp. 19-56. Lancaster:MTP Press

Carubbi, F., Guicciardi, M.E., Concari, M., Loria, P., Bertolotti, M., Carulli, N. 2002. Comparative cytotoxic and cytoprotective effects of taurohyodeoxycholic acid (THDCA) and tauroursodeoxycholic acid (TUDCA) in HepG2 cell line. *Biochim Biophys Acta* **1580:**31-9

Cazes, J. 2005. Encyclopedia of Chromatography. Taylor & Francis, London

Chen, Y., Liu, C.P., Xu, K.F., Mao, X.D., Lu, Y.B., Fang, L., Yang, J.W., Liu, C. 2008. Effect of taurine-conjugated ursodeoxycholic acid on endoplasmic reticulum stress and apoptosis induced by advanced glycation end products in cultured mouse podocytes. *Am J Nephrol* **28:**1014-22

Chen, Y., Zhang, Y., Yin, Y., Gao, G., Li, S., Jiang, Y., Gu, X., Luo, J. 2005. SPD--a web-based secreted protein database. *Nucleic Acids Res* **33:**D169-73

Chieco, P., Romagnoli, E., Aicardi, G., Suozzi, A., Forti, G.C., Roda, A. 1997. Apoptosis induced in rat hepatocytes by in vivo exposure to taurochenodeoxycholate. *Histochem J* **29:**875-83

Choi, Y.H., Im, E.O., Suh, H., Jin, Y., Lee, W.H., Yoo, Y.H., Kim, K.W., Kim, N.D. 2001. Apoptotic activity of novel bile acid derivatives in human leukemic T cells through the activation of caspases. *Int J Oncol* **18:**979-84

Choi, Y.H., Im, E.O., Suh, H., Jin, Y., Yoo, Y.H., Kim, N.D. 2003. Apoptosis and modulation of cell cycle control by synthetic derivatives of ursodeoxycholic acid and chenodeoxycholic acid in human prostate cancer cells. *Cancer Lett* **199:**157-67

Claudel, T., Staels, B., Kuipers, F. 2005. The Farnesoid X receptor: a molecular link between bile acid and lipid and glucose metabolism. *Arterioscler Thromb Vasc Biol* **25:**2020-30

Coghlan, M.J., Jacobson, P.B., Lane, B., Nakane, M., Lin, C.W., Elmore, S.W., Kym, P.R., Luly, J.R., Carter, G.W., Turner, R., Tyree, C.M., Hu, J., Elgort, M., Rosen, J., Miner, J.N. 2003. A novel antiinflammatory maintains glucocorticoid efficacy with reduced side effects. *Mol Endocrinol* **17:**860-9

Colanzi, A., Suetterlin, C., Malhotra, V. 2003a. Cell-cycle-specific Golgi fragmentation: how and why? *Curr Opin Cell Biol* **15:**462-7

Colanzi, A., Sutterlin, C., Malhotra, V. 2003b. RAF1-activated MEK1 is found on the Golgi apparatus in late prophase and is required for Golgi complex fragmentation in mitosis. *J Cell Biol* **161:**27-32

Cole, N.B., Ellenberg, J., Song, J., DiEuliis, D., Lippincott-Schwartz, J. 1998. Retrograde transport of Golgi-localized proteins to the ER. *J Cell Biol* **140:**1-15

Committee, N.R.N. 1999. A unified nomenclature system for the nuclear receptor superfamily. *Cell* **97:**161-3

Cook, J.W., Kennaway, E.L., Kennaway, N.M. 1940. Production of Tumours in Mice by Deoxycholic Acid. *Nature* **145:**627

Cortopassi, G., Danielson, S., Alemi, M., Zhan, S.S., Tong, W., Carelli, V., Martinuzzi, A., Marzuki, S., Majamaa, K., Wong, A. 2006. Mitochondrial disease activates transcripts of the unfolded protein response and cell cycle and inhibits vesicular secretion and oligodendrocyte-specific transcripts. *Mitochondrion* **6:**161-75

Costarelli, V., Key, T.J., Appleby, P.N., Allen, D.S., Fentiman, I.S., Sanders, T.A. 2002. A prospective study of serum bile acid concentrations and colorectal cancer risk in post-menopausal women on the island of Guernsey. *Br J Cancer* **86:**1741-4

Coussens, L.M., Werb, Z. 2002. Inflammation and cancer. *Nature* **420:**860-7

Crowley-Weber, C.L., Payne, C.M., Gleason-Guzman, M., Watts, G.S., Futscher, B., Waltmire, C.N., Crowley, C., Dvorakova, K., Bernstein, C., Craven, M., Garewal, H., Bernstein, H. 2002. Development and molecular characterization of HCT-116 cell lines resistant to the tumor promoter and multiple stress-inducer, deoxycholate. *Carcinogenesis* **23:**2063-80

Croxtall, J.D., Choudhury, Q., Flower, R.J. 2000. Glucocorticoids act within minutes to inhibit recruitment of signalling factors to activated EGF receptors through a receptor-dependent, transcription-independent mechanism. *Br J Pharmacol* **130:**289-98

Cunha, D.A., Hekerman, P., Ladriere, L., Bazarra-Castro, A., Ortis, F., Wakeham, M.C., Moore, F., Rasschaert, J., Cardozo, A.K., Bellomo, E., Overbergh, L., Mathieu, C., Lupi, R., Hai, T., Herchuelz, A., Marchetti, P., Rutter, G.A., Eizirik,

D.L., Cnop, M. 2008. Initiation and execution of lipotoxic ER stress in pancreatic beta-cells. *J Cell Sci* **121:**2308-18

Das, D., Chilton, A.P., Jankowski, J.A. 2009. Chemoprevention of oesophageal cancer and the AspECT trial. *Recent Results Cancer Res* **181:**161-9

De Bosscher, K. 2010. Selective Glucocorticoid Receptor modulators. *J Steroid Biochem Mol Biol* **120:**96-104

de Kok, T.M., van Faassen, A., Glinghammar, B., Pachen, D.M., Eng, M., Rafter, J.J., Baeten, C.G., Engels, L.G., Kleinjans, J.C. 1999. Bile acid concentrations, cytotoxicity, and pH of fecal water from patients with colorectal adenomas. *Dig Dis Sci* **44:**2218-25

Deasy, B.M., O'Sullivan-Coyne, G., O'Donovan, T.R., McKenna, S.L., O'Sullivan, G.C. 2007. Cyclooxygenase-2 inhibitors demonstrate anti-proliferative effects in oesophageal cancer cells by prostaglandin E(2)-independent mechanisms. *Cancer Lett* **256:**246-58

Debruyne, P.R., Bruyneel, E.A., Li, X., Zimber, A., Gespach, C., Mareel, M.M. 2001. The role of bile acids in carcinogenesis. *Mutat Res* **480-481:**359-69

DeFranco, D.B., Qi, M., Borror, K.C., Garabedian, M.J., Brautigan, D.L. 1991. Protein phosphatase types 1 and/or 2A regulate nucleocytoplasmic shuttling of glucocorticoid receptors. *Mol Endocrinol* **5:**1215-28

DeRubertis, F.R., Craven, P.A., Saito, R. 1984. Bile salt stimulation of colonic epithelial proliferation. Evidence for involvement of lipoxygenase products. *J Clin Invest* **74:**1614-24

Diaz Anel, A.M., Malhotra, V. 2005. PKCeta is required for beta1gamma2/beta3gamma2- and PKD-mediated transport to the cell surface and the organization of the Golgi apparatus. *J Cell Biol* **169:**83-91

Dittmar, K.D., Demady, D.R., Stancato, L.F., Krishna, P., Pratt, W.B. 1997. Folding of the glucocorticoid receptor by the heat shock protein (hsp) 90-based chaperone machinery. The role of p23 is to stabilize receptor.hsp90 heterocomplexes formed by hsp90.p60.hsp70. *J Biol Chem* **272:**21213-20

Dong, D., Dubeau, L., Bading, J., Nguyen, K., Luna, M., Yu, H., Gazit-Bornstein, G., Gordon, E.M., Gomer, C., Hall, F.L., Gambhir, S.S., Lee, A.S. 2004. Spontaneous and controllable activation of suicide gene expression driven by the stress-inducible grp78 promoter resulting in eradication of sizable human tumors. *Hum Gene Ther* **15:**553-61

Duggan, S.P., Behan, F.M., Kirca, M., Smith, S., Reynolds, J.V., Long, A., Kelleher, D. 2010. An integrative genomic approach in oesophageal cells identifies TRB3 as a bile acid responsive gene, downregulated in Barrett's oesophagus, which regulates NF-kappaB activation and cytokine levels. *Carcinogenesis* **31:**936-45

Duma, D., Jewell, C.M., Cidlowski, J.A. 2006. Multiple glucocorticoid receptor isoforms and mechanisms of post-translational modification. *J Steroid Biochem Mol Biol* **102:**11-21

Earnest, D.L., Holubec, H., Wali, R.K., Jolley, C.S., Bissonette, M., Bhattacharyya, A.K., Roy, H., Khare, S., Brasitus, T.A. 1994. Chemoprevention of azoxymethane-induced colonic carcinogenesis by supplemental dietary ursodeoxycholic acid. *Cancer Res* **54:**5071-4

El-Mir, M.Y., Badia, M.D., Luengo, N., Monte, M.J., Marin, J.J. 2001. Increased levels of typically fetal bile acid species in patients with hepatocellular carcinoma. *Clin Sci (Lond)* **100:**499-508

El Kihel, L., Clement, M., Bazin, M.A., Descamps, G., Khalid, M., Rault, S. 2008. New lithocholic and chenodeoxycholic piperazinylcarboxamides with antiproliferative and pro-apoptotic effects on human cancer cell lines. *Bioorg Med Chem* **16:**8737-44

Encio, I.J., Detera-Wadleigh, S.D. 1991. The genomic structure of the human glucocorticoid receptor. *J Biol Chem* **266:**7182-8

Ewerth, S., Angelin, B., Einarsson, K., Nilsell, K., Bjorkhem, I. 1985. Serum concentrations of ursodeoxycholic acid in portal venous and systemic venous blood of fasting humans as determined by isotope dilution-mass spectrometry. *Gastroenterology* **88:**126-33

Fan, J., Hu, Z., Zeng, L., Lu, W., Tang, X., Zhang, J., Li, T. 2008. Golgi apparatus and neurodegenerative diseases. *Int J Dev Neurosci* **26:**523-34

Faubion, W.A., Guicciardi, M.E., Miyoshi, H., Bronk, S.F., Roberts, P.J., Svingen, P.A., Kaufmann, S.H., Gores, G.J. 1999. Toxic bile salts induce rodent hepatocyte apoptosis via direct activation of Fas. *J Clin Invest* **103:**137-45

Fernandez, P.M., Tabbara, S.O., Jacobs, L.K., Manning, F.C., Tsangaris, T.N., Schwartz, A.M., Kennedy, K.A., Patierno, S.R. 2000. Overexpression of the glucose-regulated stress gene GRP78 in malignant but not benign human breast lesions. *Breast Cancer Res Treat* **59:**15-26

Fimognari, C., Lenzi, M., Cantelli-Forti, G., Hrelia, P. 2009. Apoptosis and modulation of cell cycle control by bile acids in human leukemia T cells. *Ann N Y Acad Sci* **1171:**264-9

Fini, A., Roda, A., Bellini, A.M., Mencini, E., Guarneri, M. 1990. Quantitative structure-antimicrobial activity relationship in 5 beta-cholanyl-24-benzylamine derivatives. *J Pharm Sci* **79:**603-5

Fiorucci, S., Mencarelli, A., Palladino, G., Cipriani, S. 2009. Bile-acid-activated receptors: targeting TGR5 and farnesoid-X-receptor in lipid and glucose disorders. *Trends Pharmacol Sci* **30:**570-80

Fitzgerald, R.C., Abdalla, S., Onwuegbusi, B.A., Sirieix, P., Saeed, I.T., Burnham, W.R., Farthing, M.J. 2002. Inflammatory gradient in Barrett's oesophagus: implications for disease complications. *Gut* **51:**316-22

Fitzgerald, R.C., Lascar, R., Triadafilopoulos, G. 2001. Review article: Barrett's oesophagus, dysplasia and pharmacologic acid suppression. *Aliment Pharmacol Ther* **15:**269-76

Fleckenstein, J.F., Paredes, M., Thuluvath, P.J. 1998. A prospective, randomized, double-blind trial evaluating the efficacy of ursodeoxycholic acid in prevention of liver transplant rejection. *Liver Transpl Surg* **4:**276-9

Florence, A.T., Attwood, D. 2006. Physicochemical Principles of Pharmacy. Pharmaceutical Press, London

Forster, A., Emmler, T., Schwalm, S., Ebadi, M., Heringdorf, D.M., Nieuwenhuis, B., Kleuser, B., Huwiler, A., Pfeilschifter, J. 2010. Glucocorticoids protect renal mesangial cells from apoptosis by increasing cellular sphingosine-1-phosphate. *Kidney Int*

Fraga, M., Laux, M., Dos Santos, G.R., Zandona, B., Dos Santos Giuberti, C., de Oliveira, M.C., da Silveira, M.U., Teixeira, H.F. 2008. Evaluation of the toxicity of oligonucleotide/cationic nanoemulsion complexes on Hep G2 cells through MTT assay. *Pharmazie* **63:**667-70

Fujiwara, T., Oda, K., Yokota, S., Takatsuki, A., Ikehara, Y. 1988. Brefeldin A causes disassembly of the Golgi complex and accumulation of secretory proteins in the endoplasmic reticulum. *J Biol Chem* **263:**18545-52

Fulda, S., Debatin, K.M. 2006. Extrinsic versus intrinsic apoptosis pathways in anticancer chemotherapy. *Oncogene* **25:**4798-811

Garidel, P., Hildebrand, A., Knauf, K., Blume, A. 2007. Membranolytic activity of bile salts: influence of biological membrane properties and composition. *Molecules* **12:**2292-326

Germain, P., Staels, B., Dacquet, C., Spedding, M., Laudet, V. 2006. Overview of nomenclature of nuclear receptors. *Pharmacol Rev* **58:**685-704

Gillen, P., Keeling, P., Byrne, P.J., Healy, M., O'Moore, R.R., Hennessy, T.P.J. 1988. Implication of duodenogastric reflux in the pathogenesis of Barrett's oesophagus. *Br. J. Surg* **75:**540-543

Glass, C.K., Rosenfeld, M.G. 2000. The coregulator exchange in transcriptional functions of nuclear receptors. *Genes Dev* **14:**121-41

Glick, B.S. 2000. Organization of the Golgi apparatus. *Curr Opin Cell Biol* **12:**450-6

Gonatas, N.K., Stieber, A., Gonatas, J.O. 2006. Fragmentation of the Golgi apparatus in neurodegenerative diseases and cell death. *J Neurol Sci* **246:**21-30

Goulding, N.J., Guyre, P.M. 1993. Glucocorticoids, lipocortins and the immune response. *Curr Opin Immunol* **5:**108-13

Graf, D., Kurz, A.K., Fischer, R., Reinehr, R., Haussinger, D. 2002. Taurolithocholic acid-3 sulfate induces CD95 trafficking and apoptosis in a c-Jun N-terminal kinase-dependent manner. *Gastroenterology* **122:**1411-27

Graves, T.K., Patel, S., Dannies, P.S., Hinkle, P.M. 2001. Misfolded growth hormone causes fragmentation of the Golgi apparatus and disrupts endoplasmic reticulum-to-Golgi traffic. *J Cell Sci* **114:**3685-94

Green, S., Kumar, V., Theulaz, I., Wahli, W., Chambon, P. 1988. The N-terminal DNA-binding 'zinc finger' of the oestrogen and glucocorticoid receptors determines target gene specificity. *EMBO J* **7:**3037-44

H.P. Rang, M.M.D., J.M. Ritter. 1999. Pharmacology. Churchill Livingstone, Edinburgh

Hakomori, S. 1996. Tumor malignancy defined by aberrant glycosylation and sphingo(glyco)lipid metabolism. *Cancer Res* **56:**5309-18

Hakomori, S. 2001. Tumor-associated carbohydrate antigens defining tumor malignancy: basis for development of anti-cancer vaccines. *Adv Exp Med Biol* **491:**369-402

Han, F.X., Lin, H., Ru, L. 2009. [MTT assay for detecting 5-fluorouracil chemosensitivity of human breast carcinoma cell line]. *Nan Fang Yi Ke Da Xue Xue Bao* **29:**97-9

Harmand, P.O., Duval, R., Delage, C., Simon, A. 2005. Ursolic acid induces apoptosis through mitochondrial intrinsic pathway and caspase-3 activation in M4Beu melanoma cells. *Int J Cancer* **114:**1-11

Haslewood, G.A. 1964a. The Biological Significance of Chemical Differences in Bile Salts. *Biol Rev Camb Philos Soc* **39:**537-74

Haslewood, G.A. 1964b. Comparative studies of bile salts. 19. The chemistry of ranol. *Biochem J* **90:**309-13

He, Y., Szapary, D., Simons, S.S., Jr. 2002. Modulation of induction properties of glucocorticoid receptor-agonist and -antagonist complexes by coactivators involves binding to receptors but is independent of ability of coactivators to augment transactivation. *J Biol Chem* **277:**49256-66

Healy, S.J., Gorman, A.M., Mousavi-Shafaei, P., Gupta, S., Samali, A. 2009. Targeting the endoplasmic reticulum-stress response as an anticancer strategy. *Eur J Pharmacol* **625:**234-46

Heck, S., Kullmann, M., Gast, A., Ponta, H., Rahmsdorf, H.J., Herrlich, P., Cato, A.C. 1994. A distinct modulating domain in glucocorticoid receptor monomers in the repression of activity of the transcription factor AP-1. *EMBO J* **13:**4087-95

Heery, D.M., Kalkhoven, E., Hoare, S., Parker, M.G. 1997. A signature motif in transcriptional co-activators mediates binding to nuclear receptors. *Nature* **387:**733-6

Heitzer, M.D., Wolf, I.M., Sanchez, E.R., Witchel, S.F., DeFranco, D.B. 2007. Glucocorticoid receptor physiology. *Rev Endocr Metab Disord* **8:**321-30

Herr, I., Ucur, E., Herzer, K., Okouoyo, S., Ridder, R., Krammer, P.H., von Knebel Doeberitz, M., Debatin, K.M. 2003. Glucocorticoid cotreatment induces apoptosis resistance toward cancer therapy in carcinomas. *Cancer Res* **63:**3112-20

Hess, L.M., Krutzsch, M.F., Guillen, J., Chow, H.H., Einspahr, J., Batta, A.K., Salen, G., Reid, M.E., Earnest, D.L., Alberts, D.S. 2004. Results of a phase I multiple-dose clinical study of ursodeoxycholic Acid. *Cancer Epidemiol Biomarkers Prev* **13:**861-7

Heuman, D. 1993. Hepatoprotective properties of ursodeoxycholic acid. *Gastroenterology* **104:**1860-1865

Heuman, D.M. 1989. Quantitative estimation of the hydrophilic-hydrophobic balance of mixed bile salt solutions. *J Lipid Res* **30:**719-30

Heuman, D.M., Pandak, W.M., Hylemon, P.B., Vlahcevic, Z.R. 1991. Conjugates of ursodeoxycholate protect against cytotoxicity of more hydrophobic bile salts: in vitro studies in rat hepatocytes and human erythrocytes. *Hepatology* **14:**920-6

Hicks, S.W., Machamer, C.E. 2005. Golgi structure in stress sensing and apoptosis. *Biochim Biophys Acta* **1744:**406-14

Higuchi, H., Gores, G.J. 2003. Bile acid regulation of hepatic physiology: IV. Bile acids and death receptors. *Am J Physiol Gastrointest Liver Physiol* **284:**G734-8

Hill, M.J. 1990. Bile flow and colon cancer. *Mutat Res* **238:**313-20

Hillaire, S., Boucher, E., Calmus, Y., Gane, P., Ballet, F., Franco, D., Moukthar, M., Poupon, R. 1994. Effects of bile acids and cholestasis on major histocompatibility complex class I in human and rat hepatocytes. *Gastroenterology* **107:**781-8

Hirano, F., Tanada, H., Makino, Y., Okamoto, K., Hiramoto, M., Handa, H., Makino, I. 1996. Induction of the transcription factor AP-1 in cultured human colon adenocarcinoma cells following exposure to bile acids. *Carcinogenesis* **17:**427-33

Hofmann, A.F. 1985. Trends in Hepatology. MTP Press, Lancaster

Hofmann, A.F. 1994. Pharmacology of ursodeoxycholic acid, an enterohepatic drug. *Scand J Gastroenterol Suppl* **204:**1-15

Hofmann, A.F. 1999. The continuing importance of bile acids in liver and intestinal disease. *Arch Intern Med* **159:**2647-58

Hofmann, A.F. 2002. Cholestatic liver disease: pathophysiology and therapeutic options. *Liver* **22 Suppl 2:**14-9

Hofmann, A.F., Hagey, L.R. 2008. Bile acids: chemistry, pathochemistry, biology, pathobiology, and therapeutics. *Cell Mol Life Sci* **65:**2461-83

Hofmann, A.F., Mysels, K.J. 1992. Bile acid solubility and precipitation in vitro and in vivo: the role of conjugation, pH, and Ca2+ ions. *J Lipid Res* **33:**617-26

Hofmann, A.F., Roda, A. 1984. Physicochemical properties of bile acids and their relationship to biological properties: an overview of the problem. *J Lipid Res* **25:**1477-89

Holthuis, J.C., Pomorski, T., Raggers, R.J., Sprong, H., Van Meer, G. 2001. The organizing potential of sphingolipids in intracellular membrane transport. *Physiol Rev* **81:**1689-723

Hong, J., Behar, J., Wands, J., Resnick, M., Wang, L.J., DeLellis, R.A., Lambeth, D., Souza, R.F., Spechler, S.J., Cao, W. 2010. Role of a novel bile acid receptor TGR5 in the development of oesophageal adenocarcinoma. *Gut* **59:**170-80

Horlein, A.J., Naar, A.M., Heinzel, T., Torchia, J., Gloss, B., Kurokawa, R., Ryan, A., Kamei, Y., Soderstrom, M., Glass, C.K., et al. 1995. Ligand-independent repression by the thyroid hormone receptor mediated by a nuclear receptor co-repressor. *Nature* **377:**397-404

Hsu, T.C., Young, M.R., Cmarik, J., Colburn, N.H. 2000. Activator protein 1 (AP-1)- and nuclear factor kappaB (NF-kappaB)-dependent transcriptional events in carcinogenesis. *Free Radic Biol Med* **28:**1338-48

Hu, P., Han, Z., Couvillon, A.D., Exton, J.H. 2004. Critical role of endogenous Akt/IAPs and MEK1/ERK pathways in counteracting endoplasmic reticulum stress-induced cell death. *J Biol Chem* **279:**49420-9

Huang, L., Sun, Y., Zhu, H., Zhang, Y., Xu, J., Shen, Y.M. 2009. Synthesis and antimicrobial evaluation of bile acid tridentate conjugates. *Steroids* **74:**701-6

Hung, J.H., Su, I.J., Lei, H.Y., Wang, H.C., Lin, W.C., Chang, W.T., Huang, W., Chang, W.C., Chang, Y.S., Chen, C.C., Lai, M.D. 2004. Endoplasmic reticulum stress stimulates the expression of cyclooxygenase-2 through activation of NF-kappaB and pp38 mitogen-activated protein kinase. *J Biol Chem* **279:**46384-92

Iguchi, Y., Yamaguchi, M., Sato, H., Kihira, K., Nishimaki-Mogami, T., Une, M. 2009. Bile alcohols function as the ligands of membrane-type bile acid-activated G protein-coupled receptor. *J Lipid Res* **51:**1432-41

Iizaka, T., Tsuji, M., Oyamada, H., Morio, Y., Oguchi, K. 2007. Interaction between caspase-8 activation and endoplasmic reticulum stress in glycochenodeoxycholic acid-induced apoptotic HepG2 cells. *Toxicology* **241:**146-56

Ikegami, T., Matsuzaki, Y., Fukushima, S., Shoda, J., Olivier, J.L., Bouscarel, B., Tanaka, N. 2005. Suppressive effect of ursodeoxycholic acid on type IIA phospholipase A2 expression in HepG2 cells. *Hepatology* **41:**896-905

Ikegami, T., Matsuzaki, Y., Shoda, J., Kano, M., Hirabayashi, N., Tanaka, N. 1998. The chemopreventive role of ursodeoxycholic acid in azoxymethane-treated rats: suppressive effects on enhanced group II phospholipase A2 expression in colonic tissue. *Cancer Lett* **134:**129-39

Im, E., Martinez, J.D. 2004. Ursodeoxycholic acid (UDCA) can inhibit deoxycholic acid (DCA)-induced apoptosis via modulation of EGFR/Raf-1/ERK signaling in human colon cancer cells. *J Nutr* **134:**483-6

Imberti, R., Nieminen, A.L., Herman, B., Lemasters, J.J. 1993. Mitochondrial and glycolytic dysfunction in lethal injury to hepatocytes by t-butylhydroperoxide: protection by fructose, cyclosporin A and trifluoperazine. *J Pharmacol Exp Ther* **265:**392-400

Innes, G.K., Nagafuchi, Y., Fuller, B.J., Hobbs, K.E. 1988. Increased expression of major histocompatibility antigens in the liver as a result of cholestasis. *Transplantation* **45:**749-52

Ishida, T., Kikuchi, Y. 1967. Keto bile acids. Tokyo Tanabe Pharmaceutical Co., Ltd

Ishigaki, S., Fonseca, S.G., Oslowski, C.M., Jurczyk, A., Shearstone, J.R., Zhu, L.J., Permutt, M.A., Greiner, D.L., Bortell, R., Urano, F. 2010. AATF mediates an antiapoptotic effect of the unfolded protein response through transcriptional regulation of AKT1. *Cell Death Differ* **17:**774-86

Iwasaki, T. 1936. Uber die konstitution der urso-desoxycholsaure. *Z Physiol Chem* **244:**181-193

Jankowski, J., Hopwood, D., Pringle, R., Wormsley, K.G. 1993. Increased expression of epidermal growth factor receptors in Barrett's esophagus associated with alkaline reflux: a putative model for carcinogenesis. *Am J Gastroenterol* **88:**402-8

Jankowski, J.A., Anderson, M. 2004. Review article: management of oesophageal adenocarcinoma -- control of acid, bile and inflammation in intervention strategies for Barrett's oesophagus. *Aliment Pharmacol Ther* **20 Suppl 5:**71-80; discussion 95-6

Jazrawi, R.P., de Caestecker, J.S., Goggin, P.M., Britten, A.J., Joseph, A.E., Maxwell, J.D., Northfield, T.C. 1994. Kinetics of hepatic bile acid handling in cholestatic liver disease: effect of ursodeoxycholic acid. *Gastroenterology* **106:**134-42

Jean-Louis, S., Akare, S., Ali, M.A., Mash, E.A., Jr., Meuillet, E., Martinez, J.D. 2006. Deoxycholic acid induces intracellular signaling through membrane perturbations. *J Biol Chem* **281:**14948-60

Jenkins, G., Hardle, L. 2008. Bile Acids: Toxicology and Bioactivity. *In:* Issues in Toxicology. D. Anderson, editor. Royal Society of Chemistry, Cambridge

Jenkins, G.J., D'Souza, F.R., Suzen, S.H., Eltahir, Z.S., James, S.A., Parry, J.M., Griffiths, P.A., Baxter, J.N. 2007. Deoxycholic acid at neutral and acid pH, is genotoxic to oesophageal cells through the induction of ROS: The potential role of anti-oxidants in Barrett's oesophagus. *Carcinogenesis* **28:**136-42

Jenkins, G.J., Harries, K., Doak, S.H., Wilmes, A., Griffiths, A.P., Baxter, J.N., Parry, J.M. 2004. The bile acid deoxycholic acid (DCA) at neutral pH activates NF-kappaB and induces IL-8 expression in oesophageal cells in vitro. *Carcinogenesis* **25:**317-23

Jesch, S.A., Mehta, A.J., Velliste, M., Murphy, R.F., Linstedt, A.D. 2001. Mitotic Golgi is in a dynamic equilibrium between clustered and free vesicles independent of the ER. *Traffic* **2:**873-84

Ji, W.J., Qu, Q., Jin, Y., Zhao, L., He, X.D. 2009. [Ursodeoxycholic acid inhibits hepatocyte-like cell apoptosis by down-regulating the expressions of Bax and Caspase-3]. *Zhonghua Yi Xue Za Zhi* **89:**2997-3001

Kast, H.R., Nguyen, C.M., Sinal, C.J., Jones, S.A., Laffitte, B.A., Reue, K., Gonzalez, F.J., Willson, T.M., Edwards, P.A. 2001. Farnesoid X-activated receptor induces apolipoprotein C-II transcription: a molecular mechanism linking plasma triglyceride levels to bile acids. *Mol Endocrinol* **15:**1720-8

Katona, B.W., Anant, S., Covey, D.F., Stenson, W.F. 2009. Characterization of enantiomeric bile acid-induced apoptosis in colon cancer cell lines. *J Biol Chem* **284:**3354-64

Kauppi, B., Jakob, C., Farnegardh, M., Yang, J., Ahola, H., Alarcon, M., Calles, K., Engstrom, O., Harlan, J., Muchmore, S., Ramqvist, A.K., Thorell, S., Ohman, L., Greer, J., Gustafsson, J.A., Carlstedt-Duke, J., Carlquist, M. 2003. The three-dimensional structures of antagonistic and agonistic forms of the glucocorticoid receptor ligand-binding domain: RU-486 induces a transconformation that leads to active antagonism. *J Biol Chem* **278:**22748-54

Kaur, B.S., Ouatu-Lascar, R., Omary, M.B., Triadafilopoulos, G. 2000. Bile salts induce or blunt cell proliferation in Barrett's esophagus in an acid-dependent fashion. *Am J Physiol Gastrointest Liver Physiol* **278:**G1000-9

Kawamata, Y., Fujii, R., Hosoya, M., Harada, M., Yoshida, H., Miwa, M., Fukusumi, S., Habata, Y., Itoh, T., Shintani, Y., Hinuma, S., Fujisawa, Y., Fujino, M. 2003. A G protein-coupled receptor responsive to bile acids. *J Biol Chem* **278:**9435-40

Kawamura, Y.I., Toyota, M., Kawashima, R., Hagiwara, T., Suzuki, H., Imai, K., Shinomura, Y., Tokino, T., Kannagi, R., Dohi, T. 2008. DNA hypermethylation

contributes to incomplete synthesis of carbohydrate determinants in gastrointestinal cancer. *Gastroenterology* **135:**142-151 e3

Keiding, S., Hockerstedt, K., Bjoro, K., Bondesen, S., Hjortrup, A., Isoniemi, H., Erichsen, C., Soderdahl, G., Ericzon, B.G. 1997. The Nordic multicenter double-blind randomized controlled trial of prophylactic ursodeoxycholic acid in liver transplant patients. *Transplantation* **63:**1591-4

Kellokumpu, S., Sormunen, R., Kellokumpu, I. 2002. Abnormal glycosylation and altered Golgi structure in colorectal cancer: dependence on intra-Golgi pH. *FEBS Lett* **516:**217-24

Khare, S., Mustafi, R., Cerda, S., Yuan, W., Jagadeeswaran, S., Dougherty, U., Tretiakova, M., Samarel, A., Cohen, G., Wang, J., Moore, C., Wali, R., Holgren, C., Joseph, L., Fichera, A., Li, Y.C., Bissonnette, M. 2008. Ursodeoxycholic acid suppresses Cox-2 expression in colon cancer: roles of Ras, p38, and CCAAT/enhancer-binding protein. *Nutr Cancer* **60:**389-400

Khatib, S., Nerya, O., Musa, R., Tamir, S., Peter, T., Vaya, J. 2007. Enhanced substituted resorcinol hydrophobicity augments tyrosinase inhibition potency. *J Med Chem* **50:**2676-81

Kihira, K., Yoshii, M., Okamoto, A., Ikawa, S., Ishii, H., Hoshita, T. 1990. Synthesis of new bile salt analogues, sodium 3 alpha, 7 alpha-dihydroxy-5 beta-cholane-24-sulfonate and sodium 3 alpha, 7 beta-dihydroxy-5 beta-cholane-24-sulfonate. *J Lipid Res* **31:**1323-6

Kim, N.D., Im, E., Yoo, Y.H., Choi, Y.H. 2006. Modulation of the cell cycle and induction of apoptosis in human cancer cells by synthetic bile acids. *Curr Cancer Drug Targets* **6:**681-9

Kisand, K.E., Karvonen, A.L., Vuoristo, M., Farkkila, M., Lehtola, J., Inkovaara, J., Kisand, K.V., Miettinen, T., Krohn, K., Uibo, R. 1996. Ursodeoxycholic acid treatment lowers the serum level of antibodies against pyruvate dehydrogenase and influences their inhibitory capacity for the enzyme complex in patients with primary biliary cirrhosis. *J Mol Med* **74:**269-72

Kitahara, K., Sato, T. 1964. Ursodeoxyholic Acid. Tokyo Tanabe Pharmaceutical Co., Ltd, Japan

Koop, I., Schindler, M., Bosshammer, A., Scheibner, J., Stange, E., Koop, H. 1996. Physiological control of cholecystokinin release and pancreatic enzyme secretion by intraduodenal bile acids. *Gut* **39:**661-7

Koumenis, C., Naczki, C., Koritzinsky, M., Rastani, S., Diehl, A., Sonenberg, N., Koromilas, A., Wouters, B.G. 2002. Regulation of protein synthesis by hypoxia via activation of the endoplasmic reticulum kinase PERK and phosphorylation of the translation initiation factor eIF2alpha. *Mol Cell Biol* **22:**7405-16

Kramer, W., Buscher, H.P., Gerok, W., Kurz, G. 1979. Bile salt binding to serum components. Taurocholate incorporation into high-density lipoprotein revealed by photoaffinity labelling. *Eur J Biochem* **102:**1-9

Kroemer, G., Galluzzi, L., Brenner, C. 2007. Mitochondrial membrane permeabilization in cell death. *Physiol Rev* **87:**99-163

Kucera, T., Waltner-Law, M., Scott, D.K., Prasad, R., Granner, D.K. 2002. A point mutation of the AF2 transactivation domain of the glucocorticoid receptor disrupts its interaction with steroid receptor coactivator 1. *J Biol Chem* **277:**26098-102

Kumar, R., Thompson, E.B. 2005. Gene regulation by the glucocorticoid receptor: structure:function relationship. *J Steroid Biochem Mol Biol* **94:**383-94

Kumar, R., Volk, D.E., Li, J., Lee, J.C., Gorenstein, D.G., Thompson, E.B. 2004. TATA box binding protein induces structure in the recombinant glucocorticoid receptor AF1 domain. *Proc Natl Acad Sci U S A* **101:**16425-30

Ladisch, S., Sweeley, C.C., Becker, H., Gage, D. 1989. Aberrant fatty acyl alpha-hydroxylation in human neuroblastoma tumor gangliosides. *J Biol Chem* **264:**12097-105

Lagorce, C., Paraf, F., Vidaud, D., Couvelard, A., Wendum, D., Martin, A., Flejou, J.F. 2003. Cyclooxygenase-2 is expressed frequently and early in Barrett's oesophagus and associated adenocarcinoma. *Histopathology* **42:**457-65

Lamireau, T., Zoltowska, M., Levy, E., Yousef, I., Rosenbaum, J., Tuchweber, B., Desmouliere, A. 2003. Effects of bile acids on biliary epithelial cells: proliferation, cytotoxicity, and cytokine secretion. *Life Sci* **72:**1401-11

Lane, J.D., Lucocq, J., Pryde, J., Barr, F.A., Woodman, P.G., Allan, V.J., Lowe, M. 2002. Caspase-mediated cleavage of the stacking protein GRASP65 is required for Golgi fragmentation during apoptosis. *J Cell Biol* **156:**495-509

Lapre, J.A., Termont, D.S., Groen, A.K., Van der Meer, R. 1992. Lytic effects of mixed micelles of fatty acids and bile acids. *Am J Physiol* **263:**G333-7

Lazaridis, K.N., Gores Gregory, Lindor K.D. 2001. Ursodeoxycholic Acid mechanisms of action and clinical use in hepatobiliary disorders. *Journal of Hepatology* **35:**134-146

Lee, A.H., Chu, G.C., Iwakoshi, N.N., Glimcher, L.H. 2005. XBP-1 is required for biogenesis of cellular secretory machinery of exocrine glands. *EMBO J* **24:**4368-80

Lee, A.S. 2007. GRP78 induction in cancer: therapeutic and prognostic implications. *Cancer Res* **67:**3496-9

Lee, A.S., Hendershot, L.M. 2006. ER stress and cancer. *Cancer Biol Ther* **5:**721-2

Lefebvre, P., Cariou, B., Lien, F., Kuipers, F., Staels, B. 2009. Role of bile acids and bile acid receptors in metabolic regulation. *Physiol Rev* **89:**147-91

Leuschner, M., Guldutuna, S., You, T., Hubner, K., Bhatti, S., Leuschner, U. 1996. Ursodeoxycholic acid and prednisone versus ursodeoxycholic acid and placebo in the treatment of early stages of primary biliary cirrhosis. *J Hepatol* **25:**49-57

Lewis-Tuffin, L.J., Cidlowski, J.A. 2006. The physiology of human glucocorticoid receptor beta (hGRbeta) and glucocorticoid resistance. *Ann N Y Acad Sci* **1069:**1-9

Lewis-Tuffin, L.J., Jewell, C.M., Bienstock, R.J., Collins, J.B., Cidlowski, J.A. 2007. Human glucocorticoid receptor beta binds RU-486 and is transcriptionally active. *Mol Cell Biol* **27:**2266-82

Lindor, K.D., Therneau, T.M., Jorgensen, R.A., Malinchoc, M., Dickson, E.R. 1996. Effects of ursodeoxycholic acid on survival in patients with primary biliary cirrhosis. *Gastroenterology* **110:**1515-8

Litwack, G. 1988. The glucocorticoid receptor at the protein level. *Cancer Res* **48:**2636-40

Liu, H., Qin, C.K., Han, G.Q., Xu, H.W., Ren, W.H., Qin, C.Y. 2008. Synthetic chenodeoxycholic acid derivative, HS-1200, induces apoptosis of human hepatoma cells via a mitochondrial pathway. *Cancer Lett* **270:**242-9

Livak, K.J., Schmittgen, T.D. 2001. Analysis of relative gene expression data using real-time quantitative PCR and the 2(-Delta Delta C(T)) Method. *Methods* **25:**402-8

Looby, E., Abdel-Latif, M.M., Athie-Morales, V., Duggan, S., Long, A., Kelleher, D. 2009. Deoxycholate induces COX-2 expression via Erk1/2-, p38-MAPK and AP-1-dependent mechanisms in esophageal cancer cells. *BMC Cancer* **9:**190

Lopez, F.J., Ardecky, R.J., Bebo, B., Benbatoul, K., De Grandpre, L., Liu, S., Leibowitz, M.D., Marschke, K., Rosen, J., Rungta, D., Viveros, H.O., Yen, W.C., Zhi, L., Negro-Vilar, A., Miner, J.N. 2008. LGD-5552, an antiinflammatory glucocorticoid receptor ligand with reduced side effects, in vivo. *Endocrinology* **149:**2080-9

Lowe, M., Rabouille, C., Nakamura, N., Watson, R., Jackman, M., Jamsa, E., Rahman, D., Pappin, D.J., Warren, G. 1998. Cdc2 kinase directly phosphorylates the cis-Golgi matrix protein GM130 and is required for Golgi fragmentation in mitosis. *Cell* **94:**783-93

Lu, N.Z., Cidlowski, J.A. 2005. Translational regulatory mechanisms generate N-terminal glucocorticoid receptor isoforms with unique transcriptional target genes. *Mol Cell* **18:**331-42

Lu, N.Z., Cidlowski, J.A. 2006. Glucocorticoid receptor isoforms generate transcription specificity. *Trends Cell Biol* **16:**301-7

Lu, T.T., Makishima, M., Repa, J.J., Schoonjans, K., Kerr, T.A., Auwerx, J., Mangelsdorf, D.J. 2000. Molecular basis for feedback regulation of bile acid synthesis by nuclear receptors. *Mol Cell* **6:**507-15

Ma, K., Saha, P.K., Chan, L., Moore, D.D. 2006. Farnesoid X receptor is essential for normal glucose homeostasis. *J Clin Invest* **116:**1102-9

Maag, R.S., Hicks, S.W., Machamer, C.E. 2003. Death from within: apoptosis and the secretory pathway. *Curr Opin Cell Biol* **15:**456-61

Madauss, K.P., Bledsoe, R.K., McLay, I., Stewart, E.L., Uings, I.J., Weingarten, G., Williams, S.P. 2008. The first X-ray crystal structure of the glucocorticoid receptor bound to a non-steroidal agonist. *Bioorg Med Chem Lett* **18:**6097-9

Maeda, K., Kambara, M., Tian, Y., Hofmann, A.F., Sugiyama, Y. 2006. Uptake of ursodeoxycholate and its conjugates by human hepatocytes: role of Na(+)-taurocholate cotransporting polypeptide (NTCP), organic anion transporting polypeptide (OATP) 1B1 (OATP-C), and oatp1B3 (OATP8). *Mol Pharm* **3:**70-7

Maeda, Y., Naganuma, S., Niina, I., Shinohara, A., Koshimoto, C., Kondo, K., Chijiiwa, K. 2010. Effects of bile acids on rat hepatic microsomal type I 11beta-hydroxysteroid dehydrogenase. *Steroids* **75:**164-8

Magnuson, B.A., Shirtliff, N., Bird, R.P. 1994. Resistance of aberrant crypt foci to apoptosis induced by azoxymethane in rats chronically fed cholic acid. *Carcinogenesis* **15:**1459-62

Maitra, U., Mukhopadhyay, S. 2004. Chemistry and Biology of Bile Acids. *Current Science* **87:**25

Makino, I., Shinozaki, K., Yoshino, K., Nakagawa, S. 1975. [Dissolution of cholesterol gallstones by long-term administration of ursodeoxycholic acid]. *Nippon Shokakibyo Gakkai Zasshi* **72:**690-702

Makishima, M., Okamoto, A.Y., Repa, J.J., Tu, H., Learned, R.M., Luk, A., Hull, M.V., Lustig, K.D., Mangelsdorf, D.J., Shan, B. 1999. Identification of a nuclear receptor for bile acids. *Science* **284:**1362-5

Mancini, M., Machamer, C.E., Roy, S., Nicholson, D.W., Thornberry, N.A., Casciola-Rosen, L.A., Rosen, A. 2000. Caspase-2 is localized at the Golgi complex and cleaves golgin-160 during apoptosis. *J Cell Biol* **149:**603-12

Martinez-Augustin, O., Sanchez de Medina, F. 2008. Intestinal bile acid physiology and pathophysiology. *World J Gastroenterol* **14:**5630-40

Martinez, J.D., Stratagoules, E.D., LaRue, J.M., Powell, A.A., Gause, P.R., Craven, M.T., Payne, C.M., Powell, M.B., Gerner, E.W., Earnest, D.L. 1998. Different bile acids exhibit distinct biological effects: the tumor promoter deoxycholic

acid induces apoptosis and the chemopreventive agent ursodeoxycholic acid inhibits cell proliferation. *Nutr Cancer* **31:**111-8

McCullough, K.D., Martindale, J.L., Klotz, L.O., Aw, T.Y., Holbrook, N.J. 2001. Gadd153 sensitizes cells to endoplasmic reticulum stress by down-regulating Bcl2 and perturbing the cellular redox state. *Mol Cell Biol* **21:**1249-59

McKay, L.I., Cidlowski, J.A. 1998. Cross-talk between nuclear factor-kappa B and the steroid hormone receptors: mechanisms of mutual antagonism. *Mol Endocrinol* **12:**45-56

McMahon, S.B., Monroe, J.G. 1996. The role of early growth response gene 1 (egr-1) in regulation of the immune response. *J Leukoc Biol* **60:**159-66

Mellman, I., Simons, K. 1992. The Golgi complex: in vitro veritas? *Cell* **68:**829-40

Milovic, V., Teller, I.C., Faust, D., Caspary, W.F., Stein, J. 2002. Effects of deoxycholate on human colon cancer cells: apoptosis or proliferation. *Eur J Clin Invest* **32:**29-34

Miura, T., Ouchida, R., Yoshikawa, N., Okamoto, K., Makino, Y., Nakamura, T., Morimoto, C., Makino, I., Tanaka, H. 2001. Functional modulation of the glucocorticoid receptor and suppression of NF-kappaB-dependent transcription by ursodeoxycholic acid. *J Biol Chem* **276:**47371-8

Monte, M.J., Marin, J.J., Antelo, A., Vazquez-Tato, J. 2009. Bile acids: chemistry, physiology, and pathophysiology. *World J Gastroenterol* **15:**804-16

Morris, C.D., Armstrong, G.R., Bigley, G., Green, H., Attwood, S.E. 2001. Cyclooxygenase-2 expression in the Barrett's metaplasia-dysplasia-adenocarcinoma sequence. *Am J Gastroenterol* **96:**990-6

Mukhopadhyay, S., Maitra, U. 2004. Facile synthesis, aggregation behavior, and cholesterol solubilization ability of avicholic acid. *Org Lett* **6:**31-4

Nagengast, F.M., Grubben, M.J., van Munster, I.P. 1995. Role of bile acids in colorectal carcinogenesis. *Eur J Cancer* **31A:**1067-70

Nakagomi, S., Barsoum, M.J., Bossy-Wetzel, E., Sutterlin, C., Malhotra, V., Lipton, S.A. 2008. A Golgi fragmentation pathway in neurodegeneration. *Neurobiol Dis* **29:**221-31

Nakamura, N., Rabouille, C., Watson, R., Nilsson, T., Hui, N., Slusarewicz, P., Kreis, T.E., Warren, G. 1995. Characterization of a cis-Golgi matrix protein, GM130. *J Cell Biol* **131:**1715-26

Nakka, V.P., Gusain, A., Raghubir, R. 2010. Endoplasmic reticulum stress plays critical role in brain damage after cerebral ischemia/reperfusion in rats. *Neurotox Res* **17:**189-202

Narisawa, T., Magadia, N.E., Weisburger, J.H., Wynder, E.L. 1974. Promoting effect of bile acids on colon carcinogenesis after intrarectal instillation of N-methyl-N'-nitro-N-nitrosoguanidine in rats. *J Natl Cancer Inst* **53:**1093-7

Natalini, B., Sardella, R., Camaioni, E., Gioiello, A., Pellicciari, R. 2007. Correlation between CMC and chromatographic index: simple and effective evaluation of the hydrophobic/hydrophilic balance of bile acids. *Anal Bioanal Chem* **388:**1681-8

Necela, B.M., Cidlowski, J.A. 2003. Crystallization of the human glucocorticoid receptor ligand binding domain: a step towards selective glucocorticoids. *Trends Pharmacol Sci* **24:**58-61

Necela, B.M., Cidlowski, J.A. 2004. Mechanisms of glucocorticoid receptor action in noninflammatory and inflammatory cells. *Proc Am Thorac Soc* **1:**239-46

Nehra, D., Howell, P., Pye, J.K., Beynon, J. 1998. Assessment of combined bile acid and pH profiles using an automated sampling device in gastro-oesophageal reflux disease. . *Br. J. Surg* **85:**134-137

Nehra, D., Howell, P., Williams, C.P., Pye, J.K., Beynon, J. 1999. Toxic bile acids in gastro-oesophageal reflux disease: influence of gastric acidity. *Gut* **44:**598-602

Newton, R., Holden, N.S. 2007. Separating transrepression and transactivation: a distressing divorce for the glucocorticoid receptor? *Mol Pharmacol* **72:**799-809

Nishigaki, Y., Ohnishi, H., Moriwaki, H., Muto, Y. 1996. Ursodeoxycholic acid corrects defective natural killer activity by inhibiting prostaglandin E2 production in primary biliary cirrhosis. *Dig Dis Sci* **41:**1487-93

Novac, N., Baus, D., Dostert, A., Heinzel, T. 2006. Competition between glucocorticoid receptor and NFkappaB for control of the human FasL promoter. *FASEB J* **20:**1074-81

Oakley, R.H., Jewell, C.M., Yudt, M.R., Bofetiado, D.M., Cidlowski, J.A. 1999. The dominant negative activity of the human glucocorticoid receptor beta isoform. Specificity and mechanisms of action. *J Biol Chem* **274:**27857-66

Oglodek, E., Augustynska, B., Araszkiewicz, A., Mos, D. 2009. [The bile acids as an example of patogens destructive hepatocytes in alcoholic liver injury]. *Pol Merkur Lekarski* **27:**346-8

Ogryzko, V.V., Schiltz, R.L., Russanova, V., Howard, B.H., Nakatani, Y. 1996. The transcriptional coactivators p300 and CBP are histone acetyltransferases. *Cell* **87:**953-9

Ogundare, M., Theofilopoulos, S., Lockhart, A., Hall, L.J., Arenas, E., Sjovall, J., Brenton, A.G., Wang, Y., Griffiths, W.J. 2010. Cerebrospinal fluid steroidomics: are bioactive bile acids present in brain? *J Biol Chem* **285:**4666-79

Okunade, G.W., Miller, M.L., Azhar, M., Andringa, A., Sanford, L.P., Doetschman, T., Prasad, V., Shull, G.E. 2007. Loss of the Atp2c1 secretory pathway Ca(2+)-ATPase (SPCA1) in mice causes Golgi stress, apoptosis, and midgestational death in homozygous embryos and squamous cell tumors in adult heterozygotes. *J Biol Chem* **282:**26517-27

Onate, S.A., Tsai, S.Y., Tsai, M.J., O'Malley, B.W. 1995. Sequence and characterization of a coactivator for the steroid hormone receptor superfamily. *Science* **270:**1354-7

Onnis, V., Kinsella, G.K., Carta, G., Jagoe, W.N., Price, T., Williams, D.C., Fayne, D., Lloyd, D.G. 2010. Virtual screening for the identification of novel nonsteroidal glucocorticoid modulators. *J Med Chem* **53:**3065-74

Ota, S., Tsukahara, H., Terano, A., Hata, Y., Hiraishi, H., Mutoh, H., Sugimoto, T. 1991. Protective effect of tauroursodeoxycholate against chenodeoxycholate-induced damage to cultured rabbit gastric cells. *Dig Dis Sci* **36:**409-16

Ozanne, B.W., McGarry, L., Spence, H.J., Johnston, I., Winnie, J., Meagher, L., Stapleton, G. 2000. Transcriptional regulation of cell invasion: AP-1 regulation of a multigenic invasion programme. *Eur J Cancer* **36:**1640-8

Pageaux, G.P., Blanc, P., Perrigault, P.F., Navarro, F., Fabre, J.M., Souche, B., Domergue, J., Larrey, D., Michel, H. 1995. Failure of ursodeoxycholic acid to prevent acute cellular rejection after liver transplantation. *J Hepatol* **23:**119-22

Pahl, H.L., Baeuerle, P.A. 1997. The ER-overload response: activation of NF-kappa B. *Trends Biochem Sci* **22:**63-7

Paolini, M., Pozzetti, L., Montagnani, M., Potenza, G., Sabatini, L., Antelli, A., Cantelli-Forti, G., Roda, A. 2002. Ursodeoxycholic acid (UDCA) prevents DCA effects on male mouse liver via up-regulation of CYP [correction of CXP] and preservation of BSEP activities. *Hepatology* **36:**305-14

Pardi, D.S., Loftus, E.V., Jr., Kremers, W.K., Keach, J., Lindor, K.D. 2003. Ursodeoxycholic acid as a chemopreventive agent in patients with ulcerative colitis and primary sclerosing cholangitis. *Gastroenterology* **124:**889-93

Pariante, C.M., Pearce, B.D., Pisell, T.L., Owens, M.J., Miller, A.H. 1997. Steroid-independent translocation of the glucocorticoid receptor by the antidepressant desipramine. *Mol Pharmacol* **52:**571-81

Pariante, C.M., Pearce, B.D., Pisell, T.L., Su, C., Miller, A.H. 2001. The steroid receptor antagonists RU40555 and RU486 activate glucocorticoid receptor translocation and are not excreted by the steroid hormones transporter in L929 cells. *J Endocrinol* **169:**309-20

Parks, D.J., Blanchard, S.G., Bledsoe, R.K., Chandra, G., Consler, T.G., Kliewer, S.A., Stimmel, J.B., Willson, T.M., Zavacki, A.M., Moore, D.D., Lehmann, J.M. 1999. Bile acids: natural ligands for an orphan nuclear receptor. *Science* **284:**1365-8

Patel T, B.S., Gores GJ. 1994. Increases of intracellular magnesium promote glycodeoxycholate-induced apoptosis in rat hepatocytes. *J Clin Invest* **94:**2183-2192

Paumgartner, G. 2006. Medical treatment of cholestatic liver diseases: From pathobiology to pharmacological targets. *World J Gastroenterol* **12:**4445-51

Pellicciari, R., Costantino, G., Camaioni, E., Sadeghpour, B.M., Entrena, A., Willson, T.M., Fiorucci, S., Clerici, C., Gioiello, A. 2004. Bile acid derivatives as ligands of the farnesoid X receptor. Synthesis, evaluation, and structure-activity relationship of a series of body and side chain modified analogues of chenodeoxycholic acid. *J Med Chem* **47:**4559-69

Pellicciari, R., Costantino, G., Fiorucci, S. 2005. Farnesoid X receptor: from structure to potential clinical applications. *J Med Chem* **48:**5383-403

Pellicciari, R., Sato, H., Gioiello, A., Costantino, G., Macchiarulo, A., Sadeghpour, B.M., Giorgi, G., Schoonjans, K., Auwerx, J. 2007. Nongenomic actions of bile acids. Synthesis and preliminary characterization of 23- and 6,23-alkyl-substituted bile acid derivatives as selective modulators for the G-protein coupled receptor TGR5. *J Med Chem* **50:**4265-8

Peracaula, R., Tabares, G., Lopez-Ferrer, A., Brossmer, R., de Bolos, C., de Llorens, R. 2005. Role of sialyltransferases involved in the biosynthesis of Lewis antigens in human pancreatic tumour cells. *Glycoconj J* **22:**135-44

Perez, M.J., Briz, O. 2009. Bile-acid-induced cell injury and protection. *World J Gastroenterol* **15:**1677-89

Perretti, M., D'Acquisto, F. 2009. Annexin A1 and glucocorticoids as effectors of the resolution of inflammation. *Nat Rev Immunol* **9:**62-70

Petrini, M., Pelosi-Testa, E., Sposi, N.M., Mastroberardino, G., Camagna, A., Bottero, L., Mavilio, F., Testa, U., Peschle, C. 1989. Constitutive expression and abnormal glycosylation of transferrin receptor in acute T-cell leukemia. *Cancer Res* **49:**6989-96

Pinho, S., Marcos, N.T., Ferreira, B., Carvalho, A.S., Oliveira, M.J., Santos-Silva, F., Harduin-Lepers, A., Reis, C.A. 2007. Biological significance of cancer-associated sialyl-Tn antigen: modulation of malignant phenotype in gastric carcinoma cells. *Cancer Lett* **249:**157-70

Plevin, M.J., Mills, M.M., Ikura, M. 2005. The LxxLL motif: a multifunctional binding sequence in transcriptional regulation. *Trends Biochem Sci* **30:**66-9

Posa, M., Kuhajda, K. 2010. Hydrophobicity and haemolytic potential of oxo derivatives of cholic, deoxycholic and chenodeoxycholic acids. *Steroids*

Poupon, R., Poupon, R.E. 1995. Ursodeoxycholic acid therapy of chronic cholestatic conditions in adults and children. *Pharmacol Ther* **66:**1-15

Poupon, R.E., Balkau, B., Eschwege, E., Poupon, R. 1991. A multicenter, controlled trial of ursodiol for the treatment of primary biliary cirrhosis. UDCA-PBC Study Group. *N Engl J Med* **324:**1548-54

Poupon, R.E., Huet, P.M., Poupon, R., Bonnand, A.M., Nhieu, J.T., Zafrani, E.S. 1996. A randomized trial comparing colchicine and ursodeoxycholic acid combination to ursodeoxycholic acid in primary biliary cirrhosis. UDCA-PBC Study Group. *Hepatology* **24:**1098-103

Poupon, R.E., Poupon, R., Balkau, B. 1994. Ursodiol for the long-term treatment of primary biliary cirrhosis. The UDCA-PBC Study Group. *N Engl J Med* **330:**1342-7

Powell, A.A., LaRue, J.M., Batta, A.K., Martinez, J.D. 2001. Bile acid hydrophobicity is correlated with induction of apoptosis and/or growth arrest in HCT116 cells. *Biochem J* **356:**481-6

Presul, E., Schmidt, S., Kofler, R., Helmberg, A. 2007. Identification, tissue expression, and glucocorticoid responsiveness of alternative first exons of the human glucocorticoid receptor. *J Mol Endocrinol* **38:**79-90

Pusl, T., Vennegeerts, T., Wimmer, R., Denk, G.U., Beuers, U., Rust, C. 2008. Tauroursodeoxycholic acid reduces bile acid-induced apoptosis by modulation of AP-1. *Biochem Biophys Res Commun* **367:**208-12

Pyrko, P., Kardosh, A., Liu, Y.T., Soriano, N., Xiong, W., Chow, R.H., Uddin, J., Petasis, N.A., Mircheff, A.K., Farley, R.A., Louie, S.G., Chen, T.C., Schonthal, A.H. 2007. Calcium-activated endoplasmic reticulum stress as a major component of tumor cell death induced by 2,5-dimethyl-celecoxib, a non-coxib analogue of celecoxib. *Mol Cancer Ther* **6:**1262-75

Qiao, D., Chen, W., Stratagoules, E.D., Martinez, J.D. 2000. Bile acid-induced activation of activator protein-1 requires both extracellular signal-regulated kinase and protein kinase C signaling. *J Biol Chem* **275:**15090-8

Qiao, D., Im, E., Qi, W., Martinez, J.D. 2002. Activator protein-1 and CCAAT/enhancer-binding protein mediated GADD153 expression is involved in deoxycholic acid-induced apoptosis. *Biochim Biophys Acta* **1583:**108-16

Qiao, D., Stratagouleas, E.D., Martinez, J.D. 2001a. Activation and role of mitogen-activated protein kinases in deoxycholic acid-induced apoptosis. *Carcinogenesis* **22:**35-41

Qiao, L., Studer, E., Leach, K., McKinstry, R., Gupta, S., Decker, R., Kukreja, R., Valerie, K., Nagarkatti, P., El Deiry, W., Molkentin, J., Schmidt-Ullrich, R., Fisher, P.B., Grant, S., Hylemon, P.B., Dent, P. 2001b. Deoxycholic acid (DCA) causes ligand-independent activation of epidermal growth factor receptor (EGFR) and FAS receptor in primary hepatocytes: inhibition of EGFR/mitogen-activated protein kinase-signaling module enhances DCA-induced apoptosis. *Mol Biol Cell* **12:**2629-45

Quist, R.G., Ton-Nu, H.T., Lillienau, J., Hofmann, A.F., Barrett, K.E. 1991. Activation of mast cells by bile acids. *Gastroenterology* **101:**446-56

Ranganathan, A.C., Zhang, L., Adam, A.P., Aguirre-Ghiso, J.A. 2006. Functional coupling of p38-induced up-regulation of BiP and activation of RNA-dependent protein kinase-like endoplasmic reticulum kinase to drug resistance of dormant carcinoma cells. *Cancer Res* **66:**1702-11

Rao, Y.P., Stravitz, R.T., Vlahcevic, Z.R., Gurley, E.C., Sando, J.J., Hylemon, P.B. 1997. Activation of protein kinase C alpha and delta by bile acids: correlation with bile acid structure and diacylglycerol formation. *J Lipid Res* **38:**2446-54

Raufman, J.P., Shant, J., Guo, C.Y., Roy, S., Cheng, K. 2008. Deoxycholyltaurine rescues human colon cancer cells from apoptosis by activating EGFR-dependent PI3K/Akt signaling. *J Cell Physiol* **215:**538-49

Raveh-Amit, H., Maissel, A., Poller, J., Marom, L., Elroy-Stein, O., Shapira, M., Livneh, E. 2009. Translational control of protein kinase Ceta by two upstream open reading frames. *Mol Cell Biol* **29:**6140-8

Ray, D.W., Suen, C.S., Brass, A., Soden, J., White, A. 1999. Structure/function of the human glucocorticoid receptor: tyrosine 735 is important for transactivation. *Mol Endocrinol* **13:**1855-63

Reddy, B.S., Watanabe, K., Weisburger, J.H., Wynder, E.L. 1977. Promoting effect of bile acids in colon carcinogenesis in germ-free and conventional F344 rats. *Cancer Res* **37:**3238-42

Reddy, R.K., Mao, C., Baumeister, P., Austin, R.C., Kaufman, R.J., Lee, A.S. 2003. Endoplasmic reticulum chaperone protein GRP78 protects cells from apoptosis induced by topoisomerase inhibitors: role of ATP binding site in suppression of caspase-7 activation. *J Biol Chem* **278:**20915-24

Regan, J., Lee, T.W., Zindell, R.M., Bekkali, Y., Bentzien, J., Gilmore, T., Hammach, A., Kirrane, T.M., Kukulka, A.J., Kuzmich, D., Nelson, R.M., Proudfoot, J.R., Ralph, M., Pelletier, J., Souza, D., Zuvela-Jelaska, L., Nabozny, G., Thomson, D.S. 2006. Quinol-4-ones as steroid A-ring mimetics in nonsteroidal dissociated glucocorticoid agonists. *J Med Chem* **49:**7887-96

Reichardt, H.M., Kaestner, K.H., Tuckermann, J., Kretz, O., Wessely, O., Bock, R., Gass, P., Schmid, W., Herrlich, P., Angel, P., Schutz, G. 1998. DNA binding of the glucocorticoid receptor is not essential for survival. *Cell* **93:**531-41

Reichardt, H.M., Tuckermann, J.P., Gottlicher, M., Vujic, M., Weih, F., Angel, P., Herrlich, P., Schutz, G. 2001. Repression of inflammatory responses in the absence of DNA binding by the glucocorticoid receptor. *EMBO J* **20:**7168-73

Reinehr, R., Becker, S., Eberle, A., Grether-Beck, S., Haussinger, D. 2005. Involvement of NADPH oxidase isoforms and Src family kinases in CD95-dependent hepatocyte apoptosis. *J Biol Chem* **280:**27179-94

Reker, C.E., LaPointe, M.C., Kovacic-Milivojevic, B., Chiou, W.J., Vedeckis, W.V. 1987. A possible role for dephosphorylation in glucocorticoid receptor transformation. *J Steroid Biochem* **26:**653-65

Renaud, J.P., Moras, D. 2000. Structural studies on nuclear receptors. *Cell Mol Life Sci* **57:**1748-69

Revollo, J.R., Cidlowski, J.A. 2009. Mechanisms generating diversity in glucocorticoid receptor signaling. *Ann N Y Acad Sci* **1179:**167-78

Rieger, A.M., Hall, B.E., Luong, L.T., Schang, L.M., Barreda, D.R. 2010. Conventional apoptosis assays using propidium iodide generate a significant number of false positives that prevent accurate assessment of cell death. *J Immunol Methods*

Rivinoja, A., Kokkonen, N., Kellokumpu, I., Kellokumpu, S. 2006. Elevated Golgi pH in breast and colorectal cancer cells correlates with the expression of oncofetal carbohydrate T-antigen. *J Cell Physiol* **208:**167-74

Roda, A., Fini, A. 1984. Effect of nuclear hydroxy substituents on aqueous solubility and acidic strength of bile acids. *Hepatology* **4:**72S-76S

Roda, A., Hofmann, A.F., Mysels, K.J. 1983. The influence of bile salt structure on self-association in aqueous solutions. *J Biol Chem* **258:**6362-70

Roda, A., Minutello, A., Angellotti, M.A., Fini, A. 1990. Bile acid structure-activity relationship: evaluation of bile acid lipophilicity using 1-octanol/water partition coefficient and reverse phase HPLC. *J Lipid Res* **31:**1433-43

Roda, A., Pellicciari, R., Cerre, C., Polimeni, C., Sadeghpour, B., Marinozzi, M., Forti, G.C., Sapigni, E. 1994. New 6-substituted bile acids: physico-chemical and biological properties of 6 alpha-methyl ursodeoxycholic acid and 6 alpha-methyl-7-epicholic acid. *J Lipid Res* **35:**2268-79

Rodrigues, C.M., Ma, X., Linehan-Stieers, C., Fan, G., Kren, B.T., Steer, C.J. 1999. Ursodeoxycholic acid prevents cytochrome c release in apoptosis by inhibiting mitochondrial membrane depolarization and channel formation. *Cell Death Differ* **6:**842-54

Rodrigues CMP, F.G., Wong PY, Kren BT, Steer CJ. . 1998. Ursodeoxycholic acid may inhibit deoxycholic acid-induced apoptosis by modulating mitochondrial transmembrane potential and reactive
oxygen species production. . *Mol Med* **4:**165-178

Rolo, A.P., Oliveira, P.J., Moreno, A.J., Palmeira, C.M. 2000. Bile acids affect liver mitochondrial bioenergetics: possible relevance for cholestasis therapy. *Toxicol Sci* **57:**177-85

Ronacher, K., Hadley, K., Avenant, C., Stubsrud, E., Simons, S.S., Jr., Louw, A., Hapgood, J.P. 2009. Ligand-selective transactivation and transrepression via the glucocorticoid receptor: role of cofactor interaction. *Mol Cell Endocrinol* **299:**219-31

Rosen, J., Miner, J.N. 2005. The search for safer glucocorticoid receptor ligands. *Endocr Rev* **26:**452-64

Rosenfeld, M.G., Glass, C.K. 2001. Coregulator codes of transcriptional regulation by nuclear receptors. *J Biol Chem* **276:**36865-8

Rubin, R.A., Kowalski, T.E., Khandelwal, M., Malet, P.F. 1994. Ursodiol for hepatobiliary disorders. *Ann Intern Med* **121:**207-18

Rudolph, G., Endele, R., Senn, M., Stiehl, A. 1993. Effect of ursodeoxycholic acid on the kinetics of cholic acid and chenodeoxycholic acid in patients with primary sclerosing cholangitis. *Hepatology* **17:**1028-32

Russell, D.W. 2003. The enzymes, regulation, and genetics of bile acid synthesis. *Annu Rev Biochem* **72:**137-74

Sambrook, J., Russel, D.W. 2001. Molecular Cloning: a laboratory manual. Cold Spring Harbour Laboratory Press, New York

Sarbu, C., Kuhajda, K., Kevresan, S. 2001. Evaluation of the lipophilicity of bile acids and their derivatives by thin-layer chromatography and principal component analysis. *J Chromatogr A* **917:**361-6

Sarbu, C., Onisor, C., Posa, M., Kevresan, S., Kuhajda, K. 2008. Modeling and prediction (correction) of partition coefficients of bile acids and their derivatives by multivariate regression methods. *Talanta* **75:**651-7

Sarkar, A., Kellogg, G.E. 2010. Hydrophobicity--shake flasks, protein folding and drug discovery. *Curr Top Med Chem* **10:**67-83

Sato, H., Macchiarulo, A., Thomas, C., Gioiello, A., Une, M., Hofmann, A.F., Saladin, R., Schoonjans, K., Pellicciari, R., Auwerx, J. 2008. Novel potent and selective bile acid derivatives as TGR5 agonists: biological screening, structure-activity relationships, and molecular modeling studies. *J Med Chem* **51:**1831-41

Scaffidi, C., Fulda, S., Srinivasan, A., Friesen, C., Li, F., Tomaselli, K.J., Debatin, K.M., Krammer, P.H., Peter, M.E. 1998. Two CD95 (APO-1/Fas) signaling pathways. *EMBO J* **17:**1675-87

Schaaf, M.J., Cidlowski, J.A. 2002. Molecular mechanisms of glucocorticoid action and resistance. *J Steroid Biochem Mol Biol* **83:**37-48

Schaffner, F., Bacchin, P.G., Hutterer, F., Scharnbeck, H.H., Sarkozi, L.L., Denk, H., Popper, H. 1971. Mechanism of cholestasis. 4. Structural and biochemical changes in the liver and serum in rats after bile duct ligation. *Gastroenterology* **60:**888-97

Schiffelers, R.M., Metselaar, J.M., Fens, M.H., Janssen, A.P., Molema, G., Storm, G. 2005. Liposome-encapsulated prednisolone phosphate inhibits growth of established tumors in mice. *Neoplasia* **7:**118-27

Schliess, F., Kurz, A.K., vom Dahl, S., Haussinger, D. 1997. Mitogen-activated protein kinases mediate the stimulation of bile acid secretion by tauroursodeoxycholate in rat liver. *Gastroenterology* **113:**1306-14

Schoch, G.A., D'Arcy, B., Stihle, M., Burger, D., Bar, D., Benz, J., Thoma, R., Ruf, A. 2010. Molecular switch in the glucocorticoid receptor: active and passive antagonist conformations. *J Mol Biol* **395:**568-77

Schteingart, C.D., Hofmann, A.F. 1988. Synthesis of 24-nor-5 beta-cholan-23-oic acid derivatives: a convenient and efficient one-carbon degradation of the side chain of natural bile acids. *J Lipid Res* **29:**1387-95

Schubert, R., Schmidt, K.H. 1988. Structural changes in vesicle membranes and mixed micelles of various lipid compositions after binding of different bile salts. *Biochemistry* **27:**8787-94

Schule, R., Rangarajan, P., Kliewer, S., Ransone, L.J., Bolado, J., Yang, N., Verma, I.M., Evans, R.M. 1990. Functional antagonism between oncoprotein c-Jun and the glucocorticoid receptor. *Cell* **62:**1217-26

Scott, D.W., Mutamba, S., Hopkins, R.G., Loo, G. 2005. Increased GADD gene expression in human colon epithelial cells exposed to deoxycholate. *J Cell Physiol* **202:**295-303

Scotti, E., Gilardi, F., Godio, C., Gers, E., Krneta, J., Mitro, N., De Fabiani, E., Caruso, D., Crestani, M. 2007. Bile acids and their signaling pathways: eclectic regulators of diverse cellular functions. *Cell Mol Life Sci* **64:**2477-91

Sequeira, S.J., Wen, H.C., Avivar-Valderas, A., Farias, E.F., Aguirre-Ghiso, J.A. 2009. Inhibition of eIF2alpha dephosphorylation inhibits ErbB2-induced deregulation of mammary acinar morphogenesis. *BMC Cell Biol* **10:**64

Serfaty, L., De Leusse, A., Rosmorduc, O., Desaint, B., Flejou, J.F., Chazouilleres, O., Poupon, R.E., Poupon, R. 2003. Ursodeoxycholic acid therapy and the risk of

colorectal adenoma in patients with primary biliary cirrhosis: an observational study. *Hepatology* **38:**203-9

Setchell, K.D., Rodrigues, C.M., Clerici, C., Solinas, A., Morelli, A., Gartung, C., Boyer, J. 1997. Bile acid concentrations in human and rat liver tissue and in hepatocyte nuclei. *Gastroenterology* **112:**226-35

Shah, S.A., Looby, E., Volkov, Y., Long, A., Kelleher, D. 2005. Ursodeoxycholic acid inhibits translocation of protein kinase C in human colonic cancer cell lines. *Eur J Cancer* **41:**2160-9

Shah, S.A., Mahmud, N., Mftah, M., Roche, H.M., Kelleher, D. 2006a. Chronic but not acute conjugated linoleic acid treatment inhibits deoxycholic acid-induced protein kinase C and nuclear factor-kappaB activation in human colorectal cancer cells. *Eur J Cancer Prev* **15:**125-33

Shah, S.A., Volkov, Y., Arfin, Q., Abdel-Latif, M.M., Kelleher, D. 2006b. Ursodeoxycholic acid inhibits interleukin 1 beta [corrected] and deoxycholic acid-induced activation of NF-kappaB and AP-1 in human colon cancer cells. *Int J Cancer* **118:**532-9

Shima, D.T., Haldar, K., Pepperkok, R., Watson, R., Warren, G. 1997. Partitioning of the Golgi apparatus during mitosis in living HeLa cells. *J Cell Biol* **137:**1211-28

Shoda, M. 1927. Uber die ursodesoxycholsaure aus barengallen und ihre physiologische wirkung. *J Biochem* **7:**505-517

Shorter, J., Warren, G. 1999. A role for the vesicle tethering protein, p115, in the post-mitotic stacking of reassembling Golgi cisternae in a cell-free system. *J Cell Biol* **146:**57-70

Shorter, J., Warren, G. 2002. Golgi architecture and inheritance. *Annu Rev Cell Dev Biol* **18:**379-420

Shorter, J., Watson, R., Giannakou, M.E., Clarke, M., Warren, G., Barr, F.A. 1999. GRASP55, a second mammalian GRASP protein involved in the stacking of Golgi cisternae in a cell-free system. *EMBO J* **18:**4949-60

Silva, R.F., Rodrigues, C.M., Brites, D. 2001. Bilirubin-induced apoptosis in cultured rat neural cells is aggravated by chenodeoxycholic acid but prevented by ursodeoxycholic acid. *J Hepatol* **34:**402-8

Sinal, C.J., Tohkin, M., Miyata, M., Ward, J.M., Lambert, G., Gonzalez, F.J. 2000. Targeted disruption of the nuclear receptor FXR/BAR impairs bile acid and lipid homeostasis. *Cell* **102:**731-44

Sinko, P.J., Singh, Y. 2006. Martin's Physical Pharmacy and Pharmaceutical Sciences. Lippincott Williams & Wilkins, a Wolters Kluwer, Philadelphia

Small, D.M. 1971. *In:* The Bile acids: Chemistry, Physiology and Metabolism. P.P. Nair and D. Kritchevsky, editors. pp. 249-356. Plenum Press, New York

Snopek, J., Smolkova-Keulemansova, E., Jelinek, I., Dohnal, J., Klinot, J., Klinotova, E. 1988. Use of cyclodextrins in isotachophoresis. VI. Cyclodextrins as leading electrolyte additives for the separation of bile acids. *J Chromatogr* **450:**373-9

Sodeman, T., Bronk, S.F., Roberts, P.J., Miyoshi, H., Gores, G.J. 2000. Bile salts mediate hepatocyte apoptosis by increasing cell surface trafficking of Fas. *Am J Physiol Gastrointest Liver Physiol* **278:**G992-9

Sokol, R.J., Dahl, R., Devereaux, M.W., Yerushalmi, B., Kobak, G.E., Gumpricht, E. 2005. Human hepatic mitochondria generate reactive oxygen species and undergo the permeability transition in response to hydrophobic bile acids. *J Pediatr Gastroenterol Nutr* **41:**235-43

Sokol, R.J., Devereaux, M., Khandwala, R., O'Brien, K. 1993. Evidence for involvement of oxygen free radicals in bile acid toxicity to isolated rat hepatocytes. *Hepatology* **17:**869-81

Sokol, R.J., Devereaux, M., Khandwala, R.A. 1991. Effect of dietary lipid and vitamin E on mitochondrial lipid peroxidation and hepatic injury in the bile duct-ligated rat. *J Lipid Res* **32:**1349-57

Sokol, R.J., McKim, J.M., Jr., Goff, M.C., Ruyle, S.Z., Devereaux, M.W., Han, D., Packer, L., Everson, G. 1998. Vitamin E reduces oxidant injury to mitochondria and the hepatotoxicity of taurochenodeoxycholic acid in the rat. *Gastroenterology* **114:**164-74

Sola, S., Amaral, J.D., Aranha, M.M., Steer, C.J., Rodrigues, C.M. 2006. Modulation of hepatocyte apoptosis: cross-talk between bile acids and nuclear steroid receptors. *Curr Med Chem* **13:**3039-51

Sola, S., Amaral, J.D., Castro, R.E., Ramalho, R.M., Borralho, P.M., Kren, B.T., Tanaka, H., Steer, C.J., Rodrigues, C.M. 2005. Nuclear translocation of UDCA by the glucocorticoid receptor is required to reduce TGF-beta1-induced apoptosis in rat hepatocytes. *Hepatology* **42:**925-34

Sola, S., Castro, R.E., Kren, B.T., Steer, C.J., Rodrigues, C.M. 2004. Modulation of nuclear steroid receptors by ursodeoxycholic acid inhibits TGF-beta1-induced E2F-1/p53-mediated apoptosis of rat hepatocytes. *Biochemistry* **43:**8429-38

Solito, E., Mulla, A., Morris, J.F., Christian, H.C., Flower, R.J., Buckingham, J.C. 2003. Dexamethasone induces rapid serine-phosphorylation and membrane translocation of annexin 1 in a human folliculostellate cell line via a novel nongenomic mechanism involving the glucocorticoid receptor, protein kinase C, phosphatidylinositol 3-kinase, and mitogen-activated protein kinase. *Endocrinology* **144:**1164-74

Soltoff, S.P. 2007. Rottlerin: an inappropriate and ineffective inhibitor of PKCdelta. *Trends Pharmacol Sci* **28:**453-8

Span, L.F., Pennings, A.H., Vierwinden, G., Boezeman, J.B., Raymakers, R.A., de Witte, T. 2002. The dynamic process of apoptosis analyzed by flow cytometry using Annexin-V/propidium iodide and a modified in situ end labeling technique. *Cytometry* **47:**24-31

Spivey, J.R., Bronk, S.F., Gores, G.J. 1993. Glycochenodeoxycholate-induced lethal hepatocellular injury in rat hepatocytes. Role of ATP depletion and cytosolic free calcium. *J Clin Invest* **92:**17-24

Stadler, J., Stern, H.S., Yeung, K.S., McGuire, V., Furrer, R., Marcon, N., Bruce, W.R. 1988. Effect of high fat consumption on cell proliferation activity of colorectal mucosa and on soluble faecal bile acids. *Gut* **29:**1326-31

Stahn, C., Lowenberg, M., Hommes, D.W., Buttgereit, F. 2007. Molecular mechanisms of glucocorticoid action and selective glucocorticoid receptor agonists. *Mol Cell Endocrinol* **275:**71-8

Stauffer, A.T., Rochat, M.K., Dick, B., Frey, F.J., Odermatt, A. 2002. Chenodeoxycholic acid and deoxycholic acid inhibit 11 beta-hydroxysteroid dehydrogenase type 2 and cause cortisol-induced transcriptional activation of the mineralocorticoid receptor. *J Biol Chem* **277:**26286-92

Stein, H.J., Kauer, W.K.D., Feussner, H., Siewert, J.R. 1998. Bile reflux in benign and malignant Barrett's esophagus: effect of medical acid suppression and nissen fundoplication. *J. Gastrointest. Surg.* **2:**333-341

Steller, H. 1995. Mechanisms and genes of cellular suicide. *Science* **267:**1445-9

Stevens, A., Garside, H., Berry, A., Waters, C., White, A., Ray, D. 2003. Dissociation of steroid receptor coactivator 1 and nuclear receptor corepressor recruitment to the human glucocorticoid receptor by modification of the ligand-receptor interface: the role of tyrosine 735. *Mol Endocrinol* **17:**845-59

Stieber, A., Gonatas, J.O., Moore, J.S., Bantly, A., Yim, H.S., Yim, M.B., Gonatas, N.K. 2004. Disruption of the structure of the Golgi apparatus and the function of the secretory pathway by mutants G93A and G85R of Cu, Zn superoxide dismutase (SOD1) of familial amyotrophic lateral sclerosis. *J Neurol Sci* **219:**45-53

Stiehl, A., Benz, C., Sauer, P. 1999. Mechanism of hepatoprotective action of bile salts in liver disease. *Gastroenterol Clin North Am* **28:**195-209, viii

Strupp, W., Weidinger, G., Scheller, C., Ehret, R., Ohnimus, H., Girschick, H., Tas, P., Flory, E., Heinkelein, M., Jassoy, C. 2000. Treatment of cells with detergent activates caspases and induces apoptotic cell death. *J Membr Biol* **175:**181-9

Suino-Powell, K., Xu, Y., Zhang, C., Tao, Y.G., Tolbert, W.D., Simons, S.S., Jr., Xu, H.E. 2008. Doubling the size of the glucocorticoid receptor ligand binding pocket by deacylcortivazol. *Mol Cell Biol* **28:**1915-23

Sun, K.H., de Pablo, Y., Vincent, F., Johnson, E.O., Chavers, A.K., Shah, K. 2008. Novel genetic tools reveal Cdk5's major role in Golgi fragmentation in Alzheimer's disease. *Mol Biol Cell* **19:**3052-69

Tamaki, N., Hatano, E., Taura, K., Tada, M., Kodama, Y., Nitta, T., Iwaisako, K., Seo, S., Nakajima, A., Ikai, I., Uemoto, S. 2008. CHOP deficiency attenuates cholestasis-induced liver fibrosis by reduction of hepatocyte injury. *Am J Physiol Gastrointest Liver Physiol* **294:**G498-505

Tanaka, H., Makino, I. 1992. Ursodeoxycholic acid-dependent activation of the glucocorticoid receptor. *Biochem Biophys Res Commun* **188:**942-8

Tanaka, H., Makino, Y., Miura, T., Hirano, F., Okamoto, K., Komura, K., Sato, Y., Makino, I. 1996. Ligand-independent activation of the glucocorticoid receptor by ursodeoxycholic acid. Repression of IFN-gamma-induced MHC class II gene expression via a glucocorticoid receptor-dependent pathway. *J Immunol* **156:**1601-8

Tao, Y., Williams-Skipp, C., Scheinman, R.I. 2001. Mapping of glucocorticoid receptor DNA binding domain surfaces contributing to transrepression of NF-kappa B and induction of apoptosis. *J Biol Chem* **276:**2329-32

Terasaki, S., Nakanuma, Y., Ogino, H., Unoura, M., Kobayashi, K. 1991. Hepatocellular and biliary expression of HLA antigens in primary biliary cirrhosis before and after ursodeoxycholic acid therapy. *Am J Gastroenterol* **86:**1194-9

Thompson, M.B. 1996. Bile acids in the assessment of hepatocellular function. *Toxicol Pathol* **24:**62-71

Tint, G.S., Salen, G., Colalillo, A., Graber, D., Verga, D., Speck, J., Shefer, S. 1982. Ursodeoxycholic acid: a safe and effective agent for dissolving cholesterol gallstones. *Ann Intern Med* **97:**351-6

Tong, J.L., Ran, Z.H., Shen, J., Fan, G.Q., Xiao, S.D. 2008. Association between fecal bile acids and colorectal cancer: a meta-analysis of observational studies. *Yonsei Med J* **49:**792-803

Trauner, M., Graziadei, I.W. 1999. Review article: mechanisms of action and therapeutic applications of ursodeoxycholic acid in chronic liver diseases. *Aliment Pharmacol Ther* **13:**979-96

Triadafilopoulos, G. 2001. Acid and bile reflux in Barrett's esophagus: a tale of two evils. *Gastroenterology* **121:**1502-6

Tsuchiya, S., Tsuji, M., Morio, Y., Oguchi, K. 2006. Involvement of endoplasmic reticulum in glycochenodeoxycholic acid-induced apoptosis in rat hepatocytes. *Toxicol Lett* **166:**140-9

Tsujii, M., DuBois, R.N. 1995. Alterations in cellular adhesion and apoptosis in epithelial cells overexpressing prostaglandin endoperoxide synthase 2. *Cell* **83:**493-501

Tsujii, M., Kawano, S., DuBois, R.N. 1997. Cyclooxygenase-2 expression in human colon cancer cells increases metastatic potential. *Proc Natl Acad Sci U S A* **94:**3336-40

Tsujii, M., Kawano, S., Tsuji, S., Sawaoka, H., Hori, M., DuBois, R.N. 1998. Cyclooxygenase regulates angiogenesis induced by colon cancer cells. *Cell* **93:**705-16

Tung, B.Y., Emond, M.J., Haggitt, R.C., Bronner, M.P., Kimmey, M.B., Kowdley, K.V., Brentnall, T.A. 2001. Ursodiol use is associated with lower prevalence of colonic neoplasia in patients with ulcerative colitis and primary sclerosing cholangitis. *Ann Intern Med* **134:**89-95

Turner, J.D., Schote, A.B., Macedo, J.A., Pelascini, L.P., Muller, C.P. 2006. Tissue specific glucocorticoid receptor expression, a role for alternative first exon usage? *Biochem Pharmacol* **72:**1529-37

Ueno, M. 1997. *In:* Structure Performance Relationships in Surfactants. K. Esumi and M. Ueno, editors. pp. 147. Marcel and Dekker

Vaezi, M.F., Singh, S., Richter, J.E. 1995. Role of acid and duodenogastric reflux in esophageal mucosal injury: a review of animal and human studies. *Gastroenterology* **108:**1897-907

van der Laan, S., Meijer, O.C. 2008. Pharmacology of glucocorticoids: beyond receptors. *Eur J Pharmacol* **585:**483-91

Varki, A., Cummings, R., Esko, J., Freeze, H., Hart, G., Marth, J. 1999. Essentials of glycobiology. Cold Spring Harbor Laboratory Press, Cold Spring Harbor, New York

Vatmurge, N.S., Hazra, B.G., Pore, V.S., Shirazi, F., Chavan, P.S., Deshpande, M.V. 2008. Synthesis and antimicrobial activity of beta-lactam-bile acid conjugates linked via triazole. *Bioorg Med Chem Lett* **18:**2043-7

Vayssiere, B.M., Dupont, S., Choquart, A., Petit, F., Garcia, T., Marchandeau, C., Gronemeyer, H., Resche-Rigon, M. 1997. Synthetic glucocorticoids that dissociate transactivation and AP-1 transrepression exhibit antiinflammatory activity in vivo. *Mol Endocrinol* **11:**1245-55

Vermes, I., Haanen, C., Reutelingsperger, C. 2000. Flow cytometry of apoptotic cell death. *J Immunol Methods* **243:**167-90

Virrey, J.J., Dong, D., Stiles, C., Patterson, J.B., Pen, L., Ni, M., Schonthal, A.H., Chen, T.C., Hofman, F.M., Lee, A.S. 2008. Stress chaperone GRP78/BiP confers

chemoresistance to tumor-associated endothelial cells. *Mol Cancer Res* **6:**1268-75

Vlahcevic, Z.R., Eggertsen, G., Bjorkhem, I., Hylemon, P.B., Redford, K., Pandak, W.M. 2000. Regulation of sterol 12alpha-hydroxylase and cholic acid biosynthesis in the rat. *Gastroenterology* **118:**599-607

Vlahcevic, Z.R., Gurley, E.C., Heuman, D.M., Hylemon, P.B. 1990. Bile salts in submicellar concentrations promote bidirectional cholesterol transfer (exchange) as a function of their hydrophobicity. *J Lipid Res* **31:**1063-71

Vyvoda, O.S., Coleman, R., Holdsworth, G. 1977. Effects of different bile salts upon the composition and morphology of a liver plasma membrane preparation. Deoxycholate is more membrane damaging than cholate and its conjugates. *Biochim Biophys Acta* **465:**68-76

Wang, H., Chen, J., Hollister, K., Sowers, L.C., Forman, B.M. 1999. Endogenous bile acids are ligands for the nuclear receptor FXR/BAR. *Mol Cell* **3:**543-53

Wang, J.C., Shah, N., Pantoja, C., Meijsing, S.H., Ho, J.D., Scanlan, T.S., Yamamoto, K.R. 2006. Novel arylpyrazole compounds selectively modulate glucocorticoid receptor regulatory activity. *Genes Dev* **20:**689-99

Wang, Q., Blackford, J.A., Jr., Song, L.N., Huang, Y., Cho, S., Simons, S.S., Jr. 2004. Equilibrium interactions of corepressors and coactivators with agonist and antagonist complexes of glucocorticoid receptors. *Mol Endocrinol* **18:**1376-95

Ward, A., Brogden, R.N., Heel, R.C., Speight, T.M., Avery, G.S. 1984. Ursodeoxycholic acid: a review of its pharmacological properties and therapeutic efficacy. *Drugs* **27:**95-131

Waris, G., Tardif, K.D., Siddiqui, A. 2002. Endoplasmic reticulum (ER) stress: hepatitis C virus induces an ER-nucleus signal transduction pathway and activates NF-kappaB and STAT-3. *Biochem Pharmacol* **64:**1425-30

Weigel, N.L., Zhang, Y. 1998. Ligand-independent activation of steroid hormone receptors. *J Mol Med* **76:**469-79

Weitzel, C., Stark, D., Kullmann, F., Scholmerich, J., Holstege, A., Falk, W. 2005. Ursodeoxycholic acid induced activation of the glucocorticoid receptor in primary rat hepatocytes. *Eur J Gastroenterol Hepatol* **17:**169-77

Wiedmann, T.S., Kamel, L. 2002. *J. Pharm. Sci* **91:**1743

Wieland, S., Schatt, M.D., Rusconi, S. 1990. Role of TATA-element in transcription from glucocorticoid receptor-responsive model promoters. *Nucleic Acids Res* **18:**5113-8

Williams, D., Lemke, T.L. 2002. Foye's Priciples of Medicinal Chemistry. Lippincott Williams & Wilkins, Philadelphia

Wlodkowic, D., Skommer, J., McGuinness, D., Hillier, C., Darzynkiewicz, Z. 2009. ER-Golgi network--a future target for anti-cancer therapy. *Leuk Res* **33:**1440-7

Wlodkowic, D., Skommer, J., Pelkonen, J. 2007. Brefeldin A triggers apoptosis associated with mitochondrial breach and enhances HA14-1- and anti-Fas-mediated cell killing in follicular lymphoma cells. *Leuk Res* **31:**1687-700

Wrange, O., Eriksson, P., Perlmann, T. 1989. The purified activated glucocorticoid receptor is a homodimer. *J Biol Chem* **264:**5253-9

Wu, J., Kaufman, R.J. 2006. From acute ER stress to physiological roles of the Unfolded Protein Response. *Cell Death Differ* **13:**374-84

Wu, J., Li, Y., Dietz, J., Lala, D.S. 2004. Repression of p65 transcriptional activation by the glucocorticoid receptor in the absence of receptor-coactivator interactions. *Mol Endocrinol* **18:**53-62

Wu, Y.M., Nowack, D., Omenn, G., Haab, B. 2009. Mucin glycosylation is altered by pro-inflammatory signaling in pancreatic-cancer cells. *J Proteome Res*

Xiao, H.Y., Wu, D.R., Malley, M.F., Gougoutas, J.Z., Habte, S.F., Cunningham, M.D., Somerville, J.E., Dodd, J.H., Barrish, J.C., Nadler, S.G., Dhar, T.G. 2010. Novel synthesis of the hexahydroimidazo[1,5b]isoquinoline scaffold: application to the synthesis of glucocorticoid receptor modulators. *J Med Chem* **53:**1270-80

Xu, H.E., Stanley, T.B., Montana, V.G., Lambert, M.H., Shearer, B.G., Cobb, J.E., McKee, D.D., Galardi, C.M., Plunket, K.D., Nolte, R.T., Parks, D.J., Moore, J.T., Kliewer, S.A., Willson, T.M., Stimmel, J.B. 2002. Structural basis for antagonist-mediated recruitment of nuclear co-repressors by PPARalpha. *Nature* **415:**813-7

Yamaguchi, H., Wang, H.G. 2004. CHOP is involved in endoplasmic reticulum stress-induced apoptosis by enhancing DR5 expression in human carcinoma cells. *J Biol Chem* **279:**45495-502

Yamaguchi, J., Toledo, A., Bass, B.L., Celeste, F.A., Rao, J.N., Wang, J.Y., Strauch, E.D. 2004. Taurodeoxycholate increases intestinal epithelial cell proliferation through c-myc expression. *Surgery* **135:**215-21

Yang-Yen, H.F., Chambard, J.C., Sun, Y.L., Smeal, T., Schmidt, T.J., Drouin, J., Karin, M. 1990. Transcriptional interference between c-Jun and the glucocorticoid receptor: mutual inhibition of DNA binding due to direct protein-protein interaction. *Cell* **62:**1205-15

Yasukawa, K., Iida, T., Fujimoto, Y. 2009. Relative inhibitory activity of bile acids against 12-O-tetradecanoylphorbol-13-acetate-induced inflammation, and chenodeoxycholic acid inhibition of tumour promotion in mouse skin two-stage carcinogenesis. *J Pharm Pharmacol* **61:**1051-6

Yin, X.M., Ding, W.X. 2003. Death receptor activation-induced hepatocyte apoptosis and liver injury. *Curr Mol Med* **3:**491-508

Yoshikawa, M., Tsujii, T., Matsumura, K., Yamao, J., Matsumura, Y., Kubo, R., Fukui, H., Ishizaka, S. 1992. Immunomodulatory effects of ursodeoxycholic acid on immune responses. *Hepatology* **16:**358-64

Yudt, M.R., Cidlowski, J.A. 2002. The glucocorticoid receptor: coding a diversity of proteins and responses through a single gene. *Mol Endocrinol* **16:**1719-26

Yui, S., Kanamoto, R., Saeki, T. 2009. Biphasic regulation of cell death and survival by hydrophobic bile acids in HCT116 cells. *Nutr Cancer* **61:**374-80

Yui, S., Saeki, T., Kanamoto, R., Iwami, K. 2005. Characteristics of apoptosis in HCT116 colon cancer cells induced by deoxycholic acid. *J Biochem* **138:**151-7

Zaal, K.J., Smith, C.L., Polishchuk, R.S., Altan, N., Cole, N.B., Ellenberg, J., Hirschberg, K., Presley, J.F., Roberts, T.H., Siggia, E., Phair, R.D., Lippincott-Schwartz, J. 1999. Golgi membranes are absorbed into and reemerge from the ER during mitosis. *Cell* **99:**589-601

Zanchi, N.E., Filho, M.A., Felitti, V., Nicastro, H., Lorenzeti, F.M., Lancha, A.H., Jr. 2010. Glucocorticoids: Extensive physiological actions modulated through multiple mechanisms of gene regulation. *J Cell Physiol*

Zhang, F., Subbaramaiah, K., Altorki, N., Dannenberg, A.J. 1998. Dihydroxy bile acids activate the transcription of cyclooxygenase-2. *J Biol Chem* **273:**2424-8

Zhang, R., Gong, J., Wang, H., Wang, L. 2005. Bile salts inhibit growth and induce apoptosis of human esophageal cancer cell line. *World J Gastroenterol* **11:**5109-16

Zhang, S., Jonklaas, J., Danielsen, M. 2007. The glucocorticoid agonist activities of mifepristone (RU486) and progesterone are dependent on glucocorticoid receptor levels but not on EC50 values. *Steroids* **72:**600-8

Zheng, H.C., Takahashi, H., Li, X.H., Hara, T., Masuda, S., Guan, Y.F., Takano, Y. 2008. Overexpression of GRP78 and GRP94 are markers for aggressive behavior and poor prognosis in gastric carcinomas. *Hum Pathol* **39:**1042-9

Zock, J.M. 2009. Applications of high content screening in life science research. *Comb Chem High Throughput Screen* **12:**870-76

APPENDICES

Appendix 1-Reagents and Antibodies

Table of Reagents

Reagent	Source
DCA	Sigma-Aldrich, Chemical Co, St. Louis, MO, USA
UDCA	Sigma-Aldrich, Chemical Co, St. Louis, MO, USA
CDCA	Sigma-Aldrich, Chemical Co, St. Louis, MO, USA
CA	Sigma-Aldrich, Chemical Co, St. Louis, MO, USA
TDCA	Sigma-Aldrich, Chemical Co, St. Louis, MO, USA
TCDCA	Sigma-Aldrich, Chemical Co, St. Louis, MO, USA
TUDCA	Sigma-Aldrich, Chemical Co, St. Louis, MO, USA
TCA	Sigma-Aldrich, Chemical Co, St. Louis, MO, USA
GDCA	Sigma-Aldrich, Chemical Co, St. Louis, MO, USA
GCDCA	Sigma-Aldrich, Chemical Co, St. Louis, MO, USA
GUDCA	Sigma-Aldrich, Chemical Co, St. Louis, MO, USA
GCA	Sigma-Aldrich, Chemical Co, St. Louis, MO, USA
LCA	Sigma-Aldrich, Chemical Co, St. Louis, MO, USA
Dehydrocholic acid	Sigma-Aldrich, Chemical Co, St. Louis, MO, USA
Dimethylsulphoxide(DMSO)	Sigma-Aldrich, Chemical Co, St. Louis, MO, USA
Methanol	Sigma-Aldrich, Chemical Co, St. Louis, MO, USA
Ammonium acetate	Sigma-Aldrich, Chemical Co, St. Louis, MO, USA
Acetic acid	Sigma-Aldrich, Chemical Co, St. Louis, MO, USA
Hanks Balance Salt solution	Sigma-Aldrich, Chemical Co, St. Louis, MO, USA
Trypsin	GIBCO, Invitrogen Ltd., Paisley, UK
Soya Bean Trypsin Inhibitor	Sigma-Aldrich, Chemical Co, St. Louis, MO, USA
Fetal Calf Serum	GIBCO, Invitrogen Ltd., Paisley, UK
PBS	Lonza Group Ltd, Switzerland
PBS Tablets	Lonza Group Ltd, Switzerland
MTT reagent	Sigma-Aldrich, Chemical Co, St. Louis, MO, USA
Propidium iodide	Sigma-Aldrich, Chemical Co, St. Louis, MO, USA
Triton-X	Sigma-Aldrich, Chemical Co, St. Louis, MO, USA
Hoechst 33342	Invitrogen, Carlsbad, CA, USA
Hoechst 33258	Invitrogen, Carlsbad, CA, USA
Paraformaldehyde	Sigma-Aldrich, Chemical Co, St. Louis, MO, USA
BSA	Sigma-Aldrich, Chemical Co, St. Louis, MO, USA
Phalloidin-TRITC	Sigma-Aldrich, Chemical Co, St. Louis, MO, USA
Brefeldin A	Sigma-Aldrich, Chemical Co, St. Louis, MO, USA

Luria Bertani broth powder	Sigma-Aldrich, Chemical Co, St. Louis, MO, USA
Ampicillin	Sigma-Aldrich, Chemical Co, St. Louis, MO, USA
Isopropanol	Sigma-Aldrich, Chemical Co, St. Louis, MO, USA
Lipofectamine	Invitrogen, Carlsbad, CA, USA
Fugene HD	Roche Diagnostics GmBH, Mannheim, Germany
OptiMem	GIBCO, Invitrogen Ltd., Paisley, UK
ONPG	Sigma-Aldrich, Chemical Co, St. Louis, MO, USA
Sodium Phosphate	Sigma-Aldrich, Chemical Co, St. Louis, MO, USA
Sodium carbonate	Sigma-Aldrich, Chemical Co, St. Louis, MO, USA
Hydrochloric acid	Sigma-Aldrich, Chemical Co, St. Louis, MO, USA
Sulphuric acid	Sigma-Aldrich, Chemical Co, St. Louis, MO, USA
Sodium hydroxide	Sigma-Aldrich, Chemical Co, St. Louis, MO, USA
B-mercaptoethanol	Sigma-Aldrich, Chemical Co, St. Louis, MO, USA
Ethanol	Sigma-Aldrich, Chemical Co, St. Louis, MO, USA
Benzylbromide	Sigma-Aldrich, Chemical Co, St. Louis, MO, USA
Cesium carbonate	Sigma-Aldrich, Chemical Co, St. Louis, MO, USA
N,N-dimethylformamide	Sigma-Aldrich, Chemical Co, St. Louis, MO, USA
Acetylchloride	Sigma-Aldrich, Chemical Co, St. Louis, MO, USA
Magnesium sulphate	Sigma-Aldrich, Chemical Co, St. Louis, MO, USA
Sodiumbicarbonate	Sigma-Aldrich, Chemical Co, St. Louis, MO, USA
Dichloromethane	Hazardous Materials facility,TCD
Acetic anhydride	Sigma-Aldrich, Chemical Co, St. Louis, MO, USA
Pyridine	Sigma-Aldrich, Chemical Co, St. Louis, MO, USA
Hexane	Hazardous Materials facility,TCD
Ethylacetate	Hazardous Materials facility,TCD
Methane sulfonylchloride	Sigma-Aldrich, Chemical Co, St. Louis, MO, USA
Sodium azide	Sigma-Aldrich, Chemical Co, St. Louis, MO, USA
Pyridinium chlorochromate	Sigma-Aldrich, Chemical Co, St. Louis, MO, USA
Diethylether	Hazardous Materials facility,TCD
Palladium on carbon	Sigma-Aldrich, Chemical Co, St. Louis, MO, USA
Formic acid	Sigma-Aldrich, Chemical Co, St. Louis, MO, USA
Perchloric acid	Sigma-Aldrich, Chemical Co, St. Louis, MO, USA
Trifluoroacetic acid	Sigma-Aldrich, Chemical Co, St. Louis, MO, USA
Sodium nitrite	Sigma-Aldrich, Chemical Co, St. Louis, MO, USA
Sodium	Sigma-Aldrich, Chemical Co, St. Louis, MO, USA
Potassium hydroxide	Sigma-Aldrich, Chemical Co, St. Louis, MO, USA
Sodium chloride	Sigma-Aldrich, Chemical Co, St. Louis, MO, USA

Trifluoroacetic anhydride	Sigma-Aldrich, Chemical Co, St. Louis, MO, USA
Thionyl chloride	Sigma-Aldrich, Chemical Co, St. Louis, MO, USA
Lithium aluminium hydride	Sigma-Aldrich, Chemical Co, St. Louis, MO, USA
Cyclopropylamine	Sigma-Aldrich, Chemical Co, St. Louis, MO, USA
Triethylamine	Sigma-Aldrich, Chemical Co, St. Louis, MO, USA
Diphenylamine	Sigma-Aldrich, Chemical Co, St. Louis, MO, USA
Phenethylamine	Sigma-Aldrich, Chemical Co, St. Louis, MO, USA
Aniline	Sigma-Aldrich, Chemical Co, St. Louis, MO, USA
Alphamethylbenzylamine	Sigma-Aldrich, Chemical Co, St. Louis, MO, USA
Benzylamine	Sigma-Aldrich, Chemical Co, St. Louis, MO, USA
Phenpropylamine	Sigma-Aldrich, Chemical Co, St. Louis, MO, USA
Morpholine	Sigma-Aldrich, Chemical Co, St. Louis, MO, USA
2-iodoaniline	Sigma-Aldrich, Chemical Co, St. Louis, MO, USA
1-BOC piperazine	Sigma-Aldrich, Chemical Co, St. Louis, MO, USA
Benzylpiperazine	Sigma-Aldrich, Chemical Co, St. Louis, MO, USA
Salubrinal	Calbiochem, Merck Chemicals Ltd. Nottingham, UK
Dexamethasone	Sigma-Aldrich, Chemical Co, St. Louis, MO, USA
Cycloheximide	Calbiochem, Merck Chemicals Ltd. Nottingham, UK
5-chloromethylfluorescein diacetate	Invitrogen, Carlsbad, CA, USA
TNF-α	R&D Systems, Minneapolis, USA

Table of Antibodies

Purified rabbit anti-human GM130 Polyclonal Antibody	Sigma-Aldrich, Chemical Co, St. Louis, MO, USA
Purified mouse anti-human Glucocorticoid receptor Antibody	BD Biosciences, San Jose, California, USA
Goat anti-rabbit Ig-G antibody Alexa Fluor 488	Molecular Probes, Invitrogen, Carlsbad, CA, USA
Goat anti-mouse Ig-G antibody Alexa Fluor 488	Molecular Probes, Invitrogen, Carlsbad, CA, USA
Goat anti-rabbit Ig-G antibody Alexa Fluor 568	Molecular Probes, Invitrogen, Carlsbad, CA, USA
Goat anti-mouse Ig-G antibody Alexa Fluor 568	Molecular Probes, Invitrogen, Carlsbad, CA, USA

Table of Primers

ABI Code	Official Symbol	Alias
Hs00358796_m1	DDIT3	CHOP
Hs02856596_m1	XBP-1	
Hs99999174_m1	HSPA5	Bip/Grp78
Hs00231069_m1	ATF3	
Hs99999905_m1	GAPDH	

Staining Solutions and Buffers

Vanillin Solution

Vanillin	6 g
Conc. H_2SO_4	1.5 ml
Acetic Acid	3.5 ml
Ethanol	95 ml

Phopshate-Buffered saline PBS 1x

PBS tablets (0.14 M NaCl, 0.01 M PO_4 Buffer, 0.003 M KCl) 5 g

Each 5 g tablet should be dissolved in 500 ml dissolved in 500 ml distilled water and sterilised by autoclaving.

BCA reagent A (Proprietary formulation)

Sodium carbonate, sodium bicarbonate, bicinchoninic acid and sodium tartrate in 0.1 M sodium hydroxide.

BCA reagent B

4% cupric sulphate

Blocking Buffer

Bovine Serum Albumin (BSA)	1.5 g
1× PBS	50 ml

Plasmid Purification Buffers

Buffer P1 (resuspension buffer)

50 mM Tris-Cl, 10 mM EDTA, 100 µg/ml RNase A.

Stored at 2-8 ºC

Buffer P2 (Lysis buffer)

200 mM NaOH, 1% SDS (w/v)

Buffer P3 (neutralisation buffer)

3 M potassium acetate, pH 5.5

Buffer QC (wash buffer)

1M NaCl, 50 mM MOPS, pH 7, 15% isopropanol

Buffer QF (elution buffer)

1.25 M NaCl, 50 mM Tris-Cl, pH 8.5, 15% isopropanol

Beta-gal Assay buffers

Magnesium Buffer

0.1 M $MgCl_2$

4.5 M β-mercaptoethanol

Sodium Phosphate Buffer

0.2 M Na_2HPO_4	41 ml
0.2 M NaH_2PO_4	9 ml
Water	50 ml

ONPG Solution

ONPG	200 mg
0.1 M Sodium phosphate buffer	50 ml

RNA Extraction Buffers

Macherey-Nagel Proprietary Buffers

Addresses of Other Suppliers

Macherey-Nagel GmBH & Co. KG, Düren, Germany

Merck, Darmstadt, Germany

Chemical Computing Group, Montreal, Canada

Nunclon, Roskilde, Denmark

Molecular Devices, Sunnyvale, CA, USA

Promega Corporation, Madison, USA

Qiagen Inc., Valencia, CA, USA

R&D Systems, Minneapolis, USA

SABiosciences Corporation, Executive Way, Frederick, USA

New England Biolabs, Ipswich, MA, USA

Pierce Biotechnology, Meridian Rd, Rockford, USA

Thermofisher Scientific, Waltham, USA

Applied Biosystems, Foster City, CA

Corning B.V. Life Sciences, Fogostraat, Amsterdam, The Netherlands

Clontech, Saint-Germain-en-Laye, France

Appendix 2-Numbering of Compounds

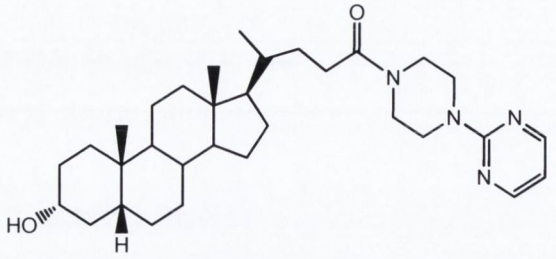

1 LCA piperazinylcarboxamide

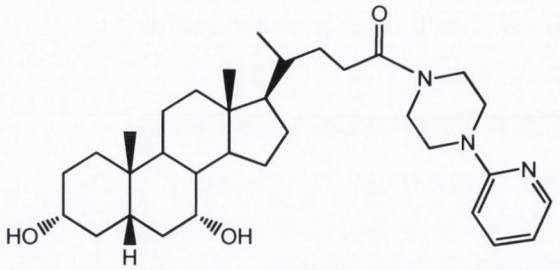

2 CDCA piperazinylcarboxamide

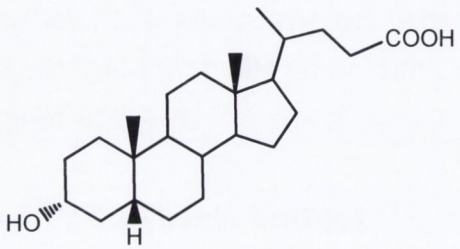

3 LCA

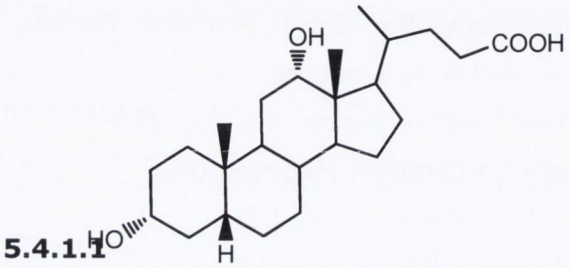

5.4.1.1

4 DCA

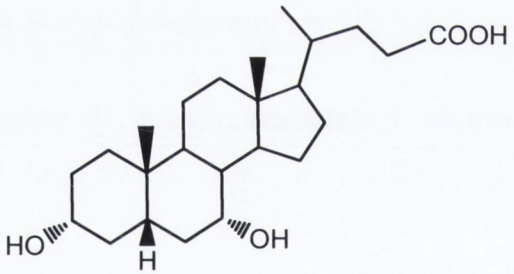

5 CDCA

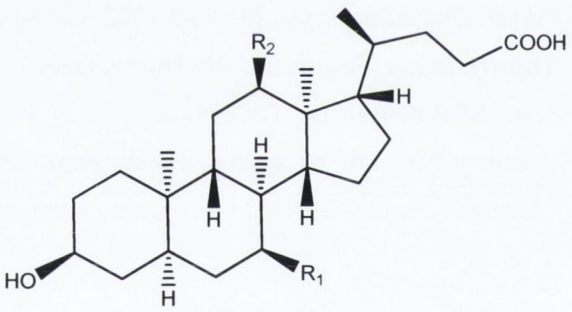

6 ent-LCA R1=H R2=H
7 ent-DCA R1=H R2=OH
8 ent-CDCA R1=OH R2=H

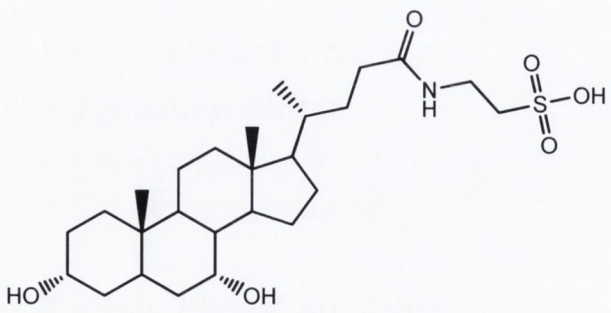

9 TCDCA

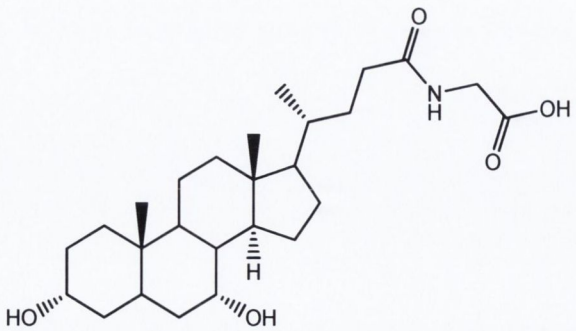

10 GCDCA

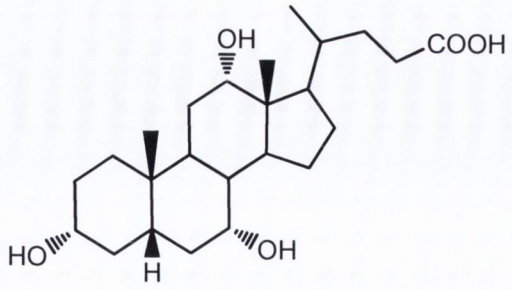

11 Cholic acid

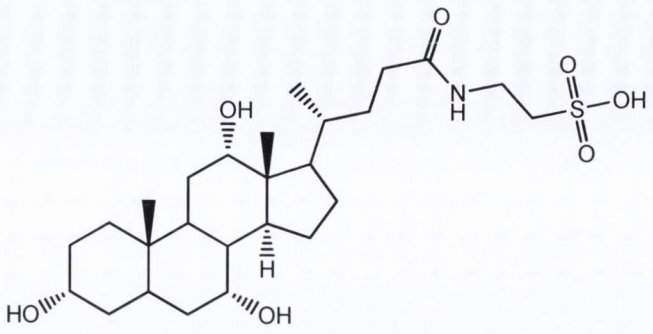

12 TCA

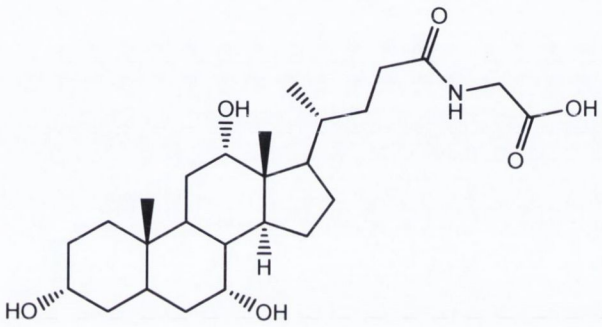

13 GCA

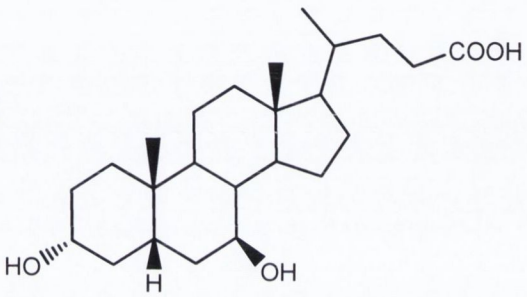

14 UDCA

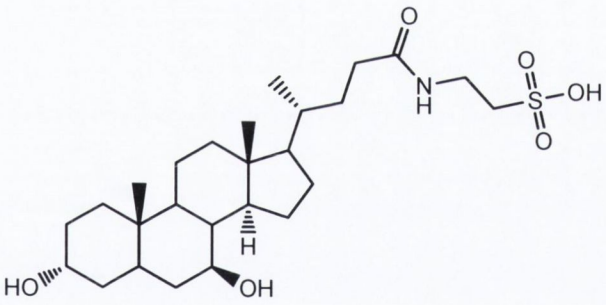

15 TUDCA

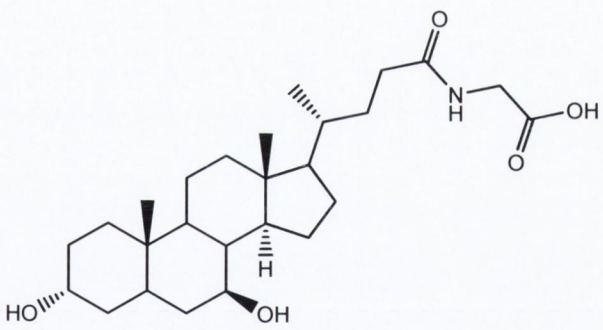

16 GUDCA

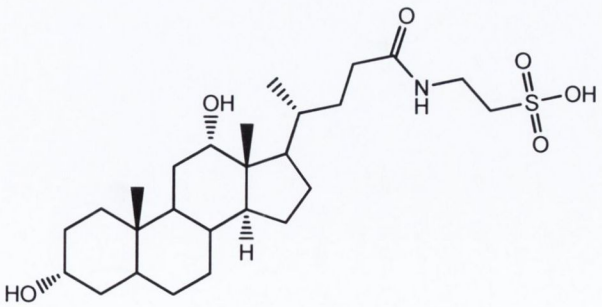

17 TDCA

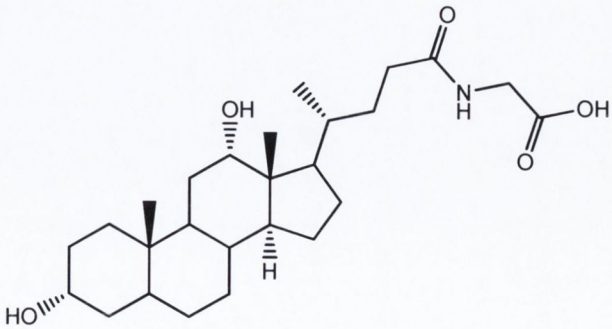

18 GDCA

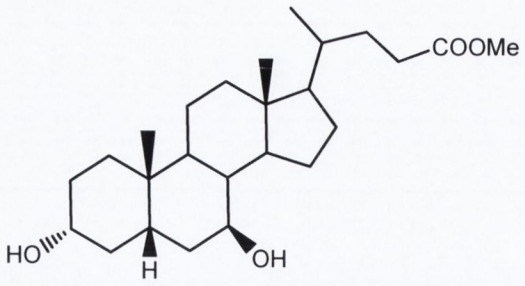

19 MeUDCA

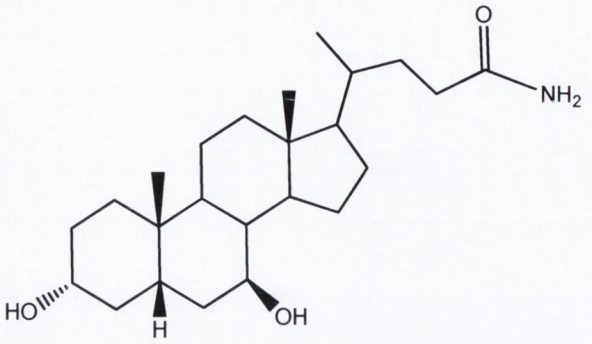

20 UDCA Amide

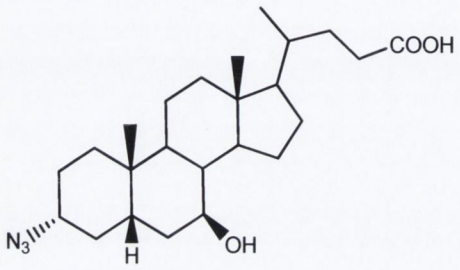

21 3α UDCA Azide

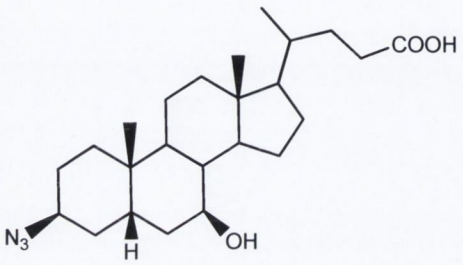

22 3β UDCA Azide

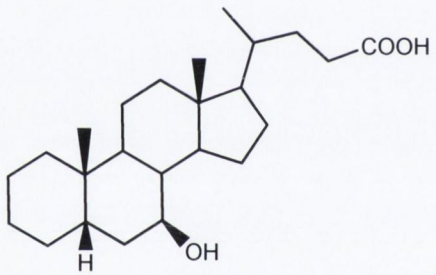

23 3-deoxy UDCA

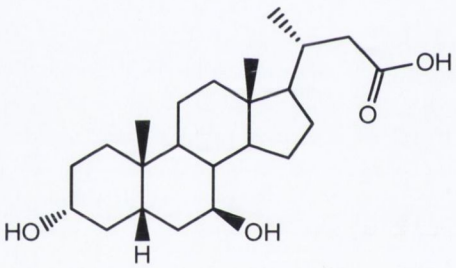

24 norUDCA

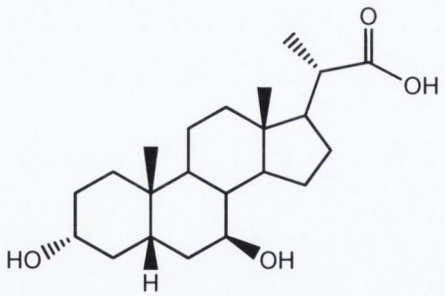

25 BisnorUDCA

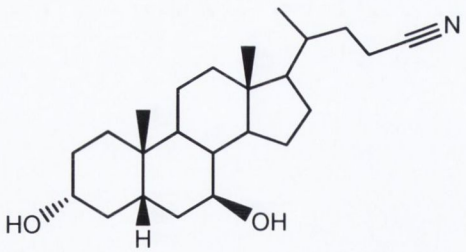

26 nitrile

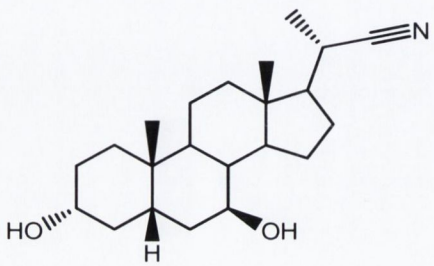

27 Bisnornitrile

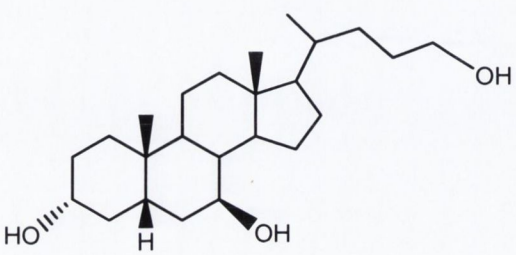

28 UDCA alcohol

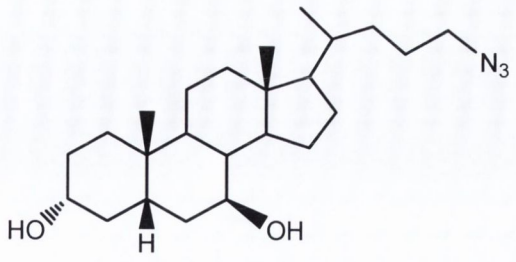

29 24-Azide

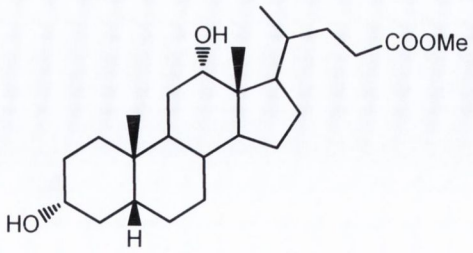

30 MeDCA

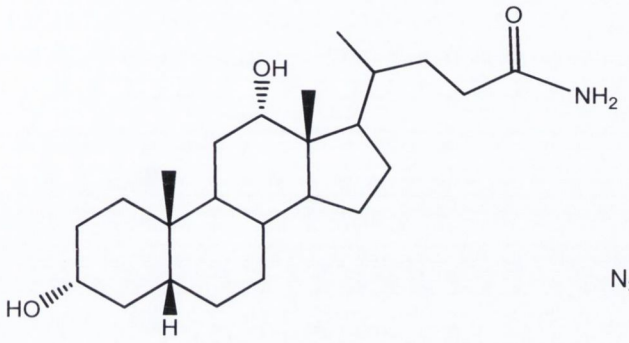

31 DCA Amide

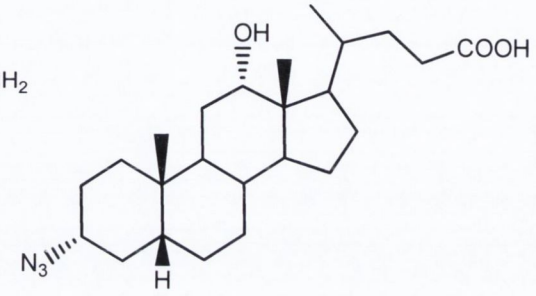

32 3α DCA Azide

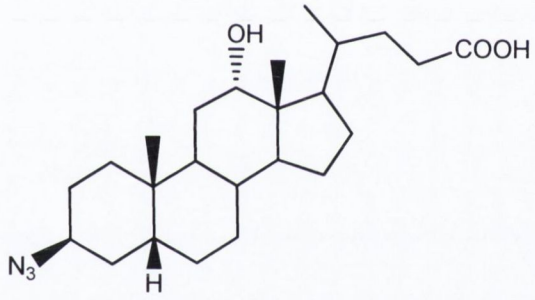

33 3β DCA Azide

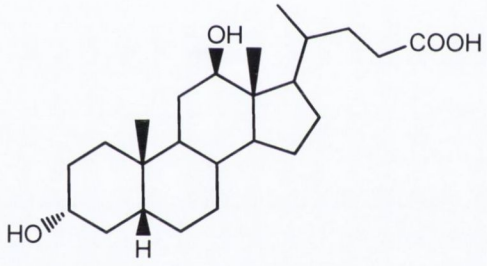

34 LagoDCA

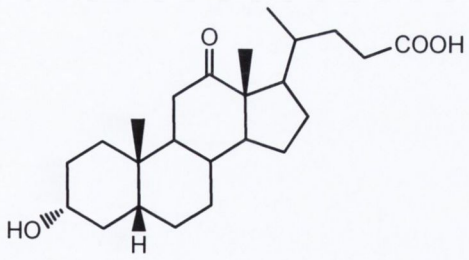

35 12 keto LCA

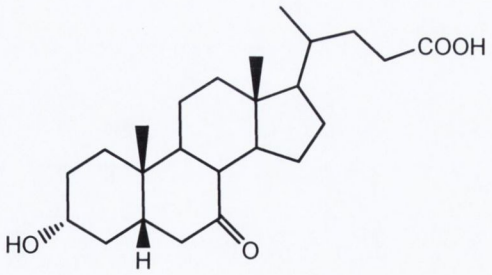

36 NCA

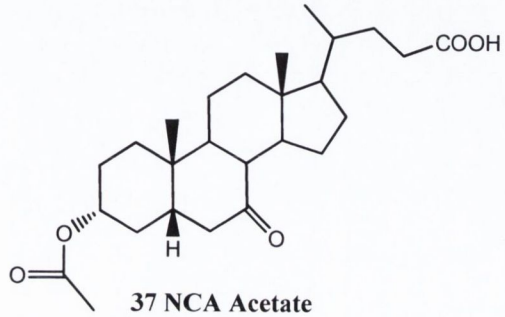

37 NCA Acetate

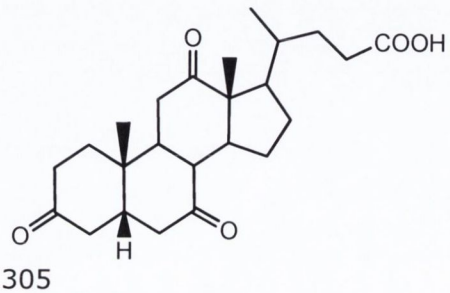

38 Triketone

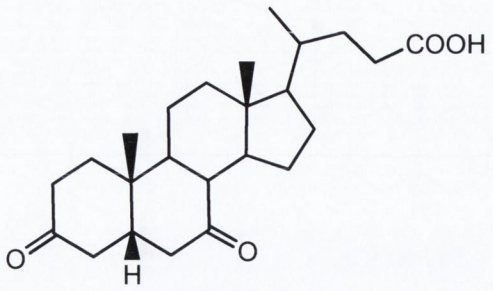

39 Diketone

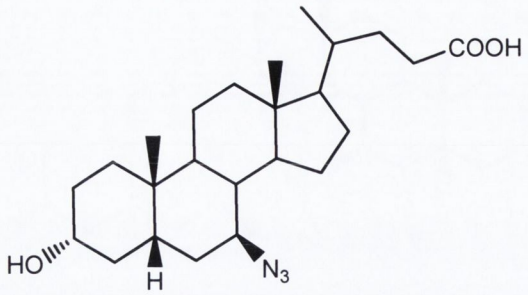

40 7β Azide

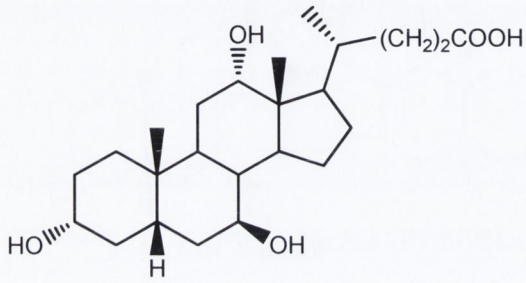

41 UCA

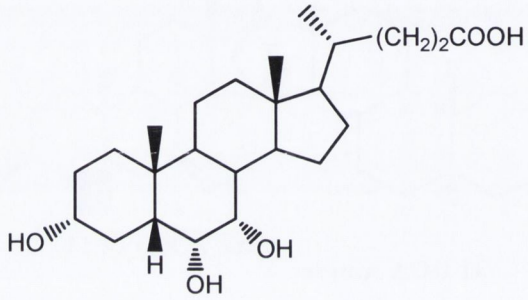

42 HCA

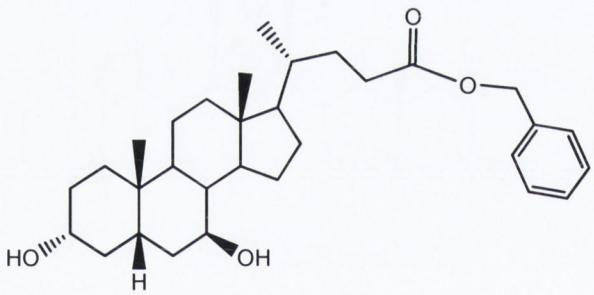

43 24-BenzylUDCA

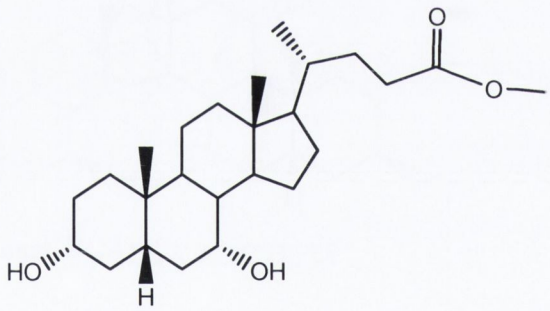

44 24-MeCDCA

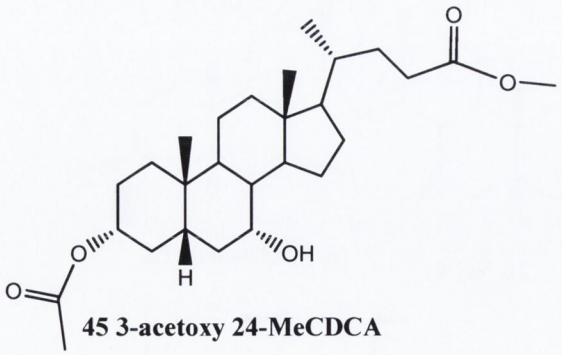

45 3-acetoxy 24-MeCDCA

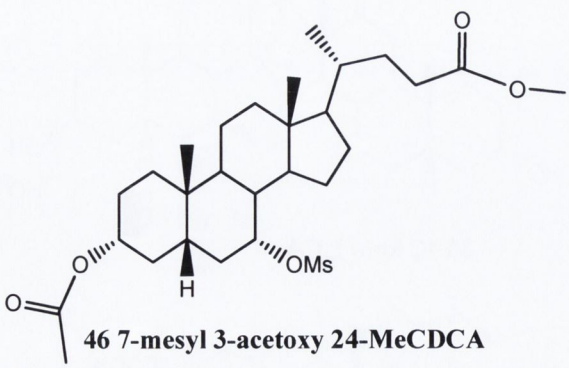

46 7-mesyl 3-acetoxy 24-MeCDCA

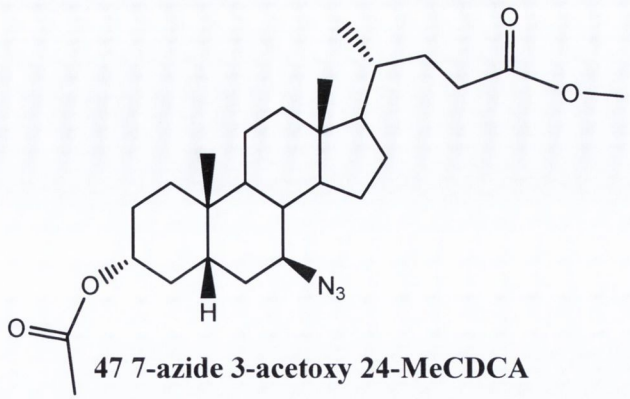

47 7-azide 3-acetoxy 24-MeCDCA

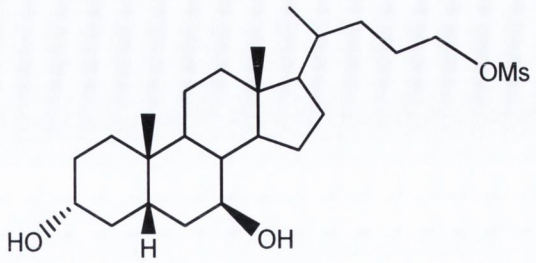

48 24-mesylUDCA

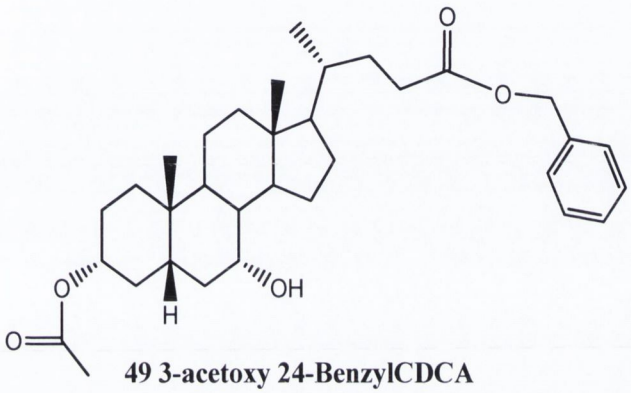

49 3-acetoxy 24-BenzylCDCA

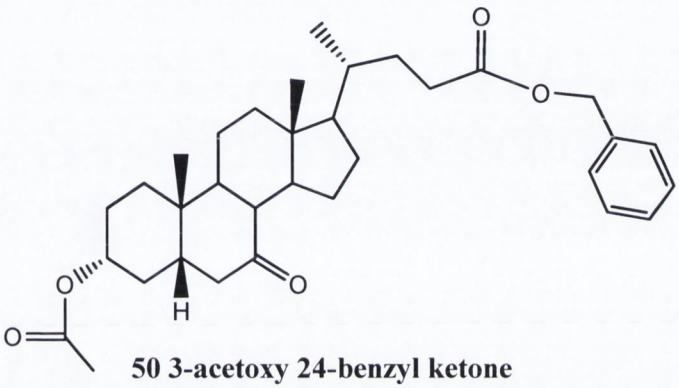

50 3-acetoxy 24-benzyl ketone

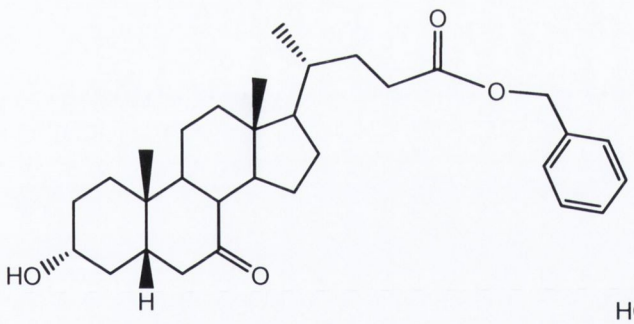

51 24-Benzyl 7-ketone

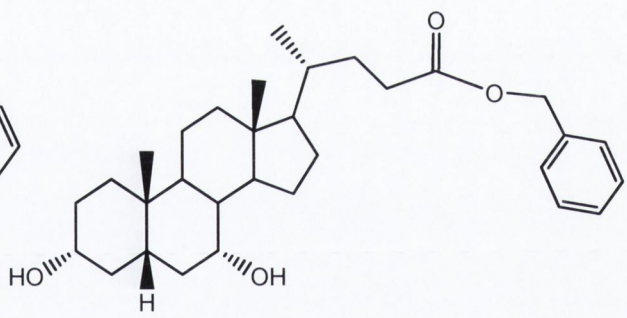

52 24-BenzylCDCA

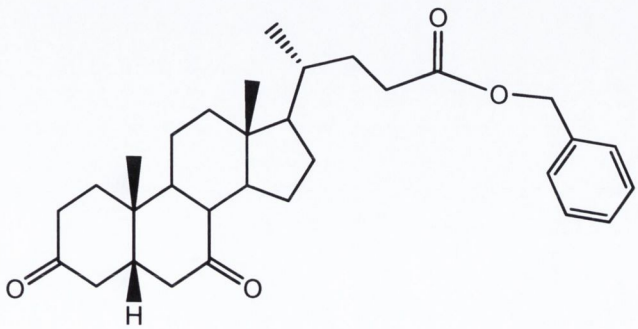

53 24-Benzyl Diketone

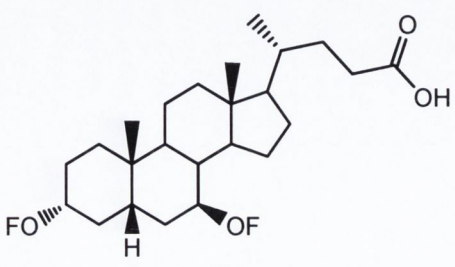

54 Formyl UDCA

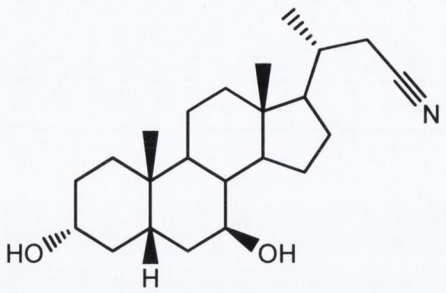

55 UDCA nornitrile

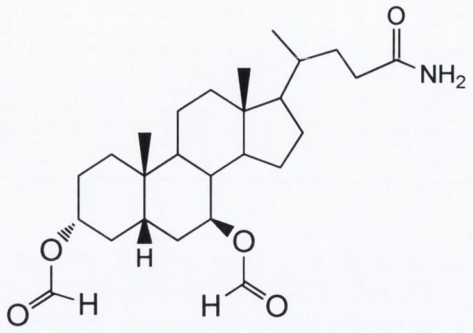

56 FormylUDCA amide

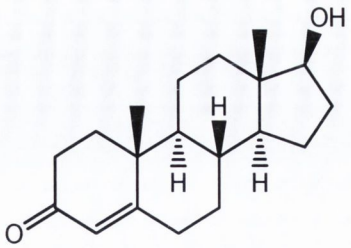

Testosterone (**57**)

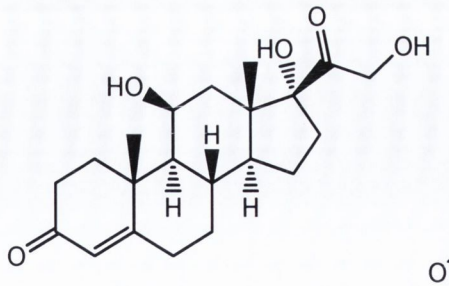

Cortisol (**58**)

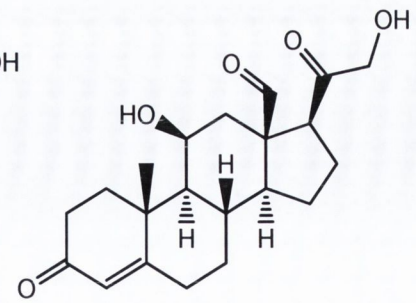

Aldosterone (**59**)

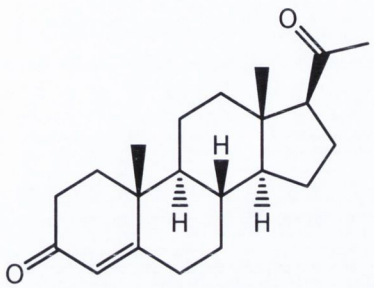

Progesterone (**60**)

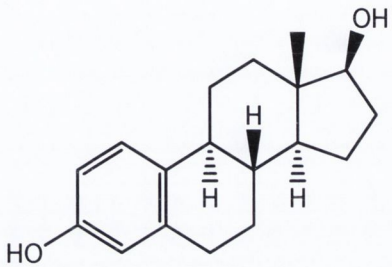

17β-estradiol (**61**)

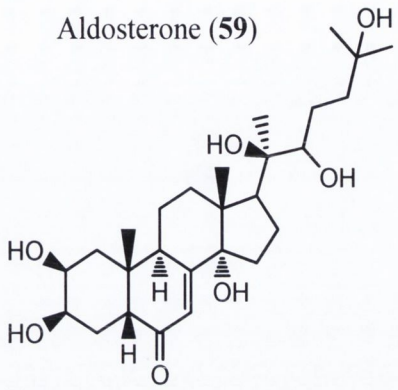

20-hydroxyecdysone (**62**)

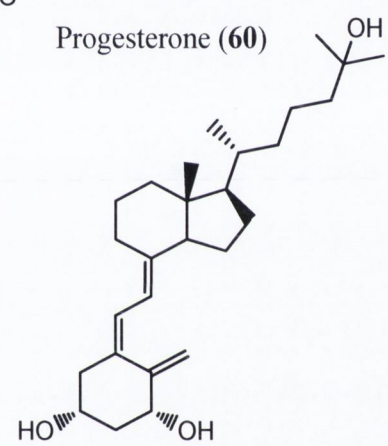

1alpha,25-dihydroxyvitamin D_3 (**63**)

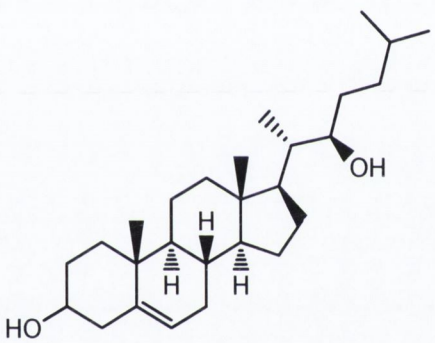

22(R)-hydroxycholesterol (**64**)

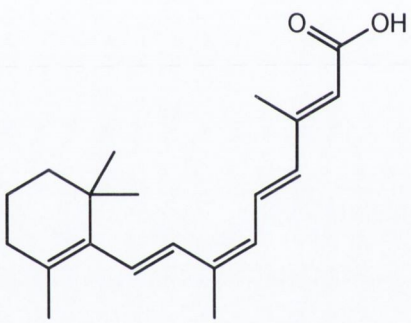

9-cis retinoic acid (**65**)

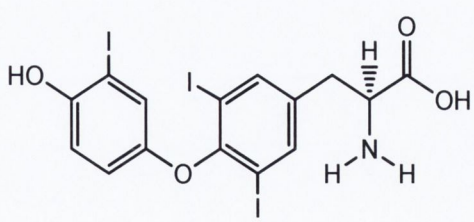

Triiodothyronine (**66**)
(TR)

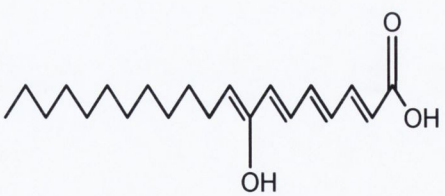

8(S)-hydroxyeicosatetraenoic acid (**67**)
(PPAR-a)

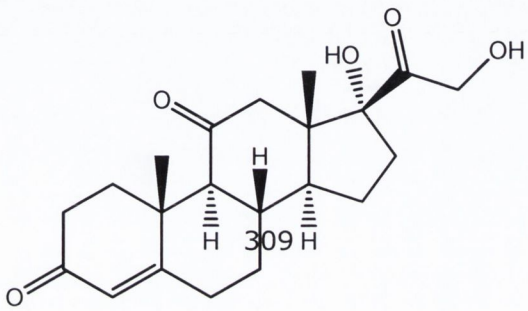

68 Cortisone

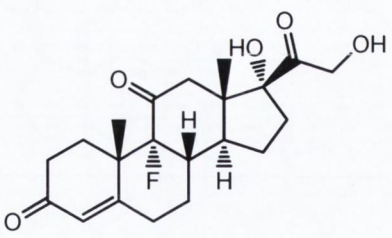

Fludrocortisone (**69**)

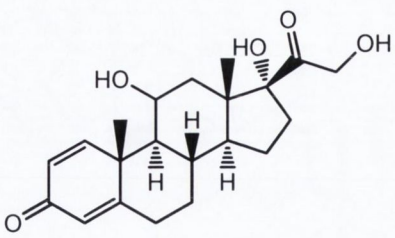

Prednisolone (**70**)

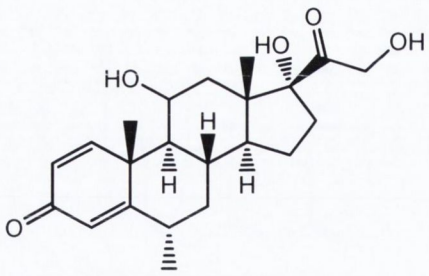

Methylprednisolone (**71**)

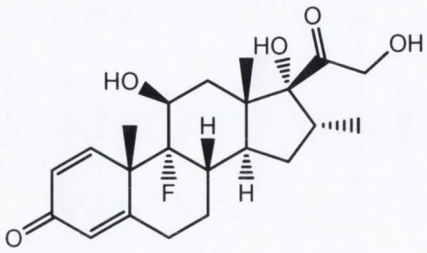

Dexamethasone (**72**)

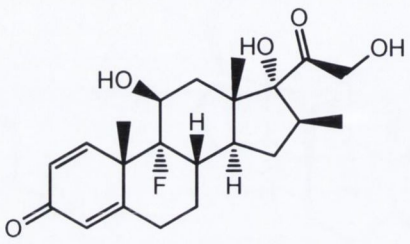

Betamethasone (**73**)

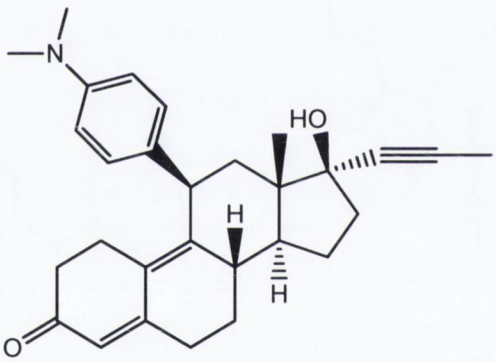

74 Mifepristone

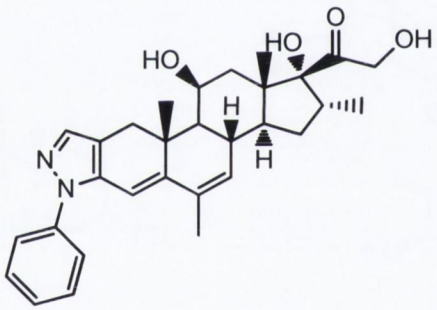

75 Deacetylcortivazol

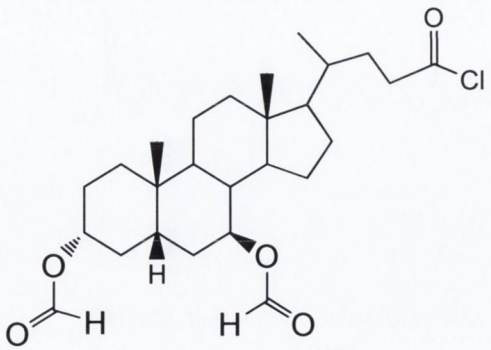

76 Formyl UDCAchloride

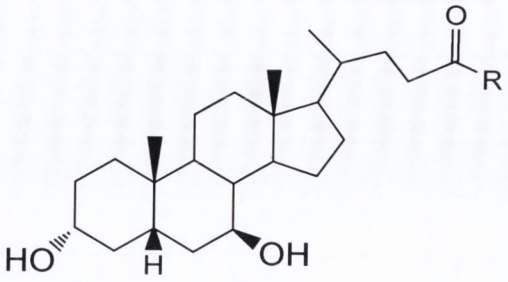

77-87

77, R= 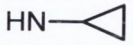

78, R= 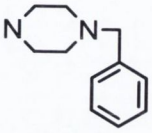

79, R= 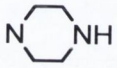

80, R= 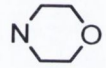

81, R= 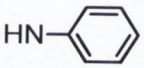

82, R= 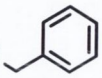

83, R= 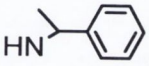

84, R= 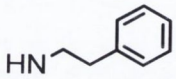

85, R= 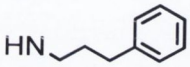

86, R= $-N(C_6H_5)_2$

87, R= 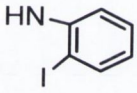

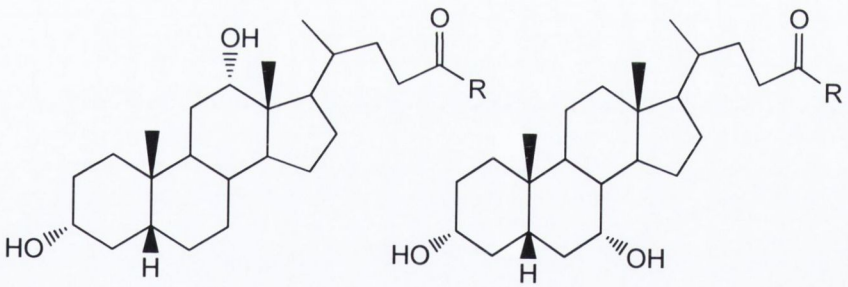

88, R= 

89, R= 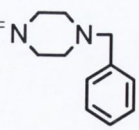

90, R= 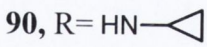

91, R= 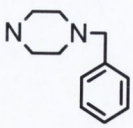

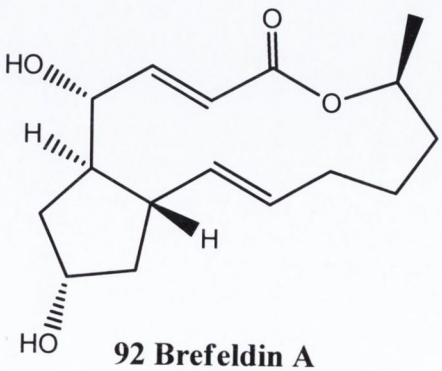

92 Brefeldin A

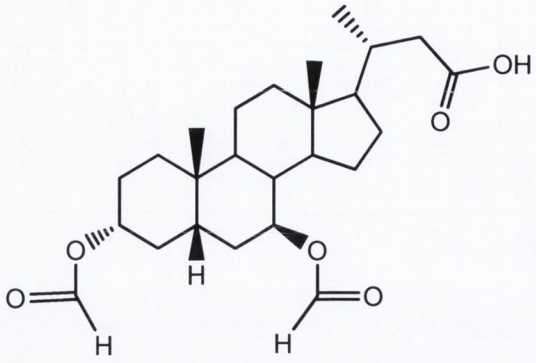

94 Formyl norUDCA

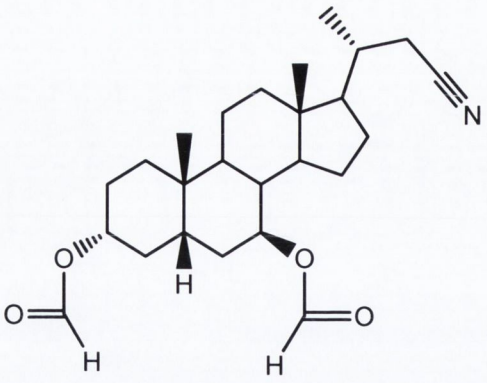

93 Formyl UDCA nornitrile

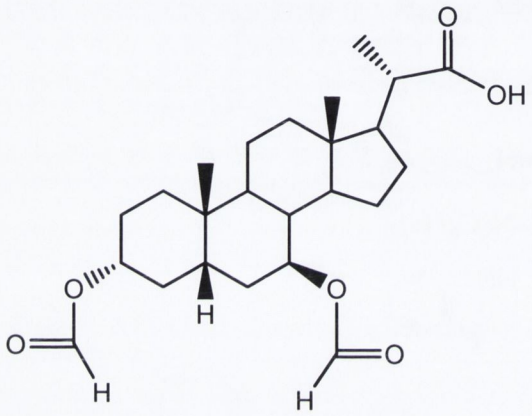

95 Formyl BisnorUDCA

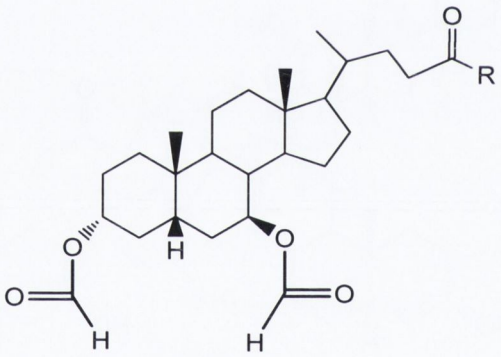

96-106

96, R= 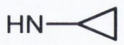

97, R= $-N(C_6H_5)_2$

98, R= 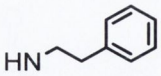

99, R= 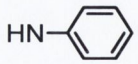

100, R= 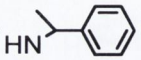

101, R= 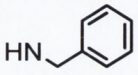

102, R= 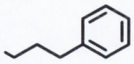

103, R= 

104, R= 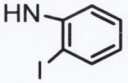

105, R= 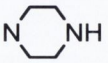

106, R= 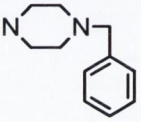

Appendix 3- Copy of Publications

Carcinogenesis vol.31 no.4 pp.737–744, 2010
doi:10.1093/carcin/bgq011
Advance Access publication January 21, 2010

Bile acids modulate the Golgi membrane fission process via a protein kinase Cη and protein kinase D-dependent pathway in colonic epithelial cells

Anne-Marie Byrne, Eilis Foran, Ruchika Sharma, Anthony Davies, Ciara Mahon, Jacintha O'Sullivan[1], Diarmuid O'Donoghue[1], Dermot Kelleher and Aideen Long*

Department of Clinical Medicine, Institute of Molecular Medicine, Trinity College Dublin, Ireland and [1]Centre for Colorectal Disease, St Vincent's University Hospital, Dublin 4, Ireland

*To whom correspondence should be addressed. Tel: +353 18962923; Fax: +353 18963503; Email: longai@tcd.ie

Deoxycholic acid (DCA) is a secondary bile acid that modulates signalling pathways in epithelial cells. DCA has been implicated in pathogenesis of colon carcinoma, particularly by activation of the protein kinase C (PKC) pathway. Ursodeoxycholic acid (UDCA), a tertiary bile acid, has been observed to have chemopreventative effects. The aim of this study was to investigate the effect of DCA and UDCA on the subcellular localization and activity of PKCη and its downstream effects on Golgi structure in a colon cancer cell model. PKCη expression was localized to the Golgi in HCT116 colon cancer cells. DCA induced fragmentation of the Golgi in these cells following activation of PKCη and its downstream effector protein kinase D (PKD). Pretreatment of cells with UDCA or a glucocorticoid, dexamethasone, inhibited DCA-induced PKCη/PKD activation and Golgi fragmentation. Knockdown of glucocorticoid receptor (GR) expression using small interfering RNA or inhibition using the GR antagonist mifepristone attenuated the inhibitory effect of UDCA on Golgi fragmentation. Elevated serum and faecal levels of DCA have been previously reported in patients with ulcerative colitis (UC) and colon cancer. Analysis of Golgi architecture *in vivo* using tissue microarrays revealed Golgi fragmentation in UC and colorectal cancer tissue. We have demonstrated that DCA can disrupt the structure of the Golgi, an organelle critical for normal cell function. Inhibition of this DCA-induced Golgi fragmentation by UDCA was mediated via the GR. This represents a potential mechanism of observed chemopreventative effects of UDCA in benign and malignant disease of the colon.

Introduction

Deoxycholic acid (DCA) is the predominant secondary bile acid implicated as a tumour promoter in colon carcinogenesis (1). Diets rich in saturated fats are linked to excessive bile acid production and associated with increased risk of progression to colon cancer (2,3). Long-term ulcerative colitis (UC) is also a risk factor for colon cancer and serum and faecal levels of DCA are elevated in patients both with UC and colon cancer (4). DCA can modulate cell signalling pathways and activity of transcription factors, such as activator protein-1 and nuclear factor-kappaB (NF-κB), shown previously to be involved in tumour progression (5). NF-κB activity is increased in most human cancers (6), whereas activator protein-1 shows increased activity in transformed cell lines and its transactivation is required for tumour promotion *in vivo* (7,8). DCA activated signalling pathways associated with tumourigenesis, including extracellular signal-regulated kinase (activated protein kinaseERK)/mitogen-activated protein kinase (MAPK)-, protein kinase B/AKT- and protein kinase C (PKC)-related pathways (9,10). The conventional and novel members of the PKC family are receptors for the tumour-promoting phorbol esters, such as phorbol 12-myristate 13-acetate. PKC expression and activity have been implicated in colon cancer promotion as it is a key regulator of proliferation in colonic epithelium (11). PKC activity has been associated with the amount and type of dietary fat where a high-fat diet containing corn oil increased colonic mucosal levels of PKC activity in a rat model (12). We have shown previously DCA-mediated activation and translocation of PKC isoenzymes implicated in tumour progression, including translocation of PKCα, PKCδ, PKCε and PKCβ1 in HCT116 colon cancer cells (13). PKCη is predominantly expressed in epithelial cells where it is localized to the Golgi apparatus and is involved in differentiation. PKCη is expressed in suprabasal layers in the intestine where cell differentiate but not in the basal layer where cells divide (14). Any change in its expression/activation would result in altered cell differentiation in the colon that potentially results in neoplastic progression. PKCη may also play a role in carcinogenesis as several studies have looked at expression levels of PKC in human colon cancer tissue and found altered levels of PKCη expression in tumour versus normal tissue (15–17). PKCη also promotes production of the pro-inflammatory cytokine interleukin-6 (18) that is up-regulated in the pre-neoplastic colon cancer diseases (19). PKCη is also important in epithelial tight junction regulation (20).

The Golgi apparatus is the organelle responsible for transport, sorting and processing of proteins from the endoplasmic reticulum. Proteins enter the *cis*-Golgi network and are sorted and packaged into carrier vesicles at the *trans*-Golgi network (TGN) ready to be transported to the plasma membrane, endosomes and endoplasmic reticulum. These carriers are dissociated from the TGN by a controlled process termed membrane fission. Once cargo accumulates at the TGN, a G-protein-coupled receptor activates a trimeric G-protein at the TGN resulting in the activation of PKCη and recruitment and phosphorylation of protein kinase D (PKD) (by PKCη). PKD then activates downstream targets to control membrane carrier fission (21). A natural marine product, ilimaquinone, overactivates the fission machinery, resulting in complete vesiculation of the Golgi via a PKD-dependent process (22–24). Golgi fragmentation, which is associated with abnormal protein processing, has been observed in the MCF-7 breast tumour cell line and also in SW480, Caco-2, HT-29 and T-84 colon cancer cell lines. In certain cases, the cause of Golgi fragmentation is thought to be associated with altered Golgi pH (25); however, factors involved in the regulation of this phenotype *in vivo* are not characterized.

Ursodeoxycholic acid (UDCA) is a tertiary bile acid traditionally used for the treatment of hepatobiliary disease, including primary biliary cirrhosis, primary sclerosing cholangitis (PSC) and gallstones (26). It is a hydrophilic non-toxic bile acid and has been shown to be cytoprotective against other more hydrophobic bile acids, such as DCA (27). We have previously demonstrated that UDCA can prevent DCA-induced translocation of PKCα, PKCδ, PKCε and PKCβ1 (13) and inhibit both cytokine- and DCA-induced activation of NF-κB and activator protein-1 (5). The therapeutic effects of UDCA have been attributed to several mechanisms including modulation of classical mitochondrial pathways of apoptosis (28) and its interaction with the glucocorticoid receptor (GR) (29,30). UDCA has immunomodulatory and anti-inflammatory effects similar to glucocorticoids and has been shown to suppress NF-κB-dependent transcriptional activity (31) and interferon-γ-induced major histocompatibility complex class II gene expression via a GR-dependent pathway (30).

The aim of this study was to investigate the effect of DCA and UDCA on the Golgi membrane fission process in colonic epithelial cells. We demonstrate that DCA induced activation of PKCη and consequently, PKD, resulting in fragmentation of the Golgi in

Abbreviations: CA, constitutively active; DAG, diacylglycerol; DEX, dexamethasone; DCA, deoxycholic acid; GFP, green fluorescent protein; GR, glucocorticoid receptor; MFT, mifepristone; NF-κB, nuclear factor-kappaB; PKC, protein kinase C; PKD, protein kinase D; PSC, primary sclerosing cholangitis; siRNA, small interfering RNA; TGN, trans-Golgi network; UC, ulcerative colitis; UDCA, ursodeoxycholic acid.

HCT116 colon cancer cells. This DCA-stimulated Golgi fragmentation can be inhibited by the hydrophilic bile acid, UDCA, in a GR-dependent manner. In a cellular context, fragmentation of the Golgi has profound implications for protein processing and may result in alterations to processes, such as signal transduction, cellular proliferation and cell–cell adhesion, all key elements of carcinogenesis. We further demonstrate increased Golgi fragmentation in tissue from UC and colon cancer patients when compared with that from normal controls.

Materials and methods

Cell culture and reagents

HCT116 colon cancer cells were obtained from American Type Culture Collection (Rockville, MD). Cells were cultured in McCoy's 5A medium supplemented with 10% (vol/vol) foetal bovine serum (Gibco BRL, Grand Island, NY). DCA, UDCA, dexamethasone (DEX), mifepristone (MFT) and dimethyl sulphoxide were all obtained from Sigma–Aldrich Chemical Co. (St Louis, MO). DCA, UDCA and MFT were solubilized in dimethyl sulphoxide, whereas DEX was dissolved in ethanol (100% vol/vol; BDH, Dorset, UK). PKCη plasmids were a gift from the late Dr F.J.Johannes (Institute of Cell Biology and Immunology, University of Stuttgart, Germany). Transient transfections were conducted using GenePORTER transfection reagent (Gene Therapy Systems, San Diego, CA), Fugene HD (Roche Diagnostics, Basel, Switzerland) or Lipofectamine 2000 (Invitrogen, Carlsbad, CA) according to the manufacturers protocols. Experiments were performed 24 h after transfection (or in some cases cells were pretreated with UDCA for 1 h prior to transfection). A Smartpool of pre-designed small interfering RNA (siRNA) oligos (ON-TARGET plus siRNA reagents) targeting the GR (siGR), scrambled control siRNA (siControl) and siRNA transfection reagent were purchased from Dharmacon (Lafayette, CO). Cells were seeded and transfected with 100 nM siGR or siControl for 24 h. Appropriate wells were pretreated with 300 μM UDCA and cells were left for a further 24 h prior to treatment with 300 μM DCA for 6 h.

Western blot analysis

Knockdown of the GR by siRNA was confirmed by western blot analysis. To investigate activation of PKD and PKCη by bile acids, lysates of stimulated cells were prepared and analysed using anti-phospho-PKD (Ser 744/748), anti-PKD (Cell Signalling Technology, Danvers, MA), anti-phosphospecific-PKCeta (pT655) (Biosource, Nivelles, Belgium) or anti-PKCη (Santa Cruz Biotechnology, Santa Cruz, CA).

Gaussia luciferase secretion assay

To determine the effects of DCA on protein secretion, we used a Gaussia luciferase assay (New England Biolabs, Ipswich, MA). Cells were transfected with a Gaussia luciferase construct using Fugene HD (Roche Diagnostics) according to the manufacturers protocol. Twenty-four hours post-transfection, cells were treated with Brefeldin as positive control, vehicle control (dimethyl sulphoxide) or DCA at indicated concentrations for either 1 or 6 h. The amount of luciferase protein secreted by the cells was quantified by measuring luminescence.

Tissue microarray construction

For all cases, haematoxylin- and eosin-stained slides from formalin-fixed paraffin-embedded tissue blocks were used to identify colonic mucosa. These areas were aligned with the tissue block and four 6 mm cores taken and transferred to a recipient block using a Tissue Microarrayer (Beecher Instruments, Silver Spring, MD). Four micrometre sections were cut for immunofluorescence studies and mounted onto SuperFrost Plus adhesive slides (Menzel-Glaser, Braunschweig, Germany).

Immunofluorescent staining

Cells were fixed with 4% paraformaldehyde and then permeabilized with 0.1% (vol/vol) Triton X-100/phosphate-buffered saline followed by blocking with 5% bovine serum albumin/phosphate-buffered saline. Cells were incubated with anti-Golgi 58K protein or anti-GM130 Golgi antibodies (Sigma–Aldrich Chemical Co.) and then incubated with AlexaFluor-488-conjugated secondary antibody (Invitrogen).

Quantification of Golgi fragmentation using high-content analysis

The GE Incell-1000 is a microscope-based screening platform capable of large-scale objective analysis of fluorescently labelled cells using automated image acquisition, data management and multiparametric analysis. For analysis of Golgi fragmentation, cells were treated in 96-well plates and stained for Golgi using a GM130 antibody as outlined above. Six fields of view per well were acquired using a ×20 objective in duplicate wells for $n = 3$ experiments. Fragmentation was measured using the Investigator software package (GE Healthcare, Piscataway, NJ) that uses an algorithm specific for detection of objects within the cell. The multi-target analysis algorithm was optimized to detect objects (Golgi fragments) within a cell using untreated cells with intact Golgi as a negative control and Brefeldin-A (1 μg/ml)-treated cells as positive control for Golgi fragmentation (32). The 'object mean area' parameter was used to classify cells as having intact Golgi (object mean area of >0.5 μm) or fragmented Golgi (object mean area of <0.5 μm) with up to 300 cells analysed per treatment group. Examples of cellular analysis are provided as supplementary material (supplementary Figure 1 is available at *Carcinogenesis* Online).

Patient tissue collection and analysis

In order to assess the clinical significance of Golgi fragmentation, we examined Golgi structure in tissues from five tissue types: (i) normal individuals ($n = 32$, 32 biopsies from 32 patients with no history of malignant disease); (ii) patients with UC without dysplasia ($n = 10$, 27 biopsies from 10 UC patients with no progression to dysplasia); (iii) patients with UC with dysplasia ($n = 6$, 18 biopsies from six UC patients with progression to dysplasia); (iv) UC-associated cancer ($n = 2$, 16 biopsies from two UC patients with progression to cancer) and (v) sporadic colonic cancer ($n = 22$, 22 biopsies from 22 patients). Normal individuals are defined as patients undergoing colonoscopy for investigation of altered bowel habit but whose histological investigations were normal and haematological indices and biochemical inflammatory markers (erythrocyte sedimentation rate and C-reactive protein) were normal. All patients were recruited by the Centre for Colorectal Disease (by D.O.D). Following endoscopy or surgery, tissues were fixed in 1% formalin and embedded in paraffin. Ethical approval was granted by the St Vincent's Hospital Ethics and Medical Research Committee to conduct this study. Tissue microarrays were stained with a TGN46 Golgi antibody. This antibody gave superior staining in paraffin-embedded tissue sections compared with either the GM130 or the 58K Golgi antibodies. A simple scoring system was devised to describe Golgi fragmentation with 0 corresponding to no Golgi fragmentation, 1 to describe partial fragmentation and 2 to describe complete Golgi fragmentation. Examples of these are included (supplementary Figure 2 is available at *Carcinogenesis* Online). The median and interquartile ranges were used for statistical analysis. Samples were coded and all stages of examination were performed blind to the tissue status.

Statistical analysis

Statistical comparison between groups for *in vitro* data was carried out using analysis of variance with least significant difference post hoc correction to examine differences between groups. Data are graphically represented as the mean ± SEM. For human tissue analyses, continuous data are presented as median and interquartile ranges. Non-parametric data were assessed using the Kruskal–Wallis test and Mann–Whitney *U*-test where appropriate. All *P*-values are two sided and *P*-values <0.05 were considered statistically significant in all analyses. All data were analysed using the SPSS™ statistical software package (SPSS, Chicago, IL).

Results

DCA altered the subcellular localization of PKCη and induced Golgi fragmentation in HCT116 colon cancer cells

DCA (300 μM) was shown previously to induce translocation of PKCα, PKCβ$_1$, PKCε and PKCδ, whereas UDCA prevented DCA-induced activation of these PKC isoenzymes (13). To investigate the effect of DCA on cellular localization of the novel PKCη isoform, HCT116 cells were transfected with PKCη-green fluorescent protein (GFP) and then treated with DCA for 1, 6 or 18 h (Figure 1A). In resting cells, PKCη was localized in a membranous stack adjacent to the cell nucleus. As PKCη was shown previously to be associated with the Golgi (15), we also stained cells using an anti-58K Golgi marker and found it colocalized with PKCη. DCA caused dispersal of the Golgi and the associated PKCη-GFP in a vesicular pattern throughout the cytoplasm demonstrating that DCA induced Golgi fragmentation in these cells. This DCA-induced Golgi fragmentation was observed over a concentration range between 50 and 300 μM (Figure 1B).

DCA-induced Golgi fragmentation was reversible

To determine whether DCA-induced Golgi fragmentation was reversible (and not an irreversible pro-apoptotic event), HCT116 cells were treated with 300 μM DCA for 6 h and then washed with phosphate-buffered saline and medium was replaced. Cells were fixed with 4%

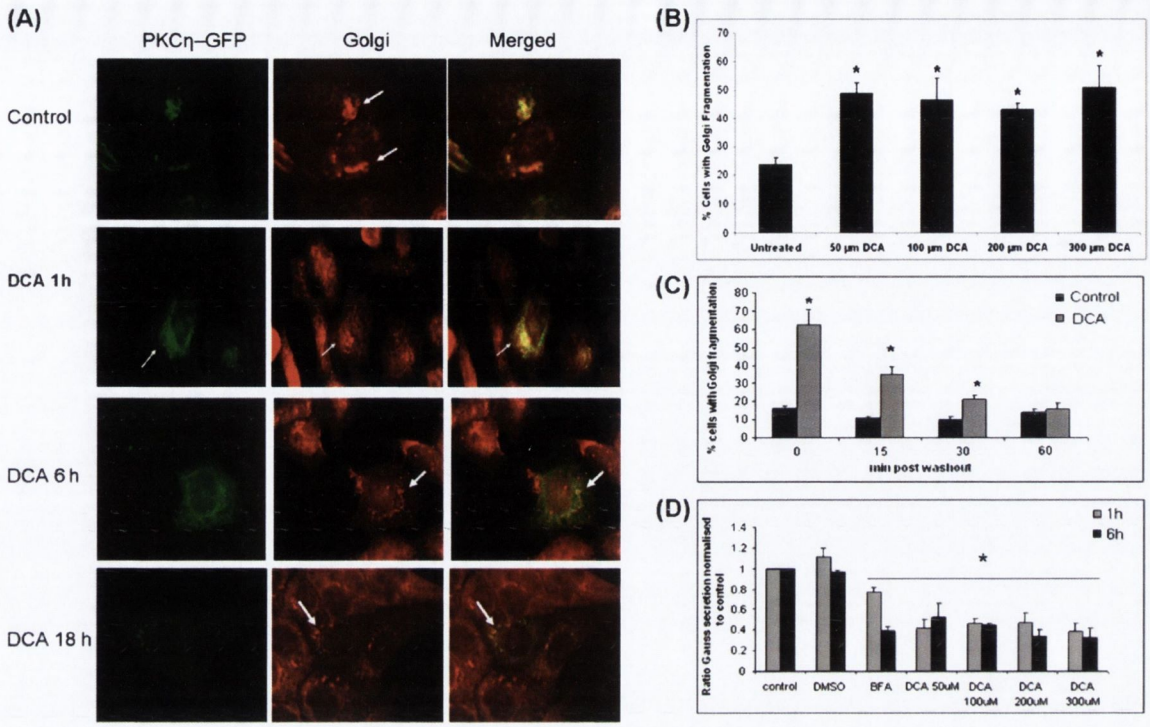

Fig. 1. DCA disrupted PKCη localization and induced Golgi fragmentation and impaired Golgi function in HCT116 cells. (**A**) Cells were transfected with PKCη-GFP (green) and then treated with 300 μM DCA for 6 or 18 h. Golgi were identified using a p58K antibody (red, indicated by white arrow) and visualized using a Nikon T800 fluorescent microscope. Original magnification ×40. (**B**) Cells were treated with 50, 100, 200 or 300 μM DCA for 6 h. Golgi were identified using the GM130 antibody. The percentage of cells with fragmented Golgi was quantified using the Incell-1000 and Investigator software package. (**C**) HCT116 cells were treated with 300 μM DCA or vehicle (control) for 6 h and then washed with phosphate-buffered saline and medium was replaced. Cells were fixed with 4% paraformaldehyde in phosphate-buffered saline at the timepoints indicated. Golgi fragmentation was quantified as in (B). (**D**) The secretory capacity of cells after treatment with DCA was assessed using a Gaussia luciferase assay. Cells were transfected with a Gaussia luciferase construct and 24 h post-transfection, cells were treated with Brefeldin-A (BFA) as positive control, vehicle control [dimethyl sulphoxide (DMSO)] or DCA at indicated concentrations for either 1 or 6 h. The amount of luciferase protein secreted by the cells was quantified by measuring luminescence. All data were expressed as the mean ± SEM and analysed by analysis of variance with least significant difference post hoc correction (*$P < 0.05$ versus control).

paraformaldehyde at various timepoints up to 1 h as indicated in Figure 1C. The percentage of cells with fragmented Golgi was quantified by high-content analysis. Consistent with visual inspection, at 6 h post-treatment, DCA induced Golgi fragmentation in 62.3 ± 8.5% cells compared with fragmentation in 16.2 ± 1.4% of untreated cells. Following removal of DCA, the Golgi reformed in a time-dependent manner. The percentage of cells with fragmented Golgi 60 min post-washout of DCA (16.0 ± 3.2%) was the same as untreated cells (14.3 ± 1.7%). In addition, cell viability was assessed using the 3-(4,5-dimethylthiazole-2-yl)-2,5-biphenyl tetrazolium bromide assay and by the propidium iodide exclusion assay. No significant changes in cell viability were observed using the 3-(4,5-dimethylthiazole-2-yl)-2,5-biphenyl tetrazolium bromide assay compared with untreated control, whereas those observed using propidium iodide were low (5.8 ± 1.7%) at the 6 h time period for 300 μM DCA (supplementary Figure 3 is available at *Carcinogenesis* Online).

DCA-induced Golgi fragmentation impairs protein secretion

To test the functional significance of the observed DCA-induced Golgi fragmentation, the secretory capacity of cells after treatment with DCA was assessed using a Gaussia luciferase assay. There was a significant decrease in secretion of luciferase into the supernatant in DCA-treated cells compared with controls (Figure 1D).

DCA induced phosphorylation and activation of PKCη and PKD

To investigate whether DCA overactivates the membrane fission process, we examined the effect of DCA on PKCη and PKD activation in HCT116 cells. Activation of PKCη is associated with phosphorylation on Ser 729 and PKD with phosphorylation on Ser 744/748. HCT116 cells were cultured in 0.5% serum for 24 h prior to the experiment. Cells were treated with 300 μM DCA for 0, 15, 30 or 60 min. Cell lysates were prepared and PKCη and PKD phosphorylation was assessed by western blot analysis (Figure 2A). DCA induced phosphorylation and therefore, activation of PKCη and PKD at 15, 30 and 60 min. To confirm the involvement of PKCη in DCA-induced Golgi fragmentation, we transfected cells with a GFP-tagged PKCη-kinase dead construct (PKCη-KD-GFP) followed by treatment with 300 μM DCA for 6 h. The number of cells expressing the PKCη-kinase dead (PKCη-KD) construct with fragmented Golgi in response to DCA treatment was significantly reduced compared with those not expressing the mutant enzyme (Figure 2B).

Pretreatment of HCT116 cells with UDCA or DEX inhibits PKCη activation and Golgi fragmentation

As we previously showed that UDCA could inhibit DCA-induced translocation of other PKC isoforms (13), we investigated if it could inhibit DCA-mediated modulation of PKCη. HCT116 cells were transfected with PKCη-GFP, pretreated with 300 μM UDCA for 1 h and then exposed to 300 μM DCA for 18 h. UDCA inhibited DCA-induced Golgi fragmentation and associated PKCη dispersal (Figure 3A).

Constitutively active (CA) PKCη was shown previously to cause Golgi fragmentation in HeLa cells (33). To determine whether UDCA or DEX can directly target this process, HCT116 cells were treated with either 300 μM UDCA or 10 nM DEX for 1 h prior to transfection

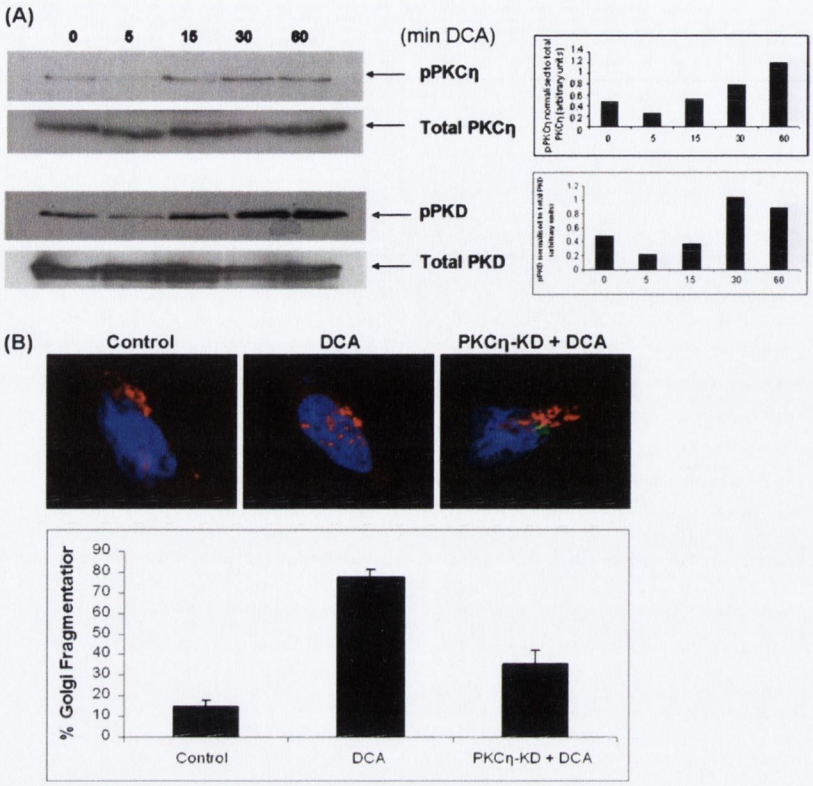

Fig. 2. DCA induced activation of PKCη and PKD in HCT116 cells. DCA could no longer induce Golgi fragmentation in cells transfected with PKCη-kinase dead (PKCη-KD) construct. (**A**) HCT116 cells were cultured in 0.5% serum for 24 h prior to stimulation for the timepoints indicated with 300 μM DCA. Cell lysates were prepared and pPKCη, total PKCη, pPKD or total PKD expression was assayed by western blot using antibodies specific to phospho-PKCη (Biosource), total PKCη (Santa Cruz Biotechnology), phospho-PKD (Ser 744/748) or total PKD (Cell Signalling Technology). Graphs of densitometry measurements are included. (**B**) HCT116 cells were transfected with PKCη-KD-GFP (green) and 24 h post-transfection, cells were treated with 300 μM DCA for 6 h. Cells were fixed and Golgi were identified using GM130 (red) antibody. Nuclei were stained with Hoechst (Invitrogen). At least 100 cells were counted for each group (control, DCA treated and DCA treatment following PKCη-KD transfection). Slides were coded and quantification was performed blind to treatment.

with a CA PKCη (stained in red). Golgi were visualized by immunofluorescence using the anti-58K Golgi antibody (green, Figure 3B). Cells transfected with CA PKCη had fragmented Golgi. Pretreatment with DEX or UDCA 1 h prior to transfection prevented CA PKCη-induced fragmentation.

UDCA displays structural similarity to glucocorticoids, exerts anti-inflammatory effects and was shown previously to activate the GR in primary rat hepatocytes (34). Therefore, the effects of DEX, a synthetic glucocorticoid, and UDCA on DCA-induced Golgi fragmentation were compared (Figure 3C). To confirm hyperactivation of the fission machinery and complete fragmentation of the Golgi, an antibody targeting a protein resident in the *cis*-Golgi network GM130 was used to examine the effect on Golgi morphology. DCA caused complete vesiculation of the Golgi structure. Both UDCA and DEX inhibited DCA-induced Golgi fragmentation.

UDCA or DEX pretreatment prevented DCA-induced PKD phosphorylation

PKD is necessary for the detachment (fission) of transport carriers from the TGN. As DCA activated PKD, we investigated if UDCA or DEX could prevent DCA-mediated activation of PKD. HCT116 cells were pretreated with UDCA (300 μM) or DEX (10 nM) for 1 or 2 h prior to treatment with DCA (300 μM) for 2 h. Cell lysates were prepared and PKD phosphorylation (pPKD) was assessed by western blot (Figure 4). Pretreatment with either UDCA or DEX prevented DCA-induced activation of PKD.

The GR is required for UDCA-mediated inhibition of DCA-induced Golgi fragmentation

Since the synthetic glucocorticoid DEX exerted the same effects as UDCA, inhibiting (i) DCA-induced Golgi fragmentation; (ii) CA PKCη-induced Golgi fragmentation and (iii) DCA-induced PKD activation, the potential involvement of the GR in these processes was investigated. When GR expression was knocked down using siRNA or when the GR was blocked using the GR antagonist, MFT, UDCA-mediated inhibition of DCA-induced Golgi fragmentation was attenuated (Figure 5A–C). There was no difference in Golgi fragmentation in cells treated with UDCA (33.8 ± 3.1%) or MFT (34.7 ± 3.3%) alone compared with untreated control cells (33.3 ± 2.2%). DCA induced Golgi fragmentation in 54.4 ± 1.2% cells. Pretreatment with UDCA inhibited DCA-induced fragmentation (42.9 ± 4.4%). UDCA could no longer overcome DCA-induced fragmentation when cells were treated with MFT (57.4 ± 3.7%) or when the GR was knocked down using siRNA (51.7 ± 4.1%), suggesting that UDCA mediates its protective effects via the GR in this system.

Golgi fragmentation is evident in vivo in patients with UC and colon cancer

To investigate whether the DCA-mediated effect on Golgi architecture observed in HCT116 cells may also be seen *in vivo* in UC (inflammatory) or cancer, Golgi structure was examined in five tissue types (i) normal; (ii) UC without dysplasia; (iii) UC with dysplasia; (iv)

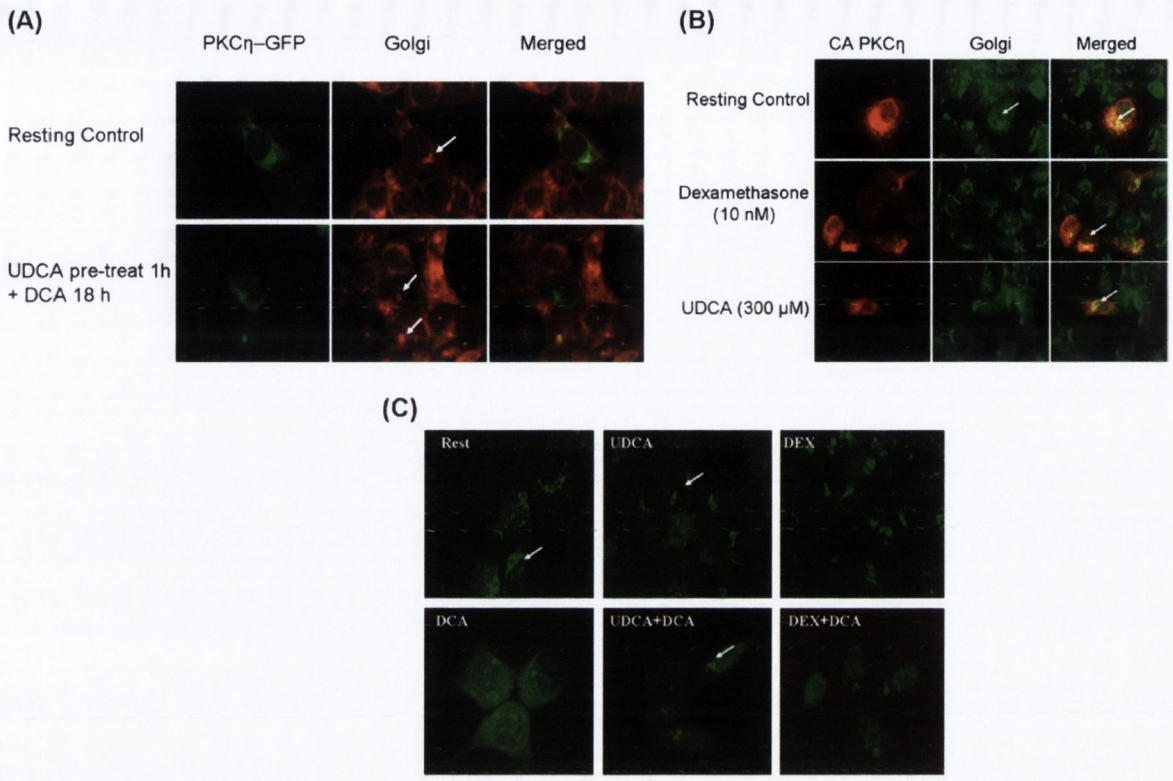

Fig. 3. UDCA and DEX inhibit both DCA-induced and PKCη-induced Golgi fragmentations. (**A**) UDCA inhibits DCA activation of PKCη. HCT116 cells were transfected with PKCη-GFP (green) or pretreated with 300 μM UDCA for 1 h followed by treatment with 300 μM DCA for 18 h. UDCA inhibited DCA-induced PKCη translocation and Golgi fragmentation (red, indicated by white arrow) throughout the cytoplasm. (**B**) DEX or UDCA inhibits CA PKCη-induced Golgi fragmentation. HCT116 cells were transfected with a CA PKCη (red) or treated with either 10 nM DEX or 300 μM UDCA for 1 h prior to transfection. (**C**) UDCA and DEX inhibit DCA-induced Golgi fragmentation. Cells were treated with 300 μM DCA, 300 μM UDCA or 10 nM DEX for 6 h or pretreated with 300 μM UDCA for 18 h or 10 nM DEX for 1 h followed by treatment with 300 μM DCA for 6 h. Golgi were identified by immunofluorescence using a GM130 antibody and visualized with a Nikon T800 fluorescent microscope. Original magnification ×40.

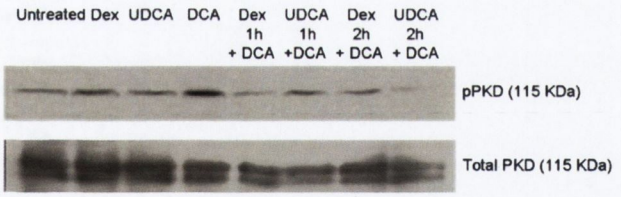

Fig. 4. UDCA and DEX inhibit DCA-induced PKD phosphorylation in HCT116 cells. HCT116 cells were cultured in 0.5% serum for 24 h prior to stimulation. HCT116 cells were treated with 10 nM DEX, 300 μM UDCA or 300 μM DCA for 2 h or pretreated with DEX (10 nM) or UDCA (300 μM) for 1 or 2 h prior to treatment with DCA (300 μM) for 2 h. Cell lysates were prepared and pPKD or total PKD expression was assayed by western blot using an antibody specific to phospho-PKD (Ser 744/748) or total PKD. Blot is representative of three independent experiments.

UC-associated cancer and (v) sporadic colon cancer (Figure 6A). Arbitrary units were used to describe Golgi fragmentation in tissues (Figure 6B). All UC and cancer tissues (both inflammatory and tumour samples) showed significant increases in Golgi fragmentation ($P < 0.005$). There was no significant difference observed between UC tissue without dysplasia, UC tissue with dysplasia or cancer.

Discussion

In this study, we have demonstrated that the bile acid, DCA, can induce Golgi fragmentation in colonic cells by activation of the membrane fission process. This observed Golgi fragmentation is a direct consequence of the activation of PKCη and phosphorylation of PKD. Our finding is consistent with the model proposed by Diaz Anel and Malhotra (33) in which the marine product ilimaquinone induced Golgi fragmentation via hyperactivation of PKD resulting in transport carriers being continuously formed from the TGN until it was reduced to small vesicles. Here, we describe a novel effect of bile acids on Golgi morphology where DCA induced Golgi fragmentation *in vitro* in the HCT116 colon carcinoma cell line. Constitutive Golgi fragmentation has previously been observed in other colonic cancer cell lines, including the SW480, Caco-2, HT-29 and T-84 colon cancer cell lines (25).

In our cell model system, this DCA-induced Golgi fragmentation is mediated by the Golgi-associated PKCη isoform. Localization of this enzyme to the Golgi and TGN appears to play a critical role in regulation of intracellular transport mechanisms. PKCη also has the capacity to translocate to the nucleus in response to signalling through tumour promoters and in this location may play a role in the nuclear machinery for cell proliferation through its interaction with, for example, cyclinE–cdk2 complex (15). Rather than translocation to the nucleus, PKCη remains localized to the Golgi in response to DCA but this change in cellular distribution could also affect cell proliferation and differentiation.

Consistent with previous studies, which have demonstrated that UDCA can antagonize the adverse biological effects of hydrophobic bile acids such as DCA, we have shown here that UDCA could prevent DCA-mediated Golgi fragmentation in colon cancer cells. At a molecular level, UDCA mediates some of its anti-inflammatory effects via activation of the GR (31,34,35) and this is consistent with

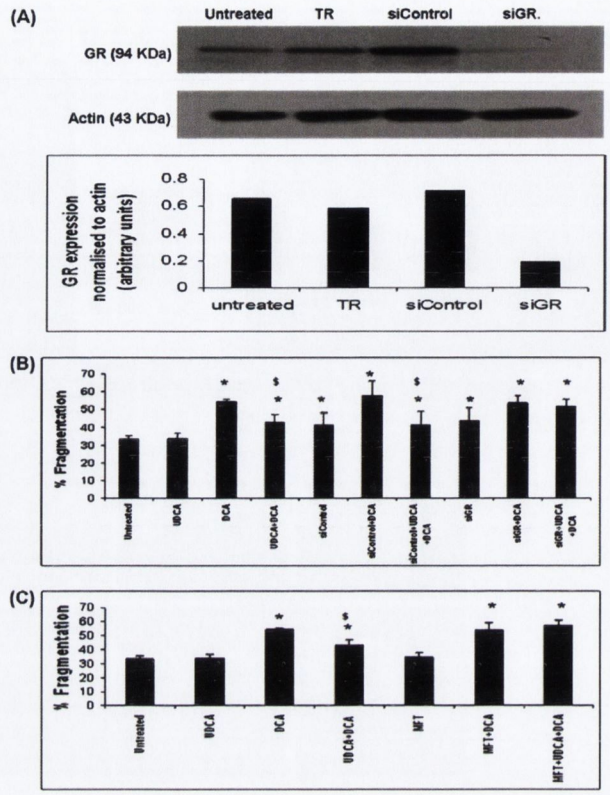

Fig. 5. UDCA-mediated inhibition of DCA-induced Golgi fragmentation was reversed by inhibiting expression of the GR (siGR) or by the glucocorticoid antagonist, MFT. (**A**) GR was knocked down in HCT116 cells using siRNA. A graph of densitometry is included. (**B**) HCT116 cells were treated with 300 μM UDCA (6 h), 300 μM DCA (6 h) or 300 μM UDCA (18 h) + 300 μM DCA (6 h) or transfected with 100 nM siRNA targeting the GR (siGR, 24 h) prior to treatment with UDCA (18 h) and DCA (6 h). Scrambled siRNA sequences (siControl) were used to control for non-specific effects due to siRNA transfection and treated as above with UDCA and DCA. (**C**) The GR was also blocked using 100 nM of the antagonist MFT for 2 h and treated as above. Golgi fragmentation was assessed by high content analysis using the Incell-1000 and Investigator software package. Data were expressed as the mean ± SEM and analysed by analysis of variance with least significant difference post hoc correction ($^{*}P < 0.05$ versus untreated and $^{\$}P < 0.05$ versus DCA treated).

our prior observations that UDCA inhibits cytokine-induced NF-κB induction (5). UDCA-mediated GR activation is ligand independent but facilitates GR translocation to the nucleus through dissociation of the GR–Heat shock protein 90 complex (35). It has previously been demonstrated that UDCA acts on a distinct region of the ligand-binding domain when compared with the classical GR agonist DEX and thus can mediate differential regulation of gene expression by the GR (31). In the current study, UDCA could no longer prevent DCA-induced Golgi fragmentation when the GR was blocked with the GR antagonist MFT or when siRNA was used to knockdown GR expression, indicating that UDCA mediates its effects on Golgi fragmentation via the GR in HCT116 colon cancer cells.

UDCA is currently used clinically for the treatment of liver diseases, such as primary biliary cirrhosis and PSC. Patients with UC and PSC are at an increased risk of developing colon cancer (36). DCA levels are elevated in the colon of patients with PSC, whereas UC patients with neoplasia have increased faecal concentrations of DCA compared with patients without neoplasia (37). UDCA has been shown to act as a chemopreventative agent decreasing the risk for developing colon cancer in these patients (36). In addition, dietary supplementation with UDCA has been shown to inhibit tumour incidence by >50% in response to cholic acid in the azoxymethane colon cancer model (38). The mechanism whereby UDCA improves liver function and DCA-induced damage is unknown. Suggested mechanisms include (i) its ability to create a more hydrophilic bile acid pool counteracting cell damage induced by a hydrophobic bile acid pool; (ii) reduction of inflammation around bile ducts; (iii) improving secretory capacity of hepatocytes in choleostasis and (iv) up-regulation of anti-apoptotic survival signalling pathways (39). We suggest a novel mechanism whereby UDCA inhibits DCA-induced Golgi fragmentation and thus the alterations in intracellular trafficking/signalling associated with this process.

The Golgi apparatus is the organelle responsible for transport, sorting and processing of proteins and lipids from the endoplasmic reticulum. The *cis*-Golgi networks, medial-Golgi networks and TGNs are rich in distinct glycosyltransferase enzymes, which modify O- and N-linked carbohydrate chains on glycoproteins and glycolipids. Disruption of Golgi architecture could therefore result in mis-localization of glycosyltransferases and dissociation from their cognate ligands resulting in alterations in normal protein/lipid processing. Terminal oligosaccharide units expressed on such proteins/lipids are highly specific in their recognition capabilities and are involved in a range of normal cell processes, such as intracellular protein sorting, cell signalling and cell–cell or cell–extracellular matrix adhesion. Alterations in the terminal oligosaccharide units can potentially alter differentiation, proliferation and promote neoplastic progression. Abnormal glycosylation of proteins and lipids is a common observation in malignant cells (40–42) with aberrant glycosylation patterns found in tissue from most colon cancer patients (43–45). Glycosylation alterations also occur in UC, Crohn's disease, UC-associated cancer and sporadic colon cancer with increased expression of Thomsen Friedenreich (TF) and sialyl tenascin

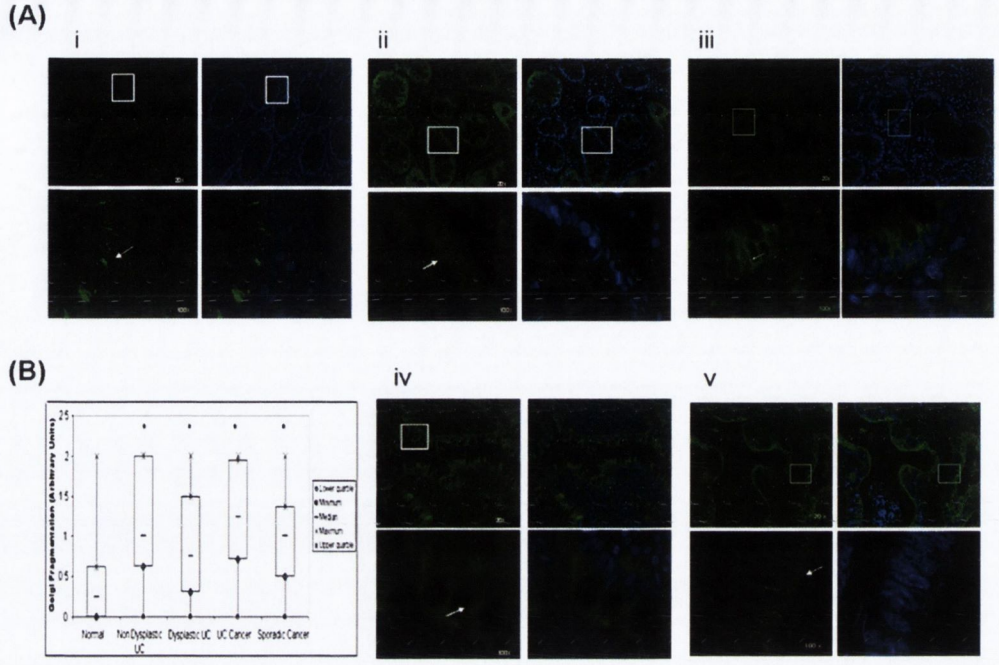

Fig. 6. Golgi fragmentation in patients with UC and colon cancer. **(A) Golgi structure was examined in five sets of tissue:** (i) no history of malignant disease (normal); (ii) UC with no progression to dysplasia (non-dysplastic); (iii) UC with progression to dysplasia (dysplastic); (iv) colorectal cancer on background of UC (UC cancer) and (v) sporadic colon cancer. Golgi (green, as indicated by white arrow) were visualized using a TGN antibody TGN46 and an AlexaFluor fluorescent secondary antibody. **(B) Biopsies classified as completely fragmented Golgi were assigned arbitrary scores of 0 for non-fragmented Golgi,** 1 for partially fragmented Golgi and 2 for fully fragmented Golgi. Data are expressed as medians and interquartile ranges; $^{*}P < 0.05$.

oncofoetal antigens that are high-risk markers for cancer progression in inflammatory bowel disease (46,47). These glycosylation changes have been observed in the absence of dysplasia and can occur prior to malignant transformation (44). Altered N-linked glycosylation leading to over-expression of sialyl Lewis A and sialyl Lewis X carbohydrates is found in tumours and correlates with metastasis (48).

Bile acids have previously been shown to activate PKCα and PKCδ in hepatocytes by facilitating enzyme association with phospholipids and increasing cell membrane diacylglycerol (DAG) content. Bile acids do not appear to bind to DAG (49) but instead stimulate its formation in rat hepatocytes (50) possibly through phospholipase C activation (51). Trichloroacetic acid and DCA have also been shown to activate DAG formation in normal colon and colonic tumour cell extracts (52). PKC activation is highly dependent on physiochemical properties of the lipid membrane and PKCη activity is more sustained at the Golgi due to prolonged DAG accumulation at this site (53).

We have observed Golgi fragmentation in biopsies obtained from patients with the inflammatory condition UC and in patients with colon cancer. We did not observe differences in levels of Golgi fragmentation between UC and cancer patients nor did we observe a progression between UC, dysplasia and cancer. It is possible that there are multiple processes that could lead to Golgi fragmentation in inflammation and cancer. It has been proposed that increased levels of bile acids may play a role in both inflammatory bowel disease and cancer (4). Hence, it is possible that Golgi fragmentation may play a role in the pathogenesis of both UC and cancer through either single or multiple mechanisms.

The effects of UDCA in inhibiting Golgi fragmentation may play a role in several of its pharmacological effects including possible effects in liver disease and chemopreventative effects in patients with premalignant colonic diseases, such as extensive UC. These studies demonstrate a potential link between bile acids and Golgi fragmentation that may be involved in the pathogenesis of both benign and malignant disease of the gastrointestinal tract.

Supplementary material

Supplementary Figures 1–3 can be found at http://carcin.oxfordjournals.org/

Funding

Cancer Research Ireland (CRI04LON) and Programme for Research in Third Level Institutions cycle 4.

Acknowledgements

Conflict of Interest Statement: None declared.

References

1. Bayerdorffer,E. *et al.* (1995) Unconjugated secondary bile acids in the serum of patients with colorectal adenomas. *Gut.*, **36**, 268–273.
2. Hori,T. *et al.* (1998) Effect of dietary deoxycholic acid and cholesterol on fecal steroid concentration and its impact on the colonic crypt cell proliferation in azoxymethane-treated rats. *Cancer Lett.*, **124**, 79–84.
3. Lapre,J.A. *et al.* (1992) Diet-induced increase of colonic bile acids stimulates lytic activity of fecal water and proliferation of colonic cells. *Carcinogenesis*, **13**, 41–44.
4. Bayerdorffer,E. *et al.* (1993) Increased serum deoxycholic acid levels in men with colorectal adenomas. *Gastroenterology*, **104**, 145–151.
5. Shah,S.A. *et al.* (2006) Ursodeoxycholic acid inhibits interleukin 1 beta [corrected] and deoxycholic acid-induced activation of NF-kappaB and AP-1 in human colon cancer cells. *Int. J. Cancer*, **118**, 532–539.
6. Karin,M. (2006) NF-kappaB and cancer: mechanisms and targets. *Mol. Carcinog.*, **45**, 355–361.
7. Eferl,R. *et al.* (2003) AP-1: a double-edged sword in tumorigenesis. *Nat. Rev. Cancer*, **3**, 859–868.

8. Young,M.R. *et al.* (1999) Transgenic mice demonstrate AP-1 (activator protein-1) transactivation is required for tumor promotion. *Proc. Natl Acad. Sci. USA*, **96**, 9827–9832.
9. Dent,P. *et al.* (2005) Conjugated bile acids promote ERK1/2 and AKT activation via a pertussis toxin-sensitive mechanism in murine and human hepatocytes. *Hepatology*, **42**, 1291–1299.
10. Qiao,D. *et al.* (2000) Bile acid-induced activation of activator protein-1 requires both extracellular signal-regulated kinase and protein kinase C signaling. *J. Biol. Chem.*, **275**, 15090–15098.
11. Craven,P.A. *et al.* (1987) Subcellular distribution of protein kinase C in rat colonic epithelial cells with different proliferative activities. *Cancer Res.*, **47**, 3434–3438.
12. Reddy,B.S. *et al.* (1996) Effect of amount and types of dietary fat on intestinal bacterial 7 alpha-dehydroxylase and phosphatidylinositol-specific phospholipase C and colonic mucosal diacylglycerol kinase and PKC activities during stages of colon tumor promotion. *Cancer Res.*, **56**, 2314–2320.
13. Shah,S.A. *et al.* (2005) Ursodeoxycholic acid inhibits translocation of protein kinase C in human colonic cancer cell lines. *Eur. J. Cancer*, **41**, 2160–2169.
14. Osada,S. *et al.* (1993) Predominant expression of nPKC eta, a Ca(2+)-independent isoform of protein kinase C in epithelial tissues, in association with epithelial differentiation. *Cell Growth Differ.*, **4**, 167–175.
15. Maissel,A. *et al.* (2006) PKCeta is localized in the Golgi, ER and nuclear envelope and translocates to the nuclear envelope upon PMA activation and serum-starvation: C1b domain and the pseudosubstrate containing fragment target PKCeta to the Golgi and the nuclear envelope. *Cell. Signal.*, **18**, 1127–1139.
16. Doi,S. *et al.* (1994) Expression of multiple isoforms of protein kinase C in normal human colon mucosa and colon tumors and decreased levels of protein kinase C beta and eta mRNAs in the tumors. *Mol. Carcinog.*, **11**, 197–203.
17. Kahl-Rainer,P. *et al.* (1994) Five of six protein kinase C isoenzymes present in normal mucosa show reduced protein levels during tumor development in the human colon. *Carcinogenesis*, **15**, 779–782.
18. Fima,E. *et al.* (1999) Expression of PKCeta in NIH-3T3 cells promotes production of the pro-inflammatory cytokine interleukin-6. *Eur. Cytokine Netw.*, **10**, 491–500.
19. Li,Y. *et al.* (2009) Disease-related expression of the IL-6 / STAT3 / SOCS3 signaling pathway in ulcerative colitis and ulcerative colitis-related carcinogenesis. *Gut* (Epub ahead of print).
20. Suzuki,T. *et al.* (2009) PKC eta regulates occludin phosphorylation and epithelial tight junction integrity. *Proc. Natl Acad. Sci. USA*, **106**, 61–66.
21. Bard,F. *et al.* (2006) The formation of TGN-to-plasma-membrane transport carriers. *Annu. Rev. Cell Dev. Biol.*, **22**, 439–455.
22. Takizawa,P.A. *et al.* (1993) Complete vesiculation of Golgi membranes and inhibition of protein transport by a novel sea sponge metabolite, ilimaquinone. *Cell*, **73**, 1079–1090.
23. Jamora,C. *et al.* (1997) Regulation of Golgi structure through heterotrimeric G proteins. *Cell*, **91**, 617–626.
24. Jamora,C. *et al.* (1999) Gbetagamma-mediated regulation of Golgi organization is through the direct activation of protein kinase D. *Cell*, **98**, 59–68.
25. Kellokumpu,S. *et al.* (2002) Abnormal glycosylation and altered Golgi structure in colorectal cancer: dependence on intra-Golgi pH. *FEBS Lett.*, **516**, 217–224.
26. Lazaridis,K.N. *et al.* (2001) Ursodeoxycholic acid 'mechanisms of action and clinical use in hepatobiliary disorders'. *J. Hepatol.*, **35**, 134–146.
27. Copaci,I. *et al.* (2005) New therapeutical indications of ursodeoxycholic acid. *Rom. J. Gastroenterol.*, **14**, 259–266.
28. Rodrigues,C.M. *et al.* (1998) Ursodeoxycholic acid may inhibit deoxycholic acid-induced apoptosis by modulating mitochondrial transmembrane potential and reactive oxygen species production. *Mol. Med.*, **4**, 165–178.
29. Tanaka,H. *et al.* (1992) Ursodeoxycholic acid-dependent activation of the glucocorticoid receptor. *Biochem. Biophys. Res. Commun.*, **188**, 942–948.
30. Tanaka,H. *et al.* (1996) Ligand-independent activation of the glucocorticoid receptor by ursodeoxycholic acid. Repression of IFN-gamma-induced MHC class II gene expression via a glucocorticoid receptor-dependent pathway. *J. Immunol.*, **156**, 1601–1608.
31. Miura,T. *et al.* (2001) Functional modulation of the glucocorticoid receptor and suppression of NF-kappaB-dependent transcription by ursodeoxycholic acid. *J. Biol. Chem.*, **276**, 47371–47378.
32. Dinter,A. *et al.* (1998) Golgi-disturbing agents. *Histochem. Cell Biol.*, **109**, 571–590.
33. Diaz Anel,A.M. *et al.* (2005) PKCeta is required for beta1gamma2/beta3-gamma2- and PKD-mediated transport to the cell surface and the organization of the Golgi apparatus. *J. Cell Biol.*, **169**, 83–91.
34. Weitzel,C. *et al.* (2005) Ursodeoxycholic acid induced activation of the glucocorticoid receptor in primary rat hepatocytes. *Eur. J. Gastroenterol. Hepatol.*, **17**, 169–177.
35. Sola,S. *et al.* (2005) Nuclear translocation of UDCA by the glucocorticoid receptor is required to reduce TGF-beta1-induced apoptosis in rat hepatocytes. *Hepatology*, **42**, 925–934.
36. Pardi,D.S. *et al.* (2003) Ursodeoxycholic acid as a chemopreventive agent in patients with ulcerative colitis and primary sclerosing cholangitis. *Gastroenterology*, **124**, 889–893.
37. Hill,M.J. *et al.* (1987) Faecal bile acids, dysplasia, and carcinoma in ulcerative colitis. *Lancet*, **2**, 185–186.
38. Earnest,D.L. *et al.* (1994) Chemoprevention of azoxymethane-induced colonic carcinogenesis by supplemental dietary ursodeoxycholic acid. *Cancer Res.*, **54**, 5071–5074.
39. Gustav Paumgartner,U.B. (2002) Ursodeoxycholic acid in cholestatic liver disease: mechanisms of action and therapeutic use revisited. *Hepatology*, **36**, 525–531.
40. Rhodes,J.M. (1996) Unifying hypothesis for inflammatory bowel disease and associated colon cancer: sticking the pieces together with sugar. *Lancet*, **347**, 40–44.
41. Petrini,M. *et al.* (1989) Constitutive expression and abnormal glycosylation of transferrin receptor in acute T-cell leukemia. *Cancer Res.*, **49**, 6989–6996.
42. Ladisch,S. *et al.* (1989) Aberrant fatty acyl alpha-hydroxylation in human neuroblastoma tumor gangliosides. *J. Biol. Chem.*, **264**, 12097–12105.
43. Rivinoja,A. (2006) Elevated Golgi pH in breast and colorectal cancer cells correlates with the expression of oncofetal carbohydrate T-antigen. *J. Cell. Physiol.*, **208**, 167–174.
44. Campbell,B.J. *et al.* (2001) Altered glycosylation in inflammatory bowel disease: a possible role in cancer development. *Glycoconj. J.*, **18**, 851–858.
45. Boland,C.R. *et al.* (1990) The carbohydrate composition of mucin in colonic cancer. *Gastroenterology*, **98**, 1170–1177.
46. Karlen,P. *et al.* (1998) Sialyl-Tn antigen as a marker of colon cancer risk in ulcerative colitis: relation to dysplasia and DNA aneuploidy. *Gastroenterology*, **115**, 1395–1404.
47. Itzkowitz,S.H. *et al.* (1995) Sialosyl-Tn antigen: initial report of a new marker of malignant progression in long-standing ulcerative colitis. *Gastroenterology*, **109**, 490–497.
48. Varki,A. *et al.* (1999) *Essentials of glycobiology.* Cold Spring Harbor Laboratory Press, Cold Spring Harbor, NY.
49. Rao,Y.P. *et al.* (1997) Activation of protein kinase C alpha and delta by bile acids: correlation with bile acid structure and diacylglycerol formation. *J. Lipid Res.*, **38**, 2446–2454.
50. Beuers,U. *et al.* (1996) Tauroursodeoxycholic acid activates protein kinase C in isolated rat hepatocytes. *Gastroenterology*, **110**, 1553–1563.
51. Takenawa,T. *et al.* (1981) Purification of phosphatidylinositol-specific phospholipase C from rat liver. *J. Biol. Chem.*, **256**, 6769–6775.
52. Nomoto,K. *et al.* (1994) The effects of bile acids on phospholipase C activity in extracts of normal human colon mucosa and primary colon tumors. *Mol. Carcinog.*, **9**, 87–94.
53. Gallegos,L.L. *et al.* (2008) Spatiotemporal dynamics of lipid signaling: protein kinase C as a paradigm. *IUBMB Life*, **60**, 782–789.

Received July 13, 2009; revised December 11, 2009; accepted January 10, 2010

Bioorganic & Medicinal Chemistry 18 (2010) 6886–6895

Contents lists available at ScienceDirect

Bioorganic & Medicinal Chemistry

journal homepage: www.elsevier.com/locate/bmc

Bile acid toxicity structure–activity relationships: Correlations between cell viability and lipophilicity in a panel of new and known bile acids using an oesophageal cell line (HET-1A)

Ruchika Sharma [a,b,*], Ferenc Majer [a], Vijaya Kumar Peta [a], Jun Wang [a], Ray Keaveney [a], Dermot Kelleher [b], Aideen Long [b], John F. Gilmer [a,*]

[a] School of Pharmacy and Pharmaceutical Sciences, Trinity College Dublin, Dublin 2, Ireland
[b] Cell Signalling, Institute of Molecular Medicine, Trinity Centre for Health Science, St. James's Hospital, Dublin 8, Ireland

ARTICLE INFO

Article history:
Received 25 March 2010
Revised 12 July 2010
Accepted 13 July 2010
Available online 19 July 2010

Keywords:
Bile acids
Lipophilicity
Physicochemical characteristics
Cell viability
Cytotoxicity
Azido steroid

ABSTRACT

The molecular mechanisms and interactions underlying bile acid cytotoxicity are important to understand for intestinal and hepatic disease treatment and prevention and the design of bile acid-based therapeutics.

Bile acid lipophilicity is believed to be an important cytotoxicity determinant but the relationship is not well characterized. In this study we prepared new azido and other lipophilic BAs and altogether assembled a panel of 37 BAs with good dispersion in lipophilicity as reflected in RPTLC R_{Mw}. The MTT cell viability assay was used to assess cytotoxicity over 24 h in the HET-1A cell line (oesophageal). R_{Mw} values inversely correlated with cell viability for the whole set ($r^2 = 0.6$) but this became more significant when non-acid compounds were excluded ($r^2 = 0.82$, $n = 29$). The association in more homologous subgroups was stronger still ($r^2 > 0.96$). None of the polar compounds were cytotoxic at 500 μM, however, not all lipophilic BAs were cytotoxic. Notably, apart from the UDCA primary amide, lipophilic neutral derivatives of UDCA were not cytotoxic. Finally, CDCA, DCA and LagoDCA were prominent outliers being more toxic than predicted by R_{Mw}. In a hepatic carcinoma line, lipophilicity did not correlate with toxicity except for the common naturally occurring bile acids and their conjugates. There were other significant differences in toxicity between the two cell lines that suggest a possible basis for selective cytotoxicity. The study shows: (i) azido substitution in BAs imparts lipophilicity and toxicity depending on orientation and ionizability; (ii) there is an inverse correlation between R_{Mw} and toxicity that has good predictive value in homologous sets; (iii) lipophilicity is a necessary but apparently not sufficient characteristic for BA cytocidal activity to which it appears to be indirectly related.

1. Introduction

Bile acids (BAs) exert multiple biological effects, non-specifically on organic solutes and membranes and specifically as signalling agents by binding to membrane and nuclear receptors.[1–3] Their peculiar effects on cell proliferation (negative and positive) attract attention because of the relevance of these phenomena to the pathogenesis of cholestatic liver diseases and intestinal carcinogenesis.[4–7] An understanding of the structural basis for the apoptotic effects of BAs is important to ongoing efforts to harness this property pharmacologically in the design of selective cytocidal and cytoprotective agents.[8–12]

A specific binding target(s) for BAs in triggering apoptotic processes remains elusive but there is substantial evidence for the involvement of membrane interactions.[13] The ability to induce necrosis through detergent effects is one manifestation of this.[14] At lower concentration, BAs can induce apoptosis through extrinsic and intrinsic pathways, and through ER stress.[7] Membrane effects are important in this context too. BAs can modify membrane fluidity and composition[15–17] as well as protein mobilization and activation[18] without directly affecting barrier function.[19] Some of these effects resemble those observed with non-BA hydrophobic solutes such as cholesterol myristate and detergents *n*-octylglycoside and Triton-X, at sub-lytic concentrations.[20]

Abbreviations: GCA, glcyocholic acid; GCDCA, glycochenodeoxycholic acid; GDCA, glycodeoxycholic acid; GUDCA, glycoursodeoxycholic acid; HSA, hydrophobic surface area; HCA, hyocholic acid; NCA, nutriacholic acid; UCA, ursocholic acid; PSA, polar surface area; TCA, taurocholic acid; TCDCA, taurochenodeoxycholic acid; TDCA, taurodeoxycholic acid; TUDCA, tauroursodeoxycholic acid.

* Corresponding authors. Tel.: +353 18963350/8962844; fax: +353 18962810 (R.S.); tel.: +353 18962795 (J.F.G.).
E-mail addresses: rsharma@tcd.ie (R. Sharma), gilmerjf@tcd.ie (J.F. Gilmer).

0968-0896/$ - see front matter © 2010 Elsevier Ltd. All rights reserved.
doi:10.1016/j.bmc.2010.07.030

An influential early observation about the SAR of BA toxicity was that deoxycholate (DCA) causes more membrane damage than cholic acid (CA) and its conjugates.[21] Numerous studies have since shown that DCA, chenodeoxycholic acid (CDCA) and lithocholic acid (LCA) have greater effects on cell viability[7] and mitochondrial function than other BAs.[22] They are also more toxic than their own glyco- and tauro-conjugates.[7,23] In partitioning experiments these BAs are lipophilic relative to other less toxic physiological BAs suggesting that lipophilicity and toxicity are associated or even correlated. The activation of PKC in vitro in constituted micelles correlated with chromatographic measures of hydrophobicity for DCA, ursodoexycholic acid (UDCA), CA and CDCA but especially with their taurine conjugates.[24] In a HCT116 cell line, growth arrest and apoptosis roughly paralleled a RPHPLC hydrophobicity ranking for a range of 16 BAs, though interestingly the behaviour of DCA and CDCA was not contiguous with the rest of the series.[25] LCA, DCA and CDCA occupy the toxic/hydrophobic end of the spectrum of common BAs but their toxicity may not be attributable to their hydrophobicity alone. In a recent study, natural bile acids LCA, CDCA and DCA were reported to initiate more apoptosis than their enantiomers *ent*-LCA, *ent*-CDCA and *ent*-DCA in HT-29 and HCT-116 cell lines. However, hydrophobic interactions are predicted to be identical in enantiomeric pairs unless the environment is itself chiral.[26,27]

In order to further explore the requirements for BA toxicity we constructed a panel of 37 naturally occurring and synthetic bile acids (Fig. 1). We sought to enrich the panel with new hydrophobic BAs. We focused especially on compounds related to UDCA and DCA being the prototypical cytoprotective and cytotoxic BAs, respectively. We were drawn in this regard towards azido analogues since the azide group is well known to enhance lipophilicity. We evaluated the relative polarity and effect on cell viability in the human oesophageal HET-1A cell line. We chose this line because of our ongoing investigation into the role of BAs in provoking oesophageal cancer. The objective of the present study was to

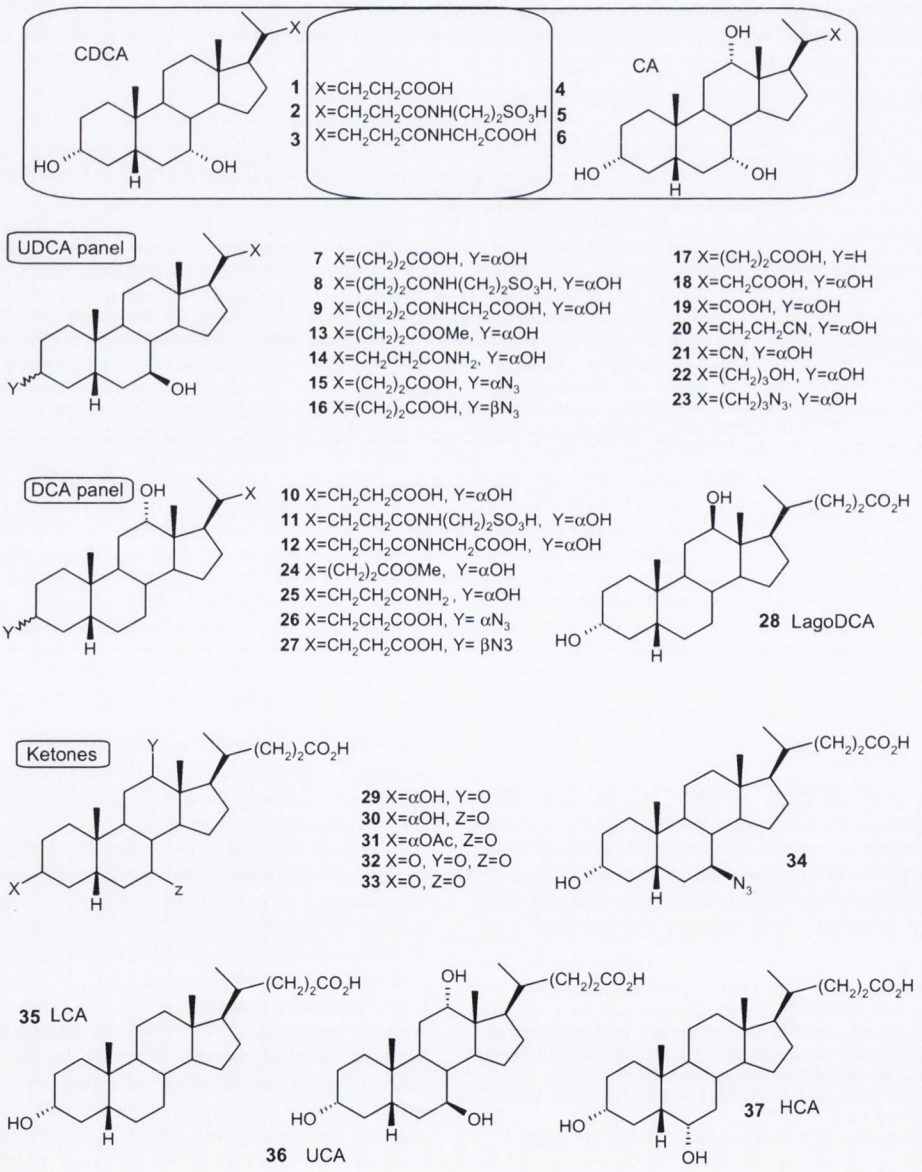

Figure 1. Structures of BAs.

characterize the relationship between cytotoxicity and polarity and to investigate if toxicity is related to functional group type and arrangement in synthetic and natural BAs.

2. Results and discussion

2.1. Synthesis

A group of 16 BAs was assembled from gifts and commercially available products. This was augmented with 21 compounds previously reported and synthesised for this study or newly prepared and characterised (compound identity synthesised using conventional methods was confirmed from references listed in Table 1). UDCA and DCA 3-azides were synthesised as outlined in Scheme 1 from the respective protected BAs **38** and **41**, which were prepared in three steps from the parent BAs. Introduction of 3α-azides (**15**, **26**) (i.e., with retention of configuration) was accomplished by generating first the β-bromides (**39**, **42**). The β-azides (**16**, **27**) could be obtained by direct SN2 substitution on the α-mesylates (**40**, **43**). Similarly, the 7-β azido analog of UDCA (**34**) was generated by treating the appropriately protected CDCA-derived mesylate (**45**) with NaN_3 in DMPU followed by deprotection in aqueous base. The 24-azido UDCA (**23**) was prepared by $LiAlH_4$ reduction of UDCA to alcohol **22** followed by regioselective mesylation of the primary alcohol in cold solvent. Chromatographic isolation yielded the 24-mesylate (**46**) (and 3α, 24 dimesyloxy UDCA) in pure form after which azide substitution with NaN_3 in DMPU afforded the 24-azide. By performing various conventional side chain (Scheme 2) and 3-OH transformations (including the 3-deoxy compound **17**), we assembled a panel of 15 UDCA analogs in which the 7-βOH group was conserved (Fig. 1). Notably, eight of these retained an ionizable side chain (**7–9**, **15–19**). For comparison, seven DCA analogs were assembled along with LagoDCA (**28**) the epimeric 12-βOH compound (Fig. 1). A third panel consisted of five oxosteroid analogues (**29–33**).

2.2. Reverse phase thin layer chromatography (RPTLC)

RPTLC has been used widely for lipophilicity determination including for BAs.[28,29] Relative to LOGP/D experiments it has the usual chromatographic advantages; relative to HPLC it has higher throughput and, for generally UV transparent analytes such as BAs, it permits simple post-chromatographic derivatization. We developed the RPTLC approach here using commercially available BAs UDCA, CDCA, CA and DCA along with their glycine and taurine conjugates (compounds **1–12**). The relationship between retention and pH was assessed in the pH range 5.4–8.4 for this group. The approach was optimised with respect to pH and solvent composition before application to the wider panel of compounds. Over four concentration levels in the organic modifier concentration range (ϕ) 50–80% the relationship with R_M was linear (r^2 >0.99) which allowed the R_{Mw} to be estimated by extrapolation:

Table 1
BAs physicochemical properties (R_{Mw}, total hydrophobic surface area (HSA), total polar surface area (PSA))

Compound number and trivial name	R_{Mw}	HSA (Å^2)	PSA (Å^2)	Cell viability at24 h 500 (μM) (HET-1A)	CC_{50} (μM) (95% CI)	Cell viability at 24 h 500 (μM) (Huh7)
1 CDCA	4.193	458	157	0.422	216 (134–346)	0.723
2 GCDCA	2.926	450	230	1.116	nd	1.146
3 TCDCA	2.597	521	233	1.300	729	1.053
4 CA	3.25	433	183	1.016	1075 (910–1270)	0.908
5 GCA	2.243	430	237	1.121	nd	0.879
6 TCA	1.908	493	254	1.052	nd	0.877
7 UDCA	3.35	452	164	0.788	1313 (997–1727)	0.740
8 GUDCA	2.124	452	234	1.073	1002 (753–1333)	1.049
9 TUDCA	1.717	520	231	1.092	nd	1.038
10 DCA	4.023	454	156	0.412	257 (199–332)	0.570
11 GDCA	2.926	455	222	1.148	nd	1.062
12 TDCA	2.529	517	229	1.113	1237	1.050
13 MeUDCA[37]	4.776	514	146	0.943	nd	0.812
14 UDCA-24NH_2[38]	4.54	447	185	0.397	161 (115–225)	0.500
15 UDCA3αN3	5.412	445	205	0.368	45 (28–70)	0.266
16 UDCA3βN3	5.452	446	194	0.303	37 (30–44)	1.009
17 3deoxyUDCA[39]	5.304	475	145	0.399	30 (22–40)	0.237
18 Nor UDCA[40]	3.395	427	158	0.888	nd	0.718
19 BisNorUDCA[41]	3.623	416	147	0.805	799	0.748
20 UDCA24CN	4.938	449	162.3	0.940	nd	0.852
21 BisNorUDCACN	3.623	413	155	0.805	nd	0.873
22 UDCA-24OH[42]	5.032	480	140	0.975	nd	0.445
23 UDCA-24N_3	5.299	476	181	0.759	688 (206–1000)	0.451
24 MeDCA[43]	4.697	512	137	0.281	46 (30–69)	0.488
25 DCA-24NH_2[38]	3.895	451	176	0.386	39 (32–49)	0.252
26 DCA3αN3	5.402	441	196	0.307	71 (59–84)	0.371
27 DCA3βN3[44]	5.454	452	193	0.354	97 (72–129)(	1.085
28 LagoDCA[45]	3.89	457	158	0.590	389 (251–601)	0.890
29 12-KetoLCA[43]	3.66	457	157	0.818	nd	0.806
30 NCA[46]	4.468	452	155	0.769	nd	0.756
31 NCA3-acetate[47]	5.638	480	172	0.472	366 (260–516)	0.777
32 3,7,12-ketone[48]	1.925	425	175	1.109	nd	0.544
33 3,7-diketone[48]	3.266	447	152	0.935	nd	0.546
34 3OH,7βN3	5.466	440	203	0.290	99 (65–147)	0.641
35 LCA	5.27	479	130	0.417	25 (17–36)	0.637
36 UCA[49]	3.011	429	186	0.808	nd	0.823
37 HCA[50]	4.407	428	188	0.882	nd	0.738

The effect on cell viability relative to control in the HET-1A cell line after 24 h incubation is shown (n = 6) along with an estimated CC_{50} for this. The effect in the hepatic Huh7 line was also evaluated. Compounds were introduced in DMSO and cell viability was normalised to control DMSO at the same concentration.

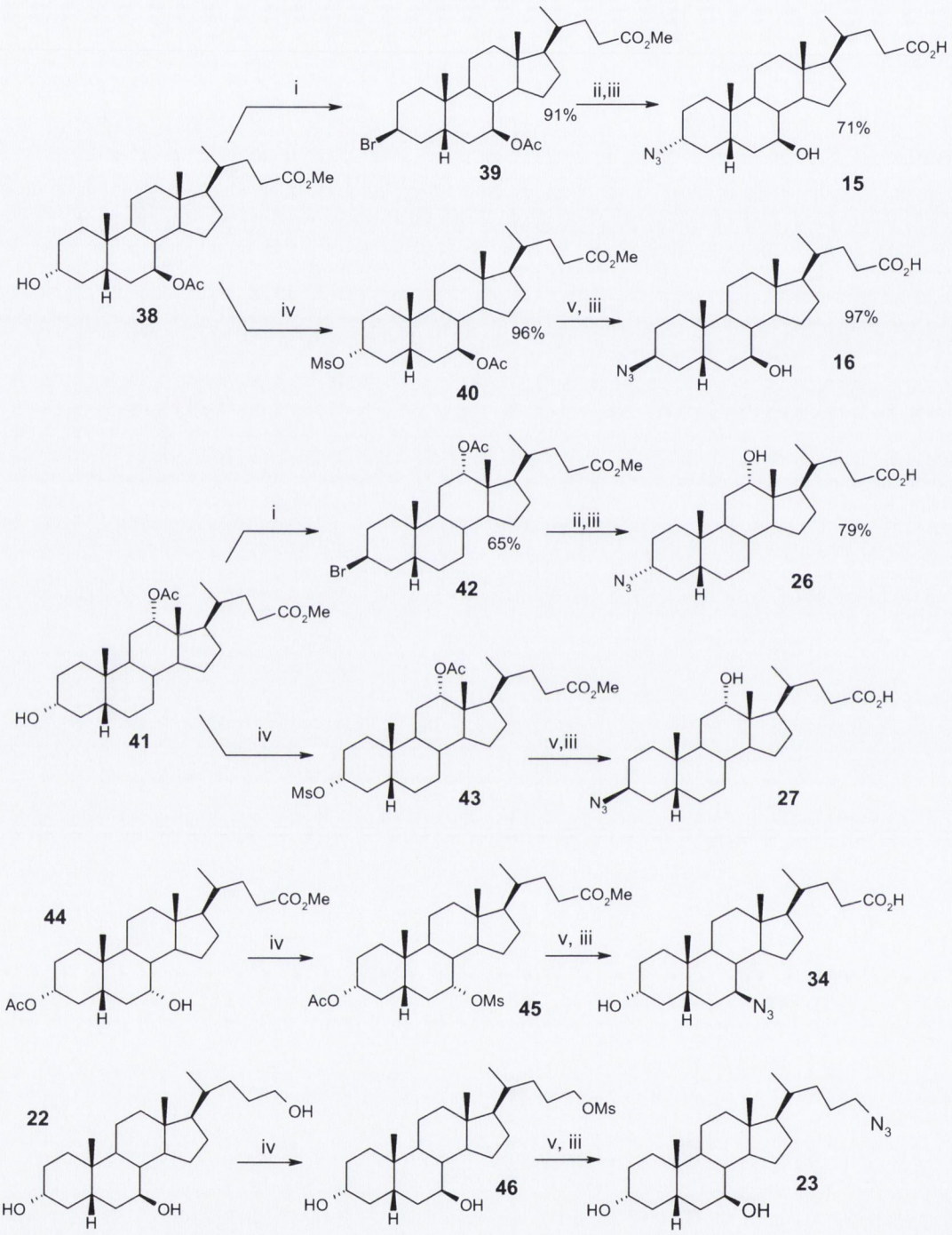

Scheme 1. Synthesis of azidobile acids. Reagents and conditions: $P(Ph_3)_3$, NBS, THF, −18 °C to rt, 1.5 h; (ii) NaN_3, DMF, 60 °C, 3 d; (iii) 2 M NaOH/MeOH (pH ~14), reflux, 24 h; (iv) MsCl, NEt_3, DCM, 0 °C, 20 min; (v) NaN_3, DMPU, 50 °C.

$$R_M = -S\phi + R_{Mw} \quad \text{where } R_M = \text{Log}(1/R_f - 1)$$

The slope S which is a measure of the degree of responsiveness to changes in mobile phase composition was found to be linear with R_{Mw} for the set. For the set of 12 development compounds R_{Mw} values were estimated at pH 5.4, 7.4, 8.4. In most cases, including, unexpectedly, the taurine conjugates, R_{Mw} values were higher at pH 5.4 than at the latter two pH values, which were similar. It was decided therefore to assess the retention for the whole group of 37 compounds at pH 7.4 since this was the pH at which toxicity was to be determined in the cell-based assay and variations due to shifts in pK_a in methanol mixtures had been shown to be marginal. The rank order at pH 7.4 for the initial test set of 12 was: CDCA~DCA≫UDCA>CA>GDCA>GCDCA>TCDCA>TDCA >GCA>GUDCA>TCA>TUDCA. This is roughly as expected and in accordance with numerous studies on the relative chromato-

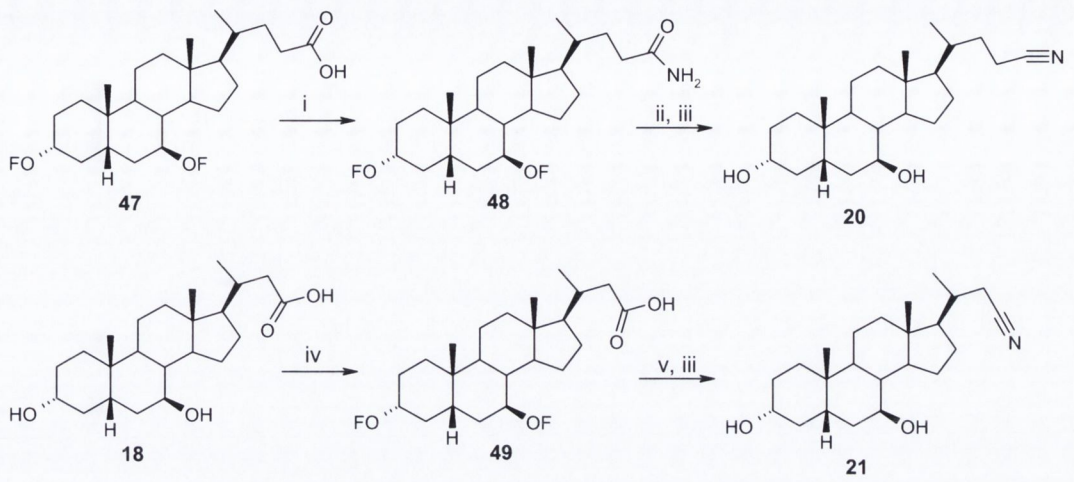

Scheme 2. Synthesis of nitriles: (i) $(BOC)_2O$, pyridine, NH_4HCO_3, rt, 24 h; (ii) trifluoroacetic anhydride/pyridine (1:1); (iii) NaOMe/MeOH reflux, 1 h; (iv) formic acid, perchloric acid 47 °C, 3 h; (v) THF, rt, 3 h. TFA, trifluoroacetic anhydride, $NaNO_2$ 0–5 °C (1 h), 38–40 °C (2 h).

graphic retention of these bile acids and their conjugates.[30,31] Retention in RP chromatographic systems is a function of the number of hydroxyl groups, their topological arrangement and extent of ionisation, bearing in mind the differences between glyco- and tauro-conjugates.[30] Relative retention of the BAs is also influenced by organic modifier and stationary phase identity.[31] The relative retention of unconjugated CA to UDCA was found to be pH dependent in our system but at pH 7.4 CA (3.25) was slightly more polar than UDCA (3.35) which accords with its greater hydrophilicity in other measures such as Log *D* and water solubility.[32] On the other hand the UDCA conjugates GUDCA and TUDCA were more polar than the corresponding CA conjugates. There was a significant inverse correlation between R_{Mw} and estimated polar surface area ($r^2 = 0.81$) in this set, little correlation with hydrophobic surface area ($r^2 = 0.15$) and a moderate positive correlation with the ratio of HSA to PSA ($r^2 = 0.65$). Associations with these global properties are strongly influenced by variation in molecular size and substitution pattern. For example, tauro- and glyco-conjugates have increased HSA and PSA relative to the unconjugated compounds and hence the HSA:PSA ratio does not reflect the decreased R_{Mw}. R_{Mw} data for the whole set at pH 7.4 is presented in Table 1.

The panel as a whole (**1–37**) exhibited satisfactory dispersion and range in lipophilicity as reflected in R_{Mw} (1.717(**9**)–5.466(**34**)) (Table 1). The six azido-analogs were highly lipophilic as expected. Indeed the azides with ionizable side chains were more highly retained than some of the non-azido neutral compounds. However, on the whole the neutral compounds such as the esters and amides yielded R_{Mw} values above the median. Introduction of keto (oxo) groups at the 3, 7 and 12 positions has the effect of depressing hydrophobicity by promoting water access to both faces of the steroid[28,29] and this had the expected effect on R_{Mw} through compounds **29–33**.

2.3. Effects on cell viability

Cell viability in the oesophageal HET-1A line was determined at an initial BA test concentration of 500 μM for all compounds in the set over 24 h (Fig. 2). This high concentration (pharmacologically) has been widely used to evaluate BA toxicity. It has been reported that 500 μM DCA causes cell death through apoptosis rather than necrosis.[19] Moreover, BAs can achieve this concentration in vivo and during UDCA treatment.[33,34] In the present case it allowed relative toxicity assessment of compounds that are moderately cytotoxic. Where we observed a significant effect on cell viability at 500 μM, the experiment was repeated at successively lower concentration in order to estimate a CC_{50} value (half maximal cytotoxic concentration). In a number of cases the experiment was repeated at increasing concentration up to 10 mM. Concentration response curves were not calculated in cases where there were poor convergence using a monophasic sigmoid function. The 500 μM cell viability values were found to be most useful therefore for comparisons and they were consistent with CC_{50} values in cases where these were estimated. It is also worth noting that while the results here for classical bile acids are consistent with reported effects on cell viability using other measures of apoptosis, the MTT assay is a reflection of mitochondrial function which could be attenuated in cells that are nonetheless alive. On the other hand BA induction of apoptosis is to a significant extent due to mitrochondrial interactions directly and indirectly.

In this context the following general structure-cytotoxicity observations can be made: (i) glycine and taurine conjugates of CA, CDCA, DCA and UDCA were not cytotoxic at 500 μM. There was in these cases a trend towards increased cell proliferation which only achieved statistical significance in the case of TDCA. Three of these compounds (**3**, **8**, **12**) did trigger cell death when the concentration was raised to >1 mM. The conjugates and least toxic unconjugated BAs caused cell death at a similar concentration suggesting that for these compounds the mechanism of cell death was not structure specific and at such high concentration attributable to detergency and necrosis. The HET-1A cell line is not known to express a BA transporter and therefore considered impermeable to the BA conjugates; (ii) CDCA, DCA and particularly LCA were potently cytotoxic as expected (Table 1); (iii) all of the ionisable azido compounds were potently cytotoxic. The UDCA and DCA 3-azido analogues were significantly more toxic than the parent compounds. Indeed the UDCA 3-azides were more toxic than the corresponding DCA compounds. The 7β-azido compound (**34**) was also cytotoxic (CC_{50} 99 μM) however the UDCA-based 24-azide had not effect on cell viability at 500 μM despite its high lipophilicity; (iv) the DCA and UDCA primary amides (**25**, **14**) markedly reduced viability (CC_{50} 39, 161 μM, respectively); (v) in contrast, the DCA methyl ester (**24**) was more toxic that DCA itself but the UDCA analogue **13** was not more toxic than UDCA. DCA methyl ester **24** was not acting as a prodrug for DCA in this context because it could be recovered unchanged from the medium at 24 h; (v) the 3-deoxy UDCA compound (**17**) (an isomer of LCA)

was highly toxic; (vi) apart from the amide **14**, the UDCA side chain analogs (**18–23**) which are neutral and hydrophobic were not cytotoxic; (vii) oxidation of the steroid secondary alcohols to ketone level was associated with a reduction in cytotoxicity. This is consistent with the reported haemolytic potential of this series.[28,29]

Overall, the most polar compounds were least cytotoxic and there was an association between lipophilicity and toxicity with some important exceptions, which are discussed below. The azido and amide analogs were stable over the time course of the experiments as evidenced by TLC/HPLC.

2.4. Relationship between lipophilicity and cell viability in the HET-1A cell line

A relationship between lipophilicity and toxicity of BAs has been speculated to exist for some time based mainly on the contrasting behaviour of LCA, DCA and CDCA and more polar di- and tri-hydroxy BAs such as UDCA and CA. In the present set of 37 compounds there was a significant negative correlation between R_{Mw} and cell viability at 24 h ($r^2 = 0.6$) (Fig. 3). A similar significance level was achieved using the sparser CC_{50} values. The strength of the association was significantly increased when the neutral

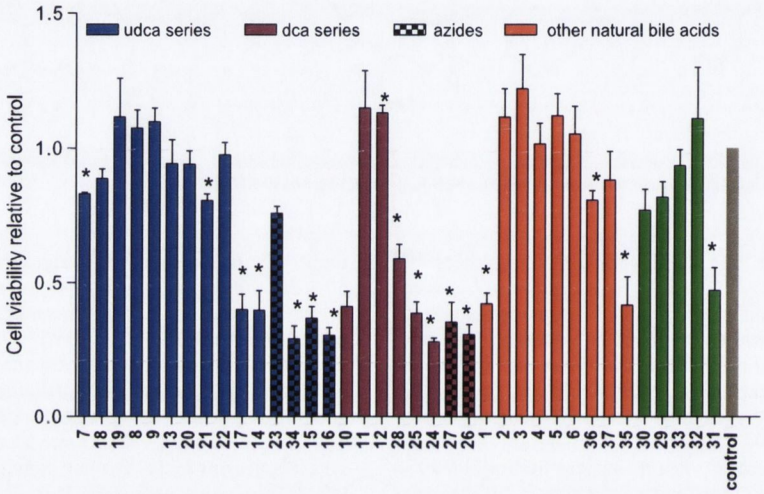

Figure 2. Effect of compounds **1–37** on HET-1A viability at 500 μM: $n = 6$, $^{*}p < 0.05$.

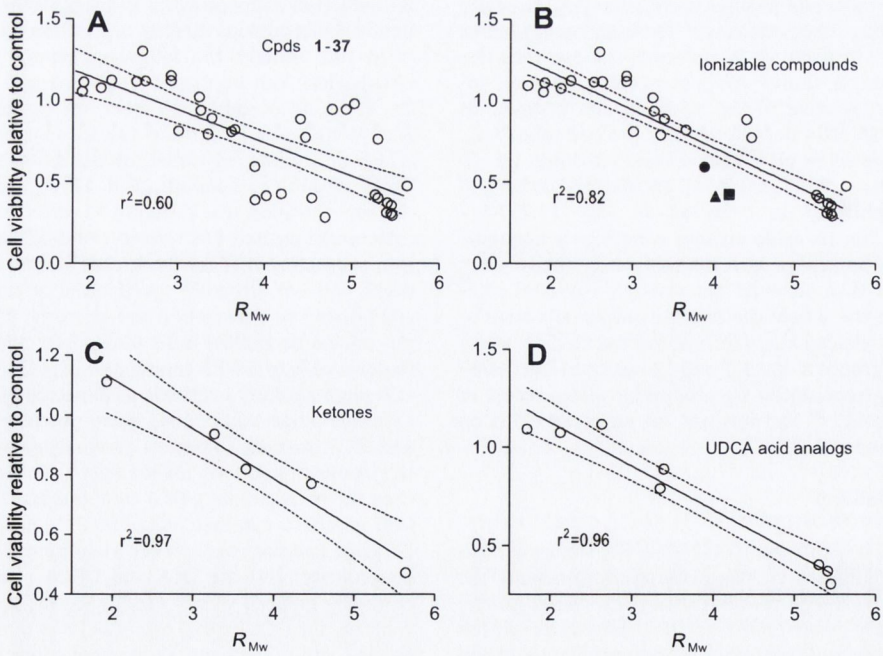

Figure 3. Linear regression lines showing 95% confidence bands for cell viability at 24 h in the HET-1A cell line and R_{Mw}. The panels show: (A) linear regression for compounds **1–37**; (B) linear regression for the ionisable (acidic) compounds **1–12, 15–19, 26–37**; CDCA (■) DCA (▲) and LagoDCA (●) are highlighted; (C) linear regression for the ketones **29–33**; (D) linear regression for the UDCA analogues with an acidic side chain.

compounds were excluded (Fig. 3B: $r^2 = 0.82$, $n = 29$). This might be explained by differences in ionization between the neutral and acid compounds that overwhelm more subtle retention interactions. However, in the group of neutral compounds ($n = 8$) there was a very weak association between R_{Mw} and cell viability ($r^2 = 0.11$). The correlation between R_{Mw} and toxicity may therefore be contingent on BA amphilicity.

It is notable that DCA, CDCA and LagoDCA are out of trend (Fig. 3B) being significantly more toxic than predicted on the basis of R_{Mw}. This may be evidence for an additional more specific mechanism for cell death induction in these cases. Interestingly, these three BAs are reported to depart from the norm in prosecretory behaviour and toxicity towards colon cells.[19,35]

Excellent correlations were obtained for the ionisable UDCA group ($r^2 = 0.96$, $n = 8$) and the ketone panel ($r^2 = 0.97$, $n = 5$) (Fig. 3C and D); focussing in this way on relatively homologous groups minimizes confounding structural factors. It would be interesting to assess correlations in even more homologous BA series with diverse lipophilicity such as fluoro- or methyl-substituted BAs. There were no significant correlations between the in silico bulk hydophobicity/polarity indices (HSA, PSA) and cell viability, consistent with the idea that (relative) BA hydrophobicity/lipophilicity is a shape dependent property[36] that is better predicted chromatographically.[28]

2.5. Relationship between lipophilicity and cell viability in the Huh7 cell line

In order to assess the generality of the findings made in the oesophageal cell line, we evaluated the effect of the compounds on the MTT signal in the Huh7 cell line at 24 h (500 μM, $n = 3$; Table 1). This cell line is a human hepatic carcinoma cell line with significantly different characteristics to the HET-1A line (hepatic versus oesophageal, cancer versus normal). Nevertheless we were able to make some interesting observations. The mean MTT signal was similar in both sets (0.75). Overall there was a weak correlation between MTT values between the two sets ($r^2 = 0.28$). There was also a weak correlation in the Huh7 set between cell viability and lipophilicity ($r^2 = 0.22$). This residual correlation appeared to be dependent on the contribution from the development set of naturally occurring BAs CA, CDCA, DCA, UDCA, their glyco- and tauro-conjugates and LCA ($r^2 = 0.52$, $n = 13$). The results for these compounds correlated well between the two cell lines ($r^2 = 0.8$). Amongst the rest of the compounds ($n = 24$), mainly synthetic BAs, there was no relationship between lipophilicity and cytotoxicity in the hepatic cell line. The cytotoxicity in the hepatic cell line seemed in general to be more structure dependent and less on lipophilicity. For example, whereas in the HET-1A cell line, the 3α- and 3β-azides of UDCA and DCA were all cytotoxic, in the Huh7 line, the α- and β-compounds diverged: the α-azides of UDCA and DCA (**15**, **26**) were toxic whereas the β-azides were not. This had a significant effect on the strength of the correlation in the UDCA set in the Huh7 cell line which was otherwise strong. The 24-azide and -alcohol compounds (**23**, **22**) were significantly more toxic in the Huh7 cell line than in the HET1-A line. Whether these observations are attributable to differences in metabolic competency (and detoxification) or to intrinsic cytocidal effect they suggest prospects for selective toxicity.

3. Conclusions

In BAs, azido substitution is associated with enhanced toxicity and the azide group may therefore be a useful design tool for BA-based cytotoxic agents. Azide orientation may be important in determining toxicity which could be useful in the design of selective cytocidal agents. Simple DCA and UDCA amides also hold promise in this regard. RPTLC retention extrapolated to zero organic modifier was predictive of BA toxicity in the HET-1A cell line and it could be a useful high throughput tool for cytotoxic BA discovery and development in this context. This is the first direct linear correlation between BA toxicity and a lipophilicity parameter that we are aware of.

The lipophilicity–toxicity correlation was strongest with acidic BAs and it was especially strong in structurally homologous subgroups. We are unable to say whether the association is due to a hidden common factor, membrane-perturbation effects or whether it is a reflection of a capacity to bind specifically to unidentified BA target proteins: correlations between lipophilicity and affinity/potency are well known. Significantly, the correlation broke down for non-ionizable lipophilic BAs, and it does not fully account for the toxicity associated with DCA, CDCA and LagoDCA. Apart from the naturally occurring bile acids and their conjugates, the correlation between lipophilicity and cytotoxicity did not hold in a hepatic carcinoma cell line (Huh7). Collectively, the results indicate that the relationship between lipophilicity and toxicity is complex, and probably indirect.

4. Experimental

4.1. Synthesis

Uncorrected melting points were obtained using a Stuart® melting point SMP11 melting point apparatus. Spectra were obtained using a Perking Elmer 205 FT Infrared Paragon 1000 spectrometer. Band positions are given in cm^{-1}. Solid samples were obtained by KBr disk; oils were analyzed as neat films on NaCl plates. ^1H and ^{13}C spectra were recorded at 27 °C on a Bruker Advance II 600 MHz spectrometer (600.13 MHz ^1H, 150.91 MHz ^{13}C) and Bruker DPX 400 MHz FT NMR spectrometer (400.13 MHz ^1H, 100.16 MHz ^{13}C), in either $CDCl_3$ or CD_3OD, (tetramethylsilane as internal standard). For $CDCl_3$, ^1H NMR spectra were assigned relative to the TMS peak at 0.00 δ and ^{13}C NMR spectra were assigned relative to the middle $CDCl_3$ triplet at 77.00 ppm. For CD_3OD, ^1H and ^{13}C NMR spectra were assigned relative to the centre peaks of the CD_3OD multiplets at 3.30 δ and 49.00 ppm, respectively. High resolution mass spectrometry (HRMS) was performed on a Micromass mass spectrophotometer (EI mode) at the Department of Chemistry, Trinity College. HPLC was performed on a reverse phase 250 mm × 4.6 mm Waters Spherisorb ODS-2, 5 μm column using a Waters Alliance 2695 chromatograph equipped with an autosampler, column oven and dual wavelength detector. The flow rate was 1 ml/min with a mobile phase consisting of 40% phosphate buffer pH 2.5 and 60% acetonitrile at time 0 and grading to 85% acetonitrile at 4 min. Injection volume was 20 μl, and areas determined at 254 nm. The isocratic HPLC method was aqueous phosphate buffer solution pH 2.5 40% and acetonitrile 60%. Flow rate was 1 ml/min. Flash chromatography was performed on Merck Kieselgel 60 particle size 0.040–0.063 mm. TLC was performed on silica gel Merck F-254 plates. Compounds were visually detected by absorbance at 254 nm and/or vanillin staining.

BAs **1–12** and **35** (Table 1) were obtained from Sigma–Aldrich Chemical Co. (St. Louis, MO, USA). UCA and HCA (**36**, **37**) were a gift from Professor B. Natalini (University of Perugia). Identity of all BAs was confirmed with ^1H NMR, ^{13}C NMR and HRMS. Purity was confirmed by HPLC and TLC.

4.1.1. 24-Methyl 3β-bromo, 7β–acetoxy-5β-cholanoate (39)

Triphenylphosphine (0.170 g) was added to a stirred solution of **38** (0.145 g) in anhydrous THF (15 ml) and the mixture was cooled to −18 °C. *N*-Bromosuccinimide (0.115 g) was added dropwise and

the mixture allowed to warm to room temperature. After 1.5 h, when TLC analysis showed no more starting material, the reaction mixture was poured into water (50 ml) and extracted with ethyl acetate (3 × 50 ml). The organic phase was dried over $MgSO_4$, filtered and the solvent was evaporated under reduced pressure. The product was separated by flash chromatography, using hexane/ethyl acetate 3:1 as mobile phase to yield colourless oil (0.151 g, 91%). ^1H NMR δ ($CDCl_3$): 4.76 (s, 1H, 3α-H), 4.69 (m, 1H, 7α-H), 3.67 (s, 3H, –O–CH_3), 2.00 (s, 3H, 7-C=OCH_3), 1.06 (s, 3H, 19-CH_3), 0.93 (d, 3H, J = 6.53 Hz, 21-CH_3), 0.69 (s, 3H, 18-CH_3). ^{13}C NMR ppm ($CDCl_3$): 174.83 (C=O, 24-C), 170.81 (C=O, 7-OC=OCH_3), 74.01 (CH, 7-C), 51.64 (CH_3, OCH_3), 21.97 (CH_3, 7-C=OCH_3). IR_{vmax} (DCM): 3435.54, 2948.89, 1729.41, 1646.49 and 1243.23 cm^{-1}. HRMS: Found: $(M-Na)^+$ = 533.2249.

4.1.2. 3α-Azido, 7β–hydroxy-5β-cholanoate (15)

To a stirred solution of **39** (1.876 g) in anhydrous *N,N*-DMF (40 ml) was added 5 equiv NaN_3 (1.192 g) at 60 °C. The mixture was stirred overnight then poured into saturated aqueous $NaHCO_3$ (150 ml) and extracted with ethyl acetate (3 × 100 ml). The organic phase was washed with brine (200 ml), dried over $MgSO_4$, filtered and the solvent was evaporated in vacuum. The product was separated on a flash column (hexane/ethyl acetate 9:1) to yield orange foam (1.258 g, 72%). The azide (0.150 g) was dissolved in methanol (15 ml) to which was added 2 M sodium hydroxide solution to pH ~14 and stirred at reflux for 1 day, when TLC analysis showed the hydrolysis was complete. Then the reaction mixture was poured into 1 M HCl solution (50 ml) and extracted with ethyl acetate (3 × 50 ml). The organic layer was washed with water (2 × 100 ml) and brine (1 × 100 ml), dried over Na_2SO_4, filtered and the solvent was removed under reduced pressure to give the product as a light yellow solid (0.131 g, 99%). ^1H NMR δ ($CDCl_3$): 3.60 (m, 1H, 7α-H), 3.30 (m, 1H, 3β-H), 0.98 (s, 3H, 19-CH_3), 0.96 (d, 3H, J = 6.53 Hz, 21-CH_3), 0.69 (s, 3H, 18-CH_3). ^{13}C NMR ppm ($CDCl_3$): 180.19 (C=O, 24-C), 71.68 (CH, 7-C), 61.30 (CH, 3-C). IR_{vmax} (KBr): 3375.06, 2934.00, 2867.03, 2093.18, 1690.57 and 1255.27 cm^{-1}. HRMS: Found: $(M-Na)^+$ = 440.2896.

4.1.3. 24-Methyl 3α-(methylsulfonyl)oxy, 7β-acetoxy-5β-cholanoate (40)

To a solution of **38** (1 g) and triethylamine (0.34 ml) in anhydrous dichloromethane (30 ml) was added methanesulfonylchloride (0.26 ml in 10 ml anhydrous DCM) dropwise at 0 °C and stirred for 20 min. Then, cooled water (50 ml) was added to the mixture, which was separated and the aqueous phase was extracted with DCM (2 × 40 ml). The organic phase was washed with brine (100 ml), dried over $MgSO_4$, filtered and the solvent was removed under reduced pressure to give colourless oil as product (1.115 g, 95%). ^1H NMR δ ($CDCl_3$): 4.77 (m, 1H, 7α-H), 4.62 (m, 1H, 3β-H), 3.68 (s, 3H, –O–CH_3), 3.02 (s, 3H, –OSO_2CH_3), 2.00 (s, 3H, 7-C=OCH_3), 0.99 (s, 3H, 19-CH_3), 0.94 (d, 3H, J = 6.02 Hz, 21-CH_3), 0.69 (s, 3H, 18-CH_3). ^{13}C NMR ppm ($CDCl_3$): 174.82 (C=O, 24-C), 170.70 (C=O, 7-OC=OCH_3), 81.72 (CH, 3-C), 73.42 (CH, 7-C), 52.68 (CH_3, –OSO_2CH_3), 51.64 (CH_3, OCH_3), 21.92 (CH_3, 7-C=OCH_3). IR_{vmax} (DCM): 3436.82, 2950.45, 2873.89, 1729.45, 1646.30 and 1173.83 cm^{-1}. HRMS: Found: $(M-Na)^+$ = 549.2858.

4.1.4. 3β-Azido, 7β-hydroxy-5β-cholanoate (16)

Compound **40** (0.705 g) and sodium azide (0.870 g) in DMPU (20 ml) were stirred at 50 °C for 11 days (TLC hexane/ethyl acetate 3:1) then poured into water (50 ml) and extracted with ethyl acetate (3 × 50 ml). The organic phase was washed with brine (100 ml) dried over $MgSO_4$, filtered and the solvent was removed under reduced pressure to give the crude product as yellow oil. This was flash columned using 5% then 10% ethyl acetate in hexane as mobile phase to yield white solid as product (0.537 g, 85%). ^1H NMR δ (400 MHz, $CDCl_3$): 4.74 (m, 1H, 7α-H), 3.95 (s, 1H, 3α-H), 3.68 (s, 3H, –O–CH_3), 2.00 (s, 3H, 7-C=OCH_3), 1.01 (s, 3H, 19-CH_3), 0.93 (d, 3H, J = 6.53 Hz, 21-CH_3), 0.69 (s, 3H, 18-CH_3). ^{13}C NMR ppm ($CDCl_3$): 174.52 (C=O, 24-C), 170.52 (C=O, 7-OC=OCH_3), 73.47 (CH, 7-C), 57.94 (CH, 3-C), 51.33 (CH_3, OCH_3), 21.65 (CH_3, 7-C=OCH_3). IR_{vmax} (DCM): 3445.10, 2946.85, 2871.37, 2102.43, 1736.79 and 1248.22 cm^{-1}. HRMS: Found: $(M-Na)^+$ = 496.3164. The crude ester azide was hydrolysed as described above (**4.1.2**) yielding the azide (**16**) as a white solid. ^1H NMR δ ($CDCl_3$): 3.93 (s, 1H, 3α-H), 3.55 (m, 1H, 7α-H), 1.00 (s, 3H, 19-CH_3), 0.96 (d, 3H, J = 6.02 Hz, 21-CH_3), 0.70 (s, 3H, 18-CH_3). ^{13}C NMR ppm ($CDCl_3$): 179.81 (C=O, 24-C), 71.54 (CH, 7-C), 58.42 (CH, 3-C). IR_{vmax} (KBr): 3330.87, 2929.30, 2867.30, 2103.92, 1687.49 and 1243.05 cm^{-1}. HRMS: Found: $(M)^-$ = 416.2913.

4.1.5. 3α,7β-Dihydroxy-5 β-cholan-24-nitrile (20)

Formyl UDCA amide (**48**) (0.42 g) was dissolved in dry THF (10 ml) at 0 °C. Pyridine (150 μl) and trifluoroacetic anhydride (270 μl) were added to this mixture. After completion of the reaction as monitored by TLC (10 h) the solvent was removed in vacuo and the residue redissolved in ethyl acetate (20 ml) which was then washed with HCl (3 × 20 ml) and water to neutrality. Chromatographic elution with ethyl acetate/hexane (1:1) afforded a white solid. Sodium (0.2 g) was added to methanol (10 ml) to form an excess of sodium methoxide. The formyl nitrile obtained in the above reaction was added to this solution which was then refluxed for 2 h. After 2 h the reaction was cooled to room temperature and added to water (20 ml). The nitrile product (**20**) was extracted with ethyl acetate. The organic layer was then washed with water (3 × 20 ml) and dried ($MgSO_4$). The solvent was removed in vacuo to yield a white solid (0.3 g, 78%). ^1H NMR δ (MeOD) 3.50 (m, 2-H, 3-β H, 7-α H), 2.8 (m, 1-H, 20-CH), 1.00 (d, 3-H, J = 6.02 Hz, 21-CH_3), 0.98 (s, 3-H, 19-CH_3), 0.75 (s, 3-H, 18-CH_3). ^{13}C NMR ppm ($CDCl_3$): 124 (CN, 22-C), 71 (3-C, 7-C). HRMS: Found: $(M-Na)^+$ 396.2867.

4.1.6. 3α,7β-Dihydroxy-24-bisnor-5β-cholane-22-nitrile (21)

Formyl protected norUDCA (3.5 g) (**18**) was stirred in trifluoroacetic acid (4 ml) and trifluoroacetic anhydride (1 ml) at 0–5 °C until dissolution was complete. Sodium nitrite (0.786 g) was then added in small portions, waiting for the salt to react between additions. After addition the mixture was stirred at 0–5 °C for 1 h. The mixture was then warmed to 38–40 °C and left to stir for another 2 h. The brown solution was cooled to room temperature and added to a mixture of water/1 M NaOH (1:1, 50 ml). The nitrile was extracted with ethyl acetate and washed with NaOH (4 × 20 ml) and water to neutrality. The ethyl acetate was dried ($MgSO_4$) and removed in vacuo to yield an off white solid. Sodium (1 g) was added to MeOH (50 ml) to form an excess of sodium methoxide. The formyl bisnornitrile obtained in the above reaction was added to this solution and refluxed for 2 h. After 2 h the reaction was cooled to room temperature and added to water (100 ml). The title compound was extracted with ethyl acetate. The organic layer was then washed with water (3 × 20 ml) and dried ($MgSO_4$). The solvent was removed in vacuo to yield a white solid (2.6 g, 94%). ^1H NMR δ ($CDCl_3$) 3.48 (m, 2-H, 3-β H, 7-α H), 2.8 (m, 1-H, 20-CH), 1.34 (d, 3-H, J = 7.02 Hz, 21-CH_3), 1.00 (s, 3-H, 19-CH_3), 0.76 (s, 3-H, 18-CH_3). ^{13}C NMR ppm ($CDCl_3$): 124 (CN, 22-C), 71 (3-C, 7-C). HRMS: Found: $(M)^-$ = 344.2590.

4.1.7. 3α,7β-Dihydroxy-5 β-cholan-24-azide (23)

3α,7β,24-Trihydroxy-5 β-cholane (0.2 g) (**22**) was dissolved in dry pyridine (4 ml) at 0 °C followed by the addition of methane sulfonyl chloride (63 μl). After 20 min the reaction was quenched by adding crushed ice and the compound was extracted with ethyl acetate (2 × 10 ml). The organic layer was washed with cold water

(2 × 20 ml), cold HCl (2 × 20 ml) and dried ($MgSO_4$) to afford a white solid (**46**). TLC of this product revealed starting material and a new product spot. Chromatographic elution with ethyl acetate afforded a white solid (0.13 g, 53%). The product was dissolved in DMPU and treated with an excess of NaN_3 at 50 °C for two days. The title compound was obtained by partitioning between ethyl acetate and water, followed by successive acid and base wash, evaporation and flash chromatography. ^{1}H NMR δ (MeOD) 3.5 (m, 2-H, 3-β H, 7-α H), 3.26 (m, 2-H, 23-CH_2), 0.99 (d, 3-H, J = 6.02, 21-CH_3), 0.95 (s, 3-H, 19-CH_3), 0.70 (3-H, s, 18-CH_3). ^{13}C NMR ppm (MeOD): 71 (3-C, 7-C), 51 (23-C), IR_{vmax} (KBr) 3341.06. 2091, HRMS: Found: $(M-Na)^+$ = 426.3096.

4.1.8. 24-Methyl 3β-bromo, 12α-acetoxy-5β-cholanoate (42)

Triphenylphosphine (0.821 g) was added to a stirred solution of **41** (1.035 g) in anhydrous THF (40 ml) and the mixture was cooled to −18 °C. *N*-Bromosuccinimide (1.210 g) was added in three parts to the reaction mixture over 1 h and it was allowed to warm to room temperature. After 1.5 h, when TLC analysis showed no more starting material, the reaction mixture was poured into 1 M HCl solution (150 ml) and extracted with ethyl acetate (3 × 100 ml). The organic phase was washed with water (2 × 100 ml) and brine (1 × 100 ml), dried over $MgSO_4$, filtered and the solvent was evaporated under reduced pressure. The product was separated by flash chromatography twice, using 30% ethyl acetate first then 0–12% ethyl acetate in hexane as mobile phase to yield colourless semi-solid (0.766 g, 65%). ^{1}H NMR δ ($CDCl_3$): 5.10 (s, 1H, 12β-H), 4.80 (s, 1H, 3α-H), 3.68 (s, 3H, –O–CH_3), 2.09 (s, 3H, 12-C=OCH_3), 1.00 (s, 3H, 19-CH_3), 0.83 (d, 3H, J = 6.28 Hz, 21-CH_3), 0.75 (s, 3H, 18-CH_3). ^{13}C NMR ppm ($CDCl_3$): 175.07 (C=O, 24-C), 170.85 (C=O, 12-OC=OCH_3), 76.41 (CH, 12-C), 51.97 (CH_3, OCH_3), 21.78 (CH_3, 12-C=OCH_3). IR_{vmax} (KBr): 3444.74, 2940.49, 2873.22, 1736.69 and 1245.03 cm^{-1}. HRMS: Found: $(M-Na)^+$ = 533.2252.

4.1.9. 3α-Azido, 12α-hydroxy-5β-cholanoate (26)

To a solution of **22** (0.150 g) in methanol (15 ml) was added 2 M sodium hydroxide solution to pH ~14 and stirred at reflux for 1 day, when TLC analysis showed the hydrolysis was complete. Then the reaction mixture was poured into 1 M HCl solution (50 ml) and extracted with ethyl acetate (3 × 50 ml). The organic layer was washed with water (2 × 100 ml) and brine (1 × 100 ml), dried over Na_2SO_4, filtered and the solvent was removed under reduced pressure to give the product as a light yellow solid (0.131 g, 99%) mp 88 °C. ^{1}H NMR δ ($CDCl_3$): 4.01 (s, 1H, 12β-H), 3.35 (m, 1H, 3β-H), 1.01 (d, 3H, J = 6.03 Hz, 21-CH_3), 0.94 (s, 3H, 19-CH_3), 0.70 (s, 3H, 18-CH_3). ^{13}C NMR ppm ($CDCl_3$): 179.80 (C=O, 24-C), 73.29 (CH, 12-C), 61.40 (CH, 3-C). IR_{vmax} (KBr): 3440.00, 2941.49, 2866.14, 2090.46, 1709.85, 1679.00 and 1246.00 cm^{-1}. HRMS: Found: $(M-Na)^+$ = 440.2878.

4.1.10. 24-Methyl 3α-azido, 7β–acetoxy-5β-cholanoate (22)

To a stirred solution of **19** (1.876 g) in anhydrous *N*,*N*-DMF (40 ml) was added 5 equiv sodium azide (1.192 g) at 60 °C. The mixture was stirred overnight then poured into std. $NaHCO_3$ (150 ml) and extracted with ethyl acetate (3 × 100 ml). The organic phase was washed with brine (200 ml), dried over $MgSO_4$, filtered and the solvent was evaporated in vacuo. The product was separated on a flash column (hexane/ethyl acetate 9:1) to yield orange foam (1.258 g, 72%). ^{1}H NMR δ ($CDCl_3$): 4.76 (6, 1H, J_1 = 5.52 Hz, J_2 = 5.53 Hz, J_3 = 5.01 Hz, 7α-H), 3.68 (s, 3H, –O–CH_3), 3.28 (m, 1H, 3β-H), 2.00 (s, 3H, 7-C=OCH_3), 0.99 (s, 3H, 19-CH_3), 0.94 (d, 3H, J = 6.53 Hz, 21-CH_3), 0.69 (s, 3H, 18-CH_3). ^{13}C NMR ppm ($CDCl_3$): 174.52 (C=O, 24-C), 170.40 (C=O, 7-OC=OCH_3), 73.31 (CH, 7-C), 60.58 (CH, 3-C), 51.32 (CH_3, OCH_3), 21.63 (CH_3, 7-C=OCH_3). IR_{vmax} (KBr): 3430.05, 2929.21, 2871.64, 2099.67, 1745.61, 1722.74, 1256.74 and 1164.61 cm^{-1}. HRMS: Found: $(M-Na)^+$ = 496.3159.

4.1.11. 3α-Hydroxy, 7β-azido-5β-cholanoate (34)

^{1}H NMR δ (MeOD) 3.6369 (m, 1-H, 3 β-H), 3.0519 (m, 1-H, 7 α-H), 0.9583 (s, 3-H, 19-CH_3), 0.9407 (d, 3-H, J = 6.02, 21-CH_3), 0.6986 (s, 3H, 18-CH_3). ^{13}C NMR ppm (MeOD): 180 (C=O, 24-C), 71 (3-C), 61 (7-C). IR_{vmax} (KBr) 3340.06, 2915.00, 2105.01, 1695.34 and 1235.21 cm^{-1}. HRMS: Found: $(M-Na)^+$ = 440.2889.

4.2. Reverse phase TLC

TLC was performed on pre-coated C18 reversed-phase HPTLC (20x10, F254) plates (Merck, Darmstadt, Germany). Test solutions were applied in DMSO. The plates were then dried at 40 °C for 1 h. Plates were developed in a closed chamber at room temperature across a development distance of 15 cm. Methanol: aqueous ammonium acetate (15 mM) adjusted to the required pH with acetic acid was used as the mobile phase. After development, the plates were dried under ambient conditions and stained with a vanillin solution to visualize spots.

4.3. Cell culture

The human oesophageal squamous epithelial cell line HET-1A was obtained from American Type Culture Collection (ATCC, Rockville, MD). Cells were cultured in bronchial epithelial cell basal medium (Lonza Group Ltd, Switzerland) supplemented with triiodothyronine, insulin, transferrin, retinoic acid, hydrocortisone, human recombinant epidermal growth factor, epinephrine and bovine pituitary extract.

The human hepatoma cell line, Huh7 was a kind gift from Dr. Ralf Bartenschlager (Department of Molecular Virology, University of Heidelberg, Germany). Cells were cultured in Dulbecco's Modified Eagle Medium (DMEM) supplemented with 10% foetal calf serum and 100 U/ml penicillin/streptomycin. Cultures were maintained at 37 °C in a humidified atmosphere containing 5% CO_2.

4.4. Calculation of physicochemical descriptors

UDCA was extracted from the X-ray crystal structure bound to AKR1C2 (PDB entry 1IHI) and visualized in molecular operating environment (MOE 2007.09, Chemical Computing Group, Montreal, Canada). Energy minima for the other test bile acids were generated from this by modification in MOE using sequential SD (100 steps) and TN (1000 steps or to an RMS gradient of <0.01 kcal/(mol*A)) using the PM3 algorithm, Stochastic searches were performed for the conjugates using PM3 over 1000 steps. Physicochemical descriptor parameters including hydrophobic surface area (ASAH) and polar surface area (ASAP) were calculated based on the minimised steroid molecules following a stochastic conformational search procedure using the database functions of MOE.

4.5. MTT assay

Cell viability was measured using the 3-[4,5-dimethylthiazol-2-yl] 2,5-diphenyltetrazolium bromide (MTT) assay. Cells were plated into 96 well plates at a concentration of 8×10^4 cells/ml (100 µl/well). After 24 h the cells were treated with various bile acids at concentrations ranging from 4 µM to 10 mM for a further 24 h in supplement free medium. Test compounds were maintained as 200 mM stock solutions in DMSO. The compounds were diluted to the required concentrations with medium. No change in pH was observed on addition of bile acids to the medium. Control wells were treated with BEBM without supplements or

with PMA 1 μg/ml as a positive control for cell death. Vehicle control wells were treated with 1% DMSO. After 22 h cells were incubated with 20 μl of MTT solution for a further 2 h. The medium was aspirated from the wells and DMSO (100 μl) added to each well to lyse the cells. The plates were shaken for 10 min to dissolve the formazan crystals and then read on a multiwell spectrophotometer at a wavelength of 570 nm. The absorbance of vehicle controls was set as 100% survival and of PMA treated wells as 0%. Cell survival rates were determined by calculating: (T − B)/(V − B), where T (treated) is the absorbance of bile acid treated cells, B (blank) is the absorbance of media plus MTT and V (vehicle) is the absorbance of vehicle control cells. Values represent the mean ± SEM of three experiments performed in triplicate. CC_{50} values were estimated from concentration–effect curves generated using nonlinear regression models in GraphPad Prism5.

4.6. Statistical analysis

Statistical comparison between groups was carried out using a one-sample *t*-test to examine differences between groups. Data are graphically represented as the mean ± standard error of the mean (SEM). All data were analysed using GraphPad Prism5. $p < 0.05$ was considered to be statistically significant.

Acknowledgements

We are most grateful to Dr. John O'Brien for NMR spectroscopy. We would also like to thank Dr. Annemarie Byrne and Dr. David Prichard for their many helpful comments and suggestions.

Funding: This work was supported by the Health Research Board [TRA/2007/11] and the Embark Initiative (IRCSET Award to Sharma, 2006).

References and notes

1. Monte, M. J.; Marin, J. J.; Antelo, A.; Vazquez-Tato, J. *World J. Gastroenterol.* **2009**, *15*, 804.
2. Zimber, A.; Gespach, C. *Anticancer Agents Med. Chem.* **2008**, *8*, 540.
3. Fiorucci, S.; Mencarelli, A.; Palladino, G.; Cipriani, S. *Trends Pharmacol. Sci.* **2009**, *30*, 570.
4. Debruyne, P. R.; Bruyneel, E. A.; Li, X.; Zimber, A.; Gespach, C.; Mareel, M. M. *Mutat. Res.* **2001**, *480–481*, 359.
5. Kim, N. D.; Im, E. O.; Choi, Y. H.; Yoo, Y. H. *J. Biochem. Mol. Biol.* **2002**, *35*, 134.
6. Amaral, J. D.; Viana, R. J.; Ramalho, R. M.; Steer, C. J.; Rodrigues, C. M. *J. Lipid Res.* **2009**, *50*, 1721.
7. Perez, M. J.; Briz, O. *World J. Gastroenterol.* **2009**, *15*, 1677.
8. Liu, H.; Qin, C. K.; Han, G. Q.; Xu, H. W.; Ren, W. H.; Qin, C. Y. *Cancer Lett.* **2008**, *270*, 242.
9. Choi, Y. H.; Im, E. O.; Suh, H.; Jin, Y.; Lee, W. H.; Yoo, Y. H.; Kim, K. W.; Kim, N. D. *Int. J. Oncol.* **2001**, *18*, 979.
10. El Kihel, L.; Clement, M.; Bazin, M. A.; Descamps, G.; Khalid, M.; Rault, S. *Bioorg. Med. Chem.* **2008**, *16*, 8737.
11. Kim, N. D.; Im, E.; Yoo, Y. H.; Choi, Y. H. *Curr. Cancer Drug Targets* **2006**, *6*, 681.
12. Choi, Y. H.; Im, E. O.; Suh, H.; Jin, Y.; Yoo, Y. H.; Kim, N. D. *Cancer Lett.* **2003**, *199*, 157.
13. Heuman, D. M. *Ital. J. Gastroenterol.* **1995**, *27*, 372.
14. Hofmann, A. F. *Arch. Intern. Med.* **1999**, *159*, 2647.
15. Garidel, P.; Hildebrand, A.; Knauf, K.; Blume, A. *Molecules* **2007**, *12*, 2292.
16. Asamoto, Y.; Tazuma, S.; Ochi, H.; Chayama, K.; Suzuki, H. *Biochem. J.* **2001**, *359*, 605.
17. Vlahcevic, Z. R.; Gurley, E. C.; Heuman, D. M.; Hylemon, P. B. *J. Lipid Res.* **1990**, *31*, 1063.
18. Gonzalez, B.; Fisher, C.; Rosser, B. G. *Mol. Cell. Biochem.* **2000**, *207*, 19.
19. Akare, S.; Martinez, J. D. *Biochim. Biophys. Acta* **2005**, *1735*, 59.
20. Strupp, W.; Weidinger, G.; Scheller, C.; Ehret, R.; Ohnimus, H.; Girschick, H.; Tas, P.; Flory, E.; Heinkelein, M.; Jassoy, C. *J. Membr. Biol.* **2000**, *175*, 181.
21. Vyvoda, O. S.; Coleman, R.; Holdsworth, G. *Biochim. Biophys. Acta* **1977**, *465*, 68.
22. Krahenbuhl, S.; Fischer, S.; Talos, C.; Reichen, J. *Hepatology* **1994**, *20*, 1595.
23. Martinez-Diez, M. C.; Serrano, M. A.; Monte, M. J.; Marin, J. J. *Biochim. Biophys. Acta* **2000**, *1500*, 153.
24. Rao, Y. P.; Stravitz, R. T.; Vlahcevic, Z. R.; Gurley, E. C.; Sando, J. J.; Hylemon, P. B. *J. Lipid Res.* **1997**, *38*, 2446.
25. Powell, A. A.; LaRue, J. M.; Batta, A. K.; Martinez, J. D. *Biochem. J.* **2001**, *356*, 481.
26. Katona, B. W.; Rath, N. P.; Anant, S.; Stenson, W. F.; Covey, D. F. *J. Org. Chem.* **2007**, *72*, 9298.
27. Katona, B. W.; Anant, S.; Covey, D. F.; Stenson, W. F. *J. Biol. Chem.* **2009**, *284*, 3354.
28. Sarbu, C.; Kuhajda, K.; Kevresan, S. *J. Chromatogr., A* **2001**, *917*, 361.
29. Posa, M.; Kuhajda, K. *Steroids* **2010**, *75*, 424.
30. Roda, A.; Minutello, A.; Angellotti, M. A.; Fini, A. *J. Lipid Res.* **1990**, *31*, 1433.
31. Natalini, B.; Sardella, R.; Camaioni, E.; Macchiarulo, A.; Gioiello, A.; Carbone, G.; Pellicciari, R. *J. Pharm. Biomed. Anal.* **2009**, *50*, 613.
32. Heuman, D. M. *J. Lipid Res.* **1989**, *30*, 719.
33. Stadler, J.; Stern, H. S.; Yeung, K. S.; McGuire, V.; Furrer, R.; Marcon, N.; Bruce, W. R. *Gut* **1988**, *29*, 1326.
34. Hess, L. M.; Krutzsch, M. F.; Guillen, J.; Chow, H. H.; Einspahr, J.; Batta, A. K.; Salen, G.; Reid, M. E.; Earnest, D. L.; Alberts, D. S. *Cancer Epidemiol. Biomarkers Prev.* **2004**, *13*, 861.
35. Keely, S. J.; Scharl, M. M.; Bertelsen, L. S.; Hagey, L. R.; Barrett, K. E.; Hofmann, A. F. *Am. J. Physiol. Gastrointest. Liver Physiol.* **2007**, G290.
36. Costantino, G.; Wolf, C.; Natalini, B.; Pellicciari, R. *Steroids* **2000**, *65*, 483.
37. Liliang, H.; Hua, Z.; Xiaoping, X.; Chunchun, Z.; Yu-Mei, S. J. *Organomet. Chem.* **2009**, *694*, 3247.
38. Bellini, A. M.; Quaglio, M. P.; Guarneri, M.; Cavazzini, G. *Eur. J. Med. Chem.* **1983**, *18*, 191.
39. Takashi, I.; Frederic, C. C. *J. Org. Chem.* **1983**, *48*, 1194.
40. Schteingart, C. D.; Hofmann, A. F. *J. Lipid Res.* **1988**, *29*, 1387.
41. Batta, A. K.; Datta, S. C.; Tint, G. S.; Alberts, D. S.; Earnest, D. L.; Salen, G. *Steroids* **1999**, *64*, 780.
42. Kihira, K.; Yoshii, M.; Okamoto, A.; Ikawa, S.; Ishii, H.; Hoshita, T. *J. Lipid Res.* **1990**, *31*, 1323.
43. Gao, H.; Dias, J. R. *Eur. J. Org. Chem.* **1998**, *4*, 719.
44. Anelli, P. L. B. M.; Morosini, P.; Palano, D.; Carrea, G.; Falcone, L.; Pasta, P.; Sartore, D. *Biocatal. Biotransform.* **2002**, *20*, 29.
45. Batta, A. K.; Aggarwal, S. K.; Salen, G.; Shefer, S. *J. Lipid Res.* **1991**, *32*, 977.
46. Gil, R. P.; Martinez, C. S. P.; Manchado, F. C. *Synth. Commun.* **1998**, *28*, 3387.
47. Snopek, J.; Smolkova-Keulemansova, E.; Jelinek, I.; Dohnal, J.; Klinot, J.; Klinotova, E. *J. Chromatogr.* **1988**, *450*, 373.
48. Bortolini, O.; Fantin, G.; Fogagnolo, M.; Forlani, R.; Maietti, S.; Pedrini, P. *J. Org. Chem.* **2002**, *67*, 5802.
49. Takashi, I.; Frederic, C. C. *J. Org. Chem.* **1982**, *47*, 2972.
50. Pedrini, P.; Andreotti, E.; Guerrini, A.; Dean, M.; Fantin, G.; Giovannini, P. P. *Steroids* **2006**, *71*, 189.

Journal of Medicinal Chemistry Article

J. Med. Chem. **XXXX,** *XXX,* 000–000 A
DOI: 10.1021/jm100860s

Ursodeoxycholic Acid Amides As Novel Glucocorticoid Receptor Modulators

Ruchika Sharma,*[,†,‡] David Prichard,[‡] Ferenc Majer,[†] Anne-Marie Byrne,[‡] Dermot Kelleher,[‡] Aideen Long,[‡] and John F. Gilmer*[,†]

[†]*School of Pharmacy and Pharmaceutical Sciences, Trinity College Dublin, Dublin 2, Ireland, and* [‡]*Cell Signalling, Institute of Molecular Medicine, Trinity Centre for Health Science, St. James's Hospital, Dublin 8, Ireland*

Received July 9, 2010

Ursodeoxycholic acid (UDCA) is used for the treatment of hepatic inflammatory diseases. Recent studies have shown that UDCA's biological effects are partly glucocorticoid receptor (GR) mediated. UDCA derivatives were synthesized and screened for ability to induce GR translocation in a high content analysis assay using the esophageal cancer SKGT-4 cell line. UDCA derivatives induced GR translocation in a time dependent manner with equal efficacy to that of dexamethasone (Dex) and with greatly increased potency relative to UDCA. The cyclopropylamide **1a** suppressed TNF-α induced NF-κB activity and it induced GRE transactivation. **1a** was unable to displace Dex from the GR ligand binding domain (LBD) in a competition experiment but was capable of coactivator recruitment in a time-resolved fluorescence energy transfer assay (TR-FRET). This represents a novel mechanism of action for a GR modulator. These derivatives could result in a new class of GR modulators.

Introduction

The glucocorticoid receptor (GR[a]) is a member of the nuclear receptor family of eukaryotic transcription regulators.[1] Classical GR agonists (glucocorticoids, GCs) include the endogenous GR ligand cortisol and its synthetic derivatives. GCs are the principal therapies in asthma, rheumatoid arthritis, and inflammatory bowel disease.[2] They also find clinical application in neurological conditions and in certain types of cancer.[3] The GR is arguably the most important pharmacological target in medicine.

The unliganded GR resides in the cytoplasm, part of a multimeric complex consisting of the GR polypeptide and chaperone proteins hsp90 and immunophilins, FKBP52, FKBP51, Cyp40, and PP5.[4] Ligand binding causes dissociation of chaperones leading to exposure of nuclear localization signals triggering nuclear translocation. Ligand-bound GR may dimerize. Homodimeric GR has direct and indirect effects on a wide spectrum of transcriptional activities.[5] Binding to glucocorticoid response elements (GREs) followed by coactivator recruitment results in transactivation of genes.[6−9] Homodimers can also bind to negative GREs, inhibiting gene expression.[10,11] Yet another pathway involves direct binding to pro-inflammatory transcription factors such as activator protein-1 (AP-1) and nuclear factor κ-light-chain-enhancer of activated B cells (NF-κB).[5,12] This "transrepression" effect is associated with GR monomers.[13] There has been in the past few years an interest in so-called "dissociated steroids" that can separate transrepression from transactivation, which is associated with steroid side effects.[14−17] Steroid antagonists also cause receptor dissociation and nuclear translocation but with limited transcription. GC antagonists are being investigated in a range of indications including, psychotic depression, diabetes, obesity, Alzheimer's disease, neuropathic pain, drug abuse, and glaucoma.[18] Thus it is possible to envisage ligands capable of inducing GR translocation but associated with a more limited repertoire of transcriptional activities than classical GC agonist. Mechanistically, such compounds should bind nonclassically, influencing GR self-association and recruitment of transcriptional machinery.[19]

UDCA (UDCA, **1**, Figure 1), a traditional medicine, is used at high dose in the treatment of primary biliary cirrhosis (PBC) and primary sclerosing cholangitis.[20] The biochemical basis for UDCA's actions remains somewhat obscure although it is the subject of extensive investigation. UDCA exhibits antiapoptotic action in hepatic[21,22] and nonhepatic cell lines,[23,24] and it has neuroprotective actions.[25−27] It has putative chemopreventative effects in colon cance,r[28] and it has been shown to attenuate carcinogenic signaling cascades induced by other bile acids. These include inhibition of protein kinase C translocation,[29] suppression of p38, MAPK, and Cox-2 expression[30] as well as reduction in activity of the transcription factors AP-1 and NF-κB.[31] UDCA treatment reduces serum antimitochondrial and immunoglobulin G antibodies.[32] It can also suppress interleukin-2[33] and interferon γ production[34] and decrease the hepatocellular and

*To whom correspondence should be addressed. For R.S.: phone, +35318963350/8962844; fax, +35318962810; E-mail, rsharma@tcd.ie. For J.F.G.: phone, +35318962795; fax, +35318962793; E-mail, gilmerjf@tcd.ie.

[a]Abbreviations: AP-1, activator protein-1; CDCA, chenodeoxycholic acid; DCA, deoxycholic acid; Dex, dexamethasone; GCs, glucocorticoids; GR, glucocorticoid receptor; GREs, glucocorticoid response elements; HRMS, high resolution mass spectrometry; HPLC, high performance liquid chromatography; HCl, hydrochloric acid; LBD, ligand binding domain; LPS, lipopolysaccharide; $MgSO_4$, magnesium sulfate; MeOH, methanol; NF-κB, nuclear factor κ-light-chain-enhancer of activated B cells; PBS, phosphate buffered saline; PLA_2IIA, phospholipase A_2 IIA; PBC, primary biliary cirrhosis; PSC, primary sclerosing cholangitis; TR-FRET, time-resolved fluorescence energy transfer; SRC1−4, steroid receptor coactivator 1−4; TLC, thin layer chromatography; TAT, tyrosine aminotransferase; UDCA, ursodeoxycholic acid.

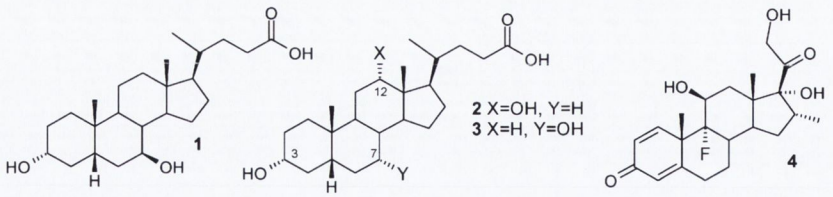

Figure 1. Structural formulas of UDCA (**1**), DCA (**2**), CDCA (**3**), and Dex (**4**).

Scheme 1. Synthesis and Structural Formulas of UDCA analogues **1a**−**1k**

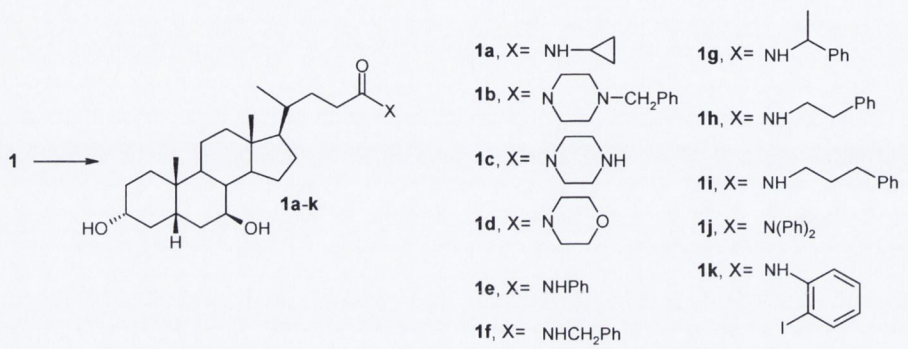

(i) Formic acid/perchloric acid, 47 °C, 3 h; (ii) $SOCl_2$, reflux, 2 h; (iii) RNH_2, NEt_3, RT; (iv) NaOMe/MeOH, 70 °C, 2 h.

biliary expression of both major histocompatibility complex class I and class II molecules in patients with PBC.[35,36] UDCA can correct the defective natural killer cell activity by inhibiting prostaglandin E_2 production in PBC patients.[37] UDCA has a suppressive effect at the transcriptional level on phospholipase A_2 IIA (PLA_2IIA) in hepatocytes.

These latter effects at a physiological and biochemical level are similar to those of GCs.[38] There is also a significant body of biochemical evidence that UDCA can activate GR pathways. UDCA has been reported to induce translocation of the GR and to activate the GR in various different cell models.[39−42] Furthermore, UDCA can suppress NF-κB activity via activation of the GR.[41] The GR-ligand binding domain (LBD) is responsible for UDCA-dependent nuclear translocation of the GR.[41] GR knockdown attenuates UDCA's inhibitory effects on PLA_2IIA.[38]

Taking these studies and UDCA's clinical history of minimal side effects into account, we decided that it would make an excellent lead for the development of a novel class of GR modulators.

In this work, a series of bile acid derivatives (Scheme 1) were synthesized in order to test this hypothesis. Chronic inflammation in the esophagus has been associated with the pathogenesis of esophageal adenocarcinoma.[43] Hence we screened our derivatives for the ability to modulate the GR in an esophageal cancer cell line. We have shown that modification at the C24-position of UDCA leads to compounds endowed with the ability to induce GR translocation in the low micromolar range. These may act as leads for development of GR modulators with new transcriptional profiles. The increased potency of these analogues makes them useful tools for further characterizing UDCA's effects on the GR and elucidating its mechanism of action.

Results and Discussion

We initially established the ability of UDCA to induce translocation of the GR from the cytoplasm to the nucleus in the esophageal SKGT-4 cell line. UDCA weakly induced translocation of the GR from the cytoplasm to the nucleus (54% efficacy of Dex 100 nM (**4**) at 300 μM (Figure 2A−C). This is a similar level of effect to that reported in other cell lines. UDCA has three readily manipulable functional groups: the C3-, C7-OH, and C24-COOH (Figure 1). UDCA's ability to induce GR trafficking is connected with its C7-β OH group because its C7-epimer chenodeoxycholic acid (CDCA, **3**) and deoxycholic acid (DCA, **2**) do not induce GR trafficking. Our initial chemistry therefore focused on manipulating the C24-COOH group. This strategy was supported by the observation that TauroUDCA (TUDCA) can induce GR and mineralocorticoid receptor (MR) translocation, illustrating that the side chain could be modified and that amide derivatives of UDCA might be active.[44,45] We therefore targeted a small chemically diverse library of UDCA amides (**1a**−**k**, Scheme 1). These were produced in four steps from UDCA by formyl protection of the steroidal −OH groups, formation of the corresponding acyl chloride ($SOCl_2$), amidation with the appropriate amine, and deformylation (NaOMe/MeOH).

We produced another set of UDCA derivatives (**1l**−**1s**, Figure 3) in which the acid group was abolished or migrated using classical bile acid chemistry.[46,47]

Analogues **1a**−**1s** were tested in a high content analysis assay using immunofluorescence to estimate the nuclear to cytoplasmic ratio (Figure 4). The experiment was carried out initially at 300 μM for 4 h and repeated at successively lower concentration where an effect was observed (Table 1). The amide series (**1a**−**1k**) exhibited the highest biochemical efficacy relative to Dex and highest potency. For example, the cyclopropyl derivative (**1a**) and **1b**, **1c**, and **1d** had similar efficacy to Dex as reflected in steady-state nuclear/cytoplasmic ratio. **1a**−**b** were the most potent compounds with EC_{50} values of 7.3 and 5.6 μM, respectively (Figure 2D). Removal of the benzyl group in **1c** maintained GR translocation efficacy but reduced potency by 10-fold (50.8 μM). The anilide (**1e**) did not induce translocation but the benzylamide (**1f**), α-methylbenzylamide (**1g**) and phenethylamide (**1h**) showed

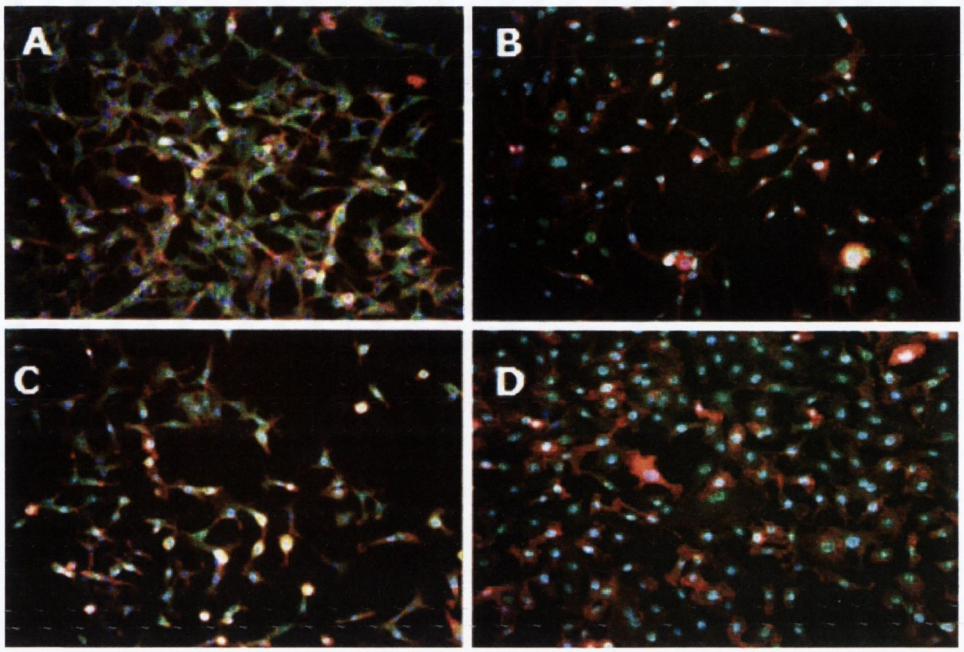

Figure 2. UDCA derivatives induce GR translocation. SKGT-4 cells were treated with (A) DMSO 1%, (B) Dex (100 nM) as a positive control, (C) UDCA (300 μM), or (D) **1a** (100 μM). Cells were fixed with paraformaldehyde 4% in PBS after 4 h. The GR was identified using a mouse monoclonal GR antibody (green.) and cells were stained with Hoechst (blue) and phalloidin (red) to identify the nucleus and actin cytoskeleton respectively. Cells were imaged using the GE IN Cell Analyzer 1000. Original magnification ×10.

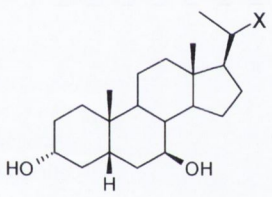

1l, X= $(CH_2)_2CN$
1m, X=CH_2CN
1n, X=CN
1o, X=$(CH_2)_3OH$
1p, X=CH_2COOH
1q, X=COOH
1r, X=$(CH_2)_2COOPh$
1s, X=$(CH_2)_2COOMe$

Figure 3. UDCA analogues **1l**–**s**.

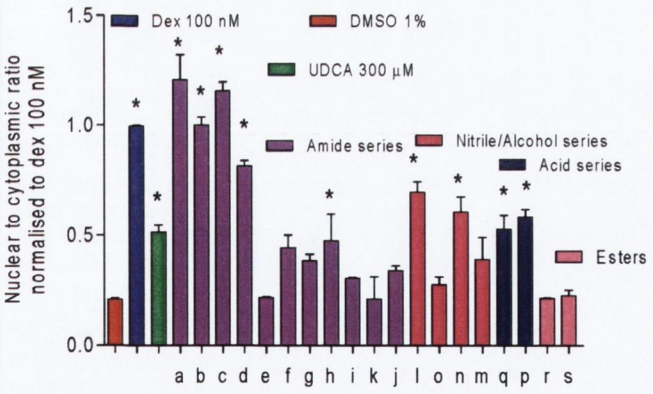

Figure 4. Analysis of GR translocation induced by UDCA derivatives. SKGT-4 cells were treated with DMSO 1%, Dex 100 nM as a positive control, UDCA 300 μM, or bile acid derivatives as indicated. All bile acid derivatives were initially screened at 300 μM. Cells were fixed, stained, and imaged as described, Original magnification, ×10. GR translocation was measured using the Investigator software package. Analysis was based on the ratio of the intensity of the GR within the nucleus and the intensity in the cytoplasm. Values are normalized to nuclear to cytoplasmic ratio of Dex 100 nM and are expressed as the mean ± SEM of two experiments performed in triplicate, * $p < 0.05$.

equal efficacy to UDCA with increased potency, 109.5, 123.5, and 109.0 μM, respectively. Extending the spacer by one carbon abolished activity (**1i**).

Table 1. EC_{50} Values for GR Translocation of UDCA (**1**) and Selected Modified Bile Acids [a]

compd	EC_{50} (μM, 95% CI) (% efficacy[b])
1	298.7 (151–432) (54)
1a	7.3 (1–14) (100)
1b	5.6 (2–10) (100)
1c	50.8 (29–88) (100)
1d	25.3 (17–31) (100)
1f	109.5 (60–149) (49)
1g	123.5 (57–191) (49)
1h	109.0 (42–168) (53)
1l	101.0 (44–168) (70)
1n	130.0 (25–181) (59)
1p	105.3 (54–161) (58)
1q	99.7 (51–154) (59)

[a] Compounds less active than UDCA are omitted. EC_{50} values for translocation after 4 h of treatment were determined from six point concentration-effect curves generated using nonlinear regression models Table 1. EC_{50} values for GR translocation of UDCA and selected modified bile acids. [b] Relative to Dex (100 nM).

Shortening the side chain but maintaining the acid functionality resulted in compounds with equal efficacy to UDCA but enhanced potency, norUDCA (**1p**) (EC_{50} of 105 μM) and bisnorUDCA (**1q**) (EC_{50} of 99.7 μM). The UDCA alcohol (**1o**) did not induce translocation, but conversion to the nitrile (**1l**) enhanced potency (EC_{50} of 100 μM, 70%). The bisnornitrile (**1n**) (EC_{50} of 130 μM, 59%) showed similar efficacy and potency to **1l** although the nornitrile (**1m**) did not induce translocation. UDCA methyl and benzyl esters (**1r**, **1s**) did not induce GR translocation.

Having shown that UDCA amides are moderately potent inducers of GR translocation, we investigated whether similar amide derivatives of DCA and CDCA could also induce translocation of the GR. The cyclopropyl and *N*-benzylpiperazine derivatives of DCA (**2**) (3α, 12α OH) and UDCA's

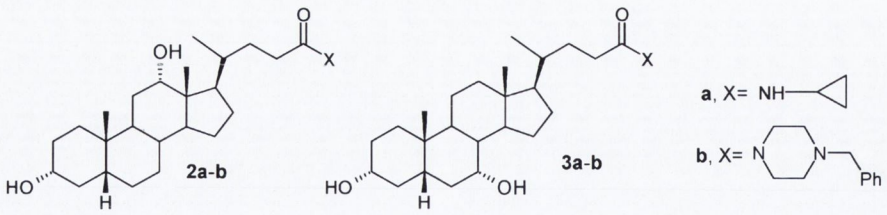

Figure 5. DCA and CDCA amides **2a**−**b**, **3a**−**b**.

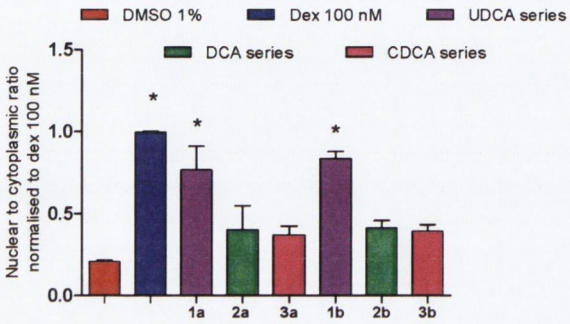

Figure 6. DCA and CDCA amides **2a**−**b**, **3a**−**b** do not induce GR translocation. SKGT-4 cells were (a) untreated or (b) treated with Dex 100 nM as a positive control, (c) cyclopropyl amide derivatives of UDCA, DCA, and CDCA (10 μM) (**1**−**3a**) or (d) benzylpiperidine derivatives of UDCA, DCA, and CDCA (10 μM) (**1**−**3b**) for 4 h and fixed, stained, and analyzed as described previously. Values are normalized to nuclear to cytoplasmic ratio of Dex (100 nM) and are expressed as the mean ± SEM of two experiments performed in triplicate, * $p < 0.05$.

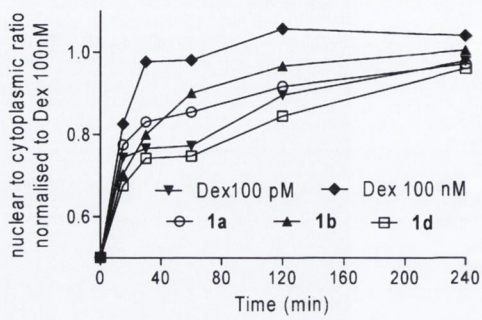

Figure 7. UDCA derivatives **1a**,**b**,**d** show similar translocation kinetics to Dex. SKGT-4 cells were treated with UDCA derivatives 100 μM or Dex at indicated concentration for 15, 30, 60, 120, or 240 min. Cells were fixed, stained, and analyzed for GR translocation as described previously. Values are normalized to nuclear to cytoplasmic ratio of Dex 100 nM and are expressed as the mean of two experiments performed in triplicate, $p < 0.05$ relative to DMSO 1%, for **1a** (120, 240 min), **1b** (60, 120, 240 min), **1d** (120, 240 min), Dex 100 pM (120, 240 min), Dex 100 nM (30, 60, 120, 240 min).

epimer CDCA (**3**) (3α, 7α OH) were prepared, Figure 5. The DCA and CDCA amides (**2a**−**b**, **3a**−**b**) did not induce translocation at 10 μM (Figure 6). This indicates that the orientation of the OH groups on the steroid nucleus exerts a strong influence on the capacity of similar amides to induce GR translocation and it is consistent with a range of observations about the effects of UDCA compared with DCA and CDCA. The latter BAs promote apoptosis, whereas UDCA is anti-apoptotic, due in part to its ability to cause GR translocation.[45] The differing biological effects of DCA and CDCA relative to UDCA are attributed to the uninterrupted hydrophobic β-face of the former pair, although it is unclear whether this affects a macroscopic biophysical property or protein binding.

We examined the time course for GR translocation in the SKGT-4 cell line following treatment with analogues **1a**, **1b**, **1d**, and Dex to help characterize the kinetics of the effect. Following treatment with the UDCA amides produced a trend toward increased nuclear GR evident at 15 min; this achieved significance in 60 min in the case of **1b** and 120 min for **1a** and **1d**. The time course of a ligand-dependent protein event such as GR translocation is a function of the affinity of the ligand for the protein and ultimately ligand concentration. Therefore, Dex (100 nM) induced significant and maximum translocation of the GR at 30 min consistent with reported values, whereas at 100 pM, nuclear trafficking kinetics were more leisurely, with ratios reaching significance at 120 min, Figure 7. Overall, the time-course experiments indicated a direct effect on GR distribution rather than one downstream of protein synthesis. Furthermore, pretreatment of SKGT-4 cells with cycloheximide, an inhibitor of protein biosynthesis, did not affect **1a** induced GR translocation (Supporting Information (SI)). Cycloheximide did not induce translocation of the GR by itself. Hence **1a** induced GR translocation occurs

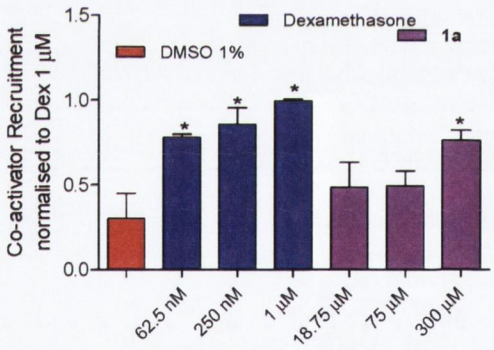

Figure 8. UDCA derivatives induce co-activator recruitment. A Lanthascreen TR-FRET GR coactivator assay was used to determine if the UDCA derivatives were capable of coactivator recruitment. Dex and **1a** were incubated at RT for 3 h with a GST-tagged GR-LBD and a mixture of the fluorescein labeled coactivator peptide and the terbium labeled anti-GST antibody. The TR-FRET ratio was calculated by dividing the emission signal at 520 nm by the emission signal at 495 nm. Values represent the mean ± SEM of three experiments performed in duplicate, normalized to positive control, Dex (1 μM).

independent of protein translation and in a similar time frame to Dex, albeit at a lower rate.

Even though UDCA and its active amides do not satisfy the classical GR pharmacophore, the most obvious explanation for their activity and time-course was ligand binding at the GR active site. However, selected active compounds (**1a**, **1p**, **1m**, **1h**) did not displace radiolabeled Dex in competition experiments at concentrations relevant to their ability to translocate. UDCA (10−50 μM) was also unable to displace Dex, consistent with previous studies.[39,41]

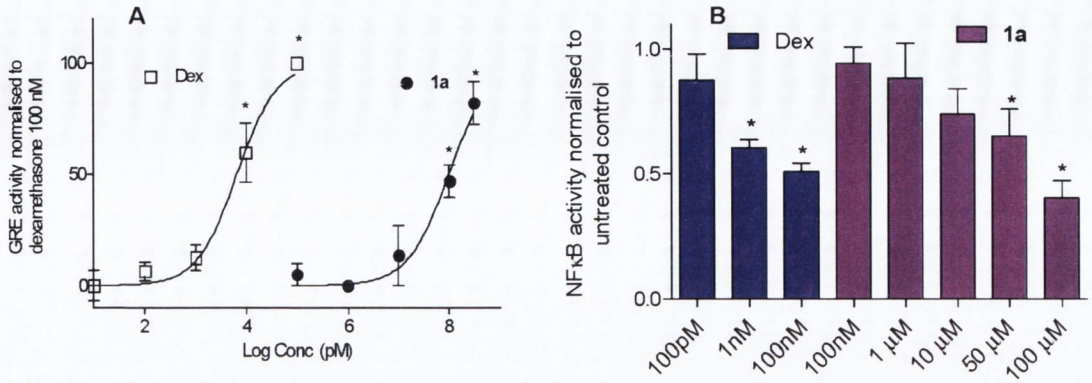

Figure 9. (A) UDCA derivatives transactivate the GR. SKGT-4 cells were transiently transfected with a mixture of an inducible glucocorticoid responsive firefly luciferase reporter and constitutively expressing Renilla construct (40:1). Cells were treated with increasing concentrations of Dex or **1a** for 16 h. Cells were then lysed and assayed for luciferase activity. Firefly luciferase activity was normalized to the internal vector control, renilla luciferase, to control for transfection efficiency. (B) UDCA derivatives decrease NFκB activity. HEK-293 cells were transiently transfected with an inducible NFκB responsive firefly luciferase reporter gene construct and a constitutively expressing β-galactosidase construct. After 24 h, the cells were treated with TNF-α 10 ng/μL alone or with TNF-α 10 ng/μL and varying concentrations of Dex or **1a**. After 16 h, the cells were lysed and the lysates assayed for firefly luciferase activity. Firefly luciferase activity was normalized to β-galactosidase activity to control for transfection efficiency. Values are expressed as the mean $\pm$ SEM of three experiments performed in duplicate, normalized to untreated control, * $p < 0.05$ relative to untreated control.

We next employed a time-resolved fluorescent energy transfer assay (TR-FRET) to try to detect an effect by UDCA or **1a** on GR coactivator recruitment which might indicate physical contact with the GR ensemble leading to conformational changes in the region of the LBD (Figure 8). **1a** (300 μM) increased the TR-FRET ratio to a significant extent, whereas UDCA (300 μM) did not. This result for UDCA is consistent with previous reports.[41] The DCA and CDCA compound **2a** and **3a** were unable to increase the TR-FRET ratio in the coactivator recruitment assay (data not shown).

Having demonstrated that the cyclopropylamide derivative (**1a**) was able to induce coactivator recruitment, our next step was to investigate whether treatment with **1a** could result in GR activation. We found that **1a** was able to induce GRE transactivation in a concentration dependent manner, reaching significance at 100 μM (Figure 9A). UDCA could only induce transactivation at 500 μM, but this did not follow a pharmacological trend (SI). The ability to attenuate NF-kB signaling is regarded as pivotal to the therapeutic actions of classical GCs. We therefore carried out a reporter assay to determine if **1a** could inhibit TNF-α induced NF-κB transcriptional activity in a HEK-293 cell line. We first showed that **1a** caused translocation of the GR in this cell line with similar potency and biochemical efficacy to the SKGT-4 cell line. Compound **1a** was capable of transrepression of NF-κB activity in a concentration dependent manner, $p < 0.05$ at 50 μM, 100 μM (Figure 9B).

The GR and MR are known to have widely overlapping ligand binding preferences and interrelated transcriptional activities, indeed, TUDCA causes translocation of both. However when MR expression was knocked down using siRNA, **1a** was still able to inhibit NF-κB transcriptional activity, whereas in the GR knock down condition, this effect was attenuated (SI). Furthermore, treatment with **1a** (50 μM) was not associated with nuclear translocation of the MR. Therefore, taking together the evidence of translocation exerted by **1a**, its ability to induce GRE transactivation and its GR dependent inhibition of NF-κB transcriptional activity, an agonist mode of action involving the GR is most likely. However, the potential involvement of other nuclear receptors merits further study.

UDCA has been shown to induce GR translocation in multiple cell models[41,42,48] at high concentrations (300 μM range). The mechanism by which UDCA induces GR translocation remains unknown despite extensive efforts over the past decade. Incubation of radiolabeled UDCA with the GR binding site expressed in a GR fusion protein yielded no specific binding of UDCA.[39] UDCA did not displace tritiated Dex from the GR binding site; furthermore, specific binding of tritiated UDCA to GR could not be detected in CHOpMTGR cells.[41] UDCA (10 and 50 μM) was unable to displace tritiated Dex in our competition binding experiment.

Despite this, UDCA requires the GR-LBD to induce GR nuclear translocation and for its subsequent biological effects.[41,45,49] Using a series of GR mutants, Miura et al showed that UDCA influences a broader region of the LBD than Dex. GR deletion mutants (1−765, 1−750, 1−740) could not be translocated by Dex but were by UDCA.[41] On the other hand, GR mutant 1−730 was unresponsive to UDCA. The specific carboxy terminal region of the LBD was identified as essential for translocation and UDCA's cytoprotective effect on TGFβ1 induced apoptosis.[49] This mutant lacks Tyr735 of the steroid binding pocket, which is necessary for hydrophobic contact between ligands and the GR.[50]

The ability of UDCA to induce GR activation downstream of translocation remains a matter of debate as studies are widely conflicted over its ability to activate GREs.[39,41,42,49] Previous investigators failed to show an interaction between UDCA and the coactivator transcription intermediary factor-2.[41] Other studies have shown that UDCA can have an additive effect with GCs in inducing gene expression. For example, UDCA increased Dex induced mRNA levels of tyrosine aminotransferase (TAT), a hepatocyte-specific marker of GC action.[51] Others have shown that combining UDCA and Dex can increase the expression of the bicarbonate carrier, AE2, altered expression of which is associated with PBC. It has been suggested that certain genes contain only half of a GRE site referred to as GRE cores. Binding of GR to GRE core sites may require further assistance in addition to the interaction with GCs which UDCA may provide.[52]

Similar to UDCA, there is not a defined mechanism for GR translocation induced by its more active amides. The most

potent GR translocator **1a** was unable to displace tritiated Dex in a competition binding experiment at similar concentration to its EC_{50} for translocation. Previous authors have suggested that UDCA may interact with the cell membrane and set up a series of cytoplasmic events through secondary signals, one of which may be GR activation.[41,45] Such an explanation cannot be ruled out for the derivatives although GR translocation by the amides displayed a similar time profile to Dex. Furthermore **1a** was able to induce coactivator recruitment in a cell free system. Recruitment of steroid receptor coactivator 1−4 (SRC1−4) by **1a** indicates that it can induce the necessary conformational change in the GR-LBD. This recruitment was specific to the UDCA core nucleus as the corresponding derivatives of DCA and CDCA did not cause coactivator recruitment.

Conclusion

We have discovered amido derivatives of UDCA that causes GR translocation in the low micromolar range in SKGT-4 cells. These compounds do no bind at the classical GC binding locus, but they affect coactivator recruitment and cause transactivation at high concentration. The most potent compound decreased NF-κB activity in a HEK-293 line with moderate potency.

Taken together, the data suggests that UDCA amides bind to the LBD but at a different site to the classical pocket, binding to which accounts for the actions of established GR modulators, including dissociated steroids which separate transactivation from transrepression.[53−56] UDCA has well established but poorly understood effects on cellular function that appear to be mediated at least in part by the GR. The amido analogues reported herein amplify this activity by about 100-fold. They hold potential in therapeutic applications and in exploring ongoing puzzles associated with the actions of UDCA.

Experimental Section

Chemistry. Uncorrected melting points were obtained using a Stuart melting point SMP11 melting point apparatus. IR spectra were obtained using a Perkin-Elmer 205 FT Infrared Paragon 1000 spectrometer. Band positions are given in cm^{-1}. Solid samples were obtained by KBr disk; oils were analyzed as neat films on NaCl plates. ^1H and ^{13}C spectra were recorded at 27 °C on a Bruker Advance II 600 MHz spectrometer (600.13 MHz ^1H, 150.91 MHz ^{13}C) and Bruker DPX 400 MHz FT NMR spectrometer (400.13 MHz ^1H, 100.16 MHz ^{13}C) in either $CDCl_3$ or CD_3OD (tetramethylsilane as internal standard). For $CDCl_3$, ^1H NMR spectra were assigned relative to the TMS peak at 0.00 δ and ^{13}C NMR spectra were assigned relative to the middle $CDCl_3$ triplet at 77.00 ppm. For CD_3OD, ^1H and ^{13}C NMR spectra were assigned relative to the center peaks of the CD_3OD multiplets at 3.30 δ and 49.00 ppm, respectively. High-resolution mass spectrometry (HRMS) was performed on a Micromass mass spectrophotometer (EI mode) at the Department of Chemistry, Trinity College. High-performance liquid chromatography (HPLC) was performed on a reversed phase 250 mm × 4.6 mm Waters Spherisorb ODS-2, 5 μm column using a Waters Alliance 2695 chromatograph equipped with an autosampler, column oven, and dual wavelength detector. The flow rate was 1 mL/min, with a mobile phase consisting of 40% phosphate buffer pH 2.5 and 60% acetonitrile at time 0 and grading to 85% acetonitrile at 4 min. Injection volume was 20 μL and areas determined at 254 nm. The isocratic HPLC method was aqueous phosphate buffer solution pH 2.5 40% and acetonitrile 60%. Flow rate was 1 mL/min. Flash chromatography was performed on Merck Kieselgel 60 particle size 0.040−0.063 mm. Thin layer chromatography (TLC) was performed on silica gel Merck F-254 plates. Compounds were visually detected by absorbance at 254 nm and/or vanillin staining. All test compounds were ≥95% purity by HPLC.

24-Cyclopropyl-3α,7β-dihydroxy-5β-cholanamide (1a). 3α,7β-Diformyloxy-5β-cholan-24-oic acid (1.0 g, 2 mmol) was dissolved in thionyl chloride (5 mL) and refluxed at 90 °C for 2 h. After 1 h, the reaction was cooled to room temperature and the thionyl chloride was removed in vacuo to leave a sticky solid which was the acid chloride. This was dissolved in dry DCM (10 mL) and cyclopropylamine (131 μL, 1.9 mmol) and triethylamine (244 μL, 1.9 mmol) were added on ice. The reaction mixture was allowed to warm to room temperature and stirred monitoring for disappearance of the starting material by TLC. After 24 h, the solvent was removed in vacuo. The residue was dissolved in ethyl acetate (20 mL) and washed with hydrochloric acid (HCl) (3 × 20 mL) for removal of unreacted amines, water (2 × 20 mL), and brine solution (2 × 20 mL). The organic layer was dried and evaporation of solvent gave the cyclopropylamide after chromatographic elution (hexane:ethyl acetate 1:1). Sodium (0.1 g) was added to HPLC grade methanol (MeOH) (10 mL) to form an excess of sodium methoxide. The formyl cyclopropylamide (0.5 g, 1 mmol) was added to this solution and refluxed for 2 h. After 2 h, the reaction was cooled to room temperature and added to water (100 mL). The amide was extracted with ethyl acetate. The organic layer was then washed with water (3 × 20 mL) and dried ($MgSO_4$). The solvent was removed in vacuo and after chromatographic elution with ethyl acetate afforded a white solid (0.4 g, 92%). ^1H NMR δ (CD_3OD): 0.49 (2-H, m), 0.65 (3-H, s), 0.92 (3-H, d, J = 6.52 Hz), 0.97 (3-H, s), 2.75 (1-H, m), 3.61 (2-H, m), 5.32 (1-H, br). ^{13}C NMR ppm (CD_3OD): 8.4, 12.4, 18.8, 22.4, 24.0, 25.2, 25.5, 28.0, 29.8, 31.1, 35.3, 36.5, 36.9, 38.1, 38.8, 40.9, 41.7, 44.1, 44.6, 44.9, 56.5, 57.8, 71.1, 175.2. HRMS: found $(M - Na)^+$ = 454.3297. Melting point 124 °C

24-*N*-Benzylpiperazine-3α,7β-dihydroxy-5β-cholanamide (1b). ^1H NMR δ (CD_3OD): 0.70 (3-H, s, 18-CH_3), 0.95 (6-H, m), 3.41−3.60 (8-H, m), 3.52 (2-H, m). ^{13}C NMR ppm (CD_3OD): 12.9, 19.0, 22.5, 24.0, 28.0, 29.8, 31.1, 32.2, 32.5, 35.1, 36.1, 36.8, 38.1, 38.9, 39.2, 40.9, 41.7, 44.2, 44.7, 44.9, 45.3, 56.6, 57.8, 71.1, 80.3, 130.2, 175.5. HRMS: found $(M - Na)^+$ = 573.4097. Melting point 116 °C.

Biochemistry. Chemicals. Dex, UDCA, and all reagents for chemical synthesis were obtained from Sigma-Aldrich Chemical Co. (St. Louis, MO, USA). Lipofectamine was purchased from Invitrogen (Carlsbad, CA, USA). TNF-α was purchased from R&D Systems and reconstituted with sterile PBS at 100 μg/mL. Cycloheximide (Calbiochem, Merck Chemicals Ltd. Nottingham, UK) was reconstituted with ethanol at a concentration of 20 mg/mL. *Escherichia coli* lipopolysaccharide was obtained from Alexis Biochemicals (San Diego, CA, USA).

Dex was dissolved in DMSO to give a 10 mM stock solution, and all other bile acids and bile acid derivatives were maintained as 200 mM stock solutions in DMSO. The compounds were diluted to the required concentrations with medium with 1% DMSO in order to maintain solubility.

A Smartpool of predesigned siRNA oligos (ON-TARGET *plus* siRNA reagents) targeting the glucocorticoid receptor (siGR), mineralocorticoid receptor (siMR), scrambled control siRNA (siScr), and siRNA transfection reagent were purchased from Dharmacon (Lafayette, CO, USA).

Cell Culture. The SKGT4 cell line, derived from a well-differentiated adenocarcinoma arising in Barrett's epithelium of the distal esophagus, was generously provided by Dr. David Schrump (Bethesda, MA).[57] Cells were maintained in RPMI 1640 medium supplemented with 10% fetal bovine serum and 4 mM L-glutamine (GIBCO-BRL, Grand Island, NY) HEK-293 cells, an adherent human embryonic kidney cell line, were grown in Dulbecco's Modified Eagle's Medium (DMEM, GIBCO, Invitrogen Ltd., Paisley, UK) supplemented with 10%

heat-inactivated FBS. Cultures were maintained at 37 °C in a humidified atmosphere containing 5% CO_2.

GR Translocation Assay. Cells were plated into 96-well plates at a concentration of 6×10^4 cells/mL (100 μL volume). Cells were serum starved for 12 h prior to bile acid treatment. After 48 h, cells were treated with bile acid derivatives in supplement free medium at the required concentration for the indicated time points. Control wells were left untreated or treated with 1% DMSO as a vehicle control or Dex 100 nM as positive control. After the appropriate treatment time, cells were fixed with 4% paraformaldehyde/phosphate buffered saline (PBS) then permeabilized with 0.1% (v/v) Triton X-100/PBS followed by blocking with 3% bovine serum albumin in PBS. Cells were incubated with purified mouse antiglucocorticoid receptor antibody (BD Transduction Laboratories) then incubated with AlexaFluor-488-conjugated secondary antibody (Invitrogen, Carlsbad, CA, USA). Images were acquired using the GE IN cell analyzer 1000, original magnification ×10. Four fields of view per well were acquired using a 10× objective, with up to 2000 cells imaged per treatment group, for $n = 3$ experiments.

Quantification of GR Translocation Using High Content Analysis. The GE IN cell analyzer 1000 is a microscope based screening platform capable of large scale objective analysis of fluorescently labeled cells using automated image acquisition, data management, and multiparametric analysis. SKGT-4s were stained for GR as outlined above. Nuclear to cytoplasmic ratio was measured using the Investigator software package (GE Healthcare, Piscataway, NJ, USA). The analysis was based on the ratio of the intensities of GR within the nucleus and cytoplasm. The multitarget analysis algorithm was optimized to detect GR within the nucleus and the cytoplasm using vehicle only treated cells as negative control and Dex treated cells as positive control. Hoechst staining enabled identification of the nucleus. The nuclear to cytoplasmic ratios were determined by calculating (nuclear Intensity of GR − background intensity)/(cytoplasmic intensity of GR − background intensity). Values represent the mean ± SEM of three experiments performed in triplicate. EC_{50} values were estimated from concentration−effect curves generated using nonlinear regression models in GraphPad Prism5.

GRE Assay. SKGT-4 cells were transiently transfected with a mixture of an inducible glucocorticoid responsive firefly luciferase reporter and constitutively expressing renilla construct (40:1) (SABiosciences Corporation, Executive Way, Frederick, MD, USA). A reverse transfection procedure was optimized using fugene HD as a transfection reagent at a ratio of 4:1 (Fugene HD:DNA). DNA and Fugene HD were diluted in OptiMem, and this mixture was added to 96-well plates to give 100 ng DNA per well. SKGT-4 cells at a density of 7×10^4 cells/mL (100 μL) were added to this mixture. After 24 h, the cells were treated with varying concentrations of Dex or **1a** for 16 h. After 16 h, the cells were lysed using passive lysis buffer 50 μL (Promega Corporation, Madison, WI, USA) and incubated at room temperature for 15 min. The lysates were then assayed for firefly and renilla luciferase activity (Promega Dual-Luciferase Reporter Assay System) using a Victor Perkin-Elmer luminometer. Values represent the mean ± SEM of three experiments performed in duplicate, normalized to Dex 100 nM as positive control.

Time-Resolved Fluorescence Resonance Energy Transfer Assay. TR-FRET is based on the principle that when a suitable pair of fluorophores is brought within close proximity of one another, excitation of the first fluorophore results in energy transfer to the second fluorophore. This can be detected by an increase in the fluorescence emission of the acceptor molecule and a decrease in the fluorescence emission of the donor molecule. We used a Lanthascreen TR-FRET glucocorticoid receptor coactivator assay kit (Invitrogen, Carlsbad, CA, USA), which provides a human GR-LBD tagged with a glutathione-*S*-transferase (GST), a terbium-labeled anti-GST antibod,y and a fluorescein labeled SRC1−4 peptide. Binding of agonist to the nuclear receptor causes a conformational change in the LBD of the GR, which results in recruitment of the coactivator peptide. When the terbium label on the anti-GST antibody is excited at 340 nm, energy is transferred to the fluorescein label on the coactivator peptide and detected as emission at 520 nm. The GR-LBD was added to the indicated concentration of Dex, **1a**, **2a**, and **3a** in a 384-well black assay plates (Corning BV Life Sciences, Fogostraat, Amsterdam, The Netherlands) followed by addition of a mixture of the fluorescein labeled coactivator peptide and the terbium labeled anti-GST antibody. The plates were incubated at room temperature for 3 h and then measured for TR-FRET activity using the LanthaScreen optic filter module on the BMG pherastar (Imgen Technologies, VA, USA). The TR-FRET ratio was calculated by dividing the emission signal at 520 nm by the emission signal at 495 nm. Values represent the mean ± SEM of three experiments performed in duplicate, normalized to positive control, Dex 1 μM.

NF-κB Assay. HEK-293 cells were transiently cotransfected with an inducible NF-κB responsive construct, which contains 3 κB elements upstream of a minimal conalbumin promoter linked to the firefly luciferase gene[58] and a constitutively expressing β-galactosidase construct (Clontech, Saint-Germain-en-Laye, France) as an internal control to monitor for transfection efficiency (ratio of 4:1). A reverse transfection procedure was carried out using lipofectamine as a transfection reagent at a ratio of 3:2 (lipofectamine:DNA). DNA and lipofectamine were diluted in OptiMem, and this mixture was added to 48-well plates to give 500 ng of DNA per well. HEK-293 cells at a density of 7×10^5 cells/mL (200 μL) were added to this mixture. After 24 h, the cells were treated with TNF-α 10 ng/μL alone or with TNF-α 10 ng/μL and varying concentrations of Dex or CPA (**1a**) for 16 h. After 16 h, the cells were lysed with Promega lysis buffer (50 μL) and the lysates assayed for firefly luciferase activity (Promega Corporation, Madison, WI, USA). The lysates were then assayed for β-galactosidase activity using *o*-nitrophenyl-β-D-galactopyranoside as a substrate following methods described by Sambrook et al.[59] Values are expressed as the mean ± SEM of three experiments performed in duplicate, normalized to untreated control, * $p < 0.05$ relative to untreated control.

Radioligand Binding Assay. Human HeLa S3 cells enriched with GRs were used in HEPES/RPMI-1640 buffer pH 7.2. Cells (3×10^6) were incubated with 3 nM [^{3}H] Dex for 120 min at 25 °C. Nonspecific binding was estimated in the presence of Dex (10 μM). Cells were filtered and washed, and the filters were then counted to determine [^{3}H] Dex specifically bound. UDCA derivatives were screened at 10 μM and UDCA at 10 and 50 μM.

Statistical Analysis. Statistical comparison between groups was carried out using one way ANOVA with Dunnett's posthoc correction. Data are graphically represented as the mean ± standard error of the mean (SEM). All data were analyzed using GraphPad Prism5.

Acknowledgment. We thank Dr. John O'Brien and Dr. Manuel Reuther for NMR spectroscopy, Dr. Martin Feeney and Dr. Dilip Rai for HRMS data, Dr. Sinead Smith for assistance with plasmids, and Ray Keaveney for HPLC work. This work was supported by the Health Research Board [TRA/2007/11, Esophageal Cancer−Toward New Therapies] and the Embark Initiative (IRCSET Award to Sharma, 2006).

Supporting Information Available: Characterization and purity data, biochemistry figures. This material is available free of charge via the Internet at http://pubs.acs.org.

References

(1) Renaud, J. P.; Moras, D. Structural studies on nuclear receptors. *Cell. Mol. Life Sci.* **2000**, *57*, 1748–1769.
(2) Stahn, C.; Lowenberg, M.; Hommes, D. W.; Buttgereit, F. Molecular mechanisms of glucocorticoid action and selective glucocorticoid receptor agonists. *Mol. Cell. Endocrinol.* **2007**, *275*, 71–78.
(3) Banciu, M.; Schiffelers, R. M.; Metselaar, J. M.; Storm, G. Utility of targeted glucocorticoids in cancer therapy. *J. Liposome Res.* **2008**, *18*, 47–57.
(4) Heitzer, M. D.; Wolf, I. M.; Sanchez, E. R.; Witchel, S. F.; DeFranco, D. B. Glucocorticoid receptor physiology. *Rev. Endocr. Metab. Disord.* **2007**, *8*, 321–330.
(5) Necela, B. M.; Cidlowski, J. A. Mechanisms of glucocorticoid receptor action in noninflammatory and inflammatory cells. *Proc. Am. Thorac. Soc.* **2004**, *1*, 239–246.
(6) Starr, D. B.; Matsui, W.; Thomas, J. R.; Yamamoto, K. R. Intracellular receptors use a common mechanism to interpret signaling information at response elements. *Genes Dev.* **1996**, *10*, 1271–1283.
(7) Smirnov, A. N. Nuclear receptors: nomenclature, ligands, mechanisms of their effects on gene expression. *Biochemistry (Moscow)* **2002**, *67*, 957–977.
(8) Jenkins, B. D.; Pullen, C. B.; Darimont, B. D. Novel glucocorticoid receptor coactivator effector mechanisms. *Trends Endocrinol. Metab.* **2001**, *12*, 122–126.
(9) Deroo, B. J.; Archer, T. K. Glucocorticoid receptor-mediated chromatin remodeling in vivo. *Oncogene* **2001**, *20*, 3039–3046.
(10) Morrison, N.; Eisman, J. Role of the negative glucocorticoid regulatory element in glucocorticoid repression of the human osteocalcin promoter. *J. Bone Miner. Res.* **1993**, *8*, 969–975.
(11) Sakai, D. D.; Helms, S.; Carlstedt-Duke, J.; Gustafsson, J. A.; Rottman, F. M.; Yamamoto, K. R. Hormone-mediated repression: a negative glucocorticoid response element from the bovine prolactin gene. *Genes Dev.* **1988**, *2*, 1144–1154.
(12) Yudt, M. R.; Cidlowski, J. A. The glucocorticoid receptor: coding a diversity of proteins and responses through a single gene. *Mol. Endocrinol.* **2002**, *16*, 1719–1726.
(13) Zanchi, N. E.; Filho, M. A.; Felitti, V.; Nicastro, H.; Lorenzeti, F. M.; Lancha, A. H., Jr. Glucocorticoids: extensive physiological actions modulated through multiple mechanisms of gene regulation. *J. Cell. Physiol.* **2010**, *224*, 311–315.
(14) Rosen, J.; Miner, J. N. The search for safer glucocorticoid receptor ligands. *Endocr. Rev.* **2005**, *26*, 452–464.
(15) Vayssiere, B. M.; Dupont, S.; Choquart, A.; Petit, F.; Garcia, T.; Marchandeau, C.; Gronemeyer, H.; Resche-Rigon, M. Synthetic glucocorticoids that dissociate transactivation and AP-1 transrepression exhibit antiinflammatory activity in vivo. *Mol. Endocrinol.* **1997**, *11*, 1245–1255.
(16) Belvisi, M. G.; Wicks, S. L.; Battram, C. H.; Bottoms, S. E.; Redford, J. E.; Woodman, P.; Brown, T. J.; Webber, S. E.; Foster, M. L. Therapeutic benefit of a dissociated glucocorticoid and the relevance of in vitro separation of transrepression from transactivation activity. *J. Immunol.* **2001**, *166*, 1975–1982.
(17) Xiao, H. Y.; Wu, D. R.; Malley, M. F.; Gougoutas, J. Z.; Habte, S. F.; Cunningham, M. D.; Somerville, J. E.; Dodd, J. H.; Barrish, J. C.; Nadler, S. G.; Dhar, T. G. Novel synthesis of the hexahydroimidazo[1,5*b*]isoquinoline scaffold: application to the synthesis of glucocorticoid receptor modulators. *J. Med. Chem.* **2010**, *53*, 1270–1280.
(18) Schoch, G. A.; D'Arcy, B.; Stihle, M.; Burger, D.; Bar, D.; Benz, J.; Thoma, R.; Ruf, A. Molecular switch in the glucocorticoid receptor: active and passive antagonist conformations. *J. Mol. Biol.* **2010**, *395*, 568–577.
(19) De Bosscher, K. Selective Glucocorticoid Receptor modulators. *J Steroid Biochem Mol. Biol.* **2009**, *120*, 96–104.
(20) Heathcote, E. J. Management of primary biliary cirrhosis. The American Association for the Study of Liver Diseases practice guidelines. *Hepatology* **2000**, *31*, 1005–1013.
(21) Azzaroli, F.; Mehal, W.; Soroka, C. J.; Wang, L.; Lee, J.; Crispe, N.; Boyer, J. L. Ursodeoxycholic acid diminishes Fas-ligand-induced apoptosis in mouse hepatocytes. *Hepatology* **2002**, *36*, 49–54.
(22) Amaral, J. D.; Castro, R. E.; Steer, C. J.; Rodrigues, C. M. p53 and the regulation of hepatocyte apoptosis: implications for disease pathogenesis. *Trends Mol. Med.* **2009**, *15*, 531–541.
(23) Rodrigues, C. M.; Ma, X.; Linehan-Stieers, C.; Fan, G.; Kren, B. T.; Steer, C. J. Ursodeoxycholic acid prevents cytochrome c release in apoptosis by inhibiting mitochondrial membrane depolarization and channel formation. *Cell Death Differ.* **1999**, *6*, 842–854.
(24) Fimognari, C.; Lenzi, M.; Cantelli-Forti, G.; Hrelia, P. Apoptosis and modulation of cell cycle control by bile acids in human leukemia T cells. *Ann. N.Y. Acad. Sci.* **2009**, *1171*, 264–269.
(25) Keene, C. D.; Rodrigues, C. M.; Eich, T.; Chhabra, M. S.; Steer, C. J.; Low, W. C. Tauroursodeoxycholic acid, a bile acid, is neuroprotective in a transgenic animal model of Huntington's disease. *Proc. Natl. Acad. Sci. U.S.A* **2002**, *99*, 10671–10676.
(26) Keene, C. D.; Rodrigues, C. M.; Eich, T.; Linehan-Stieers, C.; Abt, A.; Kren, B. T.; Steer, C. J.; Low, W. C. A bile acid protects against motor and cognitive deficits and reduces striatal degeneration in the 3-nitropropionic acid model of Huntington's disease. *Exp. Neurol.* **2001**, *171*, 351–360.
(27) Lukivskaya, O.; Zavodnik, L.; Knas, M.; Buko, V. Antioxidant mechanism of hepatoprotection by ursodeoxycholic acid in experimental alcoholic steatohepatitis. *Adv. Med. Sci.* **2006**, *51*, 54–59.
(28) Alberts, D. S.; Martinez, M. E.; Hess, L. M.; Einspahr, J. G.; Green, S. B.; Bhattacharyya, A. K.; Guillen, J.; Krutzsch, M.; Batta, A. K.; Salen, G.; Fales, L.; Koonce, K.; Parish, D.; Clouser, M.; Roe, D.; Lance, P. Phase III trial of ursodeoxycholic acid to prevent colorectal adenoma recurrence. *J. Natl. Cancer Inst.* **2005**, *97*, 846–853.
(29) Shah, S. A.; Looby, E.; Volkov, Y.; Long, A.; Kelleher, D. Ursodeoxycholic acid inhibits translocation of protein kinase C in human colonic cancer cell lines. *Eur. J. Cancer* **2005**, *41*, 2160–2169.
(30) Khare, S.; Mustafi, R.; Cerda, S.; Yuan, W.; Jagadeeswaran, S.; Dougherty, U.; Tretiakova, M.; Samarel, A.; Cohen, G.; Wang, J.; Moore, C.; Wali, R.; Holgren, C.; Joseph, L.; Fichera, A.; Li, Y. C.; Bissonnette, M. Ursodeoxycholic acid suppresses Cox-2 expression in colon cancer: roles of Ras, p38, and CCAAT/enhancer-binding protein. *Nutr. Cancer* **2008**, *60*, 389–400.
(31) Shah, S. A.; Volkov, Y.; Arfin, Q.; Abdel-Latif, M. M.; Kelleher, D. Ursodeoxycholic acid inhibits interleukin 1 beta [corrected] and deoxycholic acid-induced activation of NF-kappaB and AP-1 in human colon cancer cells. *Int. J. Cancer* **2006**, *118*, 532–539.
(32) Poupon, R. E.; Balkau, B.; Eschwege, E.; Poupon, R. A multicenter, controlled trial of ursodiol for the treatment of primary biliary cirrhosis. UDCA-PBC Study Group. *N Engl. J. Med.* **1991**, *324*, 1548–1554.
(33) Miyaguchi, S.; Mori, M. Ursodeoxycholic acid (UDCA) suppresses liver interleukin 2 mRNA in the cholangitis model. *Hepatogastroenterology* **2005**, *52*, 596–602.
(34) Saeki, R.; Ogino, H.; Kaneko, S.; Unoura, M.; Kobayashi, K. Effects of chenodeoxycholic and ursodeoxycholic acids on interferon-gamma production by peripheral blood mononuclear cells from patients with primary biliary cirrhosis. *J. Gastroenterol.* **1995**, *30*, 739–744.
(35) Calmus, Y.; Gane, P.; Rouger, P.; Poupon, R. Hepatic expression of class I and class II major histocompatibility complex molecules in primary biliary cirrhosis: effect of ursodeoxycholic acid. *Hepatology* **1990**, *11*, 12–15.
(36) Terasaki, S.; Nakanuma, Y.; Ogino, H.; Unoura, M.; Kobayashi, K. Hepatocellular and biliary expression of HLA antigens in primary biliary cirrhosis before and after ursodeoxycholic acid therapy. *Am. J. Gastroenterol.* **1991**, *86*, 1194–1199.
(37) Nishigaki, Y.; Ohnishi, H.; Moriwaki, H.; Muto, Y. Ursodeoxycholic acid corrects defective natural killer activity by inhibiting prostaglandin E2 production in primary biliary cirrhosis. *Dig. Dis. Sci.* **1996**, *41*, 1487–1493.
(38) Ikegami, T.; Matsuzaki, Y.; Fukushima, S.; Shoda, J.; Olivier, J. L.; Bouscarel, B.; Tanaka, N. Suppressive effect of ursodeoxycholic acid on type IIA phospholipase A2 expression in HepG2 cells. *Hepatology* **2005**, *41*, 896–905.
(39) Weitzel, C.; Stark, D.; Kullmann, F.; Scholmerich, J.; Holstege, A.; Falk, W. Ursodeoxycholic acid induced activation of the glucocorticoid receptor in primary rat hepatocytes. *Eur. J. Gastroenterol. Hepatol.* **2005**, *17*, 169–177.
(40) Tanaka, H.; Makino, I. Ursodeoxycholic acid-dependent activation of the glucocorticoid receptor. *Biochem. Biophys. Res. Commun.* **1992**, *188*, 942–948.
(41) Miura, T.; Ouchida, R.; Yoshikawa, N.; Okamoto, K.; Makino, Y.; Nakamura, T.; Morimoto, C.; Makino, I.; Tanaka, H. Functional modulation of the glucocorticoid receptor and suppression of NF-kappaB-dependent transcription by ursodeoxycholic acid. *J. Biol. Chem.* **2001**, *276*, 47371–47378.
(42) Tanaka, H.; Makino, Y.; Miura, T.; Hirano, F.; Okamoto, K.; Komura, K.; Sato, Y.; Makino, I. Ligand-independent activation of the glucocorticoid receptor by ursodeoxycholic acid. Repression of IFN-gamma-induced MHC class II gene expression via a glucocorticoid receptor-dependent pathway. *J. Immunol.* **1996**, *156*, 1601–1608.
(43) Abdel-Latif, M. M.; Duggan, S.; Reynolds, J. V.; Kelleher, D. Inflammation and esophageal carcinogenesis. *Curr. Opin. Pharmacol.* **2009**, *9*, 396–404.
(44) Sola, S.; Amaral, J. D.; Borralho, P. M.; Ramalho, R. M.; Castro, R. E.; Aranha, M. M.; Steer, C. J.; Rodrigues, C. M. Functional

modulation of nuclear steroid receptors by tauroursodeoxycholic acid reduces amyloid beta-peptide-induced apoptosis. *Mol. Endocrinol.* **2006**, *20*, 2292–2303.

(45) Sola, S.; Castro, R. E.; Kren, B. T.; Steer, C. J.; Rodrigues, C. M. Modulation of nuclear steroid receptors by ursodeoxycholic acid inhibits TGF-beta1-induced E2F-1/p53-mediated apoptosis of rat hepatocytes. *Biochemistry* **2004**, *43*, 8429–8438.

(46) Schteingart, C. D.; Hofmann, A. F. Synthesis of 24-nor-5 beta-cholan-23-oic acid derivatives: a convenient and efficient one-carbon degradation of the side chain of natural bile acids. *J. Lipid Res.* **1988**, *29*, 1387–1395.

(47) Liliang, H.; Hua, Z.; Xiaoping, X.; Chunchun, Z.; Yu-Mei, S. Synthesis and charcterisation of organometallic rhenium (I) and technetium (I) bile acid complexes. *J. Organomet. Chem.* **2009**, *694*, 3247–3253.

(48) Angulo, P.; Lindor, K. D. Management of primary biliary cirrhosis and autoimmune cholangitis. *Clin. Liver Dis.* **1998**, *2*, 333−351, ix.

(49) Sola, S.; Amaral, J. D.; Castro, R. E.; Ramalho, R. M.; Borralho, P. M.; Kren, B. T.; Tanaka, H.; Steer, C. J.; Rodrigues, C. M. Nuclear translocation of UDCA by the glucocorticoid receptor is required to reduce TGF-beta1-induced apoptosis in rat hepatocytes. *Hepatology* **2005**, *42*, 925–934.

(50) Stevens, A.; Garside, H.; Berry, A.; Waters, C.; White, A.; Ray, D. Dissociation of steroid receptor coactivator 1 and nuclear receptor corepressor recruitment to the human glucocorticoid receptor by modification of the ligand−receptor interface: the role of tyrosine 735. *Mol. Endocrinol.* **2003**, *17*, 845–859.

(51) Mitsuyoshi, H.; Nakashima, T.; Inaba, K.; Ishikawa, H.; Nakajima, Y.; Sakamoto, Y.; Matsumoto, M.; Okanoue, T.; Kashima, K. Ursodeoxycholic acid enhances glucocorticoid-induced tyrosine aminotransferase-gene expression in cultured rat hepatocytes. *Biochem. Biophys. Res. Commun.* **1997**, *240*, 732–736.

(52) Arenas, F.; Hervias, I.; Uriz, M.; Joplin, R.; Prieto, J.; Medina, J. F. Combination of ursodeoxycholic acid and glucocorticoids upregulates the AE2 alternate promoter in human liver cells. *J. Clin. Invest.* **2008**, *118*, 695–709.

(53) Newton, R.; Holden, N. S. Separating transrepression and transactivation: a distressing divorce for the glucocorticoid receptor? *Mol. Pharmacol.* **2007**, *72*, 799–809.

(54) Belvisi, M. G.; Brown, T. J.; Wicks, S.; Foster, M. L. New Glucocorticosteroids with an improved therapeutic ratio? *Pulm. Pharmacol. Ther.* **2001**, *14*, 221–227.

(55) Regan, J.; Lee, T. W.; Zindell, R. M.; Bekkali, Y.; Bentzien, J.; Gilmore, T.; Hammach, A.; Kirrane, T. M.; Kukulka, A. J.; Kuzmich, D.; Nelson, R. M.; Proudfoot, J. R.; Ralph, M.; Pelletier, J.; Souza, D.; Zuvela-Jelaska, L.; Nabozny, G.; Thomson, D. S. Quinol-4-ones as steroid A-ring mimetics in nonsteroidal dissociated glucocorticoid agonists. *J. Med. Chem.* **2006**, *49*, 7887–7896.

(56) Barker, M.; Clackers, M.; Copley, R.; Demaine, D. A.; Humphreys, D.; Inglis, G. G.; Johnston, M. J.; Jones, H. T.; Haase, M. V.; House, D.; Loiseau, R.; Nisbet, L.; Pacquet, F.; Skone, P. A.; Shanahan, S. E.; Tape, D.; Vinader, V. M.; Washington, M.; Uings, I.; Upton, R.; McLay, I. M.; Macdonald, S. J. Dissociated nonsteroidal glucocorticoid receptor modulators; discovery of the agonist trigger in a tetrahydronaphthalene-benzoxazine series. *J. Med. Chem.* **2006**, *49*, 4216–4231.

(57) Altorki, N.; Schwartz, G. K.; Blundell, M.; Davis, B. M.; Kelsen, D. P.; Albino, A. P. Characterization of cell lines established from human gastric−esophageal adenocarcinomas. Biologic phenotype and invasion potential. *Cancer* **1993**, *72*, 649–657.

(58) Arenzana-Seisdedos, F.; Fernandez, B.; Dominguez, I.; Jacque, J. M.; Thomas, D.; Diaz-Meco, M. T.; Moscat, J.; Virelizier, J. L. Phosphatidylcholine hydrolysis activates NF-kappa B and increases human immunodeficiency virus replication in human monocytes and T lymphocytes. *J. Virol.* **1993**, *67*, 6596–6604.

(59) Sambrook, J.; Russel, D. W. *Molecular Cloning: A Laboratory Manual*, 3rd ed.; Cold Spring Harbour Laboratory Press: New York, 2001; Vol. 2.